The functions of ICT1 and mtRbfA in the human mitochondrial ribosome

Ricarda Richter B.Sc.

Thesis submitted to Newcastle University in candidature for the degree of Doctor of Philosophy

Newcastle University
Faculty of Medical Sciences
Institute for Ageing and Health
Mitochondrial Research Group
November 2010

Abstract

During the last decades our knowledge about the human mitochondrial translation system has been expanded. However, our understanding of this unique system is far from complete. Mitochondria contain a minimal genome, whose expression is dependent on factors encoded by the nuclear genome. Derived from a bacterial ancestor it is very close to the translation system found in bacteria, but there are also a lot of differences especially the translating ribosome, which differs in a number of features including the sedimentation coefficient, protein-RNA ratio and number of tRNA sites. Available cryo-EM structures of the mitochondrial ribosome are limited, making it difficult to understand the system completely. There are still a lot of open questions concerning the composition, assembly, translation initiation or the recycling of stalled ribosomes in mammalian mitochondria. The study presented in this thesis contributes to our understanding of this unique system by the characterisation of two mitochondrial proteins, found in association with the mitochondrial ribosome, ICT1 and mtRbfA. These proteins are found in association with the mitochondrial ribosome, and were immunoprecipitated together with the mitochondrial ribosome recycling factor (mtRRF).

ICT1 as a member of the mitochondrial release factor family has been identified as a peptidyl-tRNA hydrolase. Data shown here indicates that ICT1 has been recruited into the mitochondrial ribosome and further, suggests the involvement of ICT1 in the rescue of stalled ribosomal complexes with immobilised peptidyl-tRNA.

In contrast mtRbfA was identified as a potential ribosome assembly factor rather than a permanent component. The function of this protein is still elusive, but data generated for this thesis shows that this protein is preferentially associated with the mitochondrial ribosomal small subunit at a late assembly point, suggesting possible roles of mtRbfA in quality control or in translation initiation.

Acknowledgments

First of all, I owe my gratitude to my supervisors, Bob and Zosia for giving me the opportunity to undertake this PhD in their laboratory on such an interesting project. I am very grateful for all their guidance and constructive discussions all the time. Furthermore I would like to thank Zosia for performing the *in vitro* translation assay and for proof-reading this thesis with her inspiring suggestions.

I thank all members of the Mitochondrial Research Group (MRG), present and past, for the last past four years. Especially, many thanks to Asia, who taught and helped me a lot and to Mateusz, who often answered many of my questions with his fundamental knowledge. Because of her kindness and willingness to help all the time I am very grateful to Ola, it was a pleasure to work with her. For helping me with the CLIP assay I owe many thanks to Agata. I would like to thank Sven for helping me a lot with the RNA analysis and for many interesting discussions. Thanks to Geoff for kindly performing most of the DNA sequencing reactions and to everyone else from the MRG, who helped me directly or indirectly during this time.

For an excellent collaboration I owe many thanks to Hans Wessels and Prof. Jan Smeitink (UNMC, Nijmegen, The Netherlands), who performed the LC MS/MS analysis. Also thanks to Prof. Umesh Varshney (Bangalore, India) and Dr. Nathalie Bonnefoy (CNRS, Paris, France) and their research groups for great collaboration and their investigations of ICT1 and its orthologues in the bacterial and yeast system, respectively.

I thank Mr. Ian Dimmick (Centre for Life, Newcastle University, Flow Cytometry Core Facility) for his kind assistance during FACS analysis.

Finally and most importantly I owe special thanks to my parents, for their understanding, encouragement and great support from the distance.

Author's declaration

I certify that none of the material presented in this thesis has been previously submitted by me for a degree or other qualification in this or any other university. Furthermore, it is my own independent contribution, unless stated otherwise.

These studies were carried out solely in the Institute for Ageing and Health, Mitochondrial Research Group under supervision and guidance of Dr. Zofia Chrzanowska-Lightowlers and Prof. Robert Lightowlers, between October 2007 and August 2010.

Ricarda Richter

Table of contents

List of Figures

List of Tables

Abbreviations

aa	amino acid(s)
aa-tRNA	aminoacyl-tRNA
ADP	adenosine diphosphate
Amp	ampicillin
APS	ammonium-persulphate
A-site	aminoacyl-tRNA site within the ribosome
ATP	adenosine triphosphate
BGH	Bovine growth hormone (BGH) polyadenylation signal
BN	Blue Native
bp	base pair(s)
Br-dUTP	bromolated deoxyuridine triphosphate
BSA	bovine serum albumin
c	cytochrome *c*
CBB	Coomassie Brilliant Blue
CL	cell lysate
CLIP	Crosslinking immunoprecipitation
CMV	cytomegalovirus
CO, COX	Cytochrome *c* oxidase
cpm	counts per minute
C_T	threshold cycle
C-terminus	carboxyl-terminus
cyt	cytochrome
DAB	3,3'-Diaminobenzidine tetrahydrochloride
DAPI	4'-6-Diamidino-2-phenylindole
DC	decoding centre
DEPC	diethyl pyrocarbonate
dH_2O	distilled water
D-loop	displacement loop
DMEM	Dulbecco's modified Eagle's medium
DMSO	dimethyl-sulphoxide
DNA	deoxyribonucleic acid
dNTP	deoxynucleotide triphosphate
DOX	doxacycline
dsDNA	double stranded DNA
DTT	dithiothreitol
E. coli	*Escherichia coli*
EDTA	ethylene diamine tetra-acetic acid
EF(-G/-Ts/-Tu)	elongation factor (-G/-Ts/-Tu)
EGTA	ethylene glycol tetra-acetic acid
EM	electron microscopic
EMEM	Earle's Minimal Essential Medium
EMPAI	experimental modified Protein Abundance Index (Estimation of molar abundance of proteins in a LC MS/MS analysed sample; PAI is a semi-quantitative representation of the relative amount of protein in a sample, relating the number of identified tryptic peptides to the number of theoretically observable ones)
ER	endoplasmic reticulum
E-site	exit-site within the ribosome
EtOH	ethanol
FAD	flavin-adenine dinucleotide
$FADH_2$	reduced flavin-adenine dinucleotide
FBS	foetal bovine serum
FCCP	trifluorocarbonylcyanide phenylhydrazone
Fe-S	iron-sulfur
fmet	formyl-methionine
FMN	flavine mononucleotide
FRT	Flp-recombination-target
GDP	guanine diphosphate
Glc	glucose

GST	Glutathione-S-transferase
GTP	guanine triphosphate
h	hour(s)
HEK293T	human embryonic kidney cells
HeLa	human cervical cancer carcinoma cells from Henrietta Lacks.
HRP	horseradish-peroxidase
H. sapiens	*Homo sapiens*
HSP	heavy strand promotor
H-strand	heavy strand
IAA	isoamylalcohol
IF	initiation factor
IgG	immunoglobulin type G
IMM	inner mitochondrial membrane
IMS	intermembrane space
IP	immunoprecipitation
IPTG	Isopropyl β-D-1-thiogalactopyranoside
JC 1	5,5',6,6'-tetrachloro-1,1',3,3'-tetraethylbenzimi-dazolylcarbocyanine iodide
kDa	kilo-Dalton
kb	kilo-base(pairs)
KCl	potassium chloride
KOD	DNA polymerase from *Thermococcus kodakaraensis*
LB	Luria-Bertani
LC MS/MS	liquid chromatography - tandem mass spectrometry
LSP	light strand promotor
L-strand	light strand
LSU	large subunit
M	mitochondria
MES	2-(*N*-morpholino)ethanesulfonic acid
m^7G-cap	7-methylguanosine cap
min	minute(s)
MOPS	morpholinopropanesulfonic acid
MPP	mitochondrial processing peptidase
mRNA	messenger RNA
MRP(L/S)	mitochondrial ribosomal protein (of the LSU/ SSU)
mt	mitochondrial
mtDNA	mitochondrial genome
mtPTP	mitochondrial permeability transition pore
MTT	3-(4,5-Dimethylthiazol-2-yl)-2,5-diphenyltetrazolium bromide
NAD	nicotinamide-adenine dinucleotide
$NADH+H^+$	reduced nicotinamide-adenine dinucleotide
NAO	10-n-nonyl-acridine orange
N. crassa	*Neurospora crassa*
ND	NADH dehydrogenase
nDNA	nuclear DNA
NP-40	Nonidet P-40, octyl phenoxy-polyethoxy-ethanol
nt	nucleotide(s)
NTB	NitroTetrazolium Blue
N-terminus	amino-terminus
OD	optical density
o/e	overexpressed, overexpressor
OMM	outer mitochondrial membrane
ORF	open reading frame
Ori_H	origin of heavy-strand replication
Ori_L	origin of light-strand replication
OXPHOS	oxidative phosphorylation
p	p-value
PAG(E)	polyacrylamide gel (electrophoresis)
PBS	phosphate buffered saline
PCR	polymerase chain reaction
Pfu	DNA polymerase from *Pyrococcus furiosus,*

P_i	inorganic phosphate
PI-Mix	protease inhibitor cocktail (Roche)
PMSF	phenylmethylsulphonyl fluoride
PNK	polynucleotide kinase
PPR	putative pentatricopeptide repeat
P-site	peptidyl-tRNA site within the ribosome
PTC	peptidyl-transferase centre
PTH	peptidyl-tRNA hydrolase
PVDF	polyvinyliden fluoride
Q	ubiquinone, coenzyme Q
RBP	RNA binding protein
RF	release factor
RISC	RNA-induced silencing complex
RNA	ribonucleic acid
ROS	reactive oxygen species
rpm	rounds per minute
RRF	ribosome recycling factor
rRNA	ribosomal RNA
secs	seconds
SDH	Succinate-dehydrogenase
SDS	sodium-dodecyl-sulphate
siRNA	silencing RNA, small interfering RNA
SN	supernatant
SOC	super optimal broth
SOD	superoxide dismutase
S. pombe	*Schizosaccharomyces pombe*
SSC	saline sodium citrate buffer
ssDNA	single stranded DNA
SSPE	saline sodium phosphate EDTA buffer
SSU	small subunit
SU	subunit
Su9	ATPase subunit 9
T_a	annealing temperature
TAE	tris-acetate EDTA
Taq	DNA polymerase from *Thermus aquaticus*
TBS	tris buffered saline
TBS-T	tris buffered saline, containing Tween-20
TCA	tricarboxylic acid (cycle)
TEMED	N, N, N', N'-tetramethylethylene-diamine
tet	tetracycline
TIM	translocase of the inner mitochondrial membrane
tmRNA	transfer-messenger RNA
T. maritima	*Thermotoga maritima*
TOM	translocase of the outer mitochondrial membrane
tRNA	transfer RNA
Tris	2-Amino-2-hydroxymethyl-propane-1,3-diol
Triton X-100	polyethylene glycol p-(1,1,3,3-tetramethylbutyl)-phenyl ether
T. thermophilus	*Thermus thermophilus*
Tween-20	polyoxyethylene sorbitanmonolaurate
U	unit (enzyme activity; 1U = 1µmol/ min)
UCP	uncoupling proteins
UTR	untranslated region
UV	ultra-violet
vol	volume
v/v	volume/ volume
WT	wildtype
w/v	weight/ volume
xg	relative centrifugal force

Chapter 1:

Introduction

1 Chapter 1: Introduction

1.1 Mitochondria - general aspects

Approximately 1-2 billion years ago an α-proteobacterium (symbiont) was annexed into a primitive eukaryotic cell (host) by endocytosis [Gray *et al.*, 1999; De Duve, 2007]. This endosymbiosis theory is widely accepted as the origin of mitochondria, which are ubiquitous organelles within the vast majority of eukaryotes. Over evolution a fascinating kind of symbiosis between the host cell and the symbiont has developed whose communication is in such a perfection of nature that our understanding of this complicated system is very far from complete.

The present day mitochondria are no longer autonomous, because they have transferred most of their genetic information to the nucleus of the host and therefore they are totally dependent on the host cell. The host in turn also depends on its symbiotic partner that performs many important, and for the host essential, tasks. Mitochondria are often called the power-plant of the cell as they produce the majority of cellular ATP. This is done through oxidative phosphorylation (OXPHOS), a process that includes electron transport and proton pumping by the organelle to generate an electrochemical gradient as energy force. ATP production is by far not the only function of mitochondria even if it is the most widely described. Mitochondria are also the location of many metabolic pathways such as tricarboxylic acid (TCA) cycle, β-oxidation, urea cycle or amino acid synthesis. Furthermore they are absolutely crucial for iron-sulphur biogenesis, probably the essential task of mitochondria within the eukaryotic cell [Lill, 2009]. In addition mitochondria are further involved in many cellular processes such as calcium and iron homoeostasis, ROS (reactive oxidative stress) production and apoptosis.

Human mitochondria have been studied intensively during the last decades since a dysfunction of those organelles leads to many human diseases, which are currently untreatable. Therefore it is absolutely crucial that we understand those little task-rich organelles, most of which have still their own genome, and in humans is a small minimised DNA molecule (mtDNA). The expression of mtDNA encoded proteins is dependent on nuclear encoded factors, which are synthesised in the cytosol and transported into the mitochondria. The reason for the transfer of the vast majority of genetic material (~99%) from the α-proteobacterium to the host genome is probably due to selective pressure to protect the DNA from mutagenesis within the organelle

since the uncorrected mutation rate of human mtDNA is 10- to 17-fold higher compared to the nDNA [Wallace, 2007, Tuppen *et al.*, 2010]. The reason why mitochondria continue to maintain a small genome that encodes only a limited subset of components of the OXPHOS complexes and whose expression requires a complicated coordinated expression machinery imported into the mitochondria is not clear. Strikingly all the proteins that are encoded by the human mtDNA are hydrophobic components of the OXPHOS complexes and COX1 and cytochrome *b*, which are the most hydrophobic ones, are present in every sequenced mitochondrial genome [Wallace, 2007]. Therefore it is often proposed that the difficulty in import of those hydrophobic proteins across the membrane might be the reason for maintaining the expression of those components within the organelle.

1.2 Origin of mitochondria

Although the endosymbiosis theory is widely accepted as the origin of mitochondria, there remain some controversial discussions about the host. Some groups argue that it was a amitochondriate primitive eukaryote containing already the nucleus and having the ability for phagocytosis. Others believe that it was an archaebacterium, meaning that the nucleus and mitochondria developed more or less at the same time from one event [Gray *et al.*, 1999]. De Duve (2007) argued that the host was more likely to be a eukaryotic cell with a cytomembrane and cytoskeletal machineries that were involved in the endocytic uptake of extra-cellular materials. Thus the ability of phagocytosis and the development of a nucleus, which is required for the transfer of genetic material from the symbiont to the host, must have been present before the α-proteobacterium was annexed by the host. This hypothesis was also argued for a long time with the fact that there are anaerobic eukaryotes, called Archezoa that lack mitochondria ("Archezoa model"). However, it was shown that the nucleus of those Archezoa encodes typical mitochondrial proteins (e.g. chaperones, with rickettsia like ancestry), which are then imported into an organelle. This organelle is called the "hydrogenosome" that generates ATP anaerobically, producing hydrogen as the reduced end product. Thus Martin and Müller (1998) proposed the "hydrogen hypothesis" where a common ancestor of living eukaryotes had an endosymbiont. They further described that it is very common that bacteria and archea depend on each other, where one of them is producing the waste that the other one is using as food. Furthermore it was shown that one prokaryote could live inside another, non-phagocytotic prokaryote [von Dohlen *et al.*, 2001]. Davidov and Jurkevitch (2009) suggested that since bacteria are not able to

undergo phagocytosis, a predatory interaction between the two prokaryotes might be the origin of the eukaryotic cell. Thus the predator, a small (facultative) aerobic α-proteobacterium penetrated and replicated with an archeal host periplasm (-like) space and later developed to the current mitochondrion. In addition to the hydrogenosome there are also small organelles with a double membrane called “mitosomes”, present in Archezoa such as Giardia. The real function of those mitosomes is not clear as they probably do not play any role in ATP synthesis. However, since they contain mitochondrial proteins required for the Fe-S cluster assembly [reviewed in Embley and Martin, 2006] it might be that the iron-sulphur biogenesis is the essential task of all mitochondria or mitochondria-like organelles. Therefore it was proposed that all eukaryotes contain mitochondria or mitochondria-like organelles (hydrogenosomes or mitosomes). It is possible that both the origin of the eukaryotic nucleus and the origin of anaerobic (hydrogenosome) and aerobic (mitochondria) energy metabolism arise from the same event [reviewed in Gray *et al.*, 1999; Davidov and Jurkevitch, 2009]. However, it is quite difficult to show clear evidence for an event that happened a billion years ago and therefore it is plausible that there is more than one accurate hypothesis.
What is probably in agreement of all studies is that mitochondria are from monophyletic origin and that they are closely related to the members of the rickettsial subdivision of the α-proteobacteria [Gray *et al.*, 1999]. Rickettsiales are obligate intracellular parasites of eukaryotes and their genome, which was sequenced by Andersson *et al.* in 1998, shows a great deal of reduction as does the human mitochondrial DNA [Anderson *et al.*, 1981].

1.3 Structure of mitochondria

Mitochondria were first described in 1857 as granule-like structures in muscle cells by Albert von Kolliker. In 1898 Carl Benda gave those organelles the name “mitochondria”, derived from the Greek words “mitos” (thread) and “chondros” (granules). Mitochondria are relatively large organelles in the eukaryotic cytoplasm with a diameter of 0.2 µm to 1 µm. The length can vary, but usually a single mitochondrion has a length from approximately 1 µm to 2 µm. The actual number, size and also positioning of mitochondria within the cell depends on the particular tissue, where heart, brain, skeletal muscle, kidney and liver are relatively mitochondria rich, due to the high necessity on energy production within those tissues. Mitochondria are dynamic organelles with morphological variations, but often are present as a branched reticular network that is regulated by fission and fusion events of the mitochondria. The

movement of mitochondria within the cell is strongly associated with components of the cytoskeleton, the microtubules. The cytosolic dynein is the motor protein that transports mitochondria along the microtubules in the cell.

The development of electron microscopy allowed that the structure of the mitochondrion could be more thoroughly investigated. Palade (1952) and Sjöstrand (1956) were the pioneers in electron microscopy of mitochondria. Mitochondria are usually described with four compartments: the mitochondrial outer membrane (OMM), the intermembrane space (IMS), the inner membrane (IMM), whose surface is increased by forming cristae, and the matrix. Palade developed a mitochondrial model, called “baffle model” that is actually the popular presentation of mitochondria in text books, where cristae have broad openings to the intermembrane space.

A new technique, the electron microscopic (EM) tomography shows the actual internal organisation of mitochondria in a different way. This reveals them to have extensively tubular cristae, which can merge to flattened lamellar compartments (Figure 1.1). The form and size of cristae depend on the tissue according to Frey and Mannella (2000).

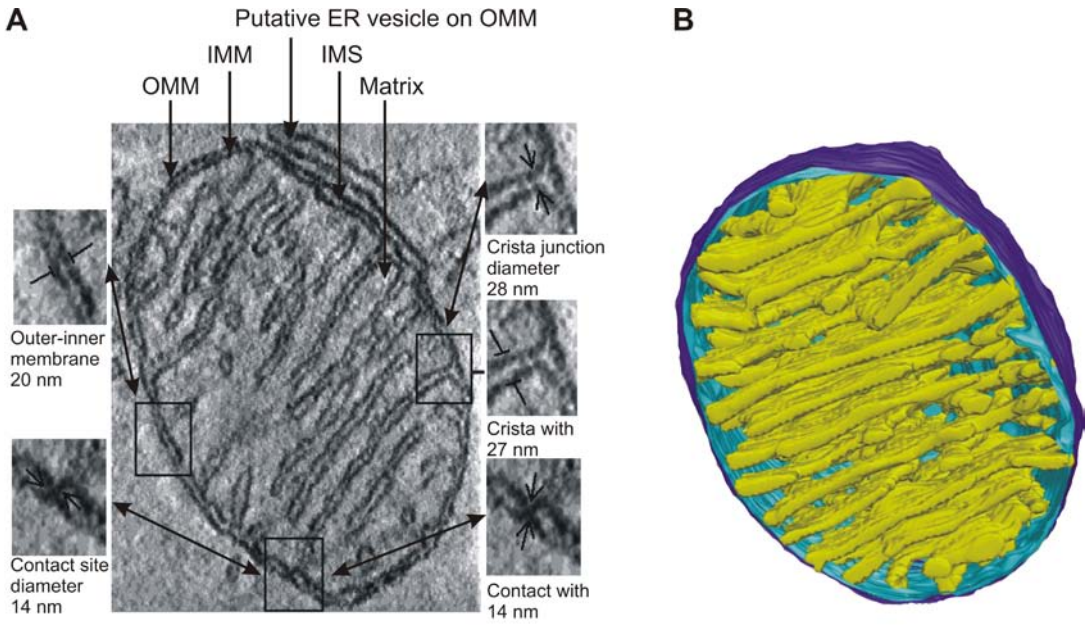

Figure 1.1: Structure of mitochondria. A) Section through a 3D tomogram of a chick cerebellum mitochondrion shows the organelle with the outer mitochondrial membrane (OMM), the inner mitochondrial membrane (IMM), the intermembrane space in between (IMS), the cristae and the matrix. The cristae are connected to the inner boundary membrane through tubular crista junctions. Image shows further an endoplasmatic reticulum (ER) vesicle in very close proximity to the outer mitochondrial membrane. **B)** Computer model generated from segmented 3D tomograms of the chick brain mitochondrion showed in (A). The model shows the outer membrane in dark blue, the inner boundary membrane in light blue and the cristae in yellow. (Images were adapted from Frey and Mannella, 2000)

What they have in common is the connection to the inner boundary membrane via tubular cristae junctions, which have a diameter of 28 nm (Figure 1.1 A). The outer membrane contains an abundance of the transport protein - porin, which forms channels through this lipid bilayer. A number of ions and small molecules can pass this permeable outer membrane and enter the intermembrane space, but they can not pass the impermeable inner membrane. The intermembrane space contains a number of proteins with cytochrome *c* as the most prominent one, which transfers electrons from Complex III to Complex IV. Additionally cytochrome *c* is also involved in apoptosis and its release from the IMS to the cytosol induces caspases-dependent apoptosis (see 1.4.3). The inner membrane is very protein rich with approximately 75% protein content (compared with most others with ~50%) [Liu and Spremulli, 2000]. It contains the abundant enzymatic complexes for oxidative phosphorylation and further channel-forming proteins and metabolite transporter proteins. The matrix harbours the majority of mitochondrial proteins that are involved in metabolic processes such as TCA cycle or β-oxidation, and iron-sulphur biogenesis. Furthermore it contains multiple copies of mtDNA, proteins that are involved in the maintenance of the mitochondrial genome, and also the mitochondrial gene expression machinery. Since the human mitochondrion comprises 1,100-1,400 proteins [Calvo and Mootha, 2010] of which only 13 are mitochondrial encoded, the majority are nuclear encoded. These are synthesised by the ribosomes in the cytosol as a precursors with a mitochondrial targeting peptides and then transported by the TOM complex through the outer membrane. In most cases they are further transported by the TIM23 through the inner membrane towards the matrix. The majority of proteins are processed by the mitochondrial processing peptidase (MPP) and folded by mitochondrial chaperones [reviewed in Neupert and Herrmann, 2007].

1.4 Functions of mitochondria

1.4.1 Oxidative phosphorylation (OXPHOS)

A major function of mitochondria is the transduction of energy into the form of ATP via oxidative phosphorylation (OXPHOS). There are five enzymatic complexes (OXPHOS complexes) in the mitochondrial inner membrane whose interplay is crucial for this task: the NADH:ubiquinone oxidoreductase (Complex I), the succinate:ubiquinone oxidoreductase (Complex II), the ubiquinol:cytochrome *c* reductase (Complex III), the cytochrome *c* oxidase (Complex IV) and the ATP synthetase (Complex V) (Figure 1.2).

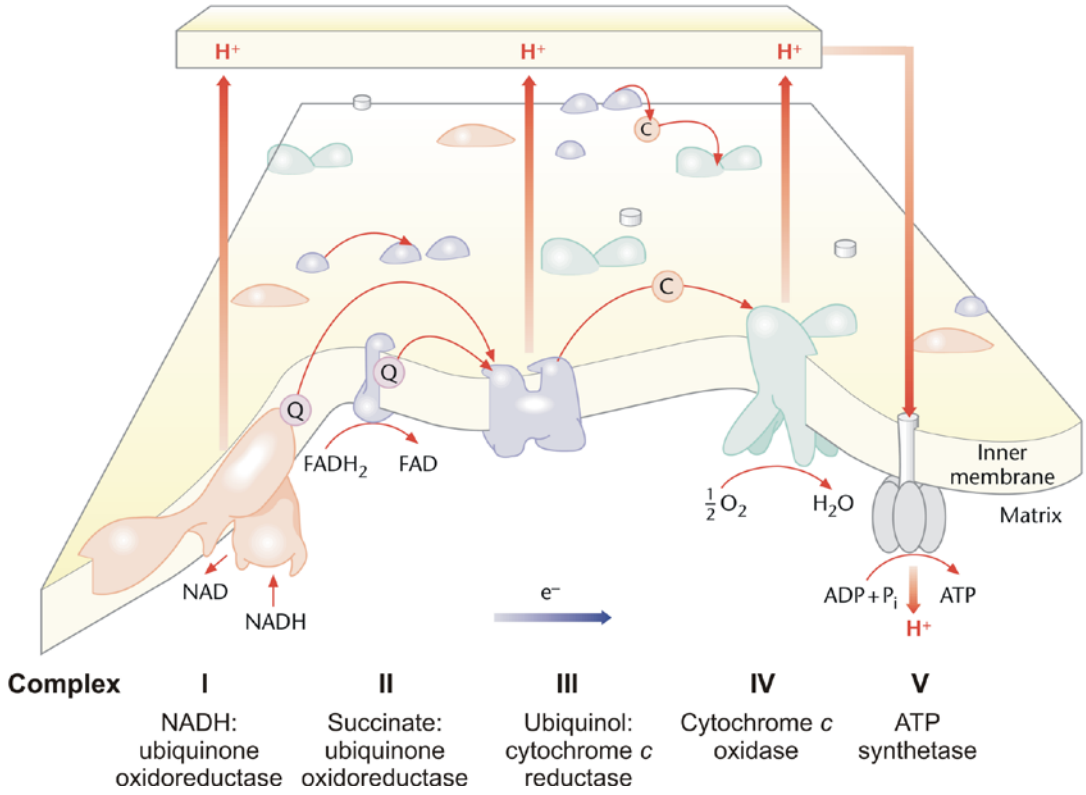

Figure 1.2: Mitochondrial oxidative phosphorylation (OXPHOS). The OXPHOS Complexes I to V are shown randomly distributed within the inner mitochondrial membrane. The mobile electron carrier ubiquinone and cytrochrome *c* are labelled as circles with single letter (Q and C, respectively). Proton pumping across the membrane into the intermembrane space by Complex I, III and IV is indicated as thick red arrows. Arrow in opposite direction reflects the force of the electrochemical gradient, used by Complex V for ATP production. (Image taken from Lightowlers *et al.*, 2001)
FAD: flavin-adenine dinucleotide; NAD: nicotinamide-adenine dinucleotide; ADP: adenosine diphosphate; P_i: inorganic phosphate; ATP: adenosine triphosphate.

The reduced co-factors $NADH+H^+$ and $FADH_2$, which are products from different pathways such as TCA cycle or β-oxidation, are oxidised by Complex I and II. Collected electrons are transferred to the lipid-soluble, electron-shuttle ubiquinone (Coenzyme Q, CoQ, Q), which is then reduced to ubiquinol (QH_2). With the transport of electrons, protons are pumped into the intermembrane space by Complex I. Ubiquinol further transfers the electrons to Complex III followed by a difficult mechanism, the Q cycle, where ubiquinol is oxidised to ubiquinone. The water soluble cytochrome *c* (cyt *c*, *c*) then transfers the electrons from Complex III to Complex IV. Both Complex III and Complex IV have also the ability to pump protons into the intermembrane space. Finally the electrons that are delivered by the reduced cyt *c*, are transferred to ½ O_2 and $2H^+$ by Complex IV with H_2O as endproduct. The protons that are pumped into the intermembrane space by Complex I, III and IV generate a pH- and thus an

electrochemical gradient that is further used as a proton motive force by Complex V to generate ATP.

Complex I

This complex is the largest of all the OXPHOS complexes with a molecular weight of approximately 980 kDa. So far there is no crystallisation of mammalian Complex I, but low-resolution three-dimensional electron microscopy shows its overall structure with a L-shape with two perpendicular arms: a hydrophobic membrane arm, which contains the mitochondrial encoded subunits and a hydrophilic matrix arm [reviewed in Vogel *et al.*, 2007]. Human Complex I contains 45 subunits, of which 38 components are nuclear encoded and the remaining 7 mitochondrial encoded (ND1, ND2, ND3, ND4, ND4L, ND5 and ND6). It further contains a non-covalently bound flavine mononucleotide (FMN) and eight iron-sulphur clusters, essential for the electron conduction. Mitochondrial disorders caused by Complex I dysfunction is very common, probably due to the large number of components that can go wrong. Pathogenic mutations have been described in every single mitochondrial encoded subunit [reviewed in Fernández-Vizarra *et al.*, 2009]. Additionally also pathogenic mutations within nuclear encoded structural subunits and further assembly factors have been reported associated with Complex I deficiency. The overall assembly of this large complex is quite complicated and even if it was intensively studied in the past few years, it is still not completely understood [Vogel *et al.*, 2007; Lazarou *et al.*, 2009].

Complex II

The Succinate:Ubiquinone oxidoreductase is the simplest of all the complexes in the respiratory chain. It is an iron-sulphur flavoenzyme that catalyses as part of the TCA cycle the oxidation of succinate to fumarate. Complex II contains four subunits, which are all nuclear encoded: SDHA, harbouring a covalently bound flavin-adenine dinucleotide (FAD), SDHB with three iron-sulphur centres, SDHC and SDHD, which together contain a cytochrome b_{560} [reviewed in Rutter *et al.*, 2010]. SDHA (70 kDa) and SDHB (27 kDa) form together the hydrophilic catalytical unit, the succinate dehydrogenase, which is located towards the matrix. However, the membrane anchor, composed by SDHC (15 kDa) and SDHD (13 kDa) is crucial for the ubiquinone binding. Complex II is only involved in the delivery of electrons to ubiquinone, but does not translocate protons into the intermembrane space.

Complex III

In 1998 the crystal structure of bovine Complex III, also called cytochrome bc_1 was published by Iwata *et al*. The mammalian Complex III is a stable dimer, of which each monomer harbours 11 subunits with an overall molecular weight of approximately 240 kDa [reviewed in Saraste, 1999]. Cytochrome *b* (cyt *b*) is the only subunit of Complex III that is mitochondrial encoded. It is one of the key elements, forming the redox centre of Complex III. Cyt *b* is very hydrophobic, containing eight transmembrane helices with two *b*-type haems (cytochrome b_L and b_H). The other two components of the redox centre are a membrane-anchored iron-sulphur protein with a Rieske Fe-S centre and cytochrome c_1. The function of Complex III requires the interaction with the electron carrier, ubiquinone/ ubiquinol at two sites: the Q_o (between the iron-sulphur protein and cyt *b*, close to the intermembrane space) and the Q_i (in cyt *b*, close to the matrix side). One ubiquinol can deliver two electrons: one of them is transferred to the Rieske Fe-S centre, further to cyt c_1 and finally to the water soluble cyt *c* in the intermembrane space. The second electron is transferred by haem b_L and b_H to Q_i. Thus after oxidation of two ubiquinols, two electrons can be delivered to Q_i and finally reduce one ubiquinone. The differences in the redox potential of the two haems are crucial for the proton motive force. Finally with each electron that is transferred to cyt *c*, two protons are pumped into the intermembrane space.

Complex IV

The X-ray crystal structure from bovine cytochrome-*c* oxidase (Complex IV, COX), which was published in 1996 by Tsukihara *et al.,* shows the enzyme as a dimer. Each monomer has a molecular weight of 204 kDa, composed by 13 subunits. The catalytic core contains the two of the three mitochondrial encoded subunits COX1 (57 kDa) and COX2 (25 kDa), which contain two type *a* haems (cytochrome *a* and a_3) and further the copper centres (Cu_A and Cu_B), essential for the electron transfer. The third mitochondrial encoded protein of Complex IV is COX3 and is part of the structural core. The other 10 subunits are nuclear encoded. Cytochrome-*c* oxidase is the terminal electron accepter of the respiratory chain and reduces oxygen to water. The electrons, delivered by cyt *c*, are first transferred to cytochrome *a* in COX1 and then to cytochrome a_3 and Cu_B, which forms a binuclear centre and is crucial for oxygen binding and reduction [reviewed in Saraste, 1999].

One of the most common defects in the respiratory chain in human pathology is COX deficiency. Quite often the reason for those defects are mutations in nuclear encoded proteins, crucial for the assembly and maturation of Complex IV (e.g. SURF1, COX10 and COX15 [Zhu *et al.*, 1998; Fernández-Vizarra *et al.*, 2009]) or for the expression of

the mitochondrial encoded ones (e.g. TACO1 and LRPPRC [Weraarpachai *et al.*, 2009, Mootha *et al.*, 2003, Sasarman *et al.*, 2010]).

Complex V

The ATP synthetase (F_oF_1-ATP synthetase, F_oF_1-ATPase) is a large complex with a molecular weight of approximately 500 kDa, composed by a water-soluble "head" complex with ~380 kDa (F_1) and the hydrophobic transmembrane portion (F_o) [reviewed in Yoshida *et al.*, 2001]. Two protein stalks connect F_1 and F_o to each other. The F_1 ATPase is composed of 5 different subunits (α, β, γ, δ and ε), where 3α and 3β subunits, arranged alternately, form a cylinder around the γ subunit [Gibbons *et al.*, 2000]. Both α and β subunits can bind nucleotides, but it is the β subunit that has the catalytic activity. This catalytic component in F_1 has three active sites and each site passes three different states: 1) "open", an empty state, 2) "loose", a state with bound ADP and P_i and 3) "tight", a state with tightly bound ATP. The F_o part of Complex V contains 8 subunits (a, b, c, d, e, f, g and A6L), where subunits a and A6L are encoded by the mitochondrial genes *MT-ATP6* and *MT-ATP8*, respectively. The proton translocation through the F_o particle causes the rotation of the γ subunit within F_1. This leads to the described conformational changes within the β subunits and therefore to ATP synthesis in F_1.

Supercomplexes

There have been a lot of investigations into how the OXPHOS complexes are organised within the inner membrane during the last decade. Usually the complexes are shown individually, randomly moving within the inner membrane, connected through the electron transfer by the mobile carriers ubiquinone and cytochrome *c*. This model is the favourite version in text books and is also called "fluid model". Following from the work of Schägger and Pfeiffer in 2000, however, there have been a lot of reports indicating that the individual complexes are assembled in larger supercomplexes [reviewed in Vonck and Schäfer, 2009], also called "respirasomes". This high degree of organisation of the complexes is also known as the "solid model". The most abundant supercomplex in bovine mitochondria was shown to be an association of one copy of Complex I, dimeric Complex III and one Complex IV ($I_1III_2IV_1$) [Schäfer *et al*., 2007]. Furthermore the ATPase was shown in a higher organisation, usually as a dimer. In 2008 Acín-Pérez *et al.* proposed a third model called "plasticity model", which suggests that most Complex IV and Complex II and some of Complex III are not within supercomplexes and that those individual complexes are likely to move freely within the mitochondrial inner membrane. In

contrast Complex I always seems to be in association either with Complex III, with Complexes III and V, with Complexes II, III, and IV, or with Complexes III and IV. Interestingly the same authors have shown for the first time that some of those supercomplexes contain ubiquinone and cytochrome *c* and further they demonstrated that those isolated supercomplexes containing Complex I, III and IV are able to transfer electrons from NADH to oxygen and therefore can be really considered as respirasome.

1.4.2 Mitochondrial Reactive Oxygen Species (ROS) production

The respiratory chain performs one of the major functions of mitochondria, where electron transfer along the complexes leads to a proton motive force that generates a membrane potential used by Complex V to produce ATP. The final electron acceptor in the respiratory chain is Complex IV, which reduces O_2 to H_2O. But electrons may leak from the respiratory chain, reacting with oxygen to form superoxide ($O_2^{\bullet -}$). The major sources producing superoxide within mitochondria are Complex I and Complex III. There are two known mechanisms of how superoxide occurs via Complex I: first, a high $NADH/NAD^+$ ratio leads to fully reduced FMN of Complex I and reacts with O_2 producing $O_2^{\bullet -}$. Thus a dysfunction within the respiratory chain can lead to increased $NADH/NAD^+$ ratio and therefore to higher superoxide production [Murphy, 2009]. The second mechanism is the reverse electron transport (RET), where electrons enter Complex I through the ubiquinone binding site [Lambert and Brand, 2004], caused by high Δp, leading to reduction of NAD^+ to NADH at FMN site. Furthermore Lambert and Brand (2004) showed that superoxide production by Complex I is dependent on the pH gradient rather than the membrane potential and that mild uncoupling which reduces the pH gradient leads to a decrease of superoxide production by Complex I during reverse electron transport. The main source of superoxide production within Complex III is probably the auto-oxidation of semiubiquinone in the Q cycle at both sites of the inner membrane (Q_o and Q_i). Superoxide is not a strong oxidant, but it is the precursor for most reactive oxygen species and therefore it needs to be eliminated [Turrens, 2003]. There are two superoxide dismutases (SOD) that can invert $O_2^{\bullet -}$ to H_2O_2, which can be further degraded by the catalase in the peroxisome [Fritz *et al.*, 2007]. The mitochondrial matrix contains a manganese-dependent SOD (MnSOD) that reacts on $O_2^{\bullet -}$ that is formed in the matrix or in the inner side of the inner mitochondrial membrane [Fridovich, 1995, Abreu and Cabelli, 2010]. The intermembrane space harbours the second SOD, which contains copper and zinc instead of manganese (CuZnSOD) [Okado-Matsumoto and Fridovich, 2001]. This enzyme is also found in the

cytosol. In addition to the CuZnSOD the reduction of cytochrome *c* by $O_2^{\cdot -}$ may also contribute to the elimination of superoxide. The reduced cytochrome *c* can then deliver the electrons further to Complex IV [Turrens, 2003]. Furthermore since a mild uncoupling of the pH gradient reduces the superoxide production by Complex I it has been proposed that uncoupling proteins (UCP) “leaking” protons across the inner membrane are important for the reduction of ROS [Brand *et al.*, 2004]. However, some superoxide can lead to the inactivation of iron-sulphur centre containing enzymes, which leads to the release of the ferrous iron that catalyses the production of hydroxyl radical ($\cdot OH$) from H_2O_2. Those hydroxyl radicals can cause damage on cellular proteins, lipids and DNA.

The overall rate of ROS generation was suggested to be ~2% of the total oxygen consumption within the mitochondria, however, this number was seen to be overestimated caused by experiments under unphysiological conditions. Therefore the rate of ROS production has been reduced to less than 0.2% of the oxygen consumption within mitochondria. However, mitochondria are still with approximately 90% the main source of cellular ROS production [Balaban *et al.*, 2005, Murphy, 2009]. Certain amounts of ROS are important for cellular signalling pathways like the initiation of apoptosis [reviewed in Circu and Aw, 2010].

1.4.3 Mitochondria and apoptosis

In multicellular organisms programmed cell death, also called apoptosis, is essential to eliminate damaged cells to inhibit further harm on other cells and therefore to lead to their survival. In addition apoptosis is very important in development to reduce cell numbers in certain tissues and to generate fully formed organs (e.g. the loss of the tissue between fingers to separate them). The intrinsic, or mitochondrial pathway of apoptosis is initiated by several apoptotic stimuli (e.g. ROS, UV radiation, DNA damage) causing the activation of caspases (cystein aspartic acid proteases) [Wang and Youle, 2009]. Apoptotic stimuli trigger the release of certain apoptogenic proteins such as cytochrome *c*, Smac/DIABLO, Omi/HtrA2, AIF and Endonuclease G (Endo G) from the mitochondria to the cytosol (Figure 1.3).

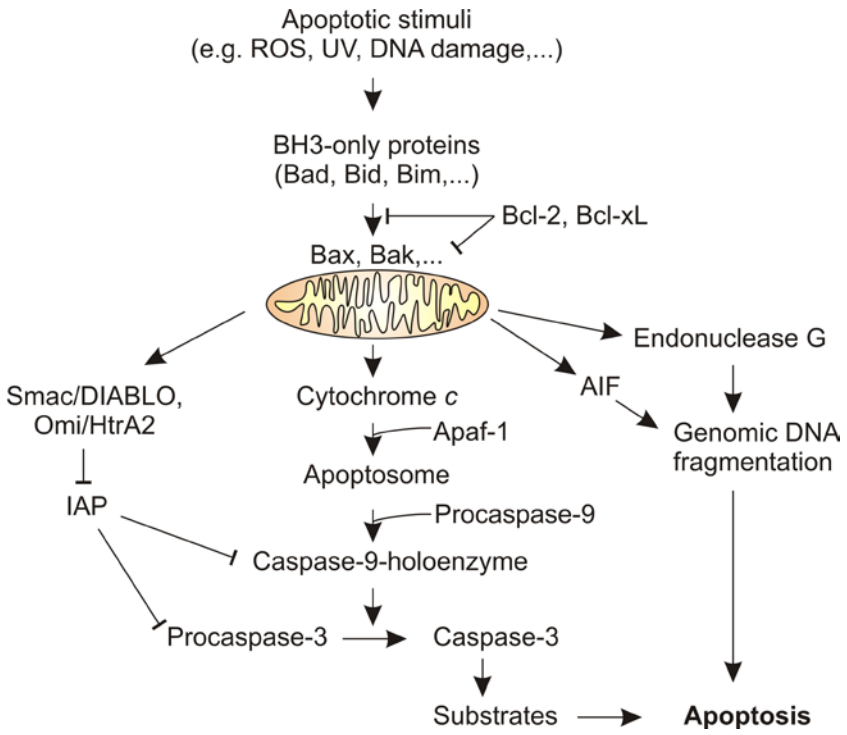

Figure 1.3: Mitochondrial pathway of apoptosis. Apoptotic stimuli induce the release of apoptotic factors over BH3-only proteins. This can cause oligomerisation of Bax or Bak and therefore changes in the outer membrane of the mitochondrion, which is shown in the centre of this image. Thus apoptotic factors such as cytochrome *c*, Smac/DIABLO, Omi/HtrA2, Endonuclease G and AIF can leave the mitochondrion, which is indicated as arrows leaving the organelle, and induce apoptosis. Cyt *c* interacts with Apaf-1 forming the apoptosome, followed by the caspase-cascade. IAP molecules (inhibitor of apoptosis protein) can inhibit this caspase pathway, however, the release of Smac/DIABLO and Omi/HtrA2 leads to inactivation of IAP molecules and therefore to enhance caspase-dependent apoptosis pathway. Endonuclease G and AIF, released to the nucleus cause DNA fragmentation. (Image was changed after Wang, 2001)

When cytochrome *c* is released from the mitochondrial intermembrane space it can initiate caspase activation [Liu *et al.*, 1996]. Together with Apaf-1, a cytosolic protein containing a caspase-recruitment domain (CARD), cytochrome *c* forms a multimeric complex, the apoptosome [Zou *et al.*, 1999]. The CARD domain of Apaf-1 recruits then procaspase 9, whose autoactivation leads to the caspase-9 holoenzyme that can then cleave further caspase such as procaspase 3 [Rodriguez and Lazebnik, 1999]. There are certain IAP molecules (inhibitor of apoptosis protein) that can bind and inhibit active caspase-9 and -3 via their BIR (baculovirus IAP repeat) domains. The release of matured Smac/DIABLO from the mitochondrial intermembrane space leads to enhanced caspase activation since this protein can competitively bind to the BIR domain of IAP [Du *et al.*, 2000, Verhagen *et al.*, 2000]. Omi/HtrA2, a serine protease, was identified as another IAP binding protein that can degrade IAP [reviewed in Wang and Youle, 2009]. The release of matured AIF from the intermembrane space and its

location to the nucleus causes chromatin condensation and DNA fragmentation [Susin *et al.*, 1999]. Endo G has nuclease activity and once released from the mitochondria it can induce nucleosomal DNA fragmentation [Li *et al.*, 2001]. How the release of certain apoptogenic factor occurs is not completely understood. However, it is believed that the mitochondrial permeability transition pore (mtPTP), a megapore spanning the outer and inner mitochondrial membranes, plays a certain role in apoptosis initiation. An opening of the mtPTP, caused by e.g. increased oxidative stress, will lead to matrix swelling, depolarization of the membrane potential, disruption of the outer membrane and therefore to the release of proteins of the intermembrane space [Wallace, 2005]. In contrast, Wang and Youle (2009) suggested that the opening of the mtPTP is more a consequence of apoptosis. Furthermore the release of all those apoptogenic proteins from the mitochondria is highly regulated by Bcl-2 (B cell lymphoma-2) family proteins [reviewed in Wang, 2001]. BH3-only proteins in the cytosol (e.g. tBid) transduce apoptotic stimuli to the mitochondria, which can be either neutralised by certain antiapoptotic proteins such as Bcl-2 and Bcl-xL, or which further induce conformational changes and oligomerisation of Bax and Bak [Eskes *et al.*, 2000] that may form a megapore, which is required for the release of apoptotic proteins [Wang and Youle, 2009].

Thus in addition to oxidative phosphorylation, the induction of apoptosis in damaged cells is one of the critical tasks of mitochondria in multicellular organism.

1.5 The structure, maintenance and replication of the mitochondrial genome

1.5.1 General aspects of the mtDNA

The size (from ~ 6 to 400 kbp), shape (linear or circular) and composition of the mitochondrial genome vary between different organisms [Lang *et al.*, 1999]. This section will describe the organisation of the human mitochondrial genome (mtDNA), which is a small double stranded, closed-circular DNA molecule of 16,569 bp (Figure 1.4). It encodes only approximately 1% of the approximately 1,400 mitochondrial proteins, of which the majority is nuclear encoded. The mtDNA is maternally inherited and its copy number varies between cell types from 1,000-10,000 in somatic cells with 2-10 copies per organelle [Satoh and Koroiwa, 1991] up to 100,000 in a mature oocyte [Shoubridge, 2000].

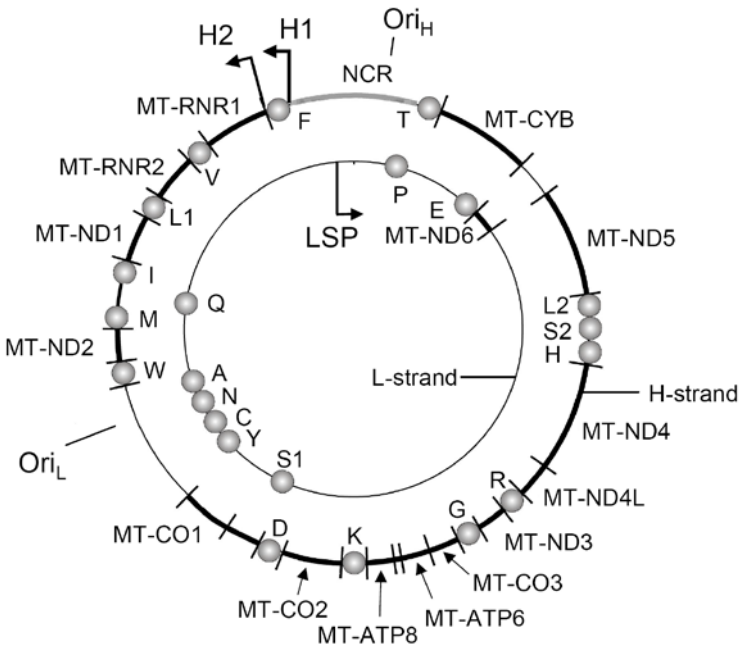

Figure 1.4: The human mitochondrial genome (mtDNA). The human mtDNA (16,569 bp) is portrayed above as a circle. The 2 ribosomal RNAs (*MT-RNR1* and *MT-RNR2*) and the open reading frames are shown as bold lines. The 22 tRNAs (grey circles) are labelled by their single letter code. There is only one non-coding region (NCR), also called D-loop. The heavy and light strand promotors are indicated as H1, H2 and LSP. (Image was kindly provided by Dr. Z. M. A. Chrzanowska-Lightowlers)

The two strands of the mtDNA differ in their density in caesium chloride gradient leading to their names [Clayton, 1982]: heavy strand (H-strand), which is guanine rich and the light strand (L-strand), which is guanine poor. The H-strand contains most of gene encoding material and codes for the two ribosomal RNAs (*MT-RNR1* (12S rRNA) and *MT-RNR2* (16S rRNA)), 14 tRNAs and 12 open reading frames [Anderson *et al.*, 1981]. The L-strand harbours the sequences for 8 tRNAs and one open reading frame. The mitochondrial genome is quite compact, lacking introns and the only non-coding region is located between $tRNA^{Phe}$ (F) and $tRNA^{Pro}$ (P) [Walberg and Clayton, 1981]. This approximately 1.1 kb large region is called displacement loop (D-loop, 7S DNA), a triple-stranded regulatory region that contains the origin of the H-strand (Ori_H) and the promotors for bi-directional transcription of the two strands (HSP1 and LSP). A second promotor for the H-strand transcription (HSP2) is located close to the 5'-end of the 12S rRNA [Montoya *et al.*, 1982]. The origin of the L-strand (Ori_L) is displaced by approximately two thirds of the genome within in cluster of five tRNAs (W, A, N, C, Y).

1.5.2 The genetic code of human mtDNA

The genetic code of mtDNA from many organisms differs from the universal code [http://www.ncbi.nlm.nih.gov/Taxonomy/Utils/wprintgc.cgi?mode=t#SG3]. Here the changes seen in the human mtDNA only are described [Anderson *et al.*, 1981]: i) there are only two codons representing stop codons (UAA and UAG) in human mitochondria. The third, present in the universal code, UGA, encodes tryptophan. ii) AUA codes for methionine instead of isoleucine and AUU codes for isoleucine during elongation but can code for methionine for initiation (*MT-ND2*). iii) AGA and AGG were presumed to be termination codons for *MT-CO1* and *MT-ND6* rather than not encoding arginine. It was shown recently, however, that those codons are not recognised by either a tRNA or a protein release factor and therefore do not represent stop codons [Temperley *et al.*, 2010a]. They are still important in acting as "hungry codons", a feature that promotes -1 frameshifting. This permits the use of UAG as a stop codon in *MT-CO1* and *MT-ND6* transcripts within the human mitochondrial ribosome.

1.5.3 The key factors of mtDNA replication

The key factors for mammalian mtDNA replication are mtPolγ, TWINKLE and mtSSB [reviewed in Wanrooij and Falkenberg, 2010]. The mitochondrial DNA polymerase γ is a heterotrimer, harbouring the catalytic subunit PolγA with polymerase, 3'-5' exonuclease and 5'-deoxyribose phosphate (dRP) lyase activities, and two copies of the accessory subunit PolγB. TWINKLE is a 5'-3' DNA helicase, which forms an hexamer in solution and is crucial for the unwinding of double stranded DNA. The mitochondrial single-stranded DNA-binding protein prevents single stranded DNA from refolding and protect against degradation. *In vitro* studies showed that mtPolγ and TWINKLE can synthesise ssDNA of ~ 2 kb length from a dsDNA template. The addition of mtSSB results in an increase of replication, generating a 16 kb DNA product [Korhonen *et al.*, 2004]. Additionally POLRMT is required for the synthesis of RNA primers, which are used for the initiation of leading-strand mtDNA synthesis at the Ori_H [Wanrooij *et al.*, 2008].

1.5.4 Organisation of mtDNA in nucleoids

The mitochondrial genome is usually clustered within a protein-DNA network called nucleoid, with 2-10 mtDNA copies per nucleoid [Spelbrink, 2010], where the mtDNA is protected by DNA-binding proteins. Mammalian nucleoids are dynamic structures, able to divide and to redistribute within the mitochondrial network. The most abundant

proteins within the nucleoids are TFAM and mtSSB. It has been suggested that TFAM protein level correlates to the relative mtDNA copy number and is therefore an important regulator of gene expression and possibly nucleoid packaging [Shen and Bogenhagen, 2001; Pohjoismaki *et al.*, 2006]. Other components of nucleoids are also key factors of the mitochondrial replication and transcription machinery. These are proteins that are permanently or temporarily directly associated with the mtDNA or with other nucleoid proteins. Bogenhagen *et al.* (2008) suggested a model of mtDNA nucleoid structure with a nucleoid core (containing 31 proteins) and a surrounding peripheral zone according to subdivision of nucleoid proteins in three classes derived from native and cross-linked preparations. However, depending on the preparation method used the resulting composition of nucleoids can be different as He *et al.* (2007) reported a more restricted set with only 6 components.

There is evidence that mtDNA/ nucleoids are bound to the inner mitochondrial membrane in close proximity of ER-mitochondrial junctions [reviewed in Spelbrink, 2010] and transcripts derived from the nucleoid are processed and translated within the peripheral zone in close vicinity to their assembly point, where also nuclear encoded proteins get coordinated imported after being translated on ER-bound cytosolic ribosomes. This model is in agreement with the fact that mitochondrial ribosomal proteins and translation factors were found in association with nucleoids [Bogenhagen *et al.*, 2008, Rorbach *et al.*, 2008]. Therefore it was proposed that there is a coupling between mtDNA maintenance and mitochondrial transcription to mitochondrial translation, cytoplasmic translation, protein import and complex assembly through the peripheral nucleoid proteins [Iborra *et al.*, 2004, Bogenhagen *et al.*, 2008, Spelbrink 2010].

1.6 Mitochondrial Transcription and mt-RNA processing

1.6.1 The mitochondrial transcription machinery

The key components of the human mitochondrial transcription machinery are the human mitochondrial RNA polymerase (POLRMT), the mitochondrial transcription factor A (TFAM) and the mitochondrial transcription factor B2.

POLRMT is a single-subunit protein of approximately 140 kDa, containing two domains [Tiranti *et al.*, 1997]: a C-terminal domain that contains conserved motifs for catalytic activity as they are found in bacteriophage polymerase, and a relatively large N-terminal domain, which harbours two putative pentatricopeptide repeat (PPR) motifs. Proteins with PPR motifs are usually involved in RNA-processing. However, it is not

known, whether the PPR motifs within the POLRMT are responsible for RNA binding. POLRMT can not initiate transcription on its own, it needs therefore the assistance of TFB2M and TFAM, where POLRMT and TFB2M forms a heterodimeric complex. Two mitochondrial transcription factors B exist, TFB1M and TFB2M. Both proteins are related to rRNA methyltransferases and were shown to be active transcription factors *in vitro* [Falkenberg *et al.*, 2002]. However, it has been demonstrated that TFB2M was the more active one. Since TFB1M was shown to be essential for the methylation of two adenines at the 3'-end of the mammalian 12S ribosomal RNA [Metodiev *et al.*, 2009], whereas the methyltransferase activity of TFB2M was less efficient [Cotney and Shadel, 2006], it has been proposed that TFB1M functions more as a ribosomal methyltransferase rather than a transcription factor. TFAM can bind and unwind DNA in a sequence independent manner. It has been therefore suggested that the binding of TFAM causes structural changes in the mtDNA such as unwinding of the promoter region for facilitating transcription initiation [Falkenberg *et al.*, 2007]. Four further transcription termination factors have been identified (MTERF, MTERFD1, -D2 and -D3), however the functions of those proteins is not completely understood [Roberti *et al.*, 2009, Hyvärinen *et al.*, 2010]. Initially MTERF was shown to bind sequence specifically to the termination site within the $tRNA^{Leu(UUR)}$ of the shorter polycistronic transcript initiated at HSP1 [Kruse *et al.*, 1989].

1.6.2 Mitochondrial RNA processing

As already described there are three promotors in human mtDNA, the initiation points of RNA synthesis. From the HSP1 promotor, located within the D-loop, a transcript containing the two ribosomal RNAs (*MT-RNR1* or 12S rRNA and *MT-RNR2* or 16S rRNA) and further $tRNA^{Phe}$ and $tRNA^{Val}$ is generated (Figure 1.5), terminating at a specific site in the $tRNA^{Leu(UUR)}$ downstream of the 16S rRNA mediated by the binding of MTERF [Montoya *et al.*, 1983, Kruse *et al.*, 1989]. The HSP2 promotor results in a polycistronic transcript that corresponds to almost the entire H-strand. The L-strand is also transcribed into a polycistronic RNA molecule starting at the LSP. It has been proposed in the so called "tRNA punctuation model" [Ojala *et al.*, 1981] that the structures of the tRNA within the polycistronic transcripts provide signals for endonucleolytic excision of the tRNA leading to most of the rRNA, tRNA and mRNA species. The processing of the polycistronic transcripts requires the mitochondrial RNase P [Holzmann *et al.*, 2008], which performs the 5'-endonucleolytic cleavage, and a tRNase Z [Levinger *et al.*, 2001, Dubrovsky *et al.*, 2004], which cleaves at the 3'-end of the tRNA.

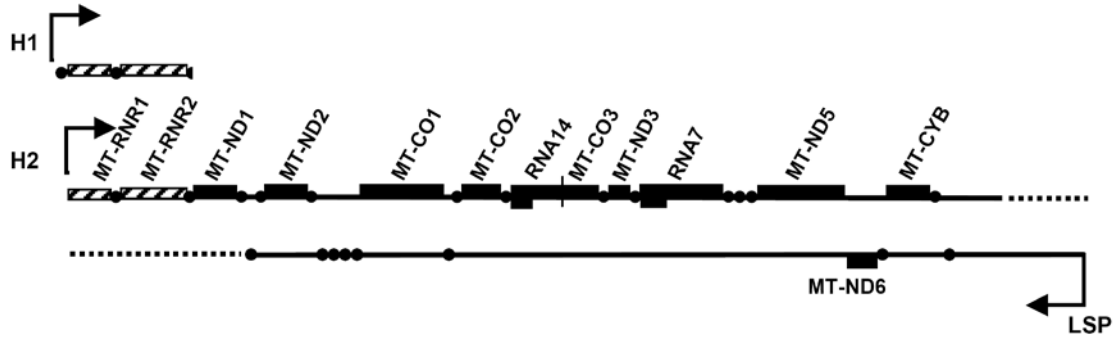

Figure 1.5: Transcription map of the human mitochondrial genome. The transcription of the human mtDNA is initiated from three promotors, leading to three polycistronic transcripts depicted above. The transcript from HSP1 (H1) is shown at the top with two ribosomal RNAs (hashed boxes) and $tRNA^{Phe}$ and $tRNA^{Val}$ as circles. The longer transcripts from HSP2 (H2) and LSP are also shown, where black boxes represent the mt-mRNAs. *RNA7* and *RNA14* indicate the two bicistrons, encoding the proteins ND4L/ND4 and ATPase8/-6. (Image was kindly provided by Dr. Z. M. A. Chrzanowska-Lightowlers)

Finally the 3'-end of each tRNA is modified by the addition of the CCA triplet, catalysed by an ATP(CTP):tRNA nucleotidyltransferase [Nagaike *et al.*, 2001]. After folding and modification of the tRNA the specific amino acid can be attached to the CCA triplet at the 3'-end by the corresponding aminoacyl-tRNA synthetase. The mitochondrial mRNAs are usually either oligo- or polyadenylated at the 3'-end, which is for some transcripts also essential to complete the stop codon (UAA), whereas the polyadenylation of mt-rRNA was suggested to be not common in cultured cells [reviewed in Temperley *et al.*, 2010b]. Finally 9 different monocistronic and 2 bicistronic (*RNA7*: *MT-ND4L/ND4*, *RNA14*: *MT-ATP8/-6*) mt-mRNAs are formed within human mitochondria, which are usually described as leaderless, meaning they either lack completely a 5'-UTR or there are only 1, 2 or 3 nucleotides upstream the start codon. The exception represents the two bicistrons, since *MT-ND4* and *MT-ATP6* harbours as 5'-UTR the out of frame sequence of *MT-ND4L* and *MT-ATP8*, respectively. However, the mt-mRNAs do not contain a sequence similar to the bacterial Shine-Dalgarno sequence at the 5'-end, which could be utilised for promoting translation initiation [Montoya *et al.*, 1981]. Furthermore there is no 5' 7-methylguanosine cap as there are in the eukaryotic cytosolic mRNAs. Therefore human mitochondrial mRNAs are unique in many aspects.

1.6.3 RNA binding proteins in human mitochondria

Yeast mitochondria contain a number of translation activators that bind the 5'-UTR of mitochondrial mRNA in yeast [Towpik, 2005]. In human mitochondria there is not much known about proteins that act as translation activators, which could be due to the

absence of specific 5'-UTRs, suggesting that there are other mechanisms that promote translation. However, TACO1 was reported to be a specific translation activator for COX1 [Weraarpachai *et al.*, 2009]. This was identified through a patient sample where a mutation in this gene caused a substantial decrease exclusively in COX1 protein level. Furthermore there have been several reports about mammalian mitochondrial PPR (pentatricopeptide repeat) proteins, which are found extensively in mitochondria and chloroplasts of land plants [Schmitz-Linneweber and Small, 2008]. Those PPR proteins have roles in RNA stability, editing, splicing, processing and possibly translational control. Because of the unique characteristics of mammalian mitochondrial transcripts as described above the function of those PPR proteins might be relatively limited. Examples for those PPR proteins in mammalian mitochondria are: POLRMT (described in 1.6.1), MRPS27 (a component of the mitochondrial ribosomal small subunit), mitochondrial RNase P protein 3 (MRPP3), LRPPRC (leucine-rich pentatricopeptide repeat cassette), PTCD1, PTCD2 and PTCD3. Patients with mutations in LRPPRC showed COX deficiency and a reduced level in mitochondrial encoded transcripts for cytochrome *c* oxidase [Xu *et al.*, 2004]. However, further studies demonstrated that all mt-mRNA were reduced in the absence of LRPPRC except *MT-ND3* and *MT-ND6* [Sarsarman *et al.*, 2010]. Additionally it has been shown that LRPPRC and SLIRP, a stem-loop RNA-binding protein, interact in a ribonucleoprotein (RNP) complex in mammalian mitochondria. The stability of both proteins was shown to be dependent on the presence of mt-mRNA, where the protein steady state level especially of SLIRP was dramatically reduced in the absence of mitochondrial transcripts [Baughman *et al.*, 2009, Sarsarman *et al.*, 2010]. Sarsarman *et al.* (2010) suggested that LRPPRC and SLIRP within the RNP complex are crucial for regulating the stability and handling of mature mt-mRNA. PTCD1 has been demonstrated to reduce the abundance of $tRNA^{Leu}$ and was therefore suggested to be a negative translation modulator [Rackham *et al.*, 2009]. Xu *et al.* (2008) have shown that a disruption in murine *PTCD2* causes a decreased level in Complex III, caused by the depletion of *MT-CYB* transcript and further accumulation of unprocessed precursor, which included *MT-ND5*. PTCD3 was shown to interact with the 12S ribosomal RNA, crucial for mitochondrial protein synthesis [Davies *et al.*, 2009]. Just recently ERAL1, a human mitochondrial protein that contains a type-II KH-domain, was shown to bind the 3'-end of the 12S rRNA and to be absolutely crucial for the stability of 12S rRNA [Dennerlein *et al.*, 2010].

Thus there are some RNA binding proteins in mammalian mitochondria, which are involved in RNA stability or processing and thus crucial for mitochondrial translation,

however, the list of those proteins is far from complete and needs further investigations in the future.

1.7 Mitochondrial Translation

The translation of a messenger RNA into a protein requires a machinery comprising a substantial number of factors: i) the ribosome, a ~2.65 MDa compound complex of rRNA and proteins, ii) the mRNA, iii) amino-acylated tRNAs and their cognate synthetases, and iv) translation factors. In human and also in other mammals all protein components within the mitochondrial translation machinery are nuclear encoded and therefore they need to be translated in the cytosol and then imported into the mitochondria.

Since mitochondria have developed from a bacterial ancestor it has been expected that its translation machinery should be relatively similar to the bacterial one. There are indeed some similarities between the mitochondrial and the bacterial protein synthesis, however, there are also substantial differences between these two systems. Furthermore the mitochondrial translation machinery between different organisms is not the same. In the following section the current knowledge about mammalian mitochondrial protein synthesis will be described and further differences to other systems will be pointed out.

1.7.1 The mammalian mitochondrial ribosome

The mammalian mitochondrial ribosome has a low sedimentation coefficient of approximately 55S, comprising a 28S small subunit (28S mt-SSU) and a 39S large subunit (39 mt-LSU) [O'Brien, 1971]. In contrast i) the eukaryotic cytosol contains a 80S ribosome with a 40S SSU and a 60S LSU ii) a bacterial ribosome is a 70S particle with a 30S SSU and a 50S LSU and iii) yeast mitochondria harbour a 70S ribosome with a 37S mt-SSU and a 54S mt-LSU. The 55S mammalian mitochondrial ribosome has a slightly higher molecular weight of approximately 2.65 MDa in comparison to the bacterial 70S ribosome with 2.3 MDa. A substantial difference between the mammalian mitochondrial ribosome and other ribosomes is the ratio of RNA:protein content, where the usual 70%:30% ratio as found in bacteria is reversed in the mammalian mitochondrial ribosome. The ribosomal RNAs, encoded by the human mitochondrial genome, are much smaller than the bacterial ones: i) the 12S mt-rRNA is with 954 nt approximately 40% shorter than the 16S rRNA of the bacterial SSU and ii) the 16S mt-rRNA with 1558 nt is only a half of the length of the 23S rRNA in the bacterial LSU

[O'Brien, 2002]. Further, it has not unequivocally confirmed whether there is a 5S rRNA present in the mammalian mitochondrial ribosome. It has been shown, however, that 5S rRNA is imported into mitochondria, but its function within the organelle is still elusive [Entelis *et al.*, 2001, Smirnov *et al.*, 2008]. Thus the RNA content within the mammalian mitochondrial ribosome is relatively low. In contrast the protein content is much higher in the 55S particle than in its bacterial counterpart or in yeast mitochondrial ribosome. Since the pioneering work of O'Brien and colleagues in 1982 [Matthews *et al.*, 1982] the list of identified mammalian mitochondrial proteins is growing [Koc *et al.*, 2010]. The more porous structure with visible voids in the cryo-EM structure of the bovine mitochondrial ribosome (Figure 1.6) [Sharma *et al.*, 2003] make it tempting to speculate that there are maybe still some proteins missing. Currently 31 proteins are known to be components of the mammalian 28S SSU, which includes 3 isoforms of MRPS18 [Koc *et al.*, 2001b]. It is still unknown whether a single ribosome contains all three isoforms of MRPS18 at the same time or only a one. However, only 14 proteins find homologues in bacteria and the others are unique for the mitochondrial 28S SSU. The 39S LSU consists 51 subunits of which 28 proteins represent homologues to components of the bacterial 50S LSU. The remainder are again unique to the mammalian mitochondrial ribosome [Koc *et al.*, 2001c; Koc *et al.*, 2010]. Most of the homologous proteins found in mammalian mitochondrial ribosomes are also present in yeast mitochondrial ribosomes, as might be predicted from a common bacterial ancestor. However, a number of the additional proteins found in the mammalian mitochondrial ribosome are absent from the yeast. This is in agreement with the hypothesis that those additional proteins within the mammalian mitochondrial ribosome replace the loss of ribosomal RNA and since yeast mitochondrial ribosomes do not show the truncated rRNAs there is no requirement for additional proteins [O'Brien, 2002]. However, Sharma *et al.* (2003) showed that only ~ 19% of the missing ribosomal RNA segments are replaced by proteins within the 28S SSU and ~ 28% within the 39S LSU. Approximately 50% of the 5S rRNA are replaced by protein mass, but as already said, the structure is relatively porous and has some open empty voids (Figure 1.6), which leads to speculations that potentially there are some proteins missing from the current structure.

These additional proteins quite often seem to be recruited pre-existing or bi-functional proteins. Examples are MRPL39, which is similar to the N-terminal region of the mitochondrial threonyl-tRNA synthetase [Spirina *et al.*, 2000], or MRPS29 (DAP3) and MRPS30 (PDCD9), which were both suggested to be involved in apoptosis [Koc *et al.*, 2001a]. Furthermore the homologous proteins present in the mammalian mitochondrial ribosome are in most cases larger than their bacterial counterparts, which also leads to

the higher protein content. This perhaps explains in part why the mammalian mitochondrial ribosome has a RNA:protein ratio of ~31%:~69%, where the bacterial ribosome shows the inverse ratio with ~67%:~33%.

Sharma *et al.* (2003) showed a cryo-EM structure of the bovine mitochondrial ribosome with a relatively porous structure. The core is relatively compact and the rRNA components within the core are surrounded by peripheral proteins (Figure 1.6). The authors have also analysed the intersubunit bridges, which hold the two subunits together. Six bridges are conserved and show similarities to the bacterial ones (Figure 1.6 C/D, green ellipses).

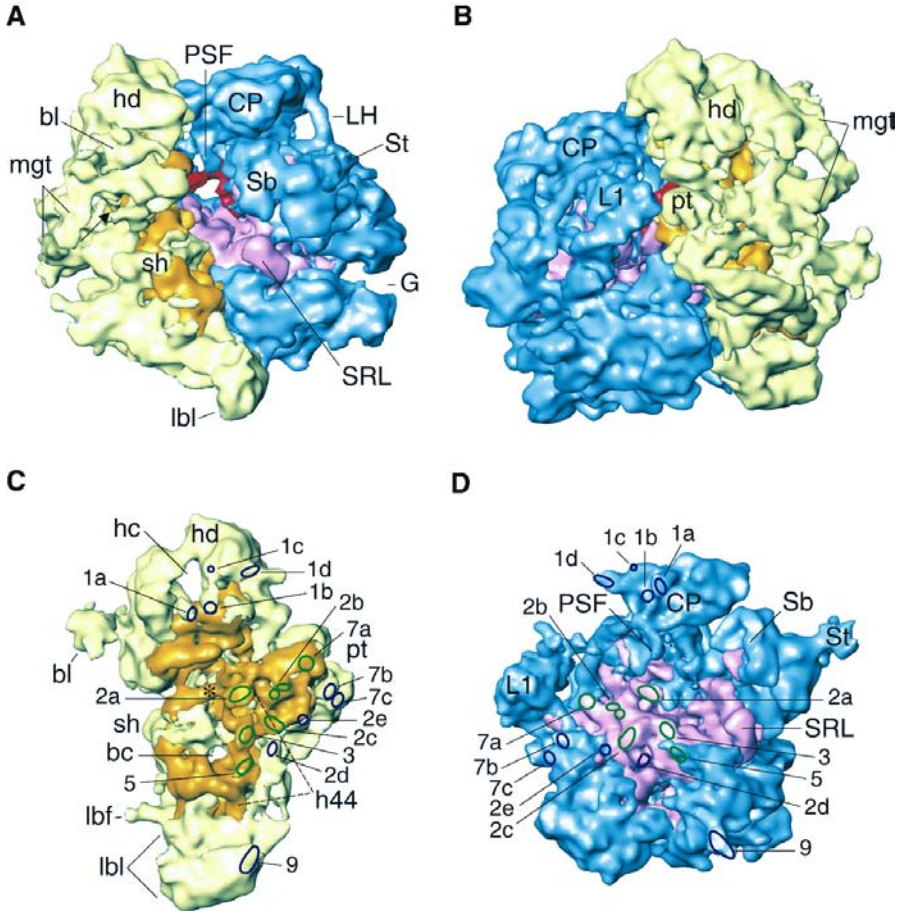

Figure 1.6: Cryo-EM structures of bovine mitochondrial ribosome. A) and **B)** The 55S ribosome is shown with the 28S SSU (protein content in yellow and RNA in orange) and the 39S LSU (protein content in blue and RNA in purple). P-site bound tRNA is shown in red. The mRNA entrance is indicated by an arrow. **C)** and **D)** The subunits are shown from the interface side with indicated locations of the intersubunit bridges, where green ellipses represent conserved bridges and dark blue ones the mitochondrial ribosome specific bridges. bc: body channel, bl: beak lobe, CP: central protuberance, G: gap, h44: rRNA helix 44, hc: head channel, hd: head, lbf: lower-body finger, lbl: lower-body lobe, LH: LSU handle, mgt: mRNA-entry gate, PSF: P-site finger, pt: platform, Sb: stalk base, sh: shoulder, SRL: α-sarcin-ricin loop (Images were taken from Sharma *et al.*, 2003)

A further nine bridges differ from the bacterial system and involve proteins. Since the mammalian mitochondrial ribosome is very protein rich its ribosomal subunits are held together by mainly protein-protein bridges. In addition to the seven protein-protein bridges there are five RNA-RNA bridges, two RNA-protein bridges and one bridge involving protein components and RNA from both subunits. The presented structure of bovine mitochondrial ribosome indicates certain unusual characteristics that may help in understanding the translation process in mammalian mitochondria in more detail. One of these particular features is a triangular gate-like structure (mRNA gate), which partially covers the mRNA entry site (Figure 1.6 A/B). Sharma *et al.* (2003) suggested since mammalian mitochondrial mRNA lack specific 5'-UTRs that when usually may facilitate translation initiation, this gate may be involved in the recruitment of mt-mRNA into the 28S SSU.

Another special feature is the "polypeptide-accessible site" (PAS) a wide opening structure just before the polypeptide exit site (PES). The authors suggested therefore that there are possibly two pathways, through which the nascent peptide chain can leave the ribosome. Furthermore an interesting characteristic of the mammalian mitochondrial ribosome is a very strongly retained tRNA in the P-site (peptidyl-tRNA site) (Figure 1.6 A/B), whereas purified bacterial ribosomes show usually a strongly bound tRNA within the E-site (exit site), a feature essentially lacking in the 55S particle. Sharma *et al.* (2003) have shown that the 39S LSU has a unique finger-like structure (P-site finger, PSF) that interacts with the P-site tRNA. This could allow a stabilisation of the bound tRNA within the P-site. Importantly most of the rRNA regions, which are crucial for the interaction of the tRNA with the E-site, are absent in the mammalian mitochondrial ribosome, suggesting that there is a rather weak E-site or even a complete loss of this site [Mears *et al.*, 2006].

To date not much is know about the assembly of the mammalian mitochondrial ribosome and the factors that may be involved in this process. So far only two polypeptides of the 28S SSU (MRPS16 and MRPS22) have been reported with mutations in patients associated with mitochondrial disorders and assembly defects of the 28S SSU [Miller *et al.*, 2004, Haque *et al.*, 2008]. Additionally two proteins have been shown to be important for the maturation or stability of the 12S rRNA and therefore for the assembly for the 28S SSU: TFB1M, which is responsible for the conserved di-methylation of the 12S rRNA [Metodiev *et al.*, 2009], and ERAL1, a 12S rRNA chaperone, which binds to the 3'-stem-loop region of the 12S rRNA [Uchiumi *et al.*, 2010, Dennerlein *et al.*, 2010]. Just recently NOA1, a mitochondrial GTPase has been demonstrated to be important for 39S LSU assembly and a loss of NOA1 leads to a substantial decrease in mitochondrial protein synthesis [Kolanczyk *et al.*, 2011].

Further for the assembly of the large subunit, MRPL32 needs to be processed by the *m*-AAA protease to become recruited into the 39S LSU as reported by Nolden *et al.* (2005). The same authors showed like other studies [Liu and Spremulli, 2000] that the mitochondrial ribosome is associated with the mitochondrial inner membrane and only membrane bound ribosomes are translational active. How the ribosome is bound to the inner membrane is not known. However, it has been shown that the inner membrane protein Oxa1 (human OXA1L), which is crucial for co-translational insertion of mitochondrial encoded proteins, interacts with the mitochondrial ribosome via proteins of the large ribosomal subunit, closely localised to the polypeptide exit tunnel [Jia *et al.*, 2003, Jia *et al.*, 2009]. Additionally, Mba1 (human MRPL45) has been shown to be a membrane-associated ribosome receptor in yeast mitochondria [Ott *et al.*, 2006], and Mdm38 also contributes to the ribosome binding at the inner mitochondrial membrane [Frazier *et al.*, 2006]. The mammalian othologue of Mdm38, LETM1 (Leucine zipper EF-hand-containing transmembrane protein 1) has been shown to interact with MRPL36 [Piao *et al.*, 2009].

1.7.2 Initiation of mitochondrial protein synthesis

The identification and characterisation of the mammalian mitochondrial initiation factors (mtIF) was predominantly done by Spremulli and colleagues. Translation initiation needs a free 28S SSU. By binding to the 28S SSU mtIF3 inhibits the association with the 39S LSU and provide therefore a pool of free 28S SSU (Figure 1.7). It has been suggested that the role of mtIF3 in translation initiation is an active one rather than a passive one, meaning that mtIF3 is directly involved in the dissociation of 55S monosome into the 28S SSU and 39S LSU and not just being an anti-association factor, bound to the 28S SSU [Christian and Spremulli, 2009]. Furthermore Bhargava and Spremulli (2005) demonstrated that mtIF3 reduces the binding of fmet-tRNA^{Met} to the 28S SSU mediated by mtIF2-GTP if there is no mt-mRNA present, which is an additional role not found in the bacterial counterpart.

As already described the mitochondrial messenger RNA does not contain a m^{7}G-cap structure at the 5'-end, or shine dalgarno sequence or other specific long UTRs that would promote translation initiation. Therefore mammalian mitochondrial ribosomes must have found another mechanism to recognise the mt-mRNA 5'-end and the start codon. One of those specific features could be the mRNA gate at the mRNA entry site [Sharma *et al.*, 2003]. Liao and Spremulli (1989) have shown that the 28S SSU is able to bind mt-mRNA in the absence of initiation factors or fmet-tRNA^{Met}, but neither the 39S LSU nor the 55S monosome showed mt-mRNA binding activity. Thus the mRNA is

at first loaded onto the 28S SSU in a sequence-independent manner. It was further suggested that the mt-mRNA is fed into the mRNA entrance gate starting with the 5'-end. After the first 17 nt have entered the ribosomal subunit there is an inspection for the start codon [Christian and Spremulli, 2010]. During this time mtIF2-GTP promotes binding of the fmet-tRNA^{Met} to the ribosome in a codon-anticodon dependent manner (Figure 1.7 (1)) [Liao and Spremulli, 1990, Ma and Spremulli, 1995, Spencer and Spremulli, 2004]. The presence of a start codon will lead to a stable initiation complex, whereas in the absence of a start codon the mRNA will pull through and possibly dissociate from the SSU [Christian and Spremulli, 2010]. Christian and Spremulli (2010) demonstrated that mt-mRNAs with more than 3-6 nt prior the start codon are very inefficiently translated by the mammalian mitochondrial ribosome and therefore the accurate processing of the mt-mRNA prior to translation initiation is crucial. After forming a stable initiation complex the 39S LSU joins the 28S SSU, forming the 55S monosome and mtIF2 can then hydrolyse GTP followed by the release of the initiation factors from the ribosome. Bacteria contain an additional initiation factor IF1 that stabilises the binding of initiator tRNA to the SSU in the presence of IF2 and furthermore it has been suggested that it blocks the ribosomal A-site during translation initiation [Carter *et al.*, 2001]. Human mitochondria do not contain a third IF, however, Gaur *et al.* (2006) have shown that an insertion of 37 residues into mtIF2 substitutes for the function of an IF1, suggesting that mtIF2 has functionally replaced the two bacterial IFs.

1.7.3 Translation elongation

For translation elongation in mammalian mitochondria three factors are required: mtEFTu, mtEFTs and mtEFG1 (Figure 1.7 (2)). All these factors have been identified in human and also mutations in each of these genes have been described in association with human diseases [reviewed in Smits *et al.*, 2010].

Many investigations analysing translation elongation were also performed by Spremulli and colleagues [Spremulli *et al.*, 2004]. For the elongation process the aminoacyl-tRNA (aa-tRNA) is delivered to the A-site by mtEFTu-GTP. An accurate recognition and codon-anticodon interaction between the aa-tRNA and the mRNA will lead to GTP hydrolysis and therefore to the release of mtEFTu-GDP. For the exchange of the GDP for a GTP mtEFTu-GDP interacts with mtEFTs, a guanine nucleotide exchange factor. The fmet (peptide chain) from the tRNA^{Met} (peptidyl-tRNA) within the P-site is then transferred to the aa-tRNA within the A-site through a catalytical action of the peptidyl-transferase centre within the 39S LSU leading to peptide bond formation.

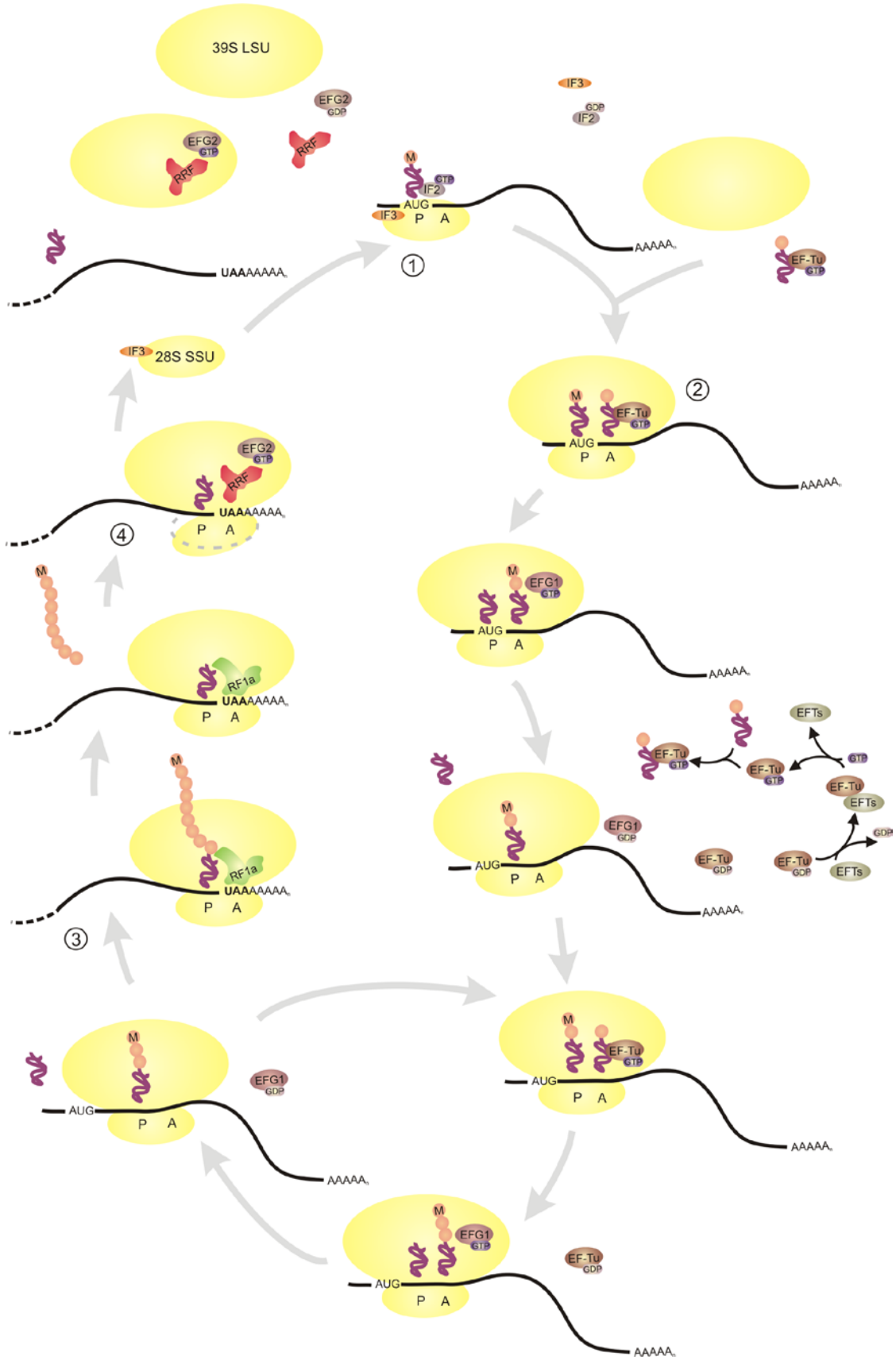

Figure 1.7: Human mitochondrial translation. (See figure legend on following page)

Legend for figure 1.7: Human mitochondrial translation. (1) Initiation: mtIF3 (orange) provides a pool of free 28S SSU (yellow). The mt-mRNA binds to the 28S SSU, where a start codon within the P-site is recognised by the cognate $tRNA^{Met}$, which carries formyl-methionine (M). For the delivery of the fmet-$tRNA^{Met}$ another initiation factor is required: mtIF2-GTP. After GTP hydrolysis the initiation factors leave the 28S SSU and the 39S LSU can associate with the 28S SSU, forming the 55S monosome. **(2)** Elongation: mtEFTu-GTP delivers the aa-tRNA to the A-site and leaves the ribosome upon GTP hydrolysis. The exchange of GDP to GTP needs the interaction with another elongation factor, mtEFTs. Then mtEFTu-GTP can interact with the next aa-tRNA and is ready for the next elongation round. The fmet of the P-site tRNA is transferred to the aa-tRNA in the A-site and after peptide bound formation mtEFG1-GTP interacts with the ribosome and causes the translocation of the peptidyl-tRNA from the A- to the P-site. The de-aminoacylated tRNA from the P-site leaves probably the ribosome immediately since the mammalian ribosome probably lacks the E-site. Then the next aa-tRNA can be delivered to the A-site and elongation carries on until a stop codon reaches the A-site. **(3)** Termination: a stop codon in the ribosomal A-site will be sequence specific recognised by mtRF1a (green), which will facilitate the catalysis of the hydrolysis of the ester bond between the peptide chain and P-site tRNA, leaving the post-termination complex. **(4)** Ribosome Recycling: mtRRF (red) and EFG2-GTP causing the release of the tRNA and the mRNA from the ribosome, exposing the binding site of mtIF3, which is required for complete dissociation of the 55S monosome into its subunits. GTP hydrolysis is required to release mtEFG2 and mtRRF from the 39S LSU.

The translocation of the peptidyl-tRNA from the A-site to the P-site is catalysed by mtEFG1-GTP. The deacylated tRNA in bacterial ribosome is usually first transferred into the E-site before it leaves the ribosome, however, since an E-site is very weak or absent in the mammalian mitochondrial ribosome [Sharma *et al.*, 2003] it is tempting to speculate whether the uncharged tRNA is released from the ribosome immediately upon translocation of the peptidyl-tRNA into the P-site. The ribosome moves then 3 nt further to expose the next codon in the A-site, which will be have delivered an aa-tRNA-mtEFTu-GTP complex. The cycle will be repeated until a stop codon reaches the A-site.

1.7.4 Translation termination in human mitochondria

In 1998 mtRF1 was suggested to be the single omnipotent class I release factor (RF) in human mitochondria [Zhang and Spremulli, 1998], however, this factor failed to show any release activity *in vitro* [Soleimanpour-Lichaei *et al.*, 2007]. In 2007 a second RF was identified, mtRF1a, which was shown to be able to recognise the stop codons UAA and UAG within the ribosomal A-site in a sequence-dependent manner *in vitro* [Soleimanpour-Lichaei *et al.*, 2007]. This release factor catalyses the hydrolysis of the peptide chain from the peptidyl-tRNA within the P-site through its highly conserved GGQ domain, which is localised into the peptidyl-transferase centre (Figure 1.7 (3)). The function of a class I release factor within the ribosome will be described in more detail later (see 1.8). Since the sequence of the human mitochondrial genome was known [Anderson *et al.*, 1981], it was for a long time suggested that there are four stop codons: UAA, UAG, AGA and AGG. Interestingly AGA and AGG would represent the

stop codons of only two mitochondrial transcripts, namely *MT-CO1* and *MT-ND6.* However, there were no reports that had identified the protein factor that could recognise these triplets as stop codons. Further studies within this laboratory have shown that AGA and AGG represent “hungry codons”, causing a pause of the mitochondrial ribosome with an empty A-site. Additionally a stable secondary structure in the 3’-UTR (in case of *MT-CO1* this is the antisense of $tRNA^{Ser(UCN)}$ and for *MT-ND6* this was a stem loop structure antisense of *MT-ND5*) downstream of both open reading frames are specific features that are crucial for a ribosome to perform frameshifting. Indeed by generating and expressing a mitochondrially targeted bacterial endonuclease, RelE, which cleaves specifically between nucleotides 2 and 3 of stop codons in the ribosomal A-site, it was proved that the human mitochondrial ribosome is able to perform a -1 frameshifting leading to an UAG stop codon of *MT-CO1* and *MT-ND6* transcripts, which can be then again recognised by mtRF1a [Temperley *et al.*, 2010a]. Thus mtRF1a is able to terminate all 13 open reading frames within human mitochondria.

In bacteria, a class II release factor (RF3) with GTPase activity is inducing a change in ribosomal conformation responsible for the dissociation of the class I RF from the ribosomal A-site after peptide release was performed [Gao *et al.*, 2007]. To date no class II RFs have been identified in human mitochondria that are able to do this job. However, a similar mechanism probably exists so that the ribosomes can be further recycled.

1.7.5 Mitochondrial Ribosome recycling

In bacteria three translation factors are required for the recycling of the ribosome: RRF, EFG and IF3 [Hirokawa *et al.*, 2006]. In 1998 the human mitochondrial ribosome recycling factor was bioinformatically identified [Zhang and Spremulli, 1998], however, its characterisation and importance for cell viability was described for the first time ten years later [Rorbach *et al.*, 2008]. It has been shown that in the absence of mtRRF mitochondrial ribosomes accumulate probably as aggregates in the densest fractions of isokinetic sucrose gradients, leading to reduced level of free individual subunits. Furthermore it has been demonstrated that mtRRF is able to co-immunoprecipitate mitochondrial ribosomal proteins and additional translation factors. Interestingly one of those associated proteins turned out to be another member of the mitochondrial release factor family, ICT1, however neither mtRF1 nor mtRF1a was found in this immunoprecipitation. The fact that ICT1 was found in this IP together with other

proteins involved in mitochondrial protein synthesis made it an interesting candidate to study and will be discussed in more detail below.

For the recycling of the ribosome an EFG is required. Most bacteria contain only one EFG, involved in both processes translation elongation and ribosome recycling. In human mitochondria two homologues of EFG were identified: mtEFG1 and mtEFG2 [Hammarsund *et al.*, 2001], which show sequence identities of approximately one third to each other [Spremulli *et al.*, 2004]. Tsuboi *et al.* (2009) demonstrated that mtEFG1 is not able to recycle the ribosome together with mtRRF, however, mtEFG2, which shows no translocation activity in the other site, was able to split the ribosome when in conjunction with mtRRF. The same authors demonstrated the importance of GTP, which is required for the action of mtEFG2 in mitochondria. The GTP hydrolysis was suggested to be crucial for the release of mtEFG2 together with mtRRF from the 39S LSU after the recycling step since mtEFG2 and mtRRF stayed on the LSU in the presence of non-hydrolysable GTP analogue, but were able to split the ribosome in its subunits. Most of this work was done *in vitro* and therefore it is still unclear whether mtEFG2 is an essential protein in mammals as mtEFG1 is. Mutations within mtEFG1 gene cause defects in mitochondrial translation, which leads to lethal mitochondrial disorders shortly after birth [Coenen *et al.*, 2004]. However, no defect in mtEFG2 has been reported so far. Furthermore mutations in yeast mtEFG2 (*MEF2*) did not show any clear phenotype, whereas mutations of mtEFG1 (*MEF1*) caused defects in mitochondrial protein synthesis *in vivo* [Winzeler *et al.*, 1999].

The third factor, essential for complete dissociation of the mitochondrial ribosome, is as already described, mtIF3. In the absence of mtIF3 the 28S SSU and 39S LSU re-associate to the 55S monosome after the release of mRNA and tRNA mediated by mtRRF and mtEFG2 [Tsuboi *et al.*, 2009]. Experiments within this laboratory showed that the addition of mtIF3 alone to mitochondrial ribosomes immunoprecipitated by mtRRF could lead to the dissociation of the ribosomal subunits [unpublished data by Dr. J. Rorbach], which supports the hypothesis of an active role of mtIF3 in the recycling event, suggested by Christian and Spremulli (2009).

1.8 Translation release factors

1.8.1 Bacterial Release Factors

Bacteria contain two classes of release factors: class I release factors (RF1 and RF2) facilitate the hydrolysis of the peptide chain from the peptidyl-tRNA in a sequence-

dependent manner [reviewed in Youngman *et al.*, 2008], and class II RF (RF3) harbours GTPase activity and stimulates the release of the class I release factor by inducing a conformational change in the ribosome [Gao *et al.*, 2007]. In contrast in the eukaryotic cytosol there is only one class I RF (eRF1), whose release activity is stimulated by the interaction with the class II RF (eRF3) [Petry *et al.*, 2008, Cheng *et al.*, 2009]. Bacteria utilise three stop codons: UAA is recognised by both RFs RF1 and RF2, whereas RF1 also interacts specifically with UAG and RF2 with UGA. There are 2 peptide motifs that are crucial for distinguishing the stop codons. These are tri-peptide motifs: PXT in RF1- and SPF in RF2-types [Ito *et al.*, 2000], and the tip of the α5-helix of RF that is localised in the decoding centre within the ribosome and therefore was proposed to be also essential for the codon recognition (Figure 1.8 D) [Petry *et al.*, 2005, Laurberg *et al.*, 2008]. The ribosome itself with its 16S rRNA within the decoding site was also suggested to be involved in the discrimination of the stop codon [Laurberg *et al.*, 2008]. For catalysing the hydrolysis of the peptide chain from the tRNA in the P-site the GGQ motif, which is conserved in all class I RFs, needs to be localised into the peptidyl-transferase centre in the ribosomal large subunit (Figure 1.8 D). Solutions structures of RFs are different from those bound to the ribosome (Figure 1.8 A/B), which shows the conformational change of domain 3 induced by the rearranged elements of the rRNA within the ribosome, where an extension of α7 will flip the domain 3 out of the core so that the GGQ motif can reach the PTC (Figure 1.8 B/D) [Petry *et al.*, 2005, Laurberg *et al.*, 2008]. It has been shown by several groups that mutations within this GGQ motif leads to dramatic loss of release activity [Frolova *et al.*, 1999, Mora *et al.*, 2003, Shaw and Green, 2007], where the two glycines seem to be the most critical residues for catalysing hydrolysis. The glutamine with less dramatic consequences for the hydrolysis activity was suggested to be crucial for the preferential selection of water for nucleophilic attack [Shaw and Green, 2007].

The overall shape of a RF within the ribosome is reminiscent to that of a tRNA within the A-site (Figure 1.8 C). The CCA extension at the 3'-end of a tRNA, localised within the PTC, causes changes of the 23S rRNA, allowing the hydrolysis of the ester bond between the peptide chain and the P-site tRNA by a nucleophilic attack through the primary amine of the incoming aa-tRNA [Schmeing *et al.*, 2005]. The GGQ motif of the RF, which is believed to mimic the CCA of the aa-tRNA in the A-site, allows similar conformational changes of the rRNA and the nucleophilic attack by water and thus the hydrolysis of the ester bond joining the peptide and the tRNA. Therefore it is a coordinated interplay between the class I RF and the ribosome that induces the peptidyl-tRNA hydrolysis and therefore a RF without the ribosome is not able to carry out its function.

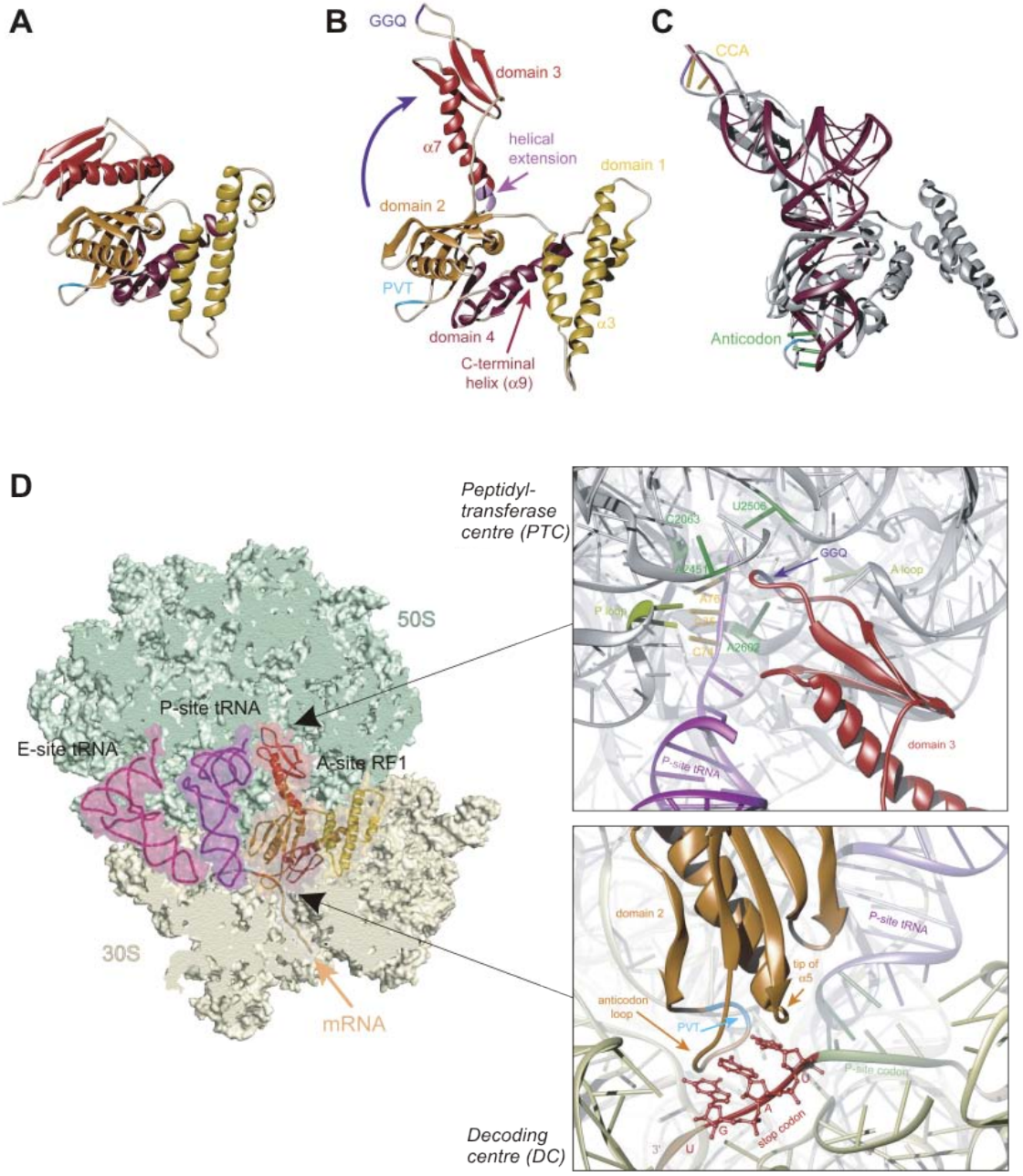

Figure 1.8: Crystal structures of bacterial RF1. A) Crystal structure of isolated RF1 from *T. maritima* **B)** Structure of ribosome bound RF1 from *T. thermophilus*. Domain 3 with α7-helix (labelled in red) flipped out of the core (indicated by an arrow) to localise the GGQ domain within the PTC in the 50S LSU. **C)** Superimposition of RF1 (grey) and an A-site bound tRNA (dark red) shows the mimic of tRNA anticodon loop (green) and the CCA triplet (yellow) at the 3'-end with the PXT tri-peptide motif and the GGQ motif of the RF, respectively. **D)** Bacterial 70S ribosome with 30S SSU and 50S LSU shows tRNAs bound to the P- (purple) and E-site (pink) and RF1 within the A-site. The right panels demonstrate the localisation of the GGQ motif (purple) within the PTC, and of the PXT tri-peptide motif (blue) and the tip of the α5-helix (brown) within the decoding centre of the 30S SSU. (Images were adapted from Petry *et al.*, 2005)

1.8.2 The human mitochondrial release factor family

As described above mtRF1a, recognising sequence specific UAA and UAG, is able to terminate all 13 open reading frames in human mitochondria [Soleimanpour-Lichaei *et al.*, 2007, Temperley *et al.*, 2010a]. This class I release factor is very similar to the bacterial RF1 with ~40% sequence identity and contains the conserved tri-peptide motif PXT. There are three further members of this family: mtRF1, ICT1 and C12orf65. Zhang and Spremulli (1998) identified mtRF1 as a mitochondrial release factor, which instead of PXT tri-peptide motif has the sequence PEVGLS and further some inserted nucleotides in the α5-helix domain. This RF completely failed to show any release activity *in vitro* [Soleimanpour-Lichaei *et al.*, 2007]. However, the conserved GGQ motif and further sequence similarity between mtRF1 and mtRF1a leads to the speculation whether this RF has adapted those changes to work as an RF under different circumstances and not in a conventional termination process. ICT1 and C12orf65 are relatively small proteins in comparison to mtRF1a and mtRF1. Both harbour the GGQ motif, but do not show any similarity over the tri-peptide motif or the α5-helix domain (Figure 1.9), indeed those regions seem to be completely absent in ICT1 and C12orf65.

Recently, mutations within the C12orf65 gene in patients with mitochondrial disorders have been reported by Antonicka *et al.* (2010). Those patients showed severe reduction in mitochondrial protein synthesis, leading to reduced level of OXPHOS complexes visualised by Blue Native PAGE and therefore to OXPHOS deficiency. However, the mt-RNA levels were relatively normal or even increased in comparison to the control. Those results strongly suggest that C12orf65 is in some way involved in mitochondrial protein synthesis, but this protein failed also to show any release activity *in vitro* using 70S *E. coli* ribosomes [Antonicka *et al.*, 2010]. Since there are significant differences between the mitochondrial ribosome and the bacterial one (see 1.7.1), it can not be excluded that C12orf65, or mtRF1, can facilitate peptidyl-tRNA hydrolysis. The fourth member, ICT1 has been identified in association with mitochondrial ribosome immunoprecipitated by mtRRF [Rorbach *et al.*, 2008]. This is very unusual for a class I RF, since in bacteria RRF and RF occupy the same site (A-site) within the ribosome, which also explains the absence of mtRF1a (or mtRF1 and C12orf65) in this IP. Alignment of all four mitochondrial RFs show some additional differences of ICT1 in comparison to the other three members (Figure 1.9), which could be due to a different function and might be in association with the fact that it was found in mtRRF-IP.

Figure 1.9: Sequence Alignment (CLUSTALW) of human mtRF1a, mtRF1, C12orf65 and ICT1. Identities are indicated by a star (*), high levels of similarity by a colon (:) and lower levels by a full stop (.). The GGQ domain is indicated in red, the PXT-motif in blue and the tip of the α5-helix in brown. Predicted mitochondrial targeting peptides are indicated italics. Residues forming an additional helix in ICT1, absent in conventional class I release factors (see chapter 6, figure 6.1) and the other members of the mitochondrial release factor family are indicated italics, underlined, bold.

Since mtRF1a is able to recognise all 13 open reading frames in human mitochondria, why do they contain three further class I release factors? The facts that mutations in C12orf65 are causing decreased *de novo* synthesis and that ICT1 was found in association with the mitochondrial ribosome (and other translation factors, respectively) suggest that both proteins are at least involved in the mitochondrial protein synthesis. These functions remain to be investigated.

1.9 Aims of this study

This PhD project contains two main parts:

Part I is focused on the characterisation of ICT1, and represents the major project of my PhD work. The following questions needed to be answered to investigate the function of ICT1 in human mitochondria:

i) *Is ICT1 a mitochondrial protein?*

ii) *Is this protein essential for life?*

iii) *Does the loss of ICT1 in human cell culture have any effect on mitochondrial protein synthesis or steady state level of mitochondrial proteins?*

iv) *Does ICT1 interact with the mitochondrial ribosome and is it important for mitochondrial ribosome biogenesis?*

v) *Is the retained GGQ motif functional, meaning does ICT1 have release activity?*

vi) *Does ICT1 have another function in the mitochondrial translation machinery, different from a conventional class I release factor?*

The characterisation of ICT1 will be represented in three result-chapters. Additionally one chapter will contribute to an initial characterisation of possible orthologues of ICT1 in other organism.

Part II, a project initiated by Dr. J. Rorbach, is an initial investigation of a possible mitochondrial ribosome assembly factor, called mtRbfA. The assembly of the mammalian mitochondrial ribosome has not been characterised. Since the bacterial ribosome can be assembled *in vitro* [reviewed in Nierhaus, 1991], it has been suggested that there are not so many factors involved in the ribosome assembly pathway in bacteria. However, those non-physiological conditions such as high temperatures and high salt concentration, used in those experiments, and further slow kinetics indicate that additional protein factors are probably required for the assembly pathway *in vivo*. There have been some proteins identified crucial for the assembly of either the 30S SSU or the 50S LSU in bacteria [reviewed in Culver, 2003, and Britton, 2009]. However, in human mitochondria this field is still elusive and needs some more attention. So far, only ERAL1 and TFB1M have been characterised and described to be essential for the stability and maturation, respectively, of the 12S rRNA of the 28S SSU and therefore are critical for the assembly of the mitochondrial SSU [Dennerlein *et al.*, 2010, Metodiev *et al.*, 2009]. The *m*-AAA protease is required for the processing of

MRPL32 and it has been therefore proposed to be essential for the complete assembly of the mitochondrial ribosome [Nolden *et al.*, 2005]. Just recently NOA1, a mitochondrial GTPase has been suggested to be important for 39S LSU assembly in mammals since a knockout of murine *Noa1* led to decreased density of the 39S LSU revealed by isokinetic sucrose gradient and consequently to impaired mitochondrial protein synthesis [Kolanczyk *et al.*, 2011]. Surprisingly its bacterial orthologue has been suggested to be involved in the assembly of the 30S SSU [Britton, 2009]. Thus NOA1 seems to have adopted a function in mammalian mitochondria different from its bacterial counterpart.

The bacterial RbfA is essential at low temperatures and has been extensively studied, which will be introduced at a later point in more detail. It was suggested to be involved in the maturation of the 16S rRNA of the 30S SSU and further in the later assembly process of the SSU in bacteria [Xia *et al.*, 2003]. Since the ribosomal RNA and the ribosome itself differs remarkably between bacteria and mammalian mitochondria it will be interesting whether mtRbfA has maintained its function or whether it has adapted a different task in human mitochondria. Thus with the investigation of the following questions it will be perhaps possible to clarify the function of mtRbfA in humans:

i) *Is mtRbfA localised within human mitochondria?*

ii) *Does this protein interact with the mitochondrial ribosome or ribosomal subunits, respectively?*

iii) *Does the depletion of mtRbfA from human cells show any effect on cell growth, mitochondrial translation, assembly of the mitochondrial ribosome or stability of mt-rRNA?*

The results of the investigations on the possible function of mtRbfA will be described and discussed in one chapter.

Chapter 2:

Materials

2 Chapter 2: Materials

2.1 Chemicals and Reagents

For this research project all chemicals and reagents were used from Sigma-Aldrich Company unless otherwise stated.

2.2 Human Cell lines

HeLa
Human cervical cancer carcinoma cells from Henrietta Lacks.

HEK293-Flp-In^{TM}T-REx^{TM} (Invitrogen)
Human Embryonic Kidney cells. This cell line contains a Tet-repressor and an integrated Flp-recombination-target (FRT) site for generating a stable cell line with Tetracycline inducible expression of the gene of interest.

143B
Human osteosarcoma cells.

143B-ρ^0 (kind gift from Prof. R. Wiesner, Cologne)
Those human osteosarcoma cells manipulated to lack mitochondrial DNA.

2.3 Bacteria strains

Strain	Genotype	Use	Company
α-select chemically competent cells	*F⁻ deoR endA1 relA1 gyrA96 hsdR17 ($r_k^-m_k^-$) phoA supE44 thi-1 Δ(lacZYA-argF)U169 Φ80δlacZΔM15*	general cloning	Bioline
Rosetta^{TM}(DE3) competent cells	*F⁻ ompT hsdS$_B$ ($r_B^-m_B^-$) gal dcm (DE3) pRARE (argU, argW, ileX, glyT, leuW, proL)*	for inducible overexpression of recombinant GST-fusion protein	Novagen

XL1-Blue supercompetent cells	*recA1 endA1 gyrA96 thi-1 hsdR17 supE44 RelA1 lac [F' proAB lacI^{q}ZΔM15 Tn10 (Tet^r)]*	for transformation of QickChange Mutagenisis reaction	Stratagene
TOPO	*F⁻ mcrA Δ(mrr-hsdRMS-mcrBC) Φ80lacZΔM15 ΔlacX74 recA1 araD139 Δ(ara-leu)7697 galU galK rpsL (Str^R) endA1 nupG*	for sequencing cloning for CLIP assay	Invitrogen

2.4 Plasmids

Plasmid	Use	Company/ source
pcDNA5/FRT/TO	Tetracycline inducible expression vector used for HEK293- Flp-In^{TM} system. Hygromycin and ampicillin resistance.	Invitrogen
pOG44	For Co-transfection with pcDNA5/FRT/TO. Expresses the Flp- recombinase. Amicillin resistance.	Invitrogen
pGex-6P-1	IPTG inducible expression vector used for N-terminus fusion of protein of interest with GST. Ampicillin resistance.	Amersham Bioscience
pTRC99A (-his-yaeJ)	IPTG inducible expression vector used for complementation assays in *E.coli* by the laboratory of Prof. Varshney (Bangalore, India). pTRC99A-his-yaeJ was used as a template for YaeJ amplification. Ampicillin resistance.	Kind gift from Prof. U. Varshney (Bangalore, India)
pFL61	*S. cerevisiae/ E. coli* shuttle vector. Contains the *URA3* gene as selection marker. Ampicillin resistance.	Kind gift from Dr. N. Bonnefoy, CNRS Paris
pTG1754	*S. pombe/ E. coli* shuttle vector. Contains the *URA3* gene as selection marker. Ampicillin resistance.	Kind gift from Dr. N. Bonnefoy, CNRS Paris
pCR4-TOPO	Sequencing vector for CLIP assay. Kanamycin and ampicillin resistance.	Invitrogen
pCMV-SPORT6-ICT1	Used as a template for ICT1-cDNA amplification. Ampicillin resistance.	Geneservice (I.M.A.G.E. ID 4418983)

Chapter 3:

Methods

3 Chapter 3: Methods

3.1 Cell culture

All cell culture methods were carried out in a class II cabinet. The inverted microscope Axiovert25 (Zeiss) was used to monitor the cells daily. For any documentation the Axiovert200M (Zeiss) with camera was used.

3.1.1 Cell culture maintenance

HeLa, 143B/ 143B-ρ^0 and HEK293-Flp-In^{TM}T-REx^{TM} cells were grown as monolayer in tissue culture flasks. HeLa cells were cultured in Earle's Minimal Essential Medium (EMEM) containing 4500 mg/l glucose, 1 mM pyruvate, non-essential amino acids and L-glutamine (Sigma, product M0643), to which 2.2 g/l sodium bicarbonate and 10 % (v/v) foetal bovine serum (FBS) were added. 143B/ 143B-ρ^0 and Hek293-Flp-In™ were grown in Dulbecco's modified Eagle's medium (DMEM) with pyruvate and L-glutamine (Sigma, product D6429), supplemented with 1 x non-essential amino acids, 50 µg/ml uridine and 10 % (v/v) FBS. Untransfected HEK293-Flp-In^{TM}T-REx^{TM} cells were routinely cultured with 10 µg/ml blasticidin and 100 µg/ml zeocin.

Usually all cells were seeded in 75 cm^2 flasks and cultured at 37°C in 5 % CO_2 humidified atmosphere. The media was changed at least every 3rd day. If a confluence of approximately 80 % was reached the cells were harvested in 1 mM EDTA/PBS. After centrifugation at 230 xg for 4 minutes the cell pellet was resuspended in fresh medium and cells were seeded into new flask(s). The size of the flask was dependent on the planned experiment.

To force cells to use oxidative phosphorylation they were cultured in glucose free media (Gibco, product 11966), containing 0.9 mg/ ml galactose, 1 mM pyruvate, 1 x non-essential amino acids, 50 µg/ml uridine and 10 % (v/v) FBS.

3.1.2 Cell storage

For longer storage, cells were harvested and the cell pellet was resuspended in 0.5 ml FBS containing 10 % (v/v) DMSO. For freezing those cells cryostorage vials were used. After 24 h storage at -80°C in a 'temperature controlled' cryo box the vials were transferred to liquid nitrogen.

To thaw cells, which should be done as fast as possible, the vial was briefly incubated in a 37°C water bath. Then pre-warmed medium was added very gently to the cells to a final volume of 5 ml. After centrifugation and resuspension the cells were transferred into a flask (same size of flask before freezing cells).

3.1.3 Mycoplasma Detection

Every 2 month or less, cells were tested for Mycoplasma infection by using MycoAlert® Mycoplasma Detection Kit (Lonza) following the manufacturer's instruction. To 25 µl of cell culture supernatant/ media an equal volume of MycoAlert reagent was added and incubated for 5 min at room temperature. A first reading in the luminometer was taken (Reading A) before adding 25 µl of MycoAlert substrate and further incubation of 10 min at room temperature. Finally the second reading was taken to calculate then the ratio of Reading B / Reading A. A ratio <1 means cells are not infected, ratio >1 should be considered as infected. In case of an infection cells were treated with Plasmocin (1:1000) for at least 2 weeks and the Mycoplasma test was repeated.

3.1.4 Cell counting

Cells were harvest as described above. The cell pellet was resuspended in a known volume of fresh media and 10 µl was added to a haemocytometer (Neubauer improved, with a 0.1 mm clearance). 4 main corner square sectors were counted. The average was multiplied by 10^4 to get the cell number per 1 ml.

3.1.5 Stable Transfection of HEK293-Flp-In^{TM}T-REx^{TM} cells

To generate a stable cell line with inducible overexpression of the gene of interest, HEK293-Flp-In^{TM}T-REx^{TM} were transfected with pcDNA5/FRT/TO (carrying the gene of interest, GOI) and pOG44 (Figure 3.1). The pOG44 vector expresses the Flp recombinase allowing the homologous recombination at the FRT sites of the pcDNA5/FRT/TO vector and the host cell line. This integration at this particular site of the genome of the host cell line will result in a zeocin sensitivity, but hygromycin resistance. The expression of the gene of interest is controlled by a Tet operator 2 ($TetO_2$). The Tet repressor (tetR) protein is expressed by the pcDNA6/TR vector (Blasticidin resistance) that was already independently integrated into the host cell line before. The adding of tetracycline (or doxacycline) to the cell culture media will result in the overexpression of the gene of interest by the hygromycin resistant cells.

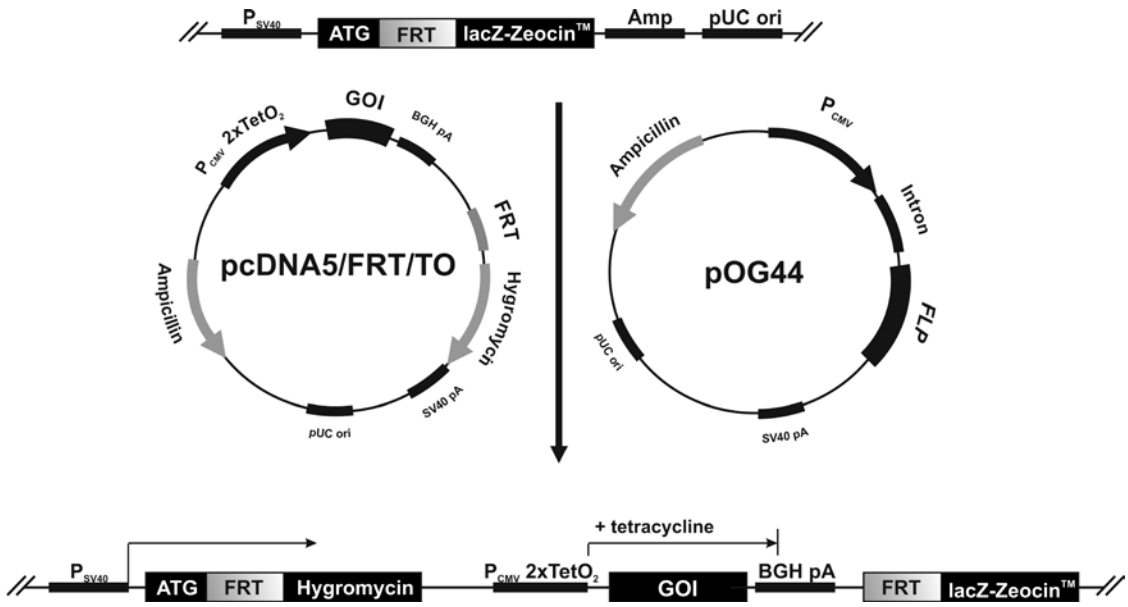

Figure 3.1: Flp-In system. To generate stable inducible expression cell line pcDNA5/FRT/TO with the gene of interest (GOI) (left circle) and pOG44 (right circle) were co-transfected into HEK293-Flp-In™T-REx™ cells. Flp recombinase, expressed by pOG44, mediates the homolog recombination via the FRT sites of the pcDNA5/FRT/TO-GOI vector and the genome of the host cell line. Successful integration (bottom) will result in hygromycin resistance and zeocin sensitivity. The expression of the GOI is controlled by CMV promotor with a Tet repressor and therefore inducible by tetracycline.

To transfect HEK293-Flp-In™T-REx™ cells (HEK293T) the protocol of "Stable Transfection of Adherent Cells" from QIAGEN was used (Superfect Transfection Reagent Handbook 12/2002).

HEK293T cells were seeded in a 6-well plate the day before transfection was carried out. For transfection the confluence was approximately 50 %. For each transfection different DNA:Superfect ratios were used: 1:5; 1:7 and 1:10, although generally the 1:7 was suitable. Tubes were prepared with 100 µl DMEM (no supplements), 2 µg of DNA (0.2 µg pcDNA5/FRT/TO-GOI + 1.8 µg pOG44) and the Superfect were added. After 10 min incubation at room temperature, 600 µl of growth media (DMEM supplemented as described in 3.1.1) were added. The media covering the cells in the 6-well plate was discarded and the transfection mix was transferred carefully to the wells. After 2.5 h at 37°C, 5% CO_2, the media with the transfection reagent was discarded and after 2 washing steps with PBS, fresh media was added. After 2 days selection was initiated by treatment with hygromycin B. As a control for antibiotic sensitivity, one well of untransfected cells was maintained under identical culture and antibiotic conditions. After approximately 2 weeks individual hygromycin resistance clones could be visualised, separated and propagated as single clonal cultures.

3.1.6 Protein-depletion: siRNA transfection of HeLa and HEK293T

By transfecting cells with synthetic siRNA duplexes it is possible to transiently deplete the protein of interest. In nature small interference RNA duplexes are the product of the dicer complex in the RNA interference process. Those siRNAs are ~ 19-24 nt long with a 2-3 nt 3'-overhang, specific features that are recognised by the RNA-induced silencing complex (RISC) within the cell (Figure 3.2). After unwinding the siRNA, separating the strands of the duplexes the siRNA/RISC complex with incorporated anti-sense strand will associate with the complementary target mRNA and finally cleave it. Thus no expression of this particular mRNA can occur.

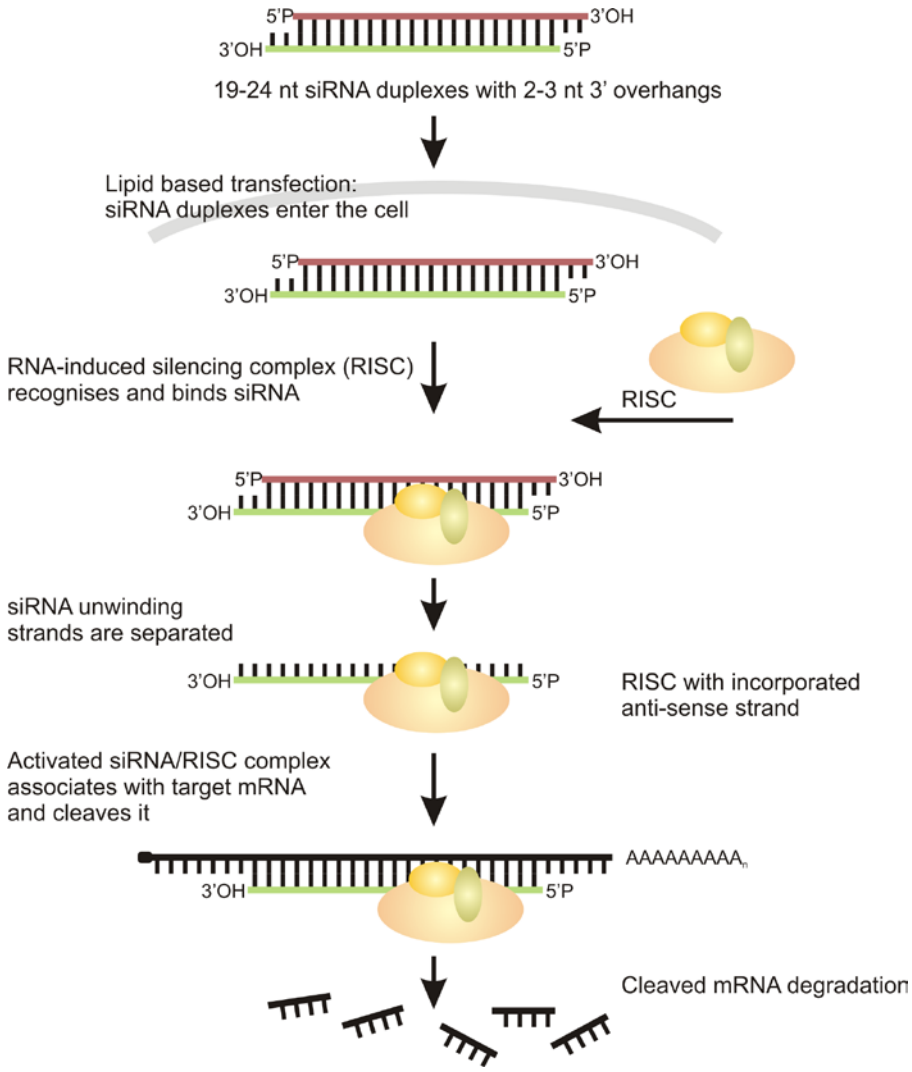

Figure 3.2: siRNA mediated gene silencing. Synthetic siRNA duplexes of 19-24 nt with 2-3 nt 3'-overhang are recognised and bound by RISC. After unwinding duplexes RISC incorporates anti-sense strand. The activated siRNA/RISC complex associates with target mRNA, followed by cleavage and degradation of the mRNA.

For growth curve analysis siRNA transfections were carried out in 6-well plates, and in 25 cm^2 or 75 cm^2 flasks for protein and / or RNA analysis. Initial analyses were performed using the 'forward' transfection method and oligofectamine as the reagent,

improved efficiency was obtained later using lipofectamine in the 'reverse' transfection method. The advantage using lipofectamine as transfection reagent is that it is possible to use less siRNA (10 nM to 50 nM final concentration), to perform reverse transfection and the transfection efficiency in case of HEK293T cells is higher.

3.1.6.1 siRNA transfection using oligofectamine™ transfection reagent (12252011, Invitrogen)

HeLa cells were seeded the day before transfection. Method and volumes are given here for 6-well plate seeded with 3x 10^4 cells per well.

For each transfection 2 tubes were prepared; tube A with 125 µl Opti-MEM®I+Glutatmax™I (Gibco 51985-026) and tube B with 15 µl. These were brought up to room temperature. To tube A 200 pmoles siRNA (= 10 µl of 20 µM stock) was added and to tube B 4 µl oligofectamine. Everything was gently mixed by pipette and after 10 min the contents of tube B was transferred to tube A, followed by another incubation time of 25 min. During this incubation step the media from the wells were discarded, the cells were washed with PBS and 800 µl of complete growth media was added. Finally the transfection mix was transferred into the wells, followed by rocking the plate carefully. After 3 days the cells were harvested or re-transfected.

For a 25 cm^2 flask all volumes were doubled transfecting ~ 1.5x 10^5 cells.

3.1.6.2 siRNA transfection using lipofectamine™ RNAiMAX (13778-150 Invitrogen)

For each transfection a tube with 250 µl Opti-MEM®I+Glutatmax™I was pre-warmed to room temperature. siRNA (15 - 75 pmoles dependent on the efficiency of the siRNA) and 2 µl lipofectamine were added, followed by an incubation of 10 - 20 min at room temperature. The transfection mix was transferred to the well and 3x 10^4 cells in 1.25 ml normal growth media were added.

For 25 cm^2 flasks all reagent and media volumes were doubled to transfect 3x 10^5 cells.

For the MTT assay as described below 96-well plates were used to transfect ~ 5,000 cells per well in a final volume of ~200 µl with appropriate amounts of siRNA and lipofectamine.

Table 3.1: Sequences of siRNA employed in this doctoral work

No	siRNA	sequence 5' → 3'
#1	si-ICT1-ORF A (220) sense	CUA GAU CGC UUG ACA AUA U dTdT
#2	si-ICT1-ORF B (419) sense	GCC GCU AUC AGU UCC GGA A dTdT
#3	si-ICT1-ORF C (179) sense	GGG UCC CGA AUG GUG CAA A dTdT
#4	si-Rbfa-ORF A (481) sense	GGA GCU GUA UGA CCU UAA C dTdT
#5	si-Rbfa-ORF B (691) sense	GGG AAA UGC AGC UCU AGC U dTdT
#6	si-Rbfa-ORF C (262) sense	GAA CUG GCU CAA GAA AUU U dTdT
#7	si-Rbfa-ORF D (862) sense	GGC GCU CAA CAA GCA GAU U dTdT
#8	si-Rbfa-ORF E (668) sense	CCG AUA GUG UUU GUU CAA G dTdT
#9	si-Rbfa-UTR F (1242) sense	GGC AGU UGA UGG AGU UAA A dTdT
#10	si-control	siRNA negative control duplex OR-0030-NEG05

siRNAs were stored as 20 µM or 100 µM stocks in RNase free water at -20°C. All siRNAs were custom synthesised by Eurogentec.

3.1.7 MTT assay

The MTT assay as a colorimetric assay can be used to measure relative cell viability in 96-well plate format. MTT (3-(4,5-Dimethylthiazol-2-yl)-2,5-diphenyltetrazolium bromide) is reduced to the purple formazan in living cells and as such can be used as an alternative to counting cells.

This assay was mostly used to determine the relative cell growth after siRNA treatment. Cells were cultured under experimental conditions as described in 3.1.6.2 until assay was performed. The MTT was always prepared fresh in PBS at a concentration of 5 mg/ ml and finally diluted to 0.5 mg/ ml in growth media. For the assay the growth media was aspirated from the plate and 200 µl of 0.5 mg/ ml MTT solution was added to each well. After 3 h incubation at 37°C the MTT solution was removed, 200 µl DMSO was added to dissolve the formazan crystals and incubated for 5 min at 37°C. The absorbance was measured at 550 nm in a microplate-reader (Bio-Tek). Each experimental sample was prepared a minimum of 4 times.

3.1.8 Flow cytometry analysis

All flow cytometry measurements were done on BD FACS CANTO II machine in the Centre for Life (Newcastle University, Flow Cytometry Core Facility) with kind assistance from Mr. Ian Dimmick.

3.1.8.1 Mitochondrial mass - NAO

To measure changes in mitochondrial mass 10-n-nonyl-acridine orange (NAO, Invitrogen A1372) can be used as an indicator, because this fluorescent dye binds specifically to negatively charged cardiolipin of the mitochondrial inner membrane.

NAO was usually prepared in DMSO at a stock concentration of 5 mM that can be stored at -20°C (light protected).

Cells were cultured as required for the experiment, harvested and resuspended at approximately 1x 10^6 cells in 0.5 ml PBS. Samples were incubated for 10 min at 37°C 5% CO_2 in the presence of 10 µM NAO. Finally the cells were washed in 1 ml PBS and resuspended in 0.5 ml PBS and green fluorescence at 530 nm was detected. The results were analysed with BD FACSDIVA™ software.

3.1.8.2 ROS species - MitoSox

MitoSox Red (Molecular Probes, M36008) can be used as a specific indicator for mitochondrial ROS production. It can be exclusively oxidised to a fluorescent form by the superoxide, which is generated in the mitochondrial matrix.

MitoSOX™ Red is delivered as 50 µg vial, to that 13 µl DMSO was added to get a stock solution of 5 mM. The stock could be stored at -20°C (light protected).

Cells were harvested and resuspended in PBS. To approximately 1x 10^6 cells in 0.5 ml PBS 5 µM MitoSOX Red was added (0.5 µl of stock reagent), followed by incubation for 10 min at 37°C 5% CO_2. Next, cells were washed in 1 ml PBS and finally resuspended in 0.5 ml PBS. The red fluorescence emission was measured at 585 nm and finally analysed using BD FACSDIVA™ software.

3.1.8.3 Mitochondrial membrane potential - JC 1

JC 1 (Molecular Probes M34152) is a cationic dye, which accumulates in the mitochondria in a membrane potential dependent manner. This can be measured in a fluorescence emission shift from green to red. A loss in the mitochondrial membrane potential will result in a decrease of the red/green fluorescence ratio.

JC 1 was usually prepared as 2 mM stock in DMSO and stored in small aliquots at -20°C (light protected). Cells were harvested and resuspended in 0.5 ml PBS. JC 1 was added to a final concentration of 2 µM. After 10 min incubation at 37°C 5% CO_2 cells were washed in 1 ml PBS and finally the fluorescence emission was measured at 530 nm (green) and 585 nm (red). As a positive control cells were treated with 2 µM to 10 µM FCCP (mitochondrial uncoupler) for 10 min at 37°C prior to JC 1 staining, which

usually results in a substantial decrease of the red/green fluorescence ratio. All the measurements were finally analysed with BD FACSDIVA™ software.

3.1.8.4 Apoptosis

To measure the level of apoptosis the APO-DIRECT™ kit (556381 from BD Biosciences Pharmingen) was used. This method measured the level of DNA fragmentation, a later step in apoptosis, by terminal deoxynucleotidyltransferase dUTP nick end labelling (TdT or "TUNEL"). TdT add bromolated deoxyuridine triphosphates (Br-dUTP) to 3'-OH of ds or ss DNA. Incorporated Br-dUTPs are then recognised by FITC-labelled monoclonal anti-BrdU antibodies.
The method was carried out following manufacturer's instruction.

Fixation
Cells (25 cm^2 flask at ~ 60% confluence) were harvested and the pellet was fixed in 1 ml 1% (w/v) paraformaldehyde in PBS (pH 7.4) for 15 min on ice. Prior to centrifugation for 5 min at 300 xg 5 ml cold PBS was added to the cells. The supernatant was discarded and the pellet was washed in 5 ml PBS. The cells were then resuspended in 0.5 ml 70% (v/v) ethanol and stored at -20°C for at least 30 min or several days.
Staining
Approximately 1x 10^6 fixed cells were centrifuged for 5 min at 300 xg followed by two washing steps with the wash buffer (provided from the kit). The pellet was then incubated in 50 µl staining solution for 1 h at 37°C. After the staining 1 ml rinse buffer was added prior to centrifugation for 5 min at 300 xg. Finally the pellet was resuspended in 0.5 ml PI/RNase staining buffer and incubated for 0.5 to 3 h prior to analysis by flow cytometry.
For the measurements two dyes were used: the FITC-dUTP (measured at 530 nm), which indicates the apoptotic cells and PI (measured at 585 nm), which stains the total DNA. Finally the measurements were analysed using BD FACSDIVA™ software.

3.1.8.5 Cell cycle

There are four main states of cell-populations: two gap-phases, G1 (between M- and S-phase) and G2 (between S-phase and mitosis), the S-phase and the M-phase. Using DNA staining methods, cells can be visualise in three categories: Cells with one copy of DNA (G1), cells with doubled amount of DNA after completed replication (G2/M), which will therefore cause a double of fluorescence intensity and cells in the S-phase, synthesising DNA will be in between the two gap phases.

To analyse the cell cycle status of cell-populations, the DNA of cells was stained with DAPI using the CyStain DNA 2 step kit from Partec (05-5005).
Approximately 5x 10^5 cells were permeabilised with 200 µl extraction buffer as provided in the kit. After 20 min incubation at room temperature 1 ml DAPI solution was added, followed by incubation for 20 min at room temperature (light protected). The stained cells were then measured at 450 nm flow cytometry. For the analysis of the flow cytometry measurements the ModFit LT V3.2 software was used.

3.2 Bacterial Culture

All bacteria were grown on LB agar plates or LB media in suspension with appropriate antibiotics at 37°C, usually overnight. For a longer storage bacteria were frozen in LB media containing 15 % (v/v) glycerol at -80°C.

LB (Luria-Bertani)

1 % (w/v)	Bacto-tryptone
0.5 % (w/v)	Yeast extract
1 % (w/v)	NaCl
(2 % (w/v)	Agar for plates)

pH 7.5 with NaOH

3.2.1 Transformation

3.2.1.1 Transformation of α-select™ competent cells (Bioline)

40 µl of α-select™ competent cells were thawed on ice. To those a maximum volume of 4 µl DNA were added. After 30 min incubation on ice the cells were placed at 42°C for 45 secs followed by 2 min on ice. Then 960 µl pre-warmed SOC medium was transferred to the bacteria, which were then incubated at 37°C for 1 h with shaking, cells were pelleted and resuspended in a final volume of 100 µl to 300 µl fresh SOC and were plated out on LB agar with appropriate antibiotics.

SOC

2 % (w/v)	Bacto-tryptone
0.5 % (w/v)	Yeast extract
0.05 % (w/v)	NaCl
2.5 mM	KCl
10 mM	$MgCl_2$
20 mM	Glc

Bacto-tryptone, yeast extract, NaCl and KCl were mixed in a final volume of 195 ml and the pH was set to 7.0 prior to autoclaving. Next, 1 ml of sterile 2M $MgCl_2$ and 4 ml of 1M Glc were added. Finally the SOC media was aliquoted à 1 ml and stored at -80°C.

3.2.1.2 Transformation of Rosetta DE3 (Novagen)

20 µl of Rosetta DE3 cells, carefully thawed on ice, were incubated with 100 ng plasmid DNA on ice, followed by a heat shock step of 30 secs at 42°C. After 2 min on ice 80 µl pre-warmed SOC medium was added to the bacteria, followed by an incubation of 1 h at 37°C. The 100 µl bacteria suspension was then plated out on LB agar containing appropriate antibiotics.

3.2.2 Colony screening

A swab of bacterial colony was transferred to an eppendorf tube and was lysed in 25 µl buffer containing 50 mM NaOH, 0.5 % (w/v) SDS, 5 mM EDTA, 10 % (v/v) glycerol and 0.025 % (w/v) bromocresol green. The lysis mixture was vortexed and heated for 30 min at 68°C, followed by centrifugation at 13,000 rpm for 8 min. 18 µl of the supernatant were loaded on a 0.75 % (w/v) agarose gel (lacking ethidium bromide). After electrophoresis of the gel at 65 V for approximately 40 min the gel was stained in 0.2 µg/ ml ethidium bromide for 15 min and washed twice in water. Finally the gel was analysed with the UV transilluminator.

3.2.3 Isolation of plasmid DNA

A 5 ml small culture of bacteria was grown overnight in LB plus appropriate antibiotics. The plasmid DNA was isolated by using the Wizard Plus® SV Minipreps kit (Promega A1460, centrifugation protocol) or (Fermentas K0503). Finally the DNA was eluted in 50 µl sterile dH_2O.

3.3 DNA manipulation

3.3.1 Isolation of DNA from human cells

Cells were harvested as already described. The pellet was resuspended in 200-400 µl 10 mM Tris/ 1 mM EDTA, lysed with 1% (w/v) SDS and treated with 2 mg/ ml proteinase K (Roche) over-night at 37°C at 1,000 rpm (Thermomixer, Eppendorf). Next day DNA was isolated by phenol/chloroform extraction followed by ethanol precipitation.

3.3.2 Phenol chloroform extraction and ethanol precipitation of nucleic acids

An equal volume of buffer saturated phenol (Sigma 108-95-2; pH 7.9 for DNA samples; pH 6.7 for RNA samples) was added to each sample, followed by vortexing and centrifugation for 2 min at 13,000 rpm. The aqueous phase was transferred to a new tube to which an equal volume of both phenol and chloroform:isoamylalcohol (24:1) was added and vortexed and centrifuged as before. This aqueous phase was transferred to a new tube containing the equal amount of chloroform:isoamylalcohol (24:1). To the final aqueous phase were added 1 µl linear acrylamide, 1/10 vol 3 M sodium acetate (pH 5.2) and 2.5 vol 100 % ethanol to precipitate the nucleic acids. After incubation at - 80°C for at least 1 h, the precipitated DNA/RNA was pelleted at 20,000 xg for 15 min at 4°C. The DNA/RNA pellet was washed with 75% (v/v) ethanol and resuspended in 10 to 20 µl sterile dH_2O.

3.3.3 DNA electrophoresis

For the DNA-gel electrophoresis 0.75 to 1.2 % (w/v) gels were used dependent on the size of the molecules to be separated and visualised. The agarose was dissolved in 1 x TAE buffer by heating in a microwave. After cooling 0.5 µg/ml ethidium bromide was added to the gels and the gel mix poured into the gel tray with comb. The DNA samples that were loaded on a gel contained 1 x DNA loading buffer. The electrophoresis was carried out in 1 x TAE at 65 to 100 V. The Invitrogen 1 kb ladder was used to estimate sizes. DNA was visualised using the UV transilluminator, and the result captured and stored with a digital camera and AlphaEasy software (Alpha Innotech).

1 x TAE	
40 mM	Tris-acetate
1 mM	EDTA (pH 8.0)

6 x DNA loading buffer	
0.2 % (w/v)	bromophenol blue
0.1 M	EDTA (pH 8.0)
30 % (v/v)	glycerol

3.3.4 DNA extraction from agarose gels

If DNA had to be extracted from agarose gels, low melting agarose was used. The DNA of interest was cut from the gel in as small a volume as possible. The gel was transferred to a 1.5 ml tube and dH_2O was added up to 400 µl final volume. Next, the gel was melted for 10 min at 65°C at 1,000 rpm using Thermomixer from Eppendorf, followed by one “hot” phenol extraction (phenol pre-heated at 65°C) and one “cold” one

(at room temperature) prior to standard phenol/chlorform extraction as described in 3.3.2.

3.3.5 Measurement of DNA concentration

To measure DNA (or RNA) concentration the absorption at 260 nm was taken by using the Spectrophotometer ND-1000 (NanoDrop). This generally used ~ 1.5 µl of undiluted sample.

3.3.6 Polymerase Chain Reaction (PCR)

The Polymerase chain reaction is a method for amplification of defined DNA regions. The PCR was performed in 0.5 ml thin walled tubes with a final volume of 20 µl or 50 µl. Each reaction generally contained the following components:

Standard PCR to investigate cloning results		PCR for cloning a gene of interest (Novagen) by using proofreading DNA polymerase	
1 µM	forward primer	1 µM	forward primer
1 µM	reverse primer	1 µM	reverse primer
0.2 mM	dNTPs	0.08 mM	dNTPs
1.5 mM	$MgCl_2$	1.5 mM	$MgSO_4$
1 x	PCR reaction buffer	1 x	PCR reaction buffer
20 - 100 ng	DNA template	20 - 100 ng	DNA template
1 U	*Taq*	1 U	*KOD* HotStart

The PCR was performed under the following conditions:

denaturation:	94°C	2 min	
denaturation:	95°C	45 sec	
annealing:	xx°C[1)]	45 sec	30 cycles
extension:	xx°C[3)]	xx sec [2)]	
extension:	xx°C[3)]	5 min	

[1)] The Annealing temperature (T_a) is specific for each oligonucleotide. It was calculated with the following formula: $T_a = 69.5 + 0.41 * GC (\%) - 500/ nt_c - 5°C$

GC (%):GC content of oligonucleotide as a percentage

nt_c: number of nucleotides which are complement to the template

[2)] The extension time is dependent on the length of PCR product, which should be amplified.

[3)] 72°C using *Taq*- and 70°C using *KOD* DNA polymerase.

Table 3.2: Oligonucleotide sequences used in this investigation

No	oligonucleotide	sequence (5' → 3')	use
#1	ICT1_FLAG (forward)	CTT TCT TAA GCT TCC ACC **ATG** GCG GCC ACC AGG TG	cloning ICT1 into pcDNA5/FRT/TO, restriction site *Hind*III (underlined), start codon (bold)
#2	ICT1_FLAG (reverse)	CTC TCC GAT ATC *CTA CTT ATC GTC GTC ATC CTT GTA ATC* GTC CAT GTC GAC CCT C	cloning ICT1 into pcDNA5/FRT/TO, restriction site *EcoR*V (underlined), primer contains FLAG sequence (italics)
#3	ICT1_GST (forward)	CTT TCT TGG ATC C**AT** **G**GC GGC CAC CAG GTG	cloning ICT1 into pGex-6P-1, restriction site *BamH*I (underlined), start codon (bold)
#4	ICT1Δ29_GST (forward)	CTT TCT TGG ATC CCT GCA CAA GCA GAA AGA CG	cloning ICT1Δ29 (truncation of the n-terminus of 29 aa) into pGex-6P-1, restriction site *BamH*I (underlined)
#5	ICT1_GST (reverse)	CTC TCC CTC GAG TCA GTC CAT GTC GAC CCT C	cloning ICT1/ ICT1Δ29 into pGex-6P-1, restriction site *Xho*I (underlined)
#6	pTRC99A_ICT1 Δ29 (forward)	CAC ACA CCA TGG *AAG GAG G*CG TA**A** **TG**C ACA AGC AGA AAG ACG GCA C	cloning ICT1Δ29 into pTRC99A, restriction site *Nco*I (underlined), *E. coli* ribosome binding site (italics) upstream of the TK1 start codon (bold)
#7	pTRC99A_ICT1 Δ29 (reverse)	CAC ACA GGA TCC TCA GTC CAT GTC GAC CCT C	cloning ICT1Δ29 into pTRC99A, restriction site *BamH*I (underlined)
#8	ICT1_yeast (forward)	CTC TCC GCG GCC GCA CGC GTC CGC TGA GC**A** **TG**	cloning ICT1 into yeast shuttle vector pFL61 or pTG1754, restriction site *Not*I (underlined), start codon (bold)
#9	ICT1_yeast (reverse)	CTC TCC GCG GCC GCG GTG TGA AAG TCC TCT CAG C	cloning ICT1 into yeast shuttle vector pFL61 or pTG1754, restriction site *Not*I (underlined)
#10	YaeJ_GST (forward)	CTT TCT TGG ATC C**AT** **G**AT TGT GAT TTC CCG ACA TG	cloning YaeJ into pGex-6P-1, restriction site *BamH*I (underlined), start codon (bold)
#11	YaeJ_GST (reverse)	ACA ACT CGA GTT ATT CCC GAC CGC TGC G	cloning YaeJ into pGex-6P-1, restriction site *Xho*I (underlined)
#12	YaeJ_FLAG (forward)	ACA AGC GCG C*CT ACT CTT CC*A TTG TGA TTT CCC GAC ATG TTG C	cloning YaeJ into pcDNA5/FRT/TO with Su9 pre-sequence (italics), restriction site *BssH*II (underlined)
#13	YaeJ_FLAG (reverse)	CTC TCC GGG CCC *CTA CTT ATC GTC GTC ATC CTT GTA ATC* TTC CCG ACC GCT GCG	cloning YaeJ into pcDNA5/FRT/TO, restriction site *Apa*I (underlined), primer contains FLAG sequence (italics)
#14	mtRbfaΔ30_ GST (forward)	CTT TCT TGG ATC CGA GCG GGG ACT TCA CTG CTC TGC TG	cloning mtRbfaΔ30 (truncation of the n-terminus of 30 aa) into pGex-6P-1, restriction site *BamH*I (underlined)
#15	mtRbfa_GST (reverse)	CTT TCT TCT CGA GGT GGG ATG GGC AGA GCC TCT CCA T	cloning mtRbfaΔ30 into pGex-6P-1, restriction site *Xho*I (underlined)
#16	pTRC99A forward	CAT CCG GCT CGT ATA ATG	for sequencing of pTRC99A
#17	pTRC99A reverse	CAA AAC AGC CAA GCT TGC	for sequencing of pTRC99A
#18	CMV forward	CGC AAA TGG GCG GTA GGC GTG	for sequencing of pcDNA5/FRT/TO

#19	BGH reverse	TAG AAG GCA CAG TCG AGG	for sequencing of pcDNA5/FRT/TO
#20	pFL61 forward	TCG TAG TTT TCA AGT TCT TAG ATG C	for sequencing of pFL61
#21	pFL61 reverse	GCG TAA AGG ATG GGG AAA GAG	for sequencing of pFL61
#22	pTG1754 forward	GAG AAT TCC ATT GTC TTG AC	for sequencing of pTG1754
#23	pTG1754 reverse	TGG CAT TGT TTG CAC ATT CC	for sequencing of pTG1754
#24	M13 forward	GTA AAA CGA CGG CCA G	colony screening in CLIP assay, sequencing primer in CLIP assay
#25	M13 reverse	CAG GAA ACA GCT ATG AC	colony screening in CLIP assay,

All oligonucleotides were custom synthesised by Eurogentec.

3.3.7 PCR product purification

For further experiments using a PCR product it was first purified using the PCR purification kit (QIAGEN 28106, centrifugation protocol). The DNA was eluted in 40 µl sterile dH_2O.

3.3.8 QuikChange Mutagenisis

To mutate particular regions of gene of interest the QuikChange® II Site-Directed Mutagenesis Kit (Stratagene 200523) was used.

The reaction was performed in 25 µl volume in 0.5 ml thin walled PCR tubes containing the following components:

2.5 µl	reaction buffer (as provided in the kit)
2.5 ng/ µl	primer forward
2.5 ng/ µl	primer reverse
0.5 µl	dNTP (as provided in the kit)
50 ng	DNA template
1.25 U	*PfuUltra*

The amplification was performed under the following conditions:

denaturation:	95°C	2 min	
denaturation:	95°C	1 min	
annealing:	xx°C[1)]	1 min	20 cycles
extension:	68°C	8 min	

After cooling down the reaction on ice, 5U *Dpn*I was added to digest the parental methylated and hemi-methylated DNA template. After 90 min at 37°C 4 µl of the reaction were added to 40 µl supercompetent cells, followed by a transformation as described in 3.2.1.

Table 3.3: Oligonucleotide sequences used for mutagenesis application

No	oligonucleotide	sequence (5' → 3')	use	T_a [1)]
#1	ICT1_AGQ_ forward	gta gtg gtc ctg cgg ggc aga atg	generating mutation in ICT1 263 G→C, 88 Gly→Ala	50°C
#2	ICT1_AGQ_ reverse	cat tct gcc ccg cag gac cac tac	generating mutation in ICT1 263 G→C, 88 Gly→Ala	50°C
#3	ICT1_GSQ_ forward	gtg gtc ctg ggt cgc aga atg tga ac	generating mutation in ICT1 265-266 GG→TC, 89 Gly→Ser	50°C
#4	ICT1_GSQ_ reverse	gtt cac att ctg cga ccc agg acc ac	generating mutation in ICT1 265-266 GG→TC, 89 Gly→Ser	50°C

3.3.9 DNA Sequencing

Most of the sequencing reactions were kindly carried out by Mr Geoff Taylor.

Briefly 450 ng plasmid DNA were cycle sequenced in a total volume of 20 µl using BigDye(R)Terminator v.3.1 from AppliedBiosystems:

450 ng	DNA
1.5 µl	5 x sequencing buffer v1.1, v3.1
1 µl	primer (3.2 µM)
3 µl	BigDyes(R)Terminator v.3.1

The reaction was performed under the following conditions:

denaturation:	95°C	5 min	
denaturation:	95°C	30 sec	
annealing:	50°C	10 sec	30 cycles
extension:	60°C	4 min	

The samples were then precipitated in a 96-well plate and 10 µl HiDi were added, followed by incubation for 2 min at 95°C just prior to running on the sequencer 3130 xl Genetic Analyzer (AppliedBiosystems). Sequences were analysed with "Sequencing Analysis software - Version 5.1 © 2001-2003" (AppliedBioSystems).

3.3.10 Restriction digest

All diagnostic restriction enzyme digestions were performed in a volume of 10 µl to 20 µl with 0.5 µg to 1.0 µg DNA. Preparatory digests were generally of ~ 4 µg plasmid DNA. 1 U restriction enzyme was used to digest 1 µg DNA. The enzymes were

supplied by Roche or New England Biolabs. The conditions chosen for each individual digestion were as recommended by the company.

3.3.11 Vector dephosphorylation

To avoid the re-ligation of a digested vector, samples were 5' dephosphorylated. Therefore digested samples were incubated at 37°C for 1-2h in the presence of 1x dephosphorylation buffer and ~1U alkaline phosphatase per 1 µg DNA. 10x buffer and enzyme were delivered by Roche (713023).

3.3.12 DNA ligation

To ligate compatible DNA fragments such as digested plasmid and PCR fragments, the two DNA components were incubated together in a volume of 10µl in the presence of 1 U T4 DNA ligase (Roche) and 1 x ligation buffer at 16°C overnight (supplemented with 1mM ATP final). Three to six fold molar access of insert to vector were used for most ligations, with usually 50 ng vector DNA.

3.4 RNA manipulation

For all work with RNA, the water used was DEPC pre-treated and autoclaved.

3.4.1 Trizol extraction

RNA from cells was isolated using Trizol from Invitrogen. Depending on the size of the cell pellet 0.5 ml or 1 ml Trizol was used to resuspend the pellet, followed by an incubation step for 5 min at room temperature. Then 0.1 ml chloroform (per 0.5 ml Trizol) was added to each sample, which was shaken by hand for 15 secs and further incubated for 3 min at room temperature. After centrifuging the samples at 12,000 xg for 15 min (4°C) the clear supernatant was transferred to a fresh tube and 250 µl isopropanol was added, mixed and incubated for 10 min at room temperature and finally centrifuged at 12,000 xg for 10 min (4°C). The pellet was washed in 75% (v/v) then 100% ethanol and then fully resuspended in 10 - 20 µl DEPC water, containing 1U RNAguard per µl. Before using or freezing the RNA, it was necessary to leave the RNA for at least 1 h on ice to ensure it had completely dissolved.

3.4.2 Northern Blot

Samples were prepared in a 20 µl volume containing 1.5 to 3 µg RNA, 1x MOPS, 5.5 % (v/v) formaldehyde and 35 % (v/v) formamide. These were denatured at 55°C for 15 min. After cooling down the samples on ice ethidium bromide (0.1 µg/ µl final) and RNA loading buffer to a 1x final concentration were added before loading on the gel.

The samples were separated on a 1.2 % (w/v) denaturing agarose gel (containing 1x MOPS and 0.9 % (v/v) formaldehyde) at 50 V for ~ 6 to 7 h. After the run the gel was rinsed 4 x in 5 volumes of DEPC water and transferred on a GeneScreen Plus membrane over-night in 10x SSPE buffer.

The next day the membrane was rinsed in 2x SSPE and then the RNA was fixed to the membrane through baking at 80°C for 2 h under a vacuum. To avoid unspecific binding of the probe the membrane was pre-hybridised in 10 ml of 50 % (v/v) formamide, 5x SSPE, 1 % (w/v) SDS and 5x Denhardt's solution for a minimum of 2 h at 42°C.

The labelled probe was prepared with 50 to 100 ng DNA fragment that was denatured in 9 µl volume at ~ 95°C for 4 min. After cooling down the DNA on ice 3 µl random hexamer mix, 5U Klenow DNA polymerase I and 2 µl of ^{32}P dCTP (~ 10-20 µCi; PerkinElmer NEG513H) were added, followed by incubation at 37°C for 1 h. The probe was then purified through a Nick column as follows: the volume of the probe was increased up to 100 µl and then added to the column and allowed to fully enter the bed volume. A 400 µl volume of DEPC water was then added and allowed to enter the column. The first flow-through was discarded and a further 400 µl were added. The second flow-through was collected in a fresh tube containing the probe. The activity was estimated using a Cerenkov counter. Approximately 2x 10^6 cpm were added per 10 ml hybridisation buffer incubating the membrane and incubated over-night at 42°C. The next day the membrane was washed twice 15 min each with 2x SSPE at room temperature, followed by at least one washing step for 15 min with 2x SSPE/ 2% (w/v) SDS at 65°C. The membrane was monitored to determine if further washes were necessary. Finally the membrane was put into Saran wrap and exposed to a Phosphor-Imager cassette. Visualization and analysis of radiolabelled RNA species employed Phosphor-Imager and Image-Quant software (Molecular Dynamics, GE Healthcare). Prior to re-probing, the membrane was stripped by washing the membrane twice with boiling 0.1x SSC and once with 0.1x SSC/ 0.1% (w/v) SDS. Then the membrane was incubated with pre-hybridisation buffer and probed as described above.

10x MOPS-buffer (pH 7.2)	
0.4 M	Morpholinopropanesulfonic acid (MOPS)
0.1 M	NaOAc
10 mM	EDTA

20x SSPE (pH 7.4)	
3 M	NaCl
0.2 M	NaH_2PO_4
20 mM	EDTA

10x RNA loading buffer	
50% (v/v)	glycerol
1 mM	EDTA
0.25% (w/v)	bromophenol blue
0.25% (w/v)	xylene cyanol

5x random hexamer mix	
250 mM	Tris/ HCl (pH 7.5)
50 mM	$MgCl_2$
5 mM	DTT
0.5 mM	dATP
0.5 mM	dGTP
0.5 mM	dTTP

50x Denhardts	
1% (w/v)	Ficoll (Type 400)
1% (w/v)	polyvinylpyrrolidone
1% (w/v)	BSA (Fraction V, Sigma)

20x SSC	
3 M	NaCl
0.3 M	Na-citrate

3.4.3 Reverse transcription

Various RNA analyses were performed including Real Time PCR for which it was necessary to synthesise a cDNA from an RNA template. The reverse transcription was performed by using "SuperScript™ First-Strand Synthesis System for RT-PCR" (Invitrogen) using the random primer protocol. The first step was to mix RNA of interest (max. 0.5 µg) with 50 ng random hexamer, 1 µl 10 µM dNTP (final concentration 0.5 µM) in a final volume of 10 µl. After an incubation at 65°C for 5 min the mixture was transferred to ice for minimum 1 min to cool. The following components were then added: 2 µl 10 x first strand buffer, 4 µl 25 mM $MgCl_2$ (final concentration 5 mM) 2 µl 0.1 M DTT (final concentration 10 mM) and 1 µl RNaseOUT Recombinant Ribonuclease Inhibitor. This was incubated for 2 min at 25°C before 50 U Superscript was applied. Finally the reaction was completed by 10 min at 25°C (specific step for random hexamer primers), 50 min at 42°C and 15 min at 70°C.

3.4.4 Real time PCR

To estimate RNA levels in the starting material, Real Time PCR was performed by using "Fast start DNA Master SYBR Green I - kit" (Roche) and the Roche Lightcycler (capillary system). All reactions were made up in 20 µl volume with the following components in the cold block:

0.5 µM	forward primer
0.5 µM	reverse primer
x mM	$MgCl_2$ (primer dependent)
1 µl	enzyme/ SYBR green mix (Roche)
2 µl	template (cDNA or 10 ng/ µl DNA)
x µl	dH_2O

Conditions:

		Temperature	Hold time (secs)	Slope (°C/ sec)
1)	Denaturation:	95°C	600	20
2)	Amplification (40 cycles)			
	Denaturation:	95°C	10	20
	Annealing:	xx°C[1)]	5	20
	Extension:	72°C	10	20
3)	Melting curve	95°C	0	20
		65°C	15	20
		95°C	0	0.1
4)	Cooling	40°C	30	20

Table 3.4: Oligonucleotides sequences used for Real Time PCR

No	Oligonucleotide	Sequence (5' → 3')	$MgCl_2$ [mM]	T_a[1)]
#1	12S forward	ACA CTA CGA GCC ACA G	3 mM	53°C
#2	12S reverse	ACC TTG ACC TAA CGT C	3 mM	53°C
#3	16S forward	CCA ATT AAG AAA GCG TTC AAG	4 mM	57°C
#4	16S reverse	CAT GCC TGT GTT GGG TTG ACA	4 mM	57°C
#5	MT-CO1 forward	AAC CCA ATA CCA AAC GC	4 mM	52°C
#6	MT-CO1 reverse	CTT CAG GGT GAC CGA AA	4 mM	52°C
#7	MT-CO2 forward	CCT AGA ACC AGG CGA C	4 mM	54°C
#8	MT-CO2 reverse	GTC GTG TAG CGG TGA A	4 mM	54°C
#9	MT-ND1 forward	AAT CGC AAT GGC ATT CC	4 mM	64°C
#10	MT-ND1 reverse	CGA TGG TGA GAG CTA AGG	4 mM	64°C
#11	β-actin forward	TGC GTT ACA CCC TTT CT	5 mM	59°C
#12	β-actin reverse	CAA CCG ACT GCT GTC A	5 mM	59°C
#13	B2M forward	CAC TGA AAA AGA TGA GTA TGC C	5 mM	64°C
#14	B2M reverse	AAC ATT CCC TGA CAA TCC C	5 mM	64°C

All the oligonucleotides for Real Time PCR were synthesised by Eurogentec or TAGN Ltd.

3.5 Protein manipulation

3.5.1 Measurement of protein concentration - Bradford Assay

The Bradford assay was performed to estimate the protein concentration. Samples were added to a final volume of 800 µl dH_2O. 200 µl Bradford (BioRad) was added. After vortexing and 5 min incubation at room temperature 200 µl were transferred in

duplicate to a flat bottomed 96-well plate. Dilutions of bovine serum albumin (BSA) were used to generate a standard curve from which to finally calculate the protein concentration of the samples. The absorbance of all samples and BSA were read at 595 nm in a microplate reader (ELx800, BioTek) and the standard curve was used to determine the concentration of samples.

3.5.2 Preparation of cell lysate

Cells were harvested as described in 3.1.1 and washed once with PBS. The volume of lysis buffer was dependent on the size of the cell pellet. Generally ~ 50 µl cold lysis buffer was added per 10 mg wet cell pellet, pipetted gently and the samples were incubated at 4°C on rotating wheel for 30 min prior to centrifugation for 10 min at 12,000 xg at 4°C. The supernatant was transferred to a pre-chilled tube. Samples were either immediately used or frozen with liquid nitrogen and stored at -20°C (for few weeks) or -80°C (for longer storage).

Lysis buffer (same as for IP and isokinetic sucrose gradient experiments)

50 mM	Tris-HCl (pH 7.4)
150 mM	NaCl
1 mM	EDTA
10 mM	$MgCl_2$
1 % (v/v)	Triton X-100
1x	PI-Mix
1 mM	PMSF (added just before use)

Lysis buffer excluding $MgCl_2$ and PMSF was usually stored as 1 ml aliquots at -20°C.

3.5.3 SDS-PAGE

The SDS-PAGE is a method to separate denatured proteins on the basis of their size. The casting and running systems were used from Hoefer/Amersham. Depending on the size of the protein(s) of interest the resolving gels were prepared with 12 % to 15 % acrylamide. The resolving gel was poured first, followed by adding dH_2O on the top to prevent inhibition of polymerization by air and to generate a clear straight interface. After the resolving gel was polymerised the stacking gel was poured on top.

Table 3.5: Components of a SDS-polyacrylamide gel

	12 % resolving gel	15 % resolving gel	3.75 % stacking gel
29:1 30 % (w/v) acryl/ bis-acrylamide	2 ml	2.5 ml	0.625 ml
3.75 M Tris/ HCl pH 8.5	0.5 ml	0.5 ml	--
0.5 M Tris/HCl pH 6.8	--	--	1.25 ml
dH_2O	2.395 ml	1.895 ml	3.02 ml
10 % (w/v) SDS	50 µl	50 µl	50 µl
TEMED	5 µl	5 µl	5 µl
10 % (w/v) APS	50 µl	50 µl	50 µl
final volume	5 ml	5 ml	5 ml

Volumes are sufficient for 1x 0.5 mm thickness gel.

The samples for the SDS-PAGE were treated with dissociation buffer (final concentration 1 x) and incubated for 3 min at 95°C or 30 min at 37°C. After cooling the samples down to room temperature, they were centrifuged at room temperature for 3 min and loaded. The SDS-PAGE was performed in 1 x running buffer at 80 V through the stacking gel and at 120 V through the resolving gel. As a size marker 5 µl Spectra^{TM} Multicolour Broad Range Protein Ladder (Fermentas, SM1841) was loaded on the gel.

2 x dissociation buffer

125 mM	Tris-HCl (pH 6.8)
4 % (w/v)	SDS
20 % (v/v)	glycerol
0.02 % (w/v)	bromophenol blue
100 mM	DTT (always added just before use)

10 x Running (Towbin-) buffer pH 8.6

1.92 M	Glycine
250 mM	Tris
1 % (w/v)	SDS

3.5.4 Staining of Polyacrylamide gels

3.5.4.1 Coomassie Brilliant Blue Staining

Proteins can be stained with Coomassie Brilliant Blue (CBB), because of the electrostatic binding of CBB to proton amino groups. The acrylamide gel was stained for ~ 15 min, at room temperature in staining solution and incubated in the destaining solution for 2 x 10 min or until banding was clear.

Staining solution

45 % (v/v)	Methanol
10 % (v/v)	Acetic acid
0.2 % (w/v)	Coomassie blue R

Destaining solution

45 % (v/v)	Methanol
10 % (v/v)	Acetic acid

3.5.4.2 SimplyBlue™ SafeStain (Invitrogen LC6060)

For staining that is more sensitive than the conventional staining with CBB it is possible to use Coomassie G-250 without containing methanol and acetic acid, enabling analysis by mass spectrometry. The protocol was carried out as provided from the company. Briefly the gel was washed 3x 5 min with dH_2O, followed by a staining step for ~ 2h. Next, the gel was washed for 1 h in dH_2O and to increase intensity 3.3 % (w/v) NaCl (final concentration) was added.

3.5.4.3 Silver Staining

For proteins samples with low nanogram concentration the proteins can be visualised after separation on acrylamide gels by silver staining. Initially the gel is incubated in 50 % (v/v) methanol for at least 1 h, followed by the staining step for 15 min. Three washing steps for 5 min each in dH_2O were necessary before the gel was developed (for a few seconds, until the wished intensity was reached). The development of the gel was stopped by adding some fixer. Then, the solution was discarded and the gel was finally fixed. The quality of the SDS used in the gels is critical otherwise the silver staining will not be successful. The SDS delivered by Sigma-Aldrich gave always good results. All the solutions used for this procedure were made up fresh, just prior to using, in nanopure dH_2O. The staining solution must be always a clear and clean liquid. A brown staining during the solution preparation should be not considered for further usage.

Staining solution		Developer		Fixer	
0.8 % (w/v)	$AgNO_3$	0.055 % (v/v)	Formaldehyde	45% (v/v)	Methanol
1.4 % (v/v)	NH_4OH	0.05 % (w/v)	Citric acid	10 % (v/v)	Acetic acid
0.075 % (w/v)	NaOH				

3.5.5 Immunodetection of proteins

3.5.5.1 Western Blot

To detect proteins with specific antibodies it is necessary to transfer them after separation by SDS-PAGE on to a PVDF membrane. After electrophoresis the SDS gel was equilibrated in transfer buffer for approximately 10 min. The PVDF membrane (Millipore) was activated for ~20 secs in 100 % methanol and washed in transfer buffer before using it for the wet transfer The gel and membrane were assembled between Whatman paper and sponges in a cassette that was then transferred to the TE22 apparatus from Hoefer. The transfer was performed for 2 h to 3 h at constant 100 Volt, 4˚C, with agitation of the buffer.

Transfer buffer (pH 8.6)

25 mM	Tris
192 mM	Glycine
0.02 % (w/v)	SDS
15 % (v/v)	Methanol

3.5.5.2 Detection

The PVDF membrane was blocked for 1 h in 5% (w/v) milk/TBS-T at room temperature with rocking to minimise unspecific binding of the antibodies. The primary antibody was usually incubated overnight at 4°C, followed by 3 x washing in TBS-T for 10 min each at room temperature. The secondary antibody used was from Dako Cytomation and was coupled to HRP for use with the ECL+ kit from Amersham (GE Healthcare) for the detection step. After 1 h incubation of the secondary antibody at room temperature the washing steps were repeated and the detection was carried out by using the ECL+ kit following manufacturer's instructions. For visualisation X-ray film or Phosphor-Imager (Storm 860 scanner) was used, the latter allowed accurate relative quantification of signals using Image-Quant software.

Table 3.6: Details of antibodies used in these investigations

antibody	dilution	company
primary antibody		
anti NDUFB8/ 20 kDa SU complex I (mouse monoclonal)	1:1000	Mitosciences (MS105)
anti NDUFA9/ 39 kDa SU complex I (mouse monoclonal)	1:1000	Mitosciences (MS111)
anti SDH/ 70 kDa SU complex II (mouse monoclonal)	1:10000	Mitosciences (MS204)
anti COX1 (mouse monoclonal)	1:1000	Molecular Probes (A6403)
anti COX2 (mouse monoclonal)	1:1000	Molecular Probes (A6404)
anti Complex V-β (mouse monoclonal)	1:2000	Mitoscience (MS503)
anti porin (mouse monoclonal)	1:10000	Molecular probes (A31855)
anti MRPL3 (goat polyclonal)	1:2000	Abcam (ab39268)
anti MRPL12 (mouse monoclonal)	1:1000	Abcam (ab58334)
anti DAP3 (mouse monoclonal)	1:1000	Abcam (ab11928)
anti-MRPS6 (goat polyclonal)	1:500	Santa Cruz (sc-67918)
anti-MRPS25 (rabbit polyclonal)	1:500	ProteinTech Group (15277-1-AP)

anti MRPS18B (rabbit polyclonal)	1:4000	ProteinTech Group (16139-1-AP)
anti ICT1 (rabbit polyclonal)	1:800	ProteinTech Group (10403-1-AP)
anti ERAL1 (rabbit polyclonal)	1:1000	ProteinTech Group (11478-1-AP)
anti FLAG (mouse monoclonal)	1:2000	Sigma (F1804)
anti β-actin (mouse monoclonal)	1:10000	Sigma (A1978)
anti mtRF1 (rabbit polyclonal)	1:3000	Custom synthesised by Eurogentec (affinity purified)
anti mtRF1a (rabbit polyclonal)	1:1000	Custom synthesised by Eurogentec (affinity purified)
anti mtRRF (rabbit polyclonal)	1:3000	Custom synthesised by Eurogentec (affinity purified)
anti mtRbfA (rabbit polyclonal)	1:1000	Custom synthesised by Eurogentec (affinity purified)
secondary antibody		
anti rabbit immunoglobulins/ HRP (swine polyclonal)	1:3000	Dako Cytomation (P0399)
anti mouse immunoglobulins/ HRP (rabbit polyclonal)	1:2000	Dako Cytomation (P0260)
anti goat immunoglobulins/ HRP (rabbit polyclonal)	1:2000	Dako Cytomation (P0449)

All antibodies were made up in 5 % (w/v) milk/ TBS-T.

10 x TBS (pH 7.6)	TBS-T	
0.2 M Tris	1 x	TBS
1.37 M NaCl	0.1 % (v/v)	Tween-20

3.5.6 Blue Native Polyacrylamide Gel Electrophoresis

The Blue Native Polyacrylamide Gel Electrophoresis (BN-PAGE) is a method to visualise whole native protein complexes like the OXPHOS complexes. It was performed as described by Nijtmans *et al*. (2002).

As it is an analysis of native complexes everything has to be chilled and any contact with SDS or ethanol has to be avoided.

3.5.6.1 Sample preparation

Cells from 2x 75 cm^2 flasks with a confluence of ~ 60-70% were harvested in 1 mM EDTA/ PBS and washed twice with 1 ml cold PBS. The pellet was resuspended in 50 µl cold PBS and cells were permeabilised by adding an equal volume of 8 mg/ ml

digitonin (final concentration 4 mg/ ml; Sigma D141). After vortexing and 10 min incubation on ice the digitonin was diluted by adding 1 ml cold PBS, followed by centrifugation at 10,000 xg for 5 min at 4°C and one washing step. Next, the pellet was resuspended in 50 µl 1.5 M AminoCaproic acid, 75 mM Bis-Tris, pH 7.0 and mitochondria were solubilised by adding 10 µl of 10 % (w/v) n-Dodecyl β-D-maltoside (Sigma, D5172), vortexing and incubating on ice for 5 min prior to centrifugation for 30 min at 10,000 xg at 4°C. The supernatant was transferred to a fresh chilled tube and protein concentration was measured by Bradford. 50 - 75 µg protein containing 1x BN sample buffer were loaded as quickly as possible on the BN gel. As a size marker Apoferretin (Sigma, A3660) was used, which migrates at 440 kDa as a monomer and at 880 kDa as a dimer.

2x Sample buffer (pH 7.0)

750 mM	AminoCaproic Acid
50 mM	Tricine
0.5 mM	EDTA
0.02 % (w/v)	Serva Blue G-250

3.5.6.2 BN PAG preparation

To prepare a 5% to 15% gradient gel a gradient mixer was used. The volumes (Table 3.7) are adjusted for one 1.5 mm thick gel, small format (Hoefer casting system).

Table 3.7: Composition of native gradient PAG

	5 % resolving gel	15 % resolving gel	4 % stacking gel
29:1 40 % (w/v) acryl/ bis-acrylamide	0.63 ml	1.88 ml	0.50 ml
Gel Buffer I	1.67 ml	1.67 ml	1.67 ml
Glycerol	--	0.79 ml	--
dH_2O	2.71 ml	0.67 ml	2.83 ml
TEMED	3.0 µl	1.5 µl	5.5 µl
10 % (w/v) APS	30 µl	15 µl	55 µl

When preparing a gradient gel it is very important to avoid any air bubbles, especially in the connection between the chambers of the gradient mixer. To prepare the 5% to 15% gradient gel the chambers of the gradient mixer were filled with 3.5 ml of each resolving gel mix. After pouring the gradient gel a thin layer of dH_2O was added on the

top of the gel as already mentioned above. When the resolving gel was solid, the water was discarded and the stacking gel was poured.

Gel-buffer I (pH 7.4)
1.5 M AminoCaproic Acid
150 mM Bis-Tris

3.5.6.3 Electrophoresis

The samples were electrophoresed at 50 V through the stacking gel and at 80 V through the resolving gel at 4°C. The Cathode buffer A was replaced by cathode buffer B as soon as the blue front was approximately 2/3 through the resolving gel. After the electrophoresis was finished the gel was either used for western blot or for enzyme *in-gel* activity assay.

Cathode buffer A (pH 7.0)		Cathode buffer B (pH 7.0)	Anode buffer (pH 7.0)
15 mM	Bis-Tris	15 mM Bis-Tris	50 mM Bis-Tris
50 mM	Tricine	50 mM Tricine	
0.02 % (w/v)	Serva Blue G-250		

3.5.6.4 Western Blot of BN-PAG

The gel was incubated in 1% (w/v) SDS/ 1% (v/v) β-mercaptoethanol for 30 min and in 1x transfer buffer for 15 min prior to transfer for 1 h at 100 V at 4°C.

3.5.6.5 Enzyme in-gel activity assay

The BN-PAG was incubated at room temperature over-night with the following substrates:

Complex I:	2 mM	Tris/HCl pH 7.4
	0.1 mg/ ml	NADH
	2.5 mg/ ml	NitroTetrazolium Blue (NTB)
Complex IV:	0.5 mg/ ml	3,3'-Diaminobenzidine Tetrahydrochloride (DAB)
	50 mM	phosphate buffer pH 7.4
	20 µg/ ml	Catalase
	1 mg/ ml	reduced cytochrome *c*
	75 mg/ ml	sucrose

3.5.7 ^{35}S metabolic labelling of mitochondrially encoded proteins

This method was used to investigate changes in translation of mitochondrially encoded proteins after siRNA treatment or overexpression of a protein of interest. The procedure was adapted from Chomyn, 1996. The method was carried out in 6-well plates or 25 cm^2 flasks.

For ^{35}S methionine/cysteine metabolic labelling it is necessary to first remove methionine by replacing the growth media with methionine/cysteine free DMEM (Sigma D0422) supplemented with L-glutamine, 50 µg/ ml uridine and 1 x non essential amino acids. The cells were incubated twice for 10 min in this methionine/cysteine free media before adding fresh methionine/cysteine free media additionally supplemented with 10 % (v/v) dialysed FBS and 100 µg/ ml emetine dihydrochloride, which was added to inhibit the cytosolic translation. After 10 min incubation 20 µl/ ml ^{35}S - methionine/ cysteine mix (~ 200 µCi/ ml; EasyTag^{TM} express^{35}S protein labelling mix - NEG772002MC from PerkinElmer) were added to the media. The labelling step was performed for 10 min to 30 min. To quench the reaction the labelling media was aspirated off and the cells were washed twice with chilled growth media containing 7.5 µg/ ml unlabelled methionine. The cells were then harvested in cold 1 mM EDTA/PBS and washed 3x in chilled PBS. Finally the cell pellet was resuspended in 30 - 50 µl PBS containing 1x PI-Mix and 1 mM PMSF.

The samples (up to 50 µg) were treated with 2 x dissociation buffer (20 % (v/v) glycerol, 4 % (w/v) SDS, 250 mM Tris-HCl pH 6.8, 100 mM DTT) and 12 U Benzonase® nuclease (Novagen). After incubation for 1 h at room temperature the denatured protein samples were separated on a 15 % SDS-PAGE. The gel was fixed overnight in 3 % (v/v) glycerol, 10 % (v/v) acetic acid, 30 % (v/v) methanol and finally dried under vacuum at 60°C for 4 h. The Phosphor-Imager system was utilised to visualise radiolabelled proteins and Image-Quant software (Molecular Dynamics, GE Healthcare) was used for analysis.

3.5.8 Isolation of mitochondria from human cell lines

Mitochondria were usually isolated from cells grown in a 300 cm^2 flask at 80 % confluence. The cells were harvested as described in 3.1.1. The cell pellet was resuspended in 2 ml ice cold homogenisation buffer containing 0.1 % (w/v) BSA and 1 mM PMSF. All subsequent steps were carried out in the cold room. The suspension was transferred into a 2 ml Glas-Col Homogeniser where it was subjected 15 passes by hand. The homogenate was then centrifuged at 400 xg for 10 min at 4°C to remove unbroken cells. The supernatant was transferred into pre-chilled tubes and the pellet

was resuspended in a further 2 ml buffer. The homogenisation and centrifugation step were repeated. The second homogenate was centrifuged at 400 xg for 10 min. Then all combined supernatants were re centrifuged at 400 xg for 5 min before the harder centrifugation step at 11,000 xg for 10 min was performed. This final mitochondrial pellet was washed in homogenisation buffer lacking BSA and also lacking PMSF if proteinase K treatment was to be performed. Depending on the size of the mitochondria pellet it was resuspended in a volume of 70 to 150 µl wash buffer.

Homogenisation buffer
0.6 M Mannitol
10 mM Tris (pH 7.4)
1 mM EGTA

Mitochondrial purification

To remove cytosolic contamination 4-5 mg mitochondria were treated with 2U RNase-free DNaseI (Epicentre Biotechnologies) in 1 ml homogenisation buffer (containing 10 mM $MgCl_2$ and 1 mM $CaCl_2$) for 15 min at room temperature prior to adding 5 µg proteinase K per 1 mg mitochondria on ice. After 30 min 1 mM PMSF (final concentration) was added to inhibit further reaction of proteinase K, followed by two washing steps with homogenisation buffer containing 1 mM PMSF. Next, mitochondria were permeabilised in 0.2 % (w/v) digitonin in homogenisation buffer for 15 min on ice, followed by 2 washing steps with homogenisation buffer and a further proteinase K treatment.

3.5.9 Immunoprecipitation

To investigate protein-protein interactions or protein-nucleic acid interactions an immunoprecipitation step was performed. Proteins of interest were inducibly expressed in HEK293T cells as C-terminal tagged with the FLAG-octapeptide. This permitted immunoprecipitation of the proteins via the FLAG tag using the Immunoprecipitation kit from Sigma (product code FLAGIPT-1). The FLAG octapeptide is very hydrophilic hence it is most probably the case that the tag is on the surface of the protein, available for the affinity purification.

The first step is the lysis of whole cells or mitochondria from a cell line expressing a FLAG tagged protein by adding 500 µl lysis buffer (supplemented with 10 mM $MgCl_2$, PI-Mix, 1 mM PMSF and 60 U RNAguard) to a cell or mitochondrial pellet. This suspension was transferred to a rotating wheel, medium speed at 4°C for 30 min followed by a centrifugation step for 10 min at 12,000 xg at 4°C. The supernatant was transferred to a pre-chilled tube. For the binding step 40 µl M2 affinity resin suspension

(containing 50 % beads) per reaction, was added to a hydrophobic tube. The beads (finally 20 µl) were washed 3 x with 1 ml 1 x washing buffer (supplemented with 10 mM $MgCl_2$, PI-Mix, 1 mM PMSF and 10 U RNAguard) before a defined protein amount of lysate was applied. The binding step was performed on a rotating wheel medium speed at 4°C for 3 h. After the binding step the beads were centrifuged for 30 secs at 5,000 xg at 4°C. The supernatant was discarded and the beads were washed at least 3 x with 1 ml 1 x washing buffer (supplemented as described above) to remove non specific binding and contamination. To elute the target protein with its interacting partners 5 µg 3 x FLAG peptide in 100 µl 1 x washing buffer was added to the beads, followed by an incubation step of 45 min, rocking gently at 4°C. After the beads were centrifuged briefly at 5,000 xg for 30 secs the elution fraction was transferred to a new pre-chilled tube. To analyse the efficiency of the elution the beads were washed again 3 times with 1 x washing buffer and finally 20 µl to 40 µl 2 x dissociation buffer (section 3.5.3) was added. The supernatant was separated on a SDS-PAGE followed by Western Blot analysis.

Lysis buffer
(Sigma product Code L 3412)

50 mM	Tris-HCl (pH 7.4)
150 mM	NaCl
1 mM	EDTA
1 % (v/v)	Triton X-100

10 x Washing buffer
(Sigma product Code W 0390)

0.5 M	Tris-HCl (pH 7.4)
1.5 M	NaCl

3 x FLAG peptide
(Sigma product Code F 4799)

ANTI-FLAG M2-Agarose Affinity Gel
(Sigma product Code A 2220)

3.5.10 Crosslinking Immunoprecipitation - CLIP

CLIP is a powerful tool to determine RNA species the potential RNA binding protein (RBP) is attached to. UV-irradiation on intact cells allows covalent binding of RNA and protein that are in close localization to each other. After covalently binding of the RNA to the protein, this particular RNA sequence is protected by the protein and thus after RNase treatment there is only this particular fragment left. With 5'-^{32}P γATP end-labelling it is possible to visualise the RNA within the protein-RNA complex on a membrane by exposing western blot membrane to X-ray film. The protein-RNA complex of interest migrates approximately 20 kDa above the molecular weight of the protein. This region of membrane is excised trying to keep the region to a minimum. Next, proteinase K is applied to the piece of membrane to remove the protein from the RNA. The independent ligation of specific RNA linkers to either the 5'- or 3'-end allows the reverse transcription and finally the amplification and cloning of the particular protected RNA species. The procedure was adapted as described in Ule *et al.* (2005).

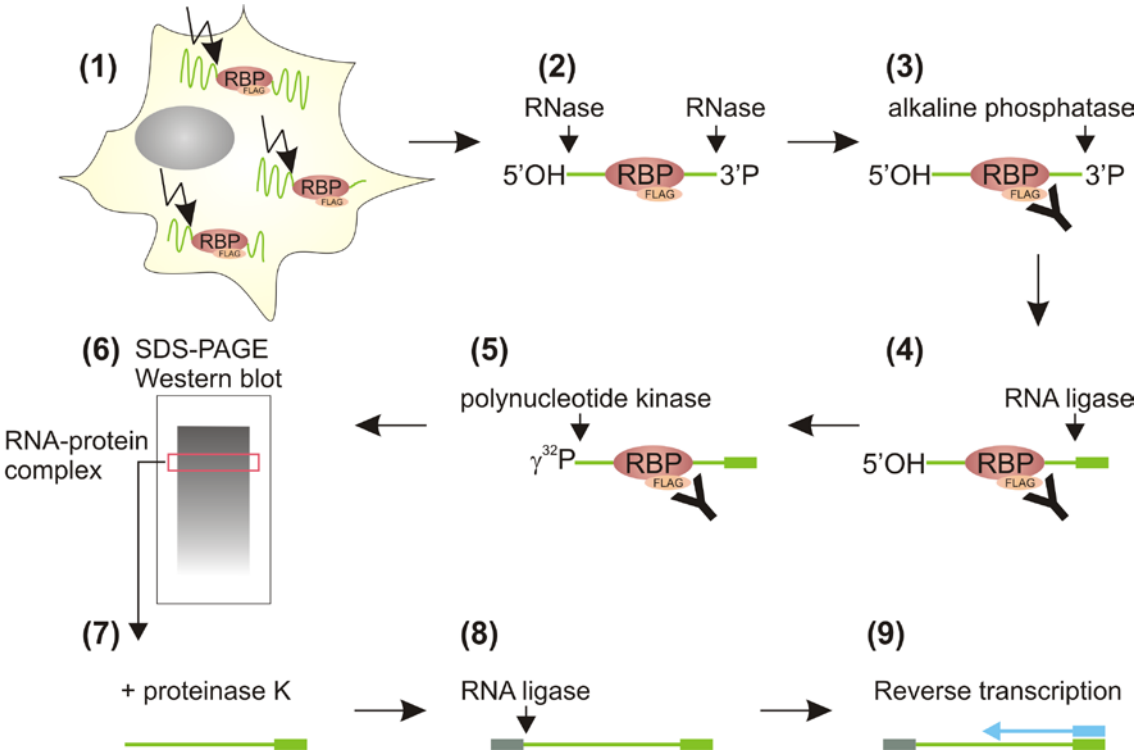

Figure 3.3: Crosslinking immunoprecipitation. Cells were UV irradiated prior to lysis (1). Cell lysate was treated with RNase (2), where the crosslinked RNA sequence is protected by the interacting RNA binding protein (RBP). The 3'-end of the RNA has to be dephosphorylated (3) before RNA linker ligation can occur (4). With the addition of $\gamma^{32}P$ by the polynucleotide kinase (5) it is possible to visualise the protein-RNA complex via western blot analysis (6). Defined bands are cut out of the membrane and proteinase K digested to remove the protein from the RNA (7). Then another RNA linker can be ligated on the 5'-end (8) and cDNA can be synthesised via reverse transcription (9). This cDNA can then be amplified by PCR and cloned for sequencing analysis. (Image was adapted from Ule *et al.,* 2005).

The CLIP assay was adapted on the FLAG-IP kit as described in 3.5.9. Cells expressing FLAG tagged protein of interest were cultured in 150 mm petri dishes until a confluence of ~ 60-70% was reached. Then cells were washed with PBS, covered with little amounts of PBS and UV cross linked on ice. For UV irradiation the Stratalinker 2400 with energy mode 4000 was used, which will deliver 400 mJ/ cm^2. After the cross linking cells were harvested in chilled PBS/ 1 mM EDTA. The pellet was lysed in 1 ml lysis buffer containing 1x PI-mix and 200 U of RNAguard (Amersham) for 30 min at rotating wheel at 4°C. Next sample was treated with 50 U RNase-free DNase I (Epicentre Biotechnologies) at 37°C 1,000 rpm for 5 min (using Eppendorf thermomixer) to remove all the DNA. Then the sample was divided into two tubes to apply different amount of RNase T1 (Ambion): 2 U and 100 U respectively. After 10 min at 37°C at 1,000 rpm 30 U SUPERase-In (Ambion) were added to each tube to inhibit further RNase T1 activity. Samples were then centrifuged for 20 min at 21,000 xg at 4°C and the supernatant was transferred to 20 µl M2-FLAG beads, which were equilibrated with five washing steps in 1x washing buffer provided from the FLAG-IP kit.

The samples were left rotating for 90 min at 4°C, followed by three washing steps with 1x washing buffer and two with PNK buffer. Next the RNA was dephosphorylated using 3 U alkaline phosphatase (Roche, 713023) in 80 µl volume containing 1x dephosphorylation buffer. The reaction was incubated in the thermomixer at 37°C for 10 min, 1,000 rpm every 3 min for 15 sec, followed by two washing steps with PNK+EDTA buffer and two with PNK buffer. Then the 3'-RNA linker ligation reaction was incubated over-night at 16°C at 1,000 rpm every 5 min for 15 secs containing 2 µM 3'-RNA linker, 20 U T4 RNA ligase (NEB M0204S) and 1x T4 RNA ligation buffer (NEB, contains ATP) in a final volume of 80 µl. The next day the beads were washed three times with PNK buffer prior to T4 polynucleotide kinase (PNK) treatment on the beads. The PNK catalyses the transfer of the ^{32}P from the γ position of ATP to the 5'-OH of the RNA: the reaction was incubated at 37˚C for 10 min (1,000 rpm every 4 min for 15 sec) containing 1 µl ^{32}P-γATP (~ 10 µCi; PerkinElmer NEG002A), 40 U T4 PNK enzyme (NEB) and 1 x T4 PNK buffer in a total volume of 80 µl. Then 1 µM and 100 µM rATP were added, followed by incubation at 37°C for 5 min each time (1,000 rpm, every 2 min for 15 sec). Next, the beads were washed with 200 µl PNK buffer, followed by two washing steps with 1 ml PNK buffer and one final washing step with 1 ml 1x washing buffer. The protein-RNA complex was eluted in 50 µl 1 x washing buffer containing 0.5 µg/ µl 3x FLAG peptide for 45 min at 1,000 rpm at room temperature. The eluted samples containing 1x sample buffer (NuPAGE LDS) and heated for 10 min at 70°C were run on a 10% Novex pre-casted gel, following manufacturer's protocol (Invitrogen, NuPAGE®Novex® Bis-Tris mini gels). The gel was electrophoresed in MES buffer at 200 V, followed by the transfer on BA-85 nitrocellulose membrane at 30 V for 1 h using the Novex wet transfer apparatus (XCell II Blot Module EI9051). The membrane was washed in PBS after transfer and wrapped in Saran wrap, followed by exposure to X-ray film over-night at -80°C. Matching the autoradiogram with the membrane allows the position of the protein-RNA complex of interest on the membrane to be identified and excised. Between the lower and higher RNase T1 digested samples there should be a shift in size of the immunoprecipitated protein which shows the protein within and without RNA-complex. The membrane was then digested in 200 µl 4 mg/ ml proteinase K solution for 20 min at 37°C at 1,000 rpm. Next 200 µl of ProtK buffer were added with 1 mM PMSF (final concentration) to inhibit further proteinase K activity, incubated for another 5 min at 37°C at 1,000 rpm. The RNA was extracted by the addition of 400 µl phenol (pH 6.7) and 130 µl chloroform/IAA (24:1), incubated for 20 min at 37°C at 1,000 rpm. After centrifugation at top speed for 3 min the aqueous phase was transferred into a new 1.5 ml tube and the RNA was precipitated over-night at -20°C by the addition of 0.3 M NaOAc pH 5.2 (final concentration), 1 µl GlycoBlue (Invitrogen)

and 2.5 vol. isopropanol/ethanol (1:1). Next day the RNA was pelleted at 21,000 xg for 15 min at 4°C and washed twice with 75 % (v/v) ethanol. The RNA was resuspended in 8 µl DEPC treated dH_2O and used for the 5'-linker ligation reaction. 7 µl RNA were incubated for 3 h at 37°C in the presence of 2 µM 5'-RNA linker, 4 U T4 RNA ligase and 1x T4 RNA ligation buffer in a total volume of 10 µl. The RNA was then again extracted and precipitated as previously described. This resulting RNA pellet was resuspended in 10 µl DEPC dH_2O, which was then used for reverse transcription. The 10 µl RNA solution was incubated with 10 pmoles P3 primer for 5 min at 65°C, followed by cooling down the tube on ice for 5 min prior to adding the master mix containing 1 µl 10 mM dNTPs, 4 µl 5x 1st strand buffer, 2 µl 0.1 M DTT and 1 µl RNAguard. After an incubation for 5 min at 42°C the Superscript II enzyme was applied to the reaction, followed by the incubation for 1 h at 42°C and 15 min at 70°C. The reaction was then used for amplification via PCR with the following composition in a total volume of 30 µl:

1x	buffer IV (ABgene)
0.4 mM	dNTP mix
2 mM	$MgSO_4$
0.4 µM	P5 primer
0.4 µM	P3 primer
3 U	*Taq* (ABgene)
3 µl	reverse transcription reaction as the template

programme:

denaturation:	95°C	5 min	
denaturation:	95°C	20 sec	
annealing:	67°C	30 sec	35 cycles
extension:	72°C	30 sec	
extension:	72°C	5 min	

The PCR product (containing 5% (v/v) glycerol instead of DNA loading buffer) was visualised on a 4% (w/v) low melting agarose gel against a 50 bp ladder (NEB). A product of ~ 80 bp was cut out and the DNA was extracted as described in 3.3.4. Finally the DNA was either directly used for cloning or it was re-amplified in a total volume of 50 µl with the following conditions:

programme:

denaturation:	95°C	5 min	
denaturation:	95°C	20 sec	
annealing:	63°C	30 sec	20 cycles
extension:	72°C	30 sec	
extension:	72°C	5 min	

For the cloning of the DNA the TOPO TA cloning kit for sequencing (Invitrogen) was used following the manufacture's instructions. Briefly 2 µl PCR product were incubated for 5-10 min in the presence of 0.2M NaCl, 10 mM $MgCl_2$ and 5 ng pCR4-TOPO vector in a total volume of 3 µl. The reaction was then transferred on ice and 1 µl was added to 25 µl TOP10 one shot chemically competent *E. coli* cells, followed by an incubation for 10 on ice and a heat shock step for 30 secs at 42°C. After cooling the reaction on ice for 2 min 125 µl SOC media was added and bacteria were incubated for 1 h at 37°C at 300 rpm prior to transfer on LB plates containing 100 µg/ ml ampicillin. Clones were screened by colony PCR using M13 primer: bacteria clones were lysed in 50 µl 10% (v/v) Triton X-100 via freeze-thawing cycle. 1.25 µl were used as a template for the PCR with the following conditions:

1x	buffer (Fermentas, containing 2 mM $MgCl_2$)
0.5 µM	dNTPs
1 µM	M13 forward
1 µM	M13 reverse
0.6 U	Dream *Taq* (Fermentas)

programme:

denaturation:	95°C	3 min	
denaturation:	95°C	45 sec	
annealing:	48°C	1 min	30 cycles
extension:	72°C	30 sec	
extension:	72°C	7 min	

The PCR products were visualised on a 2% (w/v) agarose gel against 50 bp ladder. Positive clones with an insert gave a PCR product of approximately 250 to 300 bp, of which 2.5 µl were treated with 1 µl ExoSap for 15 min at 37°C and 15 min at 80°C prior to cycle sequencing as described in 3.3.9 using M13 forward primer and 2 µl PCR product.

PNK buffer		PNK + EDTA buffer		ProtK buffer	
50 mM	Tris/HCl pH 7.4	50 mM	Tris/HCl pH 7.4	100 mM	Tris/HCl pH 7.4
10 mM	$MgCl_2$	20 mM	EDTA	50 mM	NaCl
0.5% (v/v)	NP-40	0.5% (v/v)	NP-40	10 mM	EDTA

RNA linkers (Thermo):
L5: 5′–OH AGG GAG GAC GAU GCG G 3′-OH
L3: 5′–P GUG UCA GUC ACU UCC AGC GG 3′-puromycin

DNA primers (Eurogentec):
P5: 5′-AGG GAG GAC GAT GCG G-3′
P3: 5′-CCG CTG GAA GTG ACT GAC AC-3′

3.5.11 Isokinetic sucrose gradient

The sucrose gradient was used for analysing ribosome conformation. First, 10% (w/v) and 30% (w/v) sucrose were prepared in buffer containing 50 mM Tris/HCl (pH 7.2), 40 mM NH_4Cl, 10 mM MgOAc, 0.1 M KCl, 1 mM PMSF and 50 µg/ ml chloramphenicol. 0.5 ml of 10% (w/v) sucrose was transferred to a polycarbonate centrifuge tube (Beckman 343778). With a 1 ml syringe and a needle 0.5 ml of 30% (w/v) sucrose was carefully added under the 10% (w/v) sucrose. Using the Gradient Master from Biocomp a linear gradient was prepared (Gradient Master ver 3.06L; TL55, 10-30% S1/1 0:55/85.0/22). The gradients were always left to stabilise for 1h at 4°C before use.
The samples for the gradient were either cell lysate or eluates from immunoprecipitated mitoribosomes. The cells were lysed as described in 3.5.2. The volume of lysis buffer added to the cells depended on the size of the pellet. Finally 700 µg of cell lysate or the IP-eluate (in 50 - 80 µl) was transferred to the top of the gradient.
After centrifuging the gradient at 39,000 rpm (~ 100,000 xg; Beckman Optima^{TM}TLX Ultracentrifuge, Rotor TLS 55, Accel 1, Decel 4) for 135 min at 4°C, fractions of 100 µl from top to bottom were collected. 10 µl of each fraction were separated by SDS-PAGE (followed by Western Blot or Silver Staining after IP-gradient) or RNA was extracted from each fraction using Trizol-LS (Invitrogen).

3.5.12 GST protein purification

For purification of recombinant GST tagged protein a large culture of 0.5 L was inoculated with a 10 ml small culture. The bacteria culture was grown at 37°C at 200 rpm until an OD_{600} ~ 0.4 to 0.6 was achieved. The culture was cooled down to 16°C and induced with 1 mM IPTG. The bacteria were incubated over-night at 16°C to allow controlled overexpression of recombinant protein. The following day the cells were harvested at 5,000 rpm for 15 min at 4°C. The pellet was frozen and thawed to achieve a more efficient break up of the bacteria during lysis. To lyse the cells, the pellet was

resuspended in PBS containing 1 mM PMSF, 1x PI-Mix and 50 U Benzonase and the suspension was sonicated 10 x 10 secs under chilled conditions, amplitude 18 microns (Soniprep 150). To remove insoluble particles the suspension was centrifuged at 30,000 xg for 30 min at 4°C. The supernatant was filtered through a 0.45 µm filter and finally transferred to a BioRad column containing 0.6 ml gluthathione-Sepharose beads (GE Healthcare), pre-washed with dH_2O and then PBS. The column was incubated over-night at 4°C on a rocker. The next day the beads were washed 5x with PBS containing 1 mM PMSF and PI-Mix and 5x with PBS without any Protease-Inhibitor. To elute the target protein 48 U PreScission protease was added in 0.75 ml PBS containing 1 mM DTT and 1 mM EDTA. The eluate was collected next day in a chilled 1.5 ml tube.

3.5.13 Antibody purification

To raise polyclonal antibodies against the purified recombinant protein of interest, protein was sent to Eurogentec, Belgium. Two rabbits were injected 4 times over 3 month with 100 µg protein each time. To purify the final bleed recombinant protein need to be covalently bound to NHS-activated Sepharose 4 Fast Flow.

0.6 ml of NHS-activated Sepharose beads were washed with 1 mM HCl. 1-2 mg recombinant protein (in PBS) was added to those beads over-night at 4°C. The next day the beads were blocked with 0.1 M Tris/HCl (pH 7.4), before adding the serum. 7 ml of the final bleed was filtered through a 0.45 µm and then a 0.2 µm filter. After increasing the volume up to 10 ml with PBS the serum was added to the column and left over-night rocking at 4°C. The next day the beads were washed twice with PBS, once with Tris-buffer pH 8.0 [50 mM Tris/HCl pH 8.0; 0.1% (v/v) Triton X-100; 0.5 M NaCl], followed by Tris-buffer pH 9.0 [50 mM Tris/HCl pH 9.0; 0.1% (v/v) Triton X-100; 0.5 M NaCl] and finally sodium-phosphate-buffer pH 6.3 [50 mM sodium-phosphate pH 6.3; 0.1% (v/v) Triton X-100; 0.5 M NaCl]. The antibodies were eluted with 5 ml glycine-buffer pH 2.5 [50 mM glycine pH 2.5; 0.1% (v/v) Triton X-100; 0.15 M NaCl] and immediately neutralised with 1 ml 1M Tris/HCl pH 9.0. The elution was then concentrated and buffer exchanged (to PBS) by using Amicon® Ultra-15 centrifugal filter devices (Millipore). Antibodies were stored at -20°C containing 10 % (v/v) Glycerol and 0.02 % (w/v) sodium azide.

3.5.14 *In vitro* translation termination assay

To determine whether a potential class I release factor has any peptidyl-tRNA hydrolysis activity the recombinant protein was purified from bacteria and tested in the

in vitro translation termination assay. In this experiment isolated 70S *E. coli* ribosomes were used. These were incubated with an AUG RNA triplet and an aminoacylated-tRNA^{Met} carrying ^{3}H- radiolabelled formyl-methionine to allow positioning of this substrate into the peptidyl-tRNA site (P-site). This acted as a mimic for a peptidyl-tRNA substrate for the release factor (RF). The aminoacyl-tRNA site (A-site) was then filled with the RNA triplet to be tested for recognition by the release factor.

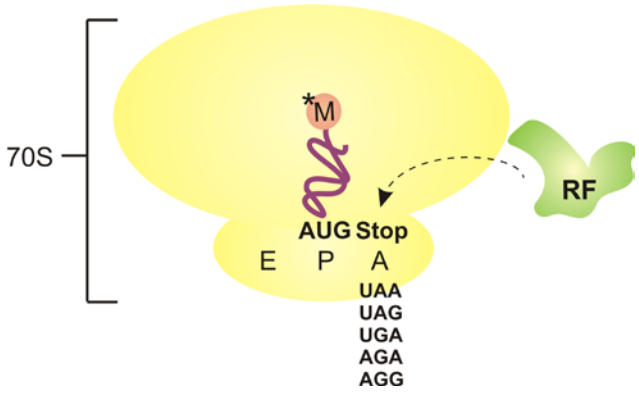

Figure 3.4: *In vitro* translation termination assay (schematic). 70S *E. coli* ribosomes are used to measure relative release activity by the applied release factor (RF). The peptidyl-tRNA (P) site carries a start codon and an aminoacylated tRNA^{Met} with ^{3}H- radiolabelled formyl-methionine (*M). The aminoacyl-tRNA (A) site is filled with a stop codon in the decoding centre. The recombinant class I RF was independently added with each RNA codon to be tested to the 70S preparation. This allowed the RF to be tested for recognition against a battery of RNA triplets.

If a class I release factor recognise the specific stop codon sequence in the decoding centre, it will catalyse the hydrolysis of the ester bond between the formyl-methionine and the tRNA, releasing the radiolabelled amino acid and the free radioactivity is measured. The *in vitro* translation termination assays were carried out by Dr. Z. M. A. Chrzanowska-Lightowlers as described in Soleimanpour-Lichaei *et al.* (2007).

3.6 Statistical evaluation

Means were usually presented with standard deviations. To examine observed differences on their significance t-test was performed using the following webpage:

http://www.graphpad.com/quickcalcs/ttest1.cfm.

Differences with $p > 0.05$ were considered as to be not statistically significant, with $p = 0.01$ to 0.05 as significant (*), $p = 0.001$ to 0.01 as very significant (**) and $p < 0.001$ as extremely significant (***).

Chapter 4:

ICT1 is an essential mitochondrial protein

4 Chapter 4: ICT1 is an essential mitochondrial protein

4.1 Introduction

As described earlier, ICT1 is one of four members of the mitochondrial release factor family. So far mtRF1a is the only mitochondrial release factor with ribosome-dependent peptidyl-tRNA hydrolysis activity with sequence specific recognition of UAA or UAG as stop codons [Soleimanpour-Lichaei *et al.*, 2007]. Recent recognition of the ability for human mitochondrial ribosome to use a -1 frameshift shows that mtRF1a is able to terminate all 13 open reading frames by recognition of UAA/UAG codons [Temperley *et al.*, 2010a]. C12orf65 was shown to have no release activity in the *in vitro* translation termination assay. It seems, however, to be crucial for mitochondrial protein synthesis as mutations of C12orf65 in two patients caused reduced level of mitochondrial translation, as monitored by ^{35}S-met *de novo* synthesis and aberrant OXPHOS complex formation shown by Blue Native PAGE [Antonicka *et al.*, 2010]. The function of C12orf65 within the mitochondria is still unknown. The fourth member of the family, mtRF1 was shown to be mitochondrial, but this candidate also did not have any release activity *in vitro* [Soleimanpour-Lichaei *et al.*, 2007]. So far it has not been reported as a protein that is involved in the mitochondrial gene expression machinery. Further characterisation of mtRF1 and C12orf65 is part of the PhD project of A. Pajak in this laboratory.

ICT1 was first described in 1995, called DS-1. Van Belzen *et al.* reported that ICT1 transcripts were down regulated during differentiation of HT29-D4 and Caco-2 colon carcinoma cells. Furthermore they showed also western blots where ICT1 could be detected at two sizes, one band at predicted size of 25 kDa and the second, more prominent one of ~ 20 kDa. The authors explained the two species may result from possible post-translational processing. With hindsight this may reflect that it has a cleavable site removing the targeting peptide.

In my host laboratory ICT1 was found in the immunoprecipitation of mtRRF-FLAG, where mitoribosomal proteins together with other translation factors and nucleoid components could be detected [Rorbach *et al.*, 2008]. The fact that ICT1 was associated with this complex pulled down via mtRRF-FLAG suggests that ICT1 is probably a mitochondrial protein, and possibly involved in the mitochondrial gene expression machinery. Combined with the fact that it is described as belonging to the

mitochondrial release factor family and because mitochondrial translation termination processes are one of the main focuses within this laboratory, means that this protein is of great interest to me. There are a few initial facts that need to be considered when investigating the possible function of ICT1: First, mtRF1a is the main release factor terminating all 13 open reading frames. Therefore there is no need for another release factor to act in the same way. Second, mtRF1a was not found in the immunoprecipitation of mtRRF-FLAG, which is not a surprise, because mtRF1a and mtRRF accommodate the same site (A-site) within the mitochondrial ribosome. Thus if mtRRF is associated with the mitochondrial ribosome there is no space for mtRF1a. The fact that ICT1 was co-immunoprecipitated with mtRRF-FLAG suggests maybe a different location and therefore function of ICT1 in comparison to mtRF1a. Third, ICT1 is a quite small protein, lacking the crucial domains for codon recognition (tip of the α5 helix and the PXT/SPF motif) within the decoding centre. Thus it seems unlikely that ICT1 can act as a conventional class I release factor like mtRF1a does.

It is therefore from great interest to identify the function of this protein. Initial investigations described in this chapter were directed at identifying i) the cellular location of ICT1 and ii) whether it is an essential protein.

4.2 Localisation of ICT1

The first aim of this investigation was to determine whether ICT1 is a mitochondrial protein. From bioinformatic studies it belongs to the prokaryotic/ mitochondrial release factor family. Different programmes like PSORT II or TargetP 1.1 can be used to predict the localisation of the protein of interest. PSORTII predicted ICT1 to be a mitochondrial protein with a probability of 73.9% with a cleavage site for the mitochondrial pre-sequence at residue 29 (RRA | LH) (subprogramme “Gavel”). TargetP 1.1 gave also the prediction that ICT1 is localised to mitochondria. This programme has 5 reliability classes (RC), where RC 1 shows the strongest prediction. ICT1 was predicted to have a mitochondrial targeting peptide with RC 1 and again it specified a cleavage site at residue 29.

To confirm the localisation of ICT1 within the mitochondria cell lysates and mitochondria were isolated from HeLa- and HEK293T cell lines and were analysed via western blot. To ensure that mitochondria were free from cytosolic contamination, these were also treated with DNase I and proteinase K, where mitochondrial proteins should be remained preserved by the intact mitochondrial membrane. The resulting data is shown in figure 4.1. Antibodies against ICT1 (ProteinTech Group 10403-1-AP)

that had been tested previously for specificity, showed a single band of ~ 20 kDa in cell lysate (lane 1 and 5), isolated mitochondria (lane 2 and 6) and was also protected against proteinase K treatment (lane 3 and 7), indicating ICT1 localisation within the mitochondria. As a control for proteinase K activity and also sensitivity of ICT1 to digestion, 1% Triton X-100 was added to mitochondria, which were treated with same amount of enzyme. After mitochondrial lysis proteinase K was able to digest ICT1 protein (lane 4 and 8), demonstrating that ICT1 is sensitive to proteinase K and thus the data in lanes 3 and 7 really reflected that ICT1 was on the inside of mitochondria.

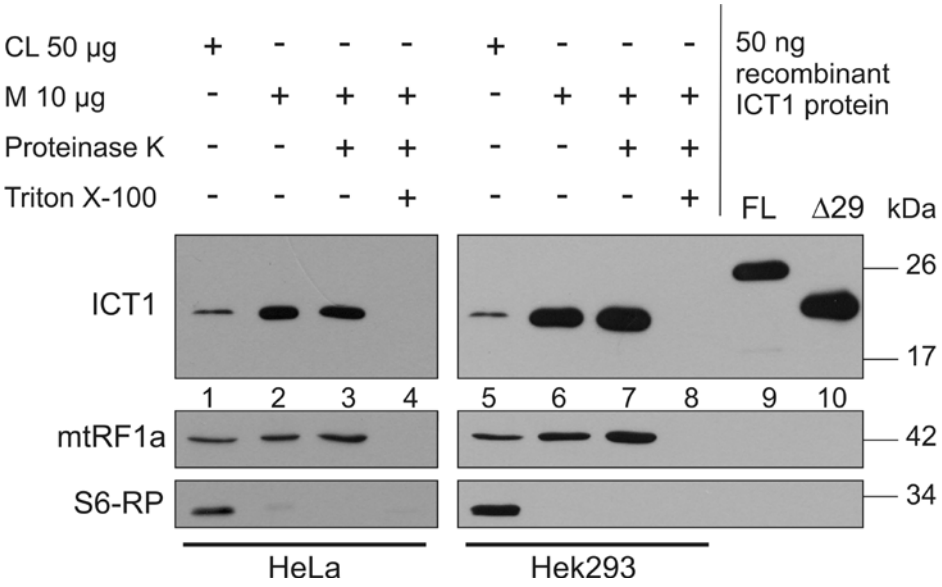

Figure 4.1: Cellular localisation of ICT1. Western Blot analysis was performed on cell lysate (50 µg, lanes 1 and 5) and isolated mitochondria (10 µg, lanes 2-4 and 6-8) from HeLa and HEK293T cell lines. Mitochondria were treated with proteinase K (4 µg per 100 µg mitochondria) and without (lanes 3 and 7) or with (lanes 4 and 8) 1% Triton X-100, to confirm the proteinase K activity and sensitivity of the 3 proteins tested. Specific antibodies against ICT1 were used to determine the presence of ICT1 in each sample. MtRF1a was used as a mitochondrial matrix marker. The western blot membrane was further probed with antibodies against a cytosolic ribosomal protein (S6-RP) as a control for the non-mitochondrial compartment of the cell. Purified full length and N-terminal truncated recombinant ICT1 (50 ng) were electrophoresed in parallel to compare migration against the endogenous and potentially cleaved ICT1.

Using antibodies against mtRF1a as a mitochondrial marker the same patterns as for ICT1 could be seen, whereas ribosomal protein S6 as a cytosolic marker could be only detected in cell lysate and was completely removed after proteinase K treatment. At this point it should be also mentioned that there was a 2-4 fold increase in the amount of ICT1 comparing cell lysate and isolated mitochondria, whereas the level of mtRF1a increased <2 folds. The cell lysates were prepared using 1% Triton X-100 followed by a centrifugation step at 12,000 xg as described in 3.5.2. Thus insolubilized membrane proteins will be removed by centrifugation whereas soluble proteins especially matrix

proteins will be recovered in the supernatant. The relatively low level of ICT1 in the cell lysate maybe already indicates a tighter association with the membrane whereas mtRF1a is clearly a soluble matrix protein. This point will be more discussed in the next chapter.

Furthermore recombinant protein, which was used for *in vitro* experiments in a later chapter, was also loaded on the western to compare migration against endogenous ICT1 in human cell samples. The full-length (FL) ICT1 migrated consistently at a higher molecular weight, which suggests a possible mitochondrial cleavable target sequence as predicted from PSORTII or TargetP 1.1. A truncation of 29 amino acids of the N-terminus resulted in a more similar size to the samples from human cell lines.

4.3 The importance of ICT1 in human cells

4.3.1 Depletion of ICT1 causes a growth defect

To investigate the possible function of ICT1, siRNAs were applied to deplete the endogenous protein from HeLa cells to determine the effect of the loss of ICT1 on cell growth and morphology and further on mitochondria function especially on mitochondrial protein synthesis.

The approach taken was to deplete endogenous protein levels using siRNA technology. Initially the oligofectamine procedure, as described in 3.1.6.1, was used to transfect HeLa cells. First three different custom synthesised, pre-annealed siRNA duplexes (Table 3.1) were used at a 0.2 µM final concentration to test the depletion efficiency of ICT1 protein. One of those (si-ICT1 C) did not show any down regulation of the protein, but also no effect on cell growth or morphology and therefore just the remaining two were used for further investigation.

As shown by western blot analysis of 20 µg and 50 µg cell lysate in figure 4.2, the endogenous ICT1 protein could be down regulated to a non-detectable level with both siRNAs within 3 days in comparison to a non-targeting siRNA (si-NT) used as control for specificity of targeted duplexes. β-actin was used as a loading control.

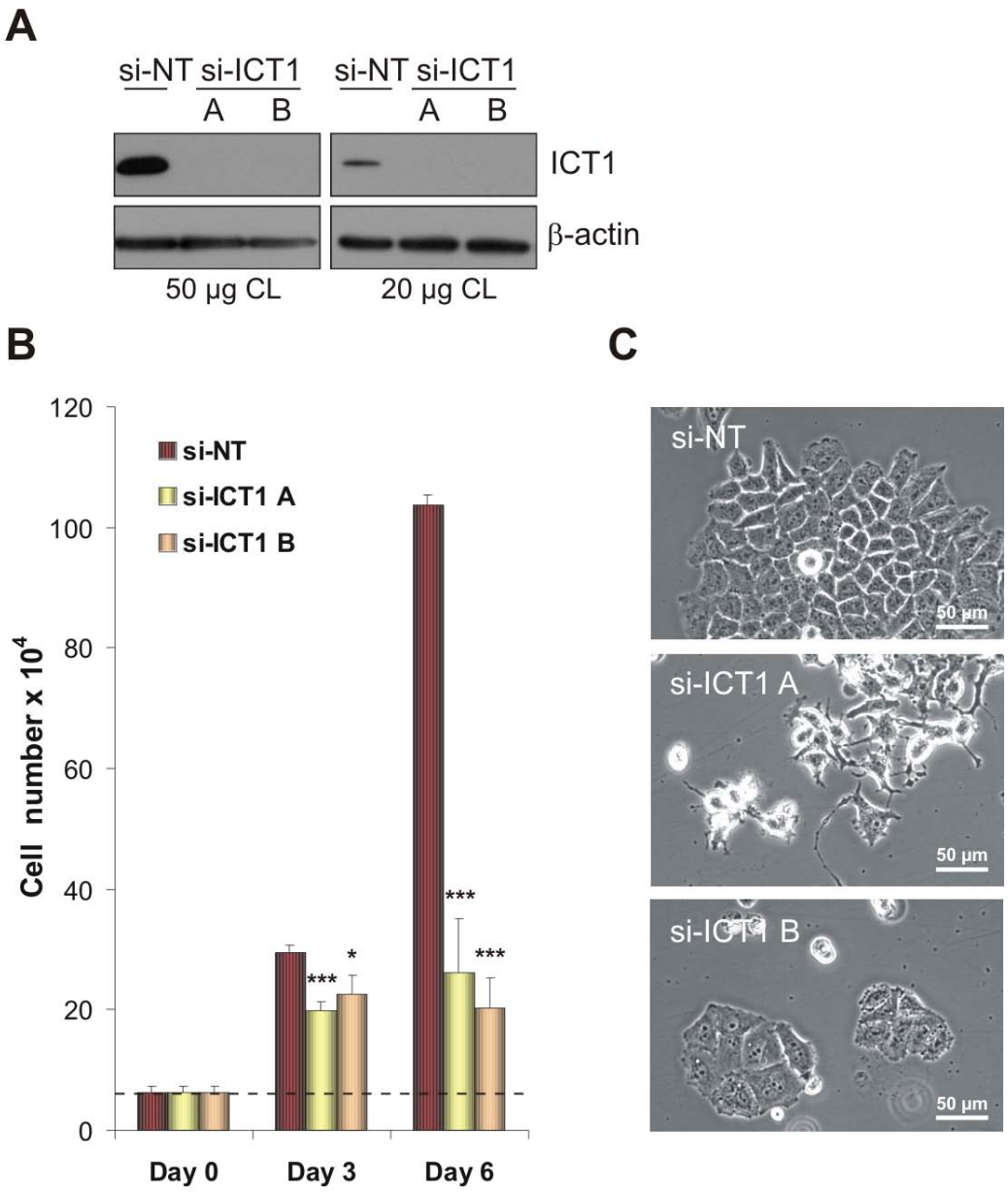

Figure 4.2: Effect of ICT1 depletion on HeLa cell growth and morphology. A) Western blot of 20 µg and 50 µg cell lysates confirmed depletion of ICT1 after 3 days transfection using 2 different siRNAs (si-ICT1 A, si-ICT1 B) in comparison to non-targeting control (si-NT). β-actin was used as a loading control. **B)** Cell counts after 3 days and 6 days siRNA transfection were performed to monitor the effect on cell growth after ICT1 depletion. Cell numbers of si-ICT1 treated samples were compared to si-NT on statistical significance using t-test. The graph represents the result from three independent experiments (n = 3; 3 days: si-ICT1 A: p = 0.0008***; si-ICT1 B: p = 0.024*; 6 days: si-ICT1 A: p = 0.0001***; si-ICT1 B: p = 0.0001***). Initial starting cell number is shown as dotted line. **C)** Images show the morphology of the cells after 3 days transfection.

Interestingly the depletion of ICT1 causes clearly a defect in cell growth (Figure 4.2 B and C). HeLa cells were treated with both siRNAs and the NT control and then counted after 3 and 6 days (Figure 4.2 B). In comparison to the control, ICT1 depleted cells showed a significant decrease in cell number after 3 days, which was even more dramatic after 6 days.

The morphology of ICT1 depleted cells was different comparing the two siRNA to each other after 3 days siRNA transfection (Figure 4.2 C). Thus it is possible that one of the siRNA is either more effective than the other or one of them is causing an off-target effect, meaning an unspecific binding of another mRNA transcript. To investigate the latter 143B-ρ^0 were transfected with the siRNAs. Since 143B-ρ^0 cells lack mitochondrial DNA, they cannot express mitochondrial encoded proteins like COX2 (Figure 4.3, A) and thus they do not need a mitochondrial gene expression machinery. Proteins which are usually involved in that machinery become redundant. Depletion of those factors should therefore not show any effect on the growth or morphology of 143B-ρ^0 cells. Furthermore the expression level of some of those proteins is highly reduced or not detectable in this cell line like it is the case for the mitochondrial ribosomal proteins DAP3 (28S SSU) and MRPL3 (39S LSU), but also for ICT1 itself (Figure 4.3 A, far right lane).

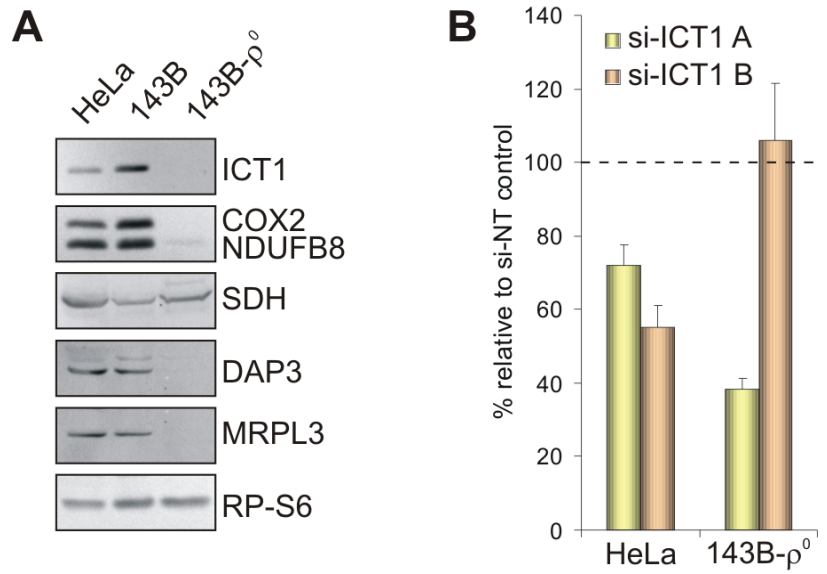

Figure 4.3 Testing the specificity of ICT1 directed siRNA duplexes. A) Western blot of 30 µg cell lysates from HeLa, 143B and 143B-ρ^0 cells probed with specific antibodies to show the relative expression level of ICT1, COX2, NDUFB8, SDH, DAP3, MRPL3 and RP-S6 (loading control) in the different cell lines. **B)** Equal numbers of HeLa- and 143B-ρ^0 cells (~5,000) were transfected with si-ICT1 (A or B) and si-NT, respectively in a 96-well plate format. After 3 days the cell growth was monitored by MTT test. The graph represents the measurements of 4 to 8 wells of each siRNA. The mean of the si-NT treated samples is marked as a dotted line.

Thus using specific siRNAs against *ICT1* should not have any effect, also because of the absence of the protein. To clarify whether this was indeed the case, the MTT-test was carried out as a relative measurement of cell numbers and it was established and optimized for the use in my host laboratory by Dr. J. Rorbach (as described in 3.1.7). This method is based on 96-well plate format and measured the absorbance of formazan which appears by reduction of MTT within the cell.

The MTT data clearly showed that using si-ICT1 A the growth of 143B-ρ^0 cells was highly reduced down to ~40% (Figure 4.3 B) whereas si-ICT1 B showed similar results on cell growth as the si-NT, indicating that si-RNA A has an off-target effect but not si-ICT1 B. The experiment also confirmed the growth defect of HeLa cells after ICT1 depletion. Because of the off-target effect of si-ICT1 A, most of the following experiments were carried out with si-ICT1 B, or both siRNAs were used.

4.3.2 ICT1 is important for mitochondrial gene expression

As has been shown above, ICT1 is not expressed or is present at non-detectable levels in 143B-ρ^0 cells. This suggests that ICT1 may be involved in the mitochondrial gene expression machinery of which many components are absent in mtDNA lacking ρ^0 cells. To investigate this possibility further ^{35}S *de novo* mitochondrial protein synthesis was carried out as described in 3.5.7. By inhibiting translation in the cytosol using emetine, it is possible to visualise the incorporation of ^{35}S-met into only the proteins encoded by the mitochondrial genome. Cells were labelled for 10 min at 37°C 5% CO_2. Samples (50 µg) were then separated through a 15% SDS-PAGE, followed by drying the gel under vacuum at 60°C for 4 h. Phosphor-Imager system was used to visualise the radiolabelled proteins and Image-Quant software for the analysis. In comparison to the si-NT control the depletion of ICT1 after 3 days causes an extremely significant decrease to < 40% in mitochondrial protein synthesis (n = 3, p = 0.0001) using both siRNAs (Figure 4.4 A). To be certain about an even loading of samples, the gel was finally re-hydrated and stained with Coomassie Brilliant Blue (CBB, Figure 4.4 A lower panel).

To see the effect of ICT1 depletion on steady state levels of mitochondrial protein, 20 µg of HeLa cell lysates were analysed by western blot after 3 days transfection from three independent experiments (Figure 4.4 B). For measurements Image-Quant software was used. ICT1 protein was depleted to a non-detectable level as before. β-actin was used as a relative loading control. There was already a significant reduction of the steady state level of the mitochondrial encoded protein COX2 after 3 days depletion (n = 3, si-ICT1 A: 71% p = 0.0197; si-ICT1 B: 69% p = 0.0222), but also of the nuclear encoded protein NDUFB8, which is frequently used as an indicator for the assembly and stability of Complex I (n = 3, si-ICT1 A: 79% p = 0.0013; si-ICT1 B: 72%, p = 0.0001).

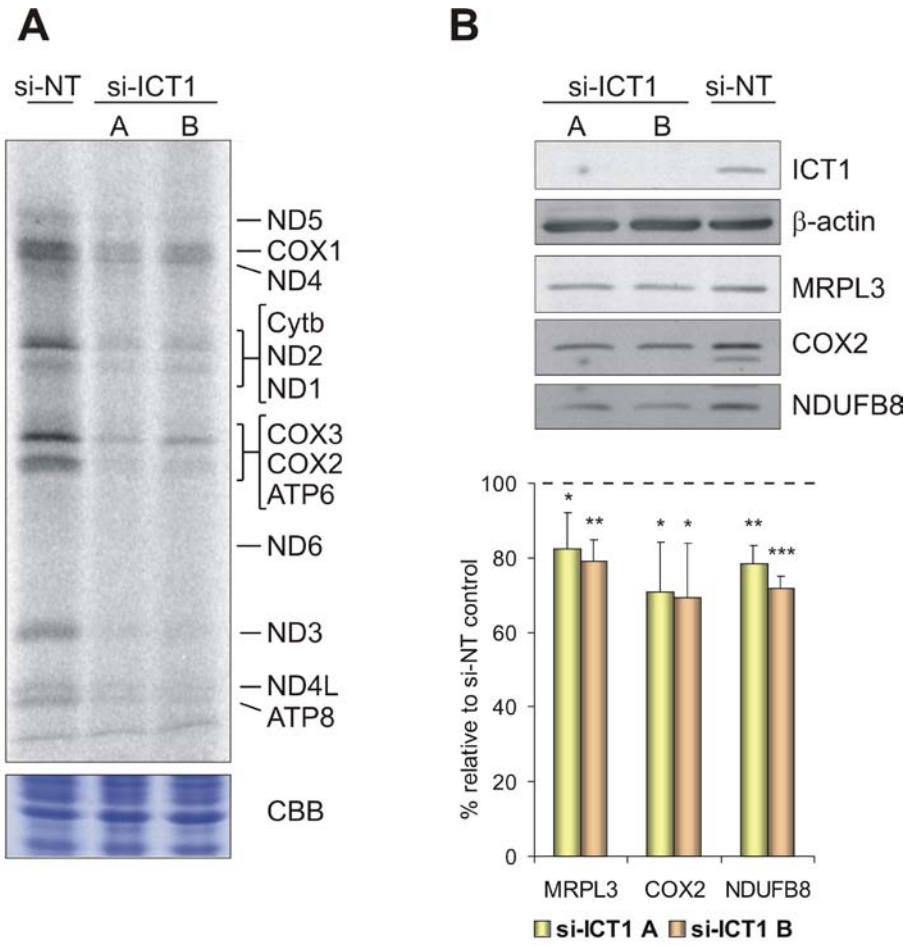

Figure 4.4: Effect of ICT1 depletion on *de novo* mitochondrial protein synthesis and protein steady state level after 3 days. HeLa cells were treated with si-NT and si-ICT1 (A or B), respectively for 3 days, followed by either ^{35}S-met *de novo* synthesis or western blot analysis **A)** ^{35}S-met labelled mitochondrial encoded proteins were separated by SDS-PAGE (15%). The gel was fixed, dried and the radiolabelled proteins were visualised using the Phosphor-Imager system. Proteins were identified by comparison to Chomyn (1996) and individual radiolabelled mitochondrial proteins were quantified using Image-Quant software with consideration of the background in each case. The image is representative for at least three independent experiments. Lower panel depicts a section of the gel after staining with Coomassie Brilliant Blue (CBB) to confirm equal loading. **B)** Western blot of 20 µg cell lysates was probed with antibodies against ICT1, to ensure depletion, proteins of the OXPHOS complexes (Complex IV: COX2; Complex I: NDUFB8) and a component of the mitochondrial ribosome (MRPL3). β-actin was used to confirm consistent loading. The image is representative for 3 independent experiments. The graph below shows the means with standard deviations of the measured signals using Image-Quant software, in comparison to the si-NT control, marked as dotted line. * significant (p = 0.01 to 0.05), ** very significant (p = 0.001 to 0.01), *** extremely significant (p < 0.001).

Often a decrease in synthesis of mitochondrial encoded proteins of Complex I, as it could be seen in the *de novo* mitochondrial protein synthesis, leads to instability of some nuclear encoded ones. Both COX2 and NDUFB8 reflect a significant decrease in the protein steady state level of the OXPHOS complexes after ICT1 depletion. Interestingly a component of the mitochondrial ribosome MRPL3 was also slightly, but

significant decreased in those samples, in comparison to the control (n = 3, si-ICT1 A: 83% p = 0.0344; si-ICT1 B: 79% p = 0.0036). Thus it may be that not only the OXPHOS complexes, but also the mitochondrial ribosome is affected by the ICT1 depletion. This possibility will be investigated and discussed in the next chapter.

4.4 Discussion

ICT1 was so far an uncharacterized protein the abundance of which altered during differentiation in colon carcinoma cells [Van Belzen *et al.*, 1995]. From bioinformatics studies ICT1 is classified as belonging to the prokaryotic/ mitochondrial release factor family as it carries the characteristic GGQ-motif, which is essential for peptidyl-tRNA hydrolysis. ICT1 is a relatively small protein in comparison to other class I release factors, comprising 206 amino acids it is approximately the half of mtRF1a (380 amino acids). The differences in size is mostly the result of the loss of the codon recognition sites (tip of α5-helix tip, PXT-motif) in ICT1 and probably suggests that there is another function for ICT1 instead of it being a typical class I release factor like mtRF1a.

In this study it has been shown that ICT1 is indeed a mitochondrial protein as predicted from several programmes like PSORTII and TargetP 1.1 with a mitochondrial cleavable target site of approximately 30 residues. There are also initial indications that unlike mtRF1a, which is a soluble matrix protein, ICT1 is a more insoluble protein resulting in less recovery of the protein in the supernatant after lysing cells in 1% Triton X-100 containing buffer followed by a hard centrifugation step.

To determine the function of ICT1, siRNAs were applied to down-regulate the endogenous protein from human cells. The depletion of ICT1 caused a decrease in growth rate so that cell number was lower after 3 days in comparison to a control. This was even more severe after 6 days. What can be the reason for this dramatic growth defect? Interestingly ICT1 is not expressed in ρ^0 cells, cells that have no mitochondrial DNA and thus a mitochondrial expression machinery is redundant in those cells. This could be already the first indication that ICT1 is involved in the mitochondrial gene expression machinery and a loss of ICT1 could result in problems in the synthesis of mitochondrial encoded proteins. Indeed this was shown via *de novo* ^{35}S metabolic labelling, the depletion of ICT1 in HeLa cells that caused a dramatic reduction in protein synthesis of mitochondrial encoded proteins. This really suggests that ICT1 is essential for mitochondrial gene expression. At this point it should be mentioned that there was no effect on ^{35}S metabolic labelling after depletion of mtRF1a [Soleimanpour-

Lichaei *et al.*, 2007], which again supports the idea that the function of ICT1 is different from mtRF1a.

Also the protein steady state level of components of Complex I (NDUFB8) and Complex IV (COX2) decreases after 3 days depletion of ICT1 and again an effect that was not seen with the mtRF1a depletion. Those results are also in agreement with those reported by Antonicka *et al.* (2010), where clearly the knockdown of ICT1 in fibroblasts caused a substantial loss and aberrance of the native OXPHOS complexes showed by Blue Native PAGE.

What is the reason of the dramatic effect on mitochondrial protein synthesis after the loss of ICT1? What is the function of ICT1 in the mitochondrial gene expression machinery? Surprisingly also the mitochondrial ribosomal protein MRPL3, a component of the 39S large subunit seemed to be reduced after ICT1 depletion. Does ICT1 cause an effect on the stability of the mitochondrial ribosome and thus on the mitochondrial protein synthesis? This possibility will be investigated and discussed in the next chapter.

Chapter 5:

ICT1 is a component of the mitochondrial ribosome

5 Chapter 5: ICT1 is a component of the mitochondrial ribosome

5.1 Introduction

As was discussed earlier ICT1 is important for human mitochondrial gene expression and a loss of ICT1 shows not only a substantial decrease in mitochondrial protein synthesis, but also a reduction in the steady state level of mitochondrial ribosomal protein MRPL3. The fact that ICT1 was detected after immunoprecipitation of the mitochondrial ribosome via mtRRF-FLAG is unusual for a class I release factor [Rorbach *et al.*, 2008], because the interaction of a release factor with the ribosome is a transient process and thus hard to detect. Furthermore none of the other members of this family were detected in this mtRRF-FLAG immunoprecipitation, not even mtRF1a. This is not a surprise, because using mtRRF-FLAG to co-immunoprecipitate the mitochondrial ribosome means the A-site is occupied and thus there is no space for mtRF1a to interact with the mitochondrial ribosome. Therefore how could ICT1 as a class I release factor be found in this immunoprecipitation? And why does the depletion of ICT1 cause just a dramatic reduction on mitochondrial protein synthesis and furthermore a decreased steady state level of MRPL3?
In this chapter the function of ICT1 in the mitochondrial protein synthesis was further investigated. The aim of this part is to show whether i) ICT1 is really associated with the mitochondrial ribosome as is reasonable to suppose from the mtRRF-FLAG-immunoprecipitation data and ii) whether the depletion of ICT1 leads to a ribosomal defect as maybe inferred from the reduced steady state level of MRPL3.

5.2 Identification of interaction partners of ICT1 via FLAG-immunoprecipitation

To determine whether there is a direct interaction between the mitochondrial ribosome and ICT1, ICT1 was used for immunoprecipitation to isolate and investigate potential interaction partners. For this approach ICT1, which was fused with a C-terminal FLAG tag, needed to be inducible expressed in HEK293T cells. First, *ICT1* cDNA was amplified using the pCMV-SPORT6-ICT1 vector (I.M.A.G.E. ID 4418983, Geneservice) as a template and the primer #1 and #2 (Table 3.2) of which the reverse primer

contains the sequence for the FLAG tag, allowing fusion of the tag to the C-terminus of ICT1. The amplicon and the target vector pcDNA5/FRT/TO were then digested with the restriction enzymes *Hind*III and *EcoR*V, followed by dephosphorylation of the vector and finally the ligation of vector and insert. After successful cloning and sequencing, HEK293-Flp-In^{TM}T-REx^{TM} cells were transfected with pcDNA5/FRT/TO-ICT1-FLAG and pOG44 as described in 3.1.5. After proving that the construct was expressed after tetracycline induction and also imported into the mitochondria, the cells were used for an immunoprecipitation via the FLAG tag as detailed in 3.5.9. As a control for unspecific binding in this experiment a mitochondrial targeted luciferase, fused with the Su9 pre-sequence from *N. crassa* [Viebrock *et al.*, 1982] and also with a C-terminal FLAG tag (mtLuc-FLAG), was used under the same conditions. This cell line was kindly provided by Dr. M. Wydro (host laboratory).

The results were analysed by silver staining and western blot, shown in figure 5.1.

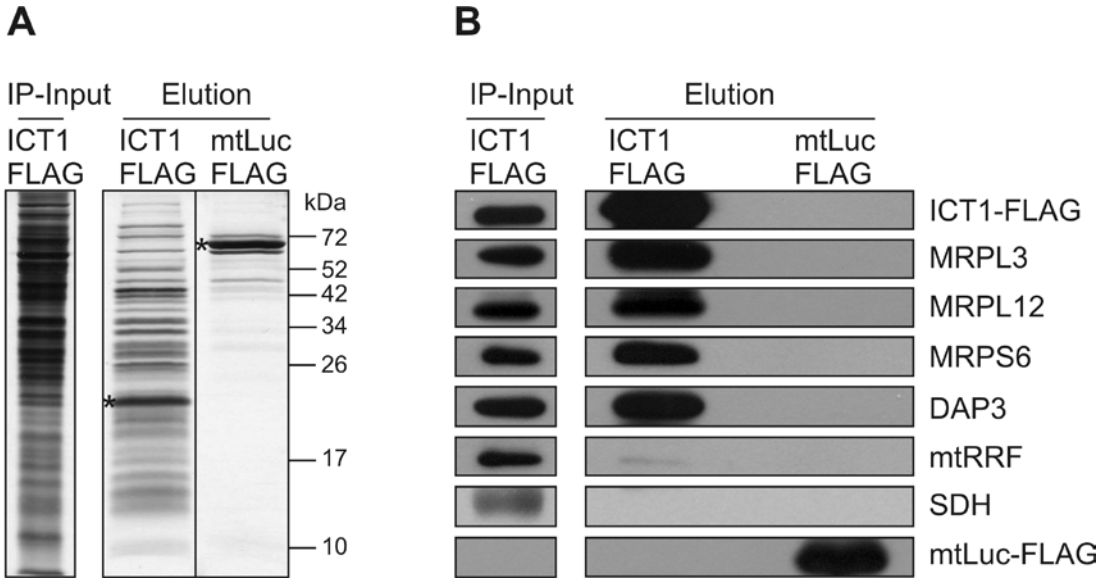

Figure 5.1: ICT1 is associated with mitochondrial ribosomal proteins. HEK293T cells expressing ICT1-FLAG were induced with 1 µg/ ml tetracycline. After 3 days cells were harvested, mitochondria isolated and purified prior to lysis. Mitochondrial lysates (3 mg) were used for immonprecipitation via FLAG tag. As a control mtLuc-FLAG was treated in the same way. Mitochondrial lysate (5 µg) of ICT1-FLAG and elution fractions (10%) of each sample were separated by SDS-PAGE (15%). **(A)** The SDS gel was analysed by silver staining, where (*) indicates the FLAG tagged protein. **B)** Western blot of the same samples was probed with antibodies against mitochondrial ribosomal proteins (39S LSU: MRPL3 and MRPL12; 28S SSU: MRPS6 and DAP3) and mtRRF. SDH, a component of Complex II, was used as a general negative control for unspecific binding. Antibodies against the FLAG epitope were used to confirm expression of the FLAG tagged protein and successful immunoprecipitation via the FLAG tag.

The 5 µg mitochondrial lysate of ICT1-FLAG sample (Figure 5.1 A, left lane) demonstrate the pattern of “input” sample in this experiment on the silver stained gel. Separating proteins from each IP elution fraction on the same gel shows clearly a lot of additional bands in the eluate of ICT1-FLAG in comparison to the negative control

mtLuc-FLAG (Figure 5.1 A, right hand lanes). To determine whether mitochondrial ribosomal proteins co-immunoprecipitate with ICT1-FLAG a western blot with the elution fractions and 5 µg of input sample was probed with antibodies against MRPL3 and MRPL12, both proteins of the mitochondrial ribosomal large subunit (39S LSU) and against MRPS6 and DAP3, components of the small subunit (28S SSU). All proteins could be detected in the elution fraction of ICT1-FLAG, but not in that of mtLuc-FLAG (Figure 5.1 B). Another test for unspecific binding was to check for an abundant protein namely the 70 kDa subunit of SDH, which was not present in either eluate, but could be detected in the input sample, proving that the antibody was working in this experiment. Additionally also the mitochondrial ribosome recycling factor (mtRRF) could be found at low level in the elution fraction of ICT1-FLAG. This is not a surprise as ICT1 was also one of the associated proteins in the mtRRF-FLAG IP [Rorbach *et al.*, 2008], where the majority of mitochondrial ribosomal proteins could be also detected. These facts suggest strongly an association of ICT1 with the mitochondrial ribosome.

Furthermore to be certain that ICT1 interacts with the whole mitochondrial ribosome as speculated the elution fraction was separated by SDS-PAGE, stained with SimplyBlue^{TM} SafeStain (Invitrogen) as described in 3.5.4.2 and the gel lane was cut into three pieces. Together with a negative control elution, samples were sent for LC MS/MS (Liquid chromatography - tandem mass spectrometry) analysis to H. Wessels courtesy of Prof. J. Smeitink at UNMC, Nijmegen. For this approach it was essential that isolated mitochondria for the IP were stringently purified prior to lysis as described in 3.5.8 to avoid as much as possible unspecific bindings of cytosolic proteins especially ribosomal ones. The results from ICT1-FLAG elution were compared to the negative control to exclude contaminations, particularly the common keratin peaks. From the final data of the LC MS/MS approximately 200 proteins could be found in the ICT1-FLAG IP (See appendix 1) where the mitochondrial ribosomal proteins were the most abundant. 26 proteins of the 28S SSU and 41 of the 39S LSU could be detected (Table 5.1), which further supports the idea that ICT1 is strongly associated with the mitochondrial ribosome.

Table 5.1: Mitoribosomal proteins identified as co-purifying components of the ICT1 immunoprecipitation

Small Subunit (28S) - SSU	**Large Subunit (39S) - LSU**
MRPS2, MRPS5, MRPS6, MRPS7, MRPS9, MRPS10, MRPS11, MRPS14, MRPS16, MRPS17, MRPS18A, MRPS18B, MRPS21, MRPS22, MRPS23, MRPS24, MRPS25, MRPS26, MRPS27, MRPS28, MRPS29/DAP3, MRPS30, MRPS31, MRPS34, MRPS35, METT11D1	MRPL1, MRPL2, MRPL3, MRPL4, MRPL9, MRPL10, MRPL11, MRPL12, MRPL13, MRPL14, MRPL15, MRPL16, MRPL17, MRPL18, MRPL19, MRPL20, MRPL21, MRPL22, MRPL23, MRPL24, MRPL27, MRPL28, MRPL31, MRPL32, MRPL37, MRPL38, MRPL39, MRPL40, MRPL41, MRPL43-a, MRPL43-b, MRPL44, MRPL45, MRPL46, MRPL47, MRPL48, MRPL49, MRPL50, MRPL51, MRPL54, MRPL55
26 MRPS of 31	41 MRPL of 50

5.3 ICT1 is associated with the 39S LSU and the 55S monosome

5.3.1 Endogenous ICT1 is associated with the 39S LSU

The advantage of expressing a FLAG tagged protein in the Flp-In system is that it provides the possibility of using it in a specific immunoprecipitation via the FLAG tag. The disadvantage is the fact that high levels of overexpression and/ or tagged proteins could cause artefactual results. Thus it has to be proved whether the endogenous ICT1 is also associated with the mitochondrial ribosome. Therefore 700 µg cell lysate were separated on an isokinetic sucrose gradient as described in 3.5.11. Fractions, which were taken from top (1) to bottom (10), were analysed by western blot. ICT1 could be clearly seen to co-sediment with components of the 39S LSU, namely MRPL3 and MRPL12 in fraction 6 (Figure 5.2). MtRRF, located in fraction 1, can be used as a soluble marker under those conditions. DAP3 as a component of the 28S SSU was more detectable in fraction 4, 5 and a little bit in 6.

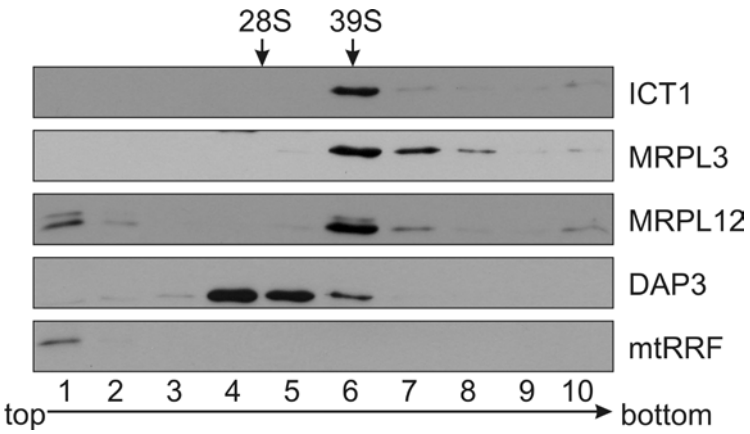

Figure 5.2: ICT1 co-migrates with components of the 39S LSU. HeLa cell lysate (700 µg) was separated on a 10 % to 30 % isokinetic sucrose gradient for 135 min at 100,000xg. Fractions (1-10) were taken from top to bottom and then analysed by western blot. The membrane was probed with antibodies against components of the 39S LSU (MRPL3 and MRPL12) and the 28S SSU (DAP3) to determine the relative sedimentation of the subunits within those gradients. Distributions of ICT1 and mtRRF are also shown.

From this result it seems that the monosome is not detectable in these gradients. From more RNA based work in this laboratory on such gradients it is known that the cytosolic ribosomal RNA from the 60S (28S rRNA) is located approximately in fractions 8 and 9, visualised by ethidium bromide stained agarose gels. From the sedimentation coefficient it would be expected that the 55S mitochondrial monosome is also migrating in approximately the same position. However, there is clearly a lack of DAP3 in the later fractions, which suggest there is no monosome and ICT1 seems to be only associated with the 39S large subunit and not with the 28S, however, IP results show both components or the monosome respectively.

5.3.2 ICT1-FLAG immunoprecipitation shows association of ICT1-FLAG with the 39S LSU and the 55S monosome

To distinguish whether ICT1 is associated with the 39S LSU or/ and with the 55S monosome, 80% of IP eluate was separated on the same range isokinetic sucrose gradient, followed by analysis via western blot (upper panels) and silver staining (lower panel) as shown in figure 5.3. On the silver stained gel the majority of co-immunoprecipitated proteins was mainly localised in the later fractions 6 to 8. Furthermore a strong band that corresponds to the overexpressed ICT1-FLAG was seen in the earlier fractions 1 and 2.

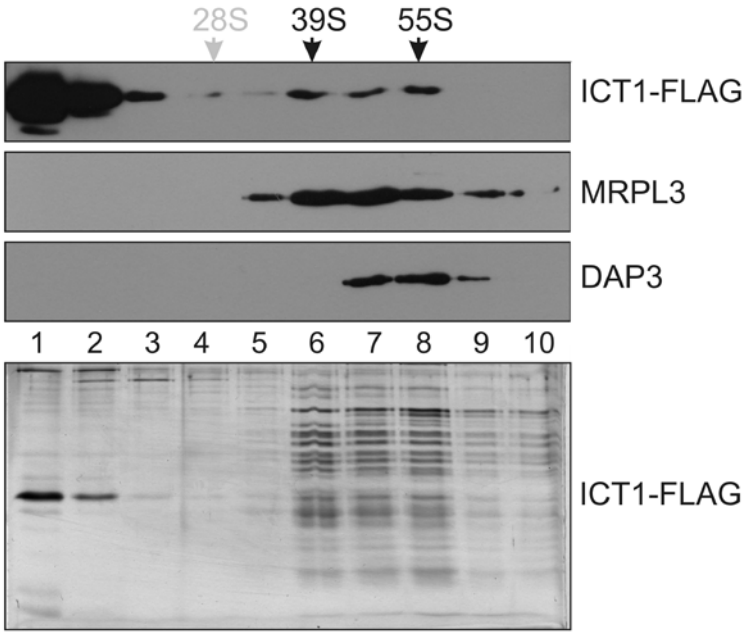

Figure 5.3: ICT1-FLAG co-sediments with 39S and 55S of the mitochondrial ribosome after immunoprecipitation. Mitochondrial lysate (3 mg) from HEK293-ICT1-FLAG was used for the IP, from which 80% of the elution were separated by isokinetic sucrose gradient. The fractions (1-10) were analysed by silver staining (lower panel) and western blot (upper panels). Antibodies against MRPL3 and DAP3 were applied to the membrane to determine the level of co-immunoprecipitated 39S LSU, 28S SSU and 55S monosome, respectively. The relative positions of the ribosomal complexes within this gradient are indicated above the image. ICT1-FLAG was detected by using antibodies against the FLAG octapeptide.

To determine further where the ribosomal proteins migrated in the gradient, a western blot with the same fractions was probed with antibodies against MRPL3 and DAP3. MRPL3 was mostly found in fractions 6 to 8. Interestingly DAP3 shifted to the later fractions 7 and 8, where it co-sediment this time with MRPL3, the component of the LSU, which suggests that the 55S monosome migrates in those fractions. ICT1-FLAG was, besides the free form in fractions 1 and 2, also detectable in fractions 6 to 8 like MRPL3. From this experiment it can be concluded that ICT1-FLAG is associated with the 39S LSU and with the 55S monosome, but not with the 28S SSU alone.

5.3.3 ICT1 is strongly associated with protein components of LSU

Besides ribosomal proteins, an intact ribosome contains also the ribosomal RNA (rRNA). The structure of the rRNA within the ribosome depends not only on the protein factors but also on Mg^{2+}.

After depletion of Mg^{2+} from the experiment, by using a chelating agent such as EDTA, it is possible to disturb the RNA structure and therefore the interactions of proteins that are more dependent on the RNA or an intact ribosome. To determine whether ICT1 is

more associated with the ribosome via the RNA or whether there are more protein-protein interactions, a similar IP as above was carried out, but instead of containing 10 mM $MgCl_2$ there was 50 mM EDTA added to the experiment. Separating this IP eluate on a gradient showed clear differences (Figure 5.4). On the silver stained gel (lower panel) the majority of proteins shifted to fraction 5 and 6, whereas they were mostly located in fraction 6 to 8 before. This is a clear indication of a substantial loss in the size of the complex, but still there were a lot of proteins co-immunoprecipitated in the ICT1-FLAG immunoprecipitation even in the presence of 50 mM EDTA.

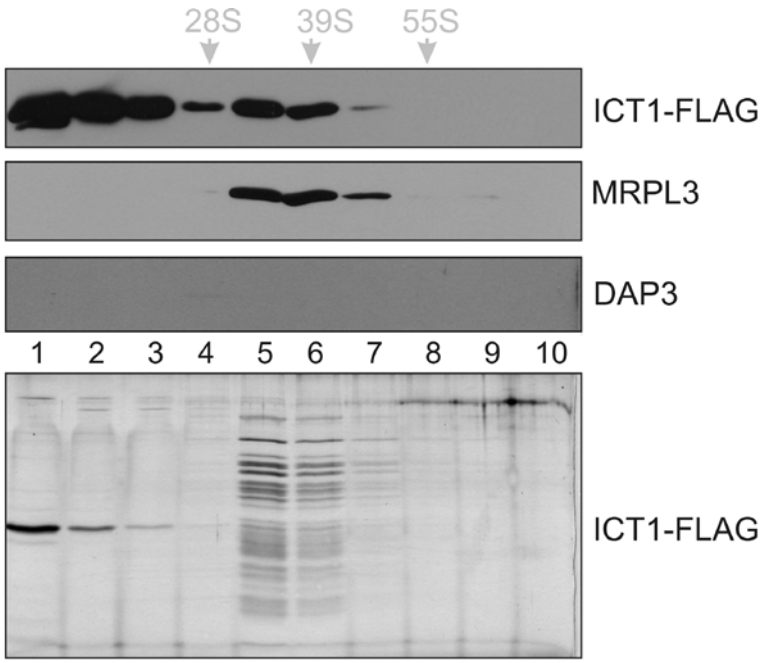

Figure 5.4: Interaction of ICT1 with components of the 39S LSU is not RNA dependent. Mitochondrial lysate (3 mg) of ICT1-FLAG overexpressor was treated with 50 mM EDTA to deplete Mg^{2+}. After IP, 80% of the eluate was separated by isokinetic sucrose gradient. Fractions were analysed by silver staining (lower panel) and western blot (upper panels). MRPL3 and DAP3 were used as before to visualise the level of co-immunoprecipitated ribosomal complexes by ICT1-FLAG, which was detected by using FLAG antibodies.

This suggests that there are several protein-protein interactions, which is one of the specific features of the mammalian mitochondrial ribosome [Sharma *et al.*, 2003]. The western blot demonstrates that there was clearly a loss of DAP3, meaning that with loss of the RNA, there is no longer a monosome. In contrast there was still a strong interaction with MRPL3. It would be interesting to know which other proteins remain associated with the ICT1-FLAG IP under these conditions, however further antibodies to MRPL peptides are not available with which to probe this blot. In conclusion ICT1 can be seen as an integral component of the mitochondrial ribosomal large subunit, because the interaction with the mitochondrial ribosome is not transient, it shows

clearly strong protein-protein interactions and the endogenous form could not be detected free, but always in association with the LSU.

5.3.4 The association of ICT1-FLAG with the 55S monosome is not caused by overexpression or by the FLAG tag

To exclude that the overexpression of ICT1-FLAG causes an accumulation of the 55S monosome, as seen in the IP eluate gradient, several control experiments needed to be done. First, 700 µg cell lysate of the ICT1-FLAG overexpressor were analysed by sucrose gradient after 3 days induction. The resulting data is shown on western blot in figure 5.5. As before, a lot of the overexpressed form was localised in the earlier fractions 1 to 4, however, in this experiment ICT1-FLAG was further only seen in fraction 6, but nothing in the later fractions. DAP3 also did not co-migrate this time with MRPL3 in the later fractions. This is a clear indication that at least the overexpression of ICT1-FLAG is not the reason for the appearance of the monosome on those gradients of IP-ed eluate.

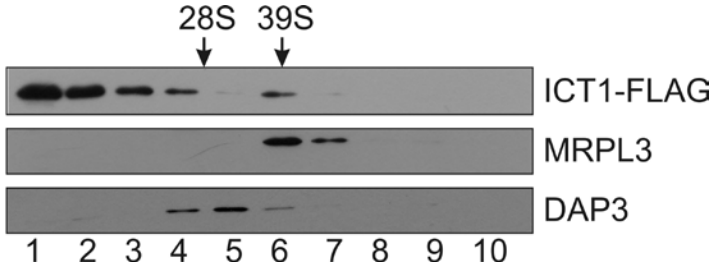

Figure 5.5: ICT1-FLAG co-migrates with 39S LSU and its overexpression causes no accumulation of 55S. HEK293-ICT1-FLAG cells were induced with 1 µg/ ml tetracycline. After 3 days cells were harvested and lysed. Cell lysate (700 µg) was separated on a 10 to 30% sucrose gradient and fractions were analysed by western blot. To determine the relative level of individual ribosomal subunits and the 55S monosome, respectively after ICT1-FLAG overexpression, antibodies against markers for the 39S LSU (MRPL3) and the 28S SSU (DAP3) were applied to the western blot membrane. The distribution of ICT1-FLAG is also shown by using FLAG antibodies.

Another control was to run similar experiments with FLAG-tagged components of the 28S SSU and the 39S LSU. Therefore overexpressed MRPS27-FLAG and MRPL20-FLAG (expressing cell lines were kindly provided by Dr. J. Rorbach and Dr. P. Smith, respectively both from host laboratory) were used to co-immunoprecipitate the mitochondrial ribosome and of course the individual intermediates, which were then separated on an isokinetic sucrose gradient as before.

Western blot in figure 5.6 A showed that MRPS27-FLAG co-immunoprecipitated a substantial amount of the 28S SSU and intermediates of it, but it did not pull down a lot

of the monosome. However, it clearly shows that also in this experiment it was possible to visualise the monosome in fraction 8, as ICT1, MRPL3, DAP3 and of course MRPS27-FLAG all co-migrated in this fraction.

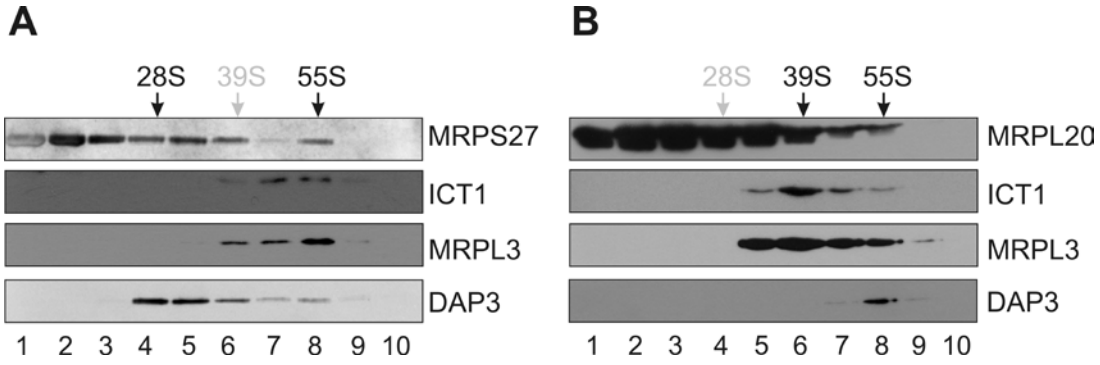

Figure 5.6: Association of ICT1 with 55S monosome is not FLAG tag dependent. Mitochondrial lysates from cells expressing MRPS27-FLAG (A) or MRPL20-FLAG (B) were used for IP, from which the elution fractions (80%) were separated on an isokinetic sucrose gradient. The distribution of co-immunoprecipitated ribosomal subunits and 55S monosome was determined by western blot using antibodies against DAP3, representing the 28S SSU, and MRPL3, a member of the 39S LSU. The migration of endogenous ICT1 within these experiments was visualised by probing the western blot membrane with specific antibodies against ICT1.

In contrast, MRPL20-FLAG shows association with the 39S LSU (Figure 5.6 B), where the main population was again located in fraction 6 with relatively strong signals of ICT1 and MRPL3. As in the gradient with ICT1-FLAG eluate, DAP3 was shifted to fraction 8, where it co-localised with ICT1, MRPL3 and MRPL20-FLAG.

In conclusion it can be said that ICT1 is an integral component of the 39S LSU and therefore of the 55S monosome. ICT1-FLAG is able to pull down the monosome, which migrates on a sucrose gradient mainly in fraction 8. The association of ICT1 with the monosome, which could not be seen before, is not a result of overexpression the protein, as the same association could be seen with the endogenous ICT1 in mitochondrial ribosome co-immunoprecipitated with MRPS27-FLAG and MRPL20-FLAG.

5.4 ICT1 depletion causes conformation changes in the 39S LSU and a loss of the 55S monosome

If ICT1 is really a component of the 39S LSU it would be important to analyse what would happen to the mitochondrial ribosome after a loss of ICT1. Therefore HeLa cells were treated with si-ICT1 B or si-NT, respectively for 3 days and the cell lysates were

separated on isokinetic sucrose gradient. The fractions were analysed by western blot as shown in figure 5.7.

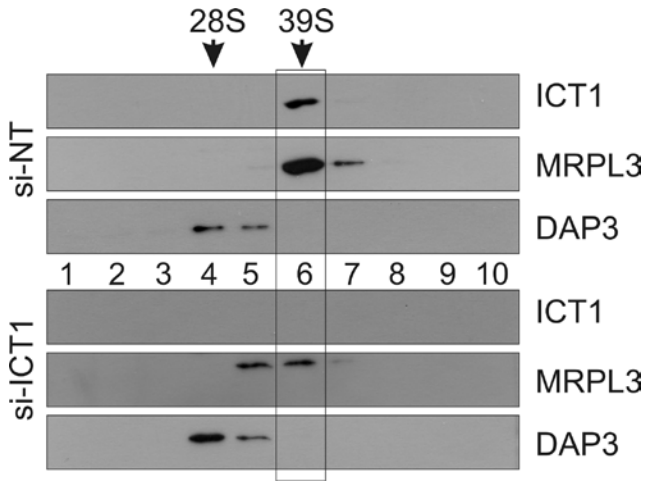

Figure 5.7: ICT1 depletion affects assembly of 39S LSU. ICT1 depleted cell lysate (600 µg) was subjected to an isokinetic sucrose gradient. The fractions (1-10) were analysed by western blot using antibodies against ICT1 to ensure depletion in the siRNA targeting sample (lower panels) and further to visualise the distribution of ICT1 in the control (upper panels). The effect of ICT1 depletion on the ribosomal profile was determined by probing the membrane with MRPL3- (39S LSU) and DAP3 (28S SSU) antibodies.

Using anti-ICT1 antibodies showed clearly successful depletion of ICT1 in samples from cells treated with si-ICT1 B, but not those treated with si-NT. Interestingly, MRPL3 showed a difference in the migration on the gradients between the two samples. In the si-NT sample it was located as usually, mainly in fraction 6 and a little in 7, whereas in the depleted sample MRPL3 shifted to fraction 5 and 6, which indicates a loss in the sedimentation of the 39S LSU. DAP3 did not show obvious differences and was located in fraction 4 and 5 as before. Those data suggests that the depletion of ICT1 causes a conformation change of the 39S LSU but not the 28S SSU which remains unchanged.

To be absolutely certain about the result that ICT1 depletion causes a defect in formation of the 39S LSU and also to analyse what would happen to the monosome, another approach needed to be used. As shown before MRPS27-FLAG can be used to co-immunoprecipitate the 55S monosome, therefore it was utilised as a tool to investigate consequences of ICT1 depletion at the level of monosome formation. The hypothesis would be that the loss of ICT1 will cause a conformation change in the 39S LSU, which would lead to a reduced ability of the 39S LSU to interact with the 28S to form a 55S monosome. Therefore the depletion of ICT1 should result a decrease amount of co-immunoprecipitated 55S monosome via MRPS27-FLAG in comparison to the si-NT control (Figure 5.8 A).

HEK293T cells expressing MRPS27-FLAG were transfected with si-ICT1 B and si-NT, respectively for 3 days using lipofectamine as described in 3.1.6.2. After one day transfection cells were induced with 1 µg/ ml tetracycline to give the cells 2 days time to overexpress MRPS27-FLAG. The elution fractions of both immunoprecipitations were analysed by western blot (Figure 5.8 B) and signals were measured using Image-Quant software.

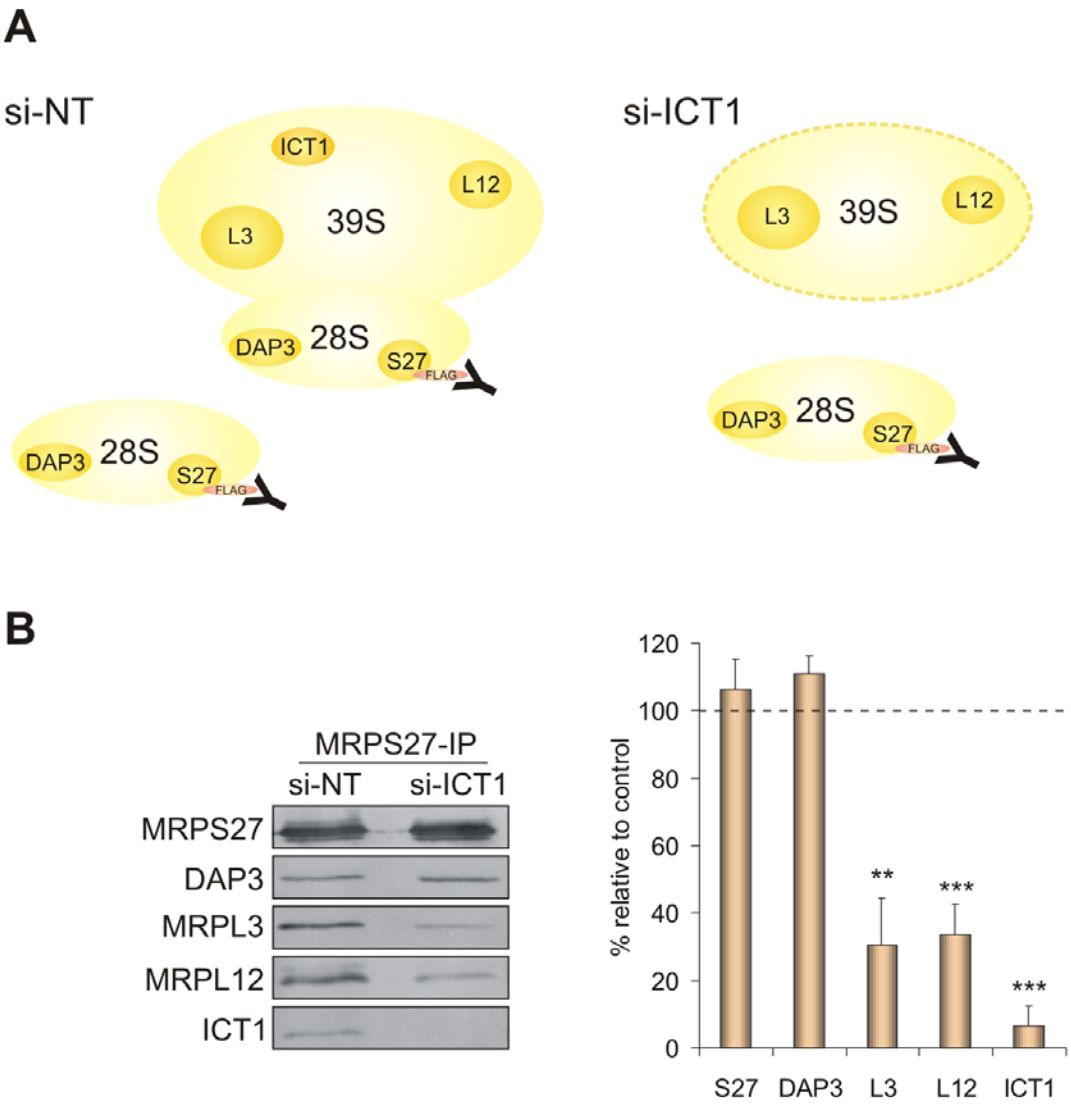

Figure 5.8: ICT1 depletion causes a loss of the 55S monosome. A) The cartoon demonstrates the loss of the ability of the 39S LSU to interact with the 28S SSU after ICT1 depletion. Using MRPS27-FLAG to co-immunoprecipitate the 55S monosome would result in decreased amounts of 39S LSU components (MRPL3 and MRPL12) in the elution fraction of ICT1 depleted samples, whereas the relative level of components of the 28S SSU (DAP3) should be unaffected. **B)** HEK293T cells expressing MRPS27-FLAG were treated with si-NT or si-ICT1 B for 3 days. Equal amounts of cell lysates (~ 2 mg) were used for immunoprecipitation via MRPS27-FLAG. The elution fractions were analysed by western blot and the relative amount of monosome was determined by measuring the level of MRPL3 and MRPL12 from 3 independent experiments. The mean of measured signals of the si-NT control is marked as a dotted line. (n = 3; MRPL3 p = 0.001; MRPL12 p = 0.0002; ICT1 p = 0.0001; ** very significant: p = 0.001 to 0.01; *** extremely significant: p < 0.001)

The results as presented in the graph in figure 5.8 B reflect three independent experiments, where after ICT1 depletion (to ~ 10%; p = 0.0001) the level of MRPL3 (p = 0.001) and MRPL12 (p = 0.0002) decreased to ~ 30%, but DAP3 remained at similar level as in si-NT treated samples (marked as dotted line).
Concluding from those results, there is not only a conformation change in the 39S LSU there is also a loss in the level of the 55S monosome after ICT1 depletion, which more strongly supports the hypothesis that ICT1 is an integral component of the mitochondrial ribosome.

5.5 Discussion

ICT1 as one of the four members of the mitochondrial release factor family was identified after immunoprecipitation of the mitochondrial ribosome via mtRRF-FLAG [Rorbach *et al.*, 2008]. None of the other members (mtRF1a, mtRF1 and C12orf65) were detectable in this IP, which is not unexpected, because the interaction of the release factor with the ribosome is usually a transient process and thus difficult to detect. Furthermore using mtRRF for immunoprecipitating the mitochondrial ribosome means that the A-site is occupied by mtRRF and thus there is no room to accommodate a class I release factor. Therefore why could ICT1 be found in the IP of mtRRF-FLAG?
In the present study it could be shown that the mitochondrial ribosome has been co-immunoprecipitated with ICT1-FLAG (Figure 5.1), which is the first time that a release factor has been shown in strong association with ribosomal proteins using immunoprecipitation procedure. Under the same conditions but using mtRF1a-FLAG, it is not possible to detect immunoprecipitation of the mitochondrial ribosome (data not shown). In addition to mitochondrial ribosomal proteins there were also trace amounts of mtRRF detectable in the elution, which was expected as mtRRF-FLAG originally immunoprecipitated ICT1. The fact that mtRRF and ICT1 can interact with the same mitochondrial ribosome, suggests that ICT1 does not occupy the A-site as either mtRRF or the class I release factor mtRF1a. This again supports the idea that ICT1 functions in another way to mtRF1a.
Furthermore it could be shown that endogenous ICT1 migrates with the 39S LSU on an isokinetic sucrose gradient (Figure 5.2), but under those conditions no 55S monosome could be detected. The western blot (Figure 5.1 B) and LC MS/MS analysis (Table 5.1) from ICT1-FLAG immunoprecipitation, however, suggested that ICT1 is associated either with the 55S monosome or with the 28S SSU and 39S LSU, respectively. Again

the fact that mtRRF, as a marker for the 55S particle, was detected within the ICT1-FLAG elution supports the hypothesis that ICT1 interacts with the 55S monosome. Separating the ICT1-FLAG IP eluate on an isokinetic sucrose gradient showed that ICT1-FLAG co-sediments with the 39S LSU and also with the 55S monosome, but not with the 28S SSU (Figure 5.3).

Why is the 55S monosome only detectable after immunoprecipitating the mitochondrial ribosome? The overexpression of ICT1 has been excluded as the reason because cell lysate of the overexpressor showed only the 39S LSU and the 28S SSU, on a sucrose gradient analysed by western blot (Figure 5.5). Furthermore with immunoprecipitation of MRPS27-FLAG and MRPL20-FLAG a purification of the 55S monosome is possible where the endogenous ICT1 was also detected within the 55S particle (Figure 5.6). The difficulty to see the monosome has also been reported in other studies [Nolden *et al.*, 2005, Williams *et al.*, 2005].

What is the difference in the gradients and what is causing the appearance of the 55S monosome only after IP? A difference of buffer conditions during lysis and the actual gradient can be excluded as they are the same. One point could be that the immunoprecipitation effectively concentrates the amount of mitochondrial ribosome in the sample, whereas in contrast the concentration of the monosome in cell lysate can be to low and therefore more below the levels of sensitivity of western detection. *This would leave the question whether a low amount of 55S monosome is the physiological situation within the mitochondria or whether it is caused by the experimental procedure?* However, the main difference between the gradient of cell lysate and IP-ed eluate is most likely the difference in incubation time of the IP-ed samples. For the binding step in the IP the samples, which are mitochondrial lysates, are left for 3 hours to allow binding of the FLAG antibody to the FLAG tag. In contrast for a standard gradient cell lysates are prepared and applied immediately to the gradient. *What can happen during those 3 hour incubation?* It is possible that mRNA is degraded and potentially mtIF3 is too diluted under those conditions to inhibit the formation of the 55S. Results from real time PCR within this study, and also those of another PhD student, A. Pajak, both showed that the mt-mRNA is indeed absent in those IP-ed monosomes, whereas mt-ribosomal RNAs were still present. The possibility that mtIF3 is not present in sufficient concentration is also in agreement with the fact that the elution fraction of immunoprecipitated mtRRF-FLAG shows substantial amounts of the associated mitochondrial ribosome. There are suggestions that mtIF3 plays an active role and is thus absolutely critical for the ribosome recycling process [Christian and Spremulli, 2009]. In addition to mtIF3, mtEFG2 (mtRRF2) [Tsuboi *et al.*, 2009] is also needed for successful disassembly of the 55S into the 28S SSU and the 39S LSU. In

summa it seems probable that the mt-mRNA is degraded during lysis and over the 3 hour incubation time, which then allows, in combination with the diluted amounts of mtIF3 and/ or mtEFG2 the ribosomal subunits to reform the 55S monosome. Another support of this theory is that the endogenous mtRRF is normally located in the earlier fractions on isokinetic sucrose gradient (Figure 5.2), but after incubating lysates for 3 hours a shift of mtRRF to the later fractions was observed, suggesting binding of this factor to the ribosome [Rorbach *et al.*, 2008].

Thus, it is possible to detect the 55S monosome under certain experimental conditions and ICT1 was shown to be associated with it. However, it is still unclear what the physiological situation is, meaning are the majority of 28S SSU and 39S LSU free and only a limiting amount of them part of a translating 55S monosome or is the 55S particle the more prominent stage within the mitochondria and only the experimental procedure is causing the disassembling of the subunits? One characteristic feature of the mitochondrial ribosome is a tight association with the inner mitochondrial membrane (IMM) [Liu and Spremulli, 2000]. It has been proposed that mitochondrially encoded proteins are translated at this site of the IMM where they will be assembled into the OXPHOS complexes allowing a co-translational insertion into the membrane [Koc *et al.*, 2010]. This might suggest that only membrane bound ribosomes are translationally active as also proposed by Nolden *et al.* (2005). Using a detergent such as Triton X-100 to lyse the cells will lead to a disruption of the interaction of most of the mitochondrial ribosomes with the inner membrane. Therefore, maybe as a consequence of losing the interaction with the inner membrane, the 55S monosome initially comes apart into the 28S SSU and 39S LSU and only by increasing the incubation time, where mRNA gets degraded and mtIF3 and/ or mtEFG2 are limited, the subunits reassemble again into the 55S monosome. Currently this is just a hypothesis, the testing of which will be challenging.

The interaction of ICT1 with the 39S LSU was shown to be RNA independent, as the presence of high EDTA concentration still allowed the co-immunoprecipitation of a large complex with ICT1-FLAG located in fractions 5 and 6 in sucrose gradient (Figure 5.4). One of the proteins that remained associated was MRPL3. It was shown previously that after treatment with EDTA the 55S monosome is no longer retained intact [Rorbach *et al.*, 2008]. Proteins such as mtRRF lose their ability to show association with the mitochondrial ribosome as their interaction are dependent on rRNA structure and/ or an intact 55S monosome. Consistent with those results, after EDTA treatment ICT1-FLAG shows no longer an association with the 55S monosome as evidenced by the loss of DAP3 from the later gradient fractions. The components of the

complex that remains after EDTA treatment, suggests that there is a tight interaction of ICT1 with mitochondrial ribosomal proteins. Thus this result and the fact that the endogenous protein was always co-migrating with MRPL3 in fraction 6 and never free (Figure 5.2) suggest that ICT1 is actually an integral component of the 39S LSU.

One of the specific characteristics of mammalian mitochondrial ribosome is that it is very protein rich (~69%) and relatively RNA poor (~31%) in comparison to the bacterial one as described in 1.7.1 [reviewed in O'Brien 2002; Sharma *et al.*, 2003] where the proportions are reversed. It was suggested that the truncations of the ribosomal RNAs within the mammalian mitochondria are compensated through an increase in size of existent homologous proteins or additional proteins [O'Brien 2002]. Therefore approximately half of the proteins are homologous to bacterial ones and the other half are specific for the mammalian mitochondrial ribosome. These additional proteins appear sometimes to pre-exist and/ or to be bi-functional. Examples for those bi-functional proteins are DAP3 (MRPS29) and PDCD9 (MRPS30), both suggested to be involved in apoptosis [Koc *et al.*, 2001a]. Another example is MRPL12 that directly interacts with POLRMT in addition to being a mitochondrial ribosomal protein of the 39S LSU [Wang *et al.*, 2007], suggesting a further function as a transcription-translation coupling factor. Another example is MRPL39, which shows similarity to the N-terminal domain of the mitochondrial threonyl-tRNA synthetase [Spirina *et al.*, 2000]. It was proposed that mitochondrial threonyl-tRNA synthetase was recruited into the mitochondrial ribosome and then lost its C-terminal domain. It is tempting to speculate that ICT1 is another example of a pre-existing protein that has been recruited into the mitochondrial ribosome. Whether the codon recognition motifs were lost before or after the recruitment of ICT1 into the mitochondrial ribosome is unclear, but the results presented in this chapter show clear evidence that ICT1 has become a mitochondrial ribosomal protein. This data was published [Richter *et al.*, 2010] prior to writing of this thesis and this finding was subsequently also the subject of a 'commentary' [Haque and Spremulli, 2010] and review by others as Koc *et al.* (2010) where ICT1 was designated MRPL58 for consistence with the accepted nomenclature.

Why was ICT1 not previously reported to be a mitochondrial ribosomal protein in mammals [O'Brien, 2002]?

There can be many reasons why so far ICT1 was missing in the screenings from O'Brien or Spremulli and colleagues [O'Brien, 2002; Koc *et al.*, 2001a/b]. It is possible that harsh isolation procedures lead to the loss of some 55S members [Matthews *et al.*, 1982]. Another possibility is that a protein like ICT1 was present, but was originally considered to be a contaminant. In the past few years bioinformatical predictions concerning mitochondrial localisation have become more sophisticated and an

advantageous tool, whereas 10 to 20 years ago those kinds of predictions were more difficult to achieve. Thus it is also possible that there are still some proteins missing. In fact the available structure of the bovine mitochondrial ribosome [Sharma *et al.*, 2003] shows a quite porous structure caused by the loss of rRNA, however, there are also gaps, where it is tempting to speculate whether there are some missing proteins that would fill these spaces.

The association of ICT1 with the mt-LSU seems to be quite late during the assembly process of the 39S. This conclusion is derived from the result in figure 5.3, where ICT1 is not interacting with a lot of large subunit intermediates as is the case with MRPL20 (Figure 5.6 B). ICT1 is likely to interact with the 39S LSU at a quite late stage, when the assembly is almost complete, because as shown in the silver stained gel in figure 5.3 the ribosomal complex co-immunoprecipitated with ICT1 is quite dense, starting in fraction 6. This would be also in agreement that the depletion of ICT1 that is causing a ribosomal defect shows “only” a shift of the mitochondrial ribosomal LSU component MRPL3 from fractions 6/7 to 5/6 (Figure 5.7), meaning there is a loss of density/ size of the 39S LSU, but there is still a quite big complex in the absence of ICT1. However, these are only suggestions according to the presented data in this chapter.
The resulting defect in the 39S LSU after depletion of ICT1 is further causing a loss of intact 55S monosome (Figure 5.8). Using MRPS27-FLAG as a tool to co-immunoprecipitate the 55S monosome it was possible to measure changes in the level of associated ribosomal components after the loss of ICT1. In comparison to the control, the depletion of ICT1 caused a decrease in the level of associated MRPL3 and MRPL12 proteins by MRPS27-FLAG to approximately 30%, whereas DAP3 remained unchanged. Those data strongly suggest that ICT1 as a ribosomal protein is essential for the assembly of the 39S LSU and a defect in the 39S LSU caused by a loss of ICT1 leads to a reduced level of translationally active monosome. This result is also in agreement with the ^{35}S-met *de novo* synthesis, where mitochondrial protein synthesis decreased to <40% after ICT1 depletion (Figure 4.4). Thus the reason for the dramatic reduction in mitochondrial translation after downregulation of ICT1 is actually the loss of the 55S monosome.
Concluding so far ICT1 was shown to be an integral component of the 39S LSU and the 55S monosome. A loss of ICT1 leads to a ribosomal defect in the 39S LSU, causing less translationally active monosome and thus a decrease in mitochondrial protein synthesis.

Chapter 6:

ICT1 is a ribosome-dependent, but codon-independent peptidyl-tRNA hydrolase

6 Chapter 6: ICT1 is a ribosome-dependent, but codon-independent peptidyl-tRNA hydrolase

6.1 Introduction

Data presented so far has shown that ICT1 is an important mitochondrial protein, essential for mitochondrial protein synthesis and a component of the mitochondrial ribosomal large subunit. This is unexpected as from the bioinformatic point of view ICT1 is defined as a member of the prokaryotic/ mitochondrial release factor family. This classification is mainly based on ICT1 harbouring the highly conserved GGQ motif (Figure 6.1), which is essential for promoting the catalysis of the peptidyl-tRNA hydrolysis within the ribosome.

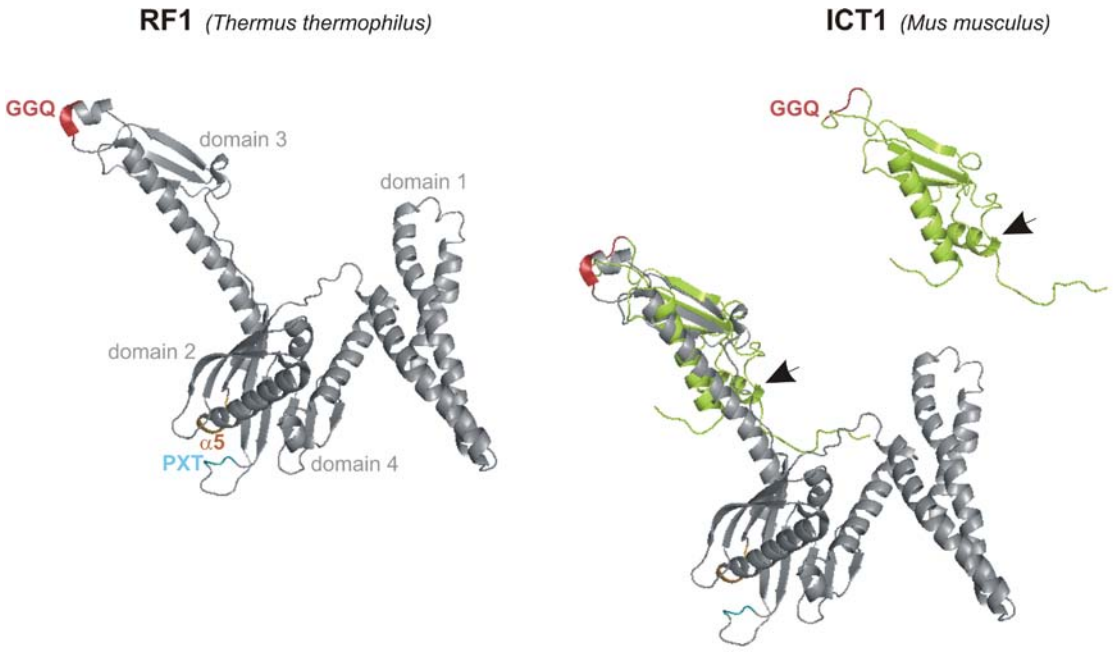

Figure 6.1: Structure alignment of RF1 (*Thermus thermophilus*) and ICT1 (*Mus musculus*). Available structures from a bacterial class I release factor RF1 (grey, *Thermus thermophilus*, PDB: 3D5A, Laurberg *et al.*, 2008) and ICT1 (green, *Mus musculus*, PDB: 1J26 unpublished) were superimposed using PyMOL. RF1 is shown with 4 domains. The GGQ motif within a flexible loop in domain 3 is labelled in red. The crucial motifs for stop codon recognition, namely the tip of the α5 helix and the PXT tripeptide motif, are shown in brown and blue, respectively within domain 2. The arrow shown within the ICT1 structure indicates an additional helix absent in bacterial RF1.

It is not only the GGQ motif that is critical for the function of a class I release factor, also the codon recognition motifs (tip of α5 helix and PXT/SPF) are absolutely crucial features for a conventional class I release factor to recognise sequence specific the stop codon in the decoding centre of the ribosomal A-site. ICT1 is a relatively small protein with 206 aa and lacks both of these motifs (Figure 6.1). Thus it is unlikely that it acts like a typical class I release factor in the manner of mtRF1a. The fact that it has become incorporated as part of the mitochondrial ribosome, a circumstance not previously reported for a release factor, strongly supports the hypothesis that ICT1 functions in a different way to a classical release factor. Two facts however indicate that ICT1 maintained its ability to catalyse peptidyl-tRNA hydrolysis activity. These are the presence of the GGQ motif in a flexible loop and also the structural similarity of ICT1 to the domain 3 of a class I release factor (Figure 6.1), which in conventional RFs flips out from the core to localise the GGQ motif in the peptidyl-transferase centre (PTC) [Petry *et al.*, 2005].

In this chapter ICT1 is further investigated on its possible function as a peptidyl-tRNA hydrolase. Therefore analysis will follow two main approaches that will be:

i) recombinant protein will be tested for release activity using the *in vitro* translation termination assay and

ii) the effect on the function of ICT1 harbouring a mutation within the conserved GGQ motif that is known to abolish activity will be investigated *in vitro* and *in vivo*.

6.2 Purification of recombinant ICT1

To investigate the possibility that ICT1 has retained the same activity as a class I release factor, a recombinant form of ICT1 needed to be recombinant generated, purified and tested in the *in vitro* translation termination assay. For this approach *ICT1* was cloned into pGex-6P-1 using primers #3 and #5 (Table 3.2) for cDNA amplification and *BamH*I and *Xho*I for restriction digest. This allowed a 5'-ligation of ICT1 to Glutathione-S-transferase (GST) tag, the expression of which is under an IPTG inducible promotor on the pGex-6P-1 vector. Rosetta^{TM}(DE3) bacteria were finally transformed with pGex-6P-1 carrying the GST-ICT1 fusion construct. The purification of recombinant full length ICT1 (ICT1 FL) was performed as detailed in 3.5.12. ICT1 FL was very insoluble, resulting in a low recovery of the protein in soluble fraction after sonication. Thus the amount of purified ICT1 FL was relatively low. Furthermore western blot as shown in chapter 4 (Figure 4.1) suggests a mitochondrial cleavable

target site approximately 30 aa from the N-terminus. Therefore a truncated version of *ICT1* using oligonucleotides #4 and #5 (Table 3.2) needed to be cloned in-frame at the C-terminus of the GST-tag in pGex-6P-1, which was then used for *E. coli* Rosetta™(DE3) transformation. The resulting amplicon excluded 87 nt from the 5'-end of the open reading frame, which leads to a truncation of 29 residues from the N-terminus (ICT1Δ29). The induced overexpression of ICT1Δ29-GST with a calculated molecular weight of 46 kDa showed more protein in the soluble fraction (Figure 6.2, "Input" lane 1), which could be successfully purified in higher yields than the full length version of ICT1 using the same condition of the protocol as described in 3.5.12 (Figure 6.2, compare lane 5 and 6).

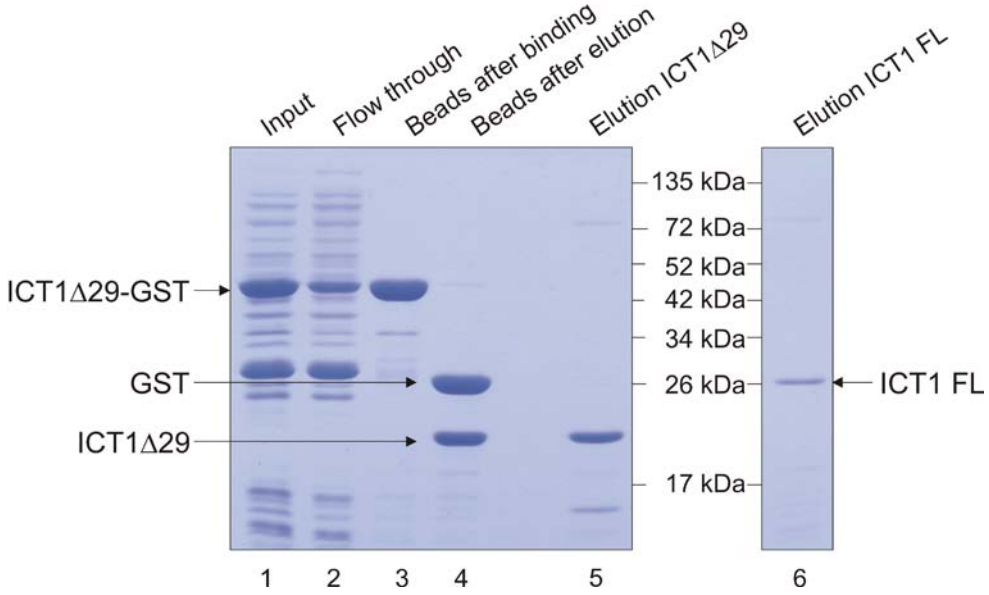

Figure 6.2: Purification of recombinant ICT1Δ29 and ICT1 full length (FL). Bacteria (OD_{600} ~ 0.4 to 0.6) were cultured at 16°C over night in the presence of 1 mM IPTG allowing overexpression of GST-ICT1Δ29 or -FL. Bacteria were sonicated and centrifuged. The soluble fraction (lane 1, Input, 5 µl of 10 ml) was subjected to equilibrated glutathione Sepharose 4B beads. The flow-through (lane 2, 5 µl of 10 ml) after the binding step showed that a reasonable amount of the fusion protein had bound to the beads (lane 3, 2.5 µl of 0.6 ml) resulting in a decreased amount of ICT1-GST in the flow-through. ICT1 was then cleaved off the GST-tag using PreScission™ Protease. The GST-tag (~ 26 kDa) stayed on the beads (lane 4), whereas ICT1 could be recovered as the elution fraction (ICT1Δ29: lane 5, 10 µl of 0.75 ml, ~ 5 µg; ICT1 FL: lane 6, 10 µl of 0.75 ml, ~ 2 µg).

In general it was noticed that the overexpression of ICT1-GST (FL and Δ29) caused some problems in the growth rate of the bacteria, whereas similar approaches to mtRF1aΔ32-GST (expressing bacteria strain was kindly provided by Dr. H. R. Soleimanpour-Lichaei) did not seem to have any change in growth pattern. The possible reason for this will be discussed later on.

6.3 ICT1 shows codon-independent, but ribosome-dependent release activity *in vitro*

To prove whether ICT1 has any release activity, 50 pmol of purified recombinant ICT1Δ29 was subjected to the *in vitro* translation termination assay using different codons in comparison to the positive control, the main mitochondrial release factor mtRF1a. For this approach mtRF1a with a truncation of 32 residues from the N-terminus (mtRF1aΔ32) was used as reported in Soleimanpour-Lichaei *et al.* (2007).

For the further analysis, the terms were simplified from ICT1Δ29 to ICT1 and mtRF1aΔ32 to mtRF1a.

For *in vitro* assay, carried out by Dr. Z. M. A. Chrzanowska-Lightowlers, 70S *E. coli* ribosomes were used with a $tRNA^{Met}$ carrying ^{3}H- radiolabelled formyl-methionine (f[^{3}H]met) in the peptidyl-tRNA (P) site and a vacant aminoacyl-tRNA (A) site. By the addition of RNA triplets, a specific codon can be added to the decoding centre. A class I release factor such as mtRF1a that has sequence specificity will recognise the stop codon and catalyse the hydrolysis of the ester bond between the f[^{3}H]met and the $tRNA^{Met}$. As shown in the graph below (Figure 6.3) mtRF1a showed release activity in the presence of UAA and UAG codons in the decoding centre, whereas other codons such as UGA (that is recognised as a stop codon in *E. coli*, but encodes for Trp in human mitochondria) UGG (encoding Trp in *E. coli* and human mitochondria), AGA or AGG (both encodes Arg in *E. coli*; no tRNA or protein recognises these codons in human mitochondria, but they are critical features for -1 frameshift within the human mitochondrial ribosome) could not cause the hydrolysis of the f[^{3}H]met from the $tRNA^{Met}$ in the presence of mtRF1a. Not surprisingly in the absence of the codon mtRF1a, as a codon-dependent release factor, did not show activity in the *in vitro* assay. In contrast ICT1 showed release activity independent of the sequence of the A-site, and also without a codon ICT1 was able to cause hydrolysis of the f[^{3}H]met from the $tRNA^{Met}$. In the absence of a 70S ribosome however, neither mtRF1a nor ICT1 can release the f[^{3}H]met from the f[^{3}H]met-$tRNA^{Met}$, suggesting that ICT1 has a codon-independent, but ribosome-dependent release activity *in vitro*.

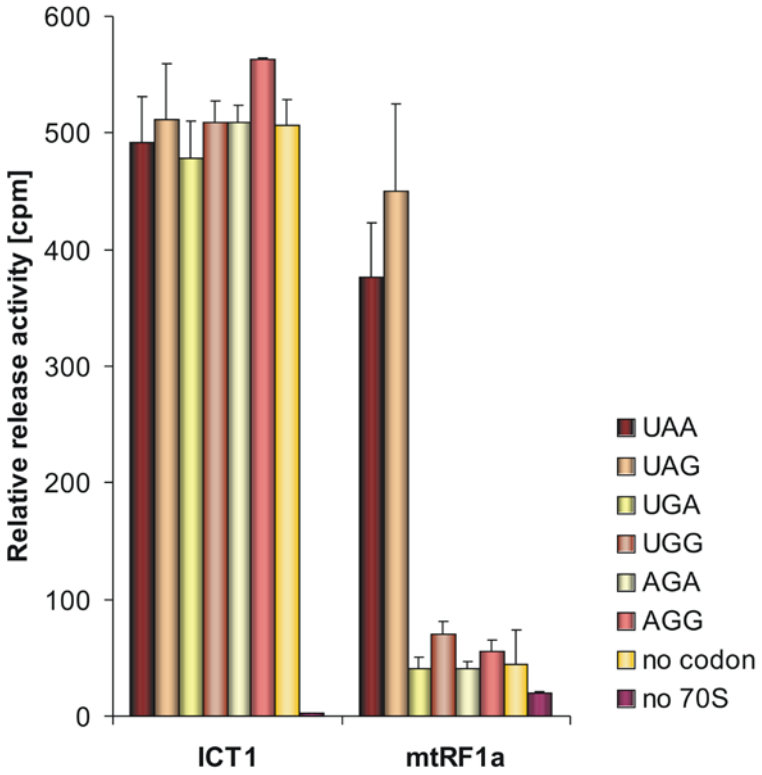

Figure 6.3: Release activity of ICT1 and mtRF1a in the *in vitro* translation termination assay. 50 pmol of recombinant ICT1 or mtRF1a were used in this *in vitro* assay, in the presence or absence of *E. coli* 70S ribosomes (5 pmol). Those ribosomes were programmed with P-site f[^{3}H]met-tRNA^{Met} and A-site codons as indicated. The reactions without 70S particle contained UAA as a stop codon. Non-limiting amounts of RNA triplet (400 pmol) were used in this assay. The relative release activity was measured as hydrolysis of the radiolabelled f[^{3}H]met from its tRNA^{Met} and is shown in counts per minute [cpm]. Means and standard deviations were calculated from at least three experiments ($n \geq 3$).

Another difference between the activity of ICT1 and mtRF1a in the *in vitro* translation termination assay is the necessity of the addition of ethanol to the reaction. Usually the class I release factor like mtRF1a needs the presence of 10 % ethanol as reported in Tate and Caskey (1990) or Soleimanpour-Lichaei *et al.* (2007). Ethanol probably helps to loosen the structure of the ribosome and more easily allows the entrance of the RF and therefore its conformation change within the ribosome. In the absence of ethanol mtRF1a does not show any significant release activity in the presence of UAG stop codon (Figure 6.4). In contrast ICT1 does not seem to require ethanol in this *in vitro* assay. This protein showed release activity in the presence, but also in the absence of 10% ethanol (Figure 6.4). It is possible that ICT1 is small enough to enter the ribosome without loosening its structure and conformational changes of ICT1 are not necessary to go in an active formation. Another possibility is that ICT1 acts from another position within the ribosome and not directly in the A-site as a conventional class I release factor. These observations will be discussed at a later point in this chapter.

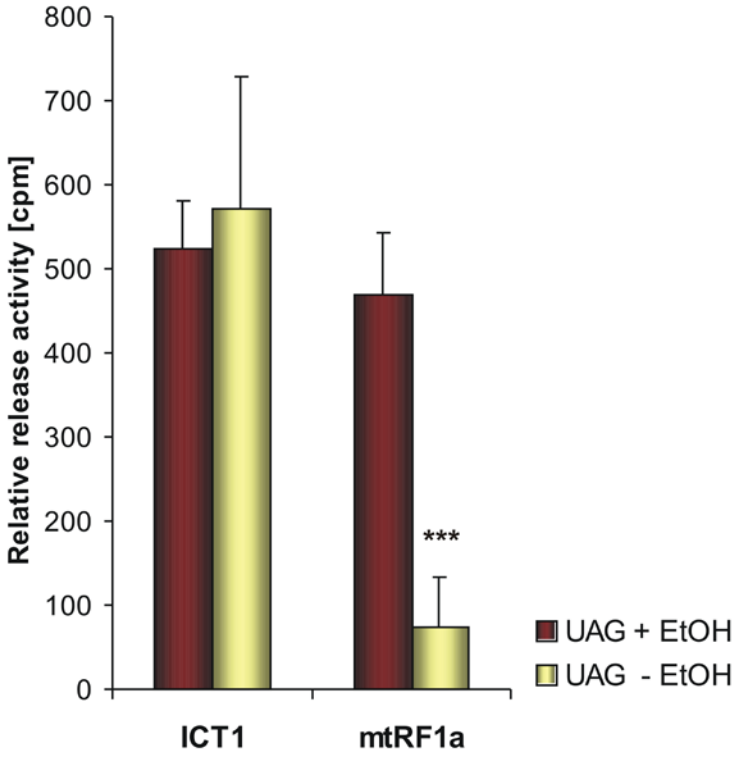

Figure 6.4: Release activity in the presence and absence of ethanol on UAG stop codon. The *in vitro* translation termination assay was performed with 50 pmol recombinant protein (ICT1 or mtRF1a), 5 pmol 70S ribosomes and 400 pmol UAG codon in the presence (red bars) or absence (yellow bars) of 10% ethanol (EtOH). The graph shows the results of 3 repeats (n = 3, $p < 0.001$***).

6.4 A mutation in the GGQ motif causes an activity loss of ICT1 *in vitro*

From the translation termination assay it seems that ICT1 has a peptidyl-tRNA hydrolase activity, which is codon-independent, but ribosome-dependent. Reason for this activity is probably the highly conserved GGQ motif in a flexible loop, which in the case of standard class I RFs is usually flipped out with respect to domain 3 and thus located in the peptidyl-transferase centre (PTC) within the ribosome. Reports from several groups [Frolova *et al.*, 1999; Mora *et al.*, 2003; Shaw and Green 2007] describe that a mutation in the GGQ motif, especially of the first or second glycine causes a loss of hydrolysis activity and it is therefore absolutely essential for the activity of a class I RF. To determine whether the GGQ motif of ICT1 has retained functionality, it was mutated by using QuikChange® II Site-Directed Mutagenisis Kit from Stratagene as described in 3.3.8. The primers listed in table 3.3 were used to generate a mutation at position 88 G → A (AGQ mutant) or at position 89 G → S (GSQ mutant), respectively.

As a template the pGex-6P-1-ICT1Δ29-GST was used to generate GST fusion products of the mutants. Purified recombinant ICT1Δ29 carrying the individual mutations were then tested in the *in vitro* translation termination assay with the GGQ wildtype as a positive control. As presented below (Figure 6.5) ICT1 mutants showed no hydrolysis activity in this assay, suggesting that the GGQ motif is necessary for the release activity of ICT1 at least *in vitro*.

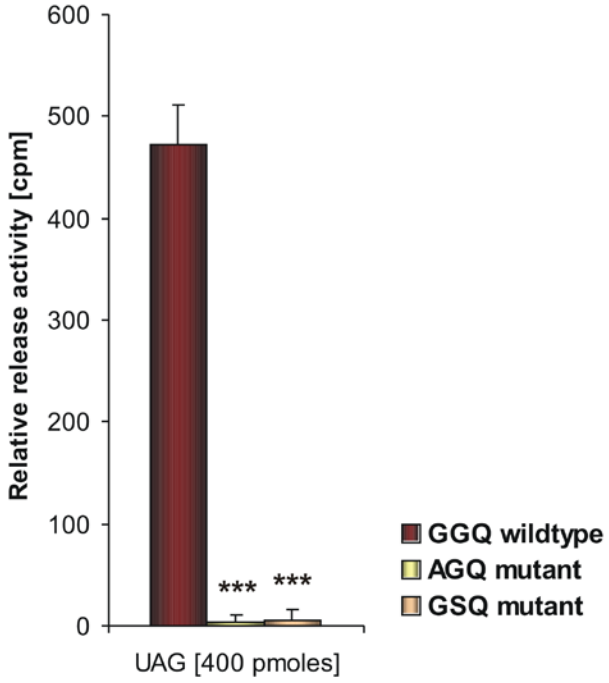

Figure 6.5: Mutation in the GGQ motif causes loss of hydrolysis activity of ICT1 *in vitro*. Purified recombinant ICT1 with mutation within the GGQ motif (AGQ- and GSQ mutant) was tested in the *in vitro* translation termination assay in the presence of 400 pmol UAG codon and 5 pmol 70S ribosomes. ICT1-GGQ wildtype was used as a positive control. (n = 3, GGQ: 100%, AGQ: 0.8%, GSQ: 1.1%, p = 0.0001***)

6.5 Mutation in the GGQ motif does not effect the interaction of ICT1 with the mitochondrial ribosome

So far it has been shown that ICT1 can act as a codon-independent peptidyl-tRNA hydrolase within a 70S *E. coli* ribosome and that a mutation in the conserved GGQ motif results in the loss of release activity *in vitro*. What happens *in vivo*? The ribosome used in the *in vitro* assay is a 70S particle and bacterial ribosomes are different in several aspects when compared to the 55S mammalian mitochondrial ribosome as described in 1.7.1 [reviewed in Koc *et al.*, 2010]. Therefore it is not the natural environment for ICT1, where it could be already shown that it has become recruited into the mitochondrial ribosome in human. The question is, has ICT1 retained its

activity also within the 55S particle or has this activity become redundant once ICT1 has become an integral component of the mitochondrial ribosome? To address those issues ICT1 mutants needed to be investigated *in vivo*. Therefore pcDNA5/FRT/TO-ICT1-FLAG was used as a template for site directed mutagenesis as it was done for pGex-6P-1-ICT1Δ29-GST using the same primers and conditions to then generate stable transfected HEK293T cells expressing ICT1^{AGQ}-FLAG and ICT1^{GSQ}-FLAG. After confirming by sequencing that the constructs carried the mutation, HEK293T cells were transfected with those plasmids as described in 3.1.5. Individual clones were then tested for overexpression of the FLAG-tagged proteins before further experiments were carried out. The first question that needed to be answered was whether the mutation in the GGQ motif causes problems in the integration of ICT1 into the mitochondrial ribosome. Therefore immunoprecipitation via the FLAG tag as described before was carried out for ICT1 mutants in comparison to ICT1 wildtype. The resulting data were analysed by silver staining and western blot as shown in figure 6.6.

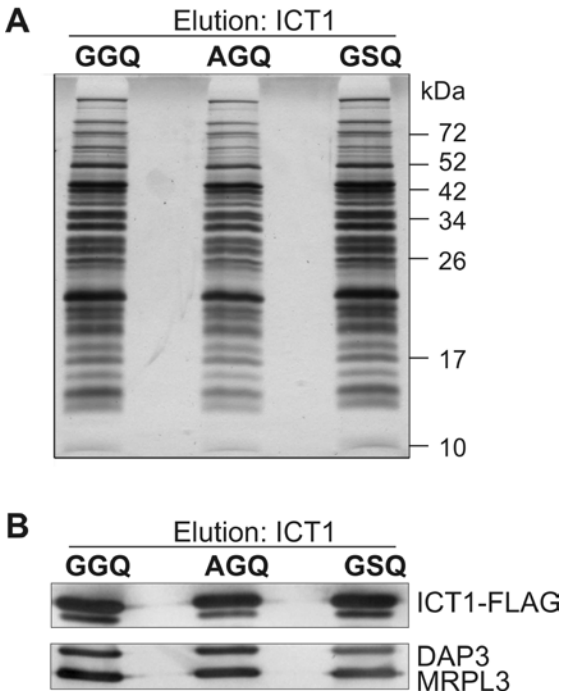

Figure 6.6: ICT1 GGQ mutants can integrate into the mitochondrial ribosome. HEK293T cells were transfected with pcDNA5/FRT/TO-ICT1-FLAG carrying the AGQ or GSQ mutation. Cells were induced with 1 µg/ ml tetracycline for 3 days and mitochondrial lysates (3 mg) were subjected to immunprecipitation via FLAG tag. The elution fractions (10% each) were separated by SDS-PAGE (15%) and further analysed by silver staining (A) or western blot (B). The western blot membrane was probed with antibodies against DAP3 (28S SSU) and MRPL3 (39S LSU) to determine the level of co-immunoprecipitated ribosomal complexes by ICT1 mutants (AGQ and GSQ) compared to the wildtype (GGQ). FLAG antibodies were used to ensure the presence of the FLAG tagged proteins in the elution fraction at relative similar level.

Silver staining of the elution fractions did not show any significant differences in the pattern of the mutants compare to the wildtype (Figure 6.6 A). Western blot analysis showed strong signals for DAP3 and MRPL3 for all three strains (Figure 6.6 B). Those results suggest that ICT1 mutants are able to interact with the mitochondrial ribosome comparable to the wildtype.

To be certain that it is not just an artefact of the conditions used in the immunoprecipitation protocol, especially concerning about the 3 h incubation time, cell lysate expressing the GGQ mutation were subjected to isokinetic sucrose gradient. The results were analysed by western blot, presented in figure 6.7.

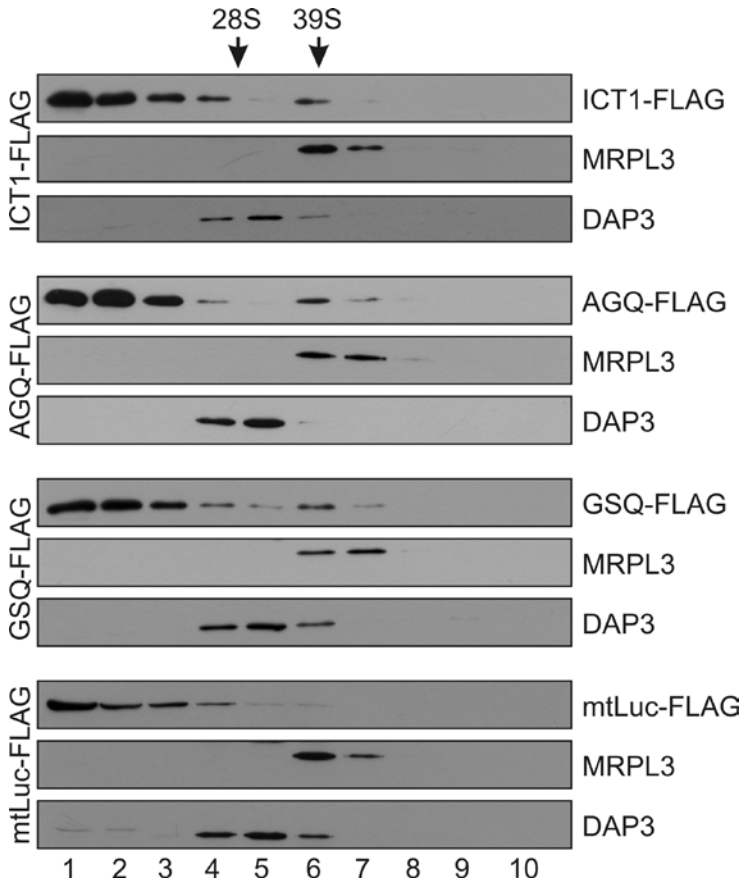

Figure 6.7: ICT1 GGQ mutants co-sediment with 39S LSU on isokinetic sucrose gradients. HEK293T cells expressing wildtype or mutant derivatives of ICT1-FLAG were induced with 1 µg/ ml tetracycline. After 3 days cells were harvested and lysates (700 µg) were subjected to isokinetic sucrose gradient. The fractions (1-10) were analysed by western blot using antibodies against MRPL3, marker for the 39S LSU, and DAP3, component of the 28S SSU. The distributions of the FLAG tagged proteins within these gradients were determined by probing the western blot membranes with FLAG antibodies. The mtLuc-FLAG, treated in the same way, was used as control for artefacts caused by overexpression.

It was shown earlier in figure 5.5 that ICT1-FLAG co-migrated with MRPL3 in fraction 6, indicating the position of 39S LSU. Due to the overexpression, in these gradients a lot of the ICT1-FLAG protein was also seen in the earlier fractions 1 to 4. Testing the AGQ

and GSQ FLAG tagged mutant in such gradients, a similar profile was observed, meaning the ICT1 mutants were also associated with the 39S LSU. As a negative control cell lysate of overexpressed mtLuc-FLAG was also subjected to a sucrose gradient. There mtLuc-FLAG was localised in fraction 1 to 4, but no signal in lane 6 was detected, which supports that the co-sedimentation of ICT1 mutants with the 39S LSU is not caused by the overexpression of any protein or the FLAG tag, respectively.

6.6 ICT1^{GSQ} mutant failed to suppress the ICT1 depletion phenotype *in vivo*

To analyse the effect of the mutation in ICT1-FLAG on the level of cell viability, it had to be investigated at first whether the overexpression of ICT1-FLAG wildtype itself has any effect on cell growth in comparison to a control. No inhibition in growth in standard glucose containing growth media was noticed for the ICT1 overexpressor. Therefore HEK293T cells expressing ICT1-FLAG were induced for 6 days, cultured in glucose-free media, supplemented with 0.9 mg/ ml galactose. Using galactose media for this kind of analysis forces the cells to generate ATP via oxidative phosphorylation and thus growth defects as a result of mitochondrial dysfunction are more obvious than in glucose media. For the experiment cells were pre-cultured in galactose media for 2-3 days prior to induction with 1 µg/ ml tetracycline. After 3 and 6 days overexpression cell growth was monitored by cell counting. As shown in the graph below (Figure 6.8) the overexpression of ICT1-FLAG is causing a decrease in cell number after 3 days, which is even more obvious and statistically significant after 6 days in comparison to untransfected HEK293T wildtype cells (WT) in galactose media.

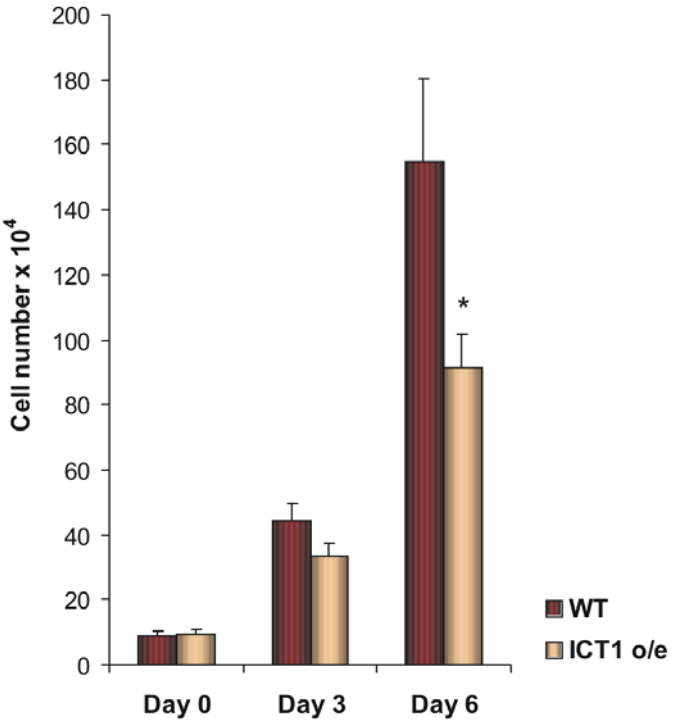

Figure 6.8: Overexpression of ICT1-FLAG causes growth defect of HEK293T cells in galactose containing media. HEK293T cells untransfected (wildtype, WT) or inducible expressing ICT1-FLAG (ICT1 o/e) were cultured in glucose free media, supplemented with galactose, and induced with 1 µg/ ml tetracycline. Cells were counted prior to induction (Day 0) and after 3 and 6 days overexpression. The graph represents the means and standard derivations of 3 experiments (n = 3; * significant, p = 0.0161).

Because there was clearly a growth defect caused by overexpression ICT1 wildtype it was necessary to manipulate the experiment in order to express only endogenous levels of mutant ICT1. Therefore different concentrations (5 nM, 10 nM and 15 nM) of siRNA B against *ICT1* were used to deplete the endogenous ICT1 from the cells and also to titrate the level of ICT1 overexpressors to a protein level equivalent to the usual endogenous form. First, cells were cultured in galactose media for at least 2 days, and then induced for 1 day prior to siRNA transfection. After siRNA application cells were cultured in the presence of 1 µg/ ml tetracycline for 3 days. Cell lysates were analysed by western blot and the protein levels were measured using Image-Quant software. The results are presented in figure 6.9, where western blot showed a slightly different migration of ICT1-FLAG in comparison to the endogenous protein. This phenomenon was noticed in previous experiments and was also seen with other FLAG tagged proteins. The reason for this is probably the positive charge of the FLAG tag, rather than the additional size of the octapeptide.

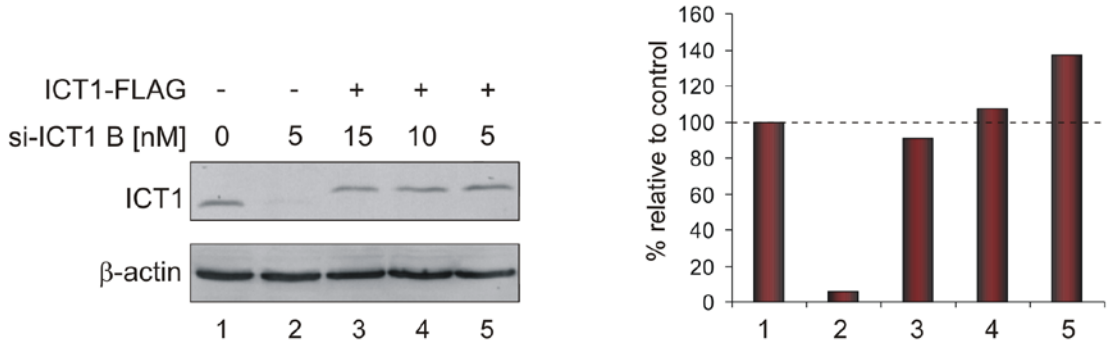

Figure 6.9: Titration of overexpressed ICT1-FLAG protein using different concentration of si-ICT1 B. HEK293T untransfected wildtype (1 and 2) or ICT1-FLAG expressing (3 to 5) cells were cultured in the presence of different amounts of si-ICT1 B (5 nM: 2 and 5; 10 nM: 4; 15 nM: 3) for 3 days and induced for 4 days with 1 µg/ ml tetracycline. Cell lysates (45 µg) of overexpressor were compared on the relative protein level via western blot to non treated wildtype cells (1). The ICT1 protein level was measured using Image-Quant software (right panel). β-actin was used as a loading control.

From the control experiment as shown above it was decided that a concentration of 10 nM gave reasonable depletion of endogenous ICT1 and a good down regulation of the ICT1 overexpressor to the relative endogenous level (Figure 6.9, lane 4). Thus for the following experiment HEK293T cells, cultured in galactose media, were induced with 1 µg/ ml tetracycline for 1 day prior to transfection with 10 nM si-ICT1 B using lipofectamine to analyse the effect of the GGQ mutations. If the GGQ motif is really essential for the function of ICT1 *in vivo*, it was expected that the overexpression of the GGQ mutants would not rescue the phenotype caused by depletion of endogenous ICT1. The graph in figure 6.10 presents the result of cell counts taken after 3 days and 6 days transfection. There is a growth defect of ICT1 depleted cells in comparison to the control wildtype HEK293T (WT) treated with NT siRNA, as was observed before in HeLa cells (Figure 6.10, compare 1 and 2: 6 days, n = 3, p = 0.0008). The overexpression of ICT1^{GGQ}-FLAG (ICT1 o/e, 3) showed a very significant suppression of the ICT1 depleted cell phenotype (compare 3 and 2: 6 days, n = 3, p = 0.004). The relative amount of ICT1 protein was analysed by western blot after 3 days (Figure 6.10, right panel), where a lower level was detected in the ICT1^{GGQ}-FLAG overexpressor (lane 3, ~ 48.9%) in comparison to the endogenous level (lane 1). This might be also the reason, why the growth phenotype could be just rescued approximately to 46%. Surprisingly a similar result was also observed using the ICT1^{AGQ}-FLAG mutant (AGQ o/e, 4), where ICT1^{AGQ}-FLAG mutant was shown a rescue of about 43%, suggesting that ICT1^{AGQ}-FLAG can also suppress the phenotype of ICT1 depleted cells (compare 4 and 2: 6 days, n = 3, p = 0.0089), whereas in the case of the ICT1^{GSQ}-FLAG mutant no rescue could be noticed (compare 5 and 2: 6 days, n = 3, p = 0.3245; 5 and 3: 6 days, n = 3, p = 0.0057).

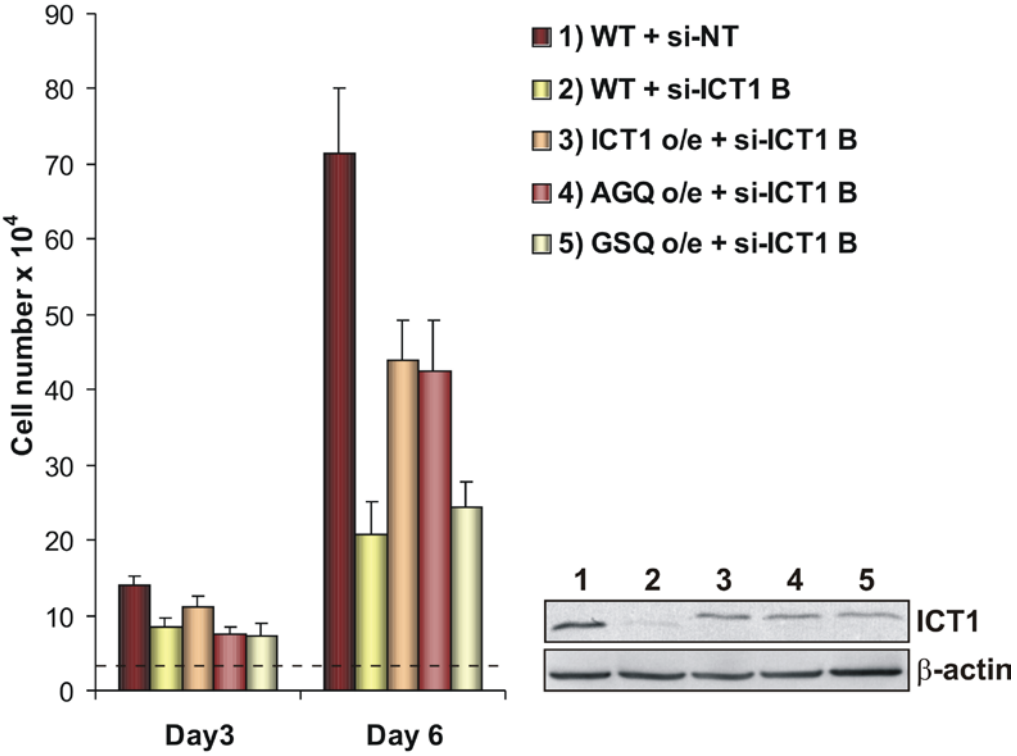

Figure 6.10: ICT1^{GSQ} mutant is not able to rescue the phenotype caused by endogenous ICT1 depletion. HEK293T cells (wildtype (WT; 1 and 2) or expressing ICT1 derivatives (3 to 5)) were cultured in galactose media, transfected with 10 nM si-NT (1) or si-ICT1 B (2 to 5), respectively. The overexpressors (3 to 5) were induced with 1 µg/ ml tetracycline 1 day prior to transfection and further cultured in the presence of inducer. Cell growth was monitored by cell counting after 3 days and 6 days transfection. For each transfection 3x 10^4 cells were used, marked as dotted line is starting cell number. The relative protein level was analysed via western blot after 3 days (25 µg cell lysates, right panel). ICT1 protein levels were measured using Image-Quant software (1: 100,0%, 2: 9,2%, 3: 48,9%, 4: 42,1%, 5: 41,1%). β-actin was used as loading control.

Interestingly the two mutants gave different results *in vivo*, whereas *in vitro* both lost the hydrolysis activity. Possible reasons will be discussed later on, but for further investigations only the GSQ mutant was used.

In a direct repeat of the experiment described above cells were counted after 4 days prior to cell lysate preparation. Those cell counts showed a 102% rescue of ICT1 depletion by the ICT1^{GGQ}-FLAG overexpressor (Figure 6.11, compare 3 to 2: n = 3, p = 0.0036; 1 to 2: n = 3, p = 0.0005), whereas the ICT1^{GSQ}-FLAG mutant failed again to suppress the phenotype (~ 6% “rescue”) (Figure 6.11, compare 4 to 2: n = 3, p = 0.8101; 4 to 1: n = 3, p = 0.0004). Thus the ability to suppress the phenotype caused by ICT1 depletion is very significant comparing the ICT1^{GGQ} wildtype and the ICT1^{GSQ} mutant (Figure 6.11, compare 3 to 4: n = 3, p = 0.0036).

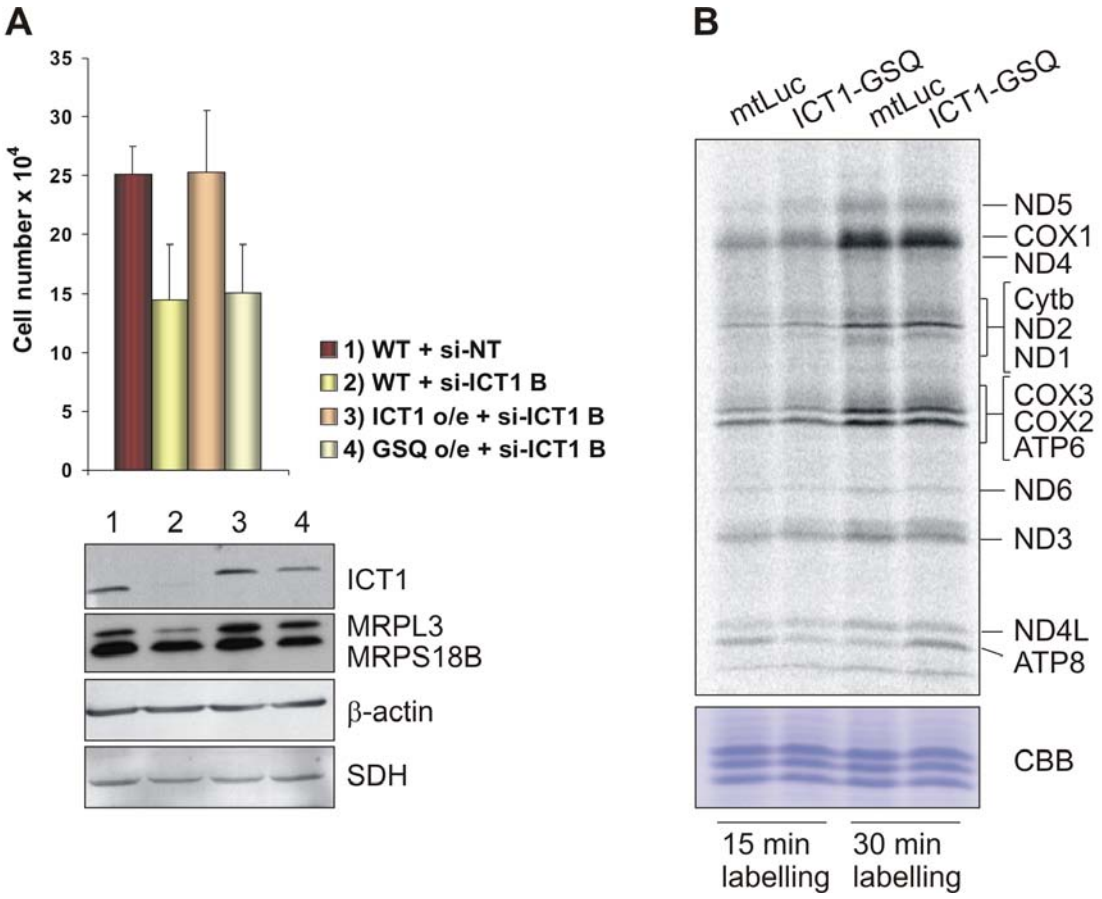

Figure 6.11: Further investigations of ICT1^{GSQ}-FLAG mutant A) HEK293T cells (WT: 1 and 2; ICT1^{GGQ} wildtype: 3; ICT1^{GSQ} mutant: 4) were cultured in galactose media and treated with 10 nM si-NT (1) or si-ICT1 B (2 to 4). Cell counts were taken after 4 days siRNA transfection and 5 days induction of ICT1 overexpressors (3 and 4). Cell lysates were analysed by western blot and ICT1 protein level was measured using Image-Quant software. β-actin and SDH were used as loading control. Western blot membrane was also probed for MRPL3 and MRPS18B to determine the relative level of ribosomal defect caused by ICT1 depletion. **B)** ^{35}S-met *de novo* synthesis of ICT1^{GSQ}-FLAG mutant in comparison to mtLuc-FLAG. Cells were labelled for 15 min and 30 min with ^{35}S-met. 50 µg of each sample were separated on a 15% PAG. After exposure on Phosphor-Image screen to visualise radiolabelled proteins, the gel was stained with CBB to prove even loading (lower panel).

In this case the relative protein level was closer to the endogenous form (ICT1^{GGQ}-FLAG: ~ 120%; ICT1^{GSQ}-FLAG: ~ 60%), probably caused by different batches of tetracycline used in those experiments. This reflects also that this approach is not the optimal way forward. Certainly it would be better to use siRNA that targets the UTR or to generate an overexpressor with silent mutations within the siRNA region, thus rendering the introduced *ICT1* sequence to be unaffected by the siRNA that targets the endogenous mRNA. However, the experiment could clearly show that GSQ mutant was not able to suppress the phenotype caused by ICT1 depletion.

Additionally the steady state level of mitochondrial ribosomal proteins were analysed by western blot and again there was a decrease in MRPL3 as it was seen before in ICT1 depleted cells (Figure 4.4), whereas MRPS18B, a component of the 28S SSU seems

to be unaffected. As it was discussed before the ICT1 depletion causes an assembly defect of the 39S LSU and therefore results in a decreased stability of MRPL3, a good marker therefore for the intact LSU. The defect in 39S LSU conformation caused by ICT1 depletion in WT seems to be rescued by the ICT1^{GGQ}-FLAG wildtype overexpressor, leading to a higher protein level of MRPL3 (Figure 6.11 A, lower panels, compare 3 and 2). Using the ICT1^{GSQ}-FLAG mutant gave a similar result (compare 4 and 2), suggesting that the mutant is able to suppress the defect on the level of mitochondrial ribosome assembling, which is in agreement with the fact that ICT1 mutants could be integrated into the mitochondrial ribosome as is the ICT1 wildtype.
To investigate whether the loss of peptidyl-tRNA hydrolysis activity is causing problems in mitochondrial protein synthesis, ICT1^{GSQ}-FLAG was also analysed by ^{35}S-met metabolic labelling in comparison to mtLuc-FLAG. Therefore cells were induced for 3 days and labelled for 15 min or 30 min, respectively as described in 3.5.7. The resulting data are shown in figure 6.11 B. There was no visible effect on *de novo* synthesis, supporting the idea that defect in mitochondrial protein synthesis is only caused by the loss of 55S particle and not by the loss of peptidyl-tRNA hydrolysis activity in ICT1 depleted cells.
However the ICT1^{GSQ} mutant showed clearly a loss of cell viability and thus it is highly likely that the GGQ motif of ICT1 is functional.

6.7 Discussion

The results presented in this chapter show evidence that ICT1 has maintained its peptidyl-tRNA hydrolysis activity. Using recombinant purified ICT1 protein in the *in vitro* translation termination assay showed that ICT1 is able to catalyse the hydrolysis of the ester bond between the tRNA (tRNA^{Met}) and the "peptide-chain" (f[^{3}H]met) at least *in vitro*. This activity was shown to be codon-independent, but ribosome-dependent (Figure 6.3). Those results are in agreement with sequence/ structure of the ICT1 protein, where it was shown in Figure 6.1 that the tip of the α5 helix and the PXT (or SPF) motif, which are crucial for codon recognition, are missing in ICT1. The presence of a GGQ motif in a flexible loop however classifies ICT1 as a member of the class I release factor family. It was proposed that the GGQ motif mimics the CCA motif of the tRNA within the A-site [reviewed in Youngman *et al.*, 2008]. Both are causing an induced fit mechanism promoting a conformational change within the ribosome, allowing new peptide bond formation (tRNA) or peptidyl-tRNA hydrolysis (release factor), respectively. The presence of the release factor with the GGQ motif within the

ribosome allows therefore the nucleophilic attack in the peptidyl-transferase centre and thus the hydrolysis of the ester bond between the P-site tRNA and the peptide chain [Schmeing *et al.*, 2005]. It is therefore not the class I release factor, which hydrolyses the peptidyl-tRNA, it is actually the ribosome. Therefore the GGQ alone is not able to hydrolyse the ester bond, only within the ribosome at the PTC can it catalyse the hydrolysis. Therefore the results of the ribosome-dependent hydrolysis activity by ICT1 stay in agreement with a functional GGQ motif.

Furthermore it was shown that a mutation in the highly conserved GGQ motif (GGQ → AGQ or GGQ → GSQ) causes a loss of the hydrolysis activity of ICT1 at least *in vitro* (Figure 6.5). However, the conditions used in the *in vitro* assay are quite different from the normal physiological environment of ICT1. As it was shown in the previous chapter ICT1 has been recruited into the 55S mitochondrial ribosome which as already described (section 1.7.1) is different in many aspects to the 70S bacterial ribosome that is used in the *in vitro* assay. To be sure that the GGQ motif is indeed functional also *in vivo,* ICT1 with mutation within this motif were tested in cell culture. At first it was shown that a GGQ mutation does not affect the integration of ICT1 in the mitochondrial ribosome (Figures 6.6 and 6.7). With siRNA technology the endogenous ICT1 was depleted and expressed ICT1-FLAG wildtype or the mutants were tested for their ability to suppress the phenotype caused by ICT1 depletion. Surprisingly the two GGQ mutants gave different results: the GSQ failed to suppress the phenotype caused by ICT1 depletion whereas the expression of the AGQ mutant showed a level of rescue similar to the ICT1 wildtype (Figure 6.10). The reason for the difference could be the 55S mitochondrial ribosome itself that is as already said different from its bacterial counterpart. Shorter ribosomal RNAs and additional proteins make it more porous than the 70S particle. As shown by Schmeing *et al.* (2005) the induced-fit mechanism within the ribosome caused by a tRNA or a class I release factor facilitates a conformation change of the ribosomal RNA and allows nucleophilic attack. Maybe ICT1 within the 55S ribosome works in a slightly different fashion. To investigate this possibility further it would be an enormous benefit if the position of ICT1 within the mitochondrial ribosome would be known.

However, it was clearly shown that the GSQ mutant was not able to rescue the phenotype caused by the ICT1 depletion (Figures 6.10 and 6.11), even if it was able to be integrated into the mitochondrial ribosome. This suggests that the GGQ motif is indeed essential for the function of ICT1 within the ribosome. It could be also shown by Shaw and Green (2007) that mutation of the second glycine has more effect on function than mutation of the first one. They demonstrated that the AGQ variant caused

loss in catalytic activity of 800-fold, whereas the GAQ mutation leaded to a decrease of 3300-fold.

Another point that is in agreement that the GGQ motif is functional, catalysing hydrolysis activity, is the actual growth rate of the ICT1 wildtype overexpressor. The overexpression of ICT1^{GGQ}-FLAG in galactose containing media caused a significant decrease in growth in comparison to the control. The reason for this could be that free ICT1 can go spontaneously into the A-site and release the nascent peptide chain in a codon-independent manner, as it was shown *in vitro*. Therefore a balanced concentration of ICT1 is crucial for cell viability. An inhibition in growth was also noticed when ICT1 was overexpressed in bacteria. Again it is reasonable to assume that a spontaneous hydrolysis of the peptidyl-tRNA catalysed by ICT1 can be the reason. Those facts also suggest that the conserved GGQ motif in ICT1 is indeed functional.
Concluding so far it was shown that ICT1 has ribosome-dependent but codon-independent peptidyl-tRNA hydrolase (PTH) activity *in vitro*. The highly conserved GGQ motif is crucial for the function of ICT1 *in vitro* and *in vivo.*

What can be the function of a ribosome bound codon-independent PTH? Besides the class I release factors there exists another class of PTH that do not have a GGQ motif and act on soluble peptidyl-tRNAs, dropped off the ribosome when elongation is disrupted [reviewed in Das and Varshney, 2006]. Those soluble peptidyl-tRNA hydrolases have two classes: the PTH1 in eubacteria and the PTH2 in archaea. They are esterases that cleave the ester bond between the C-terminus of the nascent peptide chain and the 2'OH end of the tRNA. So far there is no clear evidence of a mitochondrial PTH, but there are suggestions of candidates [De Pereda *et al.*, 2004.]. Those PTHs are essential to recycle peptidyl-tRNAs, which are released from a stalled ribosome. Sometimes ribosomes do not reach a stop codon, for example when mRNA has been degraded and the termination codon is absent. Those stalled complexes need to be recycled. Singh *et al.* (2008) proposed that those pre-termination complexes are recycled by the ribosome recycling factor (RRF) and the elongation factor G (EFG(2)) (Figure 6.12 B). The specific interaction between the two factors within the ribosome leads to a transient separation of the ribosomal subunits and to the exposure of the initiation factor 3 (IF3) binding site on the small ribosomal subunit. The binding of IF3 to the SSU leads to complete disassembly of the ribosome into the subunits and to the release of peptidyl-tRNAs, which are then recycled by the PTH (figure 6.12 B). An accumulation of peptidyl-tRNAs after inactivation of PTH was shown to be lethal in *E. coli* [Menninger, 1978]. It has been further demonstrated that those peptidyl-tRNA

hydrolases can neither act on the ribosome nor on initiator $tRNA^{fMet}$ [Das and Varshney, 2006]. The perfect substrates for those peptidyl-tRNA hydrolases are peptidyl-tRNAs containing four to five residues. What recycles peptidyl-tRNAs with longer nascent peptide chains? What happens if the ribosomal A-site runs out of RNA triplets during elongation with a peptidyl-tRNA that has a quite long peptide chain attached, which starts already folding outside the ribosome? Those “long” chain peptidyl-tRNAs can not be dropped off the ribosome so easily as the “short” ones. One mechanism that could be used under those circumstances in bacteria is the tmRNA system that mimics both tRNA and mRNA to allow coordinated translation termination and degradation of the tagged nascent peptide and leads therefore to recycling of those stalled ribosomes and peptidyl-tRNAs [reviewed in Moore and Sauer, 2007]. In mitochondria however, there is no evidence that such a tmRNA exists. This means those stalled complexes with long chain peptidyl-tRNAs must be rescued in a different way. After recycling stalled ribosomes that requires RRF (mtRRF), EFG (mtEFG2) and IF3 (mtIF3), the peptidyl-tRNA will be stuck in the ribosomal large subunit, because it can not leave the ribosome with the tRNA through the tRNA exit or the polypeptide exit tunnel/ -site (Figure 6.12 C). Thus a ribosome-dependent PTH (ICT1, Figure 6.12 C) has to catalyse the hydrolysis of the peptidyl-tRNA to recycle the ribosomal large subunit and the peptidyl-tRNA to be available for the next translation round. ICT1 as a member of the mitochondrial ribosomal large subunit carries all the features that would be required to act as such a ribosome-dependent PTH and is therefore proposed to be involved in the rescue of stalled ribosomes/ recycling of the 39S LSU. This PTH activity can not be present all the time, because this would result in an overall translation inhibition caused by uncoordinated hydrolysis of peptidyl-tRNAs. Therefore a specific signal must occur, probably a conformational change within the 39S LSU after the disassembling of the 55S monosome into its subunits that allow ICT1 to act as a PTH only under those specific circumstances.

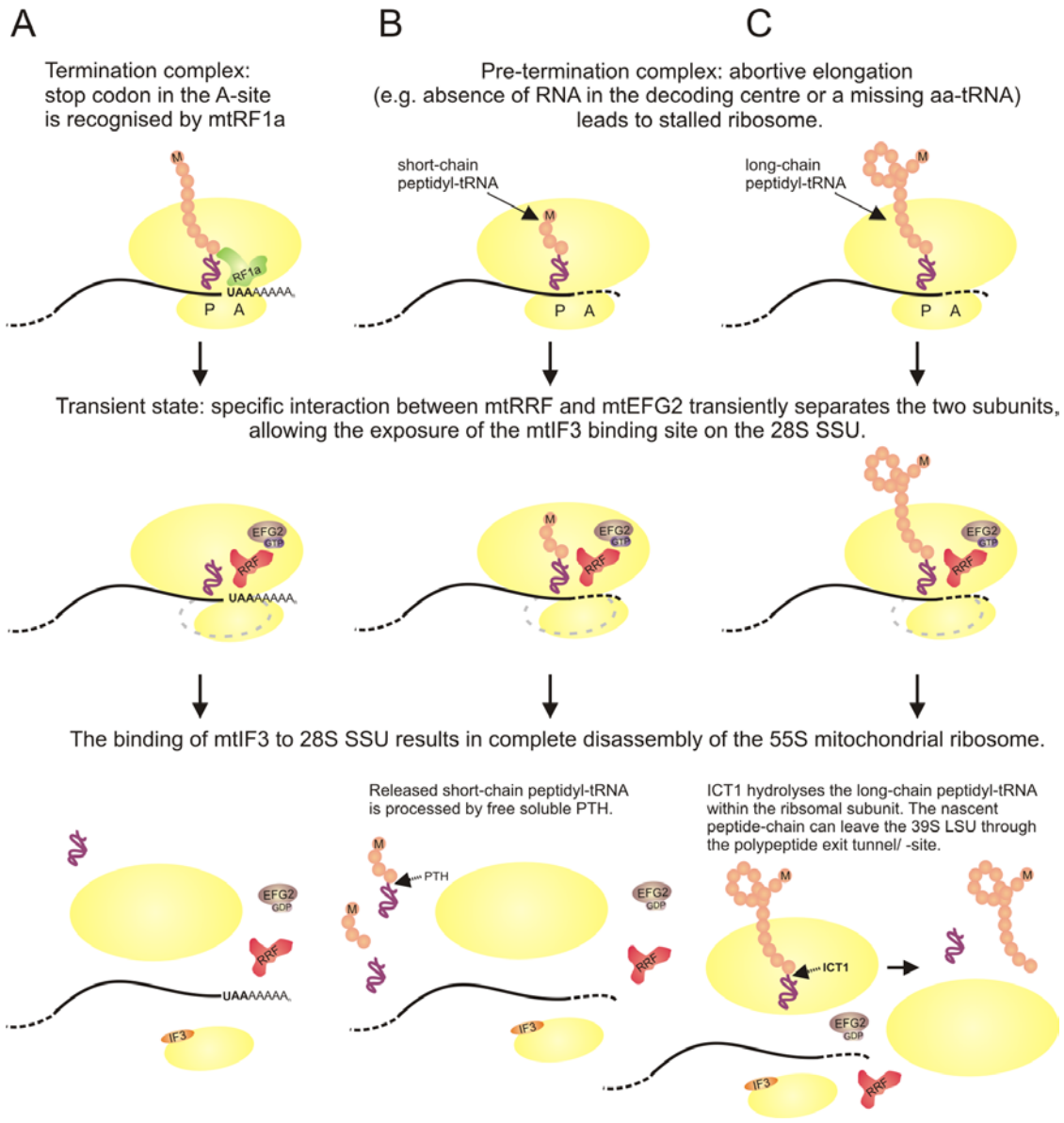

Figure 6.12: Proposed model of the function of ICT1 as ribosome-dependent peptidyl-tRNA hydrolase (PTH) involved in the recycling-process of stalled ribosomes in human mitochondria. A) When the ribosome reaches a stop codon, mtRF1a (RF1a; green) recognises this stop codon and will catalyse the hydrolysis of the peptide chain from the tRNA. The nascent peptide chain can leave the ribosome through the polypeptide exit tunnel/ -site. The post-termination complex is then further recycled by mtRRF (RRF; red) and mtEFG2 (EFG2; brown). The binding of mtIF3 (IF3; orange) to the small ribosomal subunit completes the disassembly of the 55S and inhibit the reassembling of the subunits. **B)** and **C)** Abortive elongation can occur and lead to stalled ribosomes. The reason for this can be e.g. degradation of mRNA and thus no RNA triplet in the decoding centre or no sufficient supply of amino-acylated tRNAs to the A-site. RRF and EFG2 interact with pre-termination complex. The interaction will result in a transient state, where IF3 binding site on the ribosomal small subunit is exposed. The binding of IF3 results to the complete disassembly of the ribosome into its subunits. Short-chain peptidyl-tRNAs will be released by this mechanism and can be further processed by soluble peptidyl-tRNA hydrolase (PTH) (B). In contrast long-chain peptidyl-tRNAs cannot leave the ribosome with the tRNA through the tRNA exit or through the polypeptide exit tunnel/ -site. This leads to aborted large ribosomal subunit with stuck peptidyl-tRNAs that need to be released by a ribosome-dependent codon-independent PTH: ICT1 (C). (Proposed model is based on Singh *et al.*, 2008)

How could this hypothesis be tested? Experiments using human cells expressing GSQ-mutant failed to detect an accumulation of peptidyl-tRNAs. Prof. U. Varshney (Bangalore, India) who works on peptidyl-tRNAs in *E. coli* explained that it is difficult to detect those peptidyl-tRNAs under such conditions. In the bacterial system the overexpression of AGA-minigenes or *ung*-stopless (uracil DNA glycosylase gene) constructs can be used as advantageous tool to induce artificial a high production of peptidyl-tRNAs, which can be then detected [Singh *et al.*, 2008]. An overexpression of such constructs in human mitochondria is not possible to date. Therefore collaboration with the laboratory of Prof. U. Varshney was initiated to test ICT1 in the bacterial system. There ICT1 wildtype and mutants can be tested on possible suppression of phenotype in *E. coli* strains with temperature sensitive mutations in PTH (PTH^{ts}), also in combination with a deletion in *ssrA* gene (tmRNA). Further the effect of ICT1 expression in a strain overexpressing AGA-minigene can be investigated in bacteria, which would be not possible in human mitochondria.

As it was reported by Prof. U. Varshney's group in Singh *et al.* (2008) the overexpression of AGA-minigene is toxic to *E. coli.* The overexpression of RRF can rescue the host from this toxicity by releasing the peptidyl-tRNA from the stalled ribosome (Figure 6.12). So far it was shown that ICT1 can not rescue the toxicity caused by overexpression of AGA-minigene, but it supports a weak rescue of the host if RRF is downregulated. To prove whether this weak rescue is specific for PTH activity of ICT1, ICT1 mutants need to be tested in similar experiments.

The fact that ICT1 does not show a rescue of the AGA-minigene overexpression at "normal" RRF level maybe supports the idea that it acts more on the long chain peptidyl-tRNA stacked in the ribosome or ribosomal subunit. The expression of the AGA-minigene leads to a peptidyl-tRNA with a short-peptide chain of 3 residues, which would probably drop off the ribosome after recycling by RRF and then be processed by soluble PTH. The downregulation of RRF in an overexpressing AGA-minigene strain would lead to an accumulation of more stalled ribosomes with the short-chain peptidyl-tRNA in the P-site. Maybe in the absence of RRF ICT1 can also act on those substrates and therefore at least rescue the sequestering of $tRNA^{Arg4}$, leading to the weak suppression of the phenotype.

Further it would be interesting to identify whether ICT1 would show a higher rescue if a longer stopless mRNA would be expressed as with the *ung*-stopless construct, which would result in a long-chain peptidyl-tRNA, immobilised within the ribosomal P-site after recycling the ribosome by RRF. It was already shown that the overexpression of RRF can also rescue this strain by releasing the *ung*-mRNA from the stalled ribosome, but this suppression is rather weak. Maybe this minimal rescue is caused by the peptidyl-

tRNA stuck within the large ribosomal subunit, which cannot be processed by the soluble PTH. It would be therefore interesting whether ICT1 expression under those circumstances would increase the suppression level, because of further "recycling" the ribosomal large subunit with the long-chain peptidyl-tRNA (Figure 6.12 C).

Another point that would be important to address is which protein can act as a soluble mitochondrial PTH in human. PTH2 was shown to process peptidyl-tRNAs *in vitro*, but its localisation within the mitochondrial intermembrane space makes it quite unlikely to act as a soluble PTH on matrix substrates [De Pereda *et al.*, 2004; Jan *et al.*, 2004]. Therefore which protein is responsible for this job in human mitochondria?

In conclusion it can be said that ICT1 as one of four members of the human mitochondrial release factor family has been recruited into the mitochondrial ribosome and further maintained its peptidyl-tRNA hydrolase (PTH) activity. This PTH activity is proposed to be essential for processing peptidyl-tRNAs within stalled ribosomes or within the ribosomal large subunit after recycling the pre-termination complex by mtRRF.

The highly conserved GGQ motif that is present in all four members of the mitochondrial release factor family was shown to be functional and essential for the PTH activity of ICT1. It is tempting to speculate whether the remaining two members, mtRF1 and C12orf65, have maintained a similar activity. Both were shown to be non-functional in the translation termination assay using *E. coli* ribosomes [Soleimanpour-Lichaei *et al.*, 2007; Antonicka *et al.*, 2010]. Interestingly the ^{35}S-met *de novo* syntheses from two different patient cell lines carrying a mutation within the *C12orf65* gene were dramatically reduced (~ 30%) [Antonicka *et al.,* 2010], reminiscent of the decreased level in mitochondrial protein synthesis after ICT1 depletion. The mitochondrial RNA levels were similar or even higher when compared to control. Thus it seems that also C12orf65 plays a critical role in mitochondrial translation. Surprisingly those authors showed also a partial rescue of COX activity and its assembly in those patient cell lines upon overexpression of ICT1, and suggest that C12orf65 and ICT1 may have similar or overlapping functions. Of the other two release factors, neither mtRF1a nor mtRF1 were able to suppress the phenotype, only ICT1. However, there are some major differences between ICT1 and C12orf65. ICT1 has been recruited into the human mitochondrial ribosome, whereas C12orf65 appears more like mtRF1a or mtRF1 as it was never detected within co-immunoprecipitated mitochondrial ribosomes [Rorbach *et al.*, 2008; this study]. C12orf65 did not show any activity in the translation

termination assay *in vitro*, in contrast to ICT1 that demonstrated PTH activity in a ribosome-dependent and codon-independent manner. However, there are also similarities between the two proteins: both are quite small proteins in comparison to a conventional class I release factor like mtRF1a, both have lost the crucial domains for codon recognition, and both contain the highly conserved GGQ domain. The presence of the GGQ motif within C12orf65 leads one to speculate that this protein has also maintained its ability to promote hydrolysis activity and maybe because of experimental restriction, namely using the 70S bacterial ribosome instead of the 55S mammalian mitochondrial ribosome in this assay, it is not possible to show evidence for it. However, the GGQ motif within C12orf65 suggests also in this case a ribosome-dependent PTH activity as soluble peptidyl-tRNA hydrolases do not require a GGQ motif for their function. Therefore it would be a surprise if C12orf65 with the GGQ motif would act on soluble peptidyl-tRNAs. Furthermore if C12orf65 does not have any PTH activity it would leave the question what feature of ICT1 is responsible for the partial rescue?

To investigate the possibility further whether the GGQ motif of C12orf65 is functional, causing hydrolysis activity, it would be interesting to see whether the overexpression of C12orf65 with mutation within the GGQ motif would rescue the phenotype of those patient cell lines as the wildtype form did. Additionally the expression of ICT1-GSQ mutant in comparison to ICT1 wildtype could be also tested in those patient lines with mutations in *C12orf65*. This might answer the question whether it is the PTH activity of ICT1 that can partially rescue the phenotype of the C12orf65 patient cell line. However, Antonicka *et al.* (2010) showed clearly that C12orf65 is essential for mitochondrial protein synthesis. To answer the question of its specific function within mitochondria it still needs some further investigations and these are ongoing in my host laboratory.

There is still no report whether mtRF1 is essential for the mitochondrial gene expression machinery and whether its GGQ motif is functional. The further characterisation of mtRF1 and also C12orf65 is part of the PhD project of A. Pajak within this laboratory.

Possible future experiments concerning function of ICT1 in human mitochondria:

Besides the work in the bacterial system carried out by the group of Prof. U. Varshney, there are maybe still some experiments that could be considered in the human cell system. One approach that has not been tried to investigate the role of the PTH activity of ICT1 in human cells was to use chemical crosslinking (e.g. DFDNB, BMH, DSG and MBS as reported by Gruschke *et al.*, 2010) to determine direct ICT1 interaction partners. Those results could then be used to clarify the position of ICT1 within the

mitochondrial ribosome that would be an enormous benefit. The presence of the GGQ motif leads to speculation that ICT1 is probably localised quite close to the PTC. However this fact needs also to be considered when using chemical crosslinkers as it is possible that proteins within the core of the mitochondrial ribosome are not accessible for crosslinking and only proteins closer to the surface can be investigated for direct interactions with this method.

If crosslinking of ICT1 would be possible then it would be further interesting whether also nascent peptide chains that could be labelled with ^{35}S-met are detectable after IP via ICT1-FLAG. There the ICT1^{GSQ} mutant should show more nascent peptide chains as they accumulate in the 39S LSU.

If crosslinking of ICT1 itself is not possible then proteins at the polypeptide tunnel exit (as it was reported from yeast in Gruschke *et al.*, 2010) or OXA1L could be used for crosslinking IP after ^{35}S-met labelling of the nascent peptide chain within the ribosome. Again this should show a higher accumulation of co-immunoprecipitated cross-linked nascent peptide chains in the ICT1^{GSQ} mutant than in the ICT1^{GGQ} wildtype. Those kind of experiments need at first an established system of co-expressing two construct independently in one cell line or good antibodies that allow immunoprecipitation of OXA1L or one of the mitochondrial ribosomal proteins located at the polypeptide tunnel exit.

Another possibility would be to do ^{35}S-met labelling in an ICT1^{GGQ} depleted background but expressed ICT1^{GSQ} mutant followed by separation on isokinetic sucrose gradient. There more of nascent polypeptide chain should be accumulated in fraction 6, representing immobilised nascent chain within the 39S LSU. Again, the amount of those nascent peptides could be quite limited and maybe not detectable as an artificial accumulation of non-stop mRNA within human mitochondria is so far not possible. It may be that a depletion of mtRF1a would lead to a higher accumulation of nascent peptide chain. Furthermore it is possible that because of a co-insertion of the nascent peptide chain into the membrane, one might expect to see a higher accumulation of those blocked complexes in the insolubilised membrane fraction in the pellet during preparations.

Chapter 7:

Identification of possible ICT1 orthologues in yeast (*Schizosaccharomyces pombe)* and bacteria *(Escherichia coli)*

7 Chapter 7: Identification of possible ICT1 orthologues in yeast (*Schizosaccharomyces pombe*) and bacteria (*Escherichia coli*)

7.1 Introduction

As discussed in the previous chapter the possible function of ICT1 is the rescue of stalled large ribosomal subunit with bound peptidyl-tRNA, which in the case of a long peptide chain cannot leave the ribosome with the tRNA attached through either the tRNA exit or through the polypeptide exit tunnel. The hydrolysis of the peptide chain from the tRNA that is catalysed by a ribosome-dependent, but codon-independent release factor is crucial for the recycling of those stalled complexes. ICT1 harbours all the critical features that are necessary to perform this function. The question is whether those "truncated" class I release factors are conserved or whether it is a unique class present only in mitochondria of higher eukaryotes.

By bioinformatical searches Dr. N. Bonnefoy identified MUG82 from *Schizosaccharomyces pombe* as a possible mitochondrial yeast candidate. Prof. U. Varshney and also other groups [Jiang *et al.*, 2009; Hayes and Keiler 2009] see in YaeJ the potential bacterial orthologue of ICT1.

The aim of this investigation is a first initial characterisation of those proteins. First, protein sequence alignment by using CLUSTALW was performed to establish similarity of MUG82 and YaeJ to ICT1. As shown in figure 7.1 all share the highly conserved GGQ motif. However, it is not only the GGQ tripeptide that is present, MUG82 especially shows also high similarity over the GGQ containing domain, whereas YaeJ is slightly less similar to ICT1 over this region. Overall MUG82 shares 49 identities (~27%) to ICT1 whilst YaeJ shares 31 identities (~22%) to ICT1 and 28 (20%) to MUG82.

All three proteins are relatively small: ICT1 with 206 residues is the largest of them compared to MUG82 with 182 amino acids and YaeJ with 140 amino acids. None of them show the critical features for codon recognition (tip of α5-helix and PXT/SPF) of a conventional class I release factor.

```
ICT1        MAATRCLRWGLSRAGVWLLPPPARCPRRALHKQKDGTEFKSIYSLDKLYPESQGSDTAWR 60
MUG82       -----------------MFANFRNCFKIKNSRLIYDNINKCLLTKEETNQLLKFIHLKWK 43
YaeJ        ----------------------------------------MIVISRHVAIPDG------ 13
                                                     :   ..     .

ICT1        VPNGAKQADSDIPLDRLTISYCRSSGPGGQNVNKVNSKAEVRFHLATAEWIAEPVRQKIA 120
MUG82       PAK-----------DQVQISFSRSSGPGGQNVNKLNTKVIVNLPFKQLESCIPMFLINHF 92
YaeJ        --------------ELEITAIRAQGAGGQHVNKTSTAIHLRFDIR-ASSLPEYYKERLL 57
                         .: *:  *:.*.***:*** .:   :.: :   .        .

ICT1        ITHKNKINR--LGELILTSESSRYQFRNLADCLQKIRDMITEASQTPKE--PTKEDVKLH 176
MUG82       KTCEMLRNYRIQNGIKIYSQKTRSQHKNIEDALNKISDLLNKSAETLYV--PDTPPEKIA 150
YaeJ        AASHHLISS--DGVIVIKAQEYRSQELNREAALARLVAMIKELTTEKKARRPTRPTRASK 115
             : .   .    . : : ::. * *  *   .* ::  ::.: :       *

ICT1        RIRIEN--MNRERLRQKRIHSAVKTSRRVDMD 206
MUG82       RISILKKESNEKRLSEKKYKQKKKTQRRITMD 182
YaeJ        ERRLAS---KAQKSSVKAMRGKVRSGRE---- 140
            .  : .   : ::   *  :   :: *.
```

Figure 7.1: Sequence alignment (CLUSTALW) of human ICT1, yeast MUG82 *(S. pombe)* and bacterial YaeJ *(E. coli).* Identities are indicated by a star (*) and/or grey highlighting, high level of similarity by a colon (:) and lower levels by a full stop (.). The GGQ motif is labelled in red. The region of ICT1, which does not show sequence similarities to the other human mitochondrial release factors, is shown italic, underlined.

The region from residue 107 to 132 in ICT1 (Figure 7.1 underlined, italics) does not align with the other members of the mitochondrial release factor family and forms a helix (α1) that is absent in class I release factors (Chapter 6, Figure 6.1). This may suggest that this helix is possibly responsible for ribosome interaction that occurs with ICT1 but not the other known RFs. No high similarity can be found in MUG82 or YaeJ. Just recently Handa *et al.* (2010a) proposed that the C-terminal region of ICT1, which is basic-residue-rich and unstructured or flexible, is maybe involved in ribosome binding, and once within the ribosome would become structured. The same authors speculated that the negatively charged residues over the groove between β2-(3_{10}-2)-α1-(3_{10}-3)-β3 may be interaction points with RNA or proteins. However, Handa *et al.* (2010a) do not mentioned any differences between mammalian ICT1 and the possible bacterial orthologue. Since the bacterial ribosome is already well characterised it would be a surprise if YaeJ has been recruited into the 70S ribosome and had been missing in all the analysis for such a long time. Thus MUG82 and YaeJ may perhaps act as codon-independent release factors, but the possibility that they are part of the ribosome seems quite unlikely. These are just speculations, therefore experiments would need to be done to analyse the potential release activity of MUG82 and YaeJ. Additionally it would need to be investigated as to whether they can be integrated into the ribosome.

As this is a collaborative project, some studies will be done in yeast in the laboratory from Dr. N. Bonnefoy, and others in bacteria in the laboratory from Prof. U. Varshney.

The further characterisation of ICT1 in the bacterial system allows as already discussed in the previous chapter the investigation of its function on peptidyl-tRNAs, stuck in the ribosome/ ribosomal large subunit. The study presented in this chapter will mainly contribute an initial investigation of MUG82 and YaeJ in human cell lines and further the analysis of their potential translation termination activity in the *in vitro* assay (carried out by Dr. Z. M. A. Chrzanowska- Lightowlers).

7.2 Imported MUG82 in human mitochondria is able to interact with mitoribosomal proteins

To investigate whether MUG82 is able to interact with the human mitochondrial ribosome *MUG82* was cloned into pcDNA5/FRT/TO with a C-terminal FLAG tag in two forms, either with or without Su9-presequence from *N. crassa* [Viebrock *et al.*, 1982] for mitochondrial targeting. The constructs were kindly provided by Dr. N. Bonnefoy. After transfecting HEK293T cells with the different constructs, and successful selection for hygromycin resistance, the cells were induced and tested for expression of FLAG tagged protein. The cells carrying the construct without the Su9-presequence showed expression of MUG82-FLAG at very low level, but no import into human mitochondria. In contrast Su9-targeted MUG82-FLAG (mtMUG82-FLAG) was highly expressed after induction with tetracycline and also showed import of the protein into the mitochondria, as demonstrated by the protection against proteinase K treatment of the mitochondrial preparation. As shown in figure 7.2 mtMUG82-FLAG, with a calculated molecular weight of ~ 21.5 kDa, could be detected in cell lysate, in isolated mitochondria and was also maintained after the addition of proteinase K. The lysis of mitochondria in the presence of proteinase K led to the digestion of mtMUG82-FLAG by the enzyme demonstrating both the activity of proteinase K within the whole experiment and also the sensitivity of the tested proteins to proteinase K. The molecular weight of MUG82-FLAG without the cleavage of Su9-presequence from the N-terminus would be approximately 29 kDa. The migration of mtMUG82-FLAG in the SDS-PAGE suggests that the Su9-presequence (~ 7.5 kDa) was successfully cleaved off. MRPS18B, a component of the small ribosomal subunit was used as a mitochondrial marker and showed a similar pattern as mtMUG82-FLAG.

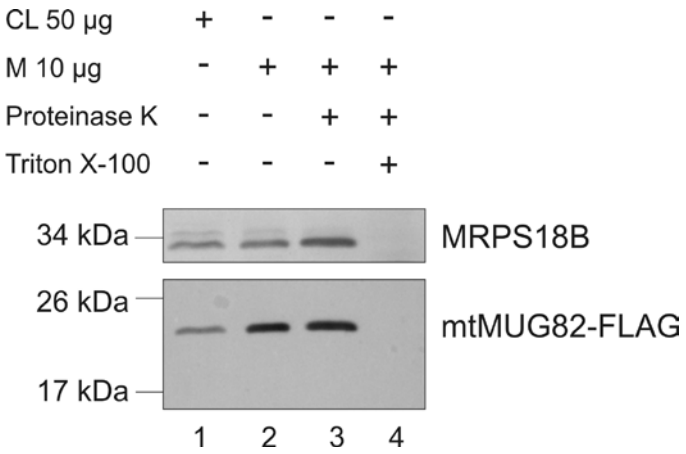

Figure 7.2: Cellular localisation of Su9-MUG82-FLAG within HEK293T cells. HEK293T cells expressing mtMUG82-FLAG were induced for 3 days. Cell lysate (50µg, lane 1) and isolated mitochondria (10 µg) untreated (lane 2) or treated with proteinase K, in the absence (lane 3) or presence of 1% Triton X-100 (lane 4) were analysed by western blot. To determine the presence of mtMUG82-FLAG in each fraction antibodies against the FLAG epitope were applied to the western blot membrane. MRPS18B, a member of the mitochondrial ribosomal small subunit was used as a positive control.

This cell line was then used for immunoprecipitation via the FLAG tag to determine whether mtMUG82-FLAG is able to interact with the human mitochondrial ribosome. To this end HEK293T-mtMUG82-FLAG cells were induced for 3 days and mitochondria were isolated. Prior to lysis, mitochondria were treated with DNase I and proteinase K to minimise unspecific binding from cytosolic proteins. The elution fraction of mtMUG82-FLAG was then analysed by silver staining and western blot in comparison to ICT1-FLAG. As shown in figure 7.3 A the elution fraction of mtMUG82-FLAG showed several bands, but the pattern was different to the ICT1-FLAG eluate and the intensity of co-immunoprecipitated proteins was also weaker. To see whether there were mitochondrial ribosomal proteins present in this elution fraction eluate was examined by western blot (Figure 7.3 B). There, components of the 39S LSU (MRPL3 and MPRL12) and of the 28S SSU (DAP3 and MRPS18B) were detected in the elution of mtMUG82-FLAG. The relative level of co-immunoprecipitated mitochondrial ribosomal proteins was lower in mtMUG82-FLAG in comparison to ICT1-FLAG, whereas the levels of FLAG tagged protein were relatively similar. Endogenous ICT1 could be not detected in the elution of mtMUG82-FLAG.

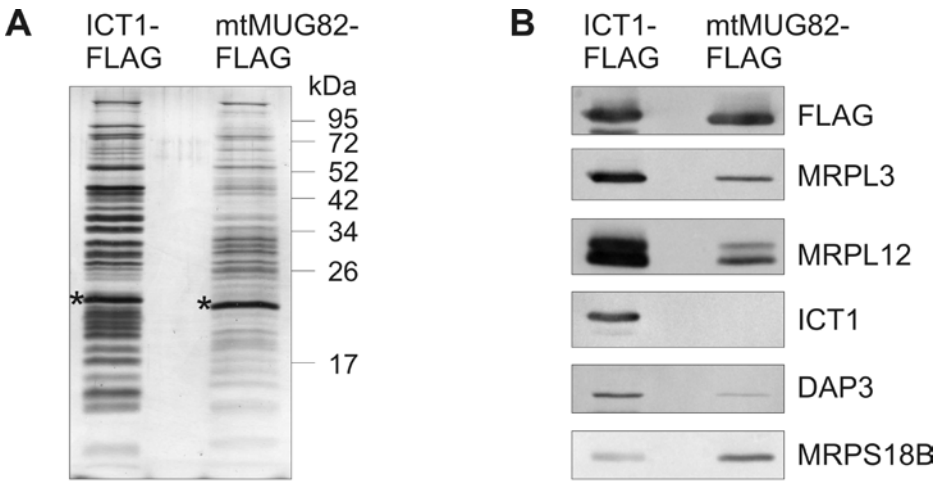

Figure 7.3: Yeast mtMUG82-FLAG is able to interact with human mitochondrial ribosomal proteins. HEK293T-mtMUG82-FLAG cell line was induced for 3 days with 1 µg/ ml tetracycline. Mitochondrial lysate was used for immunopreciptiation via the FLAG tag. The elution fraction (10%) of mtMUG82-FLAG was analysed by silver staining (A) and western blot (B) in comparison to ICT1-FLAG. **A)** * indicates FLAG tagged protein. **B)** Antibodies against MRPL3, MRPL12, ICT1, DAP3 and MRPS18B were used to determine the relative level of co-immunoprecipitated ribosomal complexes by mtMUG82-FLAG. To ensure the presence of the FLAG tagged protein in each elution fraction FLAG antibodies were applied.

Concluding from this result the possible yeast orthologue is able to interact with human mitochondrial ribosomal proteins. However, the affinity of mtMUG82-FLAG to the human mitochondrial ribosome seems to be weaker than from ICT1-FLAG.

7.3 Yeast MUG82-FLAG is not able to suppress ribosomal defects, caused by ICT1 depletion

To determine whether mtMUG82-FLAG is able to rescue the phenotype caused by ICT1 depletion, analysis of isokinetic sucrose gradient was performed. As described before in 5.4 (Figure 5.7) ICT1 depletion caused a conformation change of the 39S LSU, resulting in a shift of MRPL3 as a member of the LSU, from fractions 6/7 to 5/6. To test whether mtMUG82-FLAG can suppress this defect, HEK293T-WT- and HEK293T-mtMUG82-FLAG cells were treated with either si-NT or si-ICT1 B for 3 days. The cells were induced also for 3 days with 1 µg/ ml tetracycline. Then, cells were harvested, lysed and 700 µg of each sample was separated on a 10 to 30% sucrose gradient as described in 3.5.11. The isolated fractions were then analysed by western blot as shown in figure 7.4. The HEK293T-WT (WT) treated with si-NT showed ICT1 mostly in fraction 6, co-migrating with MRPL3, which was mainly present in fractions 6 and 7. DAP3 as member of the SSU was present in fractions 4 and 5. After ICT1 depletion in WT MRPL3 was also detectable in fraction 5. The si-NT treated mtMUG82-

FLAG samples showed a similar result as WT, where ICT1 was present mostly in fraction 6 as MRPL3. Interestingly the expressed mtMUG82-FLAG was only detectable in the earlier fractions 1 to 3, but not in fraction 6, suggesting that under those conditions mtMUG82-FLAG was not associated with the 39S LSU like ICT1. After the depletion of ICT1 in mtMUG82-FLAG expressing cells there was also MRPL3 detectable in fraction 5, whereas in si-NT samples MRPL3 migration started in fraction 6.

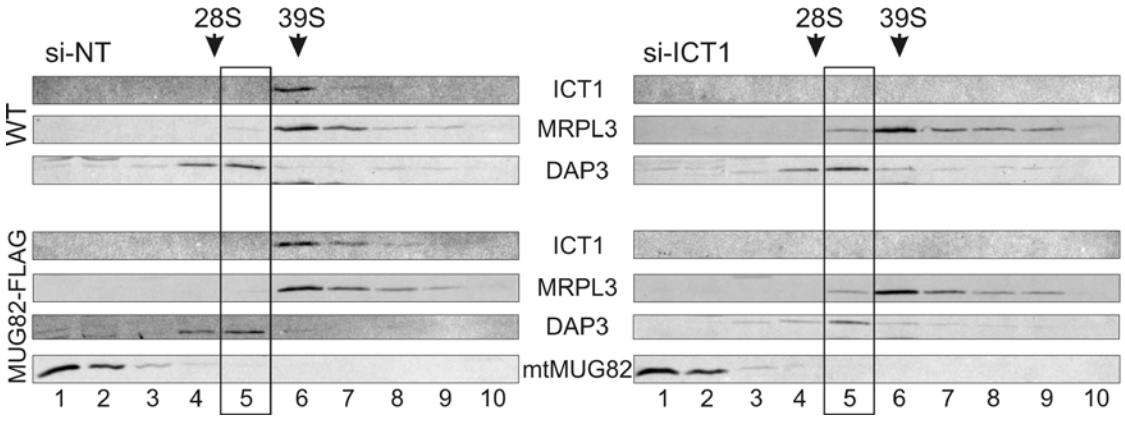

Figure 7.4: MtMUG82-FLAG cannot suppress the mitochondrial ribosomal defect caused by ICT1 depletion. HEK293T-WT- and HEK293T-mtMUG82-FLAG cells were treated with si-NT or si-ICT1 B, respectively, for 3 days. FLAG tagged protein was expressed for 3 days at the same time. Cells were then harvested and lysed. Lysates (700 µg) were subjected to sucrose gradients. The fractions (1-10) were analysed by western blot using antibodies against ICT1 to ensure ICT1 depletion in the siRNA targeting samples. The ribosomal profile in each sample was investigated by applying MRPL3 and DAP3 antibodies to all membranes. The distribution of mtMUG82-FLAG was also analysed by using antibodies against the FLAG octapeptide.

These results indicate that mtMUG82-FLAG is not able to suppress the mitochondrial ribosomal defect, which is caused by ICT1 depletion. The absence of mtMUG82-FLAG in the later fractions, where the 39S LSU sediments, suggests that under the experimental conditions mtMUG82-FLAG is not associated with the mitochondrial ribosome, despite the fact that the immunoprecipitation clearly showed some interaction with it. This phenomenon was seen previously with mtRRF-FLAG [Rorbach *et al.*, 2008] where the reason for this is believed to be the extended incubation time during IP. One explanation could be that what was visible by IP, was the interaction over this time period of mtMUG82-FLAG via the A-site of the ribosome. In order to prove this hypothesis, further experiments need to be carried out, e.g. isokinetic sucrose gradient of IP-ed eluate to analyse whether the co-immunoprecipitated complex is the 55S monosome and / or the 39S LSU. It should be further investigated whether mtRRF was present in the IP-ed ribosomal complexes. The absence of mtRRF in the IP eluate would suggest an interaction of mtMUG82-FLAG via the ribosomal A-

site. Furthermore the *in vitro* translation termination assay will answer the question as to whether MUG82 has any peptidyl-tRNA hydrolase activity.

7.4 Mitochondrial imported YaeJ is able to co-purify human mitochondrial ribosomal proteins.

For the investigation of YaeJ in human cell lines it needed first to be cloned into pcDNA5/FRT/TO with a mitochondrial targetting sequence such as the Su9-preseqence from *N. crassa* [Viebrock *et al.*, 1982]. To generate this construct primer #12 and #13 listed in table 3.2 and plasmid pTRC99A-his-YaeJ (kindly provided from Prof. U. Varshney) as the template were used for amplification of *YaeJ*. The forward primer contains the 3'-end of the Su9-preseqence and further a *BssH*II restriction site. This then allowed an in frame 5'-ligation of *YaeJ* to Su9-presequence, using as the target vector pcDNA5/FRT/TO-Su9-PARN (kindly provided by A. Bobrowicz), where the PARN insert was cut out with *BssH*II and *Apa*I. The reverse primer contains the sequence for the FLAG epitope and the *Apa*I restriction site. After successful cloning and confirmatory sequencing of the plasmid, HEK293T cells were transfected with pcDNA5/FRT/TO-Su9-YaeJ-FLAG and pOG44 to generate a stable inducible expressing cell line. HEK293T clone expressing Su9-YaeJ-FLAG, which was tested and confirmed to show inducible expression, was then used for further experiments: immunoprecipitation and isokinetic sucrose gradient. For immunoprecipitation cells were induced for 3 days with 1 µg/ ml tetracycline. Mitochondria were then isolated and treated with DNaseI and proteinase K, prior to lysis. As shown in figure 7.5 A mtYaeJ-FLAG is present in this mitochondrial lysate, which also confirmed successful import of mtYaeJ-FLAG via the Su9-presequence. YaeJ is a relatively small protein with a predicted size of 15.6 kDa. The addition of 69 amino acids from the Su9-presequence would result in a molecular weight of 23 kDa close to the size of ICT1-FLAG, but there is a substantial difference in size between ICT1-FLAG and mtYaeJ-FLAG (Figure 7.5 A). In agreement with the cleavage of the presequence are also the results shown in figures 7.5 C and 7.7, where the molecular weight of mtYae-FLAG, expressed in human cell line and recombinant YaeJ purified from *E. coli* are relatively similar. The slightly slower migration of mtYaeJ-FLAG can be caused by the FLAG tag, which is highly positively charged. A small difference in migration between endogenous and FLAG tagged protein could be also seen in case of ICT1 (Figure 6.9) and of mtRbfA in the next chapter.

The mitochondrial lysate was then incubated with M2 FLAG beads to allow immunprecipitation of mtYaeJ-FLAG via the FLAG tag. The elution fractions were then analysed by silver staining and western blot.

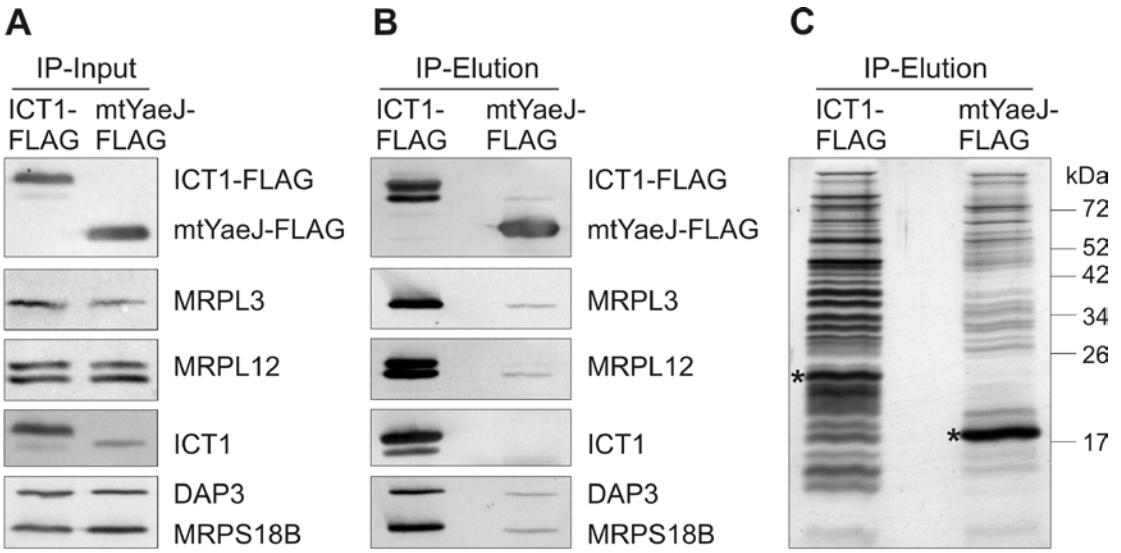

Figure 7.5: Mitochondrial imported YaeJ-FLAG shows interaction with human mitochondrial ribosomal proteins after immunoprecipition via FLAG tag. HEK293T cells expressing mtYaeJ-FLAG or ICT1-FLAG were induced with 1 µg/ ml tetracycline. After 3 days cells were harvested and mitochondria isolated, purified and finally lysed. **A)** Mitochondrial lysate (5 µg) of each sample was analysed by western blot using FLAG antibodies to ensure expression and mitochondrial import of FLAG tagged proteins. **B)** Each elution fraction (10%) was analysed by western blot on the presence of co-immunoprecipitated ribosomal proteins such as MRPL3, MRPL12, ICT1 (components of the 39S LSU), DAP3 and MRPS18B (members of the 28S SSU) and also of the FLAG tagged protein itself. **C)** As for western blot analysis 10% of each elution were analysed by silver staining. * indicates the FLAG tagged protein.

As shown in figure 7.5 C as with mtMUG82-FLAG the pattern and the intensity of co-purified proteins in mtYaeJ-FLAG elution is different from that of ICT1-FLAG. Western blot confirmed that mtYaeJ-FLAG is also able to immunprecipitate human mitochondrial ribosomal proteins of the LSU (MRPL3 and MRPL12) and of the SSU (DAP3 and MRPS18B), but with lower affinity than ICT1-FLAG. No ICT1 protein was detectable in the elution of mtYaeJ-FLAG. The lower affinity of mtYaeJ-FLAG cannot be caused by lower expression of the tagged protein, as western blot of input and elution confirms relatively similar amounts of FLAG tagged ICT1 and YaeJ.

7.5 Mitochondrial targeted YaeJ-FLAG does not co-migrate with 39S LSU on isokinetic sucrose gradient

To analyse whether the interaction of mtYaeJ-FLAG with human mitochondrial ribosomal proteins is caused by the incubation time during the immunoprecipitation, isokinetic sucrose gradients of cell lysate were performed. Thus HEK293T cells expressing mtYaeJ-FLAG were induced for 3 days with 1 µg/ ml tetracycline. The cells were then harvested and lysed as described in 3.5.2. Cell lysate (700 µg) was separated on a 10 to 30% sucrose gradient as previously described. The fractions (1-10) were analysed by western blot, shown in figure 7.6. There, mtYaeJ-FLAG, as seen with mtMUG82-FLAG, did not co-migrate with MRPL3, and thus it did not show association with the 39S LSU under those conditions. Therefore it is unlikely that mtYaeJ-FLAG would be able to rescue the ribosomal defect caused by ICT1 depletion.

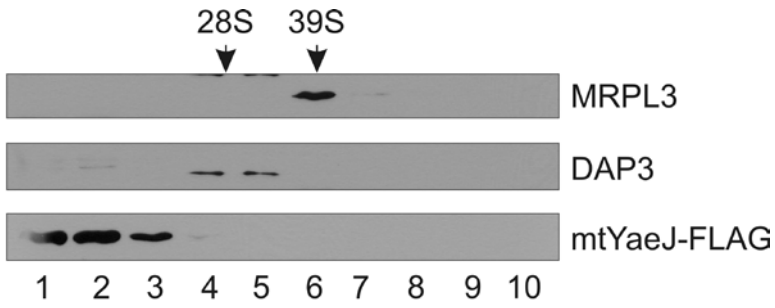

Figure 7.6: Mitochondria targeted YaeJ-FLAG does not co-migrate with the 39S LSU. Lysate (700 µg) of mtYaeJ-FLAG expressing cells was separated on an isokinetic sucrose gradient. The mitochondrial ribosomal profile within this gradient was analysed by western blot using specific antibodies against MRPL3, representing the 39S LSU, and DAP3, component of the 28S SSU. The distribution of mtYaeJ-FLAG was determined by applying FLAG antibodies to the western blot membrane.

As with MUG82 it seems highly likely that the association with the human mitochondrial ribosome after immunoprecipitation is caused by the 3 hour incubation step and it likely represents the interaction of both proteins via the A-site, where proteins that stimulate peptidyl-tRNA hydrolysis activity interact.

7.6 YaeJ shows codon-independent release activity *in vitro*

To test whether YaeJ has really peptidyl-tRNA hydrolysis activity, the recombinant protein had to be purified and then tested in the *in vitro* translation termination assay by Dr. Z. M. A. Chrzanowska-Lightowlers. Therefore *YaeJ* was amplified using primer #10

and #11 (Table 3.2) and pTRC99A-his-YaeJ as the template. The amplicon and target vector pGex-6P-1 were digested with *BamH*I and *Xho*I, allowing then 5'-ligation of *YaeJ* to the GST-tag on the pGex-6P-1 vector. Finally, *E. coli* Rosetta^{TM}(DE3) was transformed with this plasmid, allowing overexpression of YaeJ-GST under IPTG inducible promotor. The bacteria were cultured over night at 16°C in the presence of 1 mM IPTG. The next day cells were harvested and used for recombinant protein purification as detailed under 3.5.12. As shown in figure 7.7 a significant amount of the overexpressed fusion protein (~ 41.6 kDa) was recovered in the soluble fraction that was used for successful purification. The protein with a molecular weight of approximately 15.6 kDa was finally eluted by the cleavage of the GST-tag (26 kDa) by PreScission protease.

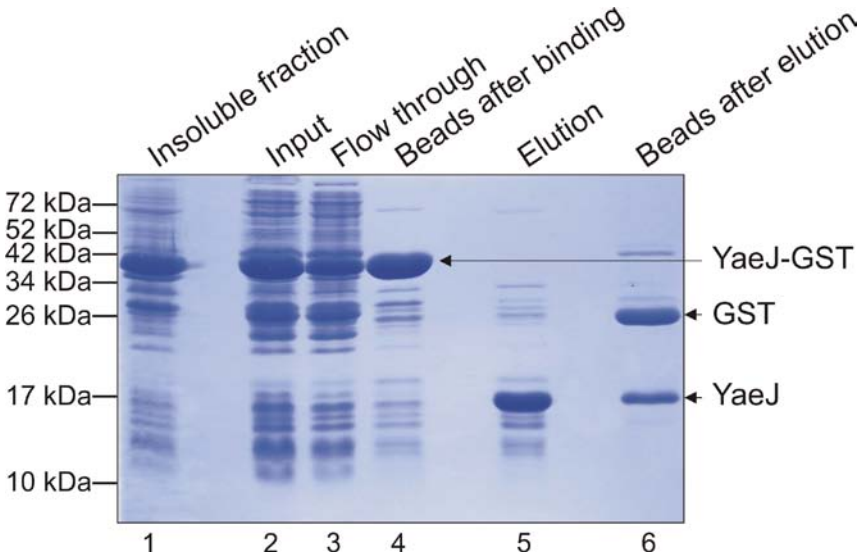

Figure 7.7: Recombinant protein purification of YaeJ. Bacteria were cultured over-night at 16°C in the presence of 1 mM IPTG allowing overexpression of YaeJ-GST (~ 41.6 kDa) fusion protein. Cells were harvested, sonicated and soluble proteins (input, 2) were separated from insoluble ones (1) by centrifugation. The soluble fraction was subjected to glutathione sepharose beads. After binding step the flow through (3) was discarded and the beads (4) washed with PBS. By the addition of PreScission protease the GST-tag was cleaved off and YaeJ (~ 15.6 kDa) could be eluted (5), whereas GST-tag (~ 26 kDa) stayed on the beads (6).

For the *in vitro* translation termination assay 50 pmol of recombinant protein were then further used. As shown in the graph in figure 7.8 YaeJ was able to cause hydrolysis of the radiolabelled f[^{3}H]met from the tRNA^{Met} in the presence, but also in the absence of a stop codon (UAA). This suggests that YaeJ has like ICT1 a codon-independent, and probably ribosome-dependent release activity. To be sure about the latter an assay in the absence of a 70S ribsome needs to be done.

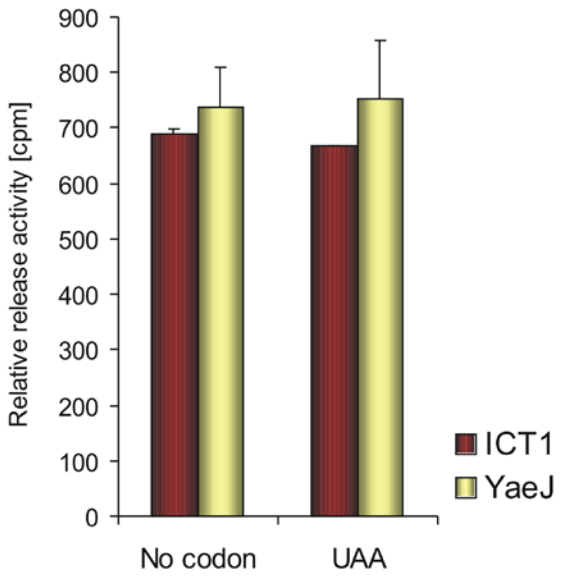

Figure 7.8: YaeJ shows release activity in the *in vitro* translation termination assay. Purified recombinant YaeJ protein (50 pmol) was tested in the *in vitro* assay. *E. coli* 70S ribosomes were programmed with f[^{3}H]met-tRNA^{Met} in the P-site and either in the presence or absence of a stop codon (400 pmol UAA) in the decoding centre. ICT1 was used as a positive control for ribosome-dependent codon-independent release activity. Means and standard deviations were calculated from three experiments.

However, it is highly likely that the function of YaeJ is also ribosome-dependent, because of the presence of the GGQ motif, which is a typical feature of a ribosome-dependent peptidyl-tRNA hydrolase. As already explained before, it is believed that the GGQ motif mimics the CCA motif of the aminoacyl-tRNA at the PTC centre within the ribosome [reviewed in Youngman *et al.*, 2008] and it is not really the class I release factor that hydrolyses the ester bond between the peptide chain and the tRNA, it is the ribosome itself that allows after conformational change with the release factor a hydrophilic attack and therefore hydrolysis [Schmeing *et al.*, 2005]. Thus hydrolysis activity catalysed by class I release factor with a GGQ motif needs the context of a ribosome. This result led to the speculation that there is possibly release activity catalysed MUG82. It is highly likely that MUG82 also shows similar activity *in vitro*. However recombinant protein needs to be purified to finally do the experiment to prove this hypothesis.

7.7 Discussion

Sequence alignment as shown in figure 7.1 demonstrates clearly similarity between human ICT1, yeast MUG82 and bacterial YaeJ. The named proteins harbour the GGQ motif that is essential for catalysing the hydrolysis of the ester bond between the P-site

tRNA and its attached peptide chain within the ribosome. Additionally MUG82 and ICT1 share 49 (~27%) identities and YaeJ and ICT1 31 (~22%). None of them shows the crucial motifs for codon recognition (tip of α5 helix and PXT/SPF tripeptide) like a conventional class I release factor. All three proteins are quite small with approximately 15 kDa to 20 kDa, whereas mtRF1a is around twice as large at ~ 40 kDa.

ICT1 was already shown in the previous chapters to be a mitochondrial ribosomal protein with ribosome-dependent, but codon-independent peptidyl-tRNA hydrolase (PTH) activity, proposed to be involved in the recycling of stalled ribosomes or abortive ribosomal large subunit with immobilised peptidyl-tRNAs.

The aim of the experiments shown in this chapter was an initial characterisation of the possible orthologues (MUG82 and YaeJ) of human ICT1 to see, whether ~

i) those orthologues can also be integrated into the human mitochondrial ribosome
ii) they show ribosome-dependent and codon-independent PTH activity in the *in vitro* translation termination assay
iii) they are able to suppress the defect caused by ICT1 depletion.

To analyse possible function of MUG82 and YaeJ, they were both targeted to human mitochondria using Su9-presequence from *N. crassa* [Viebrock *et al.*, 1982] and further fused with a C-terminal FLAG tag to allow specific immunoprecipitation via the FLAG epitope. Both, MUG82 and YaeJ were able to co-purify human mitochondrial ribosomal proteins (Figure 7.3 and 7.5), but with an overall lower affinity than ICT1. Interestingly instead of co-migrating with the 39S LSU both were located more in the earlier fractions (1 to 3) on isokinetic sucrose gradients (Figure 7.4 and 7.6). This suggests that under those conditions neither MUG82 nor YaeJ was associated with the mitochondrial ribosomal large subunit like ICT1, demonstrating that the interaction seen after IP was caused probably by the incubation time of 3 hours where MUG82 or YaeJ may be able to access the A-site as was seen before with mtRRF [Rorbach *et al.*, 2008]. Thus it seems unlikely that MUG82 or YaeJ can be integrated into the human mitochondrial ribosome as is ICT1. This is also in agreement with the fact that MUG82 was not able to suppress the ribosomal defect caused by ICT1 depletion.

It would be further interesting whether the association of both proteins with the mitochondrial ribosome is really through the A-site. Therefore it needs to be further analysed whether mtRRF is present in those immunoprecipitated ribosomal complexes. The absence of mtRRF would suggest that MUG82 or YaeJ, respectively can interact with the ribosome via the A-site.

It is further from great interest whether those two proteins interact with the yeast mitochondrial or the bacterial ribosome, respectively. An integration of YaeJ into the 70S bacterial ribosome would be a surprise, as the *E. coli* ribosome is very well characterised. However, very recently Handa *et al.* (2010b) have shown that YaeJ is most of the time associated with the 70S ribosomes and polysomes, but also with the 30S SSU in bacteria. In contrast to ICT1 YaeJ is not essential for cell growth and further a deletion of *YaeJ* in bacteria has no effect on the ribosome profile revealed by density sucrose gradients, suggesting that it is not important for ribosome assembly as is ICT1. It seems therefore that the recruitment of ICT1 into the mitochondrial ribosome is unique in mammals and that ICT1 is one example of the additional ribosomal proteins that do not have homologues in the 70S bacterial ribosome [reviewed in Koc *et al.*, 2010]. Interestingly YaeJ was also found in association with the bacterial 30S SSU, which is different from ICT1, a member of the mitochondrial ribosomal large subunit. Handa *et al.* (2010b) suggested that the C-terminus of YaeJ, which was shown to be important for ribosome binding, is maybe fixed in the 30S SSU and as soon as a ribosome gets stalled the domain 3-like portion of YaeJ with the GGQ domain will be located towards the PTC. However, the way how ICT1 and YaeJ interact with the mitochondrial ribosome or bacterial ribosome, respectively, must be different as ICT1 has been recruited into the 39S LSU and YaeJ does not represent a ribosomal protein and further shows besides interaction with 70S ribosome also an association with the 30S SSU in bacteria.

Thus far there is some evidence that also YaeJ can act as a codon-independent peptidyl-tRNA hydrolase, probably in a ribosome-dependent manner, as YaeJ showed clearly hydrolysis activity in the presence and absence of a stop codon in the *in vitro* translation termination assay using 70S *E. coli* ribosomes (Figure 7.8). Handa *et al.* (2010b) demonstrated that the GGQ motif is also essential for the PTH activity of YaeJ, however, it is unclear whether the first glycine is really important as the authors did not show results of YaeJ with mutation just in this one residue. This would be particularly interesting since the PTH activity of ICT1 seems to be the same for $ICT1^{GGQ}$ wildtype and $ICT1^{AGQ}$ mutant *in vivo*.

To determine the function of YaeJ in *E. coli in vivo* Prof. U. Varshney and his group will investigate this protein further in different bacterial background strains. Thus far they have shown that the expression of YaeJ was not able to rescue the pth^{ts} strain at nonpermissive temperatures. This could be in agreement with a ribosome-dependent PTH activity and therefore the non-ability to replace a soluble ribosome-independent PTH. The pth^{ts} strain can be rescued by the downregualtion of RRF as less peptidyl-

tRNAs are released during recycling by RRF and therefore the accumulation of peptidyl-tRNA, which is lethal [Menninger, 1978], is reduced. Under those conditions YaeJ may act as a ribosome-dependent PTH and leads to the hydrolysis of those peptidyl-tRNA within the ribosome, thus rescuing the sequestering of tRNAs. A depletion of YaeJ in a pth^{ts}-dnRRF background resulted in a growth defect again. It would be interesting whether an expression of ICT1 under those circumstances would replace YaeJ and suppress the growth defect.

Furthermore as ICT1, YaeJ was not able to rescue the host from the toxicity caused by AGA-minigene overexpression, which again supports the idea that ICT1 and YaeJ act more on long-chain peptidyl-tRNAs within the ribosome and not on dropped off short-chain peptidyl-tRNAs as discussed in the previous chapter. However, it would still be of great interest to see whether YaeJ expression would rescue the strain if RRF is downregulated as the peptidyl-tRNA would be then stuck in the ribosome and not accessible for soluble PTH.

However, it would be still from great interest to identify whether both ICT1 and YaeJ show more of an effect in the *ung*-mRNA overexpressor. Moreover this strain can be rescued by RRF the suppression is weaker than in the AGA-minigene overexpressor. It was shown that RRF overexpression releases the *ung*-mRNA [Singh *et al.*, 2008], meaning the ribosome gets recycled. The rather weak rescue of the strain by RRF expression may be due to the possibly blocked peptidyl-tRNA within the ribosomal large subunit (Figure 6.12 C). This could be tested by separating those samples on isokinetic sucrose gradients, where the peptidyl-tRNA should be detectable in the fraction where the LSU migrates. If this would be the case then it would be interesting whether ICT1 or YaeJ would suppress the phenotype further by catalysing the hydrolysis of the peptidyl-tRNA and therefore the release of the peptide chain and tRNA from the ribosomal subunit.

To date not much is known from the yeast orthologue MUG82. However, also if MUG82 was not able to rescue the ribosomal defect caused by ICT1 depletion in human mitochondria, it would be still interesting to confirm whether ICT1 could replace MUG82 in yeast.

Concluding so far ICT1 orthologues are present in yeast (*S. pombe*: MUG82) and bacteria (*E. coli:* YaeJ). It seems that these orthologues are like ICT1 ribosome-dependent, but codon-independent peptidyl-tRNA hydrolases according to the sequences and the activity of YaeJ in the *in vitro* translation termination assay. Neither YaeJ nor MUG82 can be integrated into the human mitochondrial ribosome, however,

both probably get access to the ribosomal A-site during incubation and can thus interact with human mitochondrial ribosomal proteins. As this is only an initial characterisation of MUG82 and YaeJ further experiments need to be done, especially testing MUG82 in the *in vitro* translation termination assay, and also further investigations in the yeast and bacterial system, respectively.

However, the results presented in this study and by Handa *et al.* (2010b) suggest that this class of “truncated” class I release factors including ICT1, YaeJ and potentially MUG82 represents ribosome-dependent peptidyl-tRNA hydrolases that are involved in the rescue of stalled ribosomes.

Chapter 8:

Investigation of human ribosome binding factor A

8 Chapter 8: Investigation of human ribosome binding factor A

As a consequence of the ICT1 project, where it transpired that ICT1 is a component of the mitochondrial ribosome, there was a great interest in the human mitochondrial ribosome and its assembly. Therefore the investigation of the human ribosome binding factor A (C18orf22; mtRbfA), as a potential ribosome assembly factor, that had been initiated by Dr. J. Rorbach, was continued.

8.1 Introduction

The bacterial orthologue RbfA was initially identified as a high-copy suppressor for a mutation (C23U) in the 5'-end helix of the 16S ribosomal RNA of the 30S small subunit [Dammel and Noller, 1995]. Furthermore it was shown that a pool of RbfA is associated with the 30S SSU, but not with either the 50S LSU or with the 70S ribosome or polysome [Dammel and Noller, 1995; Xia *et al.*, 2003]. Its role in the maturation of the 30S SSU is due to its processing of the 16S rRNA [Xia *et al.*, 2003]. A deletion of *RbfA* in *E. coli* leads to an accumulation of 17S rRNA, a precursor to the 16S rRNA [Inoue *et al.*, 2003; Xia *et al.*, 2003] and thus to an increased level of free 30S SSU and 50S LSU. This consequently leads to decreased amounts of translating polysomes, probably caused by the inability of the 30S SSU with precursor 16S rRNA to interact with the 50S LSU and so be incorporated into the 70S ribosome. RbfA is also a cold shock protein [Jones and Inouye, 1996; Xia *et al.*, 2003] whose abundance increases upon low temperature to adapt the translation machinery to those conditions. After a cold shock the translation rate in bacteria decreases. The upregulation of cold shock proteins such as RbfA is probably to facilitate rapid maturation of the 30S SSU and therefore to overcome the translational block. This cold shock protein, which is bound to 20% 30S SSU at 37°C, but to 40% of 30S after cold shock, is therefore crucial in *E. coli* to adapt to low temperature [Xia *et al.*, 2003].

Available structures of bacterial RbfA [Huang *et al.*, 2003; Datta *et al.*, 2007] demonstrate that RbfA has a type-II KH-domain fold, which is a characteristic of an RNA-binding domain in archaeal or bacterial proteins. It is suggested that KH folds mediate RNA-dependent protein-protein interactions. The solution structure of *E. coli* RbfA is a monomeric protein with 3 helices and 3 β-strands (α1-β1-β2-α2-α3-β3), where the βααβ subunit shows a helix-kink-helix (hkh) motif with a conserved AXG sequence.

Datta *et al.* (2007) showed that this hkh motif of *Thermus thermophilus* faces the junction between the top of helix44 (h44) and the base of helix45 (h45) of the 16S rRNA within the 30S SSU. It was further suggested that the interaction of RbfA with the neck region of the 30S SSU leads to an induced fit-like mechanism with a shift of h44 and h45. Furthermore they demonstrated that RbfA interacts with the C-terminal extension of ribosomal proteins S9 and S13 within the P-site, and the h18 and the ribosomal protein S12, which overlaps with the binding site of IF1. Because of the flexibility of the C-terminal region of RbfA it was proposed that this region relocates towards h18 and thus it can interact with the loop region of h1 at the 5'-end of the 16S rRNA. It was suggested that bound RbfA inhibits the interaction of 50S LSU with 30S SSU precursor if h1 is unformed and the 5'-end unprocessed.

Bacterial RbfA is a relatively small protein with 95 amino acids (*T. thermophilus*) or 133 amino acids (*E. coli*). The sequence identity between different RbfA homologues is very low (~20%), but the structural similarity is remarkable [Datta *et al.*, 2007].

The putative human mitochondrial orthologue (C18orf22) of bacterial RbfA was found in the immunoprecipitation of mtRRF-FLAG [Rorbach *et al.*, 2008]. C18orf22 (mtRbfA) at 343 amino acids is approximately 3 times as big as the bacterial counterpart. Sequence alignment of bacterial RbfA (*E. coli* and *T. thermophilus*) and human mtRbfA shows only a few identities (Figure 8.1 A). Low sequence similarity was also seen between other bacterial RbfA homologous as it is also shown in figure 8.1 (compare *E. coli* and *T. thermophilus*). Interestingly available structures from human mtRbfA from residue Arg86 to Asp201 demonstrate high similarity between *E. coli* RbfA and human mtRbfA over this region (Figure 8.1 B). This solution structure shows the typical type-II KH-domain fold.

Bacterial RbfA is involved in the processing of the 16S rRNA and thus in the maturation of the 30S SSU. Xia *et al.* (2003) suggested that the 16S precursor, which accumulates in RbfA depleted cells in bacteria, is potentially the pre-16S rRNA, which is processed at the RNase III site (115 nt upstream of the 5'-end of the mature form). It seems reasonable to hypothesise that mtRbfA is involved in a similar process in human mitochondria. The 12S rRNA (*MT-RNR1*) within the 28S SSU in human mitochondria, however, does not appear to have the kind of precursor form as is the case for the 16S rRNA in bacteria. In human mitochondria 12S rRNA is flanked by $tRNA^{Phe}$ (5'-end) and $tRNA^{Val}$ (3'-end) in an intronless polycistronic transcript [Anderson *et al.*, 1981; Ojala *et al.*, 1981], whose cleavage requires tRNase Z and RNase P processing at the 3'- and 5'-end, respectively of the tRNAs.

A

```
RbfA E. coli          ------------------------------------------------
RbfA T. thermophilus  ------------------------------------------------
mtRbfA H. sapiens     MWAAAGGLWRSRAGLRALFRSRDAALFPGCERGLHCSAVSCKNWLKKFAS 50

RbfA E. coli          ----------------------------------MAKEFGRPQRVAQEM 15
RbfA T. thermophilus  ----------------------------------MAYGKAH-LEAQL 12
mtRbfA H. sapiens     KTKKKVWYESPSLGSHSTYKPSKLEFLMRSTSKKTRKEDHARLRALNGLL 100
                                                         ..: : :   :

RbfA E. coli          QKEIALILQR-EIKDPRLGMMTTVSGVEMSRDLAYAKVYVTFLNDKDEDA 64
RbfA T. thermophilus  KRALAEEIQ--ALEDPRL-FLLTVEAVRLSKDGSVLSVYVEAFREEE--- 56
mtRbfA H. sapiens     YKALTDLLCTPEVSQELYDLNVELSKVSLTPDFSACRAYWKTTLSAEQN- 149
                       : ::  :    :.:    :   :. * :: * :   .*     . :

RbfA E. coli          VKAGIKALQEASGFIRSLLGKAMRLRIVPELTFFYDNSLVEGMRMSNLVT 114
RbfA T. thermophilus  --GALRALSRAERRLVAALARRVRMRRLPRLEFL---------------- 88
mtRbfA H. sapiens     -AHMEAVLQRSAAHMRHLLMSQQTLRNVPPIVFVQDKGNAALAELDQLLA 198
                            .*..:   :   *     :* :* : *.

RbfA E. coli          SVVKHDEERRVNPDDSKED------------------------------ 133
RbfA T. thermophilus  -------PWRASPA------------------------------------ 95
mtRbfA H. sapiens     VADFGPRDERDNFVQNDFRDPDAPQPCGTTEPTTSSSLCGIDHEALNKQI 248
                             * .

RbfA E. coli          ------------------------------------------------
RbfA T. thermophilus  ------------------------------------------------
mtRbfA H. sapiens     MEYKRRKDKGLGGLVWQGQVAELTTQMKKGRKRAKPRLEQDSSLKSYLSG 298

RbfA E. coli          -------------------------------------------
RbfA T. thermophilus  -------------------------------------------
mtRbfA H. sapiens     EEVEDDLDLVGAPEYECYAPDTEELEAERGGGRTEDGHSCGASRE 343
```

B

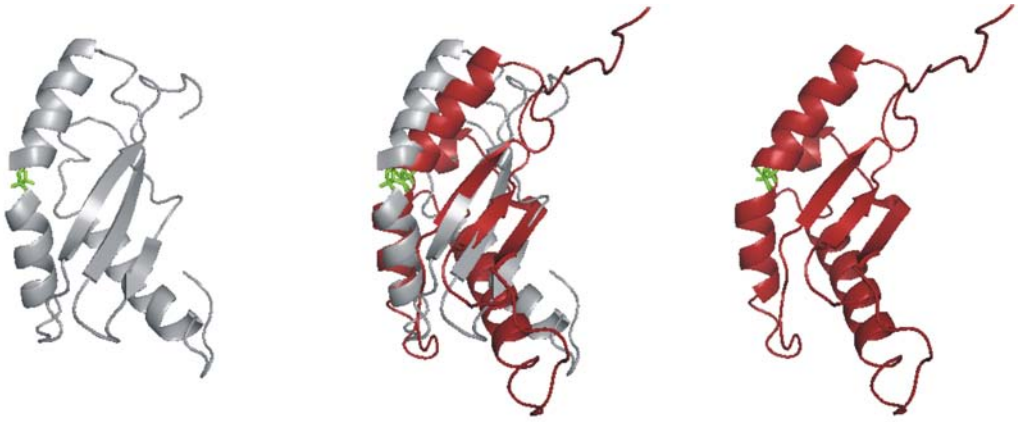

Figure 8.1: Sequence and structure alignment of bacterial RbfA and human mtRbfA. A) Sequence alignment (CLUSTALW) of RbfA from *E. coli* and *T. thermophilus* and mtRbfA from *H. sapiens*. Identities are indicated by a star (*), high level of similarity by a colon (:) and lower levels by a full stop (.). The basic residues **Arg7**, **Arg10**, **Arg45**, **Arg80**, **Lys85**, **Arg88**, **Arg90** (bold) in *E. coli* RbfA are maybe involved in RNA-binding [Huang *et al.*, 2003]. The Ala75 (green) of the AXG sequence forms an inter-helical kink (see B below). A well-conserved "sequence signature" (IRXXLXXXXXLRXVPXLXFXXD), located in the C-terminal region of *E. coli* RbfA is labelled in red. Human mtRbfA shares not all, but most of those named characteristic features of *E. coli* RbfA. **B)** Structures of *E. coli* RbfA (grey, PDB: 1KKG; Huang *et al.*, 2003) and human mtRbfA (red, PDB: 2E7G, unpublished) were superimposed using PyMOL. Both show the type-II KH-domain fold with three helices and three β-strands. Human mtRbfA shows an additional small helix, whose sequence is underlined in (A). The inter-helical kink formed by Ala75 in *E. coli* RbfA and by Ser159 in human mtRbfA is showed as green sticks.

Thus even if mtRbfA is still involved in the maturation of the ribosomal small subunit in human mitochondria, it must have adopted a distinct function. A substantial increase in the size of the protein supports the idea that mtRbfA may function in different way to its bacterial counterpart. Recently Dennerlein *et al.* (2010) reported that ERAL1 the orthologue of the bacterial Era GTPase, is a 12S rRNA chaperone in human mitochondria, binding to the 3'-end of the 12S rRNA. The loss of ERAL1 in human cells leads to a substantial reduction in the steady state level of 12S rRNA. In bacteria it has been shown that Era is also involved in the maturation of the 16S rRNA, where it facilitates the processing of the 3'-end. Datta *et al.* (2007) demonstrated that Era and RbfA interact with common elements of the 30S SSU, especially the helix 28 (h28). It was suggested that Era's interaction with h28 stabilises h1 indirectly, which is supposed to be a direct function of RbfA in bacteria. This is in agreement with the report by Inoue *et al.* (2003), where it was demonstrated that Era is able to partially suppress the cold sensitive phenotype and the defect in ribosome assembly caused by lack of RbfA in strains with deletions. Human ERAL1 has maintained its function in 28S SSU maturation operating as does its counterpart Era in bacteria. The question then is, whether the same is true for mtRbfA? Is mtRbfA involved in the maturation or assembly of the 28S SSU in human mitochondria? To answer those questions two main approaches were applied:

i) Immunoprecipitation and isokinetic sucrose gradient were utilised to investigate whether mtRbfA interacts with the 28S SSU
ii) siRNA technology was used to determine the cellular and molecular effect of mtRbfA depletion.

8.2 Localisation of the human ribosome binding factor A (mtRbfA)

The first aim of this project was to identify whether mtRbfA is really a mitochondrial protein. TargetP 1.1 predicts mitochondrial targeting of mtRbfA with RC1 and cleavage site of the targeting peptide after residue 41. The cleavage site prediction using PSORTII is quite different from TargetP 1.1. PSORTII predicts RbfA to be a mitochondrial protein with 43.5% with a possible cleavage site for mitochondrial presequence at residue 21 (subprogramme "Gavel").

To determine whether human ribosome binding factor A (mtRbfA) is a mitochondrial protein, cellular fractionation and mitochondrial preparations were made and analysed by western blotting to show whether the localisation of mtRbfA was within the

mitochondria fraction. For this approach specific antibodies against mtRbfA are essential. Therefore recombinant bacterially overexpressed protein generated by Dr. J. Rorbach was purified and sent to Eurogentec, Belgium to inject 2 rabbits 4 times over 3 months with 100 µg protein each time. The antiserum was tested on cell lysate and isolated mitochondria. As shown in figure 8.2 (left panel) the non-purified antiserum gave many non-specific interactions. Thus it needed to be purified to be useful for further investigations in this study.

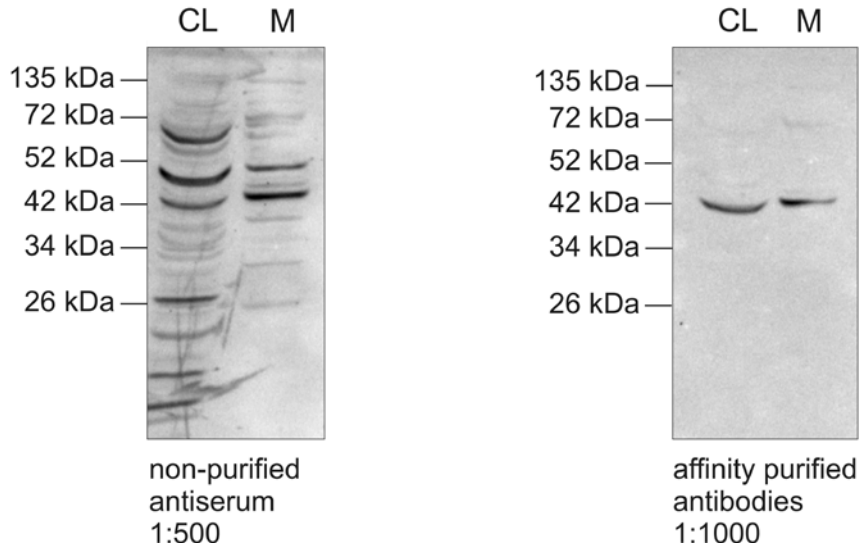

Figure 8.2: Analysis of specificity of antiserum (rabbit anti human mtRbfA polyclonal antibody). Western blot of 50 µg lysate from HEK293T cells (CL) and 10 µg isolated mitochondria (M) were probed with non-purified antiserum (dilution 1:500) and with affinity purified antibodies against human mtRbfA (dilution 1:1000).

For antibody purification approximately 1-2 mg of affinity purified recombinant protein was needed. Because the bacterially expressed full length recombinant mtRbfA-GST was mostly insoluble, a construct had to be made that would result in a higher recovery in the soluble fraction. A truncation of the N-terminus, which is usually quite hydrophobic in case of mitochondrial proteins, was made to help to resolve this problem. Therefore sequence encoding the *mtRbfA* was amplified with a truncation of 90 nucleotides at the 5'-end using the primer-pair #14/#15 (Table 3.2) and as the template pGex-6P-1-mtRbfA (containing full length *mtRbfA*; provided by Dr. J. Rorbach). The amplicon and the vector pGex-6P-1 were digested using *BamH*I and *Xho*I, the vector was dephosphorylated and finally vector and insert were ligated. After successful cloning the construct was used for *E. coli* Rosetta^{TM}(DE3) transformation. The strain was then utilised to purify a 30 amino acids N-terminus truncated recombinant mtRbfA via the GST-tag, which was then used for the antibody purification as described in 3.5.13. As shown in figure 8.2 (right panel) the purified antibodies recognised a single band in cell lysate and isolated mitochondria with the expected

molecular weight of approximately 40 kDa (Uniprot database - Q8N0V3 - calculation: 38.359 kDa of isoform 1). This result also suggests that the protein is localised to and potentially within mitochondria.
As shown later on in this study the antibodies are confirmed as specifically recognising mtRbfA, as the signal disappears after depletion of mtRbfA and furthermore increases when mtRbfA was overexpressed in cell culture.

To analyse whether mtRbfA is localised within mitochondria a western blot shown in figure 8.3 was performed with cell lysate (lane 1), isolated mitochondria (lane 2) and isolated mitochondria treated with proteinase K to remove cytosolic contaminations (lane 3). Lysed mitochondria were treated with the same amount of enzyme to be sure about the activity of proteinase K and the sensitivity of the tested proteins against the enzyme (lane 4). As a mitochondrial marker MRPS18B, a component of the mitochondrial ribosomal small subunit was used and clearly MRPS18B was detectable in cell lysate, isolated mitochondria and was also protected from the proteinase K treatment by the intact mitochondrial membrane. Mitochondria lysis allowed the digestion of MRPS18B by proteinase K, demonstrating its sensitivity to the enzyme. RP-S6 as a cytosolic marker was detectable in cell lysate, but completely disappeared in the fraction of proteinase K treated mitochondria. mtRbfA followed the same pattern as MRPS18B and thus concluding from this experiment mtRbfA is localised within the mitochondria.

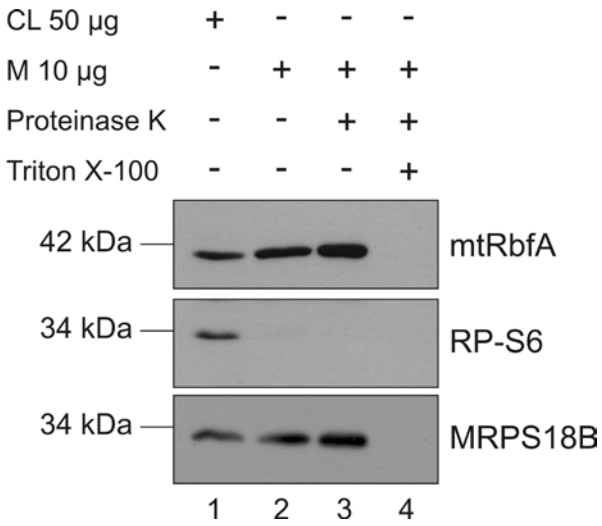

Figure 8.3: Cellular localisation of mtRbfA. Western blot shows 50 µg lysate of HEK293T cells (lane 1), 10 µg isolated mitochondria (lane 2) and 10 µg isolated mitochondria treated with proteinase K in the absence (lane 3) and presence (lane 4) of 1% Triton X-100. Using specific antibodies against mtRbfA a single band of ~ 40 kDa was detectable in cell lysate and in intact mitochondria. After mitochondrial lysis mtRbfA was no longer detected. MRPS18B was used as a mitochondrial marker and RP-S6 as a cytosolic marker.

8.3 mtRbfA is associated with the mitochondrial ribosomal small subunit

As suggested from the studies of RbfA in bacteria, the human orthologue is potentially involved in the maturation of the mitochondrial ribosomal small subunit. As a first step to investigate this possibility it had to be shown that mtRbfA is associated/ interacting in some way with the mitochondrial ribosomal small subunit. Therefore 700 µg of lysate from HEK293T cells were separated on a 10 - 30% isokinetic sucrose gradient, the fractions of which were analysed by western blot (Figure 8.4). Fraction 1 represents the top of the gradient containing particles with lighter sedimentation, whereas fraction 10, the bottom of the gradient shows complexes with heavier sedimentation.

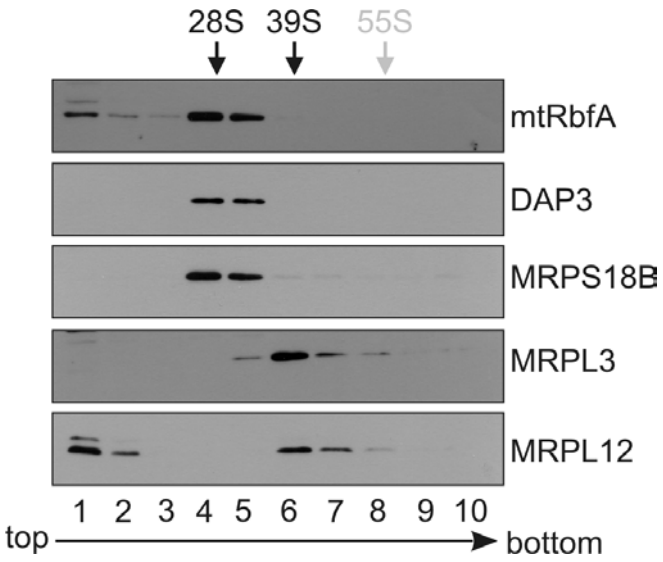

Figure 8.4: Endogenous mtRbfA co-migrates with 28S SSU on isokinetic sucrose gradient. HEK293T cell lysate (700 µg) was separated on a 10-30% sucrose gradient. Fractions, which were taken from top to bottom (labelled as 1-10 under the figure) were analysed by western blot. Using specific antibodies against components of the 28S SSU (DAP3 and MRPS18B) and the 39S LSU (MRPL3 and MRPL12) allowed the determination of the sedimentation of the ribosomal subunits within these gradients. The relative position of the mitochondrial ribosomal subunits and the monosome are indicated at the top of the image. The distribution of mtRbfA within this gradient was determined by using specific antibodies against the protein.

Under these conditions the 28S SSU was localised in fraction 4 and 5, represented by the migration of DAP3 and MRPS18B, components of the 28S SSU. MRPL3 and MRPL12, components of the 39S LSU were mostly detectable in fractions 6 and 7. MtRbfA was localised in fractions 1 (~18% of total mtRbfA protein), 2 (~9%) and also 3 (~5%), but the majority co-sediment with the 28S SSU in fractions 4 (~36%) and 5 (~26%), a first indication that mtRbfA is maybe associated with the 28S SSU.

8.4 MtRbfA-FLAG is able to co-immunoprecipitate mitochondrial ribosomal proteins

To confirm whether the observation of mtRbfA interacting with the 28S was real and also to investigate whether it is also associated with the 55S monosome, which is not visible with this kind of gradient, another experiment was performed. A cell line expressing mtRbfA-FLAG HEK293T, generated by Dr. J. Rorbach, was used to perform immunoprecipitation of mtRbfA via the FLAG tag as described in 3.5.9. As a negative control for any non-specific interaction in the immunoprecipitation, a mitochondrial targeted Luciferase (mtLuc-FLAG) was treated in the same way as mtRbfA-FLAG. To avoid unspecific interactions with cytosolic proteins mitochondria were isolated and purified as described in 3.5.8 prior to lysis. The elution fractions of mtRbfA-FLAG and mtLuc-FLAG were analysed by silver staining and western blot as presented in figure 8.5.

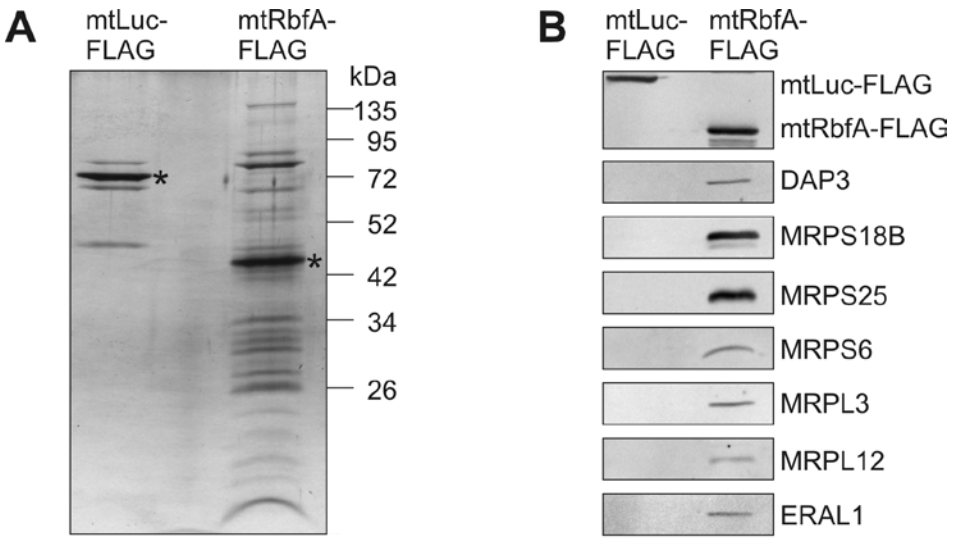

Figure 8.5: MtRbfA-FLAG is associated with mitochondrial ribosomal proteins. A) Equal amounts of each elution fraction (10%) were separated on 12% SDS-PAG followed by silver staining. * indicates the FLAG tagged protein. **B)** Western blot of the elution fractions were probed with markers of the 28S SSU (DAP3, MRPS18B, MRPS25 and MRPS6), the 39S LSU (MRPL3 and MRPL12) and with 12S rRNA chaperone ERAL1. Mitochondrial targeted Luc-FLAG was used as a control, confirming specificity of the IP. FLAG tagged proteins were detected in each elution fraction with specific antibodies against the FLAG epitope.

On the silver staining mtRbfA-FLAG showed several additional signals in comparison to the mtLuc-FLAG. The pattern is suggestive of ribosomal proteins, thus western blot of the eluates were probed with antibodies against components of the 28S SSU (DAP3, MRPS18B, MRPS25, MRPS6) and the 39S LSU (MRPL3, MRPL12), respectively. All tested components were detectable in the elution of mtRbfA-FLAG, but not in the

control of mtLuc-FLAG. ERAL1, a 12S rRNA chaperone was also associated within this immunoprecipitated complex. This result suggested that mtRbfA-FLAG is not just associated with the 28S SSU. There are also some interactions with the components of the 39S LSU or the 55S monosome.

For more detailed analysis of the elution fraction, samples were sent by Dr. J. Rorbach for LC MS/MS (Liquid chromatography - tandem mass spectrometry) analysis to H. Wessels and Prof. J. Smeitink at UNMC, Nijmegen.

The majority of co-immunoprecipitated proteins by mtRbfA-FLAG were mitochondrial ribosomal proteins as listed in table 8.1 (See also appendix 2).

Table 8.1: Mitochondrial ribosomal proteins identified as co-purified components of the mtRbfA-FLAG immunoprecipitation

Small Subunit (28S) - SSU	**Large Subunit (39S) - LSU**
MRPS2, MRPS5, MRPS6, *MRPS7*, MRPS9, MRPS10, MRPS11, MRPS16, MRPS15, *MRPS17*, MRPS18A, MRPS18B, *MRPS21*, *MRPS22*, MRPS23, MRPS25, *MRPS26*, MRPS27, MRPS28, MRPS29/DAP3, MRPS30, MRPS31, MRPS34, MRPS35, METT11D1	MRPL1, MRPL2, MRPL3, MRPL4, MRPL9, MRPL11, MRPL12, MRPL13, MRPL14, MRPL15, MRPL16, MRPL17, MRPL18, MRPL19, MRPL20, MRPL21, MRPL22, MRPL23, MRPL24, MRPL28, MRPL31, MRPL37, MRPL38, MRPL39, MRPL40, MRPL41, MRPL43a, MRPL43b, MRPL44, MRPL45, MRPL46, MRPL47, MRPL48, MRPL49, MRPL50, MRPL51, MRPL54, MRPL55, MRPL58/ICT1
25 MRPS of 31	39 MRPL of 51

Overall there was a balanced ratio of members of the 28S SSU and the 39S LSU, suggesting an interaction of mtRbfA with either the monosome or the separated subunits, respectively. However, the ribosomal proteins with the highest EMPAI value[1], were components of the 28S SSU: MRPS26, MRPS21, MRPS7, MRPS22 and MRPS17 (from high to low).

Furthermore mtIF2 was also detected within this IP, suggesting an association of mtRbfA with the translation initiation complex, which harbours the 28S SSU and mtIF2.

[1] EMPAI (experimental modified protein abundance index) value represents an estimation of molar abundance of proteins in the analysed sample, calculated by H. Wessels. The protein abundance index (PAI) is a semi-quantitative representation of the relative amount of protein in the sample, relating the number of identified tryptic peptides to the number of theoretically observable ones.

The 12S rRNA chaperone, ERAL1 [Dennerlein *et al.*, 2010] was also seen in this IP, supporting the idea that mtRbfA has a preference for the ribosomal small subunit. Another protein that was detected with a relatively high EMPAI value was SLIRP, an RNA-binding protein whose stability itself was shown to be RNA dependent [Baughman *et al.*, 2009]. Surprisingly mtRRF was absent in the mtRbfA-FLAG-IP, whereas mtRbfA was co-immunoprecipitated with mtRRF-FLAG [Rorbach *et al.*, 2008]. mtRRF is a good indicator for a 55S monosome and thus this result suggest that mtRbfA is maybe not associated with the 55S mitochondrial monosome.

To distinguish whether mtRbfA is associated with the 55S monosome or with the 39S LSU besides the 28S SSU, immunoprecipitated eluate was separated on an isokinetic sucrose gradient. Fractions were analysed by silver staining (Figure 8.6 A, lower panel) and western blot (Figure 8.6 A, upper panel). As shown in figure 8.6 mtRbfA-FLAG migrated mainly in fractions 1, 2 and 4, 5, but it was also detectable in every other fraction at lower level. Components of the 28S SSU, including DAP3, MRPS18B and MRPS25, co-sediment with mtRbfA-FLAG represented mostly in fractions 4, 5 and also 6. There was no signal in fraction 8, the approximate position of the 55S monosome, suggesting that mtRbfA-FLAG is not associated with the 55S. Components of the 39S LSU (MRPL3, MRPL12 and trace amounts of ICT1) were detectable mainly in fraction 6, which represents the 39S LSU alone and not the monosome. Interestingly, MRPL12 was also located at higher level in fractions 1 and 2. This protein was also detected with increased amounts from fraction 7 to 8, but this would make MRPL12 as the only indicator that mtRbfA is potentially associated with the 55S. ERAL1 was detected in fractions 4 and 5 with the 28S SSU, but also in relative similar intensity in fractions 1 and 2. Analysing those fractions by silver staining (Figure 8.6 A, lower panel) showed again the majority of bands, especially with lower molecular weight, in fractions 4 to 6, but not in 8. Interestingly there were also several strong bands with higher molecular weight in the earlier fractions 1 to 5. Most of the mitochondrial ribosomal proteins have a molecular weight less than 45 kDa [Koc *et al.*, 2001b/c], suggesting that those bands represent other interaction partners than components of the mitochondrial ribosome.

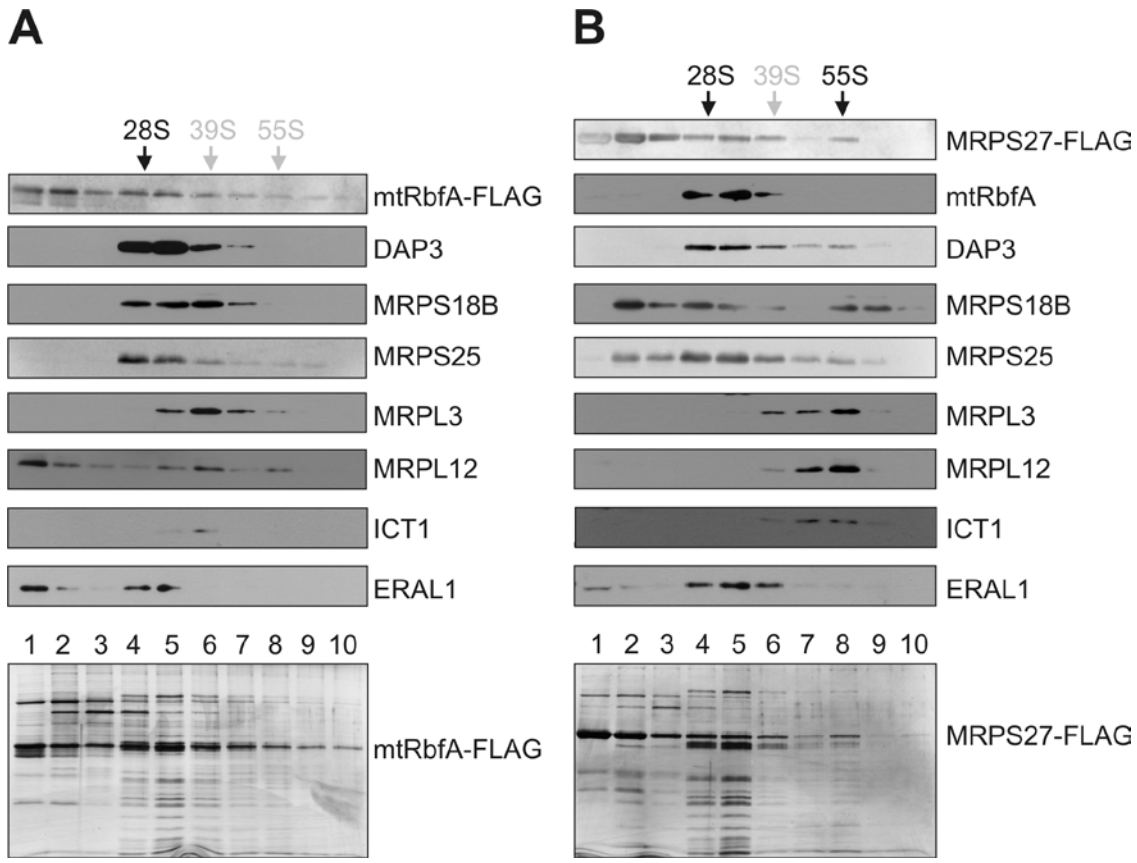

Figure 8.6: Gradients of complexes co-immunoprecipitated with mtRbfA-FLAG and MRPS27-FLAG. HEK293T cell lines expressing mtRbfA-FLAG (A) or MRPS27-FLAG (B) were induced for 3 days with 1 µg/ ml tetracycline. After a standard IP using 3 mg mitochondrial lysates, eluates (80%) were separated by isokinetic sucrose gradients. Fractions (1-10) were analysed by silver staining (lower panels) and western blot (upper panels). Immunoprecipitated ribosomal complexes were detected using antibodies against members of the 28S SSU (DAP3, MRPS18B and MRPS25) and the 39S LSU (MRPL3, MRPL12 and ICT1). The distribution of ERAL1 is also shown. To examine the presence of the FLAG tagged protein in each fraction antibodies against the FLAG octapeptide were applied to each western blot membrane.

As a control for this experiment MRPS27-FLAG was treated in the same way and IP eluate was also separated on an isokinetic sucrose gradient. MRPS27-FLAG was able to pull down the 28S SSU and the 55S monosome using anti-FLAG antibodies as was already shown in chapter 5. On this gradient DAP3 migrated mostly in fraction 4, 5 and 6, but was also detectable in fraction 8, showing the 55S monosome. MRPS18B and MRPS25 co-migrated with MRPS27-FLAG in fractions 2 and 3, representing 28S SSU intermediates. They were also detectable in fractions 4 and 5, representing the 28S SSU, and also in fraction 8, thus within the 55S monosome. MRPL3, MRPL12 and ICT1 migrated mainly in fraction 8 as part of the 55S monosome. Interestingly the endogenous mtRbfA co-sediment only with the 28S SSU in fractions 4 to 6, but not with the 55S particle in fraction 8. Similarly the 12S rRNA chaperone ERAL1 was mostly detectable in fractions 4 to 6 and just trace amounts in fractions 1 and 2.

Concluding from this experiment mtRbfA is associated with the 28S SSU, but not with the 55S. So far it can not be excluded whether mtRbfA is really interacting with the 39S LSU or whether the result of co-migrating of mtRbfA-FLAG with components of the 39S after immunoprecipitation is more unspecific binding caused by the overexpression of mtRbfA-FLAG. To exclude the latter lower amount of mtRbfA-FLAG need to be used for the same kind of experiment.

To ensure that the mtRbfA-FLAG was present at an approximately similar level to the endogenous form within the mitochondria, the latter expression levels had to be determined. This experiment might also clarify whether the majority of the expressed FLAG tagged protein is imported into the mitochondria.
To this end untransfected HEK293T cells (HEK293-wildtype; HEK293-WT) were used as the control for relative expression level of endogenous mtRbfA, in parallel HEK293T cells expressing mtRbfA-FLAG were analysed uninduced and induced with 1 ng/ ml doxycycline (DOX). The reason for using HEK293-WT cells and uninduced HEK293-mtRbfA-FLAG cells is because of possible leaky expression of trace amounts of the FLAG tagged protein without adding the inducer.
By western blot as shown in figure 8.7 cell lysate, isolated mitochondria and isolated mitochondria treated with proteinase K in the absence and presence of 1% Triton X-100 were analysed for each sample.

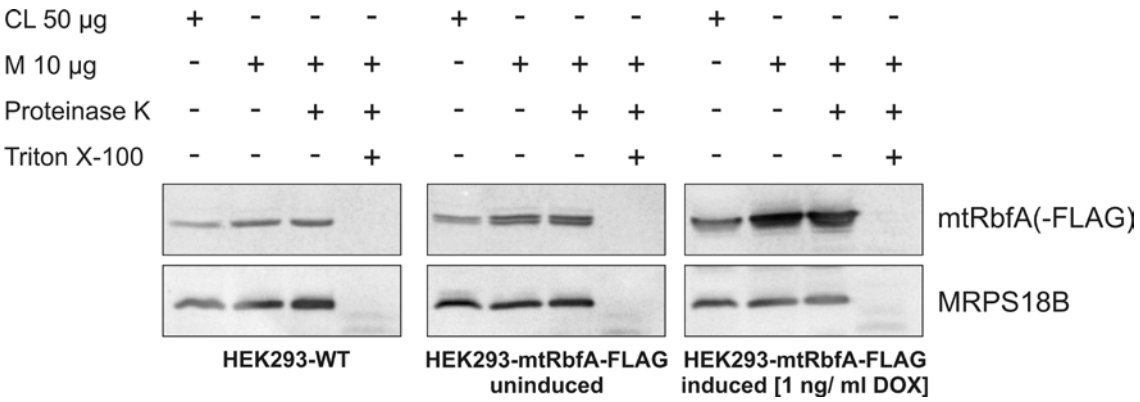

Figure 8.7: Titration of mtRbfA protein level. Western blots show samples of cell lysates (50 µg) and isolated mitochondria (10 µg) from untransfected HEK293-wildtype (HEK293-WT) cells, uninduced or induced HEK293-mtRbfA-FLAG. To ensure that mitochondria were free from cytosolic contamination mitochondria were treated with proteinase K. Lysed mitochondria were analysed in the same way to confirm the activity of the enzyme and the sensitivity of the tested proteins against it. The relative protein level of mtRbfA (±FLAG tag) in each sample was determined by using specific antibodies against mtRbfA. MRPS18B was used as a loading control.

As a loading control MRPS18B was used. The samples of HEK293-WT showed as before that the localisation of mtRbfA within the mitochondria as it was protected from

proteinase K treatment by the intact mitochondrial membrane. The uninduced HEK293-mtRbfA-FLAG samples showed a doublet when mtRbfA antibodies were used. This doublet is also resistant against proteinase K. It was noticed before that the FLAG tag can change migration of proteins (ICT1-FLAG migrated also slightly above the endogenous form, figure 6.9). Thus it was assumed that there was an expression of the mtRbfA-FLAG at a relatively similar level to the endogenous form even without adding inducer. Reason for the “leaking” can be trace amounts of tetracycline in the FBS, which is added to the culture media. Using 1 ng/ ml DOX for 3 days resulted in an increase of mtRbfA-FLAG up to 5 fold. Thus for further investigations the uninduced form was used, as it showed approximately similar expression level as the endogenous form.

Using the uninduced mtRbfA-FLAG for IP, followed by separation of the eluate on a sucrose gradient (Figure 8.8) showed clear differences to the result achieved with the induced sample earlier.

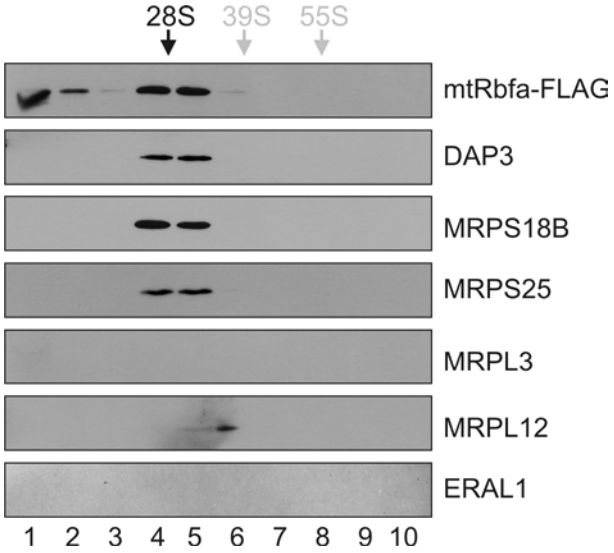

Figure 8.8: mtRbfA-FLAG is predominantly associated with the 28S SSU. Mitochondrial lysate (3 mg) from mtRbfA-FLAG expressing cells at level similar to endogenous mtRbfA were used for IP via FLAG tag. IP eluate (80%) was subjected to 10 - 30% isokinetic sucrose gradient. Isolated fractions (1-10) were analysed by western blot, using antibodies against the FLAG octapeptide to examine the distribution of mtRbfA-FLAG within this gradient. The level of co-immunoprecipitated ribosomal complexes was determined by using antibodies against components of the 28S SSU (DAP3, MRPS18B and MRPS25), the 39S LSU (MRPL3 and MRPL12) and further ERAL1.

Here the mtRbfA-FLAG was mainly detectable in fractions 1, 2 and 4, 5, whereas the highly overexpressed form was detectable in every fraction. The components of the 28S SSU DAP3, MRPS18B and MRPS25 co-migrated all in fractions 4 and 5, whereas componets of the 39S LSU (MRPL3 and MRPL12) were not detectable or only at very

low level in 5 and 6. ERAL1, which was present in 1, 2 and 4, 5 in the previous over-expressed experiment, also disappeared.

In conclusion it appear that mtRbfA does not interact with the 55S monosome, further it seems as though an association with the 39S LSU is quite unlikely. The reason for this apparent association in the previous experiment is most likely to be due to the relatively high overexpression, which might lead to artefacts.

8.5 EDTA treatment results in the loss of the association of mtRbfA-FLAG with mitochondrial ribosomal proteins

There is a possibility that the association of mtRbfA with the 28S SSU is caused by the interaction of mtRbfA with the ribosomal RNA, as it is the case for the bacterial RbfA. Therefore to destabilise the RNA structure within the ribosome EDTA was used within the immunoprecipitation samples to deplete Mg^{2+}, which is necessary for correct RNA folding. For this experiment the uninduced mtRbfA-FLAG was used for the IP rather using the high overexpressed form to avoid the artefacts previously observed and described above. As a control HEK293-WT cells were used. Mitochondria were isolated from both cell lines and purified prior to immunoprecipitation. Both were analysed in the absence and presence of 50 mM EDTA, as shown in figure 8.9.

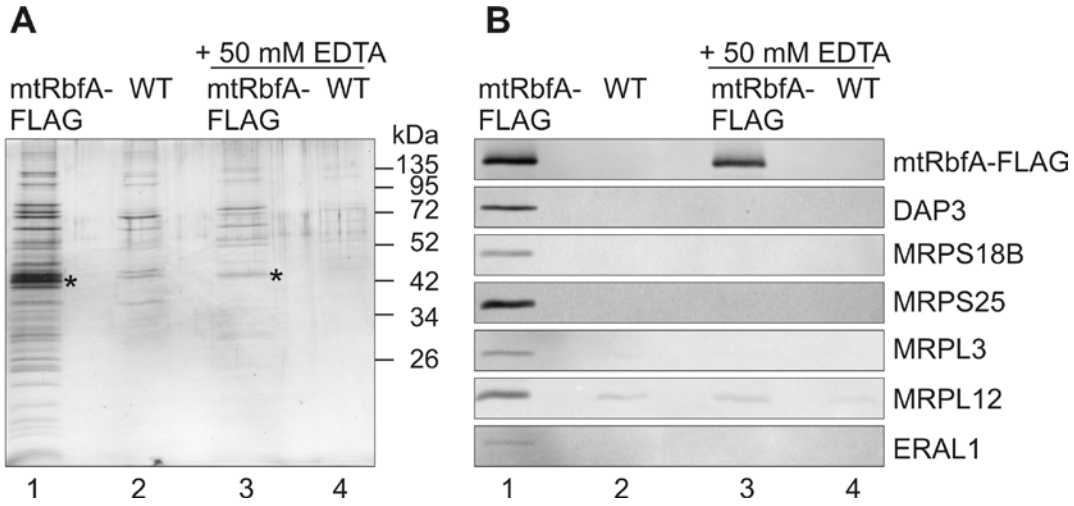

Figure 8.9: Depletion of Mg^{2+} causes a loss of mtRbfA's association with the 28S SSU. Mitochondrial lysates from HEK293-mtRbfA-FLAG (uninduced, lane 1 and 3) and HEK293-WT (lane 2 and 4) were treated with (lane 3 and 4) or without (1 and 2) 50 mM EDTA prior to immunoprecipitation. Elution fraction (10%) of each sample was analysed by silver staining (A) or western blot (B). **A)** * indicates the mtRbfA-FLAG. **B)** Antibodies against mitochondrial ribosomal proteins were applied to the western blot membrane to determine the relative level of co-immunoprecipitated ribosomal complexes in each sample. To ensure similar level of mtRbfA-FLAG in EDTA untreated and treated sample (lane 1 and 3) antibodies against the FLAG epitope were used. The level of ERAL1 was also investigated.

On silver staining the elution fraction of mtRbfA-FLAG showed again several bands, of which most of which were lost after the EDTA treatment. The negative control (WT) showed only a few bands, which represents some unspecific bindings and IgG chains. On the western blot the mitochondrial ribosomal proteins were detected in the elution fraction of mtRbfA-FLAG. There, also MRPL3 and MRPL12 could be detected, which were almost absent in the gradient of co-immunoprecipitated eluates. Therefore those signals represent no interaction complex of mtRbfA with 39S LSU.
All signals were absent in the control except trace amounts of MRPL12. After the EDTA treatment none of the mitochondrial ribosomal proteins were detectable in the elution of mtRbfA-FLAG. Only MRPL12 was present, and at low levels, which is comparable to the relative unspecific binding in the control sample (WT). This result suggest that the interaction of mtRbfA with the 28S SSU is Mg^{2+} dependent, possibly indicating that mtRbfA's association with the 28S SSU is caused by RNA-protein rather than protein-protein interaction.

8.6 Crosslinking immunoprecipitation (CLIP) failed to consistently identify interacting RNA species of mtRbfA

CLIP as described in 3.5.10 is a method to identify short RNA species that may be interacting closely with the protein of interest. Bacterial RbfA with a type-II KH-domain is responsible for the processing of 16S rRNA and thus it is possible that mtRbfA-FLAG that also contains a type-II KH-domain fold, and whose structure is very similar to bacterial RbfA, may also act as a RNA binding protein.
For the CLIP, HEK293T-mtRbfA-FLAG cells were UV irradiated to crosslink the RNA to the protein. Cells were not induced, only the "leaky" form of mtRbfA-FLAG generating approximately endogenous levels of protein. Shown in figure 8.10 is the autoradiogram post RNase T1 cleavage and end-labelling. The under-digested sample (2U T1) showed a number of bands, which made it difficult to decide with high confidence which protein-RNA complex to excise. Assuming that mtRbfA-FLAG is approximately 40 kDa, the RNA-complex should be 20 kDa above and thus around 60 kDa, where a thin band was removed of the membrane.

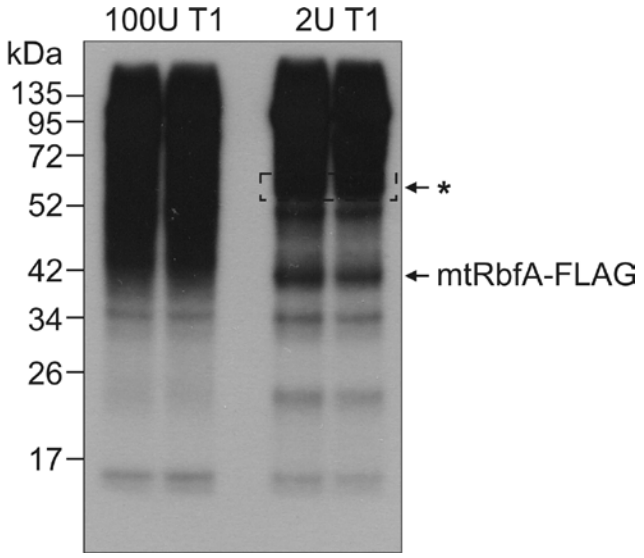

Figure 8.10: Analysis of UV crosslinked protein-RNA complexes by western blot. HEK293T cells expressing mtRbfA-FLAG were UV irradiated and used for IP. After RNase T1 treatment protein-RNA complexes of different sizes were detectable by 5'-γ^{32}P endlabelling. The potential mtRbfA-RNA complex with assumed migration of approximately 60 kDa was excised the membrane, indicated by *.

Following the protocol the final products were cloned into pCR4-TOPO vector. Individual colonies were then tested by colony PCR and products of approximately 250 to 300 bp were considered for sequencing. As shown in figure 8.11 most of the colonies produced amplicons of the expected size and were analysed by sequencing. Colonies that showed more than one product (e.g. #1 in figure 8.11) were excluded from further analysis.

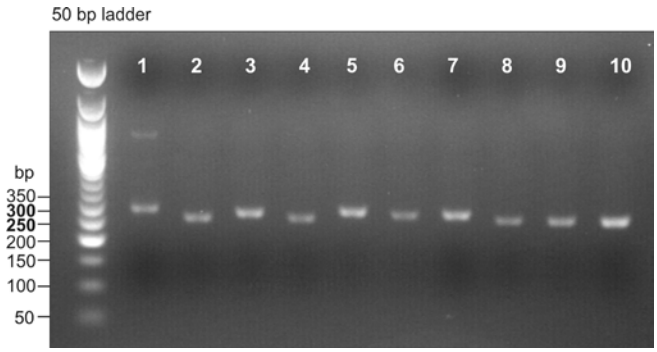

Figure 8.11: Colony PCR analysis after CLIP. Bacterial colonies derived from CLIP assay were analysed by colony PCR as described in 3.5.10. 5 µl of each reaction containing 10% glycerol were separated on a 2% agarose gel against 50 bp ladder. The image represents an example of colony PCR, with products of expected size > 250 and < 300 bp.

Most of the derived sequences could be not identified by BLAST searches or it appeared that the linkers were amplified. The only sequences that could be clearly identified were (numbers of clones with that sequence are indicated):

1x 12S mt-rRNA (*MT-RNR1*)

```
MTRNR1 1539  CATTTATATAGAGGAGACAAGTCGTAACATGGTAAGTGTACTGGAAAGTGCACTTGGAC  1597
             ||||||||||||||||||||||||||||||||||||||||||||||||||||||||||
CLIP   59    CATTTATATAGAGGAGACAAGTCGTAACATCGTAAGTGTACTGGAAAGTGCACTTGGAC  1
```

2x 5S rRNA

```
5S     2   TCTACGGCCATACCACCCTGAACGCGCCCGATCTCGTCTGATCTCGGAAGCTAAGCAGGGTCGGGCCTGG
           ||||||||||||||||||||||||||||||||||||||||||||||||||||||||||||||||||||||
CLIP  91   TCTACGGCCATACCACCCTGAACGCGCCCGATCTCGTCTGATCTCGGAAGCTAAGCAGGGTCGGGCCTGT

           TTAGTACTTGGATGGGAGACC 92
           ||||||||||||||||||||
           TTAGTACTTGGATGGGAGACC 132

5S     2   TCTACGGCCATACCACCCTGAACGCGCCCGATCTCGTCTGATCTCGGAAGCTAAGCAGGGTCGGGCCTGG  71
           ||||||||||||||||||||||||||||||||||||||||||||||||||||||||||||||||||||||
CLIP   70  TCTACGGCCATACCACCCTGAACGCGCCCGATCTCGTCTGATCTCGGAAGCTAAGCAGGGTCGGGCCTGG  1
```

2x 28S rRNA (cytosolic)

```
CLIP   1     CGAAGGATCAAAAAGCAACGTCGCTATGAACGCTTGGCTGCCAC  44
             ||||||||||||||| |||||||||||||||||||| |||||
28S    4418  CGAAGGATCAAAAAGCGACGTCGCTATGAACGCTTGGCCGCCAC  4375

CLIP   1     ATGTTCAACTGCTGT  15
             ||||||||||||||||
28S    2419  ATGTTCAACTGCTGT  2405
```

1 x EST product of unknown status

```
CLIP   1      CTGAGCAGCTCCTAGCAGTTTGGCTGTCAAAAGGCCACTGAATAAACAAATTGATAGGAATGGCGGAC  68
              ||||||||||||||||||||||||||||||||||||||||||||||||||||||||||||||||||||
EST    39135  CTGAGCAGCTCCTAGCAGTTTGGCTGTCAAAAGGCCACTGAATAAACAAATTGATAGGAATGGCGGAC  39068
```

1x SSRP1 mRNA (cytosolic)

```
CLIP   1     GTACTGGCTAGTTCTTCTTCTTCAGAGT  28
             ||||||||||||||||||||||||||||
SSRP1  2354  GTACTGGCTAGTTCTTCTTCTTCAGAGT  2327
```

The experiment was repeated twice and no improvement in terms of “real” CLIP sequences could be achieved. Also cutting slices from the nylon membrane at higher or lower molecular weight did not improve the yield of identifiable sequences.

It is still an open question whether mtRbfA acts as an RNA binding protein and whether it is important for ribosomal RNA processing (as in bacteria) or organisation. Therefore further investigations are crucial to determine the function of mtRbfA within human mitochondria.

8.7 Depletion of mtRbfA in human cell culture

8.7.1 Expression level of mtRbfA is highly reduced in mtDNA lacking ρ^0 cells

The data shown so far suggest that mtRbfA, because of its association with the 28S SSU, may be involved in the mitochondrial gene expression machinery. To address this possibility it was investigated whether mtRbfA is present in 143B-ρ^0 cells, cells that lack mtDNA and therefore do not need a mitochondrial gene expression machinery. A number of factors including certain mitochondrial ribosomal proteins are absent in such cells, e.g. DAP3 and MRPL3 as shown on the western blot in figure 8.12. Interestingly mtRbfA was almost not detectable in 143B-ρ^0 cells, further suggesting that mtRbfA may be involved in the mitochondrial gene expression and is thus redundant in 143B-ρ^0 cells.

To investigate this issue further and to analyse whether mtRbfA is important for mitochondrial function and thus for cell viability siRNA were applied to HEK293T cells to investigate the consequences of mtRbfA depletion in human cells.

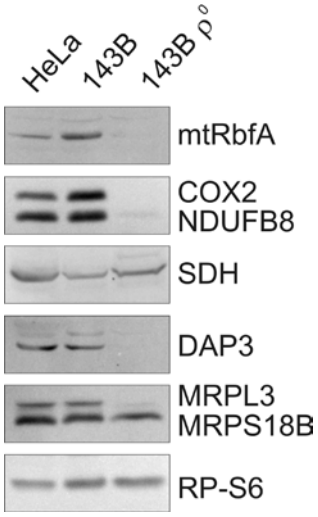

Figure 8.12: Expression level of mtRbfA protein is highly reduced in 143B-ρ^0 cells. Lysates (30 µg) from HeLa, 143B parental and -ρ^0 cells were analysed by western blot. Specific antibodies against mitochondrial proteins including mtRbfA, components of the OXPHOS complexes such as COX2, NDUFB8 and SDH, and members of the mitochondrial ribosome DAP3, MRPL3 and MRPS18B were used to determine the relative expression level in each cell line. Cytosolic marker RP-S6 was used as loading control.

8.7.2 The effect of mtRbfA depletion on cell growth

Dr. J. Rorbach has previously tested 6 different siRNAs sequences targeted to *mtRbfA* transcripts (Table 3.1) in the MTT assay to distinguish which siRNA shows an effect on

growth of 143B-ρ^0 cells. Those siRNAs that were considered to have off-target effect were not used for further analysis.

For this study si-RbfA A and B were chosen for further analysis. Neither showed a growth defect on 143B-ρ^0, whereas in HeLa cells both duplexes resulted in a decrease in growth rate after 3 days when estimated by the relative cell number compared to the si-NT control (si-RbfA A: 56%; si-RbfA B: 60%).

Next, it was tested by western blot how efficient the protein depletion was using both siRNAs independently. Therefore HEK293T cells were transfected with 50 nM siRNA using lipofectamine as transfection reagent. After 3 days cell lysates were prepared and analysed by western blot in comparison to si-NT control. As shown in figure 8.13 (top left panel) mtRbfA protein was down regulated to 10.7 % (± 5.4 %) using si-RbfA A and to 17.8% (± 10.2 %) in case of si-RbfA B compared to si-NT.

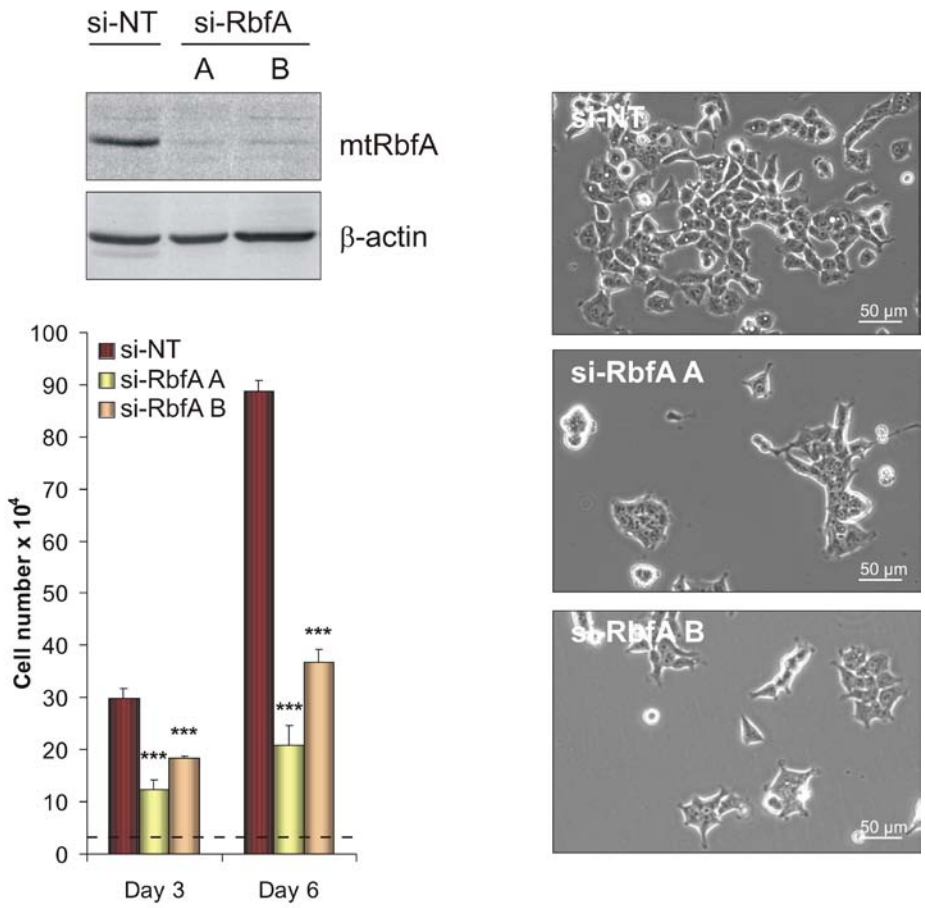

Figure 8.13: Effect of mtRbfA depletion on cell growth and morphology. HEK293T cells were treated with si-NT and si-Rbfa (A and B), respectively for 3 and 6 days. Western blot (top left panel) with 25 µg cell lysates was probed with antibodies against mtRbfA to confirm down regulation of mtRbfA protein after 3 days in comparison to si-NT. β-actin was used as loading control. The effect of mtRbfA depletion on cell growth was monitored by cell counting after 3 and 6 days siRNA treatment. For this experiment 3x 10^4 cells were used as starting point, marked as dotted line. *** extremely significant (n = 3, 3 days: si-RbfA A: p = 0.0004; si-RbfA B: p = 0.0006; 6 days: si-RbfA A: p = 0.0001; si-RbfA B: p = 0.0001). The phenotype of mtRbfA depleted cells and control was documented by using inverted microscope Axiovert200M (Zeiss) with camera (right panels).

In addition to the MTT assay, cell counts were also performed to confirm the effect on cell growth. In both cases the depletion of mtRbfA caused an extremely significant growth defect after 3 and 6 days in comparison to si-NT (Figure 8.13, graph bottom left). Cells transfected with si-RbfA B grew faster than those treated with si-RbfA A, which is probably due to the level of protein depletion as shown with the western blot analyses. Therefore si-RbfA A was considered to be more effective than si-RbfA B and was thus chosen for use in the remaining investigations, although both were used in some occasions. Both treatments showed a similar phenotype after 3 days of depletion as shown in figure 8.13, right panels.

8.7.3 No severe changes in level of mitochondrial ribosome could be observed after the loss of mtRbfA

Because of the fact that mtRbfA is associated with the 28S SSU the effect of mtRbfA depletion on the level of ribosome assembly was further investigated. Therefore cells transfected with si-RbfA A for 3 or 6 days were analysed by sucrose gradient (described in 3.5.11). The fractions were analysed by western blot in comparison to si-NT (Figure 8.14).

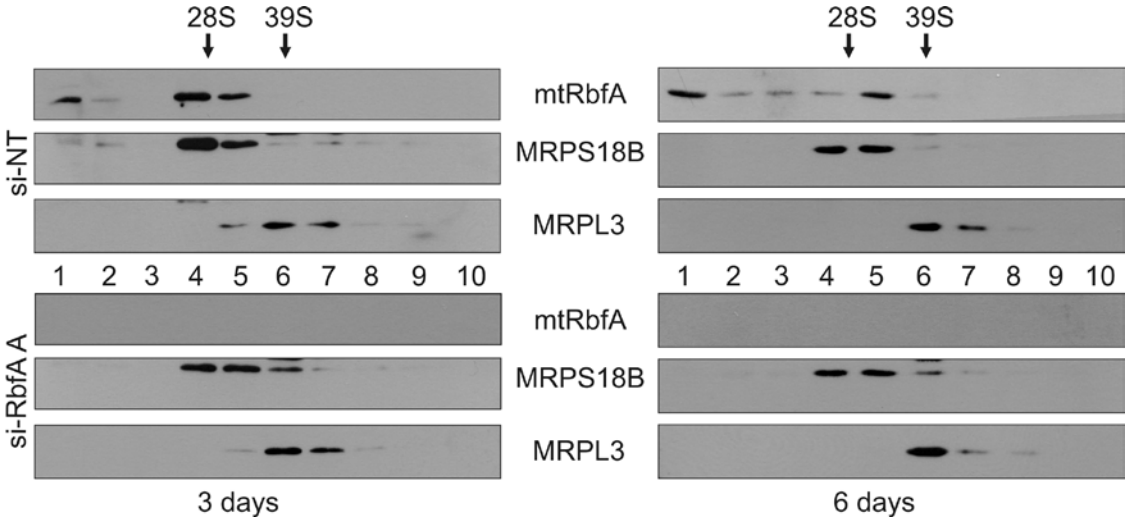

Figure 8.14: The effect of mtRbfA depletion on mitochondrial ribosomal subunits. Lysates (700 µg) of mtRbfA depleted and control cells were separated by isokinetic sucrose gradient after 3 and 6 days post siRNA transfection. Fractions (1-10) were analysed by western blot, probed with antibodies against mtRbfA to confirm successful depletion in si-RbfA treated samples. To determine changes in mitochondrial ribosomal profile, specific antibodies against MRPS18B, representing the 28S SSU and MRPL3, a member of the 39S LSU were applied to the western blots, individually.

The control showed that mtRbfA was free in fraction 1, but also associated with the 28S SSU in fractions 4 and 5. Interestingly the relative ratio of free mtRbfA to the

bound form to the 28S SSU changed between 3 and 6 days si-NT treatment. This could be due to the relatively high confluence of the cells after 6 days and possibly starvation. Thus it would be interesting to monitor the relative level of associated mtRbfA under different growth or stress situations. The 28S SSU, represented by MRPS18B, migrated mainly in fractions 4 and 5. MRPL3, a member of the 39S LSU was mostly located in fractions 6 and 7. After the depletion of mtRbfA MRPS18B migrated still in fractions 4 and 5, but was also present in relatively higher levels in comparison to si-NT in fraction 6. MRPL3 was similar between the mtRbfA depleted samples and the non-targeting control. From this experiment it cannot be shown that the depletion of mtRbfA has an effect on the 28S SSU that would cause a loss of the conformation of the 28S SSU.

To confirm the result that there was no dramatic effect of mtRbfA depletion, and also to investigate the relative level of monosome formation, immunoprecipitation of the 28S SSU and the 55S monosome was performed using the MRPS27-FLAG cell line. If the depletion of mtRbfA would have an effect on the 28S SSU that could cause a loss of the ability of the 28S SSU to interact with the 39S LSU to create an intact 55S monosome, then the prediction would be that there would be a loss of MRPL3 and MRPL12 in the elution fraction of MRPS27-FLAG.
The experiment was performed after 3 days depletion (si-RbfA A) and after 2 days induction. This was to allow overexpression of the FLAG-tagged protein and assembly into the mitochondrial ribosome. The cells were then harvested, lysed and equal amounts of cell lysate were used for the immunoprecipitations. The elution fractions were analysed by western blot. As shown in figure 8.15 MRPS27-FLAG in the si-NT treated sample is associated with DAP3 and MRPS18B, each present in both the 28S SSU and 55S monosome, and LSU components (MRPL3 and MRPL12), which represented the relative level of the monosome. The level of mtRbfA in the depleted samples was reduced to 20%. DAP3 was significant reduced to 71%, but MRPS18B with ~98% was similar to the control. MRPL3 and MRPL12 showed also a decrease to 74% and 77%, respectively, however, the result was not statistically significant.

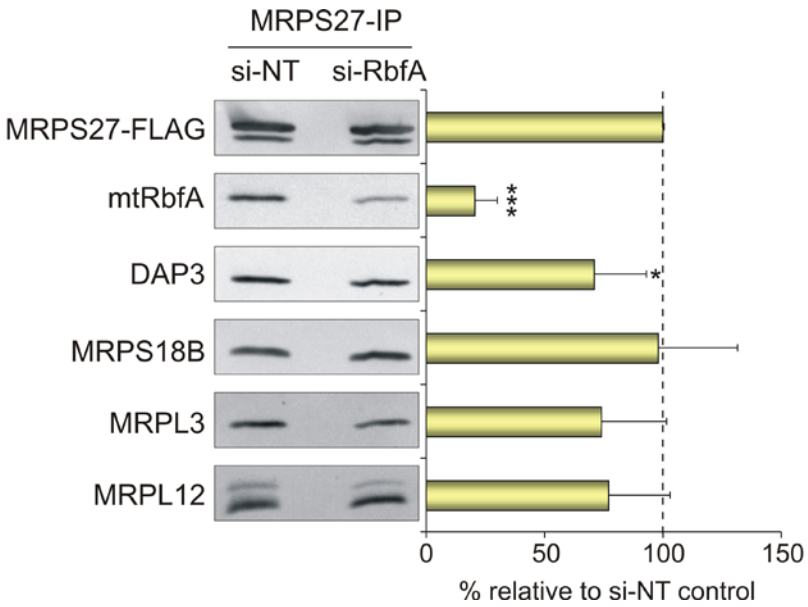

Figure 8.15: The level of 55S monosome after mtRbfA depletion. HEK293T cells expressing MRPS27-FLAG were utilised to co-immunoprecipitate the 28S SSU and the 55S monosome. Cells were transfected either with si-NT or si-RbfA for 3 days and induced with 1 µg/ ml tetracycline for 2 days. For IP equal amounts of cell lysates (2.5 mg) were applied to M2 FLAG beads. The elution fractions (10% each) were analysed by western blot and relative protein levels were measured by using Image-Quant software. Immunoprecipitated proteins in si-RbfA treated samples were compared to si-NT control, whose mean is marked as a dotted line. For statistical evaluation signals from three independent experiments of both si-RbfA and si-NT treated samples were measured and used for t-test. (n = 3; *significant p = 0.05 to 0.01; *** extremely significant p < 0.001)

Concluding from this experiment the relative level of monosome after 3 days mtRbfA depletion was unchanged or only subtly changed, under the conditions of the performed experiment.

8.7.4 Depletion of mtRbfA does not cause an instability of mitochondrial ribosomal RNAs

Since bacterial RbfA processes the 16S rRNA, I wanted to assess whether human mtRbfA played a similar role in ribosomal subunit or 12S rRNA (*MT-RNR1*) assembly or stability. Therefore the steady state levels of mitochondrial RNAs were analysed by Northern blot after 3 and 6 days mtRbfA depletion. Probes were used to detect levels of the mt-rRNAs [12S (*MT-RNR1*), 16S (*MT-RNR2*)], the mt-mRNAs and cytosolic 18S rRNA as a loading control. Figure 8.16 represents the result from three RNA isolations from independent 3 days siRNA transfections for the targeting and the non-targeting samples.

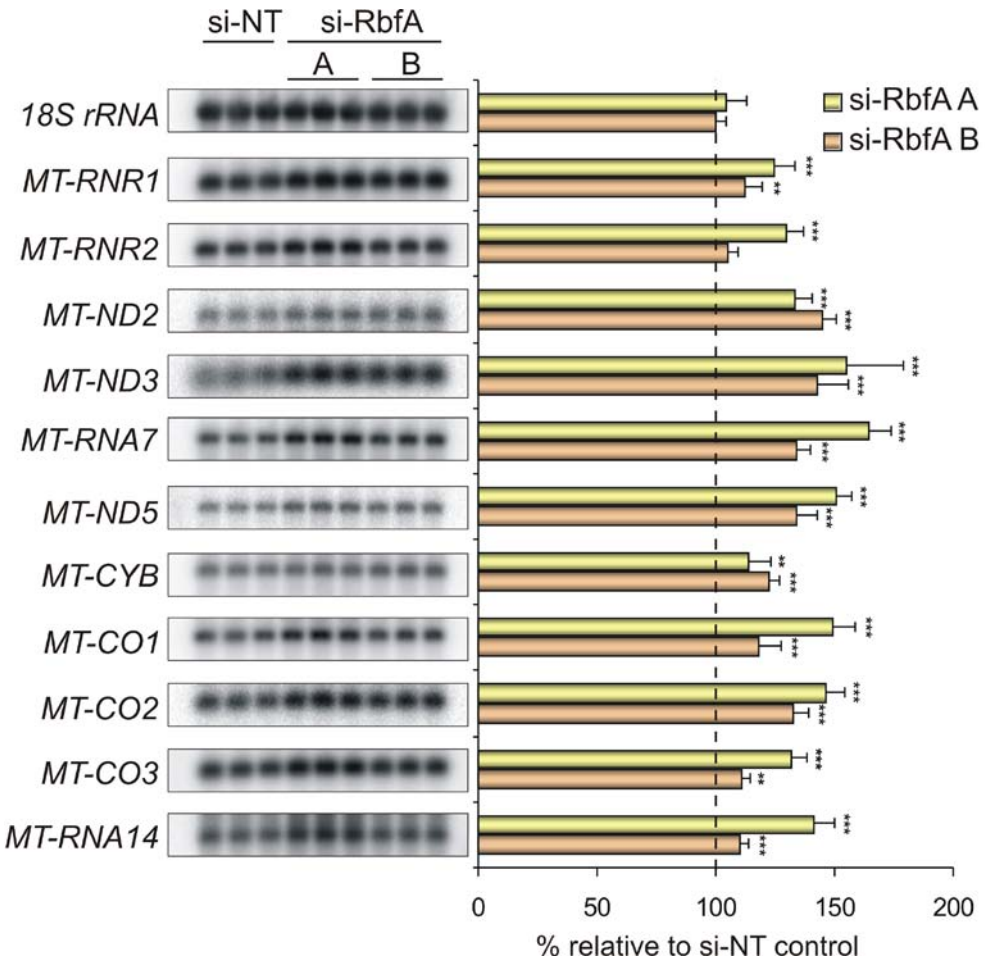

Figure 8.16: Northern blot analysis of mitochondrial RNA steady state level after 3 days mtRbfA depletion. Cells were transfected with si-RbfA-A or -B, or si-NT. After 3 days RNA (3 µg) was analysed by Northern blot. Specific probes against mitochondrial RNAs were used to visualise the transcript of interest. The cytosolic 18S rRNA was used as a loading control. The blot with graph shows the result from 3 independent experiments of each siRNA relative to the mean of signals observed in the si-NT treated samples (dotted line). (n = 3;** very significant p = 0.01 to 0.001; *** extremely significant p < 0.001)

The signals, measured by using Image-Quant software, were calculated relative to the si-NT. Both siRNAs against *mtRbfA* showed a subtle increase of the 12S rRNA steady state level up to 125% and 112%, so there was no indication that there was a loss of the stability of the 12S rRNA. Furthermore the 16S rRNA steady state level was also increased up to 129% using si-RbfA A (and 105% for si-RbfA B). The mt-mRNAs showed also no loss in the stability, all of them showed an increase, ranging from 110% to 165%. There could be no obvious pattern detected between the different transcripts.

After seen in figure 8.17, 6 days treatment, the 12S rRNA showed a modest increase in steady state levels (129% si-RbfA A; 111% si-RbfA B) indicating there was no loss of 12S rRNA stability. This was similar to that seen after 3 days mtRbfA depletion.

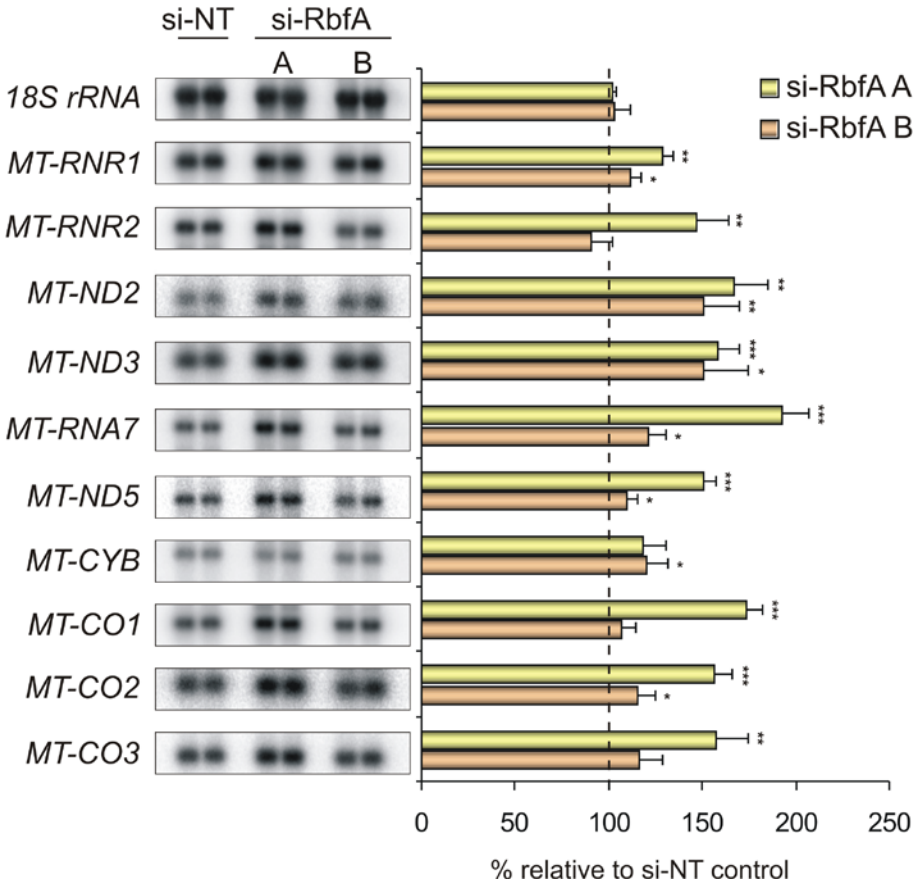

Figure 8.17: Northern blot analysis of mitochondrial RNA steady state level after 6 days mtRbfA depletion. 6 days after siRNA transfection, RNA was extracted and analysed by Northern blot (3 µg). The cytosolic 18S rRNA was used as a loading control. The blot shows the result from 2 independent experiments of each siRNA transfection in comparison to si-NT, whose mean is marked as dotted line. (n = 3; * significant p = 0.05 to 0.01; ** very significant p = 0.001 to 0.01; *** extremely significant p < 0.001)

The steady state level of 16S rRNA was not significantly changed when si-RbfA B was used, but was increased up to 147% in case of si-RbfA A. The mt-mRNAs also showed an increase, especially for si-RbfA A, where all the transcripts were up-regulated from 150% upwards, except *MT-CYB*, which was only increased to 118%. Using si-RbfA B showed an increase in the transcripts *MT-ND2* and *MT-ND3* to ~150%. *MT-RNA7* (*ND4/ND4L*) and *MT-CYB* were increased to 120% and *MT-ND5*, *MT-CO1, MT-CO2* and *MT-CO3* were just slightly up or very similar to control.

Concluding from these results it can be said that both siRNAs against *mtRbfA* caused a general but modest increase in the level of the mt-RNAs. Interestingly the 12S rRNA seems to be stable without mtRbfA, which is in contrast to the situation with ERAL1 depletion [Dennerlein *et al.*, 2010].

8.7.5 The effect of mtRbfA depletion on mitochondrial protein *de novo* synthesis

To determine whether the depletion of mtRbfA has any effect on mitochondrial protein synthesis, ^{35}S *de novo* synthesis was performed (described in 3.5.7) post 3 and 6 days si-RNA treatment. Each sample (30 µg left panels, 3 days depletion; 50 µg right panels, 6 days depletion) was separated by 15% SDS-PAGE and the results analysed using Image-Quant software (Figure 8.18). Therefore individual bands were measured with the software with considering the background in each case.

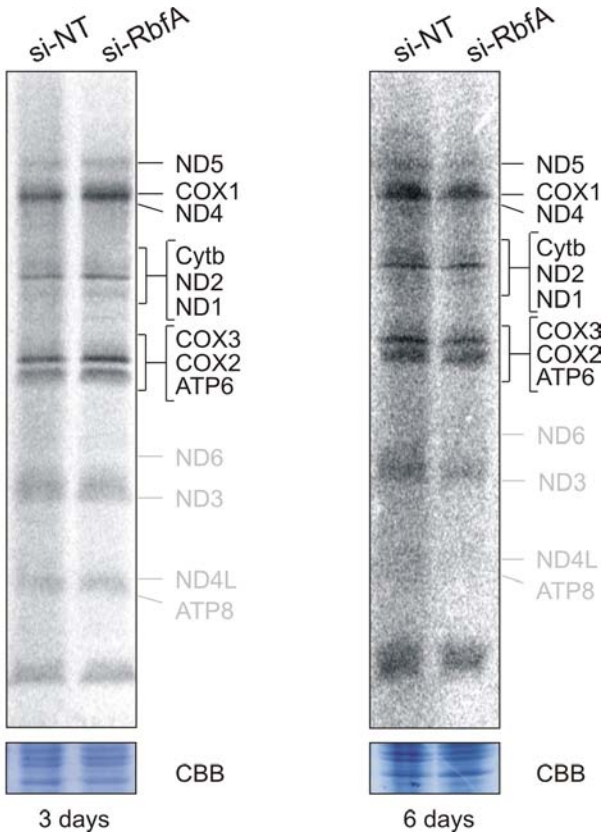

Figure 8.18: ^{35}S-met *de novo* synthesis after mtRbfA depletion. HEK293T cells were transfected with si-NT or si-RbfA A for 3 or 6 days. Mitochondrial encoded proteins were labelled with ^{35}S-met for 15 min prior to cell harvesting. Samples (30 µg left panels; 50 µg right panels) were loaded on a 15% SDS-PAG. Mitochondrial encoded proteins were identified by comparison to Chomyn (1996). Coomassie brilliant blue (CBB) staining (lower panels) confirmed the even loading. Images are representative of two independent experiments each (n = 2).

After 3 days mtRbfA depletion the mitochondrial protein synthesis was slightly upregulated of approximately 1.5 fold in comparison to si-NT. This differed from the situation after 6 days transfection where a subtle decrease in *de novo* synthesis of approximately 15 - 20% was noticed.

Concluding from this experiment, no defect in mitochondrial protein synthesis was seen after 3 days depletion of mtRbfA with a subtle decrease after 6.

Further experiments need to be done to investigate the possible function of mtRbfA within the mitochondrial gene expression machinery and furthermore to find the reason why the depletion of mtRbfA is causing a growth defect in human HEK293T cells.

8.7.6 Analysis of steady state levels of mitochondrial proteins and OXPHOS complexes after mtRbfA knockdown

In addition to the *de novo* synthesis, the steady state level of mitochondrial proteins was analysed after 3 and 6 days mtRbfA depletion. To this end treated cells were harvested, lysed and same amounts of proteins were separated by SDS-PAGE followed by western blot. As shown on figure 8.19 mtRbfA was successfully down-regulated.

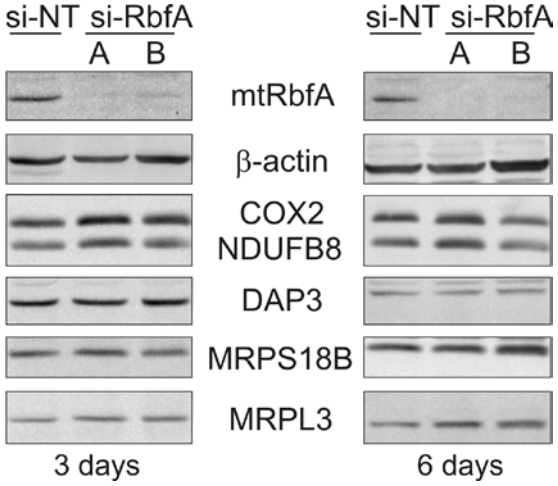

Figure 8.19: Western blot analysis of steady state levels of proteins after 3 and 6 days mtRbfA depletion. Cell lysates (25 µg) of si-NT and si-RbfA (A and B) treated samples were analysed after 3 and 6 days transfection. The western blot was probed with antibodies against a number of mitochondrial proteins including mtRbfA, components of OXPHOS (COX2 and NDUFB8) and members of the mitochondrial ribosome (DAP3, MRPS18B and MRPL3). β-actin was used as a loading control. Signals were analysed using Image-Quant software. The results are representative for at least two independent experiments of each sample ($n \geq 2$).

After 3 and 6 days depletion there was no significant change in the steady state level of mitochondrial ribosomal proteins (DAP3, MRPS18B and MRPL3) when compared to si-NT. COX2 as a mitochondrial encoded protein from Complex IV was up-regulated at 3 days (141% si-RbfA A; 123% si-RbfA B) and at 6 days increased to 122% with si-RbfA A, whilst with si-RbfA B there was a decrease to 65%. NDUFB8 as a nuclear encoded protein of Complex I was relatively similar in both cases compared to si-NT after 3 days. Again after 6 days NDUFB8 behaved in a similar way to COX2: it was slightly up-regulated to 121% using si-RbfA A, but decreased to 71% in case of si-RbfA B. However, no dramatic change in the mitochondrial protein steady state level was

observed using si-RbfA, even after 6 days depletion that could explain the growth defect.

The differences between the two mtRbfA siRNAs may be the result of the different efficiencies, or one of them may also affect levels of another unpredicted mRNA, which also encodes a mitochondrial protein. The latter cannot be excluded, because the MTT assay using 143B-ρ^0 cells can only exclude siRNAs that have an off-target effect outside the mitochondrial gene expression machinery.

A consistent observation seen with both siRNAs was that in general there was an initial increase in the steady state level of COX2, which dropped after 6 days, but was still higher in siRbfA A treated sample than in control. To determine whether the COX2 protein generated under these conditions is still incorporated and functional in the OXPHOS complexes, Blue Native acrylamide gel electrophoresis with western blot or in-gel enzyme activity assay (detailed in 3.5.6) was performed after 6 days transfection. The relative level of the complexes was determined by western blot using the following antibodies: 1) Complex I - NDUFA9, 2) Complex II - SDH 70 kDa subunit, 3) Complex IV - COX2, 4) Complex V - β-subunit. Complex I, IV and V, which all harbour mitochondrial encoded proteins were increased in comparison to si-NT, whereas Complex II (completely nuclear encoded) was similar to control (Figure 8.20). Problems with efficiency of transfer led to relatively high standard deviations of the measured level of protein complexes. The overall tendency (n = 3 independent experiments), however, was an increase in the mitochondrial encoded protein containing complexes. In-gel enzyme activities were repeatable, consistent and in agreement with the western blot, where Complexes I and IV showed a higher enzyme activity after mtRbfA depletion in comparison to si-NT.

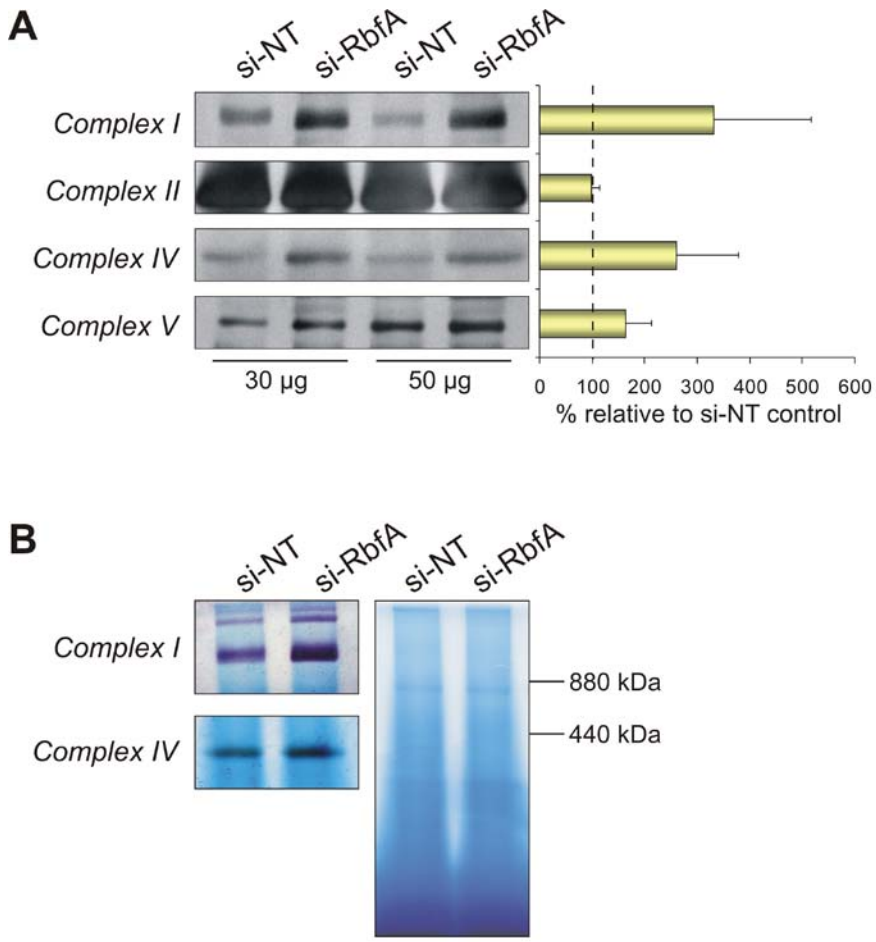

Figure 8.20: Analysis of OXPHOS complexes by Blue Native PAGE after mtRbfA depletion. Samples for BN-PAGE were 30-50 µg (western blot) and 75 µg (in gel enzyme activity). **A)** Western blot showed the relative level of the complexes using antibodies to NDUFA9 (Complex I), SDH 70 kDa (Complex II), COX2 (Complex IV) and β-subunit of Complex V. The signals were measured using Image-Quant software. Images are representative of all results n = 3 **B)** To determine the relative activity of Complex I and IV (left panels) gels were incubated over-night in specific substrate solutions (detailed in 3.5.6.5). The BN-PAG (right panel) showed migration of complex and the relative loading.

Concluding so far, the depletion of mtRbfA causes an increase in COX2 and NDUFB8 using si-RbfA A. Additionally the OXPHOS complexes, which contain mitochondrial encoded proteins, were also upregulated in comparison to the control. Complex II was present at similar levels to control, but since the signal for SDH 70 kDa was very strong and thus maybe saturated, differences cannot be distinguished when measuring with Image-Quant software. Since western blots are only semi-quantitative and there was a high standard deviation within the experiment the data have to be interpreted with caution. However, the results of the in-gel enzyme activity assay are again in agreement with the higher protein and thus complex level.

8.7.7 The mitochondrial DNA content is unchanged after mtRbfA depletion

Such an increase in the protein level as seen above can have several reasons: 1) translation is upregulated, 2) the turnover of the complexes/ protein is changed 3) mitochondrial mass is increased or 4) mtDNA copy number is higher with a commensurate increase in gene expression.

To investigate the latter mitochondrial DNA levels were measured by SYBR green Real Time PCR. Therefore DNA was extracted from cells as described in 3.3.1 after 6 days transfection (3 independent transfection experiments). Each DNA sample (10 ng) was applied to three independent PCR experiments. As a mitochondrial marker, primer pair #9/ #10 (Table 3.4) were used for one PCR reaction to amplify the *MT-ND1* region and B2M primer pair #13/ #14 to measure the relative level of nuclear DNA in a second PCR. The relative mtDNA level was calculated as followed: first, the ΔC_T of each sample was calculated [$\Delta C_T = C_T$ (B2M) - C_T (MT-ND1)], then the differences between the ΔC_T of si-NT and si-RbfA were taken [$\Delta\Delta C_T = \Delta C_T$(si-RbfA) - ΔC_T(si-NT)]. The mean $\Delta\Delta C_T$ was -0.57 cycle ($\pm$ 0.54). Due to the exponential amplification during real time PCR, one cycle represents a difference of 50% mtDNA content. Assuming that nuclear DNA stays consistent then the mtRbfA depletion resulted in an average mtDNA decrease of 28.7% ($\pm$27.1%), which can be considered as experimental error with a sensitive method such as Real Time PCR. Concluding from this experiment there is no obvious change in mtDNA after 6 days mtRbfA depletion.

8.7.8 Flow cytometry analysis: measurements of mitochondrial mass, reactive oxygen species and mitochondrial membrane potential after mtRbfA depletion

No change in the mtDNA level could be measured after RbfA depletion. Additionally it was tested whether an increase of mitochondrial mass was the reason for the increased mitochondrial protein steady state level. Therefore after 6 days siRNA transfection, cells were treated with NAO (10-n-nonyl-acridine orange), which binds specifically to cardiolipin in the inner mitochondrial membrane (described in 3.1.8.1). FACS analysis of mtRbfA depleted samples showed only a subtle increase of mitochondrial mass to 113% in comparison to the control as shown in figure 8.21.

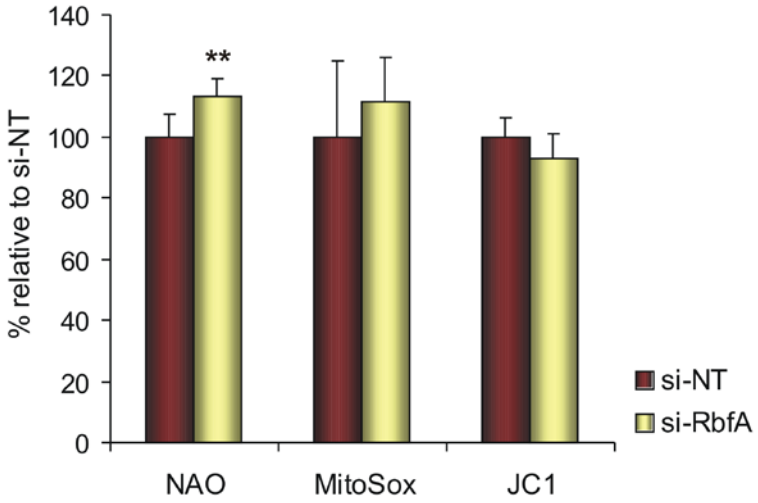

Figure 8.21: FACS analysis of mitochondrial mass (NAO), reactive oxygen species (MitoSox) and mitochondrial membrane potential (JC1) after mtRbfA depletion. HEK293T cells were treated with si-NT (red bars) or si-RbfA (yellow bars), respectively for 6 days. Cells were harvested, resuspended in PBS and treated with the dyes NAO (10 µM), MitoSox Red (5 µM) or JC1 (2 µM), respectively for 15 min at 37°C 5% CO_2 (light protected). This was followed by PBS washing step and measurements at the individual wavelengths using BD FACS CANTO II machine. The results were analysed using BD FACSDIVA^{TM} software with great support from Mr. Ian Dimmick (Centre for Life, Newcastle upon Tyne). The graph represents the results of at least 4 experiments each (NAO: n = 7, p = 0.0028**; MitoSox: n = 4, p = 0.4433; JC1: n = 4, p = 0.2180).

In addition to mitochondrial mass, mitochondrial reactive oxygen species (ROS) were measured using MitoSox Red. These parameters were analysed as unbalanced activity of the OXPHOS complexes, or increased stress within the cell could potentially result in an increase amount of ROS. There was no significant difference detected in superoxide production between si-NT and si-RbfA after 6 days treatment (Figure 8.21), suggesting that mtRbfA depletion does not cause an upregulation of ROS, which could have been reason for the growth phenotype. As a positive control for mitochondrial ROS production Guf1, a mitochondrial protein investigated by S. Dennerlein in this laboratory, was depleted and samples were treated in the same way, resulting in dramatic increase in ROS (data not shown).

The mitochondrial membrane potential, measured by JC1 as detailed in 3.1.8.3, did not show any significant alteration after the loss of mtRbfA (Figure 8.21). As a positive control for JC1 measurements, cells were uncoupled with FCCP, which resulted in a decrease of mitochondrial membrane potential (data not shown).

In summary neither mitochondrial ROS production nor mitochondrial membrane potential were altered indicating that the growth defect after mtRbfA depletion was not due to changes in either of these parameters. The mitochondrial mass was increased, but this subtle effect also cannot explain the phenotype caused by si-RbfA transfection.

8.7.9 The effect of mtRbfA depletion on the cell cycle

To investigate whether the cell cycle was disrupted following mtRbfA depletion, the state of replication of cell-populations the DNA of the cells was stained with DAPI as detailed in 3.1.8.5 and further analysed by flow cytometry.

There are four phases of the cell cycle. Cell populations tend to be distributed across these phases: the G1 phase (G = *gap*), S phase (DNA synthesis), G2 phase and M phase (mitosis). Cells in the G1 phase have one copy of DNA, whereas in the G2/M phase there are 2 copies. Thus the relative fluorescence of the G2/M is double that of G1. During the S phase cells are replicating the DNA and therefore the DNA content and value for the fluorescence intensity increases between the G1 and G2/M phases.

As shown in the graph of figure 8.22 after the depletion of mtRbfA there was an increased proportion of cells in the G1 phase (si-NT: 52.5%; si-RbfA: 60.2%) and decrease in S phase (si-NT: 42.3%; si-RbfA: 32.7%) in comparison to the si-NT. These results were statistically extremely significant and the reason for the arrest in the G1 phase could be a mitochondrial defect caused by the depletion of mtRbfA. It could also partially explain the growth defect seen resulting from mtRbfA depletion. It is unlikely that a decrease from 42.3% (si-NT) to 32.7% (si-RbfA) in the S phase would be the only reason for the growth defect seen following mtRbfA depletion. Furthermore there was a subtle increase in the G2/M phase comparing si-NT (~5.1%) to si-RbfA (~7.1%). Interestingly the amount of debris in si-RbfA treated cells was approximately 20% higher than in si-NT. Debris represent fluorescence below diploid, often arising from cell fragmentation during preparation. This explanation is unlikely to account for the difference since si-RbfA- and si-NT cells were treated in the same way. The reason may be the actual depletion of mtRbfA itself.

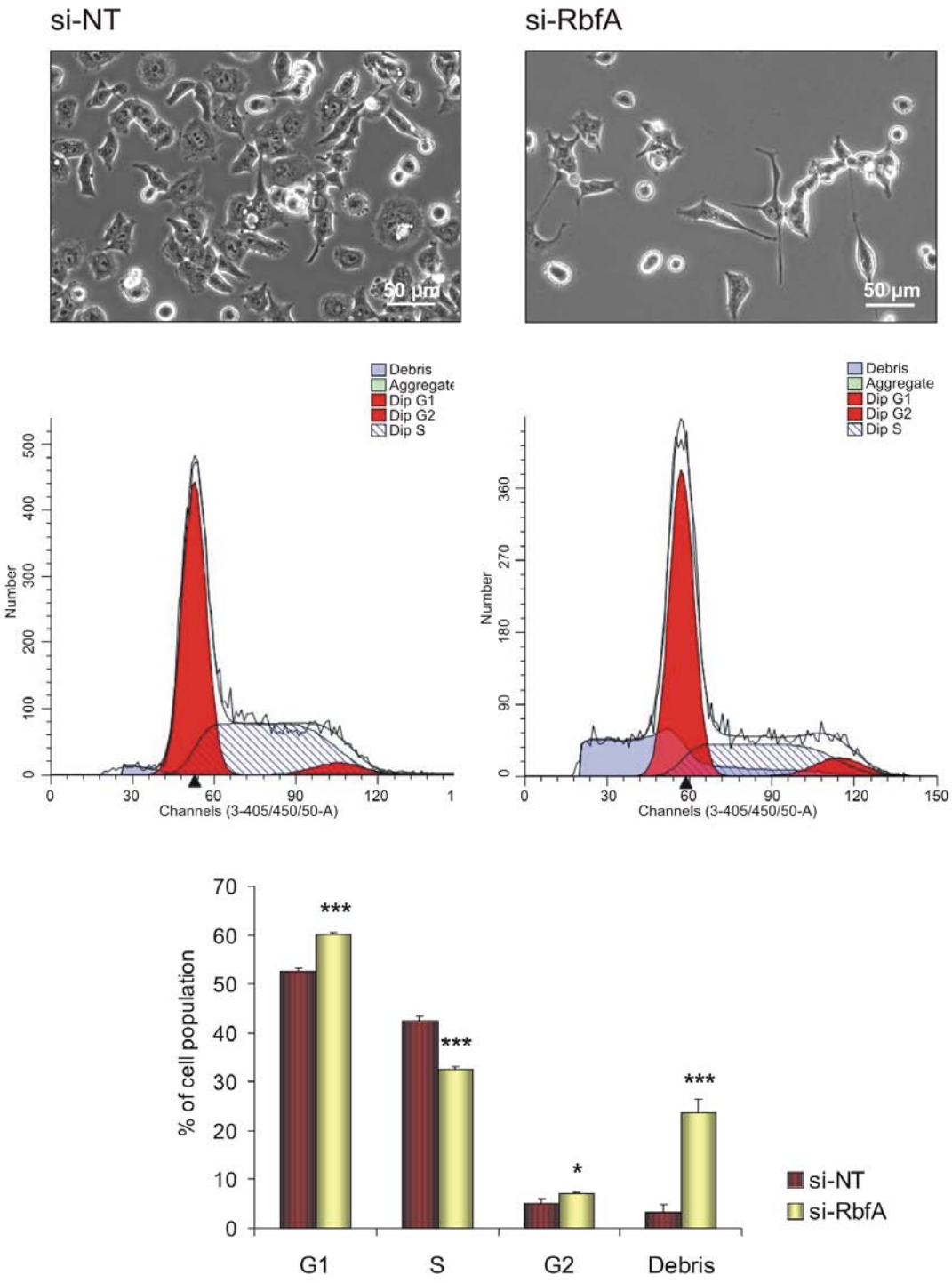

Figure 8.22: Analysis of state of cell-population after mtRbfA depletion. HEK293T cells were treated with si-NT and si-RbfA, respectively for 6 days. The phenotype was monitored by using the inverted microscope Axiovert200M (Zeiss) with camera (top panels). Cells were stained with DAPI using CyStain DNA 2 step kit (Partec), followed by flow cytometric measurements at 450 nm. The results were analysed with kind assistance from Mr. Ian Dimmick using ModFit LT V3.2 software. The images (middle panels) are representative for at least 3 experiments ($n \geq 3$) and the results are summarised in the graph below. (t-test * significant $p = 0.05$ to 0.01; *** extremely significant $p < 0.001$; G = gap; S = synthesis).

8.7.10 MtRbfA depletion does not cause high level of apoptosis

To test whether the debris in mtRbfA depleted samples described above could represent cells that are senescent or apoptotic, DNA fragmentation was measured after 6 days siRNA transfection using APO-DIRECT^{TM} kit (BD Biosciences Pharmingen) (described in 3.1.8.4). Surprisingly there was no dramatic increase (approximately 6% higher than NT control) in the amount of apoptotic cells (Figure 8.23) as had been seen with ERAL1 [Dennerlein *et al.*, 2010]. This result was statistically significant, but in comparison to the effect seen of ERAL1 depletion, where ERAL1 depletion caused ~ 35% of cells to go into apoptosis after only 3 days siRNA treatment, it can be probably excluded as the main reason for the growth defect.

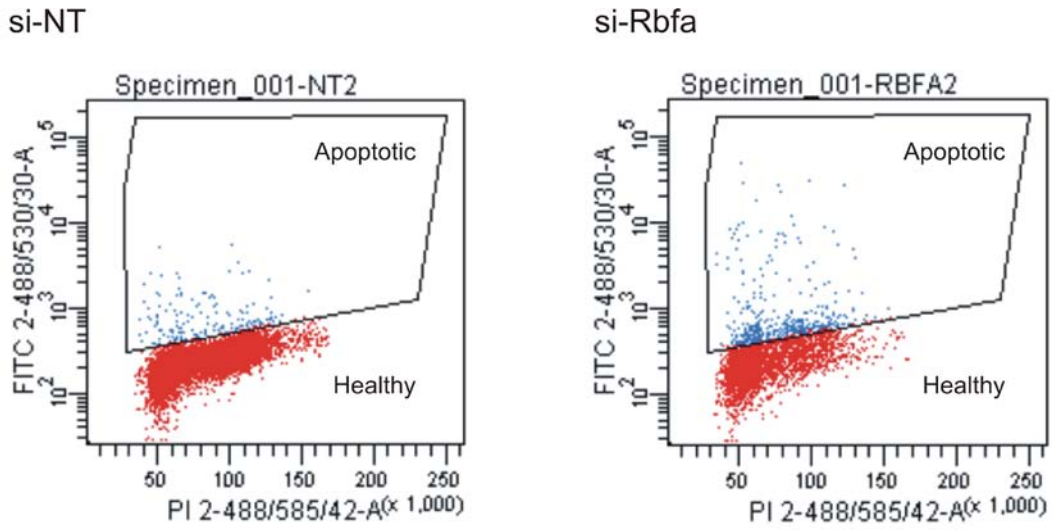

Figure 8.23: Depletion of mtRbfA does not result in high levels of apoptosis. HEK293T cells were treated for 6 days with si-NT or si-RbfA, respectively. Cells were then measured for DNA fragmentation using APO-DIRECT kit to estimate the proportion of apoptotic cells. Two dyes were used for measurements: FITC-dUTP (measured at 530 nm, y axis) indicating the apoptotic cells and PI (measured at 585 nm, x axis) staining the DNA of the whole population. The results of the flow cytometry (using ~ 5,000 cells) were analysed (assisted by Mr. Ian Dimmick) using BD FACSDivaTM software. The images are representative examples for primary FACS data for si-NT and si-RbfA treated samples. Healthy cells are labelled in red and apoptotic ones in blue. The depletion of mtRbfA resulted in 7.4% (± 3.3%) apoptotic cells, compared to si-NT with 1.7% (± 0.5%). (n = 3, p = 0.0167*)

8.8 Discussion

The data presented in this chapter represents a first characterisation of the human mtRbfA orthologue of bacterial RbfA, a cold shock protein involved in the processing of the 16S rRNA precursor (17S) and therefore maturation of the 30S SSU in bacteria. Bacterial RbfA was proposed to bind the loop region of h1 at the 5'-end of the 16S

rRNA. It therefore probably inhibits the interaction of 50S LSU with 30S SSU with 16S rRNA precursor whilst the h1 remains unformed and the 5'end unprocessed. As previously described the structure of human mtRbfA from residue Arg86 to Asp201 shows high structural similarities to that of bacterial RbfA, with a typical type-II KH-domain fold that is proposed to facilitate RNA-binding. A clear difference between bacterial RbfA and human mtRbfA is the size of the proteins. Human mtRbfA is around three times larger than its bacterial counterpart, potentially indicating adapted changes in the function. A further difference is that the human 12S rRNA is transcribed as part of a polycistronic transcript, directly flanked by $tRNA^{Phe}$ at the 5'-end and by $tRNA^{Val}$ at the 3'-end. Since the mitochondrial genome contains no introns in combination with the proposed tRNA punctuation model of RNA processing [Ojala *et al.*, 1981] the resulting cleavage by RNase P and tRNase Z would result in the excision of the fully processed 12S rRNA. Therefore a rRNA precursor such as 17S rRNA in bacteria does not exist in human mitochondria. Therefore what is the function of mtRbfA in human? My project aimed to answer whether: human mtRbfA is a mitochondrial protein? Is it important for mitochondrial function and therefore for cell viability? Has it maintained a function in the maturation of the 28S SSU?

The data presented here shows that mtRbfA is indeed a mitochondrial protein (Figure 8.3) and its depletion causes a growth defect in human HEK293T cells (Figure 8.13). It was further demonstrated by isokinetic sucrose gradients that endogenous mtRbfA co-migrates with components of the 28S SSU in fractions 4 and 5 (Figure 8.4), suggesting an association of mtRbfA with the mitochondrial SSU. These findings are similar to the situation found in the bacterial system. However, the ratio of free and associated mtRbfA is quite different compared to this one of its bacterial counterpart. In bacteria ~20% of RbfA protein are associated with the 30S SSU under normal growth conditions, which increases up to ~40% after cold shock [Xia *et al.*, 2003]. In human mitochondria the relative level of associated mtRbfA, migrating in fractions 4 and 5, seems to be higher with ~60%. This may also reflect that the overall ratio of free 28S SSU to 55S monosome is higher in human mitochondria than of the bacterial ratio of 30S SSU to 70S particle/ polysome. It would be interesting to identify whether this ratio would change under certain stress conditions such as cell culturing in galactose (glucose-free) containing medium. Under those circumstances would there be less mtRbfA associated with the 28S SSU and therefore a higher possibility to form the 55S monosome? For the future it would be sensible to investigate the level of associated mtRbfA with the 28S SSU under different growth conditions.

Surprisingly when mtRbfA-FLAG was used for immunoprecipitation there were not only components of the 28S SSU found in its elution fraction, but also a number of 39S LSU

proteins (Figure 8.5, table 8.1). However, an association of mtRbfA with the 39S LSU was not suggested from the results revealed by isokinetic sucrose gradients of cell lysates (Figure 8.4). An association of mtRbfA with the 55S monosome has now been excluded since separating co-immunoprecipitated complexes by mtRbfA-FLAG did not show co-migration of components of the 28S SSU and 39S LSU in fraction 8. This was also confirmed by the control experiment, where the eluate of MRPS27-FLAG-IP was applied to isokinetic sucrose gradient. There endogenous mtRbfA also did not co-migrate with the 55S monosome in fraction 8.

Interestingly the 28S SSU complex co-purified by mtRbfA-FLAG migrated mainly in fractions 4 and 5 (Figure 8.6 A and 8.8), suggesting an association of mtRbfA with the 28S SSU relatively late in the maturation process of the 28S SSU. In contrast MRPS27-FLAG-IP showed also some 28S SSU intermediates revealed by the co-sedimentation of MRPS27-FLAG with MRPS25 and MRPS18B in fractions 2 and 3 (Figure 8.6 B). However, there was no mtRbfA found in those earlier fractions, which is in agreement with the suggestion that mtRbfA is associated with the 28S SSU at a late assembly point. This would be similar to the situation found in bacteria, where a loss of RbfA leads to an accumulation of 50S LSU and 30S (precursor) SSU, but not to a complete loss in assembly of the ribosomal small subunit. Another interesting result of the separated immunoprecipitated eluate was the localisation of MRPL12 in the earlier fractions (Figure 8.6 A), suggesting a more direct interaction of mtRbfA with MRPL12. MRPL12 was shown to interact directly with the POLRMT [Wang *et al.*, 2003] and is therefore proposed to be a kind of transcription-translation coupler. It is possible that mtRbfA represents a similar factor. As it is potentially involved in the late maturation of the 28S SSU, it is tempting to speculate an involvement of mtRbfA in the initiation complex, where the synthesised transcript by POLRMT is loaded onto the small ribosomal subunit. Interestingly, mtIF2, which is part of the initiation complex and delivers the fmet-tRNA to the P-site in the 28S SSU [reviewed in Spremulli *et al.*, 2004], was found within the IP of mtRbfA. Furthermore POLRMT was also detectable by LC MS/MS. Another protein that was found in the mtRbfA-FLAG-IP by LC MS/MS was SLIRP, an RNA binding protein usually found in conjunction with LRPPRC. However, the latter was not detectable in mtRbfA-FLAG-IP. Sasarman *et al.* (2010) showed that both, SLIRP and LRPPRC interact in a ribonucleoprotein (RNP) complex that is important for stabilising mt-mRNA transcripts. The form of SLIRP found in the IP of mtRbfA-FLAG potentially reflects the protein stabilising mRNA, which is transported towards the 28S SSU for the translation initiation. It would be interesting to clarify whether mtRbfA could be also co-immunoprecipitated by SLIRP. This protein is being investigated further in this laboratory by Dr. P. Smith and A. Rozanska. The co-

sedimentation of ERAL1, which binds preferentially to the 28S SSU [Dennerlein *et al.*, 2010] in fractions 4 and 5, but also in the earlier fractions 1 and 2 after mtRbfA-FLAG-IP (Figure 8.6 A) suggests potentially a direct interaction of mtRbfA with ERAL1. However, it is also possible that ERAL1 has lost its association with the 28S SSU during this experimental procedure. A direct interaction between bacterial Era and RbfA has not been reported, but because of some overlapping binding sites within the 30S SSU it is difficult to exclude this possibility completely (Figure 8.24).

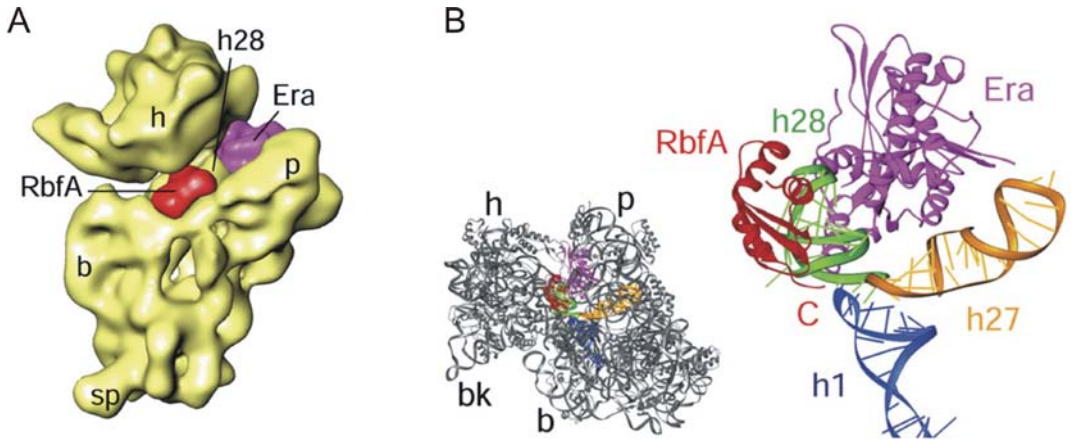

Figure 8.24: Binding sites of RbfA and Era on the 30S SSU in bacteria. A) 30S SSU (yellow) is shown with h-head, b-body, p-platform, sp-spur and bound RbfA (red) and Era (magenta). **B)** Both RbfA and Era are interacting with the helix 28 (h28; green). The C-terminus of RbfA is directed to the helix 1 (h1; blue) and facilitates its processing. Era can indirectly stabilise the h1 over its interaction with h28. (bk: beak) (Images taken from Datta *et al.*, 2007)

The possibility of an association of mtRbfA-FLAG with the 39S LSU was further examined since the results of IP and gradients were in disagreement. By decreasing the expression of mtRbfA-FLAG relatively to endogenous level led to the suggestion that the interaction of mtRbfA-FLAG with the 39S LSU was due to the high overexpression, probably causing artefacts (Figure 8.8).

Interestingly this experiment also indicated that the association with ERAL1, which was seen previously within the mtRbfA-FLAG-IP may also have been caused by the high overexpression of mtRbfA-FLAG. This result indicates that mtRbfA and ERAL1 probably interact at different stages with the 28S SSU. In contrast to mtRbfA, ERAL1 is as a 12S rRNA chaperone probably involved in an earlier assembly process.

However, the association of mtRbfA with the 28S SSU was confirmed to be real and not an overexpression artefact. What can cause those unspecific interactions seen with the 39S LSU? One possibility is that mtRbfA is indeed a KH-domain RNA-binding protein and that an excess may result in nonphysiological unspecific binding of RNA species potentially within the 39S LSU.

Is mtRbfA really a RNA-binding protein and is the type-II KH-domain functional? The loss of the ability to interact with mitochondrial ribosomal proteins in the presence of EDTA strongly suggests that the association of mtRbfA with the 28S SSU is RNA dependent. However, the CLIP (Crosslinking Immunoprecipitation) assay failed to identify with high confidence associated RNA species. Possible explanations for this could be: i) the method is not compatible with this particular protein or wrong decisions were made during the whole procedure in terms of size of RNA-complex, ii) it is also possible that even with the presence of the type-II KH-domain mtRbfA is not a RNA binding protein, and iii) the particular RNA species may not be exposed and therefore not available to be crosslinked. A further general problem occurring during the CLIP experiment with mtRbfA-FLAG could be the 28S SSU itself. If mtRbfA really interacts with either mt-rRNA or mt-mRNA only within the ribosomal subunit then it is possible that the RNase T1 digestion is not efficient enough. Liao and Spremulli (1989) showed that even with high concentration of RNase T1, the bound mRNA in a complex with the 28S SSU is protected over an approximately 45 nucleotides stretch. Therefore it is possible that the mt-rRNA, which is known to have a complex structure [Koc *et al.*, 2001b, Sharma *et al.*, 2003] within the core of the 28S SSU, is crosslinked to all its interacting protein partners and further protected against RNase T1 treatment by the intact and probably almost completely assembled 28S SSU complex. The same could be correct for the mt-mRNA if it is already loaded onto the 28S SSU in the presence of mtRbfA. Therefore the UV-crosslinked protein-RNA complex containing mtRbfA is probably much larger than predicted. It would therefore have to be first denatured so that RNase T1 would get access to the RNA species protected by the 28S SSU. Thus it is possible that most of sequences, which could not be identified by BLAST searches, represent just artefacts caused by PCR amplification.

From the sequences that were identified, 1 represented the 3'-end of the 12S rRNA, identical to the binding site of human ERAL1, and 2 of them were the 5S rRNA. The 5S rRNA in bacteria is part of the ribosomal large subunit, whereas in human mitochondria it has never been shown that the 5S rRNA is present in the human mitochondrial ribosome [Sharma *et al.*, 2003]. However, it has been shown by several groups that cytosolic 5S rRNA is imported into mitochondria [Entelis *et al.*, 2001; Smirnov *et al.*, 2010; Wang *et al.*, 2010]. Further a defect in the relevant import machinery is reported to lead to decreased imported level of 5S rRNA in mitochondria, which in turn leads to a reduced level in mitochondrial translation [Smirnov *et al.*, 2010]. This suggests an important role of the 5S rRNA within the mitochondrial gene expression machinery. However, the precise role of the 5S rRNA in human mitochondria is still unknown. It is an exciting possibility that the sequences of 5S rRNA found with the mtRbfA CLIP are

relevant and specific protein-RNA interactions within the mitochondria and further experiments needs to be addressed to this question in the future.

Even if the CLIP failed under those conditions, probably caused by inefficient access of the RNase T1 as already discussed, it cannot be excluded that mtRbfA is a RNA-binding protein. It would undoubtedly be better to use the endogenous mtRbfA instead of the FLAG tagged protein. It can never be ruled out that the FLAG tag can cause problems with some approaches, however both FLAG tagged and endogenous mtRbfA showed a similar association with the 28S SSU, and did not impede efficient CLIP in other mitochondrially targeted-FLAG tagged proteins. Thus the FLAG tag can realistically be eliminated as a possibility for unsuccessful CLIP assay.

Generation of mutations within the KH-domain could potentially answer whether this proposed RNA-binding domain is really functional. If this would be the case then a mutation within this domain would be predicted to cause a dominant negative effect on cell growth. Another possibility to investigate the possible RNA-binding activity of mtRbfA would be to perform IP of UV-crosslinked samples under denaturing conditions, followed by real time PCR to determine the presence of mt-rRNAs or mt-mRNA in comparison to a non-crosslinked sample or a control such as mtLuc-FLAG.

Another way forward would be to investigate possible direct protein interaction partners by using chemical crosslinking. In bacteria RbfA interacts in the head of the SSU with ribosomal protein S9, S13 and further with S12, which is located in the body of the SSU (Figure 8.25) [Datta *et al.*, 2007].

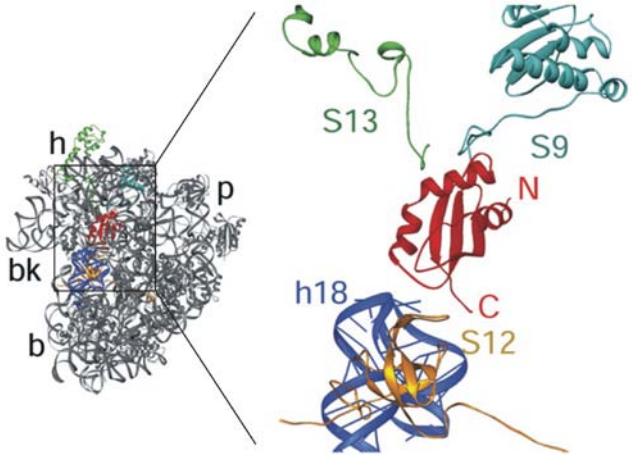

Figure 8.25: Protein interaction partners of bacterial RbfA in the 30S SSU. The C-terminal extension of bacterial ribosomal proteins S13 (green) and S9 (cyan) are located towards the P-site of the 30S SSU and interact with RbfA (red). The other binding site of RbfA within the SSU involves helix18 (h18, blue) and the ribosomal protein S12 (yellow), which overlaps with the interaction site of IF1. In human mitochondria a bacterial homologue for S13 is absent [Koc *et al.*, 2010] and there is no mitochondrial IF1. An additional domain in mtIF2 substitutes for the function of IF1 in human mitochondria [Gaur *et al.*, 2008]. (Image was taken from Datta *et al.*, 2007)

As previously described the mammalian mitochondrial ribosome differs in a many aspects to its bacterial counterpart. It is therefore highly likely that the way in which mtRbfA is associated with the mitochondrial ribosome, including the potentially interacting ribosomal proteins may not be the same as in the bacterial system.

In the LC MS/MS analysis of mtRbfA-FLAG-IP MRPS9 (orthologue of bacterial S9) was detectable, but no MRPS12, which is the most highly conserved protein of the SSU with 48% identity to *E. coli* S12. Curiously MRPS12 was not found in the LC MS/MS analysis of any mitochondrial samples that were sent from this laboratory for mass spectrometry analysis (not in mtRRF, ICT1, ERAL1 or in MRPS27). Thus it is possible that MRPS12 is present and just not detectable as it is also a quite small protein with a calculated molecular weight of 12.5 kDa as mature protein [Koc *et al.*, 2001b]. Further in the head of the mitochondrial 28S SSU a homologue for bacterial S13 is absent, one of the described differences between the mitochondrial and bacterial ribosome. Therefore it would be interesting to identify how mtRbfA has adapted to those changes. Once the protein interaction partners are identified, it could indicate whether any RNA structure would be close enough for mtRbfA to bind.

Thus far it cannot be answered whether mtRbfA is involved in SSU maturation in way that involves rRNA processing or stabilisation within the SSU. However the results represented in this chapter show clear evidence that mtRbfA interacts mainly with the 28S SSU. To determine the function of mtRbfA within the 28S SSU further experiments need to be done. One approach presented in this study was the investigation of the effect of mtRbfA depletion at the cellular and molecular level. It was shown that the loss of mtRbfA leads clearly to a growth defect (Figure 8.13), yet the reason for this defect is still not clear. On isokinetic sucrose gradient no obvious defect on the conformation of the ribosomal subunit could be observed (Figure 8.14). The protein steady state level of the mitochondrial ribosomal proteins was also not altered after 6 days mtRbfA depletion. These results are in agreement with the hypothesis that mtRbfA is associated with the 28S SSU at a very late maturation point. Since the 28S SSU to which mtRbfA is bound might be almost completely assembled, it cannot unequivocally be expected that mtRbfA depletion would lead to a complete loss of 28S SSU assembly.

It was expected that analogous to the situation in bacteria, the loss of mtRbfA would lead to an accumulation of SSU and LSU and thus to a reduced level of 55S monosome. After 3 days however, there was no significant loss of the 55S particle (Figure 8.15). One explanation may be that it would need more time to see a significant decrease in 55S monosome after mtRbfA depletion. Therefore it would be probably sensible to repeat the MRPS27-FLAG-IP after 6 days transfection. Another protein that

immunoprecipitates the 55S monosome at higher levels than MRPS27 such as ICT1, should be used for IP after mtRbfA depletion. This may give clearer results and would deliver another control.

Since bacterial RbfA is important for the processing of the 16S rRNA, it was expected that mtRbfA is in some way involved in the assembly of the mitochondrial SSU by binding/ stabilising the 12S rRNA. However, mtRbfA depletion did not cause any loss of mt-RNAs (Figure 8.16 and 8.17). If there was any change in the relative level of mt-RNA then there was more an increase instead of a decrease. Even the level of the 12S rRNA was slightly increased, which is in complete contrast to the situation after ERAL1 depletion, which leads to a dramatic reduction in the 12S rRNA level [Dennerlein *et al.*, 2010]. What is in common between mtRbfA and ERAL1 depletion is the increased steady state level of the mt-mRNA transcripts. This phenomenon was also reported by Metodiev *et al.* (2007). This group showed that the knockout of murine *Tfb1m*, which is required for dimethylation on A1006 and A1007 on 12S rRNA, leads to a reduced stability of 12S rRNA, whereas mt-mRNA transcripts are either almost unaffected or also increased. The remained stability of mt-mRNA transcripts in cells with a ribosome assembly defect is probably caused by the association of the RNA with the RNP complex. This reflects potentially a form of temporary store for transcripts before being loaded onto the 28S SSU. The similar increase in the transcripts after mtRbfA depletion was observed with ERAL1 knockdown and partially with the *Tfb1m* knockout mice leads to the speculation whether this reflects also a ribosome assembly defect. However, since mtRbfA is probably associated with the 28S SSU at a late maturation phase, it is also possible that the mt-mRNA transcripts are already bound to the 28S SSU. It is therefore likely that the transcripts are stabilised by the ribosomal subunit itself.

There was no dramatic loss of ^{35}S-met *de novo* synthesis even after 6 days depletion of mtRbfA, which was reminiscent to the results found after down-regulation of mtRF1a [Soleimanpour-Lichaei *et al.*, 2007], mtRRF [Rorbach *et al.*, 2008] and ERAL1 [Dennerlein *et al.*, 2010]. These are all proteins that are involved in the mitochondrial gene expression machinery and yet their loss did not show significant decrease in *de novo* mitochondrial protein synthesis. Thus it can be sometimes relatively difficult to interpret results from ^{35}S-met labelling experiments. Clearly, if there is a loss in *de novo* synthesis as it was the case e.g. after ICT1 depletion, in patient samples with MRPS16 or C12orf65 mutations [Miller *et al.*, 2004, Antonicka *et al.*, 2010] or in the *Tfb1m* knockout mice [Metodiev *et al.*, 2009] then it can be concluded that there is indeed a defect in mitochondrial protein synthesis. However, if there is no change in synthesis

then it is hard to conclude (not exclude) a defect in the mitochondrial translation machinery.

Surprisingly the steady state level of COX2 and partially also of NDUFB8 were upregulated. Additionally also the complexes of which they are components, namely Complex I and IV were increased and showed a higher in-gel activity (Figure 8.20). The reason for the increased level of mitochondrial proteins or complexes is still unknown, since mtDNA level was similar to control, the mitochondrial mass revealed by NAO measurements was not dramatically increased and also the mitochondrial translation seemed not to be changed in way that would explain the increased level of OXPHOS complexes. What was not investigated in this study and needs to be addressed in the future is the actual turnover of the proteins. It is possible that an overall change in the turnover of the components of the OXPHOS complexes occurred and is causing an increased amount of OXPHOS complexes. To address this possibility translation needs to be inhibited (e.g. by thiamphenicol treatment) and the decay of the existing protein monitored. A “positive” change in the turnover should lead to an increased stability/ half-life of the proteins. Another possibility to prove this hypothesis would be a ^{35}S-met pulse-chase experiment.

However, none of these discussed results can explain the growth defect after mtRbfA depletion. Interestingly an increased amount of cells was detected in the G1 phase after the loss of mtRbfA and further approximately 25% less in the S phase in comparison to the control (Figure 8.22). This could reflect a mitochondrial dysfunction where less energy production leads to a reduced DNA synthesis within the cell. Those results however, are relatively subtle and probably cannot be the main reason for the growth defect. The proportion of apoptotic cells after 6 days si-RbfA transfection was only slightly increased compared to the control. In comparison to the results that were observed after 3 days ERAL1 depletion [Dennerlein *et al.*, 2010], it can be considered as a minimal effect and not as the main reason for the growth defect. Thus it is still not clear what is causing the growth defect in the mtRbfA depleted cells. However, it still needs to be considered whether si-RbfA A, which was used for most of the experiments, has an off target effect. As previously described the reason for chosen this particular siRNA was the high efficiency in down-regulating the endogenous mtRbfA protein. Additionally this siRNA did not show any effect on 143B-ρ^0 cells, suggesting that it does not target another protein coding transcript with an important function outside mitochondria. Therefore it should be analysed in the future whether this phenotype caused by si-RbfA A is really specific, by testing if it can be rescued by the expression of mtRbfA with a silent mutation within the siRNA region.

What can be the function of mtRbfA in human mitochondria?

In summary, it was shown that mtRbfA is associated preferentially with the 28S SSU, probably at a quite late assembly point. Furthermore the virtually non-detectable level of mtRbfA protein in mtDNA lacking ρ^0 cells suggests a role in the mitochondrial gene expression machinery. Its presence therefore in mtDNA lacking cells becomes redundant as was also found with other proteins including mitochondrial ribosomal ones. It is possible that mtRbfA is directly or indirectly involved in the translation initiation, where it dissociates from the 28S SSU just when everything is correctly placed for the start of protein synthesis. In agreement with this idea was the presence of mtIF2 in the LC MS/MS analysis after mtRbfA-FLAG-IP but not in IP analyses from mtRRF, ICT1, ERAL1 or MRPS27. In human mitochondria mRNA are not modified, containing neither a 5'-cap structure nor a Shine-Dalgarno sequence that would facilitate the correct positioning of the mRNA within the ribosomal SSU. The human mitochondrial mRNAs are leaderless and their start codon is generally located within the first 3 nucleotides at the 5'-end [Montoya *et al.*, 1981; Anderson *et al.*, 1981]. There are still a lot of questions how the mammalian mitochondrial ribosome can preferentially select the first AUG at the 5'-end of those leaderless mRNAs. It is possible that some additional factors are required for this step. As described in chapter 1, Christian and Spremulli (2010) proposed a model where the mRNA starting with the 5'-end enters the 28S SSU through the mRNA entrance gate, which is unique to the mammalian mt-SSU. After the first 17 nucleotides have entered the 28S SSU, there appears to be an inspection on the codon at the 5'-end of the mRNA, causing a pause. The authors suggested that this step gives mtIF2 time to promote binding of the fmet-tRNA in a codon-anticodon dependent manner to the AUG start codon, which then leads to the formation of a stable initiation complex. It is possible that mtRbfA plays a critical quality control role within this initiation complex before the 28S SSU is then released to interact with the 39S LSU to perform translation elongation.

However, so far there is no clear evidence for such a role of mtRbfA in translation initiation control. Certainly it would be a great benefit to know the position of mtRbfA within the 28S SSU and furthermore whether it has maintained its RNA-binding function. Besides the suggested future experiments in the human cell system it might be also interesting to identify whether the human mtRbfA is able to replace RbfA in bacteria. This could potentially also answer the question whether it can still function as a RNA-binding protein. However, the substantial increase in size has to be considered. Therefore only the domain from residue Arg86 to Asp201 should be used for this kind of analysis.

Chapter 9:

Concluding remarks

9 Chapter 9: Concluding remarks

This PhD project was focused mainly on the characterisation of two proteins, **ICT1** and **mtRbfA,** both of which were found in association with the human mitochondrial ribosome initially co-immunoprecipitated with mtRRF [Rorbach *et al.*, 2008]. I will make concluding remarks for each of these sections individually below.

9.1 Part I: ICT1 - a functional peptidyl-tRNA hydrolase that has been recruited into the human mitochondrial ribosome

ICT1 studies constituted the main part of this PhD project. Results from this study revealed the first indication that a rescue system for stalled ribosomes exists in human mitochondria, for which ICT1 is probably indispensable.

My experiments have defined the following characteristics of ICT1, which is described as a member of the mitochondrial release factor family. ICT1 is:

i) localised within human mitochondria

ii) important for cell life

iii) essential for mitochondrial protein synthesis

iv) a previously unidentified member of the mitochondrial ribosomal large subunit

v) a ribosome-dependent, but codon-independent peptidyl-tRNA hydrolase (PTH), whose GGQ motif is both functional and essential for cell viability.

The function of ICT1 with its PTH activity within the mitochondrial ribosome is still not clear. The data presented here and further the investigations of ICT1 orthologues (also by other groups) however, strongly suggest an involvement of ICT1 in the recycling of stalled mitochondrial ribosomes and/ or 39S LSU with bound peptidyl-tRNA. Further experiments need to be done to prove this hypothesis. The determination of the localisation of ICT1 within the mitochondrial ribosome would be particularly beneficial in elucidating its function.

If I had the time I would have liked in particular to perform the following experiments:

i) Chemical crosslinking immunoprecipitation to identify direct protein interaction partners of ICT1. This would help to of where ICT1 is integrated within the mitochondrial ribosome.

ii) Isokinetic sucrose gradients after ^{35}S-met labelling for ICT1^{GGQ} wildtype and ICT1^{GSQ} mutant samples (potentially after mtRF1a depletion). This experiment may permit visualisation of the peptidyl-tRNA bound to the ribosome. It may be that the level of peptidyl-tRNAs is too low for detection using Phosphor-Imaging, however, utilising a scintillation counter after precipitating the relevant fraction may resolve this problem.

9.2 Part II: Human ribosome binding factor A is associated with the 28S mitochondrial ribosomal small subunit

As a potential mitochondrial ribosome assembly factor **mtRbfA** was investigated with respect to its function in human mitochondria. The work presented in this thesis has demonstrated that mtRbfA is:

i) a mitochondrial protein

ii) important for cell growth

iii) present in much lower steady state level in cells lacking mtDNA than in control cells

iv) preferentially associated with the 28S SSU, probably at a point late in subunit assembly.

The characteristics of mtRbfA that I have defined do not, however, clarify the precise function of mtRbfA within human mitochondria. The presence of a type-II KH-domain is known in other cases to facilitate RNA-binding, and such a fold is clearly present within the mtRbfA structure. It is of great interest, therefore, to identify whether mtRbfA is also able to bind RNA. This could be not answered with the experiments shown within the time limit of this study. However, there is still the possibility that with the optimisation of the CLIP assay specific RNA species can be identified, to which mtRbfA may bind. Generations of mutations within this KH-domain would also address the question as to whether this domain is really important for mtRbfA function.

Since bacterial RbfA is a cold shock protein, which is essential for bacteria growth at low temperature permitting adaptation of the translation machinery at those conditions, it would be interesting to investigate whether mtRbfA can also act as a kind of a stress response factor. To address this I would liked to have been able to analyse the

expression level and ratio of free and 28S SSU bound mtRbfA under different growth and stress conditions (using conditions such as low temperature, FBS starvation or cell culturing in glucose-free galactose containing media).

Even if the function of mtRbfA within human mitochondria is still elusive it seems highly likely that it is involved in the mitochondrial gene expression machinery, possibly in the late maturation of the 28S SSU as a potential quality control factor for translation initiation. However, this is a hypothesis that needs to be tested in the future. I would have planned various experiments to further this investigation that would have included:

i) perform CLIP under denaturing conditions
ii) examine the effect of mutations in the KH domain on cellular and molecular level
iii) determine the function of mtRbfA as a potential stress response factor
iv) extend experiments to have longer mtRbfA depletion, which may lead to clearer results (e.g. level of immunoprecipitated 55S by MRPS27 after mtRbfA depletion).

In summary mitochondrial translation in humans clearly requires quality control mechanisms to ensure that mitochondrial encoded proteins, which are all components of the OXPHOS complexes, are correctly expressed and assembled in the individual complexes. To prevent the occurrence or accumulation of failed translation events control mechanism are absolutely crucial. Defects in the translation machinery can cause mitochondrial dysfunction, harm to the cell and further human diseases, which are currently untreatable. Many mutations in patients associated with OXPHOS defects have been identified in mtDNA encoded tRNAs and rRNAs. However, in the past few years there were many reports of mutations in nDNA encoded proteins, functioning in the mitochondrial translation machinery [reviewed in Smits *et al.*, 2010]. These defects are usually associated with combined OXPHOS deficiencies. The understanding of the basic biology of the human translation machinery with all its components and control mechanisms is therefore essential to understand also the disease state and possibly to develop a way of treatment. The investigations presented here contribute with the characterisation of two proteins involved in this machinery some aspects concerning mitochondrial ribosome composition, assembly and possibly recycling when stalled.

References

References

Abreu IA, Cabelli DE (2010) Superoxide dismutases-a review of the metal-associated mechanistic variations. *Biochim Biophys Acta* **1804**(2)**:** 263-274

Acin-Perez R, Fernandez-Silva P, Peleato ML, Perez-Martos A, Enriquez JA (2008) Respiratory active mitochondrial supercomplexes. *Mol Cell* **32**(4)**:** 529-539

Anderson S, Bankier AT, Barrell BG, de Bruijn MH, Coulson AR, Drouin J, Eperon IC, Nierlich DP, Roe BA, Sanger F, Schreier PH, Smith AJ, Staden R, Young IG (1981) Sequence and organization of the human mitochondrial genome. *Nature* **290**(5806)**:** 457-465

Andersson SG, Zomorodipour A, Andersson JO, Sicheritz-Ponten T, Alsmark UC, Podowski RM, Naslund AK, Eriksson AS, Winkler HH, Kurland CG (1998) The genome sequence of *Rickettsia prowazekii* and the origin of mitochondria. *Nature* **396**(6707)**:** 133-140

Antonicka H, Ostergaard E, Sasarman F, Weraarpachai W, Wibrand F, Pedersen AM, Rodenburg RJ, van der Knaap MS, Smeitink JA, Chrzanowska-Lightowlers ZM, Shoubridge EA (2010) Mutations in C12orf65 in patients with encephalomyopathy and a mitochondrial translation defect. *Am J Hum Genet* **87**(1)**:** 115-122

Balaban RS, Nemoto S, Finkel T (2005) Mitochondria, oxidants, and aging. *Cell* **120**(4)**:** 483-495

Baughman JM, Nilsson R, Gohil VM, Arlow DH, Gauhar Z, Mootha VK (2009) A computational screen for regulators of oxidative phosphorylation implicates SLIRP in mitochondrial RNA homeostasis. *PLoS Genet* **5**(8)**:** e1000590

Benda C (1898) Über die Spermatogenese der Vertebraten und höherer Evertebraten, II. Theil: Die Histiogenese der Spermien. *Arch Anat Physiol* **73:** 393-398

Bhargava K, Spremulli LL (2005) Role of the N- and C-terminal extensions on the activity of mammalian mitochondrial translational initiation factor 3. *Nucleic Acids Res* **33**(22)**:** 7011-7018

Bogenhagen DF, Rousseau D, Burke S (2008) The layered structure of human mitochondrial DNA nucleoids. *J Biol Chem* **283**(6)**:** 3665-3675

Brand MD, Affourtit C, Esteves TC, Green K, Lambert AJ, Miwa S, Pakay JL, Parker N (2004) Mitochondrial superoxide: production, biological effects, and activation of uncoupling proteins. *Free Radic Biol Med* **37**(6)**:** 755-767

Britton RA (2009) Role of GTPases in bacterial ribosome assembly. *Annu Rev Microbiol* **63:** 155-176

Calvo SE, Mootha VK (2010) The mitochondrial proteome and human disease. *Annu Rev Genomics Hum Genet* **11:** 25-44

Carter AP, Clemons WM, Jr., Brodersen DE, Morgan-Warren RJ, Hartsch T, Wimberly BT, Ramakrishnan V (2001) Crystal structure of an initiation factor bound to the 30S ribosomal subunit. *Science* **291**(5503)**:** 498-501

Cheng Z, Saito K, Pisarev AV, Wada M, Pisareva VP, Pestova TV, Gajda M, Round A, Kong C, Lim M, Nakamura Y, Svergun DI, Ito K, Song H (2009) Structural insights into eRF3 and stop codon recognition by eRF1. *Genes Dev* **23**(9)**:** 1106-1118

Chomyn A (1996) *In vivo* labeling and analysis of human mitochondrial translation products. *Methods Enzymol* **264:** 197-211

Christian BE, Spremulli LL (2009) Evidence for an active role of IF3mt in the initiation of translation in mammalian mitochondria. *Biochemistry* **48**(15)**:** 3269-3278

Christian BE, Spremulli LL (2010) Preferential selection of the 5'-terminal start codon on leaderless mRNAs by mammalian mitochondrial ribosomes. *J Biol Chem* **285**(36)**:** 28379-28386

Circu ML, Aw TY (2010) Reactive oxygen species, cellular redox systems, and apoptosis. *Free Radic Biol Med* **48**(6)**:** 749-762

Clayton DA (1982) Replication of animal mitochondrial DNA. *Cell* **28**(4)**:** 693-705

Coenen MJ, Antonicka H, Ugalde C, Sasarman F, Rossi R, Heister JG, Newbold RF, Trijbels FJ, van den Heuvel LP, Shoubridge EA, Smeitink JA (2004) Mutant mitochondrial elongation factor G1 and combined oxidative phosphorylation deficiency. *N Engl J Med* **351**(20)**:** 2080-2086

Cotney J, Shadel GS (2006) Evidence for an early gene duplication event in the evolution of the mitochondrial transcription factor B family and maintenance of rRNA methyltransferase activity in human mtTFB1 and mtTFB2. *J Mol Evol* **63**(5)**:** 707-717

Culver GM (2003) Assembly of the 30S ribosomal subunit. *Biopolymers* **68**(2)**:** 234-249

Dammel CS, Noller HF (1995) Suppression of a cold-sensitive mutation in 16S rRNA by overexpression of a novel ribosome-binding factor, RbfA. *Genes Dev* **9**(5)**:** 626-637

Das G, Varshney U (2006) Peptidyl-tRNA hydrolase and its critical role in protein biosynthesis. *Microbiology* **152**(Pt 8)**:** 2191-2195

Datta PP, Wilson DN, Kawazoe M, Swami NK, Kaminishi T, Sharma MR, Booth TM, Takemoto C, Fucini P, Yokoyama S, Agrawal RK (2007) Structural aspects of RbfA action during small ribosomal subunit assembly. *Mol Cell* **28**(3)**:** 434-445

Davidov Y, Jurkevitch E (2009) Predation between prokaryotes and the origin of eukaryotes. *Bioessays* **31**(7)**:** 748-757

Davies SM, Rackham O, Shearwood AM, Hamilton KL, Narsai R, Whelan J, Filipovska A (2009) Pentatricopeptide repeat domain protein 3 associates with the mitochondrial small ribosomal subunit and regulates translation. *FEBS Lett* **583**(12)**:** 1853-1858

de Duve C (2007) The origin of eukaryotes: a reappraisal. *Nat Rev Genet* **8**(5)**:** 395-403

De Pereda JM, Waas WF, Jan Y, Ruoslahti E, Schimmel P, Pascual J (2004) Crystal structure of a human peptidyl-tRNA hydrolase reveals a new fold and suggests basis for a bifunctional activity. *J Biol Chem* **279**(9)**:** 8111-8115

Dennerlein S, Rozanska A, Wydro M, Chrzanowska-Lightowlers ZM, Lightowlers RN (2010) Human ERAL1 is a mitochondrial RNA chaperone involved in the assembly of the 28S small mitochondrial ribosomal subunit. *Biochem J* **430**(3)**:** 551-558

Du C, Fang M, Li Y, Li L, Wang X (2000) Smac, a mitochondrial protein that promotes cytochrome *c*-dependent caspase activation by eliminating IAP inhibition. *Cell* **102**(1)**:** 33-42

Dubrovsky EB, Dubrovskaya VA, Levinger L, Schiffer S, Marchfelder A (2004) *Drosophila* RNase Z processes mitochondrial and nuclear pre-tRNA 3' ends *in vivo*. *Nucleic Acids Res* **32**(1)**:** 255-262

Embley TM, Martin W (2006) Eukaryotic evolution, changes and challenges. *Nature* **440**(7084)**:** 623-630

Entelis NS, Kolesnikova OA, Dogan S, Martin RP, Tarassov IA (2001) 5 S rRNA and tRNA import into human mitochondria. Comparison of *in vitro* requirements. *J Biol Chem* **276**(49)**:** 45642-45653

Eskes R, Desagher S, Antonsson B, Martinou JC (2000) Bid induces the oligomerization and insertion of Bax into the outer mitochondrial membrane. *Mol Cell Biol* **20**(3)**:** 929-935

Falkenberg M, Gaspari M, Rantanen A, Trifunovic A, Larsson NG, Gustafsson CM (2002) Mitochondrial transcription factors B1 and B2 activate transcription of human mtDNA. *Nat Genet* **31**(3)**:** 289-294

Falkenberg M, Larsson NG, Gustafsson CM (2007) DNA replication and transcription in mammalian mitochondria. *Annu Rev Biochem* **76:** 679-699

Fernandez-Vizarra E, Tiranti V, Zeviani M (2009) Assembly of the oxidative phosphorylation system in humans: what we have learned by studying its defects. *Biochim Biophys Acta* **1793**(1)**:** 200-211

Frazier AE, Taylor RD, Mick DU, Warscheid B, Stoepel N, Meyer HE, Ryan MT, Guiard B, Rehling P (2006) Mdm38 interacts with ribosomes and is a component of the mitochondrial protein export machinery. *J Cell Biol* **172**(4)**:** 553-564

Frey TG, Mannella CA (2000) The internal structure of mitochondria. *Trends Biochem Sci* **25**(7)**:** 319-324

Fridovich I (1995) Superoxide radical and superoxide dismutases. *Annu Rev Biochem* **64:** 97-112

Fritz R, Bol J, Hebling U, Angermuller S, Volkl A, Fahimi HD, Mueller S (2007) Compartment-dependent management of H(2)O(2) by peroxisomes. *Free Radic Biol Med* **42**(7)**:** 1119-1129

Frolova LY, Tsivkovskii RY, Sivolobova GF, Oparina NY, Serpinsky OI, Blinov VM, Tatkov SI, Kisselev LL (1999) Mutations in the highly conserved GGQ motif of class 1 polypeptide release factors abolish ability of human eRF1 to trigger peptidyl-tRNA hydrolysis. *RNA* **5**(8)**:** 1014-1020

Gao H, Zhou Z, Rawat U, Huang C, Bouakaz L, Wang C, Cheng Z, Liu Y, Zavialov A, Gursky R, Sanyal S, Ehrenberg M, Frank J, Song H (2007) RF3 induces ribosomal conformational changes responsible for dissociation of class I release factors. *Cell* **129**(5)**:** 929-941

Gaur R, Grasso D, Datta PP, Krishna PD, Das G, Spencer A, Agrawal RK, Spremulli L, Varshney U (2008) A single mammalian mitochondrial translation initiation factor functionally replaces two bacterial factors. *Mol Cell* **29**(2)**:** 180-190

Gibbons C, Montgomery MG, Leslie AG, Walker JE (2000) The structure of the central stalk in bovine F(1)-ATPase at 2.4 A resolution. *Nat Struct Biol* **7**(11)**:** 1055-1061

Gray MW, Burger G, Lang BF (1999) Mitochondrial evolution. *Science* **283**(5407)**:** 1476-1481

Gruschke S, Grone K, Heublein M, Holz S, Israel L, Imhof A, Herrmann JM, Ott M (2010) Proteins at the polypeptide tunnel exit of the yeast mitochondrial ribosome. *J Biol Chem* **285**(25)**:** 19022-19028

Hammarsund M, Wilson W, Corcoran M, Merup M, Einhorn S, Grander D, Sangfelt O (2001) Identification and characterization of two novel human mitochondrial elongation factor genes, hEFG2 and hEFG1, phylogenetically conserved through evolution. *Hum Genet* **109**(5)**:** 542-550

Handa Y, Hikawa Y, Tochio N, Kogure H, Inoue M, Koshiba S, Guntert P, Inoue Y, Kigawa T, Yokoyama S, Nameki N (2010a) Solution structure of the catalytic domain of the mitochondrial protein ICT1 that is essential for cell vitality. *J Mol Biol* **404**(2)**:** 260-273

Handa Y, Inaho N, Nameki N (2010b) YaeJ is a novel ribosome-associated protein in *Escherichia coli* that can hydrolyze peptidyl-tRNA on stalled ribosomes. *Nucleic Acids Res*

Haque ME, Grasso D, Miller C, Spremulli LL, Saada A (2008) The effect of mutated mitochondrial ribosomal proteins S16 and S22 on the assembly of the small and large ribosomal subunits in human mitochondria. *Mitochondrion* **8**(3)**:** 254-261

Haque ME, Spremulli LL (2010) ICT1 comes to the rescue of mitochondrial ribosomes. *EMBO J* **29**(6)**:** 1019-1020

Hayes CS, Keiler KC (2010) Beyond ribosome rescue: tmRNA and co-translational processes. *FEBS Lett* **584**(2)**:** 413-419

He J, Mao CC, Reyes A, Sembongi H, Di Re M, Granycome C, Clippingdale AB, Fearnley IM, Harbour M, Robinson AJ, Reichelt S, Spelbrink JN, Walker JE, Holt IJ (2007) The AAA+ protein ATAD3 has displacement loop binding properties and is involved in mitochondrial nucleoid organization. *J Cell Biol* **176**(2)**:** 141-146

Hirokawa G, Demeshkina N, Iwakura N, Kaji H, Kaji A (2006) The ribosome-recycling step: consensus or controversy? *Trends Biochem Sci* **31**(3)**:** 143-149

Holzmann J, Frank P, Loffler E, Bennett KL, Gerner C, Rossmanith W (2008) RNase P without RNA: identification and functional reconstitution of the human mitochondrial tRNA processing enzyme. *Cell* **135**(3)**:** 462-474

Huang YJ, Swapna GV, Rajan PK, Ke H, Xia B, Shukla K, Inouye M, Montelione GT (2003) Solution NMR structure of ribosome-binding factor A (RbfA), a cold-shock adaptation protein from Escherichia coli. *J Mol Biol* **327**(2)**:** 521-536

Hyvarinen AK, Pohjoismaki JL, Holt IJ, Jacobs HT (2010) Overexpression of MTERFD1 or MTERFD3 impairs the completion of mitochondrial DNA replication. *Mol Biol Rep* **38**(2)**:** 1321-1328

Iborra FJ, Kimura H, Cook PR (2004) The functional organization of mitochondrial genomes in human cells. *BMC Biol* **2:** 9

Inoue K, Alsina J, Chen J, Inouye M (2003) Suppression of defective ribosome assembly in a *rbfA* deletion mutant by overexpression of Era, an essential GTPase in Escherichia coli. *Mol Microbiol* **48**(4)**:** 1005-1016

Ito K, Uno M, Nakamura Y (2000) A tripeptide 'anticodon' deciphers stop codons in messenger RNA. *Nature* **403**(6770)**:** 680-684

Iwata S, Lee JW, Okada K, Lee JK, Iwata M, Rasmussen B, Link TA, Ramaswamy S, Jap BK (1998) Complete structure of the 11-subunit bovine mitochondrial cytochrome bc1 complex. *Science* **281**(5373)**:** 64-71

Jan Y, Matter M, Pai JT, Chen YL, Pilch J, Komatsu M, Ong E, Fukuda M, Ruoslahti E (2004) A mitochondrial protein, Bit1, mediates apoptosis regulated by integrins and Groucho/TLE corepressors. *Cell* **116**(5)**:** 751-762

Jia L, Dienhart M, Schramp M, McCauley M, Hell K, Stuart RA (2003) Yeast Oxa1 interacts with mitochondrial ribosomes: the importance of the C-terminal region of Oxa1. *EMBO J* **22**(24)**:** 6438-6447

Jia L, Kaur J, Stuart RA (2009) Mapping of the Saccharomyces cerevisiae Oxa1-mitochondrial ribosome interface and identification of MrpL40, a ribosomal protein in close proximity to Oxa1 and critical for oxidative phosphorylation complex assembly. *Eukaryot Cell* **8**(11)**:** 1792-1802

Jiang L, Schaffitzel C, Bingel-Erlenmeyer R, Ban N, Korber P, Koning RI, de Geus DC, Plaisier JR, Abrahams JP (2009) Recycling of aborted ribosomal 50S subunit-nascent chain-tRNA complexes by the heat shock protein Hsp15. *J Mol Biol* **386**(5)**:** 1357-1367

Jones PG, Inouye M (1996) RbfA, a 30S ribosomal binding factor, is a cold-shock protein whose absence triggers the cold-shock response. *Mol Microbiol* **21**(6)**:** 1207-1218

Koc EC, Burkhart W, Blackburn K, Moseley A, Spremulli LL (2001b) The small subunit of the mammalian mitochondrial ribosome. Identification of the full complement of ribosomal proteins present. *J Biol Chem* **276**(22)**:** 19363-19374

Koc EC, Burkhart W, Blackburn K, Moyer MB, Schlatzer DM, Moseley A, Spremulli LL (2001c) The large subunit of the mammalian mitochondrial ribosome. Analysis of the complement of ribosomal proteins present. *J Biol Chem* **276**(47)**:** 43958-43969

Koc EC, Ranasinghe A, Burkhart W, Blackburn K, Koc H, Moseley A, Spremulli LL (2001a) A new face on apoptosis: death-associated protein 3 and PDCD9 are mitochondrial ribosomal proteins. *FEBS Lett* **492**(1-2)**:** 166-170

Koc EC, Haque ME, Spremulli LL (2010) Current Views of the Structure of the Mammalian Mitochondrial Ribosome. *Israel Journal of Chemistry* **50:** 45-59

Kolanczyk M, Pech M, Zemojtel T, Yamamoto H, Mikula I, Calvaruso MA, van den Brand M, Richter R, Fischer B, Ritz A, Kossler N, Thurisch B, Spoerle R, Smeitink J, Kornak U, Chan D, Vingron M, Martasek P, Lightowlers RN, Nijtmans L, Schuelke M, Nierhaus KH, Mundlos S (2011) NOA1 is an essential GTPase required for mitochondrial protein synthesis. *Mol Biol Cell* **22**(1)**:** 1-11

Korhonen JA, Pham XH, Pellegrini M, Falkenberg M (2004) Reconstitution of a minimal mtDNA replisome *in vitro*. *EMBO J* **23**(12)**:** 2423-2429

Kruse B, Narasimhan N, Attardi G (1989) Termination of transcription in human mitochondria: identification and purification of a DNA binding protein factor that promotes termination. *Cell* **58**(2)**:** 391-397

Lambert AJ, Brand MD (2004) Superoxide production by NADH:ubiquinone oxidoreductase (complex I) depends on the pH gradient across the mitochondrial inner membrane. *Biochem J* **382**(Pt 2)**:** 511-517

Lang BF, Gray MW, Burger G (1999) Mitochondrial genome evolution and the origin of eukaryotes. *Annu Rev Genet* **33:** 351-397

Laurberg M, Asahara H, Korostelev A, Zhu J, Trakhanov S, Noller HF (2008) Structural basis for translation termination on the 70S ribosome. *Nature* **454**(7206)**:** 852-857

Lazarou M, Thorburn DR, Ryan MT, McKenzie M (2009) Assembly of mitochondrial complex I and defects in disease. *Biochim Biophys Acta* **1793**(1)**:** 78-88

Levinger L, Jacobs O, James M (2001) *In vitro* 3'-end endonucleolytic processing defect in a human mitochondrial tRNA(Ser(UCN)) precursor with the U7445C substitution, which causes non-syndromic deafness. *Nucleic Acids Res* **29**(21)**:** 4334-4340

Li LY, Luo X, Wang X (2001) Endonuclease G is an apoptotic DNase when released from mitochondria. *Nature* **412**(6842)**:** 95-99

Liao HX, Spremulli LL (1989) Interaction of bovine mitochondrial ribosomes with messenger RNA. *J Biol Chem* **264**(13)**:** 7518-7522

Liao HX, Spremulli LL (1990) Identification and initial characterization of translational initiation factor 2 from bovine mitochondria. *J Biol Chem* **265**(23)**:** 13618-13622

Lightowlers RN, Selwood SP, Chrzanowska-Lightowlers ZMA (2001) Genetic Disease: Nonmendelian. *Encyclopedia of life sciences*

Lill R (2009) Function and biogenesis of iron-sulphur proteins. *Nature* **460**(7257)**:** 831-838

Liu M, Spremulli L (2000) Interaction of mammalian mitochondrial ribosomes with the inner membrane. *J Biol Chem* **275**(38)**:** 29400-29406

Liu X, Kim CN, Yang J, Jemmerson R, Wang X (1996) Induction of apoptotic program in cell-free extracts: requirement for dATP and cytochrome *c*. *Cell* **86**(1)**:** 147-157

Ma J, Spremulli LL (1996) Expression, purification, and mechanistic studies of bovine mitochondrial translational initiation factor 2. *J Biol Chem* **271**(10)**:** 5805-5811

Martin W, Muller M (1998) The hydrogen hypothesis for the first eukaryote. *Nature* **392**(6671)**:** 37-41

Matthews DE, Hessler RA, Denslow ND, Edwards JS, O'Brien TW (1982) Protein composition of the bovine mitochondrial ribosome. *J Biol Chem* **257**(15)**:** 8788-8794

Mears JA, Sharma MR, Gutell RR, McCook AS, Richardson PE, Caulfield TR, Agrawal RK, Harvey SC (2006) A structural model for the large subunit of the mammalian mitochondrial ribosome. *J Mol Biol* **358**(1)**:** 193-212

Menninger JR (1979) Accumulation of peptidyl tRNA is lethal to *Escherichia coli*. *J Bacteriol* **137**(1)**:** 694-696

Metodiev MD, Lesko N, Park CB, Camara Y, Shi Y, Wibom R, Hultenby K, Gustafsson CM, Larsson NG (2009) Methylation of 12S rRNA is necessary for *in vivo* stability of the small subunit of the mammalian mitochondrial ribosome. *Cell Metab* **9**(4)**:** 386-397

Miller C, Saada A, Shaul N, Shabtai N, Ben-Shalom E, Shaag A, Hershkovitz E, Elpeleg O (2004) Defective mitochondrial translation caused by a ribosomal protein (MRPS16) mutation. *Ann Neurol* **56**(5)**:** 734-738

Montoya J, Christianson T, Levens D, Rabinowitz M, Attardi G (1982) Identification of initiation sites for heavy-strand and light-strand transcription in human mitochondrial DNA. *Proc Natl Acad Sci U S A* **79**(23)**:** 7195-7199

Montoya J, Gaines GL, Attardi G (1983) The pattern of transcription of the human mitochondrial rRNA genes reveals two overlapping transcription units. *Cell* **34**(1)**:** 151-159

Montoya J, Ojala D, Attardi G (1981) Distinctive features of the 5'-terminal sequences of the human mitochondrial mRNAs. *Nature* **290**(5806)**:** 465-470

Moore SD, Sauer RT (2007) The tmRNA system for translational surveillance and ribosome rescue. *Annu Rev Biochem* **76:** 101-124

Mootha VK, Lepage P, Miller K, Bunkenborg J, Reich M, Hjerrild M, Delmonte T, Villeneuve A, Sladek R, Xu F, Mitchell GA, Morin C, Mann M, Hudson TJ, Robinson B, Rioux JD, Lander ES (2003) Identification of a gene causing human cytochrome *c* oxidase deficiency by integrative genomics. *Proc Natl Acad Sci U S A* **100**(2)**:** 605-610

Mora L, Heurgue-Hamard V, Champ S, Ehrenberg M, Kisselev LL, Buckingham RH (2003) The essential role of the invariant GGQ motif in the function and stability *in vivo* of bacterial release factors RF1 and RF2. *Mol Microbiol* **47**(1)**:** 267-275

Murphy MP (2009) How mitochondria produce reactive oxygen species. *Biochem J* **417**(1)**:** 1-13

Nagaike T, Suzuki T, Tomari Y, Takemoto-Hori C, Negayama F, Watanabe K, Ueda T (2001) Identification and characterization of mammalian mitochondrial tRNA nucleotidyltransferases. *J Biol Chem* **276**(43)**:** 40041-40049

Neupert W, Herrmann JM (2007) Translocation of proteins into mitochondria. *Annu Rev Biochem* **76:** 723-749

Nierhaus KH (1991) The assembly of prokaryotic ribosomes. *Biochimie* **73**(6)**:** 739-755

Nijtmans LG, Henderson NS, Holt IJ (2002) Blue Native electrophoresis to study mitochondrial and other protein complexes. *Methods* **26**(4)**:** 327-334

Nolden M, Ehses S, Koppen M, Bernacchia A, Rugarli EI, Langer T (2005) The *m*-AAA protease defective in hereditary spastic paraplegia controls ribosome assembly in mitochondria. *Cell* **123**(2)**:** 277-289

O'Brien TW (1971) The general occurrence of 55 S ribosomes in mammalian liver mitochondria. *J Biol Chem* **246**(10)**:** 3409-3417

O'Brien TW (2002) Evolution of a protein-rich mitochondrial ribosome: implications for human genetic disease. *Gene* **286**(1)**:** 73-79

Ojala D, Montoya J, Attardi G (1981) tRNA punctuation model of RNA processing in human mitochondria. *Nature* **290**(5806)**:** 470-474

Okado-Matsumoto A, Fridovich I (2001) Subcellular distribution of superoxide dismutases (SOD) in rat liver: Cu,Zn-SOD in mitochondria. *J Biol Chem* **276**(42)**:** 38388-38393

Ott M, Prestele M, Bauerschmitt H, Funes S, Bonnefoy N, Herrmann JM (2006) Mba1, a membrane-associated ribosome receptor in mitochondria. *EMBO J* **25**(8)**:** 1603-1610

Palade GE (1952) The fine structure of mitochondria. *Anat Rec* **114**(3)**:** 427-451

Petry S, Brodersen DE, Murphy FVt, Dunham CM, Selmer M, Tarry MJ, Kelley AC, Ramakrishnan V (2005) Crystal structures of the ribosome in complex with release factors RF1 and RF2 bound to a cognate stop codon. *Cell* **123**(7)**:** 1255-1266

Petry S, Weixlbaumer A, Ramakrishnan V (2008) The termination of translation. *Curr Opin Struct Biol* **18**(1)**:** 70-77

Piao L, Li Y, Kim SJ, Byun HS, Huang SM, Hwang SK, Yang KJ, Park KA, Won M, Hong J, Hur GM, Seok JH, Shong M, Cho MH, Brazil DP, Hemmings BA, Park J (2009) Association of LETM1 and MRPL36 contributes to the regulation of mitochondrial ATP production and necrotic cell death. *Cancer Res* **69**(8)**:** 3397-3404

Pohjoismaki JL, Wanrooij S, Hyvarinen AK, Goffart S, Holt IJ, Spelbrink JN, Jacobs HT (2006) Alterations to the expression level of mitochondrial transcription factor A, TFAM, modify the mode of mitochondrial DNA replication in cultured human cells. *Nucleic Acids Res* **34**(20)**:** 5815-5828

Rackham O, Davies SM, Shearwood AM, Hamilton KL, Whelan J, Filipovska A (2009) Pentatricopeptide repeat domain protein 1 lowers the levels of mitochondrial leucine tRNAs in cells. *Nucleic Acids Res* **37**(17)**:** 5859-5867

Richter R, Rorbach J, Pajak A, Smith PM, Wessels HJ, Huynen MA, Smeitink JA, Lightowlers RN, Chrzanowska-Lightowlers ZM (2010) A functional peptidyl-tRNA hydrolase, ICT1, has been recruited into the human mitochondrial ribosome. *EMBO J* **29**(6)**:** 1116-1125

Roberti M, Polosa PL, Bruni F, Manzari C, Deceglie S, Gadaleta MN, Cantatore P (2009) The MTERF family proteins: mitochondrial transcription regulators and beyond. *Biochim Biophys Acta* **1787**(5)**:** 303-311

Rodriguez J, Lazebnik Y (1999) Caspase-9 and APAF-1 form an active holoenzyme. *Genes Dev* **13**(24)**:** 3179-3184

Rorbach J, Richter R, Wessels HJ, Wydro M, Pekalski M, Farhoud M, Kuhl I, Gaisne M, Bonnefoy N, Smeitink JA, Lightowlers RN, Chrzanowska-Lightowlers ZM (2008) The human mitochondrial ribosome recycling factor is essential for cell viability. *Nucleic Acids Res* **36**(18)**:** 5787-5799

Rutter J, Winge DR, Schiffman JD (2010) Succinate dehydrogenase - Assembly, regulation and role in human disease. *Mitochondrion* **10**(4)**:** 393-401

Saraste M (1999) Oxidative phosphorylation at the fin de siecle. *Science* **283**(5407)**:** 1488-1493

Sasarman F, Brunel-Guitton C, Antonicka H, Wai T, Shoubridge EA (2010) LRPPRC and SLIRP interact in a ribonucleoprotein complex that regulates posttranscriptional gene expression in mitochondria. *Mol Biol Cell* **21**(8)**:** 1315-1323

Satoh M, Kuroiwa T (1991) Organization of multiple nucleoids and DNA molecules in mitochondria of a human cell. *Exp Cell Res* **196**(1)**:** 137-140

Schafer E, Dencher NA, Vonck J, Parcej DN (2007) Three-dimensional structure of the respiratory chain supercomplex I1III2IV1 from bovine heart mitochondria. *Biochemistry* **46**(44)**:** 12579-12585

Schagger H, Pfeiffer K (2000) Supercomplexes in the respiratory chains of yeast and mammalian mitochondria. *EMBO J* **19**(8)**:** 1777-1783

Schmeing TM, Huang KS, Strobel SA, Steitz TA (2005) An induced-fit mechanism to promote peptide bond formation and exclude hydrolysis of peptidyl-tRNA. *Nature* **438**(7067)**:** 520-524

Schmitz-Linneweber C, Small I (2008) Pentatricopeptide repeat proteins: a socket set for organelle gene expression. *Trends Plant Sci* **13**(12)**:** 663-670

Sharma MR, Koc EC, Datta PP, Booth TM, Spremulli LL, Agrawal RK (2003) Structure of the mammalian mitochondrial ribosome reveals an expanded functional role for its component proteins. *Cell* **115**(1)**:** 97-108

Shaw JJ, Green R (2007) Two distinct components of release factor function uncovered by nucleophile partitioning analysis. *Mol Cell* **28**(3)**:** 458-467

Shen EL, Bogenhagen DF (2001) Developmentally-regulated packaging of mitochondrial DNA by the HMG-box protein mtTFA during Xenopus oogenesis. *Nucleic Acids Res* **29**(13)**:** 2822-2828

Shoubridge EA (2000) Mitochondrial DNA segregation in the developing embryo. *Hum Reprod* **15 Suppl 2:** 229-234

Singh NS, Ahmad R, Sangeetha R, Varshney U (2008) Recycling of ribosomal complexes stalled at the step of elongation in Escherichia coli. *J Mol Biol* **380**(3)**:** 451-464

Sjöstrand FS (1956) The ultrastructure of cells as revealed by the electron microscope. *Int Rev Cytol* **5:** 455-533

Smirnov A, Comte C, Mager-Heckel AM, Addis V, Krasheninnikov IA, Martin RP, Entelis N, Tarassov I (2010) Mitochondrial enzyme rhodanese is essential for 5 S ribosomal RNA import into human mitochondria. *J Biol Chem* **285**(40)**:** 30792-30803

Smirnov AV, Entelis NS, Krasheninnikov IA, Martin R, Tarassov IA (2008) Specific features of 5S rRNA structure - its interactions with macromolecules and possible functions. *Biochemistry (Mosc)* **73**(13)**:** 1418-1437

Smits P, Smeitink J, van den Heuvel L (2010) Mitochondrial translation and beyond: processes implicated in combined oxidative phosphorylation deficiencies. *J Biomed Biotechnol* **2010:** 737385

Soleimanpour-Lichaei HR, Kuhl I, Gaisne M, Passos JF, Wydro M, Rorbach J, Temperley R, Bonnefoy N, Tate W, Lightowlers R, Chrzanowska-Lightowlers Z (2007) mtRF1a is a human mitochondrial translation release factor decoding the major termination codons UAA and UAG. *Mol Cell* **27**(5)**:** 745-757

Spelbrink JN (2010) Functional organization of mammalian mitochondrial DNA in nucleoids: history, recent developments, and future challenges. *IUBMB Life* **62**(1)**:** 19-32

Spencer AC, Spremulli LL (2004) Interaction of mitochondrial initiation factor 2 with mitochondrial fMet-tRNA. *Nucleic Acids Res* **32**(18)**:** 5464-5470

Spirina O, Bykhovskaya Y, Kajava AV, O'Brien TW, Nierlich DP, Mougey EB, Sylvester JE, Graack HR, Wittmann-Liebold B, Fischel-Ghodsian N (2000) Heart-specific splice-variant of a human mitochondrial ribosomal protein (mRNA processing; tissue specific splicing). *Gene* **261**(2)**:** 229-234

Spremulli LL, Coursey A, Navratil T, Hunter SE (2004) Initiation and elongation factors in mammalian mitochondrial protein biosynthesis. *Prog Nucleic Acid Res Mol Biol* **77:** 211-261

Susin SA, Lorenzo HK, Zamzami N, Marzo I, Snow BE, Brothers GM, Mangion J, Jacotot E, Costantini P, Loeffler M, Larochette N, Goodlett DR, Aebersold R, Siderovski DP, Penninger JM, Kroemer G (1999) Molecular characterization of mitochondrial apoptosis-inducing factor. *Nature* **397**(6718)**:** 441-446

Tate WP, Caskey CT (1990) Termination of protein synthesis. In *Ribosomes and Protein Synthesis: A Practical Approach,* Spedding G (ed) Oxford: Oxford University Press: 81-100

Temperley R, Richter R, Dennerlein S, Lightowlers RN, Chrzanowska-Lightowlers ZM (2010a) Hungry codons promote frameshifting in human mitochondrial ribosomes. *Science* **327**(5963)**:** 301

Temperley RJ, Wydro M, Lightowlers RN, Chrzanowska-Lightowlers ZM (2010b) Human mitochondrial mRNAs--like members of all families, similar but different. *Biochim Biophys Acta* **1797**(6-7)**:** 1081-1085

Tiranti V, Savoia A, Forti F, D'Apolito MF, Centra M, Rocchi M, Zeviani M (1997) Identification of the gene encoding the human mitochondrial RNA polymerase (h-mtRPOL) by cyberscreening of the Expressed Sequence Tags database. *Hum Mol Genet* **6**(4)**:** 615-625

Towpik J (2005) Regulation of mitochondrial translation in yeast. *Cell Mol Biol Lett* **10**(4)**:** 571-594

Tsuboi M, Morita H, Nozaki Y, Akama K, Ueda T, Ito K, Nierhaus KH, Takeuchi N (2009) EF-G2mt is an exclusive recycling factor in mammalian mitochondrial protein synthesis. *Mol Cell* **35**(4)**:** 502-510

Tsukihara T, Aoyama H, Yamashita E, Tomizaki T, Yamaguchi H, Shinzawa-Itoh K, Nakashima R, Yaono R, Yoshikawa S (1996) The whole structure of the 13-subunit oxidized cytochrome *c* oxidase at 2.8 A. *Science* **272**(5265)**:** 1136-1144

Tuppen HA, Blakely EL, Turnbull DM, Taylor RW (2010) Mitochondrial DNA mutations and human disease. *Biochim Biophys Acta* **1797**(2)**:** 113-128

Turrens JF (2003) Mitochondrial formation of reactive oxygen species. *J Physiol* **552**(Pt 2)**:** 335-344

Uchiumi T, Ohgaki K, Yagi M, Aoki Y, Sakai A, Matsumoto S, Kang D (2010) ERAL1 is associated with mitochondrial ribosome and elimination of ERAL1 leads to mitochondrial dysfunction and growth retardation. *Nucleic Acids Res* **38**(16)**:** 5554-5568

Ule J, Jensen K, Mele A, Darnell RB (2005) CLIP: a method for identifying protein-RNA interaction sites in living cells. *Methods* **37**(4)**:** 376-386

van Belzen N, Diesveld MP, van der Made AC, Nozawa Y, Dinjens WN, Vlietstra R, Trapman J, Bosman FT (1995) Identification of mRNAs that show modulated expression during colon carcinoma cell differentiation. *Eur J Biochem* **234**(3)**:** 843-848

Verhagen AM, Ekert PG, Pakusch M, Silke J, Connolly LM, Reid GE, Moritz RL, Simpson RJ, Vaux DL (2000) Identification of DIABLO, a mammalian protein that promotes apoptosis by binding to and antagonizing IAP proteins. *Cell* **102**(1)**:** 43-53

Viebrock A, Perz A, Sebald W (1982) The imported preprotein of the proteolipid subunit of the mitochondrial ATP synthase from *Neurospora crassa*. Molecular cloning and sequencing of the mRNA. *EMBO J* **1**(5)**:** 565-571

Vogel RO, Smeitink JA, Nijtmans LG (2007) Human mitochondrial complex I assembly: a dynamic and versatile process. *Biochim Biophys Acta* **1767**(10)**:** 1215-1227

von Dohlen CD, Kohler S, Alsop ST, McManus WR (2001) Mealybug β-proteobacterial endosymbionts contain γ-proteobacterial symbionts. *Nature* **412**(6845)**:** 433-436

Vonck J, Schafer E (2009) Supramolecular organization of protein complexes in the mitochondrial inner membrane. *Biochim Biophys Acta* **1793**(1)**:** 117-124

Walberg MW, Clayton DA (1981) Sequence and properties of the human KB cell and mouse L cell D-loop regions of mitochondrial DNA. *Nucleic Acids Res* **9**(20)**:** 5411-5421

Wallace DC (2005) A mitochondrial paradigm of metabolic and degenerative diseases, aging, and cancer: a dawn for evolutionary medicine. *Annu Rev Genet* **39:** 359-407

Wallace DC (2007) Why do we still have a maternally inherited mitochondrial DNA? Insights from evolutionary medicine. *Annu Rev Biochem* **76:** 781-821

Wang C, Youle RJ (2009) The role of mitochondria in apoptosis*. *Annu Rev Genet* **43:** 95-118

Wang G, Chen HW, Oktay Y, Zhang J, Allen EL, Smith GM, Fan KC, Hong JS, French SW, McCaffery JM, Lightowlers RN, Morse HC, 3rd, Koehler CM, Teitell MA (2010) PNPASE regulates RNA import into mitochondria. *Cell* **142**(3)**:** 456-467

Wang X (2001) The expanding role of mitochondria in apoptosis. *Genes Dev* **15**(22)**:** 2922-2933

Wang Z, Cotney J, Shadel GS (2007) Human mitochondrial ribosomal protein MRPL12 interacts directly with mitochondrial RNA polymerase to modulate mitochondrial gene expression. *J Biol Chem* **282**(17)**:** 12610-12618

Wanrooij S, Falkenberg M (2010) The human mitochondrial replication fork in health and disease. *Biochim Biophys Acta* **1797**(8)**:** 1378-1388

Wanrooij S, Fuste JM, Farge G, Shi Y, Gustafsson CM, Falkenberg M (2008) Human mitochondrial RNA polymerase primes lagging-strand DNA synthesis *in vitro*. *Proc Natl Acad Sci U S A* **105**(32)**:** 11122-11127

Weraarpachai W, Antonicka H, Sasarman F, Seeger J, Schrank B, Kolesar JE, Lochmuller H, Chevrette M, Kaufman BA, Horvath R, Shoubridge EA (2009) Mutation in *TACO1*, encoding a translational activator of COX I, results in cytochrome *c* oxidase deficiency and late-onset Leigh syndrome. *Nat Genet* **41**(7)**:** 833-837

Williams EH, Bsat N, Bonnefoy N, Butler CA, Fox TD (2005) Alteration of a novel dispensable mitochondrial ribosomal small-subunit protein, Rsm28p, allows translation of defective *COX2* mRNAs. *Eukaryot Cell* **4**(2)**:** 337-345

Winzeler EA, Shoemaker DD, Astromoff A, Liang H, Anderson K, Andre B, Bangham R, Benito R, Boeke JD, Bussey H, Chu AM, Connelly C, Davis K, Dietrich F, Dow SW, El Bakkoury M, Foury F, Friend SH, Gentalen E, Giaever G, Hegemann JH, Jones T, Laub M, Liao H, Liebundguth N, Lockhart DJ, Lucau-Danila A, Lussier M, M'Rabet N, Menard P, Mittmann M, Pai C, Rebischung C, Revuelta JL, Riles L, Roberts CJ, Ross-MacDonald P, Scherens B, Snyder M, Sookhai-Mahadeo S, Storms RK, Veronneau S, Voet M, Volckaert G, Ward TR, Wysocki R, Yen GS, Yu K, Zimmermann K, Philippsen P, Johnston M, Davis RW (1999) Functional characterization of the *S. cerevisiae* genome by gene deletion and parallel analysis. *Science* **285**(5429)**:** 901-906

Xia B, Ke H, Shinde U, Inouye M (2003) The role of RbfA in 16S rRNA processing and cell growth at low temperature in Escherichia coli. *J Mol Biol* **332**(3)**:** 575-584

Xu F, Ackerley C, Maj MC, Addis JB, Levandovskiy V, Lee J, Mackay N, Cameron JM, Robinson BH (2008) Disruption of a mitochondrial RNA-binding protein gene results in decreased cytochrome *b* expression and a marked reduction in ubiquinol-cytochrome *c* reductase activity in mouse heart mitochondria. *Biochem J* **416**(1)**:** 15-26

Xu F, Morin C, Mitchell G, Ackerley C, Robinson BH (2004) The role of the *LRPPRC* (leucine-rich pentatricopeptide repeat cassette) gene in cytochrome oxidase assembly: mutation causes lowered levels of *COX* (cytochrome *c* oxidase) *I* and *COX III* mRNA. *Biochem J* **382**(Pt 1)**:** 331-336

Yoshida M, Muneyuki E, Hisabori T (2001) ATP synthase--a marvellous rotary engine of the cell. *Nat Rev Mol Cell Biol* **2**(9)**:** 669-677

Youngman EM, McDonald ME, Green R (2008) Peptide release on the ribosome: mechanism and implications for translational control. *Annu Rev Microbiol* **62:** 353-373

Zhang Y, Spremulli LL (1998) Identification and cloning of human mitochondrial translational release factor 1 and the ribosome recycling factor. *Biochim Biophys Acta* **1443**(1-2)**:** 245-250

Zhu Z, Yao J, Johns T, Fu K, De Bie I, Macmillan C, Cuthbert AP, Newbold RF, Wang J, Chevrette M, Brown GK, Brown RM, Shoubridge EA (1998) *SURF1*, encoding a factor involved in the biogenesis of cytochrome *c* oxidase, is mutated in Leigh syndrome. *Nat Genet* **20**(4)**:** 337-343

Zou H, Li Y, Liu X, Wang X (1999) An APAF-1.cytochrome *c* multimeric complex is a functional apoptosome that activates procaspase-9. *J Biol Chem* **274**(17)**:** 11549-11556

Appendices

Appendix 1: LC MS/MS analysis – ICT1-FLAG IP

The LC MS/MS was carried out and analysed by H. Wessels (UNMC, Nijmegen).

The identified proteins are listed in the table below from high (green) to low (red) EMPAI value. Contaminants such as keratin, but also cytosolic ribosomal proteins were not included. Proteins with uncertain prediction for mitochondrial localisation are written in grey.

PROTEIN IDENTIFICATION INFORMATION					EMPAI VALUES	
	Gene	UNIPROT	PROT ID	PROT NAME	control	ICT1
1	ICT1	Q14197	NP_001536.1	immature colon carcinoma transcript 1	0.221677349	26.21338768
2	MRPS21	P82921	NP_061870.1	mitochondrial ribosomal protein S21	0.333521432	16.7827941
3	SSBP1	Q04837	NP_003134.1	single-stranded DNA binding protein 1	0.668100537	13.67799268
4	MRPL15	Q9P015	NP_054894.1	mitochondrial ribosomal protein L15	0.311133937	13.03003723
5	MRPL11	Q9Y3B7	NP_057134.1	mitochondrial ribosomal protein L11 isoform a	0	11.45197085
6	MRPL28	Q13084	NP_006419.2	mitochondrial ribosomal protein L28	0	9.926008611
7	MRPL47	Q9HD33	NP_065142.2	mitochondrial ribosomal protein L47 isoform a	0	8.006280202
8	MRPL17	Q9NRX2	NP_071344.1	mitochondrial ribosomal protein L17	0.274274986	7.858667904
9	MRPS26	Q9BYN8	NP_110438.1	mitochondrial ribosomal protein S26	0.311133937	7.733261624
10	MRPL55	Q7Z7F7	NP_852130.1	mitochondrial ribosomal protein L55 isoform a	0	7.376776401
11	HSPD1	P10809	NP_955472.1	chaperonin	1.392147081	6.564633276
12	MRPL51	Q4U2R6	NP_057581.2	mitochondrial ribosomal protein L51	0	5.812920691
13	MRPL24	Q96A35	NP_663781.1	mitochondrial ribosomal protein L24	0	5.628703162
14	MRPL43	Q8N983-4	NP_115488.2	mitochondrial ribosomal protein L43 isoform a	0.245197085	5.449466771
15	LRPPRC	P42704	NP_573566.2	leucine-rich PPR motif-containing protein	2.346494873	5.43788433
16	MRPS9	P82933	NP_872578.1	mitochondrial ribosomal protein S9	0.158323286	5.434438263
17	MRPS6	P82932	NP_115865.1	mitochondrial ribosomal protein S6	0.389495494	5.105402297
18	C14orf156	Q9GZT3	NP_112487.1	SRA stem-loop-interacting RNA-binding protein	1.894266125	4.878016072
19	MRPL1	Q9BYD6	NP_064621.2	mitochondrial ribosomal protein L1	0.258925412	4.843414134
20	MRPL12	P52815	NP_002940.2	mitochondrial ribosomal protein L12	0.930697729	4.779692884
21	MRPL43	Q8N983	NP_789762.1	mitochondrial ribosomal protein L43 isoform b	0.245197085	4.779692884
22	MRPS22	P82650	NP_064576.1	mitochondrial ribosomal protein S22	0.350314038	4.76593265
23	MRPL22	Q9NWU5	NP_054899.2	mitochondrial ribosomal protein L22 isoform a	0.100694171	4.623413252
24	MRPS7	Q9Y2R9	NP_057055.1	mitochondrial ribosomal protein S7	0.185971012	4.504789808
25	MRPL4	Q9BYD3	NP_057040.2	mitochondrial ribosomal protein L4 isoform a	7.01E-02	4.43618362
26	MRPL21	A6NKU0	NP_852615.1	mitochondrial ribosomal protein L21 isoform d	0	4.379838403
27	HSPA9	P38646	NP_004125.3	heat shock 70kDa protein 9B precursor	0.803422821	4.24218321
28	MRPL19	P49406	NP_055578.2	mitochondrial ribosomal protein L19	6.42E-02	4.043159487
29	MRPP2	Q99714	NP_004484.1	mitochondrial ribonuclease P protein 2, HSD17B10	0.711328304	4.011872336
30	MRPS25	P82663	NP_071942.1	mitochondrial ribosomal protein S25	0.122018454	4.011872336
31	MRPS17	Q9Y2R5	NP_057053.1	mitochondrial ribosomal protein S17	0.584893192	4.011872336
32	MRPL2	Q5T653	NP_057034.2	mitochondrial ribosomal protein L2	0.193776642	3.923882632
33	MRPS31	Q92665	NP_005821.1	mitochondrial ribosomal protein S31	0.188502227	3.73151259
34	MRPL44	Q9H9J2	NP_075066.1	mitochondrial ribosomal protein L44	0.136463666	3.641588834
35	MRPL16	Q9NX20	NP_060310.1	mitochondrial ribosomal protein L16	0	3.641588834
36	MRPL39	Q9NYK5-2	NP_542984.2	mitochondrial ribosomal protein L39 isoform b	0	3.555505605
37	MRPL41	Q8IXM3	NP_115866.1	mitochondrial ribosomal protein L41	1.275845926	3.393970561
38	MRPL20	Q9BYC9	XP_001125910.1	mitochondrial ribosomal protein L20	0	3.393970561
39	PTCD3	Q96EY7	NP_060422.4	Pentatricopeptide repeat domain 3	0.250898933	3.354004654
40	MRPL49	Q13405	NP_004918.1	mitochondrial ribosomal protein L49	0.232846739	3.328761281
41	MRPS34	P82930	NP_076425.1	mitochondrial ribosomal protein S34	0.100694171	3.216965034
42	MRPL38	B2R894	NP_115867.1	mitochondrial ribosomal protein L38	0.154781985	3.216965034
43	MRPL9	Q9BYD2	NP_113608.1	mitochondrial ribosomal protein L9	0.172102298	3.175318937
44	GADD45GIP1	Q8TAE8	NP_443082.2	growth arrest and DNA-damage-inducible, gamma interacting protein 1	0.193776642	3.124626383
45	MRPL23	Q16540	NP_066957.2	mitochondrial ribosomal protein L23	0.291549665	3.084238653
46	MRPS35	P82673	NP_068593.2	mitochondrial ribosomal protein S35	6.80E-02	2.981071706
47	MRPL45	Q9BRJ2	NP_115727.3	mitochondrial ribosomal protein L45	6.42E-02	2.931828756
48	MRPL13	Q9BYD1	NP_054797.2	mitochondrial ribosomal protein L13	9.26E-02	2.775053205
49	RNMTL1	Q9HC36	NP_060616.1	RNA methyltransferase like 1	0	2.62095835
50	MRPL48	Q96GC5	NP_057139.1	mitochondrial ribosomal protein L48	0.291549665	2.593813664
51	MRPL10	Q7Z7H8	NP_660298.2	mitochondrial ribosomal protein L10 isoform a	8.57E-02	2.433320018
52	MRPS16	Q9Y3D3	NP_057149.1	mitochondrial ribosomal protein S16	0	2.383855153
53	MRPL37	Q9BZE1	NP_057575.2	mitochondrial ribosomal protein L37	0.193776642	2.305451348
54	ATP5A1	P25705	NP_001001937.1	ATP synthase, H+ transporting, mitochondrial F1 complex, alpha subunit prec.	0.77827941	2.16227766
55	MRPS14	O60783	NP_071383.1	mitochondrial ribosomal protein S14	0.211527659	2.16227766
56	MRPL40	Q9NQ50	NP_003767.2	mitochondrial ribosomal protein L40	0.110336318	2.16227766
57	MRPL18	Q9H0U6	NP_054880.2	mitochondrial ribosomal protein L18	0.110336318	2.16227766
58	MRPL50	Q8N5N7	NP_061924.1	mitochondrial ribosomal protein L50	0	2.16227766
59	NME4	O00746	NP_005000.1	nucleoside-diphosphate kinase 4	0	1.993577295
60	MRPL14	Q6P1L8	NP_115487.2	mitochondrial ribosomal protein L14	0.274274986	1.976351442
61	COX2	P00403	NP_536846.1	cytochrome c oxidase subunit II	0.311133937	1.955209235
62	MRPS2	Q9Y399	NP_057118.1	mitochondrial ribosomal protein S2	0.333521432	1.942727176
63	MRPL54	Q6P161	NP_758455.1	mitochondrial ribosomal protein L54	0.193776642	1.894266125
64	MRPS30	Q9NP92	NP_057724.2	mitochondrial ribosomal protein S30	0	1.861025569
65	MRPS18A	Q9NVS2	NP_060605.1	mitochondrial ribosomal protein S18A	0.110336318	1.848035868
66	MRPS27	Q92552	NP_055899.1	mitochondrial ribosomal protein S27	0.304321387	1.768902684
67	MRPS28	Q9Y2Q9	NP_054737.1	mitochondrial ribosomal protein S28	0.221677349	1.721338768
68	MRPL46	Q9H2W6	NP_071446.2	mitochondrial ribosomal protein L46	0.218187912	1.682695795
69	DAP3	P51398	NP_387506.1	death-associated protein 3	0.264855217	1.559547923
70	TUFM	P49411	NP_003312.3	Tu translation elongation factor, mitochondrial	0.536174947	1.55140652
71	MRPS5	P82675	NP_114108.1	mitochondrial ribosomal protein S5	0	1.536619456
72	CHCHD1	Q96BP2	NP_976043.1	coiled-coil-helix-coiled-coil-helix domain containing 1	0	1.511886432
73	MRPS10	P82664	NP_060611.2	mitochondrial ribosomal protein S10	8.57E-02	1.470911228

74	MRPL3	P09001	NP_009139.1	mitochondrial ribosomal protein L3	0	1.32195425
75	COX4I1	P13073	NP_001852.1	cytochrome c oxidase subunit IV isoform 1 precursor	0	1.3101297
76	MRPS23	Q9Y3D9	NP_057154.2	mitochondrial ribosomal protein S23	0.445439771	1.290867653
77	GRPEL1	Q9HAV7	NP_079472.1	GrpE-like 1, mitochondrial	9.65E-02	1.290867653
78	DHX30	Q7L2E3	NP_619520.1	DEAH (Asp-Glu-Ala-His) box polypeptide 30 isoform 1	0.14504757	1.15443469
79	PRDX3	P30048	NP_006784.1	peroxiredoxin 3 isoform a precursor	0.467799268	1.15443469
80	NDUFAF3	Q9BU61	NP_951032.1	NADH dehydrogenase [ubiquinone] 1 alpha subcomplex assembly factor	0.165914401	1.15443469
81	DDX28	Q9NUL7	NP_060850.1	DEAD (Asp-Glu-Ala-Asp) box polypeptide 28	0	1.127496491
82	TFB1M	Q9Y384	NP_057104.1	transcription factor B1, mitochondrial	0	1.075263132
83	MRPS18B	Q9Y676	NP_054765.1	mitochondrial ribosomal protein S18B	9.26E-02	1.030917621
84	PGAM5	Q96HS1-2	NP_612642.1	Bcl-XL-binding protein v68	0.291549665	1.020949938
85	MTERFD1	Q96E29	NP_057026.3	MTERF domain containing 1	0	1.005975301
86	PHB2	Q99623	NP_009204.1	prohibitin 2	0.110336318	0.974488213
87	VDAC1	P21796	NP_003365.1	voltage-dependent anion channel 1 (porin)	0	0.930697729
88	ATP5L	O75964	NP_006467.4	ATP synthase, H+ transporting, mitochondrial F0 complex, subunit G	0	0.930697729
89	MRPL32	Q9BYC8	NP_114109.1	mitochondrial ribosomal protein L32	0	0.895735652
90	PYCR2	Q96C36	NP_037460.2	pyrroline-5-carboxylate reductase family, member 2	0	0.887391822
91	MRPL27	Q9P0M9	NP_057588.1	mitochondrial ribosomal protein L27 isoform a	0.165914401	0.847849797
92	UQCRC2	P22695	NP_003357.2	ubiquinol-cytochrome c reductase core protein II	0	0.802245515
93	SLC25A5	P05141	NP_001143.1	solute carrier family 25, member 5	0.211527659	0.77827941
94	ISCA1	Q9BUE6	NP_112202.2	HESB like domain containing 2	0	0.77827941
95	ALDH2	P05091	NP_000681.2	mitochondrial aldehyde dehydrogenase 2 precursor	4.44E-02	0.759069582
96	OAT	P04181	NP_000265.1	ornithine aminotransferase precursor	0.264855217	0.757510625
97	SLC25A6		NP_001627.1	solute carrier family 25, member A6	0.132541315	0.750827032
98	TRUB2	O95900	NP_056494.1	TruB pseudouridine (psi) synthase homolog 2	0	0.750827032
99	DHX30	Q7L2E3-2	NP_619519.1	DEAH (Asp-Glu-Ala-His) box polypeptide 30 isoform 3	0.102943312	0.714125253
100	NDUFS3	O75489	NP_004542.1	NADH dehydrogenase (ubiquinone) Fe-S protein 3, 30kDa	0	0.711328304
101	POLRMT	O00411	NP_005026.3	mitochondrial DNA-directed RNA polymerase precursor	0	0.70125428
102	HADHA	P40939	NP_000173.2	mitochondrial trifunctional protein, alpha subunit precursor	0.193776642	0.70125428
103	YARS2	Q9Y2Z4	NP_001035526.1	tyrosyl-tRNA synthetase 2 (mitochondrial)	0	0.684283113
104	PTCD1	O75127	NP_056360.2	pentatricopeptide repeat domain 1	0	0.668100537
105	DLD	B2R5X0	NP_000099.2	dihydrolipoamide dehydrogenase precursor	0.148153621	0.659586907
106	MRRF	Q96E11	NP_620132.1	mitochondrial ribosome recycling factor isoform 1	0	0.637893707
107	ACOT9		NP_001028755.2	acyl-Coenzyme A thioesterase 2, mitochondrial isoform b	8.41E-02	0.623776739
108	MRPS11	P82912	NP_073750.2	mitochondrial ribosomal protein S11 isoform a	0.128837892	0.623776739
109	MTERFD2	Q7Z6M4	NP_872307.2	MTERF domain containing 2	0	0.619206824
110	C6orf203	Q9P0P8	NP_057571.1	hypothetical protein LOC51250	0	0.615598098
111	MDH2	P40926	NP_005909.2	mitochondrial malate dehydrogenase precursor	0.193776642	0.603718744
112	GTPBP10	A4D1E9	NP_149098.2	claudin 12 isoform 2	0	0.598467106
113	ATP5O	P48047	NP_001688.1	mitochondrial ATP synthase, O subunit precursor	0	0.584893192
114	PRDX5	P30044	NP_036226.1	peroxiredoxin 5 precursor, isoform a	0	0.557068405
115	CECR5	Q9BXW7-2	NP_060299.4	cat eye syndrome chromosome region, candidate 5 isoform 1	6.42E-02	0.545927736
116	SARS2	Q9NP81	NP_060297.1	seryl-tRNA synthetase 2	7.46E-02	0.539926526
117	SLC25A1	P53007	NP_005975.1	solute carrier family 25 (mitochondrial carrier; citrate transporter), member 1	0	0.539926526
118	NSUN4	Q96CB9	NP_950245.2	NOL1/NOP2/Sun domain family 4 protein	0	0.539926526
119	TRAP1	Q12931	NP_057376.1	TNF receptor-associated protein 1	0.174268583	0.534781344
120	UQCRFS1	A8K519	NP_005994.1	ubiquinol-cytochrome c reductase, Rieske iron-sulfur polypeptide 1	0	0.508590709
121	MRPS24	Q96EL2	NP_114403.1	mitochondrial ribosomal protein S24	0.105295141	0.492495545
122	MRPP1	Q7L0Y3	NP_060289.2	Mitochondrial ribonuclease P protein 1, RG9MTD1	0	0.4896249
123	ATP5C1	P36542	NP_001001973.1	ATP synthase, H+ transporting, mitochondrial F1 complex, gamma subunit iso. L	0.172102298	0.487352107
124	NGRN	Q9NPE2	NP_001028260.2	mesenchymal stem cell protein DSC92 isoform 2	0	0.483981789
125	THNSL1	Q8IYQ7	NP_079114.2	threonine synthase-like 1	0	0.474601593
126	SLC25A4	P12235	NP_001142.2	solute carrier family 25 (mito. carrier; adenine nucleotide translocator), mem. 4	6.61E-02	0.467799268
127	ATP5H	O75947	NP_006347.1	ATP synthase, H+ transporting, mitochondrial F0 complex, subunit d isoform a	0	0.467799268
128	PGAM5		XP_001126125.1	PREDICTED: similar to phosphoglycerate mutase family member 5	8.73E-02	0.457593301
129	METT11D1	Q9H7H0	NP_073571.1	methyltransferase 11 domain containing 1 isoform 2	0	0.456348478
130	C7orf30	Q96EH3	NP_612455.1	hypothetical protein LOC115416	0	0.44974067
131	DBT	Q5VVL8	NP_001909.2	dihydrolipoamide branched chain transacylase precursor	0	0.447819047
132	STOML2	Q9UJZ1	NP_038470.1	stomatin (EPB72)-like 2	0.128837892	0.438449888
133	WBSCR16	Q96I51	NP_110425.1	Williams-Beuren syndrome chromosome region 16	0	0.430722989
134	MTG1	Q9BT17	NP_612393.2	GTP_binding protein	0	0.430722989
135	SFXN1	Q9H9B4	NP_073591.2	sideroflexin 1	0	0.42510267
136	C4orf14	Q8NC60	NP_115689.1	hypothetical protein LOC84273	0	0.422136151
137	NDUFS1	P28331	NP_004997.4	NADH dehydrogenase (ubiquinone) Fe-S protein 1, 75kDa precursor	0	0.422136151
138	NDUFA13	Q9P0J0	NP_057049.3	cell death-regulatory protein GRIM19	0	0.417474163
139	LOC729317	A6NLE7	XP_001133585.1	PREDICTED: similar to voltage-dependent anion channel 2	0	0.417474163
140	ALDH1L2	Q3SY69	NP_001029345.1	aldehyde dehydrogenase 1 family, member L2	0	0.415121244
141	LONP1	P36776	NP_004784.2	mitochondrial lon peptidase 1	2.51E-02	0.414287277
142	FASTKD2	Q9NYY8	NP_055744.2	FAST kinase domains 2	0	0.409081686
143	C17orf42	Q6PJ19	NP_078959.2	hypothetical protein LOC79736	0	0.406527242
144	PUSL1	Q8N0Z8	NP_699170.1	pseudouridylate synthase-like 1	0	0.403003723
145	ALDH18A1	P54886	NP_002851.2	pyrroline-5-carboxylate synthetase isoform 1	4.71E-02	0.380384265
146	UQCRC1	P31930	NP_003356.2	ubiquinol-cytochrome c reductase core protein I	0	0.380384265
147	SLC25A3	Q00325-2	NP_002626.1	solute carrier family 25 member 3 isoform b precursor	6.61E-02	0.376857165
148	HADHB	P55084	NP_000174.1	mitochondrial trifunctional protein, beta subunit precursor	9.45E-02	0.371686619
149	SHMT2	P34897	NP_005403.2	serine hydroxymethyltransferase 2 (mitochondrial)	3.78E-02	0.345960324
150	RPUSD3	Q6P087	NP_775930.1	RNA pseudouridylate synthase domain containing 3	0	0.333521432
151	MMAB	Q96EY8	NP_443077.1	cob(I)alamin adenosyltransferase precursor	0	0.318256739

152	MCCC2	Q9HCC0	NP_071415.1	methylcrotonoyl-Coenzyme A carboxylase 2 (beta)	3.98E-02	0.314147363
153	PAPD1	Q9NVV4	NP_060579.2	Poly(A) RNA polymerase (PAP) associated domain containing 1	0	0.305996548
154	PMPCA	Q10713	NP_055975.1	peptidase (mitochondrial processing) alpha	0	0.302429122
155	SLC25A11	Q02978	NP_003553.2	solute carrier family 25 (mitochondrial carrier; oxoglutarate carrier), member 11	0	0.301025217
156	ATAD3A	Q8N275	NP_060658.2	ATPase family, AAA domain containing 3A	6.80E-02	0.301025217
157	ACAD9	Q9H845	NP_054768.2	acyl-Coenzyme A dehydrogenase family, member 9	3.61E-02	0.281422389
158	C18orf22	Q8N0V3	NP_079081.1	Putative ribosome-binding factor A, mitochondrial	0	0.274274986
159	NDUFV1	P49821	NP_009034.2	NADH dehydrogenase (ubiquinone) flavoprotein 1, 51kDa	0	0.264855217
160	DNAJA3	Q96EY1	NP_005138.2	DnaJ (Hsp40) homolog, subfamily A, member 3	0	0.24782547
161	TARS2	Q9BW92	NP_079426.2	threonyl-tRNA synthetase-like 1	0	0.2466504
162	VDAC3	Q9Y277	NP_005653.3	voltage-dependent anion channel 3	0	0.240937761
163	SLC25A13	Q9UJS0	NP_055066.1	solute carrier family 25, member 13 (citrin)	0	0.239747763
164	MCAT	Q8IVS2	NP_775738.3	mitochondrial malonyltransferase isoform a precursor	0	0.238862924
165	PMPCB	O75439	NP_004270.2	mitochondrial processing peptidase beta subunit precursor	0	0.237635028
166	PNPT1	Q8TCS8	NP_149100.1	polyribonucleotide nucleotidyltransferase 1	2.68E-02	0.235816596
167	LOC648605		XP_944686.1	PREDICTED: similar to Trimethyllysine dioxygenase, mitochondrial precursor	0	0.232846739
168	ACADVL	P49748	NP_000009.1	acyl-Coenzyme A dehydrogenase, very long chain isoform 1 precursor	5.85E-02	0.220168343
169	CCDC109A	Q8NE86	NP_612366.1	coiled-coil domain containing 109A	0	0.218187912
170	PCCB	P05166	NP_000523.2	propionyl Coenzyme A carboxylase, beta polypeptide	0	0.204051772
171	MTERF	Q99551	NP_008911.1	mitochondrial transcription termination factor precursor	0	0.197929811
172	ERAL1	O75616	NP_005693.1	Era G-protein-like 1	0	0.193776642
173	ETFA	P13804	NP_000117.1	electron transfer flavoprotein, alpha polypeptide	0	0.193776642
174	NDUFS2	O75306	NP_004541.1	NADH dehydrogenase (ubiquinone) Fe-S protein 2, 49kDa	0	0.189793791
175	ALDH1B1	Q8WX76	NP_000683.3	aldehyde dehydrogenase 1B1 precursor	0	0.189793791
176	SDHA	P31040	NP_004159.1	succinate dehydrogenase complex, subunit A, flavoprotein precursor	3.39E-02	0.181581733
177	RPUSD4	Q96K56	NP_116184.1	RNA pseudouridylate synthase domain containing 4	0	0.174308583
178	VIM	P08670	NP_003371.2	vimentin	0	0.173467208
179	HARS2	P49590	NP_036340.1	histidyl-tRNA synthetase-like	0	0.168951816
180	AGK	Q53H12	NP_060708.1	multiple substrate lipid kinase	0	0.158323286
181	KARS	Q15046	NP_005539.1	lysyl-tRNA synthetase	3.72E-02	0.157422881
182	SUPV3L1	Q8IYB8	NP_003162.2	suppressor of var1, 3-like 1	0	0.152732121
183	AARS2	A2RRN5	NP_065796.1	alanyl-tRNA synthetase like	0	0.142068906
184	ATAD3B	Q5T9A4	NP_114127.3	AAA-ATPase TOB3	3.30E-02	0.13851309
185	NDUFA9	Q16795	NP_004993.1	NADH dehydrogenase (ubiquinone) 1 alpha subcomplex, 9, 39kDa	0	0.133823501
186	RHOT1	Q8IXI2-3	NP_001028740.1	ras homolog gene family, member T1 isoform 1	0	0.132541315
187	MUT	P22033	NP_000246.1	methylmalonyl Coenzyme A mutase precursor	0	0.122018454
188	PUS1	Q9Y606	NP_079491.2	pseudouridylate synthase 1 isoform 1	0	0.122018454
189	AASS	Q9UDR5	NP_005754.2	aminoadipate-semialdehyde synthase	0	0.099606032
190	SLC25A12	O75746	NP_003696.2	solute carrier family 25 (mitochondrial carrier, Aralar), member 12	0	9.26E-02
191	PEO1	Q96RR1	NP_068602.2	twinkle	0	9.14E-02
192	GLDC	Q2M2F8	NP_000161.2	glycine dehydrogenase (decarboxylating)	0	8.99E-02
193	VARS2	Q5ST30	NP_065175.3	valyl-tRNA synthetase 2-like	0	8.49E-02
194	FASTKD1	Q8TEA9	NP_078898.2	FAST kinase domains 1	0	7.38E-02
195	MOV10	Q9HCE1	NP_066014.1	Mov10, Moloney leukemia virus 10, homolog	0	6.08E-02
196	KIAA0564	A3KMH1	NP_055873.1	hypothetical protein LOC23078 isoform a	0	3.93E-02
197	TTN		NP_596869.3	titin isoform N2-A	0	2.40E-02

Appendix 2: LC MS/MS analysis – mtRbfA-FLAG IP

The LC MS/MS was carried out and analysed by H. Wessels (UNMC, Nijmegen).

The identified proteins are listed in the table below from high (green) to low (red) EMPAI value. Contaminants such as keratin, but also cytosolic ribosomal proteins were not included. Proteins with uncertain prediction for mitochondrial localisation are written in grey.

PROTEIN IDENTIFICATION INFORMATION					EMPAI VALUES	
	Gene	UNIPROT	PROT ID	PROT NAME	control	mtRbfa
1	MRPS26	Q9BYN8	NP_110438.1	mitochondrial ribosomal protein S26	1.253933905	21.53933905
2	MRPS21	P82921	NP_061870.1	mitochondrial ribosomal protein S21	0	12.33521432
3	C18orf22	Q8N0V3	NP_079081.1	Putative ribosome-binding factor A, mitochondrial	0	7.858667904
4	MRPS7	Q9Y2R9	NP_057055.1	mitochondrial ribosomal protein S7	0.531740464	7.431909293
5	HSPA9	P38646	NP_004125.3	heat shock 70kDa protein 9B precursor	0.961927374	6.551770453
6	HSPD1	P10809	NP_955472.1	chaperonin	2.274549163	4.925530976
7	C14orf156	Q9GZT3	NP_112487.1	SRA stem-loop-interacting RNA-binding protein	0.42510267	4.878016072
8	MRPS22	P82650	NP_064576.1	mitochondrial ribosomal protein S22	0.916940777	4.216645252
9	MRPS17	Q9Y2R5	NP_057053.1	mitochondrial ribosomal protein S17	0.584893192	4.011872336
10	PTCD3	Q96EY7	NP_060422.4	Pentatricopeptide repeat domain 3	0.250898933	3.948168092
11	MRPL11	Q9Y3B7	NP_057134.1	mitochondrial ribosomal protein L11 isoform a	0.245197085	3.641588834
12	MRPS34	P82930	NP_076425.1	mitochondrial ribosomal protein S34	0.100694171	3.641588834
13	GADD45GIP1	Q8TAE8	NP_443082.2	growth arrest and DNA-damage-inducible, gamma interacting protein 1	0.193776642	3.506570338
14	MRPL28	Q13084	NP_006419.2	mitochondrial ribosomal protein L28	0	3.506570338
15	MRPS31	Q92665	NP_005821.1	mitochondrial ribosomal protein S31	0.333521432	3.466835922
16	SLC25A5	P05141	NP_001143.1	solute carrier family 25, member 5	6.61E-02	3.354004654
17	MRPL1	Q9BYD6	NP_064621.2	mitochondrial ribosomal protein L1	0.165914401	3.298662347
18	MRPS35	P82673	NP_068593.2	mitochondrial ribosomal protein S35	0.692666615	3.251786303
19	MRPL15	Q9P015	NP_054894.1	mitochondrial ribosomal protein L15	0.403003723	3.14616956
20	MRPL48	Q96GC5	NP_057139.1	mitochondrial ribosomal protein L48	0.467799268	3.084238653
21	SLC25A6		NP_001627.1	solute carrier family 25, member A6	0	2.931828756
22	MRPL47	Q9HD33	NP_065142.2	mitochondrial ribosomal protein L47 isoform a	0.232846739	2.898603703
23	MRPL22	Q9NWU5	NP_054899.2	mitochondrial ribosomal protein L22 isoform a	0.333521432	2.83118685
24	MRPL21	A6NKU0	NP_852615.1	mitochondrial ribosomal protein L21 isoform d	9.26E-02	2.775053205
25	MRPS9	P82933	NP_872578.1	mitochondrial ribosomal protein S9	0.158323286	2.753773682
26	MRPL41	Q8IXM3	NP_115866.1	mitochondrial ribosomal protein L41	0.930697729	2.72759372
27	ATP5A1	P25705	NP_001001937.1	ATP synthase, H+ transporting, mitochondrial F1 complex, alpha subunit prec.	0.995262315	2.686945065
28	SLC25A1	P53007	NP_005975.1	solute carrier family 25 (mitochondrial carrier; citrate transporter), member 1	0	2.651741273
29	MRPL39	Q9NYK5-2	NP_542984.2	mitochondrial ribosomal protein L39 isoform b	0.251875026	2.63894599
30	MRPL24	Q96A35	NP_663781.1	mitochondrial ribosomal protein L24	0	2.433320018
31	PRDX3	P30048	NP_006784.1	peroxiredoxin 3 isoform a precursor	0.995262315	2.414548874
32	MRPL4	Q9BYD3	NP_057040.2	mitochondrial ribosomal protein L4 isoform a	0.311133937	2.383855153
33	MRPL43	Q8N983-4	NP_115488.2	mitochondrial ribosomal protein L43 isoform a	0.55051578	2.340484984
34	MRPL49	Q13405	NP_004918.1	mitochondrial ribosomal protein L49	0.232846739	2.16227766
35	MRPS25	P82663	NP_071942.1	mitochondrial ribosomal protein S25	0.995262315	2.16227766
36	MRPS6	P82932	NP_115865.1	mitochondrial ribosomal protein S6	0.930697729	2.16227766
37	SLC25A4	P12235	NP_001142.2	solute carrier family 25 (mitochondrial carrier; adenine nucleotide translocator)	0	2.16227766
38	MRPL9	Q9BYD2	NP_113608.1	mitochondrial ribosomal protein L9	0.268961003	2.039195382
39	MRPL12	P52815	NP_002940.2	mitochondrial ribosomal protein L12	0.730195739	1.993577295
40	MRPL43	Q8N983	NP_789762.1	mitochondrial ribosomal protein L43 isoform b	0.55051578	1.993577295
41	MRPL44	Q9H9J2	NP_075066.1	mitochondrial ribosomal protein L44	0.211527659	1.966348839
42	C1QBP	Q07021	NP_001203.1	complement component 1, q subcomponent binding protein precursor	0.193776642	1.894266125
43	MRPL55	Q7Z7F7	NP_852130.1	mitochondrial ribosomal protein L55 isoform a	0	1.894266125
44	HADHA	P40939	NP_000173.2	mitochondrial trifunctional protein, alpha subunit precursor	0.163949307	1.894266125
45	MRPL45	Q9BRJ2	NP_115727.3	mitochondrial ribosomal protein L45	6.42E-02	1.880444153
46	MRPS15	P82914	NP_112570.2	mitochondrial ribosomal protein S15	0.333521432	1.872984833
47	MRPL40	Q9NQ50	NP_003767.2	mitochondrial ribosomal protein L40	0.110336318	1.848035868
48	DAP3	P51398	NP_387506.1	death-associated protein 3	0.389495494	1.811768698
49	MRPS5	P82675	NP_114108.1	mitochondrial ribosomal protein S5	0	1.797747463
50	TUFM	P49411	NP_003312.3	Tu translation elongation factor, mitochondrial	0.726983291	1.758531618
51	MRPP2	Q99714	NP_004484.1	Mitochondrial ribonuclease P protein 2, HSD17B10	0.711328304	1.712272579
52	HADHB	P55084	NP_000174.1	mitochondrial trifunctional protein, beta subunit precursor	0.435035831	1.700054616
53	MRPL16	Q9NX20	NP_060310.1	mitochondrial ribosomal protein L16	0	1.682695795
54	MRPL2	Q5T653	NP_057034.2	mitochondrial ribosomal protein L2	0	1.648969288
55	ATAD3A	Q8N275	NP_060658.2	ATPase family, AAA domain containing 3A	0.103715503	1.595886586
56	MRPS16	Q9Y3D3	NP_057149.1	mitochondrial ribosomal protein S16	0.311133937	1.58086154
57	MRPL18	Q9H0U6	NP_054880.2	mitochondrial ribosomal protein L18	0.110336318	1.565020906
58	MRPL19	P49406	NP_055578.2	mitochondrial ribosomal protein L19	0	1.543345761
59	MRPS27	Q92552	NP_055899.1	mitochondrial ribosomal protein S27	0.363375184	1.534230736
60	MRPL46	Q9H2W6	NP_071446.2	mitochondrial ribosomal protein L46	0	1.511886432
61	SLC25A11	Q02978	NP_003553.2	solute carrier family 25 (mitochondrial carrier; oxoglutarate carrier), member 11	0	1.511886432
62	SSBP1	Q04837	NP_003134.1	single-stranded DNA binding protein 1	0.668100537	1.448436747
63	SLC25A3	Q00325-2	NP_002626.1	solute carrier family 25 member 3 isoform b precursor	6.61E-02	1.448436747
64	MRPL37	Q9BZE1	NP_057575.2	mitochondrial ribosomal protein L37	0.142068906	1.424462017
65	MRPS18B	Q9Y676	NP_054765.1	mitochondrial ribosomal protein S18B	0	1.424462017
66	MRPL14	Q6P1L8	NP_115487.2	mitochondrial ribosomal protein L14	0.438449888	1.335721469
67	MRPL17	Q9NRX2	NP_071344.1	mitochondrial ribosomal protein L17	0.274274986	1.335721469
68	MRPL50	Q8N5N7	NP_061924.1	mitochondrial ribosomal protein L50	0.110336318	1.3101297

69	ICT1	Q14197	NP_001536.1	immature colon carcinoma transcript 1	0.221677349	1.227542952
70	TFAM	Q00059	NP_003192.1	transcription factor A, mitochondrial	0.304321387	1.218982341
71	MRPS2	Q9Y399	NP_057118.1	mitochondrial ribosomal protein S2	0	1.206734069
72	NDUFAF3	Q9BU61	NP_951032.1	NADH dehydrogenase [ubiquinone] 1 alpha subcomplex assembly factor 3	0	1.15443469
73	MRPL23	Q16540	NP_066957.2	mitochondrial ribosomal protein L23	0.467799268	1.15443469
74	GRPEL1	Q9HAV7	NP_079472.1	GrpE-like 1, mitochondrial	0.318256739	1.089296131
75	ATAD3B	Q5T9A4	NP_114127.3	AAA-ATPase TOB3	3.30E-02	1.041075901
76	MRPL13	Q9BYD1	NP_054797.2	mitochondrial ribosomal protein L13	0.42510267	1.030917621
77	MRPL54	Q6P161	NP_758455.1	mitochondrial ribosomal protein L54	0	1.030917621
78	MRPS28	Q9Y2Q9	NP_054737.1	mitochondrial ribosomal protein S28	0.492495545	1.015337686
79	SLC25A13	Q9UJS0	NP_055066.1	solute carrier family 25, member 13 (citrin)	0	0.96486779
80	IDH2	P48735	NP_002159.2	isocitrate dehydrogenase 2 (NADP+), mitochondrial precursor	0.042753889	0.953930405
81	MRPS10	P82664	NP_060611.2	mitochondrial ribosomal protein S10	0.279802214	0.930697729
82	NME4	O00746	NP_005000.1	nucleoside-diphosphate kinase 4	0	0.930697729
83	MRPL20	Q9BYC9	XP_001125910.1	mitochondrial ribosomal protein L20	0	0.930697729
84	MRPL38	B2R894	NP_115867.1	mitochondrial ribosomal protein L38	0.240937761	0.910952975
85	MRPS23	Q9Y3D9	NP_057154.2	mitochondrial ribosomal protein S23	0.445439771	0.905460718
86	NDUFS3	O75489	NP_004542.1	NADH dehydrogenase (ubiquinone) Fe-S protein 3, 30kDa	0.258925412	0.847849797
87	AFG3L2	Q9Y4W6	NP_006787.1	AFG3 ATPase family gene 3-like 2	2.62E-02	0.813121744
88	PGAM5	Q96HS1-2	NP_612642.1	Bcl-XL-binding protein v68	6.61E-02	0.77827941
89	DCI	P42126	NP_001910.2	dodecenoyl-Coenzyme A delta isomerase precursor	0	0.77827941
90	MRPL10	Q7Z7H8	NP_660298.2	mitochondrial ribosomal protein L10 isoform a	0	0.77827941
91	MRPL51	Q4U2R6	NP_057581.2	mitochondrial ribosomal protein L51	0	0.77827941
92	PHB2	Q99623	NP_009204.1	prohibitin 2	0.36887451	0.77827941
93	ACOT9		NP_001028755.2	acyl-Coenzyme A thioesterase 2, mitochondrial isoform b	0	0.760410844
94	MRPS30	Q9NP92	NP_057724.2	mitochondrial ribosomal protein S30	5.13E-02	0.734324802
95	MCCC2	Q9HCC0	NP_071415.1	methylcrotonoyl-Coenzyme A carboxylase 2 (beta)	3.98E-02	0.726983291
96	ACAD9	Q9H845	NP_054768.2	acyl-Coenzyme A dehydrogenase family, member 9	3.61E-02	0.70125428
97	DHX30	Q7L2E3	NP_619520.1	DEAH (Asp-Glu-Ala-His) box polypeptide 30 isoform 1	0.14504757	0.693394598
98	COX4I1	P13073	NP_001852.1	cytochrome c oxidase subunit IV isoform 1 precursor	0	0.687612476
99	MRPS18A	Q9NVS2	NP_060605.1	mitochondrial ribosomal protein S18A	0.110336318	0.687612476
100	ATP5H	O75947	NP_006347.1	ATP synthase, H+ transporting, mitochondrial F0 complex, subunit d isoform a	0.136463666	0.668100537
101	AIFM1	O95831	NP_004199.1	programmed cell death 8 isoform 1	0	0.668100537
102	MRPL3	P09001	NP_009139.1	mitochondrial ribosomal protein L3	5.78E-02	0.657723886
103	ATP5L	O75964	NP_006467.4	ATP synthase, H+ transporting, mitochondrial F0 complex, subunit G	0	0.637893707
104	PMPCB	O75439	NP_004270.2	mitochondrial processing peptidase beta subunit precursor	0	0.598467106
105	SLC25A10	Q9UBX3	NP_036272.2	solute carrier family 25 (mitochondrial carrier; dicarboxylate transporter)	0	0.561523006
106	DNAJA3	Q96EY1	NP_005138.2	DnaJ (Hsp40) homolog, subfamily A, member 3	0	0.557068405
107	MRPP1	Q9NRG5	NP_060289.2	Mitochondrial ribonuclease P protein 1, RG9MTD1	4.53E-02	0.557068405
108	TRUB2	O95900	NP_056494.1	TruB pseudouridine (psi) synthase homolog 2	0	0.545927736
109	YME1L1	Q96TA2	NP_647473.1	YME1-like 1 isoform 1	0	0.539926526
110	POLDIP2	Q9Y2S7	NP_056399.1	DNA polymerase delta interacting protein 2	0	0.519911083
111	LOC729317	A6NLE7	XP_001133585.1	PREDICTED: similar to voltage-dependent anion channel 2	0.149756995	0.519911083
112	ALDH18A1	P54886	NP_002851.2	pyrroline-5-carboxylate synthetase isoform 1	4.71E-02	0.513561248
113	TI21L	Q9BVV7	NP_054896.1	TIM21-like protein, mitochondrial	0	0.508590709
114	GBAS	O75323	NP_001474.1	nipsnap homolog 2	0.14504757	0.501310729
115	ATP5C1	P36542	NP_001001973.1	ATP synthase, H+ transporting, mitochondrial F1 complex, gamma subunit iso. L	8.26E-02	0.487352107
116	CCDC109A	Q8NE86	NP_612366.1	coiled-coil domain containing 109A	0	0.483981789
117	VDAC1	P21796	NP_003365.1	voltage-dependent anion channel 1 (porin)	0.218187912	0.483981789
118	SLC25A12	O75746	NP_003696.2	solute carrier family 25 (mitochondrial carrier, Aralar), member 12	0	0.467799268
119	NDUFS8	O00217	NP_002487.1	NADH dehydrogenase (ubiquinone) Fe-S protein 8, 23kDa	9.65E-02	0.445439771
120	MRPS11	P82912	NP_073750.2	mitochondrial ribosomal protein S11 isoform a	0	0.438449888
121	NIPSNAP1		NP_003625.1	nipsnap homolog 1	7.46E-02	0.43301257
122	SARS2	Q9NP81	NP_060297.1	seryl-tRNA synthetase 2	0	0.43301257
123	ERAL1	O75616	NP_005693.1	Era G-protein-like 1	0	0.42510267
124	C4orf14	Q8NC60	NP_115689.1	hypothetical protein LOC84273	2.75E-02	0.422136151
125	HARS2	P49590	NP_036340.1	histidyl-tRNA synthetase-like	0	0.420830833
126	ME2	P23368	NP_002387.1	malic enzyme 2, NAD(+)-dependent, mitochondrial	0	0.410112399
127	GTPBP10	A4D1E9	NP_149098.2	claudin 12 isoform 2	0	0.406527242
128	POLRMT	O00411	NP_005026.3	mitochondrial DNA-directed RNA polymerase precursor	1.62E-02	0.402339435
129	TIMM50	Q3ZCQ8-2	NP_001001563.1	translocase of inner mitochondrial membrane 50 homolog	0.18350673	0.400688179
130	PGAM5		XP_001126125.1	PREDICTED: similar to phosphoglycerate mutase family member 5	0.042753889	0.397830607
131	MCAT	Q8IVS2	NP_775738.3	mitochondrial malonyltransferase isoform a precursor	0	0.378906706
132	PHB	P35232	NP_002625.1	prohibitin	0	0.376857165
133	PNPT1	Q8TCS8	NP_149100.1	polyribonucleotide nucleotidyltransferase 1	8.26E-02	0.373823796
134	YARS2	Q9Y2Z4	NP_001035526.1	tyrosyl-tRNA synthetase 2 (mitochondrial)	0	0.355424938
135	GLUD1	P00367	NP_005262.1	glutamate dehydrogenase 1	0.14280206	0.350314038
136	PAPD1	Q9HA74	NP_060579.2	Poly(A) RNA polymerase (PAP) associated domain containing 1	0	0.350314038
137	SFXN1	Q9H9B4	NP_073591.2	sideroflexin 1	6.08E-02	0.343399333
138	DHX30	Q7L2E3-2	NP_619519.1	DEAH (Asp-Glu-Ala-His) box polypeptide 30 isoform 3	0	0.341712835
139	CLPX	O76031	NP_006651.2	ClpX caseinolytic protease X homolog	0	0.333521432
140	NSUN4	Q96CB9	NP_950245.2	NOL1/NOP2/Sun domain family 4 protein	0	0.333521432
141	METT11D1	Q9H7H0	NP_073571.1	methyltransferase 11 domain containing 1 isoform 2	0	0.325711366
142	TFB1M	Q9Y384	NP_057104.1	transcription factor B1, mitochondrial	0	0.324192792
143	DLD	B2R5X0	NP_000099.2	dihydrolipoamide dehydrogenase precursor	9.65E-02	0.318256739
144	MTERFD1	Q96E29	NP_057026.3	MTERF domain containing 1	0	0.30701048
145	PMPCA	Q10713	NP_055975.1	peptidase (mitochondrial processing) alpha	3.85E-02	0.302429122
146	PCCB	P05166	NP_000523.2	propionyl Coenzyme A carboxylase, beta	0	0.296890252

				polypeptide		
147	SHMT2	P34897	NP_005403.2	serine hydroxymethyltransferase 2 (mitochondrial)	3.78E-02	0.296890252
148	PTCD1	O75127	NP_056360.2	pentatricopeptide repeat domain 1	0	0.291549665
149	OXA1L	Q15070	NP_005006.1	oxidase (cytochrome c) assembly 1-like, mitochondrial inner membrane protein	0	0.282649831
150	VARS2	Q5ST30	NP_065175.3	valyl-tRNA synthetase 2-like	0	0.277011153
151	AARS2	A2RRN5	NP_065796.1	alanyl-tRNA synthetase like	0	0.275760733
152	SLC25A40	Q8TBP6	NP_061331.2	mitochondrial carrier family protein	0	0.274274986
153	MRS2	Q9HD23	NP_065713.1	MRS2-like, magnesium homeostasis factor	0	0.264855217
154	HK1	P19367	NP_000179.1	hexokinase 1 isoform HKI	0	0.261856883
155	DDX28	Q9NUL7	NP_060850.1	DEAD (Asp-Glu-Ala-Asp) box polypeptide 28	3.85E-02	0.254182266
156	ECSIT	Q9BQ95	NP_057665.2	evolutionarily conserved signaling intermediate in Toll pathway	0	0.253254336
157	C7orf30	Q96EH3	NP_612455.1	hypothetical protein LOC115416	0	0.249609141
158	LONP1	P36776	NP_004784.2	mitochondrial lon peptidase 1	7.71E-02	0.249609141
159	NDUFS2	O75306	NP_004541.1	NADH dehydrogenase (ubiquinone) Fe-S protein 2, 49kDa	0	0.242623672
160	RARS2	Q96FU5	NP_064716.1	arginyl-tRNA synthetase-like	0	0.236247035
161	NDUFA13	Q9P0J0	NP_057049.3	cell death-regulatory protein GRIM19	0	0.232846739
162	ECHS1	P30084	NP_004083.2	mitochondrial short-chain enoyl-coenzyme A hydratase 1 precursor	0	0.232846739
163	LOC648605		XP_944686.1	PREDICTED: similar to Trimethyllysine dioxygenase, mitochondrial precursor	0	0.232846739
164	IMMT		NP_006830.1	inner membrane protein, mitochondrial	2.62E-02	0.22995052
165	DBT	Q5VVL8	NP_001909.2	dihydrolipoamide branched chain transacylase precursor	4.20E-02	0.228247006
166	RNMTL1	Q9HC36	NP_060616.1	RNA methyltransferase like 1	0	0.226279857
167	RHOT2	Q8IXI1	NP_620124.1	ras homolog gene family, member T2	0	0.223824937
168	FASTKD2	Q9NYY8	NP_055744.2	FAST kinase domains 2	0	0.216483949
169	C3orf58	Q8NDZ4	NP_775823.1	hypothetical protein LOC205428	0	0.216483949
170	AGK	Q53H12	NP_060708.1	multiple substrate lipid kinase	5.02E-02	0.216483949
171	TARS2	Q9BW92	NP_079426.2	threonyl-tRNA synthetase-like 1	0	0.216483949
172	AASS	Q9UDR5	NP_005754.2	aminoadipate-semialdehyde synthase	0	0.209133425
173	NDUFS1	P28331	NP_004997.4	NADH dehydrogenase (ubiquinone) Fe-S protein 1, 75kDa precursor	0	0.208795797
174	SLC30A9	Q6PML9	NP_006336.3	solute carrier family 30 (zinc transporter), member 9	0	0.206792641
175	SLC25A18	Q9H1K4	NP_113669.1	solute carrier	0	0.205260937
176	SLC25A21	Q9BQT8	NP_085134.1	solute carrier family 25 (mitochondrial oxodicarboxylate carrier), member 21	0	0.205260937
177	ERLIN2	O94905	NP_009106.1	SPFH domain family, member 2 isoform 1	0	0.205260937
178	EFHA1	Q8IYU8	NP_689939.1	EF hand domain family, member A1	0	0.203764435
179	MTERF	Q99551	NP_008911.1	mitochondrial transcription termination factor precursor	0	0.197929811
180	ECH1	Q13011	NP_001389.2	peroxisomal enoyl-coenzyme A hydratase-like protein	0	0.193776642
181	CLPB	Q9H078	NP_110440.1	suppressor of potassium transport defect 3	0	0.193776642
182	ACSS1	Q9NUB1	NP_115890.2	acyl-CoA synthetase short-chain family member 1	0	0.190577239
183	ALDH1B1	Q8WX76	NP_000683.3	aldehyde dehydrogenase 1B1 precursor	4.44E-02	0.189793791
184	RPUSD3	Q6P087	NP_775930.1	RNA pseudouridylate synthase domain containing 3	0	0.188602527
185	GRSF1	Q12849-2	NP_002083.2	G-rich RNA sequence binding factor 1	0	0.185971012
186	FLAD1	Q8NFF5	NP_079483.3	flavin adenine dinucleotide synthetase isoform 1	0	0.181581733
187	PCCA	Q8WXQ7	NP_000273.2	propionyl-Coenzyme A carboxylase, alpha polypeptide precursor	0	0.180769016
188	CABC1	Q8NI60	NP_064632.2	chaperone, ABC1 activity of bc1 complex like precursor	0	0.178768635
189	LETM1	O95202	NP_036450.1	leucine zipper-EF-hand containing transmembrane protein 1	2.75E-02	0.176489987
190	KIAA0564	A3KMH1	NP_055873.1	hypothetical protein LOC23078 isoform a	5.95E-02	0.166663489
191	PUS1	Q9Y606	NP_079491.2	pseudouridylate synthase 1 isoform 1	0	0.165914401
192	PCK2	Q6IB91	NP_004554.2	mitochondrial phosphoenolpyruvate carboxykinase 2 isoform 1 precursor	0.030355309	0.161274969
193	DDOST	B2RDQ4	NP_005207.2	dolichyl-diphosphooligosaccharide-protein glycosyltransferase precursor	0	0.151295339
194	TBRG4	Q969Z0	NP_004740.2	cell cycle progression 2 protein isoform 1	0	0.147564722
195	AP2M1	Q96CW1	NP_004059.2	adaptor-related protein complex 2, mu 1 subunit isoform a	0	0.142058806
196	ALDH2	P05091	NP_000681.2	mitochondrial aldehyde dehydrogenase 2 precursor	0	0.139209961
197	GLDC	Q2M2F8	NP_000161.2	glycine dehydrogenase (decarboxylating)	0	0.137823152
198	RHOT1	Q8IXI2-3	NP_001028740.1	ras homolog gene family, member T1 isoform 1	0	0.132541315
199	PITRM1		NP_055704.2	metalloprotease 1	0	0.126481692
200	DNAJC11	Q9NVH1	NP_060668.1	DnaJ (Hsp40) homolog, subfamily C, member 11	0	0.124210035
201	MTIF2		NP_002444.2	mitochondrial translational initiation factor 2 precursor	0	0.122018454
202	MRPP3	O15091	NP_055487.2	Mitochondrial ribonuclease P protein 3, KIAA0391	0	0.110336318
203	LARS2	Q15031	NP_056155.1	leucyl-tRNA synthetase 2, mitochondrial precursor	0	0.106511785
204	FASTKD5	Q7L8L6	NP_068598.1	FAST kinase domains 5	0	0.100694171
205	FASTKD1	Q8TEA9	NP_078898.2	FAST kinase domains 1	0	0.099606032
206	NLRX1	Q86UT6	NP_078894.2	NLR family member X1 isoform 1	0	9.26E-02
207	SUPV3L1	Q8IYB8	NP_003162.2	suppressor of var1, 3-like 1	0	8.90E-02
208	GARS		NP_002038.2	glycyl-tRNA synthetase	0	8.68E-02
209	GCS1	Q13724	NP_006293.1	mannosyl-oligosaccharide glucosidase	0	7.89E-02
210	ALDH1L2	Q3SY69	NP_001029345.1	aldehyde dehydrogenase 1 family, member L2	0	7.58E-02
211	ELAC2	Q6IA94	NP_060597.3	elaC homolog 2	0	7.30E-02

Publications arising:

Mateusz Kolanczyk*, Markus Pech*, Tomasz Zemojte, Hiroshi Yamamoto, Ivan Mikula, Maria-Antonietta Calvaruso, Ricarda Richter, Björn Fischer, Anita Ritz, Nadine Kossler, Boris Thurisch, Ralf Spörle, Jan Smeitnik, Uwe Kornak, Danny Chan, Martin Vingron, Pawel Martasek, Robert N. Lightowlers, Leo Nijtmans, Markus Schülke-Gerstenfeld, Knud H. Nierhaus, Stefan Mundlos. (2011) NOA1 is an essential GTPase required for mitochondrial protein synthesis and apoptosis. *Molecular Biology of the Cell,* **22**(1):1-11 (*These authors contributed equally to this work.)

Ricarda Richter, Aleksandra Pajak, Sven Dennerlein, Agata Rozanska, Robert N. Lightowlers, and Zofia M. A. Chrzanowska-Lightowlers. (2010) Translation Termination in human mitochondrial ribosomes. *Biochem Soc Trans*, **38**(6):1523-1526

Ricarda Richter, Joanna Rorbach, Aleksandra Pajak, Hans J. Wessels, Martijn A. Huynen, Jan A. Smeitink, Robert N. Lightowlers, Zofia M. Chrzanowska-Lightowlers. (2010) A functional peptidyl-tRNA hydrolase, ICT1, has been recruited into the human mitochondrial ribosome. *The EMBO Journal* **29**(6):1116-25**

This publication was selected as the subject for "Did you see...?" commentary: Md Emdadul Haque, Linda L. Spremulli (2010) ICT1 comes to the rescue of mitochondrial ribosomes. *The EMBO Journal* **29(6)**:** 1019-1020

Richard Temperley*, Ricarda Richter*, Sven Dennerlein, Robert N. Lightowlers, Zofia M. Chrzanowska-Lightowlers. (2010) Hungry Codons Promote Frameshifting in Human Mitochondrial Ribosomes. *Science* **327**, p. 301 (* These authors contributed equally to this work.)

Joanna Rorbach, Ricarda Richter, Hans J. Wessels, Mateusz Wydro, Marcin Pekalski, Murtada Farhoud, Inge Kühl, Mauricette Gaisne, Nathalie Bonnefoy, Jan A. Smeitink, Robert N. Lightowlers, Zofia M.A. Chrzanowska-Lightowlers. (2008) The human mitochondrial ribosome recycling factor is essential for cell viability. *Nucleic Acids Research* **36**, 5787-99.

NOA1 is an essential GTPase required for mitochondrial protein synthesis

Mateusz Kolanczyk[a,b,*], Markus Pech[c,*], Tomasz Zemojtel[d], Hiroshi Yamamoto[c], Ivan Mikula[e], Maria-Antonietta Calvaruso[f], Mariël van den Brand[f], Ricarda Richter[g], Bjoern Fischer[a,b], Anita Ritz[a,b], Nadine Kossler[a,b], Boris Thurisch[a,b], Ralf Spoerle[h], Jan Smeitink[f], Uwe Kornak[a,b], Danny Chan[i], Martin Vingron[d], Pavel Martasek[e], Robert N. Lightowlers[g], Leo Nijtmans[f], Markus Schuelke[j], Knud H. Nierhaus[c], and Stefan Mundlos[a,b]

[a]Development & Disease Group, Max Planck Institute for Molecular Genetics, 14195 Berlin, Germany; [b]Institute for Medical Genetics, Charité University Medical Center, 13353 Berlin, Germany; [c]AG Ribosomen, Max Planck Institute for Molecular Genetics, 14195 Berlin, Germany; [d]Department of Computational Molecular Biology, Max Planck Institute for Molecular Genetics, 14195 Berlin, Germany; [e]Department of Pediatrics and Center for Applied Genomics, Ist Faculty of Medicine, Charles University, 12109 Prague, Czech Republic; [f]Nijmegen Centre for Mitochondrial Disorders at the Department of Pediatrics, Radboud University Nijmegen Medical Centre, Nijmegen, The Netherlands; [g]Mitochondrial Research Group, Institute for Ageing and Health, Newcastle University, Newcastle upon Tyne, United Kingdom NE2 4HH; [h]Department of Developmental Genetics, Max Planck Institute for Molecular Genetics, 14195 Berlin, Germany; [i]Department of Biochemistry, the University of Hong Kong, Hong Kong, China; [j]Department of Neuropediatrics and NeuroCure Clinical Research Center, Charité University Medical Center, 13353 Berlin, Germany

ABSTRACT **Nitric oxide associated-1 (NOA1) is an evolutionarily conserved guanosine triphosphate (GTP) binding protein that localizes predominantly to mitochondria in mammalian cells. On the basis of bioinformatic analysis, we predicted its possible involvement in ribosomal biogenesis, although this had not been supported by any experimental evidence. Here we determine NOA1 function through generation of knockout mice and in vitro assays. NOA1-deficient mice exhibit midgestation lethality associated with a severe developmental defect of the embryo and trophoblast. Primary embryonic fibroblasts isolated from NOA1 knockout embryos show deficient mitochondrial protein synthesis and a global defect of oxidative phosphorylation (OXPHOS). Additionally, *Noa1–/–* cells are impaired in staurosporine-induced apoptosis. The analysis of mitochondrial ribosomal subunits from *Noa1–/–* cells by sucrose gradient centrifugation and Western blotting showed anomalous sedimentation, consistent with a defect in mitochondrial ribosome assembly. Furthermore, in vitro experiments revealed that intrinsic NOA1 GTPase activity was stimulated by bacterial ribosomal constituents. Taken together, our data show that NOA1 is required for mitochondrial protein synthesis, likely due to its yet unidentified role in mitoribosomal biogenesis. Thus, NOA1 is required for such basal mitochondrial functions as adenosine triphosphate (ATP) synthesis and apoptosis.**

Monitoring Editor
M. Bishr Omary
University of Michigan

Received: Jul 28, 2010
Revised: Oct 27, 2010
Accepted: Nov 5, 2010

This article was published online ahead of print in MBoC in Press (http://www.molbiolcell.org/cgi/doi/10.1091/mbc.E10-07-0643) on November 30, 2010.

*These authors contributed equally to this paper.

The authors declare no competing financial interests.

Address correspondence to: Mateusz Kolanczyk (kolanshy@molgen.mpg.de) or Tomasz Zemojtel (zemojtel@molgen.mpg.de).

Abbreviations used: 3D, three dimensions; DAP3, death-associated protein 3; DAPI, 4′,6-diamidino-2-phenylindole; DNP, 2,4-dinitrophenol; dsRNA, double-stranded RNA; FBS, fetal bovine serum; GTP, guanosine triphosphate; MEF, mouse embryonic fibroblast; mtDNA, mitochondrial DNA; MuLV, murine leukemia virus; nDNA, nuclear DNA; NOA, nitric oxide associated; OPT, optical tomography; OXPHOS, oxidative phosphorylation; PBS, phosphate-buffered saline; PFA, paraformaldehyde; PMSF, phenylmethylsulfonyl fluoride; PVDF, polyvinylidene fluoride; qPCR, quantitative PCR; RIPA, radioimmunoprecipitation assay; siRNA, small interfering RNA; TCA, trichloroacetic acid; TEM, transmission electron microscopy; TGC, trophoblast giant cell; TRAFAC, translation factors.

INTRODUCTION

Mitochondria are the principal energy-producing organelles believed to have evolved from eubacteria that were engulfed by primordial eukaryotic cells (Gray *et al.*, 2001). In the course of evolution mitochondria retained rudimentary genomes, whereas most of the other necessary genetic information was relocated to the nucleus of the host cell. As a result, in mammalian cells only

13 proteins (all of which are translated by mitochondrial and not cytosolic ribosomes) are encoded by mitochondrial DNA (mtDNA). Mitochondrial ribosomes (mitoribosomes) are assembled from more than 70 nuclearly encoded proteins (at least 29 in the 28S small subunit and 48 in the 39S large subunit) and 2 species of mitochondrially encoded rRNA (Koc *et al.*, 2001). Relatively little is known about how these multiple components assemble into a catalytically active complex and what factors are required for completion of this process. We identified nitric oxide-associated-1 (NOA1) as a predominantly mitochondrially localized guanosine triphosphate (GTP) binding protein, homologous to the essential *Bacillus subtilis* GTPase, YqeH (Zemojtel *et al.*, 2006b). YqeH defines a subfamily of circularly permutated GTPases conserved in some species of bacteria and all known eukaryotic organisms (Leipe *et al.*, 2002). The protein belongs to a larger family of YlqF/YawG translation factors (TRAFAC), whose members, such as YlqF, have been implicated in ribosomal assembly in *B. subtilis* (Kim do *et al.*, 2008). Independent of homology to bacterial YqeH, a possible involvement of NOA1 in mitoribosome function has been implicated by data from the yeast protein interactome (Zemojtel *et al.*, 2006a). Here the NOA1 yeast homologue YOR205C was shown to be a part of a protein complex associated with the S5 protein of the small mitoribosomal subunit. YqeH has been suggested to participate in the biogenesis of the 30S ribosomal subunit and to assist in 50S ribosomal subunit assembly (Loh *et al.*, 2007; Uicker *et al.*, 2007). In a recent study, human NOA1 was shown to interact with complex I of the electron transport chain and with three mitoribosomal proteins, MRPL12, MRPS27, and MRPS29 (also known as death-associated protein 3 [DAP3]), indicating that NOA1 may interact with the mitoribosome (Tang *et al.*, 2009). To date, however, no experimental data were available to support a role for NOA1 in mitochondrial protein synthesis. Similarly, a physiological role of the protein in mammalian development was also unknown. Here we present a comprehensive analysis of the cellular and developmental role of mammalian NOA1. We show that NOA1 inactivation impairs mitochondrial protein synthesis and causes global defect of oxidative phosphorylation (OXPHOS), defective apoptosis, and midgestation lethality of knockout mice.

RESULTS

Noa1 gene inactivation results in midgestation lethality

To experimentally address the function of NOA1 in a physiological in vivo context, we generated mice in which *Noa1* was inactivated (Figure 1). Mutant embryos appeared growth retarded and at E9.5 a maximum of nine somites was observed (Figure 1, E–G, and Figure 2A). At E10.5 many embryos were necrotic, and no viable *Noa1–/–*embryos were detected thereafter, indicating midgestation lethality (Table 1). Cell proliferation as measured by bromodeoxyuridine (BrdU) incorporation was drastically reduced in E9.5 *Noa1–/–* embryos (Figure 2A), and few areas of apoptotic cell death were observed (Figure 2, B and C), indicating that cell proliferation as well as apoptosis was severely impaired. Transmission electron microscopy (TEM) of *Noa1–/–* embryos revealed abnormal mitochondria with characteristically swollen cristae (Figure 2D) but no abnormalities in other organelles. In addition, we observed severe defects of the placenta with a reduction of all three trophoblast layers, including the trophoblast giant cell (TGC) layer (Figure 3, Supplemental Figure S1). This finding was in line with *Noa1* being expressed in the trophoblast but not in the maternal part of the placenta (Figure 3A). Together these results indicated that *Noa1* is indispensable for normal development of the embryo and the placenta possibly due to an important function in mitochondria.

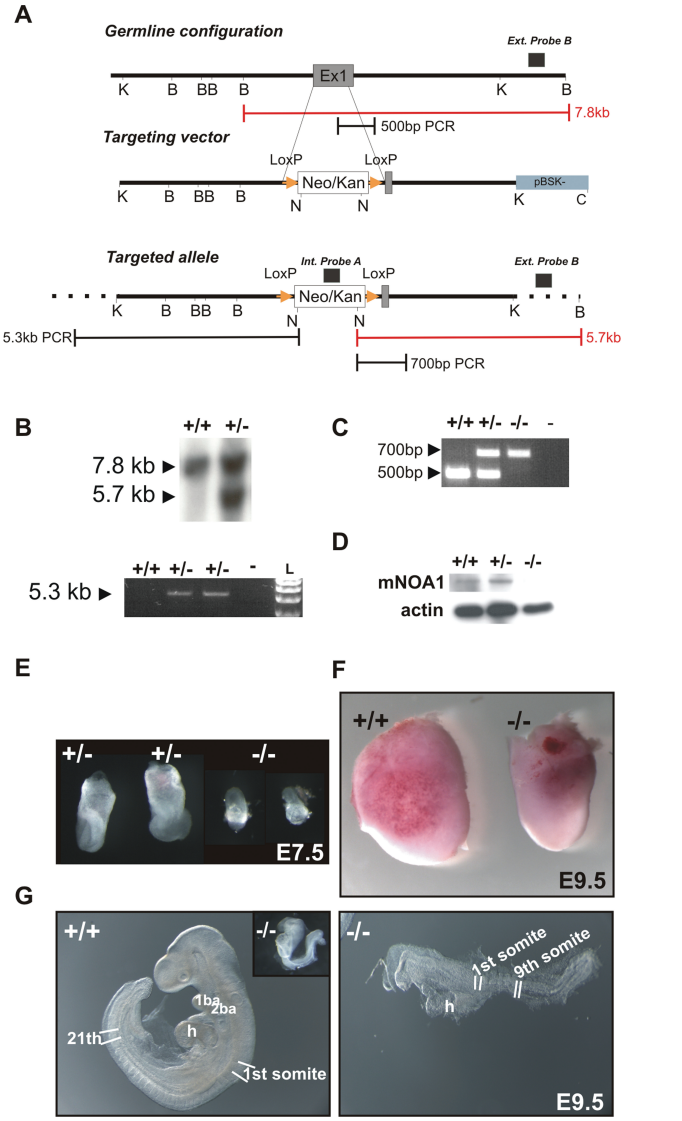

FIGURE 1: Generation of the *Noa1* knockout mice. (A) Strategy of *Noa1* gene targeting. The top bar indicates the enzymatic cleavage sites at the *Noa1* genomic locus (*Bam*HI), K (*Kpn*I), N (*Not*I), and C (*Cla*I). GTPase domain encoding Exon1 (dark grey segment) was targeted. Homologous recombination using this construct (middle bar) resulted in a targeted allele (bottom bar) where a large part of exon1 was replaced by the *loxP* flanked, PGK-gb2 promoter driven, neomycin/kanamycin resistance cassette (white segment – Neo/Kan; yellow triangles – *loxP* sites). Insertion of the selection cassette introduced a *Not*I endonuclease recognition site enabling Southern blot–based detection of homologous recombination with the internal and external probes (black boxes above the panels). Red rulers indicate expected *Bam*HI/*Not*I fragment sizes for the wild-type locus as well as the altered fragment size in the homologously targeted locus. Black rulers indicate lengths of the long-range PCR products obtained from the wild type and homologously targeted locus. (B) Southern blot and long-range-PCR–based detection of the homologous recombination. (C) PCR-based genotyping strategy. (D) Western blot analyses of E9.5 wild type, *Noa+/–*, and *Noa1–/–* embryo lysates with β-actin as loading control. (E) Appearance of *Noa1* knockout embryos at E7.5. (F) A comparison of the intact embryos at E9.5 is shown to illustrate the difference in size. (G) *Noa1* knockout embryo development is arrested at prerotation stage (inset). E9.5 wild-type embryo displays 21 somites whereas NOA1-deficient littermate (magnified) reaches maximally a 9-somite stage. See also Supplemental Movies S1 and S2 available online.

Stage	Litters	*Noa1*+/+	*Noa1*+/–	*Noa1*–/–	Total
E7.5	2	2 (10%)	13 (65%)	5 (25%)	20
E8.5	7	14 (25%)	32 (58%)	9 (16%)	55
E9.5	16	21 (17%)	80 (66%)	20 (17.0%)	121
E10.5	5	6 (17%)	22 (61%)	8 (22%)	36
E14.5	1	2 (33.3%)	4 (66.6%)	0	6
E15.5	6	16 (31%)	36 (69%)	0	52
E16.5	2	5 (33.3%)	10 (66.6%)	0	15
P1	5	9 (25%)	27 (75%)	0	36
P28	11	32 (38%)	52 (62%)	0	84

TABLE 1: Intercross of *Noa1*+/– mice – offspring genotype distribution. Knockout embryos could not be detected beyond E10.5, indicating midgestation lethality. Heterozygous animals were born in the expected Mendelian ratio. No overt lethality of heterozygotes was observed in the postnatal period.

Global OXPHOS defect in the *Noa1–/–* cells

To gain further information on the biochemical consequences of *Noa1* inactivation we isolated primary embryonic fibroblasts from E9.5 *Noa1–/–* embryos. *Noa1*-deficient cells grew in a medium known to compensate for mitochondrial respiratory deficiency and showed no overt abnormalities in the mitochondrial network (Supplemental Figure S3A). To test mitochondrial function we measured cellular respiration by polarographic assays in digitonin-permeabilized cells. Complex I–, III–, and IV–dependent oxygen consumption was severely reduced in mutant cells (Figure 4A), indicating a global OXPHOS defect. Consequently, *Noa1* knockout cells showed reduced viability and cellular ATP content when grown under nutrient restriction (Figure 4, B and C). Similar results were obtained after *NOA1* depletion in HeLa cells (Supplemental Figure S2).

Because the results of polarographic measurements are influenced by mitochondrial substrate import, we further addressed OXPHOS complex function in direct biochemical assays. Spectroscopic assays revealed that the activity of complexes I, III, IV, and V was strongly reduced in *Noa1–/–* cells, whereas the activity of complex II was increased (Figure 4D). Blue-native electrophoresis of isolated mitochondria showed a decreased amount of assembled complex I, III, IV, and V (Figure 4E) and an accumulation of the unassembled complex V (F1), whereas no free F1 subunit was detected in wild-type cells. Confirmatory to this, in-gel activity of complex I measured by the colorimetric enzymatic assay (immunoglobulin E [IgE]) was also strongly reduced (Figure 4E, top stripe). These findings suggested a general defect of mitochondrial protein synthesis in *Noa1–/–* cells, as complex I, III, IV, and V all include proteins encoded by the mtDNA, whereas all proteins of complex II are encoded in the nucleus and imported into the mitochondrium.

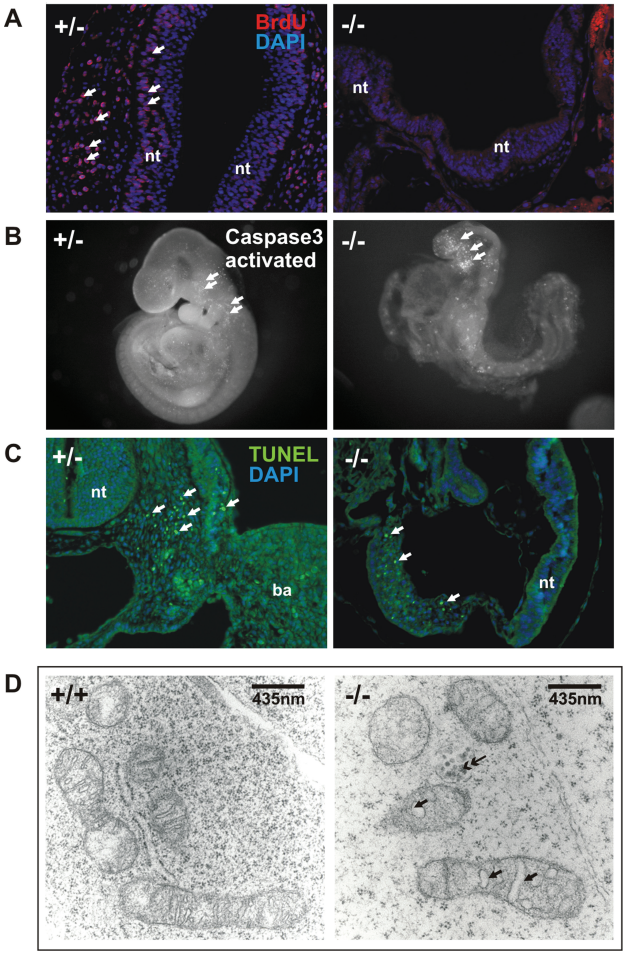

FIGURE 2: Phenotype of *Noa1* knockout mice. (A) BrdU in-vivo labeling reveals arrest of proliferation in the E9.5 *Noa–/–* embryos. (B and C) Apoptosis in the E9.5 *Noa1–/–* embryos visualized by anti-activated caspase-3 immunolabeling in the whole mount preparations (B) and TUNEL staining on paraffin sections (C). Data are representative of at least three embryos analyzed for each genotype. (D) Electron microscopic analysis of the *Noa1–/–* embryos. Many mitochondria show aberrant morphology characterized by swollen intracristal spaces (single-headed arrows). Some appear collapsed into electron dense, shrunken remnants (double-headed arrow). Endoplasmic reticulum and other organelles appear normal in *Noa1–/–* embryos (data not shown). ba – branchial arche, h – heart, nt – neural tube.

Compromised mitochondrial protein synthesis in Noa1–/– cells

To test this possibility, *Noa1–/–* cells were assayed for mitochondrial protein synthesis. Radioactive methionine labeling showed a deficiency in de novo mitochondrial protein synthesis (Figure 5A). Normal copy number and integrity of mtDNA were confirmed by quantitative PCR (qPCR) and long-range PCR, excluding defects of replication and/or mtDNA repair as a cause of compromised protein synthesis (Supplemental Figure S3, B and C). Expression of genes encoding proteins of the electron transport chain or mitoribosomal function was increased in the mutant cells, indicating that mtDNA transcription in the knockout cells was maintained, increased expression likely being compensatory to the protein synthesis defect (Figure 5B). Interestingly, 16S rRNA transcript level from the large ribosomal subunit was increased twofold in mutant cells whereas 12S rRNA remained at the control level indicative of a possible defect of mitoribosome biogenesis (Uicker *et al.*, 2007). These results are consistent with NOA1 being required for mitochondrial protein synthesis.

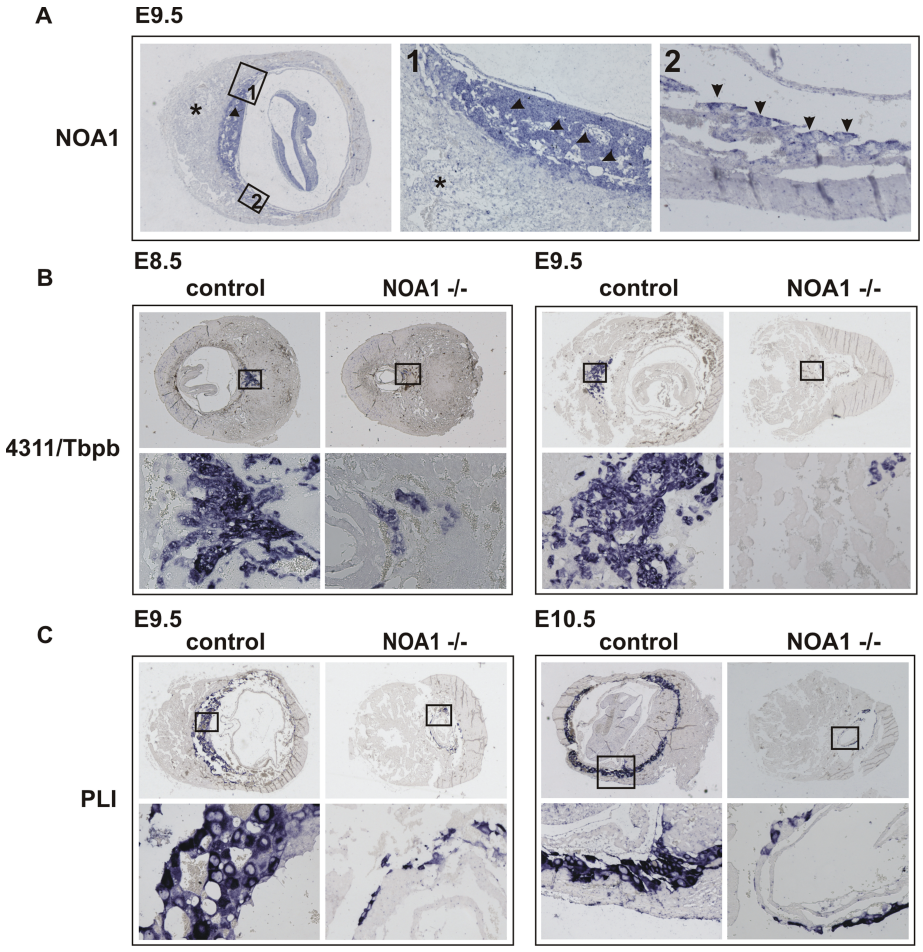

FIGURE 3: *Noa1* is indispensable for placental trophoblast development. In situ hybridization on the sections of E8.5, E9.5, and E10.5 wild type and mutant littermate embryos at the implantation sites. Boxed areas in the top panels are enlarged in bottom panels. (A) *Noa1* expression is restricted to the placental trophoblast at E9.5 (arrow). Intense expression in the labyrinth and spongiotrophoblast (arrowheads – magnification 1×) and in the trophoblast giant cells (arrows – magnification 2×). *Noa1* expression could not be detected in the maternal part of the placenta (star) or in the knockout embryos (data not shown). (B) Defect of the trophoblast progenitor cell differentiation in the *Noa1–/–* mice. 4311/Tbpb is expressed in the trophoblast progenitor cells which give rise to glycogen cells and secondary giant trophoblast cells. Diminished 4311/Tbpb expression in the E8.5, E9.5 ectoplacental cone. (C) Defect of trophoblast giant cell differentiation in E9.5 and 10.5 *Noa1–/–* embryos visualized by diminished expression of placental lactogen I (PLI).

Altered mitoribosomal profile in the *Noa1–/–* cells

Protein synthesis within mitochondria is performed by 55S mitoribosomes, each of which consists of a small 28S subunit and a large 39S subunit. To determine whether the observed mitochondrial protein synthesis defect was due to a ribosomal dysfunction, we compared the mitoribosome sucrose density profiles of wild type or rescued cells and those lacking *Noa1*. The small subunit was traced with antibodies against the mitochondrial protein S18b (MRPS18b), which consistently revealed a similar profile between wild type (NOA1+/+) and knockout cells (NOA1–/–). Similar levels of the 28S small subunit were found in fractions 4 and 5 in the wild type, knockout (NOA1–/–), and complemented cells (NOA1–/– Comp.), but no 55S ribosomes could be visualized (Figure 5C, fractions 8–10). Antibodies against the mitochondrial protein L12 (MRPL12), which reacted with the large 39S subunit (fractions 6 and 7), revealed the decrease in 55S ribosomes in the NOA1–/– cell line (fractions 8–10). Furthermore, although *Noa1* deficiency had only a minimal effect on the position or band intensity of the small subunit in the sucrose gradient (Figure 4C, bottom panels), the large subunits showed a marked shift to the slower migrating particles (lane 5, NOA1–/– *cf.* NOA1+/+); these effects were rescued by adding *Noa1* in trans (NOA1–/– comp. in Figure 5C). Additionally, NOA1 complementation led to increased abundance of L12 protein in fractions 9 and 10. In line with the observed partial rescue of mitoribosomal assembly, retroviral complementation resulted in reactivation of mitochondrial protein synthesis, normalization of respiratory chain complex assembly, and improved viability of the knockout cells (Supplemental Figure S4). These data strongly suggest that inactivation of *Noa1* resulted in an impaired assembly of the 55S mitoribosome.

The GTPase activities of mammalian NOA1 and its bacterial homologue YqeH are stimulated by ribosomal components from *Escherichia coli*

To gain further insight into NOA1 function, we purified mammalian NOA1 as well as its bacterial homologue YqeH from *B. subtilis*. Both mitochondrial NOA1 and bacterial YqeH showed a high and comparably strong intrinsic GTPase activity (Figure 6A). This observation was not made with other G-factors involved in translation, such as elongation factor G (EF-G), which can be stimulated exclusively by 70S ribosomes during protein synthesis and is boosted by empty 70S uncoupled from protein synthesis (Gordon, 1970; Qin *et al.*, 2006). In line with a previously proposed role in 30S assembly, YqeH GTPase activity could be stimulated by *E. coli* 16S rRNA, more than twofold, whereas the addition of 23S rRNA had no effect (Figure 6B), similar to poly(U) addition (data not shown).

In addition, 21S precursor particles of the 30S subunit stimulated the YqeH GTPase activity rather than mature 30S and 50S subunits or 70S ribosomes (Figure 6C). In contrast, NOA1 activity was stimulated by rRNAs of the small and large ribosomal subunits from both mammalian (human) mitochondria (12S and 16S rRNAs) and *E. coli* (16S and 23S rRNAs) by 40% (Figure 6D). Precursor of the 30S *E. coli* ribosome, the 21S particle prepared by total reconstitution (Nierhaus, 1990), stimulated NOA1 activity with approximately the same intensity (Figure 6E). Total reconstituted 30S particles as well as native 30S subunits induced a striking twofold increase of GTPase activity. Interestingly, the strongest effect was observed with 50S particles, whereas 70S ribosomes showed four times less stimulation underlining the specificity of the observed effects. These results suggest an involvement of both bacterial YqeH and mammalian NOA1 in ribosomal biogenesis.

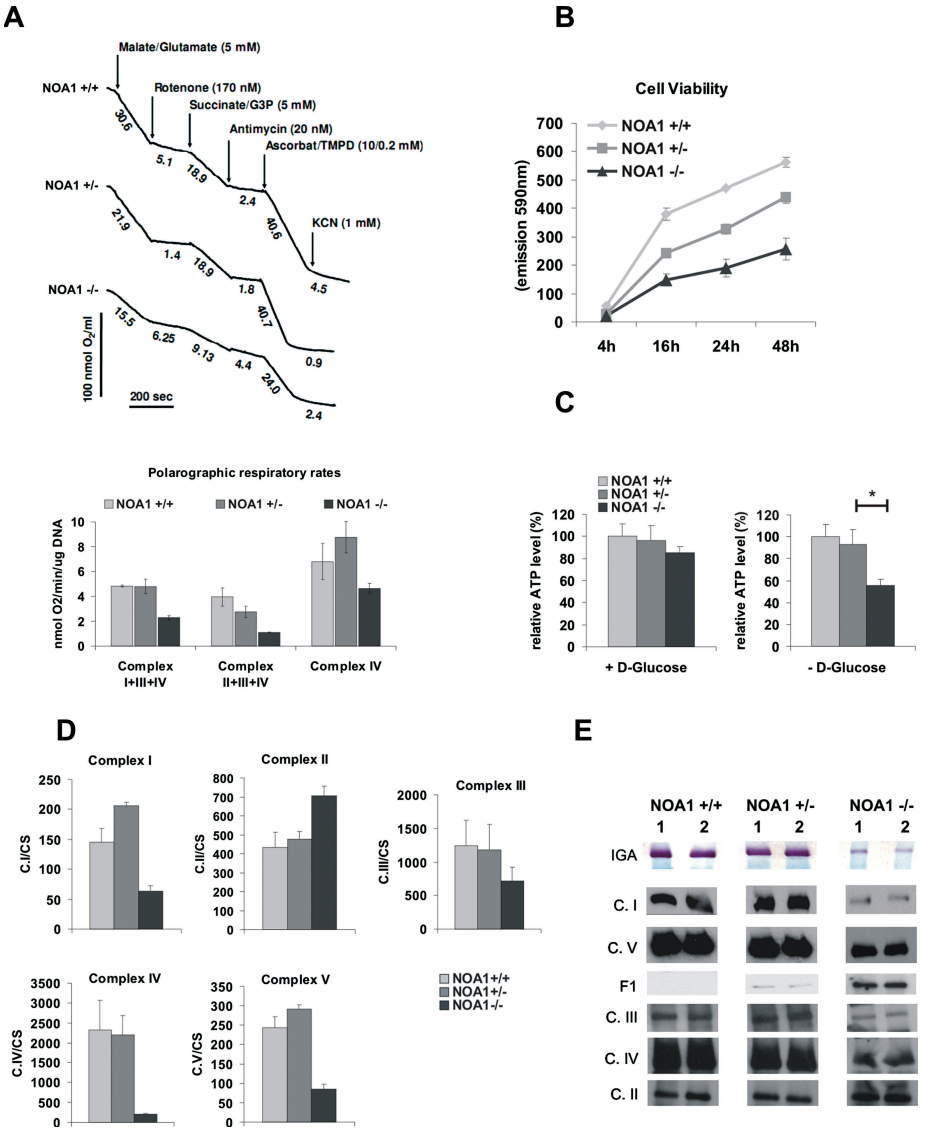

FIGURE 4: OXPHOS deficiency in *Noa1–/–* cells. (A) Cells were permeabilized with digitonin, and oxygen consumption was monitored polarographically in the presence of respiratory chain substrates and inhibitors. Note a marked decrease of the complex I–, III–, and IV–dependent oxygen consumption but not complex II–dependent oxygen consumption. Results represent mean ± SD of three independent experiments. (B) Reduced viability of the NOA1-deficient cells was determined with Alamarblue. (C) *Noa1–/–* cells show reduced ATP levels upon glucose deprivation. See also Supplemental Figure S6 for genetic complementation data. (D) Reduced enzymatic activities of the mitochondrial complexes I, III, IV, and V in the knockout cells. In contrast, complex II activity was increased. The enzymatic assay values are shown standardized to CS E3 activity. Results represent mean ± SD of three independent experiments. (E) In-gel activity (IGA) of complex I is decreased in knockout cells. Blue native electrophoresis (BN) showing reduction in quantities of the assembled complexes I, III, IV, and V and accumulation of the unassembled complex V intermediate (F1) in the homozygous *Noa1* mutant cells.

Noa1–/– cells are resistant to staurosporine-induced apoptosis

NOA1 was previously reported to be involved in regulation of apoptosis in HeLa cells (Tang *et al.*, 2009). To verify whether the mitochondrial defects in NOA1-deficient cells would also be accompanied by the impairment of apoptosis, embryonic fibroblasts were treated with staurosporine and apoptosis was monitored by accumulation of the cleaved caspase-3. A robust caspase-3 activation was detected 24 h postinduction in the control cells but was entirely absent in the mutant cells (Figure 7). Retroviral reconstitution of NOA1 expression partially restored caspase-3 activation in *Noa1–/–* cells (Supplemental Figure S4E). Additionally, mitochondrial membrane potential determined with JC-1 staining was increased in knockout cells corroborating the observed apoptosis defect (Supplemental Figure S4F). Thus, NOA1 is necessary for activation of caspase-dependent apoptosis.

DISCUSSION

In the current study we address both the cellular and the developmental function of NOA1 by inactivating the gene in mice. The vital role of *Noa1* was underlined by a massively restricted growth and arrested proliferation at ~E9.5 followed by the death of *Noa1–/–* mice at ~E10.5 (Table 1 and Figures 1 and 2A). The mitochondria in these developing embryos showed aberrations of cristae morphology, whereas other organelles appeared not to be affected (Figure 2D). Thus, both the timing of the lethality as well as the results of electron microscopic analysis reflect the important mitochondrial function of NOA1. Interestingly, the developmental defect extended to the placental trophoblast, which constitutes the interface between maternal and embryonic circulation (Figure 3B, Supplemental Figure 1) (Red-Horse *et al.*, 2004). The defect occurs at a relatively early stage of trophoblast differentiation as revealed by the diminished expression of 4311/Tbpb, demarcating the population of trophoblast progenitor cells at E8.5. The dependence of trophoblast development on NOA1 function exposes a crucial role of mitochondria in the development of the maternal–fetal interface. The importance of mitochondrial function in this process is further supported by the observation that knockouts of mitochondrial fusion factor Mtf2 as well as of mito-division factor Drp1 result in a deficiency of trophoblast giant cells (Chen *et al.*, 2003; Wakabayashi *et al.*, 2009).

The nature of NOA1 mitochondrial function was investigated in primary knockout mouse embryonic fibroblast (MEF) cells. *Noa1–/–* cells were shown to have impaired activities of the electron transfer chain complexes I, III, IV, and V but not of complex II, which lends strong support to NOA1 being required for expression of the mitochondrial genome. We therefore analyzed all stages of mtDNA expression and determined that NOA1 deficiency impairs protein synthesis but does not cause loss of mtDNA and/or transcription. Thus, NOA1 appears to be specifically required for mitochondrial protein synthesis. Sucrose gradient centrifugation and Western blot experiments revealed that knockout cells exhibit an aberrant migration of the large mitoribosomal subunit, indicating that NOA1 is required for correct mitoribosome assembly (Figure 5D). Involvement of NOA1 in the biogenesis of the small mitoribosomal subunit cannot be ruled out at present,

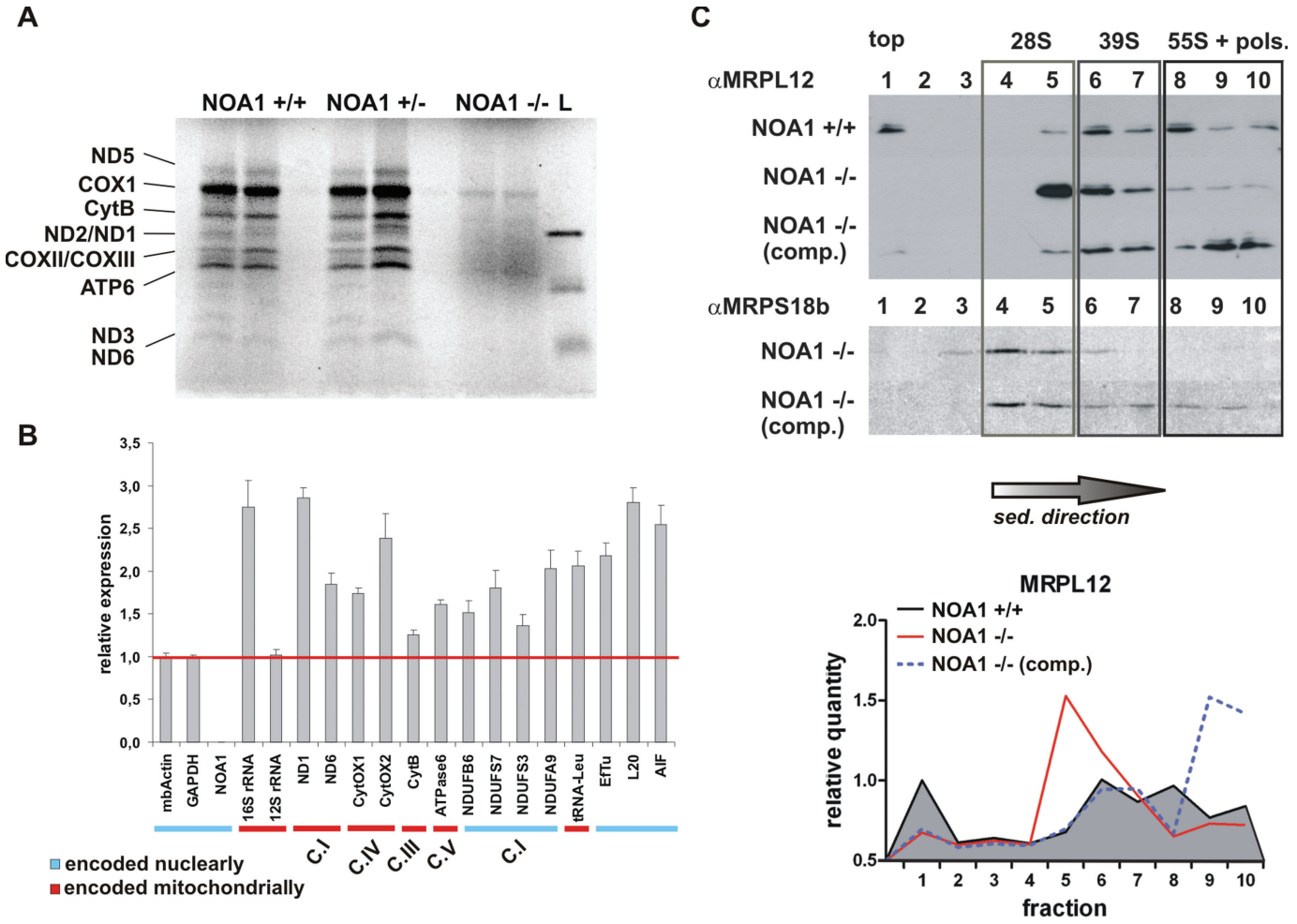

FIGURE 5: NOA1 deficiency impairs mitochondrial protein synthesis. (A) [^{35}S]methionine labeling of mitochondrial protein synthesis in primary embryonic fibroblasts reveals deficient translation in NOA1 knockout cells. Concentrations of protein lysates were calculated by the bicinchoninic acid (BCA) method, and equal loading was confirmed by Coomassie staining following exposure (data not shown). (B) Real-time PCR quantification of the mitochondrial gene transcript levels. RNA species encoded by mitochondrial (underlined red) and nuclear (underlined blue) DNA were quantified. Data were normalized against glyceraldehyde-3-phosphate dehydrogenase (GAPDH) and actin expression. (C) Cell lysates were fractionated in the 10–30% (vol/vol) isokinetic sucrose gradients and analyzed by Western blots with antibodies against MRPL12 (39S mitoribosomal subunit) or MRPS18b (28S mitoribosomal subunit). Representative blots were analyzed densitometrically (bottom panel). See also Supplemental Figure S4 for genetic complementation data. comp. – knockout cells with retroviral complementation of NOA1 expression.

however. In this study our choice of antibodies against mouse small mitoribosomal subunit was limited to anti-MRPS18b, which did not show any defect. Several other commercially available anti-MRP antibodies were tested, but none were capable of cross-reactivity with murine MRPs (data not shown).

Our knowledge about mitochondrial ribosome biogenesis and function is essentially based on the studies of bacterial and yeast model systems. Ribosome assembly comprises the processing and folding of pre-RNA and its concomitant assembly with ribosomal proteins. A large number of ribosomal constituents as well as non-ribosomal factors are involved. Among these factors, the GTPases (a family of energy-consuming enzymes characterized by the so-called G-domain) have been shown to play key roles in the assembly of ribosomes in bacteria (Karbstein, 2007; Britton, 2009). As shown here, mitochondrial NOA1, similarly to its bacterial homologue YqeH, has GTPase activity. The intrinsic GTPase activity of the *B. subtilis* YqeH is strongly and specifically stimulated by 16S rRNA of the small subunit from *E. coli* as well as by the 21S reconstitution intermediate of the small subunit, which is highly similar to the native 21S precursor particle (for a review, see Nierhaus, 1991). The strong stimulation contrasts with the effects of 23S rRNA and the mature ribosomal subunits, which did not stimulate the intrinsic activity of YqeH. This finding supports the notion that the major activity of the bacterial YqeH is related to the early assembly phase of the small subunit. Interestingly, mammalian NOA1 was stimulated both by the bacterial 50S large ribosomal subunit and by the 30S small subunit. To a lesser degree, NOA1 was also stimulated by naked rRNAs and precursor 21S particles, whereas only residual stimulation was observed with full 70S ribosomes. These data show that NOA1, like its bacterial homologue YqeH, has GTPase activity that is stimulated by the bacterial ribosomal constituents. The apparent difference in NOA1 and YqeH specificity likely reflects their evolutionary divergence. Indeed, NOA1 contains an ~100-amino-acid insertion in the GTP-binding domain, which is absent from bacterial YqeH and *Arabidopsis* NOA1 proteins. The latter could explain the differences in protein

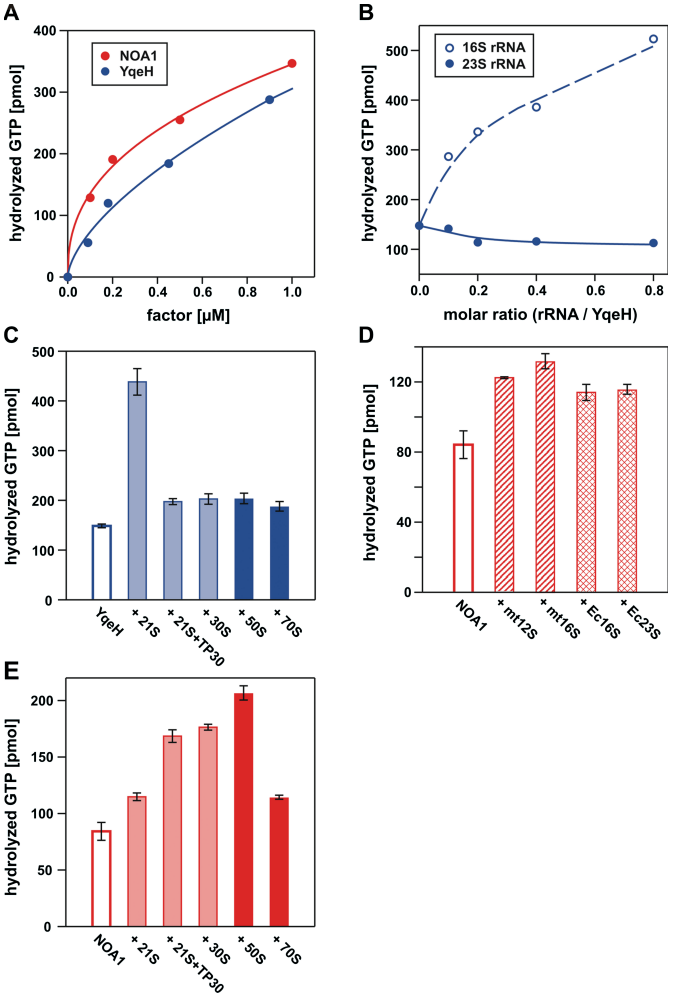

FIGURE 6: GTPase activities of NOA1 and YqeH are differently stimulated by ribosomal components from *E. coli*. (A) Intrinsic GTPase activities of NOA1 and YqeH at 30°C. (B) Specific stimulation of YqeH GTPase activity by *E. coli* 16S rRNA at 30°C. (C) Specific stimulation of YqeH GTPase by equimolar amounts of *E. coli* 30S precursors (21S) in comparison to total reconstituted 30S subunits (21S+TP30), ribosomal subunits (30S, 50S), and 70S ribosomes at 20°C. (D) Stimulation of NOA1 GTPase by equimolar amounts of mitochondrial rRNA (mt12S, mt16S) and *E. coli* rRNA (Ec16S, Ec23S) at 20°C. (E) Stimulation of NOA1 GTPase by equimolar amounts of *E. coli* 30S precursors before (21S) and after total reconstitution of 30S particles (21S+TP30), ribosomal subunits (30S, 50S), and 70S ribosomes at 20°C.

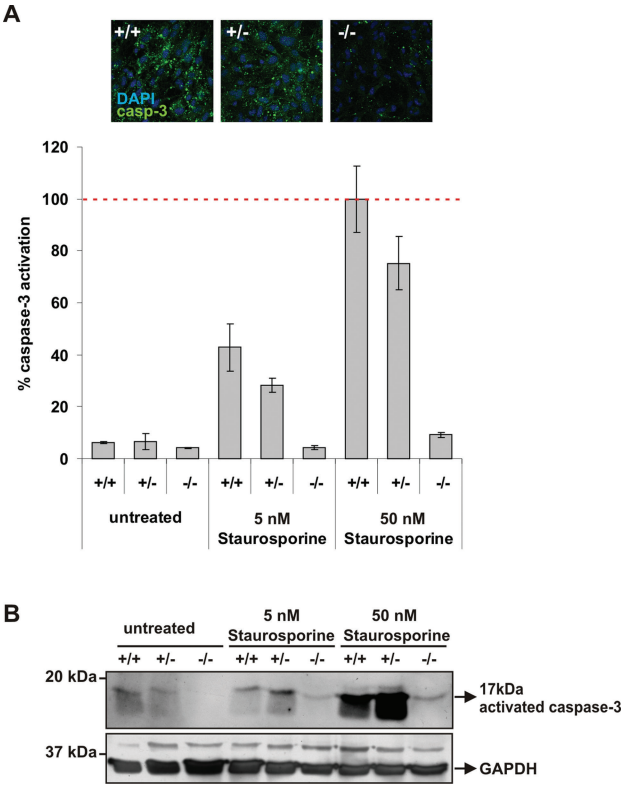

FIGURE 7: *Noa1*-deficient cells are resistant to staurosporine-induced apoptosis. Embryonic fibroblasts were cultured on coverslips in the presence of increasing concentrations of staurosporine. Apoptosis was monitored by measuring activation of the caspase-3. (A) The caspase-3–positive area was quantified using ImageJ software and corrected for the cell number. Representative microscopic pictures are shown (data represent mean of at least 10 evaluated images with SEM as error bars). (B) Western blot with anti-activated caspase-3 antibodies. Blots were stripped and probed with the antibody against GAPDH for loading control.

target recognition (Zemojtel *et al.*, 2004). These data, together with the observed aberrant migration of the large ribosomal subunit in the *Noa1* knockout cells, further suggest a possible involvement of NOA1 in the mitoribosome biogenesis.

Several proteins involved in mitochondrial protein synthesis have been shown to be involved in the process of apoptosis. Among them were mitoribosomal GTP-binding protein MRPS29/DAP3 (death-associated protein 3), MRPS30/PDCD9 or p52 (programmed cell death protein 9), and a protein with an apparent dual cell protective as well as pro-apoptotic function PDCD8/AIF (apoptosis-inducing factor) (Cavdar Koc *et al.*, 2001; O'Brien, 2002; Cheung *et al.*, 2006). Interestingly, DAP3 was among several ribosomal proteins recently shown to interact with NOA1 (Tang *et al.*, 2009).

Similarly to DAP3, NOA1 appears to be necessary for mitochondria-dependent apoptosis. The primary fibroblasts isolated from the knockout embryos were impaired in staurosporine-induced apoptosis (Figure 7A), and retroviral complementation partially reversed this phenotype (Supplemental Figure S4E). Importantly, NOA1 inactivation results in hyperpolarization of mitochondria, which likely contributes to the phenotype of defective apoptosis (Supplemental Figure S4F). In line with that, NOA1 knockdown in neuroblastoma cells was reported to result in mitochondrial hyperpolarization, preventing cytochrome *c* release (Parihar *et al.*, 2008). Thus, although the exact molecular mechanism remains to be discovered, it is increasingly clear that a group of mitoribosome-associated proteins, including NOA1, is required for the execution of programmed cell death.

Interestingly, NOA1 appears to play a similar role in plants, as *Arabidopsis* NOA1 (formerly atNOS1 [*Arabidopsis thaliana* nitric oxide synthase 1]) was shown to localize to plastids, where it is necessary for protein synthesis (Flores-Perez *et al.*, 2008). Similarly, plastidial NOA1 localization was shown in the phytoplankton diatom *Phaeodactylum tricornutum* (Vardi *et al.*, 2008). Remarkably, deficient growth and the greening phenotype of atNOA1-deficient plants could be complemented by *B. subtilis* YqeH fused to the *Arabidopsis* NOA1 organelle localization sequence (Flores-Perez *et al.*, 2008), clearly demonstrating that YqeH is a functional orthologue of plastid-localizing atNOA1. Like mitochondria, plastids are believed to have originated from

eubacterial endosymbionts. Thus mammalian NOA1 is an evolutionarily extremely conserved GTPase, required for protein synthesis in prokaryote-derived organelles. Further investigation into NOA1 structure and function is needed to unravel the exact mechanisms of its function in relation to mitoribosome and apoptotic action. The *Noa1* inactivation in mouse, however, demonstrates that this gene product plays a vital role in mitochondrial homeostasis and mammalian development.

MATERIALS AND METHODS

Tissue isolation and processing

BrdU solution (10 µl of 10 mM solution/1 g of mouse body weight) was injected intraperitoneally into pregnant mice 1 h before the mice were killed. Embryos were dissected from deciduas using an inverted microscope (Leica, Wetzlar, Germany). Whole embryos were photographed in phosphate-buffered saline (PBS) using a microscope-mounted digital camera (Leica, Germany). Embryonic stages were estimated by timed pregnancies and somite counts. The embryos were fixed in 4% paraformaldehyde (PFA) pH 7.4, dehydrated in ethanol, and paraffin embedded. The specimens were sectioned at 6 µm, stained with hematoxylin–eosin or processed for immunohistochemical staining.

MEF culture

Eviscerated embryos were collected in U-bottomed 96-well plates, cut into small fragments with dissection forceps, and digested in 25-µl of cell culture grade, 0.5% wt/vol trypsin at 37°C for 20 min. Subsequently, they were dispersed by pipetting and plated into one well of the 96-well, flat-bottomed plate in 200 µl of fresh DMEM containing glucose at 1 g/l, 10% fetal bovine serum (FBS), 2% penicillin/streptomycin, L-uridine at 50 µg/ml (Sigma, St. Louis, MO), 0.1 mM nonessential amino acids (Invitrogen, Carlsbad, CA), 1 mM sodium pyruvate (Sigma), and 10% Amniomax C-100 supplement (Invitrogen). The medium was changed every second day until cells reached confluence. Cells were subsequently expanded and continuously passaged until spontaneously immortalized colonies were derived. Cells were cultured at 37°C in 95% air / 5% CO_2.

Retroviral infection

BOSC23 packaging cells were transiently transfected with a retroviral vector expressing mouse *Noa1* (pQCXIP-mNOA1) using the CalPhos Mammalian Transfection Kit (Clontech Laboratories, Mountain View, CA). Retroviral stocks were collected 48 h post-transfection. *Noa1*-deficient MEFs were infected with the retrovirus in the presence of 6 µg of polybrene and selected for 4 days with puromycin at 2.5 µg/ml.

Immunofluorescence

For BrdU detection, sections were pretreated by 2N HCl treatment and incubated with a monoclonal antibody against BrdU (1:50; Roche Diagnostics, Indianapolis, IN). Apoptotic cell death was visualized in the whole mount specimens with antibodies against activated caspase-3 (Cell Signaling Technology, Danvers, MA). Terminal deoxynucleotidyl transferase dUTP nick end labeling (TUNEL) assays on the paraffin sections were performed using the In Situ Cell Death Detection Kit (Roche Diagnostics) following the manufacturer's protocol. Alexa-568 and/or Alexa-488 conjugated goat anti–rabbit secondary antibodies were used in all experiments.

Quantification of immunofluorescence staining

Embryonic fibroblasts were seeded on coverslips. After 12 h, the cells were treated with increasing concentrations of staurosporine (Sigma). Cells were processed 18 h later for immunofluorescence by fixing in 4% PFA and 1× PBS for 10 min and permeabilizing with 0.4% Triton X-100, 3% BSA, and 1× PBS for 10 min at 4°C. Incubation with an antibody against activated caspase-3 (Cell Signaling Technology) 1:400 was performed overnight in 3% BSA at 4°C. For visualization, an anti–rabbit immunoglobulin G (IgG) Alexa Fluor 488 (Invitrogen, Molecular Probes) conjugate was applied. Nuclei were stained with 4′,6-diamidino-2-phenylindole (DAPI), and cells were mounted in Fluoromount (Scientific Services, Sparrow Bush, NY). Cells were photographed using a fluorescence microscope (BX60; Olympus, Center Valley, PA) or scanning microscope (LSM510meta; Zeiss, Jena, Germany). For each treatment, at least 10 images were evaluated with ImageJ software. Experiments were repeated at least three times, and more than 1,000 cells per sample were counted.

Immunocytochemistry

Cells grown on gelatin-coated coverslips were fixed with 4% PFA and permeabilized in PBS/0.1% Triton X-100. Nonspecific binding was reduced by blocking with 5% bovine calf serum in PBS, and the cells were incubated with primary antibody in 1% BSA/PBS.

In situ hybridization

Embryos in deciduas were fixed overnight at 4°C in 4% PFA, dehydrated through an ethanol and xylene series, and embedded in paraffin blocks. Sections (6 µm) were cut in a transverse plane with respect to the placenta. Slides were processed for hematoxylin–eosin staining and in situ hybridization as previously described (Vortkamp *et al.*, 1996). Riboprobe template vectors were provided by Malgorzata Gasperowicz and James Cross, University of Calgary, Canada. For genotyping, embryonic tissue was scraped off unstained slides. DNA was recovered and genotyped by PCR.

HeLa cell culture and small interfering RNA (siRNA) transfections

HeLa human cervical carcinoma cells were maintained in DMEM medium (4.5 g/l glucose) supplemented with 10% fetal calf serum (FCS), penicillin G at 100 IU/ml, streptomycin at 100 g/ml, and 2 mM L-glutamate and cultured at 37°C in a humidified atmosphere containing 5% CO_2 and 95% air. The sequence of the sense strand of the NOA1 targeting siRNA was (GGUCAUACGUUACUCCAGA) dTdT. siRNA was transfected using DreamFect (Oz Biosciences, Marseille, France). 60% confluent cells were transfected with 1 µM siRNA (20 nmol of double-stranded RNA [dsRNA]) according to supplied protocol. Following transfection, cells were cultured in DMEM containing 10% FCS for 3 days. Cells were harvested 72 h post-transfection for analysis. HeLa cells transfected with scrambled siRNA were used as control.

Western blotting

Protein lysates were prepared in SDS radioimmunoprecipitation assay (SDS RIPA) buffer supplemented with a complete proteinase tablet (Roche), 1 mM phenylmethylsulfonyl fluoride (PMSF), 1 mM sodium vanadate, and 1 mM sodium fluoride. The lysate concentrations were determined using the Bradford assay (Bio-Rad, Hercules, CA). Lysates (40 µg of protein per well) were resolved in 10% SDS–PAGE and subsequently transferred to polyvinylidene fluoride (PVDF) membranes. The blots were probed with the rabbit anti-NOA1 polyclonal antibody generated against peptide: CVNVKGQRMKKSVAYK (1:100). Other antibodies used were: rabbit anti-actin (1:1,000; Sigma). Blots were developed with the Western Lightning® Plus–ECL system (PerkinElmer).

TEM

Whole E9.5 embryos were fixed with 2.5% glutaraldehyde in 0.1 M cacodylate buffer solution (pH 7.3) at 4°C, washed, and postfixed in 2% osmium tetroxide in the same buffer. Samples were dehydrated in ethanol, then embedded in Eponate 12 epoxy resin (Serva, Heidelberg, Germany) and sectioned on a Reichert-Jung Ultracut microtome (Leica, Wetzlar, Germany). Semithin sagittal sections of whole embryos were stained with methylene blue-azure to locate and mark the somite regions. The ultrathin sections were prepared, stained with uranyl acetate followed by lead citrate, and imaged using an EM906 Zeiss (Oberkochen, Germany) electron microscope at 80 kV.

Optical tomography (OPT)

The OPT method was used to visualize embryos in three dimensions (3D). The method accumulates projection images of an entire specimen from many different angles, and recalculates the original 3D structure by using a "back-projection" reconstruction algorithm (Sharpe *et al.*, 2002). OPT scans were performed in UV light using a GFP1 filter for detection of the embryos' autofluorescence using IPLab software from Scanalytics (Rockville, MD). Results were exported to QuickTime movies.

Polarography

MEFs and siRNA-treated HeLa cells were trypsinized, washed twice with PBS, and permeabilized with digitonin at 50 µg/ml. The optimum incubation time for permeabilization (50 s for MEFs; 120 s for HeLa) was determined in separate time series for each cell line and defined as the shortest duration after which 99% of the cells were trypan blue positive. Additionally, we verified adequate mitochondrial coupling by measuring the increase of respiration after decoupling with DNP (2,4-dinitrophenol) in comparison to the state IV respiration without ADP. The DNP / state IV respiration rates were 1.7 ± 0.1 in wild-type cells and 1.8 ± 0.2 in the knockout MEF cells. The cells (1×10^7) were resuspended in reaction buffer and introduced into the reaction chamber of a Clark-type electrode (Hansatech Instruments, Norfolk, England), and oxygen concentrations were measured in 1-ml volumes at 37°C with substrates and inhibitors according to standard protocols (Hofhaus *et al.*, 1996). After completion of the polarographic measurement, cells were collected and DNA quantified using a Quant-iT PicoGreen DNA kit (Invitrogen) according to the supplied protocol. Oxygen consumption was given as mean ± SD nmol O_2 per minute per µg of DNA ($n \geq 4$).

Blue-native PAGE and complex I in-gel activity assay

Blue-native PAGE was used for separation of the OXPHOS complexes on 5–15% polyacrylamide-gradient gels as described before (Calvaruso *et al.*, 2008). After electrophoresis of 40 µg of protein from MEFs, gels were further processed for in-gel activity assays and Western blotting. Assembly of the OXPHOS complexes was analyzed using monoclonal antibodies against subunits of complex I (NDUFA9, NDUFS3), complex III (Core2), complex V (α-ATPase) (Molecular Probes, Leiden, The Netherlands), and complexes II (SDHA) and IV (CoxVa) (MitoSciences, Eugene, OR).

OXPHOS enzyme complex measurements

The activities of the OXPHOS enzyme complexes were measured in MEFs as described previously (Lazarov and Cooperstein, 1951; Smeitink *et al.*, 2001; Janssen *et al.*, 2003, 2007). Citrate synthase (CS) activities were determined in cultured fibroblast as previously described (Srere, 1969).

Analysis of mitochondrial protein synthesis

In vitro pulse labeling of mitochondrial translation products was performed as described elsewhere (Boulet *et al.*, 1992), with a few adaptations. In brief, cells were labeled for 60 min at 37°C in L-methionine–free and L-cysteine–free DMEM with 10% dialyzed FCS, [^{35}S]methionine and [^{35}S]cysteine at 200 µCi/ml (Tran35S-Label; MP Biomedicals, Eindhoven, The Netherlands), and emetine at 100 µg/ml, and were subsequently chased for 10 min in regular DMEM with 10% FCS. Total cellular protein was resuspended and incubated for 10 min in PBS containing 2% lauryl maltoside. Unsolubilized material was removed by centrifugation at 10,000 × *g* for 10 min. The protein concentration was determined (Micro BSA Protein Assay Kit; Pierce) and loading buffer was added to the supernatant 1:1 (Tricine Sample Buffer; Thermo Fisher Scientific, Rockford, IL). The samples were separated through 16% polyacrylamide gels and subsequently scanned on a FLA5100 (Fujifilm Life Science, Düsseldorf, Germany). Equal protein loading was confirmed using colloidal Coomassie Blue staining (data not shown).

Isokinetic sucrose gradient analysis of mitochondrial ribosomes

Cell lysis was performed in 50 mM Tris-HCl pH 7.4, 150 mM NaCl, 1 mM EDTA, 1% Triton X-100, + PI-Mix, 1 mM PMSF, and 10 mM $MgCl_2$ for 30 min at 4°C. After a 10-min incubation, lysate was clarified by centrifugation at 12,000 × *g* at 4°C. Approximately 0.9 mg of supernatant was loaded onto a linear sucrose gradient (10–30% [vol/vol], 1 ml) in 50 mM Tris-HCl, pH 7.2, 10 mM $Mg(OAc)_2$, 40 mM NH_4Cl, 100 mM KCl, 1 mM PMSF, and chloramphenicol at 50 µg/ml and centrifuged for 2 h 15 min at 100,000 × *g* at 4°C. Fractions of 100 µl were collected, and 10 µl of each fraction was analyzed by Western blot. Antibodies used were anti-MRPS18b (ProteinTech Group, Chicago, IL) and anti-MRPL12 (Abcam, Cambridge, MA).

Quantitative RT–PCR

cDNAs were synthesized from 1 µg total RNAs with murine leukemia virus (MuLV) reverse transcriptase (Applied Biosystems, Carlsbad, CA). TaqMan universal PCR was then performed on an ABI PRISMs 7900 cycler (Applied Biosystems), using the SYBR green method according to the manufacturer's instructions. Transcripts of the following genes were monitored: NOA – NOA1, 16S RNA, 12S RNA, ND1 – NADH dehydrogenase subunit 1; ND6 – NADH dehydrogenase subunit 6, CytOx1 – Cyt *c* oxidase subunit 1, CytOx2 – Cyt *c* oxidase subunit 2, cytB – cytochrome *b*, ATP6 – ATP synthase F0 subunit 6, EF-Tu – Elongation Factor Tu, L20 – mitochondrial ribosomal protein L20, AIF – apoptosis inducing factor (see also supplemental primer list).

mtDNA analysis

The mtDNA/nuclear DNA (mtDNA/nDNA) ratio was estimated using qPCR with primers specific for mtDNA-encoded *Cox1* gene (subunit 1 of cytochrome *c* oxidase) and nuclearly encoded *Ndufv1* gene (NADH:ubiquinone oxidoreductase) (see supplemental primer list). DNA quantification was repeated five times in independent qPCR reactions, and an average mtDNA/nDNA ratio was calculated. All values were expressed as means ± SD.

Mitochondrial genome integrity was tested using primers listed in the supplement and the Expand Long Template PCR System (Roche) according to the manufacturer's protocol. PCR conditions were: 94°C for 3 min; 10 cycles: 94°C for 10 s, 65°C for 30 s, 68°C for 16 min; 20 cycles: 94°C for 10 s, 65°C for 30 s, 68°C for 16 min

(+20 s/cycle). For detection of shorter products, elongation time was reduced to 8 min.

ATP assay

ATP levels were measured with the ATPlite Bioluminescence Assay kitSystem (Roche). Cells were trypsinized after a 36-h incubation time in culture medium with (4.5 g/l) or without glucose. The cells were washed once in PBS and resuspended in the kit's dilution buffer.

Viability assay

Viability was measured with an alamarBlue assay according to supplied protocol (Invitrogen). Defined cell numbers were plated in 96-well formats, and the resazurin substrate reduction was monitored in the cell culture medium by measuring the accumulation of the fluorescent resorufin (excitation at 530 nm, emission at 590 nm).

Preparation of rRNA

16S rRNA and 23S+5S rRNA of *E. coli* were prepared by phenol extraction followed by ethanol precipitation starting with purified 30S and 50S ribosomal subunits, respectively (Lietzke and Nierhaus, 1988). The genes coding for the mitochondrial 12S and 16S rRNA were amplified from human mtDNA using the primers mt12S fw and mt12S rev or mt16S fw and mt16S rev, leading to the fusion of a T7 promoter sequence at the 5′-end of the genes. PCR fragments were digested with *Hind*III and *Eco*RI and cloned into pSP65 cleaved with the same enzymes. Transcription of the genes was performed in vitro using T7 RiboMAX Express (Promega, Madison, WI) with the new constructed plasmids (linearized with *Eco*RI) as template. Transcribed RNA was purified by gel filtration and ethanol precipitation.

Cloning, expression, and purification of *B. subtilis* YqeH and human NOA1

The gene coding for *B. subtilis* YqeH was amplified from genomic DNA by PCR and cloned into pET28a (Novagen, Merck KGaA, Darmstadt, Germany) via *Nde*I and *Xho*I, leading to an N-terminal His-tag fusion. The correct sequence was confirmed by sequencing. The gene was expressed in BL21(DE3) and the protein purified via Ni-NTA agarose (Qiagen, Valencia, CA, according to the manufacture's manual) followed by anion exchange chromatography (MonoQ, GE Healthcare, Piscataway, NJ). The protein was finally dialyzed against 20 mM HEPES·KOH (pH 8.0 at 0°C), 6 mM $Mg(acetate)_2$, 150 mM K(acetate), and 4 mM β-mercaptoethanol.

Full-length cDNAs for human NOA (IRALp962E057Q2) was obtained from the German Resource Center for Genome Research (RZPD, Berlin). The gene coding for Δ25a.a.-hNOA1 protein (hNOA1 without mitochondria targeting sequence – 25 amino acids of N terminus) was amplified by PCR and cloned into pGEX-6P (Amersham Pharmacia Biotech, Buckinghamshire, UK) via *Eco*RI and *Xho*I leading to an N-terminal GST-tag fusion. The gene was expressed in BL21-CodonPlus (DE3)-RP (Stratagene, Santa Clara, CA), and the protein was purified via Glutathione Sepharose 4B (Amersham Pharmacia Biotech, Piscataway, NJ) using PBS buffer pH 6.2 supplemented with 1% Triton X-100, according to the manufacture's manual. The protein was finally dialyzed against 50 mM Tris, pH 7.0, at 4°C, 150 mM NaCl and concentrated using Centriprep YM-10 (Amicon, Bedford, MA).

30S reconstitution and poly(Phe) synthesis

0.125 A_{260} unit of 16S *E. coli* rRNA equivalent to 9 pmol was incubated with 0.05 equivalent units (e.u.) of total proteins of the 30S subunit (TP30) for 30 min at 40°C in 15 ml of Rec20 buffer: 20 mM HEPES-KOH (pH 7.6 at 0°C), 20 mM $Mg(acetate)_2$, 400 mM $NH_4(acetate)$, and 4 mM β-mercaptoethanol (for details, see Nierhaus, 1990). Subsequently, poly(U)-dependent poly(Phe) synthesis was performed with 6 pmol of reconstituted particles, which were incubated at 37°C for 1 h in 40 μl with 6 pmol of 50S subunits, 13.4 μg of bulk transfer RNA ($tRNA^{bulk}$), 33.4 μg of poly(U), 10 nmol of phenylalanine (23 dpm/pmol), 3.33 μl of S100 enzymes in the presence of 20 mM HEPES-KOH (pH 7.6 at 0°C), 6 mM $Mg(acetate)_2$, 150 mM $NH_4(acetate)$, 4 mM β-mercaptoethanol, 2 mM spermidine, 0.05 mM spermine, 3 mM ATP, 1.5 mM GTP, and 5 mM acetyl phosphate. The reaction mix (35 μl) was subjected to hot trichloroacetic acid (TCA) precipitation and filtered through glass filters. Control reconstitutions were performed at 20°C for 1 h, but otherwise under identical conditions in the presence and absence of 9 pmol of YqeH. The *B. subtilis* YqeH factor did not accelerate the *E. coli* reconstitution process of the 30S subunit.

Preparation of 21S particle

600 A_{260} units of 16S rRNA and 240 e.u. of TP30 were reconstituted for 30 min in ice water. The incubated sample was centrifuged through a 10–30% sucrose gradient containing Rec20 in a Beckman Zonal rotor at 24,000 rpm for 19 h at 4°C. Fractions containing the heavy shoulder of the 21S peak were collected and the particles were pelleted and resuspended in Rec20 buffer. Protein content of the 21S particles was determined by two-dimensional electrophoresis, and the following proteins were detected: S4, S5, S7, S8, S9, S13, S14, S15, S16, and S18. The proteins S1 and S20 could not be resolved on the 30S control. The intactness of the rRNA was confirmed by RNA electrophoresis. Controls containing the 21S particles were subjected to a reconstitution incubation in the presence of TP30 and checked for poly(Phe) synthesis in the presence of mature 50S subunits. The results confirmed that the 21S particles were authentic intermediates, which could be processed to active 30S subunits.

GTPase assay

The assay was performed in a 50-μl reaction volume under optimized ion conditions (20 mM HEPES-KOH [pH 8.0 at 0°C], 4.5 mM $Mg(acetate)_2$, 150 mM K(acetate), 2 mM spermidine, 0.05 mM spermine, and 4 mM β-mercaptoethanol). The incubation mixture contained 10 pmol of YqeH or NOA1, 2.5 nmol of [γ^{32}P]GTP (20 dpm/pmol), and the indicated amounts of rRNA, 21S particles, or ribosomal subunits. Samples were incubated either 1 h at 30°C or 6 h at 20°C, and the reaction was stopped by the addition of 120 μl of 0.5 M H_2SO_4 and 1.5 mM NaH_2PO_4. The released γ-phosphate was extracted by mixing the samples with 30 μl of 200 mM $MoNaO_4$ and 800 μl of water-saturated 2-butanol. Samples were vortexed for 1 min followed by centrifugation at 16,000 × *g* for 10 min at 4°C. The radioactivity obtained in the butanol phase was measured in a Wallac 1409 Liquid Scintillation Counter.

All animal experimental procedures were approved by the local animal ethics commission, State Office of Health and Welfare Berlin (LAGeSo).

ACKNOWLEDGMENTS

We thank Monika Osswald, Petra Schrade, and Carola Dietrich for excellent technical assistance. We also thank Malgorzata Gasperowicz and James Cross for providing template vectors for placenta specific riboprobes. We also acknowledge Laurene Marchand for her contribution in establishing mitochondrial membrane potential assay. M. K. and N. K. were supported by a Young Investigator

Award (Grant 2007–01-038) from the Children's Tumor Fundation, New York, and by Bundesministerium für Bildung und Forschung Grant NF1–01GM0844. This work was also supported by the Sixth Framework of the European Commission, EuroGrow project LSHM-CT-2007–037471. M. P. was supported by a German Academic Exchange Service (DAAD, New York) grant and H. Y. by an Alexander-von-Humboldt stipendium. R.N.L. was supported by grant number BB/F011520/1 from the Biotechnology and Biological Sciences Research Council. I. M. and P. M. are supported by grants 1 M 6837805002 and 0021620806 from the Ministry of Education, Youth and Sports and by grant 252021 102107 from GAUK. M. S. was supported by the Deutsche Forschungsgemeinschaft, Neuro-Cure Exc 257 and is a member of the German network for mitochondrial disorders (mitoNET, 01GM0862), funded by the German Ministry of Education and Research (BMBF).

REFERENCES

Boulet L, Karpati G, Shoubridge EA (1992). Distribution and threshold expression of the tRNA(Lys) mutation in skeletal muscle of patients with myoclonic epilepsy and ragged-red fibers (MERRF). Am J Hum Genet 51, 1187–1200.

Britton RA (2009). Role of GTPases in bacterial ribosome assembly. Annu Rev Microbiol 63, 155–176.

Calvaruso MA, Smeitink J, Nijtmans L (2008). Electrophoresis techniques to investigate defects in oxidative phosphorylation. Methods 46, 281–287.

Cavdar Koc E, Ranasinghe A, Burkhart W, Blackburn K, Koc H, Moseley A, Spremulli LL (2001). A new face on apoptosis: death-associated protein 3 and PDCD9 are mitochondrial ribosomal proteins. FEBS Lett 492, 166–170.

Chen H, Detmer SA, Ewald AJ, Griffin EE, Fraser SE, Chan DC, (2003). Mitofusins Mfn1 and Mfn2 coordinately regulate mitochondrial fusion and are essential for embryonic development. J Cell Biol 160, 189–200.

Cheung EC *et al*. (2006). Dissociating the dual roles of apoptosis-inducing factor in maintaining mitochondrial structure and apoptosis. EMBO J 25, 4061–4073.

Flores-Perez U, Sauret-Gueto S, Gas E, Jarvis P, Rodriguez-Concepcion M (2008). A mutant impaired in the production of plastome-encoded proteins uncovers a mechanism for the homeostasis of isoprenoid biosynthetic enzymes in Arabidopsis plastids. Plant Cell 20, 1303–1315.

Gordon J (1970). Regulation of the in vivo synthesis of the polypeptide chain elongation factors in Escherichia coli. Biochemistry 9, 912–917.

Gray MW, Burger G, Lang BF (2001). The origin and early evolution of mitochondria. Genome Biol 2, reviews1018.1–reviews1018.5.

Hofhaus G, Shakeley RM, Attardi G (1996). Use of polarography to detect respiration defects in cell cultures. Methods Enzymol 264, 476–483.

Janssen AJ, Smeitink JA, Van Den Heuvel LP (2003). Some practical aspects of providing a diagnostic service for respiratory chain defects. Ann Clin Biochem 40, 3–8.

Janssen AJ, Trijbels FJ, Sengers RC, Smeitink JA, Van Den Heuvel LP, Wintjes LT, Stoltenborg-Hogenkamp BJ, Rodenburg RJ (2007). Spectrophotometric assay for complex I of the respiratory chain in tissue samples and cultured fibroblasts. Clin Chem 53, 729–734.

Karbstein K (2007). Role of GTPases in ribosome assembly. Biopolymers 87, 1–11.

Kim do J, Jang JY, Yoon HJ, Suh SW (2008). Crystal structure of YlqF, a circularly permuted GTPase: implications for its GTPase activation in 50 S ribosomal subunit assembly. Proteins 72, 1363–1370.

Koc EC, Burkhart W, Blackburn K, Moyer MB, Schlatzer DM, Moseley A, Spremulli LL (2001). The large subunit of the mammalian mitochondrial ribosome. Analysis of the complement of ribosomal proteins present. J Biol Chem 276, 43958–43969.

Lazarov A, Cooperstein SY (1951). Studies on the isolated islet tissue of fish. I. The cytochrome oxidase and succinic dehydrogenase contents of normal toadfish (Opsonus tau). Biol Bull 100, 191–198.

Leipe DD, Wolf YI, Koonin EV, Aravind L (2002). Classification and evolution of P-loop GTPases and related ATPases. J Mol Biol 317, 41–72.

Lietzke R, Nierhaus KH (1988). Total reconstitution of 70S ribosomes from Escherichia coli. Methods Enzymol 164, 278–283.

Loh PC, Morimoto T, Matsuo Y, Oshima T, Ogasawara N (2007). The GTP-binding protein YqeH participates in biogenesis of the 30S ribosome subunit in Bacillus subtilis. Genes Genet Syst 82, 281–289.

Nierhaus K (1990). Spedding G, Reconstitution of ribosomes. In: Ribosomes and Protein Synthesis A Practical Approach, Oxford, UK: IRL Press at Oxford University Press, 161–189.

Nierhaus KH (1991). The assembly of prokaryotic ribosomes. Biochimie 73, 739–755.

O'Brien TW (2002). Evolution of a protein-rich mitochondrial ribosome: implications for human genetic disease. Gene 286, 73–79.

Parihar MS, Parihar A, Chen Z, Nazarewicz R, Ghafourifar P (2008). mAtNOS1 regulates mitochondrial functions and apoptosis of human neuroblastoma cells. Biochim Biophys Acta 1780, 921–926.

Qin Y, Polacek N, Vesper O, Staub E, Einfeldt E, Wilson DN, Nierhaus KH (2006). The highly conserved LepA is a ribosomal elongation factor that back-translocates the ribosome. Cell 127, 721–733.

Red-Horse K, Zhou Y, Genbacev O, Prakobphol A, Foulk R, McMaster M, Fisher SJ (2004). Trophoblast differentiation during embryo implantation and formation of the maternal-fetal interface. J Clin Invest 114, 744–754.

Sharpe J, Ahlgren U, Perry P, Hill B, Ross A, Hecksher-Sorensen J, Baldock R, Davidson D (2002). Optical projection tomography as a tool for 3D microscopy and gene expression studies. Science 296, 541–545.

Smeitink J, Sengers R, Trijbels F, Van Den Heuvel L (2001). Human NADH:ubiquinone oxidoreductase. J Bioenerg Biomembr 33, 259–266.

Srere P (1969). Citrate synthase, EC 4.1.3.7, citrate oxaloacetate lyase (CoA-acetylating). Methods Enzymol 13, 3–11.

Tang T, Zheng B, Chen SH, Murphy AN, Kudlicka K, Zhou H, Farquhar MG (2009). hNOA1 interacts with complex I and DAP3 and regulates mitochondrial respiration and apoptosis. J Biol Chem 284, 5414–5424.

Uicker WC, Schaefer L, Koenigsknecht M, Britton RA (2007). The essential GTPase YqeH is required for proper ribosome assembly in Bacillus subtilis. J Bacteriol 189, 2926–2929.

Vardi A, Bidle KD, Kwityn C, Hirsh DJ, Thompson SM, Callow JA, Falkowski P, Bowler C (2008). A diatom gene regulating nitric-oxide signaling and susceptibility to diatom-derived aldehydes. Curr Biol 18, 895–899.

Vortkamp A, Lee K, Lanske B, Segre GV, Kronenberg HM, Tabin CJ (1996). Regulation of rate of cartilage differentiation by Indian hedgehog and PTH-related protein. Science 273, 613–622.

Wakabayashi J, Zhang Z, Wakabayashi N, Tamura Y, Fukaya M, Kensler TW, Iijima M, Sesaki H (2009). The dynamin-related GTPase Drp1 is required for embryonic and brain development in mice. J Cell Biol 186, 805–816.

Zemojtel T *et al*. (2006a). Plant nitric oxide synthase: a never-ending story?. Trends Plant Sci 11, 524–525; author reply 526–528.

Zemojtel T, Penzkofer T, Dandekar T, Schultz J (2004). A novel conserved family of nitric oxide synthase? Trends Biochem Sci 29, 224–226.

Zemojtel T *et al*. (2006b). Mammalian mitochondrial nitric oxide synthase: characterization of a novel candidate. FEBS Lett 580, 455–462.

transactions

Translation termination in human mitochondrial ribosomes

Ricarda Richter, Aleksandra Pajak, Sven Dennerlein, Agata Rozanska, Robert N. Lightowlers and Zofia M.A. Chrzanowska-Lightowlers[1]

Mitochondrial Research Group, Institute for Ageing and Health, Newcastle University Medical School, Framlington Place, Newcastle upon Tyne NE2 4HH, U.K.

Abstract

Mitochondria are ubiquitous and essential organelles for all nucleated cells of higher eukaryotes. They contain their own genome [mtDNA (mitochondrial DNA)], and this autosomally replicating extranuclear DNA encodes a complement of genes whose products are required to couple oxidative phosphorylation. Sequencing of this human mtDNA more than 20 years ago revealed unusual features that included a modified codon usage. Specific deviations from the standard genetic code include recoding of the conventional UGA stop to tryptophan, and, strikingly, the apparent recoding of two arginine triplets (AGA and AGG) to termination signals. This latter reassignment was made because of the absence of cognate mtDNA-encoded tRNAs, and a lack of tRNAs imported from the cytosol. Each of these codons only occurs once and, in both cases, at the very end of an open reading frame. The presence of both AGA and AGG is rarely found in other mammals, and the molecular mechanism that has driven the change from encoding arginine to dictating a translational stop has posed a challenging conundrum. Mitochondria from the majority of other organisms studied use only UAA and UAG, leaving the intriguing question of why human organelles appear to have added the complication of a further two stop codons, AGA and AGG, or have they? In the present review, we report recent data to show that mammalian mitochondria can utilize a −1 frameshift such that only the standard UAA and UAG stop codons are required to terminate the synthesis of all 13 polypeptides.

Introduction

Mitochondria are vital organelles that are present in all nucleated cells of higher eukaryotes. They play critical roles in many processes, including calcium homoeostasis, apoptosis, Fe–S cluster formation and oxidative phosphorylation. Mitochondria contain their own genome (mtDNA, where mt is mitochondrial) encoding mt-mRNAs that are translated within the organelle [1]. In humans, these transcripts encode 13 proteins that are all components of the oxidative phosphorylation machinery, in addition to the two mt-rRNAs and 22 mt-tRNAs, which are required for the intramitochondrial translation of the mt-mRNAs. The remaining protein components required for intra-organellar translation and mitochondrial biogenesis are nuclear-encoded and need to be imported from the cytosol. Human mtDNA is a relatively small genome (16 569 bp) and is found in many copies per mononucleate cell. A minimal non-coding sequence is present, which contains regions that control the initiation of mtDNA replication and transcription. From these regions, this compact genome is almost fully transcribed from both strands [2]. As a consequence, long polycistronic transcriptional units are generated, which are subsequently processed to separate the mt-rRNA, mt-tRNAs and mt-mRNAs, and are then matured [2,3]. For the mt-tRNAs, this involves the addition of -CCA to the 3′-teminus of the precursor by the tRNA-nucleotidyltransferase, a protein encoded by *TRNT1* [4]. The 3′-termini of the mt-mRNAs are also matured, but by the addition of a poly(A) tail. This modification appears to be constitutive and is effected by mtPAP, a nuclear-encoded poly(A) polymerase that is specific to mitochondria [5]. In contrast with cytosolic mRNAs, their mitochondrial counterparts lack any modification to the 5′-termini and remain as a simple 5′-PO_4. Another contrasting feature is the relative lack of UTRs (untranslated regions), leaving most ORFs (open reading frames) unflanked. Thus initiation commences at or within three nucleotides of the extreme 5′-termini for all except two of the ORFs, whereas completion of the UAA stop codon is facilitated by the addition of 'A' residues as a consequence of polyadenylation of seven ORFs.

Protein synthesis in the human mitochondrion

Initiation of protein synthesis occurs mainly at AUG codons, but AUA and AUU can also be decoded as initiating methionines [1]. Compared with translation in the eukaryotic cytosol, where there are many IFs (initiation factors) that come together to form the initiation complex, there appears to be a much reduced system in mammalian mitochondria. In the latter, the initiation complex appears to have retained only two homologues: IF2 and IF3 [6,7]. It does appear, however, that mtIF2 may have taken on the functions of

Key words: mitochondrion, protein synthesis, release factor, stop codon, translation termination.
Abbreviations used: IF, initiation factor; mt, mitochondrial; ORF, open reading frame; RF, release factor; RRF, ribosome recycling factor; UTR, untranslated region.
[1]To whom correspondence should be addressed (email Z.Chrzanowska-Lightowlers@ncl.ac.uk).

Biochemical Society Transactions www.biochemsoctrans.org

bacterial IF1 [8]. Elongation proceeds along the mt-mRNA facilitated by mtEF-Tu, mtEF-Ts and mtEF-G1 [9–12]. Another major difference lies in the general structure of the mammalian mitochondrial ribosome when compared with the more familiar bacterial 70S and eukaryotic cytosolic 80S counterparts [13]. Rather than a predominance of rRNA, mammalian mitochondrial ribosomes have reduced the RNA component to two shorter rRNA species, 12S and 16S, while concomitantly increasing the number of protein components, thus reversing the conventional ratio to ~70% protein and only ~30% rRNA. As a consequence, the structure is more open and porous with no conventional E-site and with altered sedimentation values of 28S and 39S for the small and large subunits respectively and 55S for the complete monosome [13].

Termination of protein synthesis in human mitochondria

The 55S particle continues protein synthesis until a stop codon is reached and positioned within the A-site. Sequencing of the human mtDNA almost 30 years ago [1] revealed the features mentioned above. This included the reassignment of the standard stop codon UGA as a tryptophan, a not uncommon reassignment in mitochondrial genetic codes. Strikingly, it also indicated the apparent recoding of AGA and AGG as stop signals since each of these triplets is found only once and, in both cases, only at the very end of the ORFs of mitochondrial transcripts *MTCO1* or *MTND6* respectively. The conclusion that these were now stop signals was driven by the fact that the mtDNA does not code for any tRNA that could decode either AGA/AGG triplets and no tRNA has been shown to be imported physiologically into the human organelle [14]. The remaining 11 mitochondrial ORFs terminate in either of the two standard stops, UAA or UAG. The original dilemma was therefore what form of the class I RF (release factor) would be required to promote peptidyl-tRNA hydrolysis at these stop codons? Do human mitochondria follow the bacterial paradigm where two RFs are required to decode the three stop codons (RF1 recognizing UAA/UAG, and RF2 showing specificity for UGA/UAA [15,16]), or do they utilize a single RF more akin to eRF1 (eukaryotic RF1)/aRF1 (archaeal RF1) in the eukaryotic or archaeal cytosol respectively [17,18]? A single mitochondrial RF, however, would have to recognize an unusual and expanded repertoire of four triplets.

Over 12 years ago, bioinformatic mining identified an encouraging candidate for the role of human mtRF1. This protein contained a predicted decoding tripeptide motif (comprising proline and threonine with a variable amino acid between the two and thus designated the 'PXT' motif) which, although divergent, aligned more closely with that of bacterial RF1 than RF2 [19]. The PXT motif in mtRF1 is made up of six amino acids, PEVGLS, rather than just the three, thus differing from the accepted RF1 type PXT consensus in both length and sequence. It was considered that these differences, when taken with a second sequence variation at the tip of the α-5 helix, could have evolved to allow recognition of this extended repertoire of stop triplets. Subsequent biochemical analysis with mtRF1, however, failed to identify any release activity with any codons. A more recent search for a further candidate identified a protein, mtRF1a, with high overall identity with mtRF1 [20]. Analysis of the codon recognition domains revealed greater similarity to that of the bacterial RF1 homologue and consensus sequences, with PKT as the sequence constituting the tripeptide motif. Activity assays demonstrated that mtRF1a has a specificity for the standard UAA and UAG codons, but fails to recognize AGA/AGG or any other codon tested [20]. Since the *in vitro* assays are performed with 70S bacterial ribosomes, the lack of recognition of AGA/AGG by mtRF1 or mtRF1a could have been the consequence of using a heterologous system, especially in the light of the significant differences between 55S and 70S particles described above. Further bioinformatic searches have now revealed a family of four predicted mitochondrial RFs, with ICT1 and C12orf65 adding to the previously described mtRF1 and mtRF1a. Intriguingly, these two new members, ICT1 and C12orf65, both lack the two regions involved in codon recognition and are therefore unlikely candidates for AGA/AGG recognition [21].

Reanalysis of the two transcripts containing the AGA or AGG codons indicated that each of these triplets is directly preceded by a 'U' nucleotide, which, following procession of the mitochondrial ribosome to the end of the reading frame, would be placed immediately adjacent, in the P-site [1]. Thus, by invoking a single nucleotide shift, a conventional UAG stop signal would be positioned in the A-site. In support of this hypothesis, although 3′-UTRs are unusual in human mt-mRNAs, these are present in both of the transcripts containing in-frame AGA or AGG, and are predicted to form stable secondary structures [22]. Frameshifting on mitochondrial mRNAs is not common and no examples have been identified previously in mammalian mitochondria. Indeed there are only very few examples in mitochondria, all of which thus far are in the +1 direction and occur within the mt-ORFs [23–25]. The frameshifting proposed in human mitochondria would contrast not only with these other mitochondrial examples (as it is in the -1 direction), but also with all standard frameshifts, as it would occur after protein synthesis has been completed. Furthermore, many frameshifts offer an inefficient alternative to readthrough [26], which can be regulated by changes in physiological conditions [27]. In the instance of this human mitochondrial example, there would be no possibility for readthrough, as there is no cognate mt-tRNA for the AGA/AGG triplets. We have been able to test this hypothesis by combining the use of a mitochondrially targeted bacterial A-site-specific endonuclease, mtRelE, together with sequence analysis of the resultant cleaved RNA [22]. These fine mapping data revealed the A-site codon at termination and confirmed that a -1 frameshift does indeed occur. Thus the human mitochondrial translation system only requires the more standard UAG and UAA codons for termination. Moreover, as a consequence,

only a single RF is required, mtRF1a, which has already been characterized to show selectivity and specificity for these two termination signals [20].

Recycling of the human mitochondrial ribosome following translation termination

No orthologue of a class II RF has been identified in human mitochondria, leaving the question of how mtRF1a is removed from the mitoribosome after translation. Recycling of the post-termination complex to release the deacylated mt-tRNA, mt-mRNA and separation of the monosome into the two subunits is effected by the mitochondrial ribosome recycling factor, mtRRF, in conjunction with mt-EF-G2 and mt-IF3 [28–31]. This second elongation factor mt-EF-G2 was characterized recently and appears to play no role in elongation, but co-operates exclusively with mtRRF in the recycling process [29]. The eukaryotic 80S and bacterial 70S ribosomes were believed to employ only a single EF-G for both processes. However, bioinformatic, *in vitro* and *in vivo* data now show that in fact it is not uncommon for bacteria to have separated the elongation and recycling activities and have two EF-G paralogues, as is the case in human mitochondria [32]. Human mtRRF has an N-terminal presequence that targets the protein to the mitochondrion, but this is not cleaved after successful import into the matrix of the organelle, as is the case for many of the nuclear-encoded but mitochondrially destined proteins [28]. Alignment with numerous RRF sequences suggests that the human mtRRF has a 79-amino-acid N-terminal extension that lacks homology with other proteins [28]. Since this is retained in the mature protein, it is tempting to speculate that it may contain as yet uncharacterized functional domains. Investigations are ongoing in our group to determine whether such domains are present and, if so, what their contribution might be to the process of mitoribosomal recycling.

In conclusion, mitochondrial translation and termination, particularly in humans, shares a number of similarities, but also differs in many ways from these processes in bacteria and the eukaryotic cytosol. This is perhaps not surprising, as it has become clear over the last 30 years that the mitochondrial protein synthesis machinery has an essential association with the membrane, reflecting the highly hydrophobic nature of its translation products, exclusively so in mammals. A greater understanding of this process is hampered by a lack of two important factors. First, our inability to manipulate the mitochondrial genome, which means that it is currently not possible to investigate the role of any *cis*-acting elements in mitochondrial translation. Second, although impressive reconstituted protein synthesis systems have been reported, these are essentially hybrid systems and we therefore lack a faithful reconstituted mitochondrial translation system. If either of these two issues can be resolved in the near future, our in-depth understanding of these processes will increase rapidly.

Funding

R.N.L. and Z.M.A.C.-L. thank The Wellcome Trust [grant number 074454/Z/04/Z], Biotechnology and Biological Sciences Research Council [grant number BB/F011520/1] and the Medical Research Council [grant number G0700718] for continuing support.

References

1 Anderson, S., Bankier, A.T., Barrell, B.G., De Bruijn, M.H.L., Coulson, A.R., Drouin, J., Eperon, I.C., Nierlich, D.P., Roe, B.A., Sanger, F. et al. (1981) Sequence and organization of the human mitochondrial genome. Nature **290**, 457–465
2 Falkenberg, M., Larsson, N.G. and Gustafsson, C.M. (2007) DNA replication and transcription in mammalian mitochondria. Annu. Rev. Biochem. **76**, 679–699
3 Ojala, D., Montoya, J. and Attardi, G. (1981) tRNA punctuation model of RNA processing in human mitochondria. Nature **290**, 470–474
4 Nagaike, T., Suzuki, T., Tomari, Y., Takemoto-Hori, C., Negayama, F., Watanabe, K. and Ueda, T. (2001) Identification and characterization of mammalian mitochondrial tRNA nucleotidyltransferases. J. Biol. Chem. **276**, 40041–40049
5 Tomecki, R., Dmochowska, A., Gewartowski, K., Dziembowski, A. and Stepien, P.P. (2004) Identification of a novel human nuclear-encoded mitochondrial poly(A) polymerase. Nucleic Acids Res. **32**, 6001–6014
6 Grasso, D.G., Christian, B.E., Spencer, A. and Spremulli, L.L. (2007) Overexpression and purification of mammalian mitochondrial translational initiation factor 2 and initiation factor 3. Methods Enzymol. **430**, 59–78
7 Koc, E.C. and Spremulli, L.L. (2002) Identification of mammalian mitochondrial translational initiation factor 3 and examination of its role in initiation complex formation with natural mRNAs. J. Biol. Chem. **277**, 35541–35549
8 Gaur, R., Grasso, D., Datta, P.P., Krishna, P.D., Das, G., Spencer, A., Agrawal, R.K., Spremulli, L. and Varshney, U. (2008) A single mammalian mitochondrial translation initiation factor functionally replaces two bacterial factors. Mol. Cell **29**, 180–190
9 Xin, H., Woriax, V., Burkhart, W. and Spremulli, L.L. (1995) Cloning and expression of mitochondrial translational elongation factor Ts from bovine and human liver. J. Biol. Chem. **270**, 17243–17249
10 Woriax, V.L., Burkhart, W. and Spremulli, L.L. (1995) Cloning, sequence analysis and expression of mammalian mitochondrial protein synthesis elongation factor Tu. Biochim. Biophys. Acta **1264**, 347–356
11 Gao, J., Yu, L., Zhang, P., Jiang, J., Chen, J., Peng, J., Wei, Y. and Zhao, S. (2001) Cloning and characterization of human and mouse mitochondrial elongation factor G, *GFM* and *Gfm*, and mapping of *GFM* to human chromosome 3q25.1-q26.2. Genomics **74**, 109–114
12 Bhargava, K., Templeton, P. and Spremulli, L.L. (2004) Expression and characterization of isoform 1 of human mitochondrial elongation factor G. Protein Expression Purif. **37**, 368–376
13 O'Brien, T.W. (2003) Properties of human mitochondrial ribosomes. IUBMB Life **55**, 505–513
14 Kolesnikova, O.A., Entelis, N.S., Jacquin-Becker, C., Goltzene, F., Chrzanowska-Lightowlers, Z.M., Lightowlers, R.N., Martin, R.P. and Tarassov, I. (2004) Nuclear DNA-encoded tRNAs targeted into mitochondria can rescue a mitochondrial DNA mutation associated with the MERRF syndrome in cultured human cells. Hum. Mol. Genet. **13**, 2519–2534
15 Petry, S., Brodersen, D.E., Murphy, 4th, F.V., Dunham, C.M., Selmer, M., Tarry, M.J., Kelley, A.C. and Ramakrishnan, V. (2005) Crystal structures of the ribosome in complex with release factors RF1 and RF2 bound to a cognate stop codon. Cell **123**, 1255–1266
16 Laurberg, M., Asahara, H., Korostelev, A., Zhu, J., Trakhanov, S. and Noller, H.F. (2008) Structural basis for translation termination on the 70S ribosome. Nature **454**, 852–857
17 Song, H., Mugnier, P., Das, A.K., Webb, H.M., Evans, D.R., Tuite, M.F., Hemmings, B.A. and Barford, D. (2000) The crystal structure of human eukaryotic release factor eRF1: mechanism of stop codon recognition and peptidyl-tRNA hydrolysis. Cell **100**, 311–321
18 Dontsova, M., Frolova, L., Vassilieva, J., Piendl, W., Kisselev, L. and Garber, M. (2000) Translation termination factor aRF1 from the archaeon *Methanococcus jannaschii* is active with eukaryotic ribosomes. FEBS Lett. **472**, 213–216

19 Zhang, Y. and Spremulli, L.L. (1998) Identification and cloning of human mitochondrial translational release factor 1 and the ribosome recycling factor. Biochim. Biophys. Acta **1443**, 245–250
20 Soleimanpour-Lichaei, H.R., Kuhl, I., Gaisne, M., Passos, J.F., Wydro, M., Rorbach, J., Temperley, R., Bonnefoy, N., Tate, W., Lightowlers, R. and Chrzanowska-Lightowlers, Z. (2007) mtRF1a is a human mitochondrial translation release factor decoding the major termination codons UAA and UAG. Mol. Cell **27**, 745–757
21 Richter, R., Rorbach, J., Pajak, A., Smith, P.M., Wessels, H.J., Huynen, M.A., Smeitink, J.A., Lightowlers, R.N. and Chrzanowska-Lightowlers, Z.M. (2010) A functional peptidyl-tRNA hydrolase, ICT1, has been recruited into the human mitochondrial ribosome. EMBO J. **29**, 1116–1125
22 Temperley, R., Richter, R., Dennerlein, S., Lightowlers, R.N. and Chrzanowska-Lightowlers, Z.M. (2010) Hungry codons promote frameshifting in human mitochondrial ribosomes. Science **327**, 301
23 Harlid, A., Janke, A. and Arnason, U. (1997) The mtDNA sequence of the ostrich and the divergence between paleognathous and neognathous birds. Mol. Biol. Evol. **14**, 754–761
24 Mindell, D.P., Sorenson, M.D. and Dimcheff, D.E. (1998) An extra nucleotide is not translated in mitochondrial ND3 of some birds and turtles. Mol. Biol. Evol. **15**, 1568–1571
25 Russell, R.D. and Beckenbach, A.T. (2008) Recoding of translation in turtle mitochondrial genomes: programmed frameshift mutations and evidence of a modified genetic code. J. Mol. Evol. **67**, 682–695
26 Dinman, J.D. and Wickner, R.B. (1992) Ribosomal frameshifting efficiency and *gag/gag-pol* ratio are critical for yeast M_1 double-stranded RNA virus propagation. J. Virol. **66**, 3669–3676
27 Higashi, K., Kashiwagi, K., Taniguchi, S., Terui, Y., Yamamoto, K., Ishihama, A. and Igarashi, K. (2006) Enhancement of +1 frameshift by polyamines during translation of polypeptide release factor 2 in *Escherichia coli*. J. Biol. Chem. **281**, 9527–9537
28 Rorbach, J., Richter, R., Wessels, H.J., Wydro, M., Pekalski, M., Farhoud, M., Kuhl, I., Gaisne, M., Bonnefoy, N., Smeitink, J.A. et al. (2008) The human mitochondrial ribosome recycling factor is essential for cell viability. Nucleic Acids Res **36**, 5787–5799
29 Tsuboi, M., Morita, H., Nozaki, Y., Akama, K., Ueda, T., Ito, K., Nierhaus, K.H. and Takeuchi, N. (2009) EF-G2mt is an exclusive recycling factor in mammalian mitochondrial protein synthesis. Mol. Cell **35**, 502–510
30 Christian, B.E. and Spremulli, L.L. (2009) Evidence for an active role of IF3mt in the initiation of translation in mammalian mitochondria. Biochemistry **48**, 3269–3278
31 Haque, M.E., Grasso, D. and Spremulli, L.L. (2008) The interaction of mammalian mitochondrial translational initiation factor 3 with ribosomes: evolution of terminal extensions in IF3mt. Nucleic Acids Res. **36**, 589–597
32 Suematsu, T., Yokobori, S.I., Morita, H., Yoshinari, S., Ueda, T., Kita, K., Takeuchi, N. and Watanabe, Y.I. (2010) A bacterial elongation factor G homologue exclusively functions in ribosome recycling in the spirochaete *Borrelia burgdorferi*. Mol. Microbiol. **75**, 1445–1454

Received 26 April 2010
doi:10.1042/BST0381523

The EMBO Journal (2010) 29, 1116–1125 | © 2010 European Molecular Biology Organization | Some Rights Reserved 0261-4189/10
www.embojournal.org

THE EMBO JOURNAL

EMBO open

A functional peptidyl-tRNA hydrolase, ICT1, has been recruited into the human mitochondrial ribosome

Ricarda Richter[1], Joanna Rorbach[1], Aleksandra Pajak[1], Paul M Smith[1], Hans J Wessels[2], Martijn A Huynen[3], Jan A Smeitink[2], Robert N Lightowlers[1,*] and Zofia M Chrzanowska-Lightowlers[1,*]

[1]Mitochondrial Research Group, Institute for Ageing and Health, Medical School, Newcastle University, Newcastle upon Tyne, UK, [2]Nijmegen Centre for Mitochondrial Disorders, Radboud University Nijmegen Medical Centre, Nijmegen, The Netherlands and [3]Center for Molecular and Biomolecular Informatics, NCMLS, Radboud University Nijmegen Medical Centre, Nijmegen, The Netherlands

Bioinformatic analysis classifies the human protein encoded by immature colon carcinoma transcript-1 (ICT1) as one of a family of four putative mitochondrial translation release factors. However, this has not been supported by any experimental evidence. As only a single member of this family, mtRF1a, is required to terminate the synthesis of all 13 mitochondrially encoded polypeptides, the true physiological function of ICT1 was unclear. Here, we report that ICT1 is an essential mitochondrial protein, but unlike the other family members that are matrix-soluble, ICT1 has become an integral component of the human mitoribosome. Release-factor assays show that although ICT1 has retained its ribosome-dependent PTH activity, this is codon-independent; consistent with its loss of both domains that promote codon recognition in class-I release factors. Mutation of the GGQ domain common to ribosome-dependent PTHs causes a loss of activity *in vitro* and, crucially, a loss of cell viability, *in vivo*. We suggest that ICT1 may be essential for hydrolysis of prematurely terminated peptidyl-tRNA moieties in stalled mitoribosomes.

The EMBO Journal (2010) **29,** 1116–1125. doi:10.1038/emboj.2010.14; Published online 25 February 2010
Subject Categories: proteins
Keywords: mitoribosomes; peptidyl-tRNA hydrolase; translation release factor

*Corresponding authors. ZM Chrzanowska-Lightowlers or RN Lightowlers, Mitochondrial Research Group, Institute for Ageing and Health, Medical School, Newcastle University, Newcastle upon Tyne NE2 4HH, UK.
Tel.: +44 191 222 8028; Fax: +44 191 222 8553;
E-mails: Z.Chrzanowska-Lightowlers@ncl.ac.uk or R.N.Lightowlers@ncl.ac.uk

Received: 17 December 2009; accepted: 25 January 2010; published online: 25 February 2010

Introduction

Human mitochondria are ubiquitous organelles that are essential for cell viability. Among many crucial functions, mitochondria couple the process of oxidative phosphorylation, where cellular respiration is harnessed to generate ATP. This demanding mechanism requires the synthesis and import of many nucleus-encoded proteins as well as the intramitochondrial production of 13 polypeptides that are encoded by the mitochondrial genome, mtDNA. Consequently, correct maintenance and expression of mtDNA is essential for cell viability. Although we are gradually learning more about the principal factors and mechanisms underlying the maintenance and transcription of mtDNA, the process of mitochondrial translation has proven extremely difficult to be characterised in detail. This is in part because isolated mitochondria lose their capacity to synthesise proteins after solubilisation of the inner membrane, consistent with loss of crucial membrane-associated factors. Furthermore, despite impressive efforts to reconstitute *in vitro* mitochondrial translation systems (Yasukawa *et al*, 2001; Takemoto *et al*, 2009), results have been limited. Invaluable contributions from the laboratories of Spremulli, Watanabe and O'Brien have identified or characterised constituents of both the bovine small 28S (mt-SSU) (Suzuki *et al*, 2001) and large 39S (mt-LSU) (Koc *et al*, 2001) mitoribosomal subunits and many proteins involved in translational initiation and elongation (Spremulli *et al*, 2004), but important factors remain to be unearthed.

To improve our understanding of this process, we have started to identify other principal components in mitochondrial protein synthesis. We have focused our efforts on a previous report where tagged mitochondrial ribosome recycling factor (mtRRF) was shown to immunoprecipitate mitoribosomes and associated proteins from mitochondrial lysates (Rorbach *et al*, 2008). Proteomic analysis uncovered a large number (73) of mitoribosomal proteins (MRPs). In addition, another 94 polypeptides were identified, a number of which have been tentatively identified as nucleoid proteins. Immature colon carcinoma transcript-1 (ICT1) was consistently associated with immunoprecipitation (IP), but it was neither known to be mitochondrial nor have an experimentally verified function, although it is predicted to be a member of the prokaryote/mitochondrial release factor family (uniprot Q14197). This family is intriguing. We have recently been able to show that of the four family members, only mtRF1a is necessary and sufficient to terminate the translation of all 13 mitochondrially encoded polypeptides (Soleimanpour-Lichaei *et al*, 2007; Temperley *et al*, 2010). What, therefore, is the function, if any, of the three remaining family members? We report here that a second member of

this family, ICT1, is a component of the 39S mt-LSU. It has retained its ribosome-dependent peptidyl-tRNA hydrolase (PTH) activity that is essential for cell viability. Furthermore, this ribosome-dependent PTH activity is codon-non-specific. We speculate that this ribosome-associated activity may be involved in the hydrolysis of peptidyl-tRNAs that have been prematurely terminated and thus in the recycling of stalled mitoribosomes.

Results

ICT1 is an essential mitochondrial protein

To determine the subcellular location of ICT1, western blot analysis was performed using cell lysate and enriched mitochondria. As shown in Figure 1A, a 3- to 5-fold enrichment was seen for the mitochondrial matrix protein mtRF1a along with concomitant increase in ICT1. Crucially, ICT1 was resistant to addition of proteinase-K to intact mitochondria, but was lost on solubilisation of the organelle. To assess whether ICT1 is processed on import into mitochondria, full-length ICT1 (FL) or a truncated form lacking the N-terminal 29 residues (Δ29) were prepared. Both proteins were expressed in *Escherichia coli* as N-terminal glutathione-*S*-transferase (GST)-fusion proteins before cleavage and purification as detailed under Materials and methods. Migration of endogenous ICT1 in comparison with recombinant proteins (FL/Δ29) is consistent with cleavage on mitochondrial import, with the loss of ∼30 residues.

To assess whether ICT1 serves an essential function in mitochondria, siRNAs were designed to target the transcript. Two siRNAs were highly efficient in depleting ICT1 from cells (Figure 1B), causing a morphological alteration and a reduc-

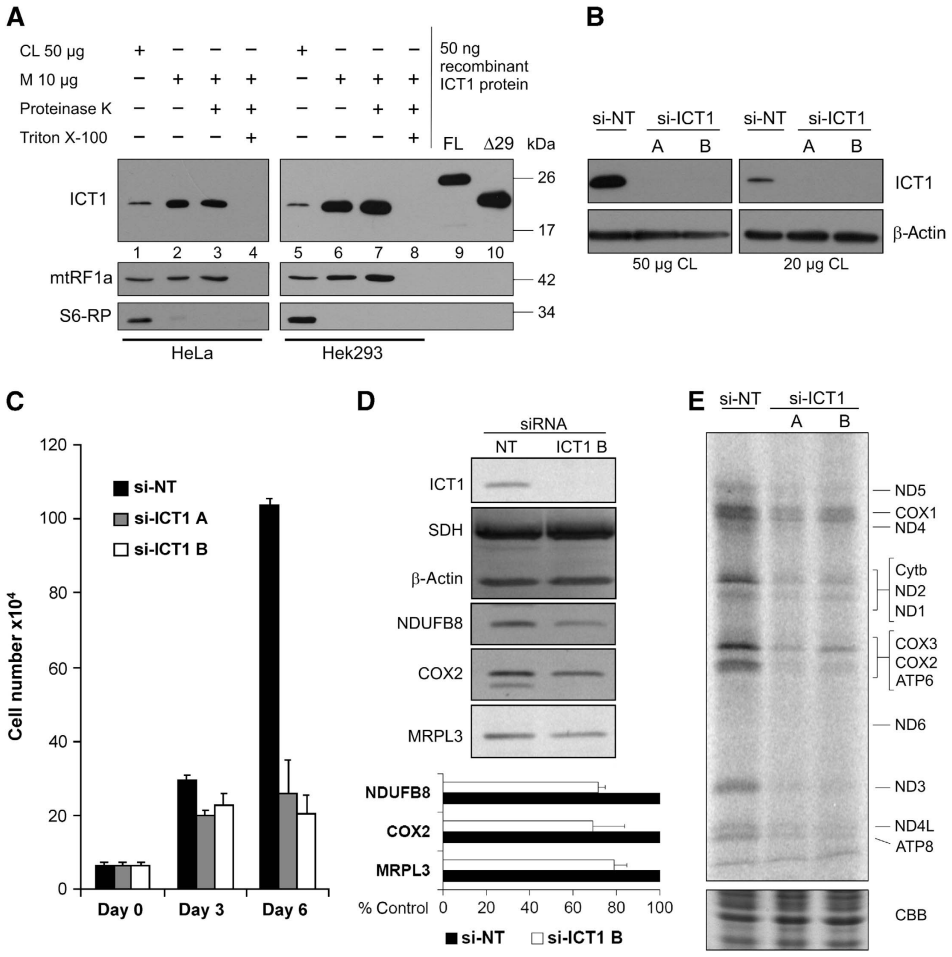

Figure 1 ICT1 is an essential protein necessary for mitochondrial protein synthesis. (**A**) Human ICT1 is a mitochondrial protein. Cell lysate (CL 50 µg, lanes 1, 5) or mitochondria (10 µg, lanes 2–4, 6–8) were isolated from HeLa and HEK293T cells and subjected to western blot analysis either immediately (lanes 1, 2; 5, 6) or after treatment with proteinase-K (lanes 3, 7). Mitochondria were lysed with Triton X-100 to confirm the sensitivity of marker proteins to the protease (lanes 4, 8). Mitochondrial release factor-1a (mtRF1a) was used as a mitochondrial matrix marker and ribosomal protein-S6 (S6-RP) as a cytosolic marker. Purified FL (lane 9) and an ICT1 deleted of N-terminal 29 residues (Δ29, lane 10) are shown in comparison with the endogenous protein. (**B**–**E**) Depletion of ICT1 inhibits cell growth, impairs mitochondrial protein synthesis and decreases mitochondrial respiratory chain complexes. HeLa cells in standard glucose media were transfected with either of two siRNAs directed to ICT1 transcript (si-ICT1A or B) or a non-targeting control (si-NT), and cell numbers were counted at 3-day intervals. Standard errors were derived from three independent experiments (**C**). Cell lysates were isolated from non-targeting and ICT1-depleted cells (3 days) and subjected to western blotting for ICT1 (**B**) and various markers (**D**). The relative levels for the MRP MRPL3 and respiratory components NDUFB8 or COX2 were quantified (lower panel) with standard errors derived from three independent repeats. (**E**) After 3-day siRNA-mediated depletion, cells were subjected to metabolic labelling of mitochondrial proteins for 15 min after inhibition of cytosolic protein synthesis. Aliquots (50 µg) were separated by 15% SDS–PAGE and exposed to a PhosphorImager. Proteins are identified by comparison against those reported by Chomyn (1996). A section of the gel stained with Coomassie blue (CBB) following exposure is shown to indicate even loading of cell lysate.

tion in cell number even when grown on standard, mainly glycolytic media (Figure 1C). To confirm that effects were specific and not off-target, cells lacking mtDNA (rho^0 cells) were also transfected with ICT1-specific siRNA and control siRNAs. The rationale being, as rho^0 cells lack mitochondrial gene expression and are still able to grow on glucose media supplemented with uridine and pyruvate, depletion of any protein involved solely in mitochondrial gene expression should have minimal effect. Accordingly, siRNA-mediated depletion of β-actin or HSP70 severely compromised the growth of rho^0 cells, whereas growth was unaffected by depletion of ICT1 or the mitochondrial translation factor mtEF-Tu (Supplementary Figure S1). These data are strongly indicative that ICT1 functions in mitochondrial gene expression.

After only 3 days of ICT1 depletion, a decrease in the markers of the highly stable mitochondrial respiratory chain complex-I (NDUFB8) and IV (COX2) was confirmed by western blotting of HeLa lysates (Figure 1D). Interestingly, a similar decrease was also noted for the MRP MRPL3, indicating that levels of mitoribosome and possibly rates of mitochondrial protein synthesis may be compromised. Therefore, *de novo* synthesis of mitochondrial translation products was assessed by *in vivo* metabolic labelling. Figure 1E shows that in the ICT1-depleted cells ^{35}S-met incorporation is indeed reduced.

ICT1 is a member of the large mitoribosomal subunit

Why does loss of ICT1 lead to reduction in mitochondrial protein synthesis? To investigate this question and to determine what components of the mitochondrial matrix associated with ICT1, a FLAG-tagged ICT1 was inducibly expressed in human HEK293T cells, facilitating IP. As shown in Figure 2A, silver staining uncovered a large number of proteins, similar to a previous profile where tagged mtRRF had immunoprecipitated the mitoribosome and associated proteins (Rorbach *et al*, 2008). Western blot analysis (Figure 2B) confirmed the presence of numerous MRPs and the predicted trace amounts of mtRRF. From proteomic data of the complete eluate, more than 200 mitochondrial proteins were identified (Supplementary Table S1), the MRPs being the most abundant (Supplementary Table S2); consistent with ICT1 interacting with entire mitoribosomes. As a second method to determine whether ICT1 was a component of the mitoribosome, complexes from untransfected cells were separated by isokinetic sucrose density gradients and fractions were subjected to blotting (Figure 2C). ICT1 co-sediments with MRPL3 and MRPL12, both components of the 39S mt-LSU. As has been found in other reports (Nolden *et al*, 2005; Williams *et al*, 2005), the mitochondrial monosome is not easily identified in cell or mitochondrial lysates by western blot after density-gradient centrifugation. This was also evidenced here by the lack of detectable small subunit marker DAP3 in the more dense fractions (Figure 2C, fractions 7–10). Therefore, to resolve this issue, we pre-concentrated samples by first immunoprecipitating mt-LSU and monosomes from mitochondrial lysates using FLAG-ICT1 and subjected the entire eluate to an identical gradient centrifugation. Fractions were then assessed by silver staining and western blotting. A similar distribution profile is still seen for ICT1 and MRPL3 (excluding free ICT1 caused by overexpression) (Figure 2D). Crucially, however, DAP3 is now visible in fractions 7–9, defining the monosomal fractions. Therefore, ICT1 behaves as an integral member of the 39S mt-LSU and a component of the intact 55S monosome.

Further support for ICT1 being an integral component of the 39S mt-LSU, was obtained from ICT1-depleted HeLa cells. Lysate was subjected to a similar isokinetic gradient, showing that the mt-LSU marker MRPL3, although present, was shifted into less dense fractions as compared with that in cells treated with non-targeting control siRNA (si-NT; Figure 2E). By contrast, the profile of the 28S mt-SSU protein DAP3 was unchanged, implying that only assembly of the mt-LSU and not the mt-SSU is affected on ICT1 depletion.

To confirm that the decrease in mt-LSU assembly observed in ICT1-depleted cells caused a concomitant decrease in the level of intact monosome, we used a cell line that expresses a FLAG-tagged component of the mt-SSU, MRPS27, that was able to IP both mt-SSU and entire monosome. After 3 days of ICT1 depletion and MRPS27-FLAG induction, FLAG-IP was performed and eluates were blotted (Figure 2F). Levels of DAP3 were unaffected by ICT1 depletion. However, anti-MRPL3 and MRPL12 antibodies showed a 60% reduction of each of these proteins in the ICT1-depleted cells, consistent with a decrease in the monosome formation, presumably due to decreased mt-LSU assembly. This was also consistent with the decreased ^{35}S metabolic labelling of mitochondrial proteins as shown in Figure 1E. Finally, to show that mitoribosomal association of ICT1 was not simply mediated by the FLAG tag, similar isokinetic gradients were used to separate the immunoprecipitated eluate from cells expressing MRPL20-FLAG. When correctly assembled, this FLAG-tagged protein was able to IP mt-LSU, assembly intermediates and intact monosome. As show in Figure 2G, ICT1 was clearly associated with mt-LSU and monosome. These data confirm that ICT1 is an important component of the complete monosome.

ICT1 is a ribosome-bound, codon-independent PTH

ICT1 is an integral component of the mitoribosome, but on the basis of homology it is predicted to be a ribosome-dependent PTH/translation release factor. This is surprising, as to our knowledge, no other PTH has been shown to be an integral ribosomal component. There are now four proteins classified as members of the mitochondrial release factor family, namely mtRF1a, mtRF1, ICT1 and another uncharacterised protein C12orf65 (Figure 3B). Curiously, both ICT1 and C12orf 65 have lost the two domains involved in codon recognition (α5 and PXT/SPF domain), potentially resulting in the dangerous situation of release factors that lack codon specificity. However, none of our previous IPs identified C12orf65 as a co-precipitant with mitoribosome components (data not shown). To determine whether ICT1 could promote hydrolysis of the ester bond between the growing peptide and the P-site tRNA, we used a well-established assay using isolated *E. coli* ribosomes, tritiated fmet-$tRNA^{Met}$, synthetic codons and purified ICT1 (Caskey *et al*, 1971; Tate and Caskey, 1990; Soleimanpour-Lichaei *et al*, 2007). In comparison to the exquisite codon selectivity of mtRF1a, ICT1 promiscuously promoted the release of formylmethionine from its P-site tRNA irrespective of the codon sequence used to programme the assay and indeed even in the absence of codons in the A-site (Figure 3C). To determine whether ICT1 possessed a direct ribosome-independent PTH activity, or whether it functioned specifically to promote ribosome-

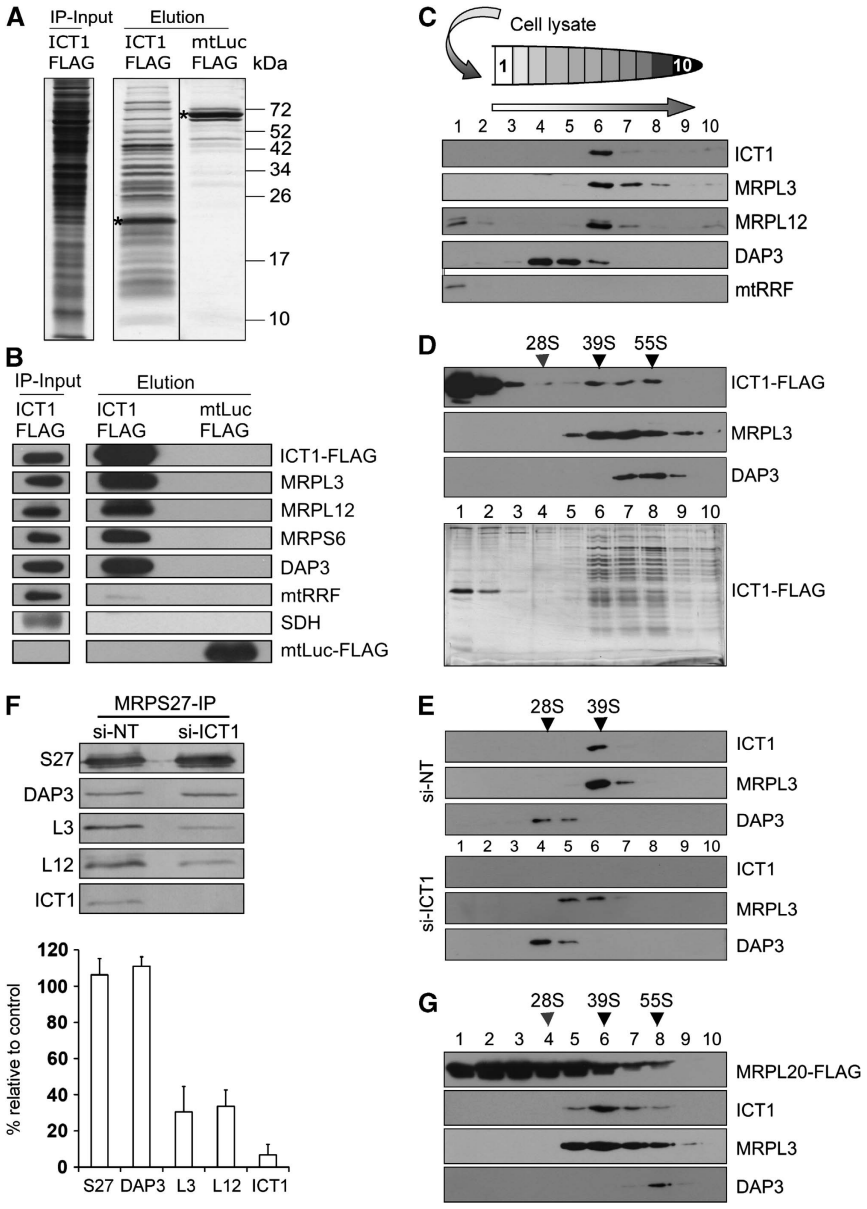

Figure 2 ICT1 is an integral component of the mitoribosome. (**A**, **B**) FLAG-tagged ICT1 immunoprecipitates mitoribosomes. HEK293T cells expressing FLAG-tagged ICT1 or mitochondrially localised luciferase (mtLuc-FLAG) were induced for 3 days; mitochondria were isolated, lysed and subjected to IP as detailed. The eluate and mitochondrial lysate before IP (IP-input) were separated by 15% SDS–PAGE and visualised by silver staining. * designates the FLAG protein. (**B**) Aliquots of the eluates were also subjected to western blot analysis with the indicated antibodies: MRPL3, MRPL12, MRPS6 and DAP3 as mitoribosomal markers; mtRRF, mitoribosome recycling factor; SDH, 70-kDa component of complex-II. (**C**) ICT1 co-sediments with the large mitoribosomal subunit. HeLa cells were lysed (600 μg), separated through a 10–30% sucrose gradient and fractionated as detailed (HeLa and HEK293T lysates gave identical separations). Components of the 39S mt-LSU (MRPL3, MRPL12) and 28S mt-SSU (DAP3) mitoribosomal subunits were visualised by western blotting. On immediate lysis, mtRRF is used as a matrix-soluble marker. (**D**) ICT1 also co-sediments with the intact monosome. Mitochondria (3 mg) of ICT1-FLAG-expressing HEK293T cells were subjected to FLAG IP; the entire eluate was separated by isokinetic density gradients and fractions were blotted as detailed above or visualised by silver staining (lower panel). Mitochondrial SSU (DAP3) and mt-LSU (MRPL3) MRPs are visualised. The approximate indicators for 28S mt-SSU, 39S mt-LSU and 55S monosome are shown and were determined as described under Materials and methods. (**E**) ICT1 is an integral member of 39S mt-LSU. Cell lysates (600 μg) from ICT1-depleted (si-ICT1B) or non-targeted control cells (si-NT) were separated by isokinetic gradients and proteins were visualised in the fractions by western blotting as described. Sedimentation markers were identified as above. (**F**) Loss of ICT1 causes depletion of the monosome. Cells expressing MRPS27-FLAG were treated with si-NT or si-ICT1B, after which IP was performed. To assess monosome formation, levels of MRPL3 and MRPL12 were quantified by western blotting of three individual experiments (right panel; MRPL3 $P=0.001$, MRPL12 $P<0.001$, MRPS27 $P=0.3$). (**G**) ICT1's association with mitoribosomes is not FLAG-dependent. Mitochondria from cells expressing MRPL20-FLAG were subjected to FLAG IP and the eluate was analysed by western blotting after isokinetic density gradients as described in panel **D**.

dependent hydrolysis, purified ICT1 was incubated with f[^{3}H]met tRNA^{met} in the absence of ribosomes before extraction and estimation of standard release factor activity. No significant increase in counts was noted over background, confirming that no significant hydrolysis of the substrate occurred in the absence of the ribosome (Figure 3C).

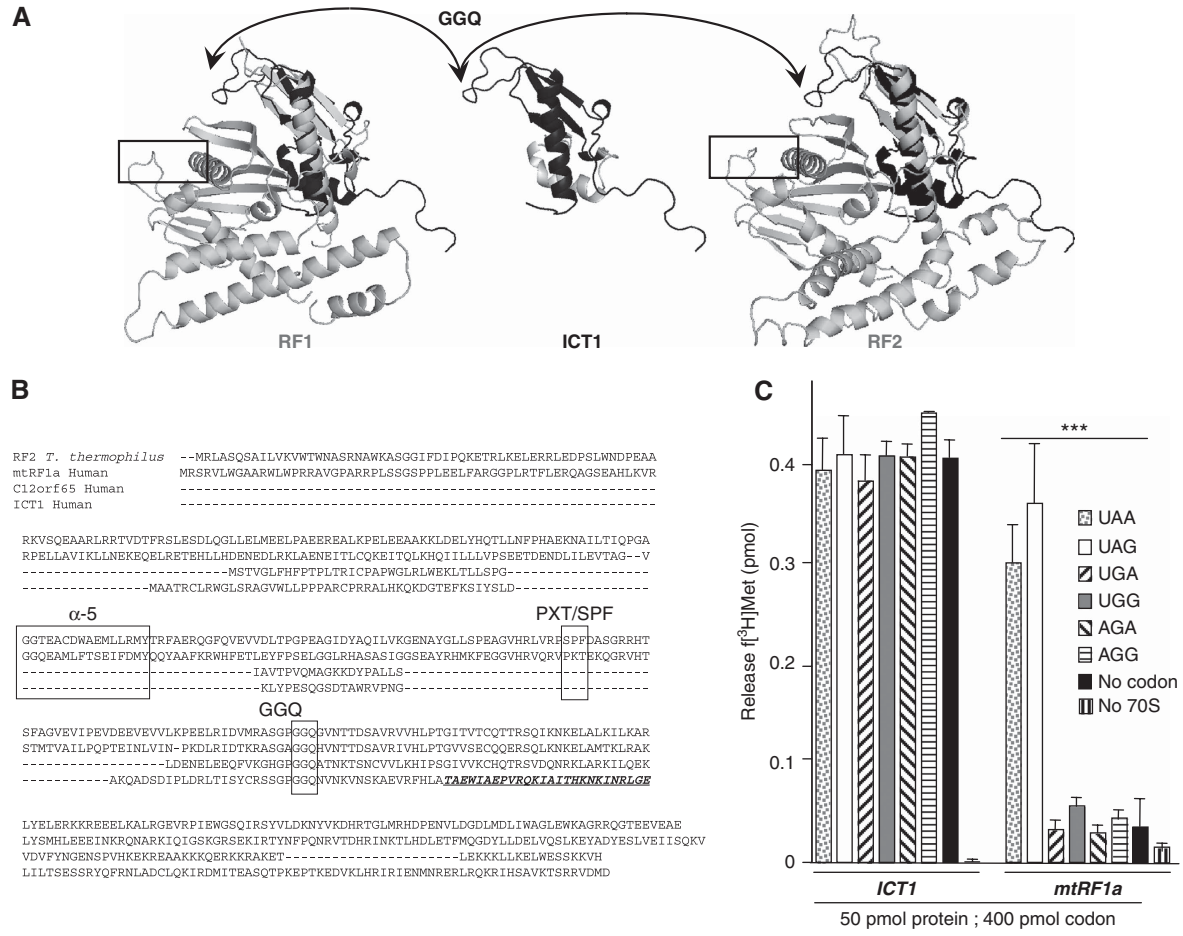

Figure 3 ICT1 is a codon-independent PTH. (**A**) Structural comparisons between ICT1 and members of RF1 or RF2. Only limited structure is available for murine ICT1 (centre, PDB 1J26 unpublished structural genomics output), but this can be superimposed using Topmatch (Sippl and Wiederstein, 2008) onto either RF family (left *T. maritima* PDB 1RQ0 (Shin *et al*, 2004); right *T. thermophilus* PDB 2IHR (Zoldak *et al*, 2007)), making it unclear as to its evolutionary origin. The arrows show the ICT 1GGQ motif and the boxes enclose the codon recognition domains (Ito *et al*, 2000; Laurberg *et al*, 2008). (**B**) Primary sequence comparisons of ICT1 and translation release factor members. Representatives of the release factor families are shown; RF1 (human mtRF1a), RF2 (*T. thermophilus*) aligned with human sequences for ICT1 and a fourth member of the mitochondrial release factor family, C12orf65. Three regions are highlighted; the GGQ motif conferring PTH activity, and α-5/tripeptide domains that are implicated in codon recognition. The latter two domains are absent in ICT1 and C12orf65. There are two other families of PTHs, PTH1 and PTH2 (reviewed by Das and Varshney, 2006), which are predicted to be represented in the human mitochondrion by PTRH1 and PTRH2 (uniprot Q86Y79 and Q9Y3E5, respectively). These protein families function independently of the ribosome and on the basis of comparison of their three-dimensional structures (data not shown), are not homologous to the ribosome-dependent PTH family that contains ICT1. (**C**) ICT1 has codon-independent and ribosome-dependent translation release factor activity. *E. coli* ribosomes were programmed with tritiated P-site fmet-tRNA^{Met} and A-site codons as indicated (detailed under Materials and methods). Activity was measured as hydrolysis of f[^{3}H]met from its cognate tRNA^{Met} and is represented as pmol f[^{3}H]met released. Non-limiting amounts of protein (50 pmol) and RNA triplet (400 pmol) were used in the assay where required, with mtRF1a as a positive control. Activities are also evident where ribosomes were programmed with no codon or were absent from the assay, entirely. Reactions lacking 70S ribosomes contained the UAA triplet. Standard errors were calculated from a minimum of eight repeats; $***P<0.001$.

A mutation of the GGQ domain of ICT1 causes loss of cell viability

ICT1 is an essential MRP with a ribosome-dependent yet codon-independent PTH activity, *in vitro*. Is it possible that ICT1 needs to maintain this activity when it is assembled into the mitoribosome, *in vivo*?

PTH activity of release factors is mediated by the domain containing the tripeptide motif GGQ (Frolova *et al*, 1999; Figure 3A and B). It has been shown that mutations in either of the two glycine residues completely abolishes *in vitro* PTH activity while retaining the structural integrity of the protein (Frolova *et al*, 1999). To determine whether the GGQ domain is critical for ICT1's function, we reproduced two of these GGQ mutants by site-directed mutagenesis. First, recombinant ICT1^{GSQ} and ICT1^{AGQ} were purified, monodispersion was confirmed by dynamic light scattering, and then they were subjected to the release assay described above (Figure 4A). Each retained ~1% of peptide-release activity (GSQ 1.1%, AGQ 0.8% residual activity). Having confirmed the requirement of the GGQ domain for the PTH activity of ICT1, it was then possible to assess the importance of the PTH activity *in vivo*. If PTH activity is crucial then replacement of wild-type ICT1 with ICT1^{GSQ} would be predicted to compromise mitochondrial gene expression, leading to reduced growth on galactose. Consequently, an HEK293T cell line was engineered to

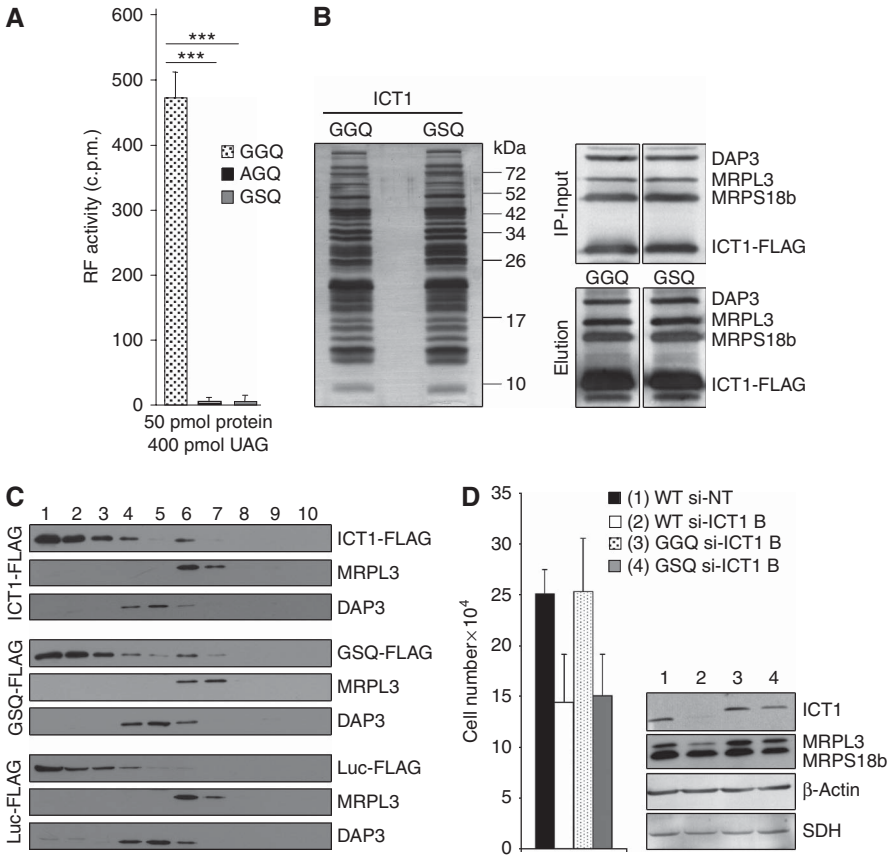

Figure 4 Mutations of the GGQ domain can affect cell viability. (**A**) GGQ-mutant derivatives of ICT1 have lost PTH activity. Wild type and mutant derivatives (AGQ, GSQ) of Δ29 ICT1 were expressed as GST-fusion proteins, cleaved and assayed for f[^{3}H]met release as described in Figure 3. All assays were performed with UAG codons and purified proteins, all equally monodispersed as assessed by dynamic light scattering (data not shown); ***$P<0.001$. (**B**, **C**) Mutated ICT1 is assembled into the mitoribosome. (B) FLAG-tagged wild-type (GGQ) and mutant (GSQ) ICT1 were expressed in HEK293T cells and the eluate from FLAG IP was subjected to silver staining (left panel) or western blotting (right panels) after denaturing gel electrophoresis. Molecular weight markers are indicated. The western blots of mitochondrial lysates shown are those before (IP-input) and after (Elution) FLAG IP of the wild type and mutated ICT1 derivatives. (**C**) Cell lysates were subjected to isokinetic gradient analysis before fractionation and western blotting, as described. The upper three panels are from wild-type ICT1-FLAG, the middle panels from mutated GSQ ICT1-FLAG and the lower panels from control mtLuc-FLAG. (**D**) A mutation of the GGQ domain affects cell growth. Non-targeting si-RNA-treated cells served as negative control (1, WT si-NT). Cells with only endogenous ICT1 (WT), or overexpressing normal (GGQ) or mutated (GSQ) ICT1 were treated for 4 days with 10 nM si-ICT1B to deplete endogenous ICT1 (2–4), whereas lane-2 represented the fully depleted control (WT si-ICT1B). Growth rates were compared by counting populations after 3 days of siRNA treatment; 3 versus 4: $P<0.01$; 1 versus 4: $P<0.001$. Western blots of lysates (4 days of siRNA treatment) after interrogation with the indicated antibodies are shown to the right.

express a FLAG-tagged version of ICT1^{GSQ} and compared with the wild-type ICT1-FLAG expressor. On induction, the ICT1 mutant was incorporated into mitoribosomes, which were assembled at levels similar to that in the wild-type transfected control (Figure 4B and C), but induction resulted in a substantial overexpression of ICT1^{GSQ} such that the majority of the protein remained free and not mitoribosome-bound (Figure 4C). A similar overexpression was also noted on induction of wild-type ICT1-FLAG (Figure 4C, upper panels), which in itself produced a mild growth phenotype. To reduce the levels of the overexpressed protein to that of the endogenous untransfected controls and concomitantly deplete the endogenous ICT1, serial dilutions of si-ICT1B were used. A concentration of siRNA was achieved that resulted in levels of FLAG-tagged ICT1 equivalent to that of the untransfected controls (10 nM; Supplementary Figure S2). Using this strategy, growth rates of these various cell lines were compared, uncovering a slower doubling time in the ICT1^{GSQ} mutant, confirming that ICT1 requires a functional GGQ domain to maintain cell viability (Figure 4D, 3 *cf.* 4).

Discussion

Following stringent purification methods, isolation of bovine mt-SSU, mt-LSU and the 55S monosome has allowed characterisation of many constituents and a low-resolution structure (Sharma *et al*, 2003). These data are in agreement that the mammalian mitoribosome differs substantially from other ribosomes that have been characterised. In particular, the 30:70 (w:w) protein-to-RNA ratio is reversed, with only one reduced rRNA component for each subunit and an increased number of protein factors, as determined by initial LCMS, resulting in a larger, more porous structure (O'Brien, 2002). Were some MRPs missed in this original screen? Our data indicates that ICT1 is indeed one such protein.

ICT1 is classified bioinformatically as one of four members of the prokaryotic/mitochondrial release factor family. It is

now known that all 13 mitochondrial encoded polypeptides terminate translation with the aid of mtRF1a (Soleimanpour-Lichaei *et al*, 2007; Temperley *et al*, 2010). A third member, mtRF1, has yet to be shown to have release-factor activity, but, similar to ICT1 and mtRF1a, is an essential mitochondrial protein. The final member, C12orf65 currently has an unknown function, although with a mitochondrial location (unpublished observation). ICT1 and C12orf65 are significantly smaller than the RF1 and RF2 types of class-I bacterial release factors. Alignments highlight that this loss occurs in three main regions: the N-terminus and the two sections (tripeptide motif and the tip of the α-5 helix) that come into close contact with the mRNA in the ribosomal A-site and determine the STOP codon specificity (Figure 3). Lack of these domains is consistent with the loss of codon specificity noted for ICT1 in this study. By contrast, there is striking sequence conservation of the GGQ motif. By superimposing the available structure of the mouse ICT1 on RF1 (*Thermotoga maritima*) and RF2 (*Thermus thermophilus*), it is clear that in all three proteins the GGQ motif reside in a flexible loop (Figure 3A). Furthermore, although there is reduced sequence identity in this domain, the structural features surrounding this motif are highly conserved and important in positioning the GGQ at the surface of the RF (Frolova *et al*, 1999). This suggests that maintaining the way in which the GGQ motif is presented to the substrate is important. Curiously, ICT1 contains a stretch of 25 residues that has no sequence similarity to C12orf65 or the other RFs (Figure 3B, bold, italics). In the structural superimpositions, this feature can also be distinguished, primarily in the unmatched horizontal helix in ICT1. As this feature is lacking in release factors that interact transiently with the ribosome and also from C12orf65 that does not IP with the mitoribosome, it is possible that this feature is involved in the integration of ICT1 into the mt-LSU.

What could be the function of a ribosome-bound, codon-independent PTH and how could its capacity for indiscriminate peptide release be controlled and positively harnessed? There are several possibilities. First, if mitoribosomes initiate translation on 3′ truncated or mutated mt-mRNA that lack termination codons, the terminus of the mRNA will eventually reach the P-site and be retained by the anchoring peptidyl-tRNA but will leave an A-site devoid of mRNA or release factors to trigger recycling. In the absence of a mitochondrial analogue to the bacterial tmRNA system that rescues stalled ribosomes (Keiler *et al*, 1996), PTH activity will be needed to liberate the peptide from the peptidyl-tRNA, forming a substrate that can be recycled. A similar activity would be necessary to help recycle mitoribosomes that have prematurely stalled. Alternatively, many genetic studies have highlighted the necessity of salvaging tRNA species from prematurely released peptidyl-tRNAs generated through abortive elongation events during protein synthesis, a function normally provided by a freely soluble PTH (reviewed by Das and Varshney, 2006). To date no human mitochondrial protein is known to show this activity (although candidates exist). Our data are consistent with mammalian mitoribosomes streamlining this process by incorporation of a codon-independent PTH activity that can recognise and hydrolyse peptidyl-tRNAs caught during their premature release from the mitoribosome (or even from the mt-LSU if the stalled ribosome dissociates, as has been suggested for *E. coli* ribosomes by Varshney and co-workers (Singh *et al*, 2008)).

Cryo-EM data of mammalian mitoribosomes uncovers a feature absent in the bacterial ribosomes. This is a surface cavity in the mt-LSU near the exit tunnel, described as the polypeptide-accessible site (PAS) that prematurely exposes the nascent peptide to the solvent (Sharma *et al*, 2003; Figure 5A). It is created by loss of rRNA regions and proteins orthologous to bacterial components (O'Brien, 2002). Integration of ICT1 at this mitoribosomal site could allow access to peptidyl-tRNAs caught on release from the mitoribosome after aborted elongation (Figure 5C). Ribosomes use substrate-induced fit mechanisms to promote conformation changes that facilitate either peptide bond formation or hydrolysis (Schmeing *et al*, 2005). Premature release of a peptidyl-tRNA may cause ribosomal distortion, resulting in

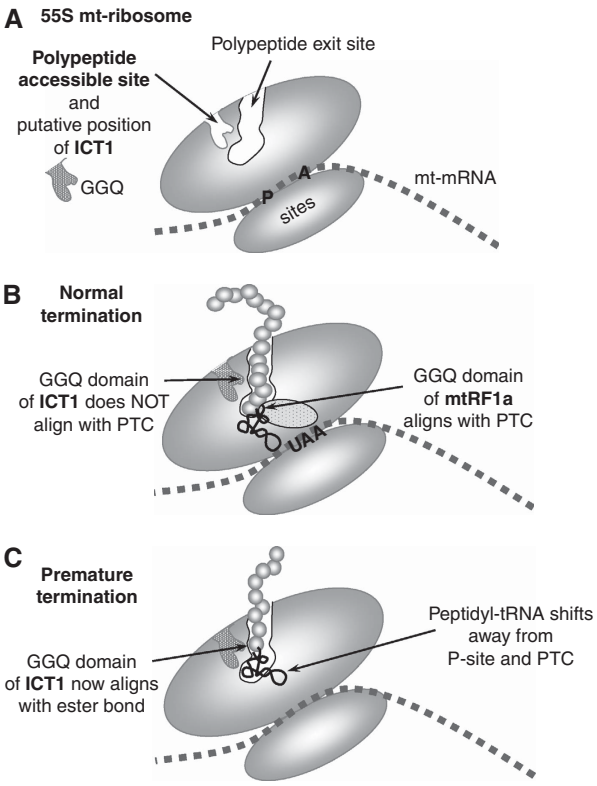

Figure 5 A schematic representation of the putative position and function of ICT1 in the human mitochondrial ribosome. (**A**) A simplified cartoon of the 55S mitochondrial ribosome indicating the polypeptide exit tunnel and site (PES) and the PAS in the large subunit as defined by Sharma *et al* (2003). No orthologues of the proteins that would occupy the PAS have been found in mammalian mitochondria, and we postulate that is where ICT1 is positioned with the GGQ domain inserted deep into the pocket. Sites for the aminoacyl (A) and peptidyl (P) tRNAs are shown. The mt-mRNA is depicted between the large and small mt-ribosomal subunits. (**B**) Under conditions of normal termination, the ester bond of the peptidyl-tRNA is positioned close to the peptidyl-transferase centre (PTC); the release factor, mtRF1a, enters through the A-site, recognising the stop codon (UAA) and aligning the GGQ domain at the PTC to promote hydrolysis of the ester bond and release of the nascent peptide. (**C**) Where abortive elongation occurs, the peptidyl-tRNA may drop away from the P-site towards the PES, aligning the ester bond close to the GGQ domain of ICT1, promoting cleavage of the tRNA, which allows both mt-tRNA and truncated peptide to be released from the mitochondrial monosome (or potentially from dissociated 39S mt-LSU).

the juxtaposition of the GGQ motif and peptidyl-tRNA, promoting ester bond hydrolysis in a codon-independent manner. Crucially, this would release the tRNA for recharging. Clearly, to support any of these hypotheses, it would be of enormous benefit to generate high-resolution structural data to identify exactly where in the mitoribosome ICT1 is found. To date, there are only very limited structural data concerning the mammalian mitoribosome and producing such structural data is beyond the scope of this paper. Further experiments will be necessary to elucidate the exact role of this PTH activity; however, it is interesting to note that ICT1 is mitochondrial, has become incorporated into the mitoribosome, lost all stop codon specificity, but has acquired another function of equal importance to mitochondrial translation. Contrastingly, mtRF1a has retained its RF activity. It is tempting to speculate on what diverging fates may also have befallen the other two members of this family.

Materials and methods

Cell culture

Human HeLa cells were cultured (37°C, humidified 5% CO_2) in Eagle's MEM (Sigma) supplemented with 10% (v/v) foetal calf serum (FCS), 1 × non-essential amino acids (NEAA) and 2 mM L-glutamine. 143B.206 rho^0 osteosarcoma cells (provided by R Wiesner, University of Koeln) were propagated in Dulbecco's modified Eagle's medium supplemented with 10% (v/v) FCS, 50 μg/ml uridine and 1 × NEAA. Flp-InT-Rex-293 cells (HEK293T; Invitrogen) were grown in identical media supplemented with 10 μg/ml $Blasticidin^S$ and 100 μg/ml Zeocin (Invitrogen). Post-transfection selection was performed with $Hygromycin^B$ (100 μg/ml). For growth on respiratory substrates, the medium contained glucose-free DMEM (Gibco), 0.9 mg/ml galactose, 1 mM sodium pyruvate, 10% (v/v) FCS, NEAA and 2 mM L-glutamine. For growth curve analyses, the galactose medium included 50 μg/ml uridine.

Subcellular localisation

Human mitochondria or cell lysates were prepared in a homogenisation buffer (10 mM Tris–HCl (pH 7.4), 0.6 M mannitol, 1 mM EGTA) by differential centrifugation. Aliquots of mitochondria were treated with proteinase-K (4 μg/100 μg protein) for 30 min at 4°C and either lysed (1% final v/v Triton X-100) or treated with 1 mM PMSF before separation through 15% PAG and transfer to a PVDF membrane. Western blots were performed and developed as described by Soleimanpour-Lichaei *et al* (2007).

siRNA constructs and transfection

Three sequences targeting ICT1 were tested for efficiency of protein depletion. The nucleotide positions are relative to the reference sequence NM_001545.1; sense strands were as follows:

si-ICT1A 5′ CUAGAUCGCUUGACAAUAU dTdT 3′ (nt 222–240);
si-ICT1B 5′ GCCGCUAUCAGUUCCGGAA dTdT 3′ (nt 421–439) and
si-ICT1C 5′GGGUCCCGAAUGGUGCAAA dTdT 3′ (nt 181–199).

Experiments were performed with si-ICT1B unless otherwise specified. si-ICT1C was found to be ineffective. Transfections were performed with 20% confluent HeLa cells using Oligofectamine (Invitrogen) in Optimem-I medium (Gibco) with 0.2 μM siRNA. Reverse transfections were performed as described by Ovcharenko *et al* (2005) using approximately 12 000 HEK293T cell per cm^2 using Lipofectamine RNAiMAX (Invitrogen) in Optimem-I medium (10–33 nM siRNA). Custom and control non-targeting (NT; ref.: OR-0030-neg05) duplex siRNAs were purchased pre-annealed from Eurogentec.

In vivo mitochondrial protein synthesis

Mitochondrial protein synthesis in cultured cells was performed as described by Chomyn (1996) after addition of emetine and pulsed with [^{35}S]-methionine for 15 min. Aliquots (50 μg) of total cell protein were separated by 15% (w/v) SDS–PAGE. The gels were exposed to PhosphorImage cassettes and visualised using the ImageQuant software.

Production of FLAG- and GST-fusion constructs, transfection, expression and purification

The original human ICT1 clone was obtained from MGC (MGC:21251; accession no. BC015335) and encodes the only isoform to be described. All constructs were prepared by PCR using the MGC clone as template. Constructs to facilitate inducible expression of C-terminal FLAG-tagged ICT1 were prepared by generating an amplicon from nt 2 to 620 using the following primers: 5′-CTTTCTTAAGCTTCCACCATGGCGGCCACCAGGTG-3′ and 5′-CTCTCCGATATCCTACTTATCGTCGTCATCCTTGTAATCGTCC ATGTCGACCCTC-3′. The amplicon and pcDNA5/FRT/TO (Invitrogen) were digested with *Hin*dIII/*Eco*RV and ligated. C-terminal FLAG-tagged MRPS27 and MRPL20 were constructed by PCR amplification from MGC clones 6009616 and 3542715 (accession nos. BC064902 and BC009515), respectively, using primers 5′-CTTT CTTGGATCCCCACCATGGCTGCCTCCATAGTGCG-3′ and 5′-CTCTCT CTCGAGCTACTTATCGTCGTCATCCTTGTAATCGGCAGATGCCTTTGC TGCTT-3′ (MRPS27 Forward and Reverse) or 5-TACTATAAGCTTAC CATGGTCTTCCTCACCG-3 and 5-ATACTACTCGAGCTACTTATCGTC GTCATCCTTGTAATCGTGGTACTGCACCACTC-3 (MRPL20 Forward and Reverse). The amplicons were digested with *Bam*HI/*Xho*I or *Hin*dIII/*Xho*I, respectively, and ligated into similarly digested pcDNA5/FRT/TO. The GST-fusion constructs were made of the FL or N-terminal-deleted (Δ29) ICT1. These were generated by amplifying nt 2 or 90–623, respectively. The forward primers incorporated a *Bam*HI site (FL Forward 5′-CTTTCTTGGATCCAT GGCGGCCACCAGGTG-3′; Δ29 Forward 5′-CTTTCTTGGATCCCTG CACAAGCAGAAAGACG-3′) and the same reverse primer was used for both amplification reactions (Reverse 5′-CTCTCCCTCGAGT CAGTCCATGTCGACCCTC-3′ containing an *Xho*I site). The amplicons and vectors were digested to allow in-frame downstream fusion of ICT1-GST in pGEX-6P-1 (GE Healthcare). The constructs derived from pGEX-6P-1 or pcDNA5/FRT/TO were used for transfection of *E. coli* Rosetta pLysS (Merck Biosciences) or HEK293T cells, respectively. Bacteria were induced, and protein was purified and cleaved from GST using PreScission Protease exactly as previously described for mtRRF (Rorbach *et al*, 2008). Bacterial expression of both FL GST-ICT1-fusion protein and Δ29 was deleterious to growth, but was not lethal. Human HEK293T cells were transfected at ~50% confluence with the vectors pOG44 and pcDNA5/FRT/TO containing sequences of the genes to be expressed (FLAG-tagged ICT1, mtLuc and derivatives) as previously described (Soleimanpour-Lichaei *et al*, 2007).

Dynamic light scattering

Dynamic light scattering measurements were performed using a commercial Zetasizer 1600 (Malvern Instruments) equipped with a He–Ne laser (633 nm, 5 mW). Aliquots (20 μl) of protein samples (concentrations of 0.1–1 mg/ml) were pipetted into low-volume glass cuvettes and equilibrated for 3 min in the apparatus before measurement. All samples were measured a minimum of five times at 25°C for 70 s.

Affinity purification and elution of FLAG peptides

Mitochondria were isolated from HEK293T cells expressing FLAG derivatives and treated with DNase-I (0.5 U/mg mitochondria; 15 min RT) and proteinase-K (5 μg/mg mitochondria; 30 min 4°C) followed by 1 mM PMSF inhibition. The pelleted mitochondria were washed in a homogenisation buffer, treated with digitonin to remove the outer membrane (400 μg/mg mitochondria), washed and resuspended in a lysis buffer (50 mM Tris–HCl (pH 7.4), 150 mM NaCl, 10 mM $MgCl_2$, 1 mM EDTA, 1% (v/v) TX-100, 1 × protease inhibitor cocktail (Roche), 1 mM PMSF). IP was performed using an anti-FLAG M2-agarose affinity gel following manufacturer's recommendations (Sigma Aldrich, St Louis, MO, USA). Elution was performed using 5 μg of 3 × FLAG peptide per 100 μl of an elution buffer.

LC MS/MS analysis of negative control and ICT1 IP

The immunopurification of ICT1 and negative control (IP eluate from the lysate of untransfected HEK293T cells subjected to the identical IP protocol with anti-FLAG M2-agarose) were separated using SDS–PAGE. Individual gel lanes were cut into three bands and were in-gel digested as described elsewhere (Wilm *et al*, 1996). The resulting peptide solutions were desalted and concentrated offline using STAGE tips (Rappsilber *et al*, 2003). Measurements were performed using an Agilent 1100 nanoflow system connected

through a nano-electrospray ion source to a 7T linear ion-trap Fourier transform ion cyclotron resonance mass spectrometer (LTQ FT ULTRA; Thermo Scientific). Peptide separations were performed using a 15-cm fused silica emitter (New Objective, PicoTip Emitter; tip: 8 ± 1 μm, ID: 100 μm, FS360-100-8-N-5-C15) packed with reversed-phase ReproSil-Pur C18AQ 3-μm resin purchased from Dr Maisch GmbH. Samples were loaded directly onto the analytical column at a flow of 600 nl/min eluent-A (3% acetonitrile, 0.5% acetic acid). Bound peptides were eluted from the column at a rate of 300 nl/min using an LC gradient of 10–40% eluent-B (80% v/v acetonitrile, 0.5% acetic acid) in 60 min, followed by a steep gradient of 40–100% eluent-B in 5 min. The mass spectrometer was programmed to select the top four most abundant ions from each survey scan in the ICR cell for subsequent fragmentation analysis using collision-induced dissociation (CID) in the linear ion trap. Only double and triple charged ions were selected for CID analysis, and dynamic exclusion with early expiration was enabled to prevent re-selection of previously fragmented ions.

MRP identification and data analysis

Precursor and fragment ions were extracted from raw data files using ExtractMSn (Thermo Scientific). Individual LC MS/MS data files of all three gel slices were combined for each sample before database search. Peptides were identified by automated database searches using Mascot (Matrix Science Mascot version 2.2) against the Refseq database (release 29) and a Refseq reverse database for automated validation using false-discovery rate calculations. Database searches were performed with a 20-p.p.m. precursor ion tolerance and 0.8-Da tolerance for MS/MS fragment ions using the following specifications: tryptic cleavage allowing one missed cleavage, carbamidomethylation (C) as fixed modification, and allowing deamidation (NQ) and oxidation (M) as variable modifications. Subsequent peptide identifications were blasted against the Refseq database and validated by false-discovery rate calculation using the PROVALT software (Weatherly *et al*, 2005). PROVALT was set to calculate peptide score cut-offs to achieve a calculated $<1\%$ false-discovery rate. Protein abundances were calculated as exponentially modified Protein Abundance Index (emPAI) values according to Ishihama *et al* (2005). MRPs were marked as enriched if (i) they were identified with at least three unique peptides and (ii) when emPAI values were at least twofold higher in the ICT1 IP sample as compared with that in the negative control. The table represents only identified human MRPs that appear in the Refseq database.

Isokinetic sucrose-gradient analysis of mitochondrial ribosomes

Total cell lysates (0.5–0.7 mg in lysis buffer) or eluted immunoprecipitates were loaded on a linear sucrose gradient (1 ml 10–30% (v/v)) along with 50 mM Tris–HCl (pH 7.2), 10 mM $Mg(OAc)_2$, 40 mM NH_4Cl, 0.1 M KCl, 1 mM PMSF, and 50 μg/ml chloramphenicol, and centrifuged for 2 h 15 min at 100 000 g at 4°C. Fractions (100 μl) were collected and 10-μl aliquots were analysed directly by western blotting or silver staining as follows: PAG were fixed in 50% methanol for 1 h, followed by 15-min incubation in staining solution (0.8% (w/v) $AgNO_3$; 1.4% (v/v) NH_4OH; 0.075% (w/v) NaOH), three washes of 5 min each in nanopure dH_2O, and then developed in 0.055% (v/v) formaldehyde/0.005% (w/v) citric acid and fixed in 45% methanol/10% acetic acid.

Northern blot analysis for mitoribosomal subunit markers in gradient gel fractions

To identify the 28S mt-SSU and 39S mt-LSU in gradient fractions, the 12S and 16S mt-rRNA were visualised by northern blotting. RNA was prepared by phenol extraction from half of each gradient fraction. Northern blots were performed as described by Chrzanowska-Lightowlers *et al* (1994). Briefly, aliquots of RNA (5 μg) were electrophoresed through 1.2% agarose under denaturing conditions and transferred to GenescreenPlus membrane (NEN duPont) following the manufacturer's protocol. Probes were generated using random hexamers on PCR-generated templates corresponding to the internal regions of the 12S and 16S mt-rRNA. An estimate of 55S monosome was made from the position of the cytosolic 28S rRNA (representing the 60S cytosolic LSU) visualised on ethidium bromide staining of the agarose gel.

Mutagenesis of ICT1

Mutations in the GGQ tripeptide were introduced into the bacterial (AGQ, GSQ) and human (GSQ) ICT1 expression constructs following the QuikChange II site-directed mutagenesis protocol (Stratagene). The following primers and their complements were used; base changes from wild type are underlined: AGQ, 5′-GTA GTGGTCCTGCGGGGCAGAATG-3′; GSQ, 5′-GTGGTCCTGGGTCGCA GAATGTGAAC-3′.

In vitro release-factor assay

E. coli ribosomes were purified and assays were performed essentially as described by Tate and Caskey (1990) with modifications as detailed in reference Soleimanpour-Lichaei *et al* (2007). Briefly, an f[^{3}H]met-$tRNA^{met}$ substrate was made by combining 3.8 nmol L-[methyl-^{3}H]-methionine (GE Healthcare) and cold methionine up to a concentration of 21.8 nmol, 3.5 mM leucovorin (Sigma) as the formyl donor, 20 μM amino acids (Promega), 0.3 mg *N*-formylmethionine-specific tRNA (Sigma), 1.2 mM ATP, 1 mM DTT, 10 mM $MgCl_2$, in cacodylate buffer (100 mM, pH 6.8), and incubating for 30 min at 37°C. The ribosomal substrate (amounts given are per 50 μl of assay) was prepared by incubation of 70S ribosomes (5 pmol) with AUG (250 pmol) and f[^{3}H]met-$tRNA^{met}$ (2.5 pmol) in 20 mM Tris–HCl (pH 7.4), 10 mM $Mg(OAc)_2$ and 150 mM NH_4Cl at 30°C for 20 min. This 'activated' ribosomal substrate was stored on ice before interrogation with release factors for activities with selected codons. Reactions that lacked the 70S were otherwise identical.

Supplementary data

Supplementary data are available at *The EMBO Journal* Online (http://www.embojournal.org).

Acknowledgements

This work was supported by the Wellcome Trust (grant number 074454/Z/04/Z), Biotechnology and Biological Sciences Research Council (grant number BB/F011520/1) and the Netherlands Genomics Initiative (Horizon Programme).

Conflict of interest

The authors declare that they have no conflict of interest.

References

Caskey CT, Beaudet AL, Scolnick EM, Rosman M (1971) Hydrolysis of fMet-tRNA by peptidyl transferase. *Proc Natl Acad Sci USA* **68:** 3163–3167

Chomyn A (1996) *In vivo* labeling and analysis of human mitochondrial translation products. *Methods Enzymol* **264:** 197–211

Chrzanowska-Lightowlers ZM, Preiss T, Lightowlers RN (1994) Inhibition of mitochondrial protein synthesis promotes increased stability of nuclear-encoded respiratory gene transcripts. *J Biol Chem* **269:** 27322–27328

Das G, Varshney U (2006) Peptidyl-tRNA hydrolase and its critical role in protein biosynthesis. *Microbiology* **152:** 2191–2195

Frolova LY, Tsivkovskii RY, Sivolobova GF, Oparina NY, Serpinsky OI, Blinov VM, Tatkov SI, Kisselev LL (1999) Mutations in the highly conserved GGQ motif of class 1 polypeptide release factors abolish ability of human eRF1 to trigger peptidyl-tRNA hydrolysis. *RNA* **5:** 1014–1020

Ishihama Y, Oda Y, Tabata T, Sato T, Nagasu T, Rappsilber J, Mann M (2005) Exponentially modified protein abundance index (emPAI) for estimation of absolute protein amount in proteomics by the number of sequenced peptides per protein. *Mol Cell Proteomics* **4:** 1265–1272

Ito K, Uno M, Nakamura Y (2000) A tripeptide 'anticodon' deciphers stop codons in messenger RNA. *Nature* **403:** 680–684

Keiler KC, Waller PR, Sauer RT (1996) Role of a peptide tagging system in degradation of proteins synthesized from damaged messenger RNA. *Science* **271:** 990–993

Koc EC, Burkhart W, Blackburn K, Moyer MB, Schlatzer DM, Moseley A, Spremulli LL (2001) The large subunit of the mammalian mitochondrial ribosome. Analysis of the complement of ribosomal proteins present. *J Biol Chem* **276:** 43958–43969

Laurberg M, Asahara H, Korostelev A, Zhu J, Trakhanov S, Noller HF (2008) Structural basis for translation termination on the 70S ribosome. *Nature* **454:** 852–857

Nolden M, Ehses S, Koppen M, Bernacchia A, Rugarli EI, Langer T (2005) The m-AAA protease defective in hereditary spastic paraplegia controls ribosome assembly in mitochondria. *Cell* **123:** 277–289

O'Brien TW (2002) Evolution of a protein-rich mitochondrial ribosome: implications for human genetic disease. *Gene* **286:** 73–79

Ovcharenko D, Jarvis R, Hunicke-Smith S, Kelnar K, Brown D (2005) High-throughput RNAi screening *in vitro*: from cell lines to primary cells. *RNA* **11:** 985–993

Rappsilber J, Ishihama Y, Mann M (2003) Stop and go extraction tips for matrix-assisted laser desorption/ionization, nanoelectrospray, and LC/MS sample pretreatment in proteomics. *Anal Chem* **75:** 663–670

Rorbach J, Richter R, Wessels HJ, Wydro M, Pekalski M, Farhoud M, Kuhl I, Gaisne M, Bonnefoy N, Smeitink JA, Lightowlers RN, Chrzanowska-Lightowlers ZM (2008) The human mitochondrial ribosome recycling factor is essential for cell viability. *Nucleic Acids Res* **36:** 5787–5799

Schmeing TM, Huang KS, Strobel SA, Steitz TA (2005) An induced-fit mechanism to promote peptide bond formation and exclude hydrolysis of peptidyl-tRNA. *Nature* **438:** 520–524

Sharma MR, Koc EC, Datta PP, Booth TM, Spremulli LL, Agrawal RK (2003) Structure of the mammalian mitochondrial ribosome reveals an expanded functional role for its component proteins. *Cell* **115:** 97–108

Shin DH, Brandsen J, Jancarik J, Yokota H, Kim R, Kim SH (2004) Structural analyses of peptide release factor 1 from *Thermotoga maritima* reveal domain flexibility required for its interaction with the ribosome. *J Mol Biol* **341:** 227–239

Singh NS, Ahmad R, Sangeetha R, Varshney U (2008) Recycling of ribosomal complexes stalled at the step of elongation in *Escherichia coli*. *J Mol Biol* **380:** 451–464

Sippl MJ, Wiederstein M (2008) A note on difficult structure alignment problems. *Bioinformatics* **24:** 426–427

Soleimanpour-Lichaei HR, Kuhl I, Gaisne M, Passos JF, Wydro M, Rorbach J, Temperley R, Bonnefoy N, Tate W, Lightowlers R, Chrzanowska-Lightowlers Z (2007) mtRF1a is a human mitochondrial translation release factor decoding the major termination codons UAA and UAG. *Mol Cell* **27:** 745–757

Spremulli LL, Coursey A, Navratil T, Hunter SE (2004) Initiation and elongation factors in mammalian mitochondrial protein biosynthesis. *Prog Nucleic Acid Res Mol Biol* **77:** 211–261

Suzuki T, Terasaki M, Takemoto-Hori C, Hanada T, Ueda T, Wada A, Watanabe K (2001) Proteomic analysis of the mammalian mitochondrial ribosome. Identification of protein components in the 28S small subunit. *J Biol Chem* **276:** 33181–33195

Takemoto C, Spremulli LL, Benkowski LA, Ueda T, Yokogawa T, Watanabe K (2009) Unconventional decoding of the AUA codon as methionine by mitochondrial tRNAMet with the anticodon f5CAU as revealed with a mitochondrial *in vitro* translation system. *Nucleic Acids Res* **37:** 1616–1627

Tate WP, Caskey CT (1990) Termination of protein synthesis. In *Ribosomes and Protein Synthesis: a Practical Approach*, Spedding G (ed) Oxford: Oxford University Press, pp 81–100

Temperley R, Richter R, Dennerlein S, Lightowlers RN, Chrzanowska-Lightowlers ZMA (2010) Hungry codons promote frameshifting in human mitoribosomes. *Science* **327:** 301

Weatherly DB, Atwood III JA, Minning TA, Cavola C, Tarleton RL, Orlando R (2005) A Heuristic method for assigning a false-discovery rate for protein identifications from Mascot database search results. *Mol Cell Proteomics* **4:** 762–772

Williams EH, Bsat N, Bonnefoy N, Butler CA, Fox TD (2005) Alteration of a novel dispensable mitochondrial ribosomal small-subunit protein, Rsm28p, allows translation of defective COX2 mRNAs. *Eukaryot Cell* **4:** 337–345

Wilm M, Shevchenko A, Houthaeve T, Breit S, Schweigerer L, Fotsis T, Mann M (1996) Femtomole sequencing of proteins from polyacrylamide gels by nano-electrospray mass spectrometry. *Nature* **379:** 466–469

Yasukawa T, Suzuki T, Ishii N, Ohta S, Watanabe K (2001) Wobble modification defect in tRNA disturbs codon–anticodon interaction in a mitochondrial disease. *EMBO J* **20:** 4794–4802

Zoldak G, Redecke L, Svergun DI, Konarev PV, Voertler CS, Dobbek H, Sedlak E, Sprinzl M (2007) Release factors 2 from *Escherichia coli* and *Thermus thermophilus*: structural, spectroscopic and microcalorimetric studies. *Nucleic Acids Res* **35:** 1343–1353

Hungry Codons Promote Frameshifting in Human Mitochondrial Ribosomes

Richard Temperley,* Ricarda Richter,* Sven Dennerlein, Robert N. Lightowlers, Zofia M. Chrzanowska-Lightowlers†

Ribosome frameshifting, although rare, must occur in mitochondrial (mt) translation systems with interrupted open reading frames (ORFs) (*1*), but all human mt-ORFs are unbroken. However, we show that human mitoribosomes do invoke –1 frameshift at the AGA and AGG codons predicted to terminate the two ORFs in *MTCO1* and *MTND6*, respectively. As a consequence, both ORFs terminate in the standard UAG codon, necessitating the use of only a single mitochondrial release factor (*2*).

Frameshifting could be promoted by (i) paused mitoribosomes on AGA or AGG triplets, because no mt-tRNAs exist that recognize these codons; (ii) upstream "slippery" sequences that are poorly defined in human mt-mRNA; or (iii) a downstream stable secondary structure predicted for both *MTCO1* and *MTND6* (fig. S1) (*3*). To demonstrate that –1 frameshifting occurs in human mitochondria, we targeted RelE, a bacterial endoribonuclease that specifically cleaves mRNA in the ribosomal A site, to the mitochondrion [mtRelE (*4, 5*), fig. S2]. This enzyme shows marked sequence preference for standard termination codons UAG and UAA with negligible predicted recognition of AGA and AGG (*4*). On induction, the majority of *MTCO1* (68 ± 1.73%, $n = 3$) and *MTCO2* (70 ± 1.4%, $n = 3$) were intact (Fig. 1A, lanes 1 and 3), ruling out nonspecific transcript degradation by mtRelE. However, mitochondrial translation was reduced for most mt-proteins, including COX1 and ND6 (Fig. 1B). Depletion of the mitochondrial release factor mtRF1a stabilizes transcripts through extended association with the mitoribosome, whereas RelE promotes release of cleaved mRNA from bacterial ribosomes (*4*). Therefore, mtRelE expression would be predicted to abrogate mitoribosome-mediated protection. mtRF1a depletion in tandem with mtRelE expression does reduce the amounts of full-length mt-transcripts and markedly so for *MTCO1* (Fig. 1A, lanes 2 and 4), indicating both recognition and cleavage by mtRelE.

Northern analysis could not resolve whether the short 3′ untranslated regions (3′UTRs) present in *MTCO1* [72 nucleotides (nt)] had been lost post–mtRelE cleavage. *MTND5*, however, possesses a longer 3′UTR (568 nt). On mtRelE induction, a species was detected that is consistent with cleavage at the stop codon and loss of this 3′UTR (Fig. 1A, lanes 3 and 4 indicated by asterisks). Human mtDNA encodes two transcripts with overlapping ORFs, one containing *MTATP8/6* (*RNA14*) and one *MTND4L/4* (*RNA7*). Cleavage at the stop codon of the upstream ORF would release an RNA with a 5′-truncated downstream ORF. As with *MTND5*, novel species were detected on mtRelE expression. This was particularly apparent for *RNA14*, where *MTATP8* terminates in UAG, a preferred stop codon for RelE (Fig. 1A).

Fine mapping was performed on *MTCO2* and the 5′ truncated site of *MTATP6* in the bicistronic *RNA14* (fig. S3). This revealed mtRelE cleavage in the UAG termination codon uniquely between nucleotides 2 and 3 before readenylation. This result therefore allowed us to determine unequivocally whether termination of *MTCO1* occurred at the AGA or UAG codon; AGA termination codon would result in –AAAAUCUAGA$_n$, whereas UAG would produce –AAAAUCUAA$_n$. On sequencing, 10 clones from control cells reflected full-length 3′UTR containing *MTCO1* transcripts; two were truncations in the antisense tRNA^{Ser}, a commonly identified expressed sequence tag. This species was also found in two of the mtRelE samples. However, all the remaining 33 mtRelE clones terminated in –AAAAUCUA followed by readenylation (Fig. 1C), signifying that *MTCO1* terminates at UAG rather than AGA. These data suggest that mtRF1a is sufficient to terminate all 13 human mt-ORFs.

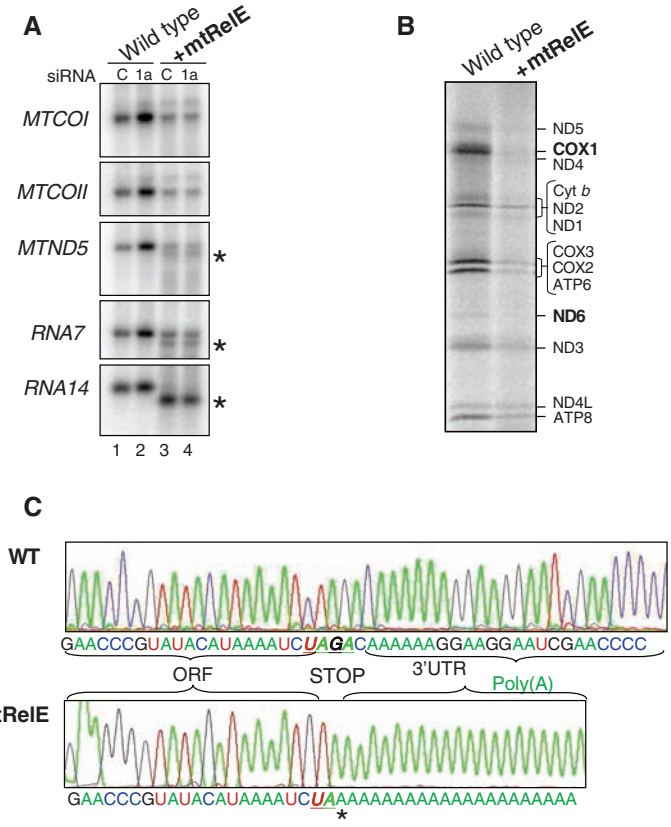

Fig. 1. Expression of mtRelE results in specific cleavage of mt-mRNA stop codons. Cells expressing mtRelE show (**A**) specific cleavage of mt-mRNA, generating novel products indicated by asterisks in both wild-type (WT) cells and those treated with siRNA to mtRF1a; (**B**) reduced metabolic labeling of mtDNA encoded gene products; and (**C**) cleavage of *MTCO1* transcripts specific at the UAG codon (33/35 clones, 2 were common truncated WT sequences) whereas WT cells retained the 3′UTR.

References and Notes

1. R. D. Russell, A. T. Beckenbach, *J. Mol. Evol.* **67**, 682 (2008).
2. H. R. Soleimanpour-Lichaei *et al.*, *Mol. Cell* **27**, 745 (2007).
3. R. F. Gesteland, R. B. Weiss, J. F. Atkins, *Science* **257**, 1640 (1992).
4. K. Pedersen *et al.*, *Cell* **112**, 131 (2003).
5. Materials and methods are available as supporting material on *Science* Online.

6. This work was supported by the Wellcome Trust (074454/Z/04/Z) and Biotechnology and Biological Sciences Research Council (BB/F011520/1). We thank K. Gerdes for kindly providing the clone and antibodies to bacterial RelE.

Supporting Online Material

www.sciencemag.org/cgi/content/full/327/5963/301/DC1
Materials and Methods
SOM Text
Figs. S1 to S4
Table S1
References and Notes

17 August 2009; accepted 30 November 2009
10.1126/science.1180674

The Mitochondrial Research Group, Institute for Ageing and Health, Newcastle University, Framlington Place, Newcastle upon Tyne NE2 4HH, UK.

*These authors contributed equally to this work.
†To whom correspondence should be addressed. E-mail: Z.Chrzanowska-Lightowlers@ncl.ac.uk

Published online 9 September 2008 *Nucleic Acids Research, 2008, Vol. 36, No. 18* ***5787–5799***
doi:10.1093/nar/gkn576

The human mitochondrial ribosome recycling factor is essential for cell viability

Joanna Rorbach[1], Ricarda Richter[1], Hans J. Wessels[2], Mateusz Wydro[1], Marcin Pekalski[3], Murtada Farhoud[2], Inge Kühl[4], Mauricette Gaisne[4], Nathalie Bonnefoy[4], Jan A. Smeitink[2], Robert N. Lightowlers[1,*] and Zofia M.A. Chrzanowska-Lightowlers[1]

[1]Mitochondrial Research Group, Institute of Cellular Medicine, Medical School, Newcastle University, Framlington Place, Newcastle upon Tyne, NE2 4HH, UK, [2]Nijmegen Centre for Mitochondrial Disorders, Radboud University Nijmegen Medical Centre, 6500 HB Nijmegen, The Netherlands, [3]Institute of Cellular Medicine, Medical School, Newcastle University, Framlington Place, Newcastle upon Tyne, NE2 4HH, UK and [4]Centre de Génétique Moléculaire, CNRS Batiment 26, Avenue de la Terrasse, 91198 Gif sur Yvette Cedex, France

Received June 9, 2008; Revised August 12, 2008; Accepted August 27, 2008

ABSTRACT

The molecular mechanism of human mitochondrial translation has yet to be fully described. We are particularly interested in understanding the process of translational termination and ribosome recycling in the mitochondrion. Several candidates have been implicated, for which subcellular localization and characterization have not been reported. Here, we show that the putative mitochondrial recycling factor, mtRRF, is indeed a mitochondrial protein. Expression of human mtRRF in fission yeast devoid of endogenous mitochondrial recycling factor suppresses the respiratory phenotype. Further, human mtRRF is able to associate with *Escherichia coli* ribosomes *in vitro* and can associate with mitoribosomes *in vivo*. Depletion of mtRRF in human cell lines is lethal, initially causing profound mitochondrial dysmorphism, aggregation of mitoribosomes, elevated mitochondrial superoxide production and eventual loss of OXPHOS complexes. Finally, mtRRF was shown to co-immunoprecipitate a large number of mitoribosomal proteins attached to other mitochondrial proteins, including putative members of the mitochondrial nucleoid.

INTRODUCTION

Mitochondria play a vital role in a wide variety of cellular processes in eukaryotic cells. They possess their own genomic DNA (mtDNA) that encodes 13 proteins, along with 22 tRNA and 2 ribosomal RNA (1). All protein products of the mitochondrial genome are part of the multi-subunit complexes involved in oxidative phosphorylation. Synthesis of these proteins is carried out on a specialized translational apparatus located within the organelle. The components of the mitochondrial translational machinery—translational factors and mitoribosomes—are distinct from those in the cytosol and generally resemble bacterial counterparts (2).

Our understanding of the mechanisms of mitochondrial translation is far from complete. A limited number of factors involved in mitochondrial translation initiation, elongation and termination have been identified and characterized (3–7). The mechanism of the last step of protein synthesis, the disassembly of the post-termination complex, has not yet been explored in human mitochondria.

Due to the monophyletic α-proteobacterial origin of mitochondria, our knowledge of ribosome recycling in prokaryotes can serve as a rough model for mitochondrial processes, although it is highly likely that they will prove to be important variations. In the bacterial system, when a ribosome reaches a stop codon, the nascent polypeptide is released by the coordinated actions of a sequence-specific class I release factor (RF1 or RF2) and a sequence-independent class II release factor [RF3, (8)]. The resulting post-termination complex containing mRNA and deacylated tRNA in the P/E site (9), has to be disassembled and ribosomal subunits need to be recycled to initiate a new round of protein synthesis. This process is catalysed by the ribosome recycling factor (RRF). RRF is universally conserved in eubacteria and deletion of the gene-encoding RRF (*frr*) has been shown to be lethal for *Escherichia coli* (10). *Mycoplasma genitalium*, with one of the smallest genomes reported to date, retains RRF despite losing RF2 and RF3, further supporting a key role for this factor in prokaryotic translation (11).

*To whom correspondence should be addressed. Tel: +44 191 222 8028; Fax: +44 191 222 8553; Email: r.n.lightowlers@ncl.ac.uk

The mechanism of bacterial ribosome recycling has been addressed by several independent laboratories [for example, (12–14)]. Conformational changes mediated by RRF bound to the 70S ribosome can disrupt the intersubunit bridges leading to separation of the monosome. This process requires GTP hydrolysis that is triggered by elongation factor G (EFG). Subsequently, initiation factor 3 (IF3) binds to the 30S subunit preventing re-association of the free subunits. More recently, emphasis has been placed on the exact role played by bacterial RRF in this process. Cryoelectron microscopy data on *E. coli* RRF binding to 70S post-termination complexes is consistent with a spontaneous movement of RRF from around the peptidyltransferase centre in the monosome to a site on the 50S subunit, resulting in the cleavage of intersubunit bridges and subunit dissociation (15). However, no such structural reorganization was found on X-ray crystallography of a similar but not identical *Thermus thermophilus* system (16).

To date, no human mitochondrial ribosome recycling factor has been characterized. A candidate, mtRRF, was proposed several years ago from bioinformatic analyses of several overlapping EST sequences (7) but with no supportive functional studies or investigation of subcellular localization. In this article, we report that this putative mitochondrial recycling factor is indeed a mitochondrial protein. Furthermore, we show a direct interaction of purified mtRRF with ribosomes of both bacterial and mammalian mitochondrial origin *in vitro* and *in vivo*. To assess the physiological function of mtRRF, we have examined the ability of human mtRRF to rescue yeast strains deleted of their endogenous factor and the effect of mtRRF depletion in cultured human cells. We observed aggregation of mitoribosomes, increased ROS and profound changes in mitochondrial morphology. Our results imply that analogous to the bacterial situation, this protein is essential for mitochondrial function and viability of human cells.

METHODS

Tissue culture manipulations

Human HeLa cells were cultured (37°C, humidified 5% CO_2) in Eagle's modified essential medium (Sigma-Aldrich Co.Ltd, Dorset, UK) supplemented with 10% (v/v) fetal calf serum (FCS), 1 × non-essential amino acids and 2 mM L-glutamine. Flp-In™T-Rex™-293 cells (HEK293T, Invitrogen Ltd, Paisley, UK) were grown in Dulbecco's modified Eagle's medium (DMEM) supplemented with 10% FCS, 50 μg/ml uridine and 1 × non-essential amino acids in the presence of 10 μg/ml Blasticidin S and 100 μg/ml Zeocin (Invitrogen). Post-transfection selection was effected with Hygromycin B (100 μg/ml). For growth on respiratory substrates, medium was glucose-free DMEM (Gibco, UK), 0.9 mg/ml galactose, 1 mM sodium pyruvate, 10% (v/v) FCS, non-essential amino acids and 2 mM L-glutamine. For growth-curve analyses, galactose medium included 50 μg/ml uridine.

Production of GFP-, FLAG- and GST-fusion constructs and cloning into yeast expression vectors

The original human mtRRF clone was obtained from MGC (MGC:17776; Acc No BC013049), but primer positions described below are relative to the reference sequence NM_138777.2.

To generate a fusion construct that would allow expression of mtRRF with GFP at the C-terminus, nucleotides 102–894 of the mtRRF cDNA were amplified using primers for 5′-CACACATGATCAGATTGTCTTCAGTCATGG-3′ and Rev 5′-CACACATGATCAAGTTCTTTGGTCTTCACTGC-3′ (BclI sites underlined). This was digested and cloned in-frame upstream of GFP in pGFP3 (pcDNA3.1 Invitrogen, containing the GFP open reading frame (ORF) and multiple cloning site kindly donated by Dr D Elliott, Newcastle University).

The glutathione-S-transferase (GST)-fusion constructs were made of the full-length (FL) or N-terminal deleted (NDel) mtRRF. These were generated by amplifying nucleotide 116 or nucleotides 324–940, respectively. The FL forward primer incorporated a BclI site, whilst the NDel included an EcoR1 site (FL for 5′-CACACCTGATCAATGGCCTTGGGATTAAAG-3′; NDel for 5′-CACACCGAATTCCCAGAGTGAATATTAATGCT-3′) and the same reverse primer was used for both amplification reactions (Rev 5′-AATTATGCGGCCGCACTGGGCTCTGGAGTATT-3′ containing a NotI site). Amplicons and vectors were digested to allow in-frame downstream fusion of mtRRF-GST in pGEX-6P-1 or pGEX-6P-2, respectively (GE Healthcare, Amersham, UK).

To generate a FLAG-tagged mtRRF construct, the following primers were used to amplify nucleotides 115–900. The region corresponding to the FLAG tag is italicized and *Eco*RV sites are underlined for 5′-CTTTCTTGATATCCCACCATGGCCTTGGGATTAAAGTGCTTCCGCATGGTCCA-3′ and Rev 5′-CTCTCCGATATC*CTACTTATCGTCGTCATCCTTGTAATC*TCCAAGGAGTTCTTTGG-3′.

A FL mtRRF PCR product (nucleotides 101–980) was generated using primers for 5′-CACACCTGATCAGGAUUGUCUUCAGUCAUG-3′ and Rev 5′-CACACCTGATCAGAGAGAAGTCCCAATGTGC-3′ (BclI site underlined). This product was cloned into pGEM-Teasy (Promega, Southampton,UK), excised by NotI digestion and subcloned into NotI-digested *Saccharomyces cerevisiae* URA3 expression vector pFL61 (17) or the *Schizosaccharomyces pombe* ura4 expression vector pTG1754 [a gift from Transgene, (18)], which both contain a strong constitutive promoter.

Transient transfection of HeLa cells, microscopy and image capture

HeLa cells were grown on coverslips to 50% confluency, transfected with GFP fusion vector (1 μg) using SuperFect (Qiagen, Sussex, UK) as recommended and cultured for a further 24 h prior to incubation with Mitotracker Red CM-H2XRos (1 μM final, Invitrogen). After brief fixation (4% paraformaldehyde/PBS, 15 min at room temperature), cells were mounted in Vectashield (H-1200 Vector Laboratories Ltd, Peterborough, UK) and visualized by

fluorescence microscopy using a Leica (Nussloch, Germany) DMRA. Images were recorded as a *Z*-series (0.5 μm slices) using a cooled CCD camera and imaging system (Spot–II Diagnostics Instruments, Sterling Heights, MI, USA).

Immunocytochemistry

HeLa cells (3×10^5) plated on coverslips were incubated with Mitotracker Red CMH2XRos, as described above, fixed in 3% paraformaldehyde, incubated with anti-mtRRF polyclonal antibodies (1/300) for 4 h, washed, and then incubated with AlexaFluor-488 conjugated anti-rabbit antibodies (Molecular Probes, Invitrogen, Paisley, UK) for 1 h. Signals were visualized by microscopy as described above.

Mitochondrial import assays

Assays were performed and assessed using isolated rat liver mitochondria following the methods described in ref. (6) but with reticulocyte lysates programmed with the relevant RNA species.

Over-expression and purification of mtRRF–GST

Escherichia coli strain Rosetta(DE3)pLysS (Novagen, Merck Biosciences Ltd, Nottingham, UK) was transformed with constructs for the over-expression of the human mitochondrial RRF. Bacteria were induced at 0.5 A_{600} with 1 mM IPTG, overnight at 16°C. Pelleted cells were resuspended in 50 mM Tris–HCl pH 7.4, 150 mM NaCl, 1 mM lysozyme, 1 mM EDTA, 1 mM PMSF and sonicated on ice 10×10 s (Soniprep 150). Post-centrifugation (30 000*g* for 20 min, 4°C), the supernatant was filtered (0.45 μm Corning) and incubated for 3 h at 4°C with glutathione Sepharose 4B beads (GE Healthcare). Beads were extensively washed prior to elution in 50 mM Tris–HCl pH 7.8, 150 mM NaCl, 20 mM reduced glutathione, 1 mM PMSF.

For cleavage and removal of the GST on the Sepharose, beads were incubated at 4°C overnight in 50 mM Tris–HCl pH 7.8, 150 mM NaCl, 1 mM PMSF supplemented with 1 mM EDTA, 1 mM DTT and 24 μl/ml PreScission Protease (GE Healthcare). Eluted recombinant protein was stored at 4°C.

Production of anti-mtRRF antibodies

Recombinant human mtRRF purified as described above was used as an antigen to raise rabbit antisera. Antibody generation and affinity purification was performed by Eurogentec, Belgium.

In vitro ribosome binding assay

Escherichia coli ribosomes were prepared as described in ref. (6). Reactions (50 μl) combined purified recombinant mtRRFΔ69 and 70S ribosomes (1 μM) in 10 mM Tris–HCl pH 7.2, 10 mM $Mg(OAc)_2$, 80 mM NH_4Cl, 1 mM DTT at room temperature for 30 min. The mixture was centrifuged through 10% (v:v) sucrose (150 μl in binding buffer) for 1 h in Beckman–Coulter air-driven ultracentrifuge (30 p.s.i.). Fractions (4×50 μl) were collected and analysed by western blot.

Stable transfection of HEK293T cells with FLAG-tagged mitochondrially targeted proteins

Cells were transfected at ~30% confluency using Superfect (Qiagen). The vectors, pOG44 expressing FRT recombinase, and pcDNA5/FRT/TO containing sequences of the genes to be expressed (FLAG-tagged mtRRF or mitochondrially targeted luciferase) were combined to give a total of 2 μg DNA in a 9:1 ratio, and mixed with Superfect prior to a 3-h incubation with the cells. Selection with Hygromycin B (100 μg/ml) commenced 2 days later. Independent colonies were isolated, propagated and analysed for induction (1 μg/ml tetracycline) by western analysis using anti-FLAG antibodies (Sigma).

Isokinetic sucrose-gradient analysis of mitochondrial ribosomes

Total cell lysates (0.5 mg) were loaded on a linear sucrose gradient [10–30% (v:v), 1 ml] in 10 mM Tris–HCl pH 7.2, 10 mM $Mg(OAc)_2$, 80 mM NH_4Cl, 1 mM PMSF and centrifuged for 2 h at 100 000*g* at 4°C. Fractions of 100 μl were collected and analysed by western blot.

Affinity purification and elution of FLAG peptides

Mitochondria were isolated from HEK293T cells over-expressing FLAG-mtRRF or -mtLUC essentially as described in ref. (6) and treated with proteinase K (5 μg/1 mg of mitochondria; 30 min 4°C) followed by PMSF (1 mM) inhibition. Pelleted mitochondria were resuspended in lysis buffer (supplemented with 10 mM $Mg(OAC)_2$ as indicated, although no difference in the composition of protein precipitate could be measured without supplement). Immunoprecipitation was performed with a-FLAG-Gel following manufacturer's recommendations (Sigma Aldrich, St Louis, MO, USA). Elution was effected with FLAG peptide. RNase A (5 μg/ml) and EDTA (50 mM) were added as indicated.

Mass spectrometry analysis and protein identification

Mass spectrometric analysis of immunoprecipitated complexes was performed as described in Supplementary Material.

Yeast growth conditions, plasmid and general strain constructions and complementation assays

All yeast strains used in this study are detailed in Table S2. General yeast media and genetic techniques/transformation protocols were as described in ref. (18). In brief, fermentable media contained 2% glucose, non-fermentable conditions were 3% (v:v) glycerol/ethanol or 2% (v:v) glycerol with 0.1% glucose or for *S. pombe* only 2% (w:v) galactose/0.1% (w:v) glucose.

Production of *S. pombe* Δ*rrf1* strain

A single *S. pombe* protein, encoded by the gene SPBC1709.09, was found to have significant similarities to both *S. cerevisiae* Rrf1 (Figure S4) and *E. coli* RRF.

The ORF was PCR amplified from genomic DNA and cloned into the NotI site of the pTG1754 and pFL61 expression plasmids for *S. pombe* and *S. cerevisiae*, respectively. An *S. pombe Δrrf1::Kan*^{R} strain (NB331) was constructed in the wild-type recipient strain NB205-6A by using a PCR disruption strategy with hybrid *rrf1-Kan*^{R} oligonucleotides as described in ref. (19), removing 629 bp encompassing the 735 bp *rrf1Sp* ORF (starting 8 bp before the ATG). Of 50, 22 clones showed delayed growth on glycerol medium and were proved to contain the correct insertion by PCR. Crossing to wild-type followed by sporulation and tetrad analysis showed a 2:2 cosegregation of the geneticin resistance and slow glycerol growth. Transformation with the Rrf1pSp-encoding plasmid restored growth on galactose, confirming that the mitochondrial DNA was intact in this strain.

Spectroscopic analyses

Cells from *Δrrf1Sp* transformants were dried, mixed with sodium dithionite to fully reduce the cytochromes and frozen in liquid nitrogen before recording the absorbance of the samples at wavelengths from 630 nm to 490 nm (spectrophotometer Cary 400Ò, Varian, San Fernando, CA). Peaks were the following: cytochrome *c* (548 nm), cytochrome c_1 (554 nm), cytochrome *b* (560 nm) and cytochrome aa_3 (603 nm).

siRNA constructs, transfection and RT–PCR analysis

The following sequences targeting mtRRF were tested for efficiency of mRNA and protein depletion. Nucleotide positions are relative to reference sequence NM_138777.2, siRNA ORF1 5′ GGACACCAUUAGGCUAAUA dTdT 3′ (nucleotides 211–229); siRNA ORF2 5′ GAGAAAUGCUGGUGAAACU dTdT 3′ (nucleotides 684–702); siRNA ORF3 5′ GACAGUGCAUGAAAGACAA dTdT 3′ (nucleotides 799–817). Experiments were performed with siRNA ORF2 unless otherwise specified. Treatment of stably transfected and induced HEK293T cells was performed with siRNA UTR1 5′ GUAUUCUUGUUGCACUUAA dTdT 3′ (nucleotides 1633–1651) targeting the 3′-UTR region that was absent in the inducibly expressed form of mtRRF. Transfections were performed on 20% confluent cells with Oligofectamine (Invitrogen) in Optimem-I medium (Gibco) with final concentrations of 0.2 μM siRNA. Control non-targetting siRNA and custom siRNA duplexes were purchased, purified and pre-annealed from Eurogentec. Quantification of mtRRF mRNA was performed with TaqMan Gene Expression Assay (Applied Biosystems, Warrington, UK) using ABI Prism sequence detector system. Data were normalized to GAPDH as an endogenous control. Probe kits were ordered from Applied Biosystems—HS01067555_g1 (mtRRF) and HS999999905_m1 (GAPDH).

Cell preparations, western analysis and Blue Native-PAGE

Schizosaccharomyces pombe mitochondria was purified from cells grown either in complete glucose medium or in minimal glucose medium lacking uracil as described in ref. (19) with Roche protease inhibitors present at all stages. Yeast proteins were separated by 12% SDS–PAGE and immobilized on nitrocellulose (Schleicher & Schuell, London, UK) by wet transfer in 25 mM Tris, 192 mM glycine, 0.02% (w/v) SDS and 20% (v/v) ethanol. Blots were hybridized with mouse (anti-human Hsp60, Sigma H-3525; anti-FLAG, Sigma H-1804) or rabbit antibodies [anti-mtRRFHs (this work); -Cox2Sp, (20) -Arg8Sc (21); -EFTuSp (18)].

Human cell lysates were prepared, separated by SDS–PAGE and immobilized by wet transfer as described (6). Proteins of interest were bound by overnight incubation (4°C) with antibodies [mtRRF, GDH (Lightowlers Group, Newcastle); Porin, COX I, COX II, SDH 70K and ND6 (MitoSciences, Eugene, OR); β-actin (Sigma); DAP3, MRLP3 (Abcam, Cambridge, UK)] followed by HRP-conjugated secondary antibodies (DAKO) and visualized by ECL-plus (GE Healthcare).

Blue native gel electrophoresis was performed as described in ref. (22) with 30 μg protein loaded per lane and wet transfer as above.

Free radicals and mitochondrial mass measurements

MitoSOX (Molecular Probes) prepared in DMSO, diluted to 5 μM in DMEM medium-lacking serum was added to cells for 10 min at 37°C. Cells were washed before re-suspension in 2 ml DMEM-lacking serum and passed through a FACScan flow cytometer (Becton Dickinson Ltd, Oxford, UK, equipped with 488 nm Argon laser). Data were collected for forward and side scatter together with autofluorescence of unstained cells, gating eliminated debris and apoptotic cells from the analyses. After acquisition, data were analysed by WinMDI software (version 2.8). Experiments were performed on four independent occasions with triplicate measurements based on 10 000 events. Dihydrorhodamine 123 (DHR, Molecular Probes) and nonyl acridine orange (NAO, Molecular Probes) were resuspended in DMSO, diluted to 30 mM (DHR) or 10 mM (NAO) in DMEM-lacking serum and incubated with cells at 37°C for 30 (DHR) min or 10 (NAO) min. Cells were then washed before resuspension in 2 ml DMEM-lacking serum and green fluorescence emission analysed as above.

Electron microscopy studies

Cells were grown as detailed above, pelleted and fixed in 2% glutaraldehyde in Sorensen's phosphate buffer. Samples were than post-fixed in 1% osmium tetroxide in the same buffer, dehydrated in alcohol and embedded in Epoxy resin (TAAB). Ultrathin sections were stained with 2% aqueous uranyl acetate and lead citrate and examined using a Philips CM100 transmission electron microscope (EM Research Services, Newcastle University).

In vivo mitochondrial protein synthesis

Protein translation in HeLa cells was performed essentially as described (23). Cells were incubated with radiolabelled methionine for 15 min.

Respirometry

High-resolution respirometry was performed at 37°C with an Oroboros Oxygraph-2K (Oroboros Instruments, Austria) essentially as detailed in ref. (6).

Statistical analysis

Students unpaired *t*-tests were used to determine the significance of values as indicated in the figure legends. Values of $P < 0.05$ were recorded as statistically significant.

RESULTS

MtRRF, the human homologue of bacterial RRF, is a mitochondrial protein

To confirm mitochondrial localization of the putative human mtRRF predicted by *in silico* studies (7), a mtRRF–GFP fusion construct was used to transfect HeLa cells. This chimera included all but the terminal 2 residues of mtRRF fused N-terminal to GFP. Cells were cultured for 24 h prior to staining with Mitotracker CM-H_2XRos, to visualize mitochondria. Fluorescence microscopy images and line scan analysis (Figure 1A, left panels) of transfected cells demonstrated co-localization of mtRRF–GFP with Mitotracker Red. In contrast to the well-defined, discrete pattern produced by mtRRF–GFP, expression of the GFP protein alone produced a diffuse stain (data not shown).

To verify, if localization of the mtRRF–GFP fusion protein reflects the behaviour of the endogenous protein, immunocytochemistry was performed. Polyclonal antisera against FL recombinant protein were raised and anti-mtRRF antibodies affinity were purified. Immunocytochemistry (Figure 1A, right panels) indicated similar mitochondrial localization of both the endogenous and mtRRF–GFP.

To confirm that mtRRF is indeed imported into the mitochondrial matrix and not merely localized to the organelle, import assays were performed with isolated

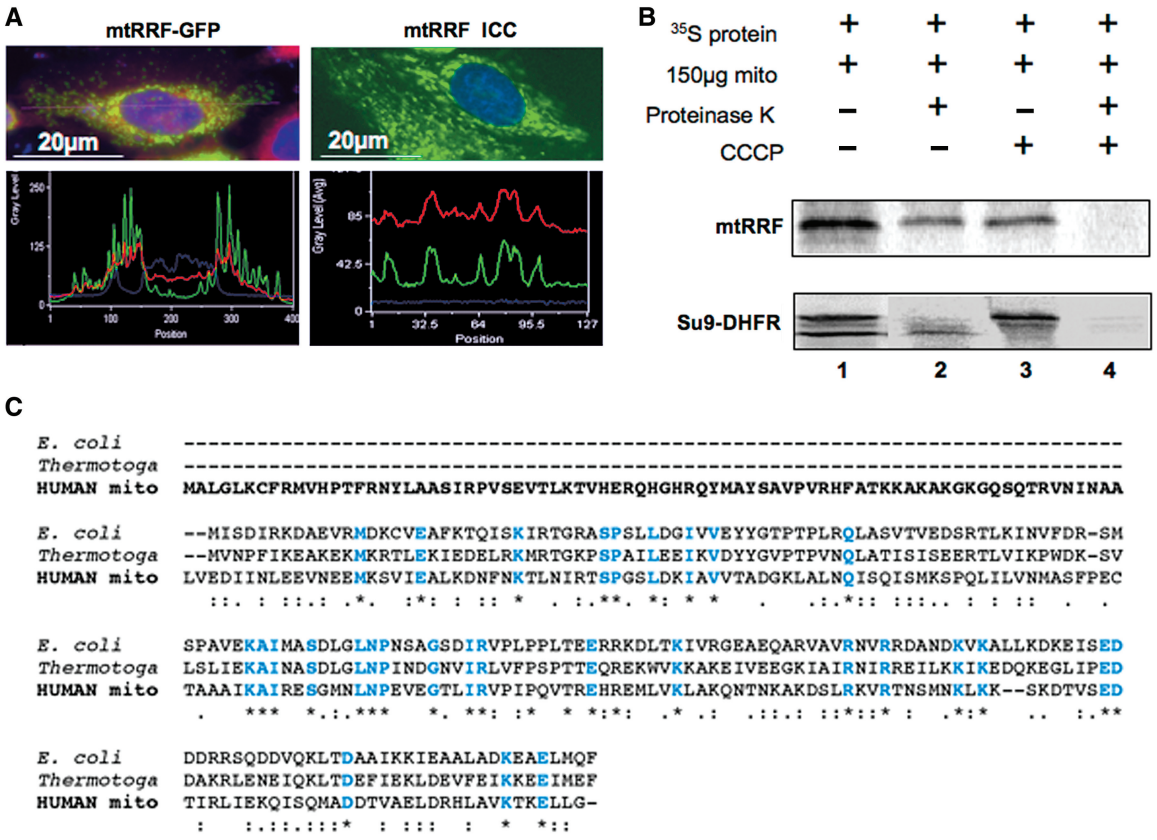

Figure 1. mtRRF is a mitochondrial protein with an extended N-terminal pre-sequence. (**A**) Human mtRRF is targeted to mitochondria. Left panels show HeLa cells transiently transfected (24 h) with a mtRRF–GFP fusion construct. Cells were stained to visualize nuclei (DAPI blue) and mitochondria (Mitotracker red). Fluorescence images and linescans confirmed mitochondrial localization of mtRRF–GFP by superimposition of green and red signals (lower left). The image reflects three-independent transfections. Endogenous mtRRF in HeLa cells was visualized by immunocytochemistry (upper right) using affinity purified anti-mtRRF and FITC secondary. DAPI-stained nuclei (blue) and Mitotracker the mitochondria (red). Mitochondrial localization of mtRRF was confirmed by superimposition of linescan green and red fluorescence (lower right). The image reflects three-independent transfections. (**B**) Human mtRRF is imported into mitochondria. FL ^{35}S-radiolabelled mtRRF was *in vitro* synthesized and incubated with rat liver mitochondria (lane 1). Under import conditions a single product is visible (lane 2) that is protected from proteinase K (lane 3), but degraded by treatment with proteinase K and FCCP uncoupler (lane 4). Control import reactions contained DHFR with a mitochondrial pre-sequence (Su9) showing the FL pre-protein and the matured form under import conditions. (**C**) Sequence alignment (CLUSTALW) indicates an extensive N-terminal pre-sequence when compared with *E. coli* or *Thermotoga maritima*. Identity to these RRFs is indicated in blue and by *, high levels of similarity by a colon ':' and lower levels by a fullstop '.'.

mitochondria and *in vitro* translated ^{35}S-labelled mtRRF (Figure 1B). Resistance of the radiolabelled protein to proteinase K (lane 2) confirmed successful mitochondrial uptake. Import resulted in cleavage of the mitochondrial targeting pre-sequence of Su9-DHFR but interestingly not of mtRRF. This is consistent with bioinformatic predictions (www.cbs.dtu.dk/services/TargetP) being unable to identify a clear cleavage signal in the mtRRF sequence (7). Alignment of the mtRRF sequence with bacterial counterparts indicates that optimal alignment begins at position 80 of the FL mtRRF (Figure 1C). Since our results show that this long N-terminal extension is not a cleavable import signal but an integral part of the mature protein, it suggests that it may be of functional importance specific to mitochondria.

mtRRF binds *E. coli* ribosomes *in vitro* and can associate with human mitoribosomes

Direct interaction of prokaryotic RRF with ribosomes in the absence of other translation factors has been demonstrated (16,24). Binding experiments were therefore performed to determine if human mtRRF could play a similar role to its bacterial homologues. Isolation of FL over-expressed mtRRF showed that the protein tended to aggregate (Figure S1). Therefore, a short N-terminal truncation mtRRFΔ69 was used as this deletion significantly increased solubility of the recombinant protein. Comparative circular dichroism analysis of both the FL and truncated mtRRF confirmed that removal of the N-terminus did not cause any major structural changes (data not shown). *In vitro* binding assays showed that mtRRF localized to the rapidly sedimenting ribosomal fraction only in the presence of *E. coli* ribosomes (Figure 2A), indicating a direct interaction.

To determine whether mtRRF could interact with mitoribosomes in isolated organelles, FLAG epitope-tagged mtRRF was inducibly expressed in human Flip-In T-REx HEK293 cells (HEK293T) as described in procedures. Subsequently, complexes containing the fusion protein were isolated from solubilized mitochondria by anti-FLAG affinity purification and FLAG peptide elution. To control for non-specific binding, FLAG-tagged mitochondrially targeted luciferase (mtluc) was expressed in cells and immunoprecipitated by the same procedure. Western analysis revealed a specific interaction of mtRRF and mitoribosomal proteins (Figure 2B). Mitoribosomes were very efficiently precipitated with FLAG-mtRRF. Taken together these data show that mtRRF can tightly associate with mitoribosomes.

Bacterial RRF is only transiently associated with ribosomes *in vivo*, partially occluding the P and A sites on binding to the post-termination complex (9,15) so it was surprising to find that the majority of mtRRF was bound to mitoribosomes. To investigate this further, HEK293T cells were induced as above and lysates were immediately subjected to isokinetic sucrose-gradient centrifugation. This mtRRF over-expression was not deleterious to cell growth (data not shown) but led to a slight decrease in mitoribosome formation (Figure 2C cf. Figure 5A). No association of mtRRF with mitoribosomes at steady state was detectable. However, binding became evident on incubation (3 h) of the lysate prior to centrifugation (mimicking the IP procedure) potentially due to dissociation or hydrolysis of charged tRNAs that would naturally occupy most A/P sites. This dependence on pre-incubation was not a consequence of mtRRF over-expression, as a similar effect was noted with HeLa cell lysate (Figure 5A, data not shown). Further, association was not due to non-specific interactions promoted by the pre-incubation step as interactions were lost either on RNase or EDTA treatment (Figure 2E, lanes 1 and 2).

Mitoribosomes associated with numerous mitochondrial proteins are co-immunoprecipitated with mtRRF

Immunoprecipitation (IP) experiments using mtRRF as bait revealed an association with two mitoribosomal proteins, presumably indicating the presence of the large (39S) and small (28S) ribosomal subunits (MRPs) (Figure 2B). To confirm the presence of other MRPs and determine which if any additional proteins were present, IP experiments were performed on lysates from a protease/DNase-treated HEK293T mitoplast fraction. After elution of specifically bound proteins with FLAG peptide, the eluant was separated by gel electrophoresis and gel slices subjected to LC-MS/MS as detailed in Supplementary Material. The mitoplast enrichment procedure yielded a total of 167 identified mitochondrial proteins (Tables 1 and S1), 73 of which were indeed MRPs. Although MRPs constituted most of the purified immunoprecipitated proteins, detailed LC-MS/MS analysis revealed some remaining cytosolic contaminants (data available on request) but also allowed us to identify other mitochondrial proteins that co-immunoprecipitated with mtRRF (Table 1). The second largest group were proteins that had been previously reported as components of human mitochondrial nucleoids (25–27). Among other proteins interacting with mitoribosomes were factors involved in intra-organellar translation, nucleic acid binding proteins and chaperones/proteases, all proteins that might be expected to associate with ribosomal components or nascent peptides. Several polypeptides known to be involved in metabolism were also identified.

Human mtRRF improves the respiratory competence of *S. pombe* Δ*rrf1*

To gain insight into the *in vivo* function of human mtRRF, we first examined whether it could replace the endogenous mtRRF of the budding yeast *S. cerevisiae*. Respiratory deficiency due to loss of *S. cerevisiae* mtRRF (Δ*rrf1Sc*) was reportedly associated with depletion of cytochrome *c* oxidase activity (28) or total loss of mtDNA (29). Thus, for complementation analysis we used Δ*rrf1Sc* strains with different nuclear and mitochondrial backgrounds (Supplementary Material). In the W303 background, Δ*rrf1Sc* cells showed a mild to pronounced respiratory deficiency depending on the mitochondrial intron content (Figure S2), but retained wild-type mtDNA. This allowed direct complementation tests by transformation with expression plasmids carrying either the natural *S. cerevisiae* gene, or human or *S. pombe* (fission yeast)

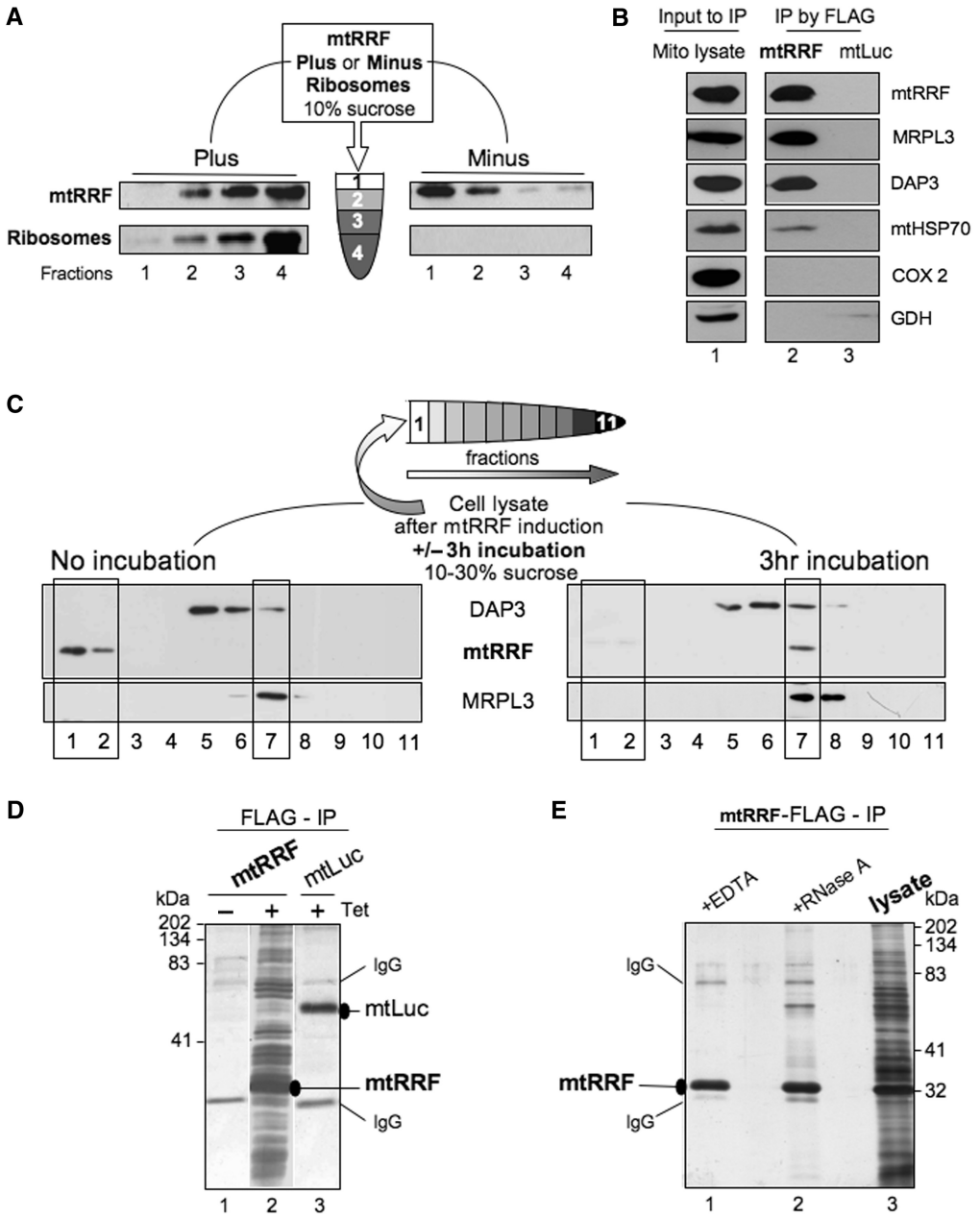

Figure 2. Human mtRRF associates with bacterial ribosomes *in vitro* and mitoribosomes *in vivo*. (**A**) Human mtRRF binds *E. coli* ribosomes. Recombinant mtRRF (mtRRFΔ69) was incubated with or without 70S ribosomes prior to sedimentation through 10% (w:v) sucrose. Fractions were subjected to western analysis. (**B**) mtRRF associates with mitoribosomes. FLAG-mtRRF and mtLuc HEK293T cells were induced, mitochondria isolated. Lysate was prepared (lane 1) from which proteins were immunoprecipitated via the FLAG epitope (lanes 2–3). Western blot analysis used antibodies to mtRRF, large 39S and small 28S mitoribosomal subunits (MRPL3, DAP3), mitochondrial chaperone (mtHSP70), complex IV (COX 2) and a matrix protein (glutamate dehydrogenase -GDH). (**C**) Pre-incubation of mitochondria allows detection of mtRRF binding to mitoribosomes. Lysate was prepared from HEK293T cells after induction of FLAG-mtRRF and was either separated immediately or post 3 h incubation on a 10–30% (v:v) isokinetic sucrose gradient. Fractions were analysed by western blot with antibodies to mtRRF, MRPL3 (39S mitoribosomal subunit) or DAP3 (28S mitoribosomal subunit). A similar time-dependent mitoribosomal association in HeLa cell lysate was noted for the endogenous mtRRF (data not shown). (**D**) HEK293T cells were induced (±Tet) for FLAG-mtRRF (lanes 1–2) or control mtluc (lane 3) expression and mitochondria isolated. Co-immunoprecipitating proteins were separated through a 12% SDS–PAG and visualized by silver stain. mtRRF, mtluc and anti-FLAG IgG are indicated. (**E**) Preparations of the mtRRF IP were also treated with EDTA (lane 1) or RNase A (lane 2). Mitochondrial lysate is shown in lane 3.

homologues. However, neither the *S. pombe* nor the human homologue complemented the *S. cerevisiae* mutant (Figure 3A, data not shown).

As the fission yeast *S. pombe* is regarded as a closer evolutionary relative to human than *S. cerevisiae*, particularly in mitochondrial physiology (19), we inactivated the gene coding the *S. pombe* mtRRF homologue (*rrf1Sp*) to test if it could be replaced by human mtRRF. Deletion of *rrf1Sp* slightly but significantly impaired growth on non-fermentable carbon sources (Figure 3B),

Table 1. Predicted function of the mitochondrial proteins identified after anti-FLAG mtRRF affinity precipitation

Protein type[a]	Immunoprecipitation		
	mtRRF[b]	mtRRF + EDTA[c]	mtRRF + RNase[d]
Mitoribosomal proteins[e]	73	1	0
Nucleoid[f]			
Class I	25 (31)	2	0
Class II	6 (10)	0	0
Class III	6 (16)	0	0
Nucleoid[g]	5 (6)	1	0
Translation associated	6	1[h]	1[h]
Nucleic acid binding/modifying	13	0	0
Metabolic	23	0	0
Chaperone/protease	5	0	0
Transporter	4	0	0
Unknown function	6	0	0
TOTAL	167[j]	7[i]	1

[a]Known or predicted function of identified mitochondrial proteins.
[b]Immunoprecipitation from mitoplasts after protease and DNase shaving.
[c]EDTA-washed immunoprecipitant from crude mitochondria.
[d]RNase-treated immunoprecipitant from crude mitochondria.
[e]Mitoribosomal subunits identified by Koc *et al.* 2001 (39) and Cavdar Koc *et al.* (40).
[f]Putative nucleoid proteins as recently classified by Bogenhagen *et al.* (25) (of total proteins).
[g]Putative nucleoid proteins as identified by He *et al.* (26) (of total proteins).
[h]Mitochondrial ribosomal recycling factor, mtRRF.
[i]Three cytosolic ribosomal proteins were identified in the precipitation following EDTA treatment.
[j]Does not include any non-mitochondrial, hypothetical or predicted proteins that were found.

lowered overall content of mt-encoded cytochromes (Figure 3C) and decreased steady-state levels of mt-encoded Cox2 protein (Figure 3D), consistent with a role in mitochondrial translation. In addition, western analysis of *S. pombe* mtRRF protein confirmed mitochondrial location (Figure S3). Transfectants of this strain expressing FL human mtRRF were able to fully restore normal growth on non-fermentable medium, levels of mt-encoded cytochromes and Cox2 protein, correlating with weak but reproducibly detectable mtRRFHs in only the mitochondrial fraction (Figure 3B–D). Thus, human mtRRF clearly performs the same function as *S. pombe* mtRRF consistent with interaction with the *S. pombe* mitochondrial translation machinery.

Loss of mtRRF in human cells results in reduced growth rate and cell death

To determine the function of mtRRF in human mitochondria, three siRNA specific to the human *mtRRF* mRNA were designed and used to transfect HeLa and HEK293T cells. A non-targeting siRNA (*NT*) was used to confirm specificity. A reduction of 80–90% of *mtRRF* mRNA levels were observed 2 days post-transfection with a consequent dramatic reduction in mtRRF protein by day 3 (Figure 4A). To investigate the long-term effect of mtRRF depletion, HeLa cells were retransfected with siRNA on the third day of the experiment. Interestingly, the cells transfected with *mtRRF* siRNA(ORF2) showed a significant reduction in growth compared to *NT* controls (Figure 4B). After 3 days of *mtRRF* siRNA treatment, cells developed morphological changes and depletion for more than 6 days was lethal. If cells were cultured in glucose-free media supplemented with galactose to force dependence on oxidative phosphorylation, the effect of mtRRF depletion was even more profound (Figure 4B). These observations suggest that mtRRF is an essential protein and its loss affects mitochondrial functions.

To further ensure that the growth phenotype was specific to mtRRF depletion, an siRNA designed against the 3′-UTR of *mtRRF* was introduced to HEK293T cells, concomitant with inducible expression of the exogenous *FLAG-mtRRF* lacking this 3′-UTR. Expression of mtRRF after transfection of the cells with 3′-UTR-specific *mtRRF* siRNA restored normal growth (Figure 4B) consistent with the growth phenotype being solely due to depletion of mtRRF.

Depletion of mtRRF partially affects mitochondrial translation and inhibits mitoribosomal disassembly

What is the mechanism causing the growth phenotype? It has been shown that in bacteria and yeast mitochondria, inactivation of RRF inhibits protein synthesis (12,29). To determine if the same is true for the mtRRF, we investigated the effect of protein depletion on an *in vivo* mitochondrial protein synthesis. In the presence of *mtRRF* siRNA, there was partial inhibition of mitochondrial protein translation (Figure 4C). Although the effect was not as dramatic as in *S. cerevisiae Δrrf1* (29), it must be recognized that even partial translation defects result in instability and loss of mtDNA, which in turn produce a greater impairment of mitochondrial protein synthesis. The relative synthesis of most of the components was significantly altered (Figure 4C, data not shown). Consequently, the steady-state levels of mtDNA-encoded proteins were progressively affected as detected by western blot (Figure 4D). Although we did not observe significant reduction of the protein levels after short siRNA treatment (2–3 days), longer treatment resulted in decreased steady-state levels of mitochondrially encoded proteins of up to 40% when compared to non-targeting controls (day 6). These results were consistent with the decreased levels of fully assembled OXPHOS complexes after 6 days siRNA treatment, as revealed by Blue Native gel electrophoresis (Figure 4E). Moreover, polarographic measurements showed that respiration rates of the siRNA-treated cells decreased, consistent with affected function of OXPHOS complexes (Figure 4F).

To further decipher the exact mechanism of mtRRF function in mitochondrial translation, we looked at the sedimentation profile of HeLa cell mitoribosomes in isokinetic sucrose density gradients following mtRRF depletion. Western analysis of mitoribosomes from cells treated for 4 days with *NT* or *mtRRF* siRNA (Figure 5A) showed a striking contrast in distribution of DAP3 representing the small ribosomal subunit. *mtRRF* siRNA caused a shift from fractions 5–8 to mainly 7. This fraction has proteins

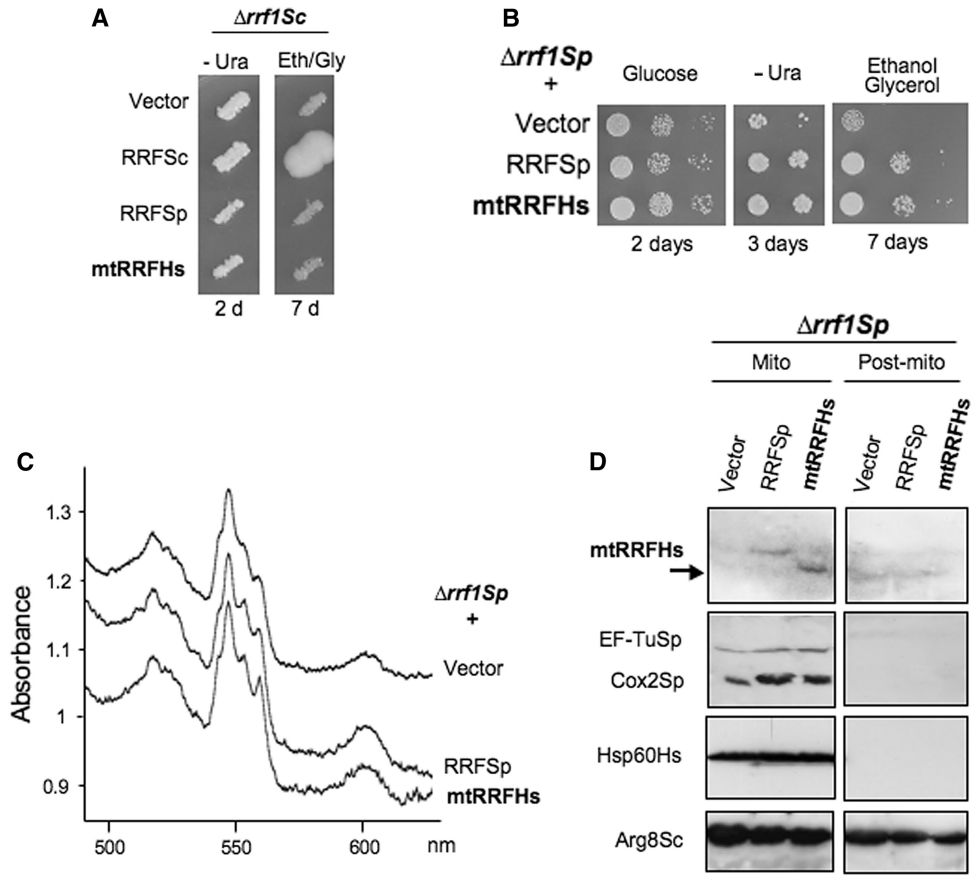

Figure 3. Human mtRRF suppresses a partial respiratory deficiency in *Δrrf1* fission yeast. (**A**) Human mtRRF cannot rescue the Δrrf respiratory defect in budding yeast. *Saccharomyces cerevisiae* transformants of *Δrrf1* strain MG38 carrying the control vector pFL44L or *URA3* plasmids producing the *S. cerevisiae*, *S. pombe* or human mtRRF were replica-plated on non-fermentable media (eth/gly + glycerol 0.1% glucose) and incubated at 28°C. (**B–D**) Human mtRRF restores respiratory capacity in Δrrf1 fission yeast. *Schizosaccharomyces pombe* lacking endogenous RRF (*Δrrf1Sp*, NB331) was transformed with vector alone (vector) or expressing human (RRFHs) or *S. pombe* (RRFSp) mtRRF (B). Serial dilutions of three *Δrrf1Sp* transformants were spotted on complete glucose, uracil-free minimal or complete gly/eth media and grown at 28 °C for the times indicated. (**C**) *Δrrf1Sp* transformants were grown on 2% glycerol/0.1% glucose (vector) or ethanol/glycerol medium (RRFSp or RRFHs) before recording whole-cell cytochrome spectra. Cytochrome $b + c_1$ and aa_3 correspond to Complex III and Complex IV, respectively. (**D**) Mitochondria and post-mitochondrial supernatants from transformants grown in glucose medium minus uracil were separated by 12% PAGE and analysed by western blot with antibodies recognizing human mtRRF, *S. pombe* mtEF-Tu and mt-encoded Cox2, human mt-Hsp60 and *S. cerevisiae* mtArg8 (this also recognizes *S. pombe* Arg1 in mitochondria and an unknown protein in the supernatant).

from both mitochondrial ribosomal subunits and represents monosome accumulation. Moreover, only after mtRRF depletion where both ribosomal subunits detected in the heaviest fraction (F11), suggesting aggregation of the ribosomal proteins. We conclude that on depletion of mtRRF, monosomes are poorly dissociated into single subunits and non-functional monosomes accumulate, producing aggregates. These data are consistent with mtRRF functioning as a factor responsible for disassembly of ribosomes in human mitochondria.

Depletion of mtRRF causes increased mitochondrial ROS and changes in mitochondrial morphology

The observed aggregation of mitoribosomes may have a direct influence on mitochondrial function and may be a primary cause of cell death. Stress conditions in mitochondria are frequently associated with elevated levels of reactive oxygen species (ROS). To assess stress due to ROS accumulation in siRNA-treated cells, superoxide and peroxide/peroxynitrite levels were measured by mitoSOX and DHR, respectively. A statistically significant increase of ROS levels over the *NT* control was seen at day 3, a difference that was maintained through to day 6 (Figure 5B).

Increased ROS is often paralleled by augmented mitochondrial biogenesis and mtRRF depletion also resulted in a significant increase of mitochondrial mass as measured by NAO fluorescence, a dye that binds selectively to cardiolipin in the mitochondrial inner membrane (Figure 5B).

These abnormalities were reflected in the progressive morphological changes of mitochondria revealed by EM (Figure 5C 3 days and 6 days *mtRRF* siRNA) where the longer treatment resulted in a dramatic increase in mitochondrial density. Many more tightly packed membranous sheets were observed, which was consistent with increased mitochondrial biogenesis, whereas the numerous 'black spots' detected in the matrix compartment are consistent with mitoribosome aggregates.

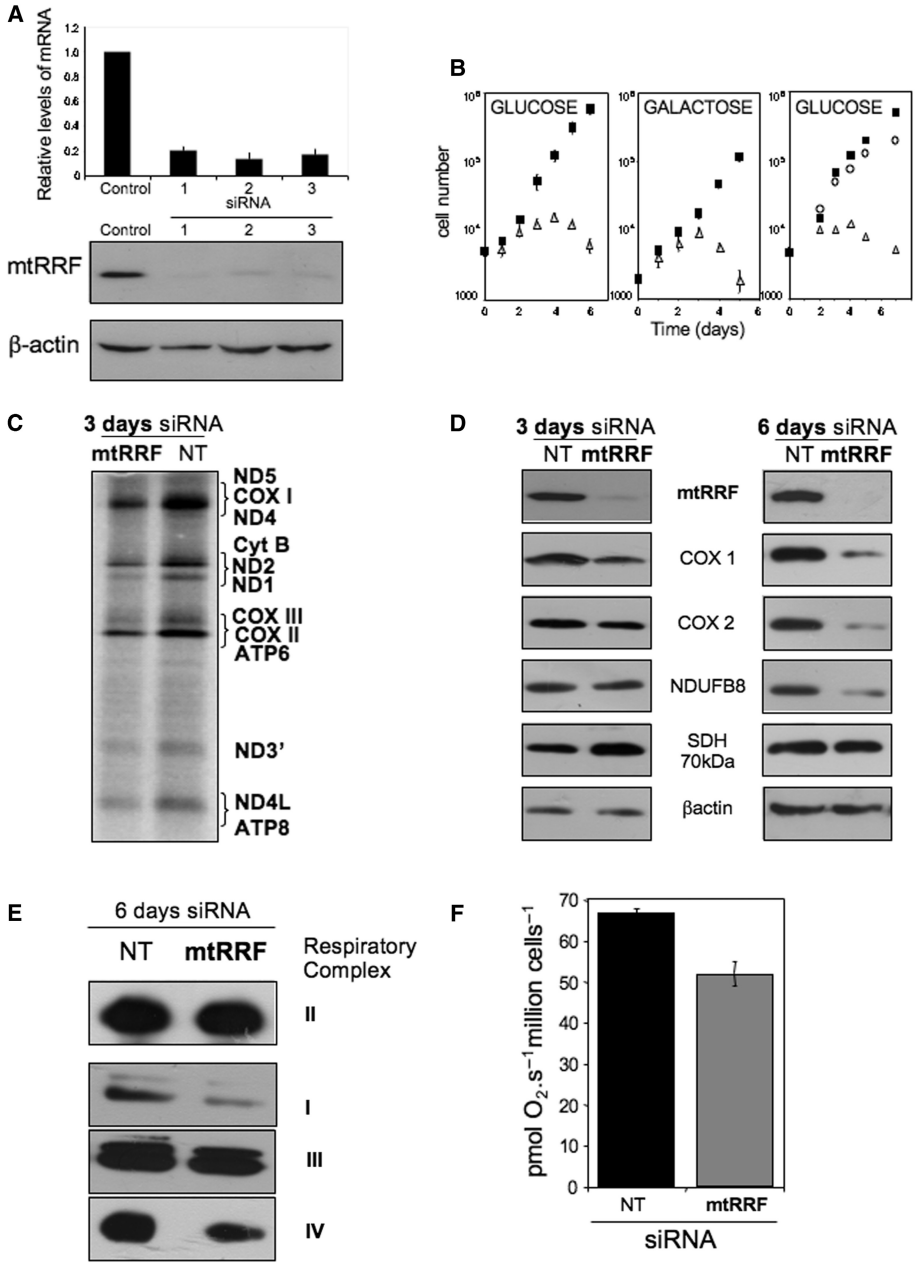

Figure 4. Depletion of human mtRRF severely affects cell viability and compromises mitochondrial translation. (**A**) siRNA-mediated depletion of human mtRRF. HeLa cells were exposed to three different siRNA molecules all in the *mtRRF*-coding sequence or an control siRNA for 6 days and RNA or cell lysates were prepared. Levels of mtRRF transcript compared to control siRNA transfected cells were quantified by real-time PCR (upper graph, mean ± SEM from four-independent transfections). Western blots (30 μg lysate/lane) in the lower panel were performed with antibodies against mtRRF to confirm depletion and β-actin as a loading. The blot accurately reflects three experiments. (**B**) Depletion of mtRRF causes a severe growth defect. Multiple aliquots of HeLa cells (left and centre panels) were exposed to targeted (*mtRRF*, open triangles) or non-targeted (*NT*, black squares) siRNA for 6 days in glucose (left) or galactose (centre) media, cells counted and presented in a semi-log plot. Counts were made of HEK293T transfectants (right panel) treated with non-targeted siRNA (*NT*, black squares) or siRNA directed against the endogenous *mtRRF* 3′-UTR with (open circles) or without (open triangles) concomitant inducible expression of FLAG-mtRRF. Numbers are a mean ± SEM of four independent wells. (**C**) *In vivo* mitochondrial proteins synthesis is partially affected by mtRRF depletion. HeLa cells were grown in the presence of control (*NT*) or targeted (*mtRRF*) siRNA. Cytosolic protein synthesis was inhibited with emetine prior to labelling mitochondrial proteins with ^{35}S-methionine (15 min). Equal amounts of lysate (20 μg) were separated by 15% SDS–PAGE and gels analysed by PhosphorImager. Polypeptides designation is as described in ref. (23). (**D**) Steady-state levels of mtDNA-encoded proteins are affected by depletion of mtRRF. Western blots show analysis of cell lysates after 3 or 6 days siRNA treatment (*mtRRF* or *NT*) with antibodies against mitochondrial translation products or proteins sensitive to mitochondrial translation inhibition (cytochrome *c* oxidase subunits I and II—COX I and 2; complex I subunit NDUFB8) or nuclear-encoded complex II SDH 70 kDa protein and β-actin as a loading control. The blot accurately reflects three repeat experiments. (**E**) OXPHOS complexes are reduced at steady-state levels after mtRRF depletion. HeLa cells were exposed (6 days) to *mtRRF*- or *NT*-targeted siRNA prior to BN–PAGE. Complexes were visualized with antisera to complex I, anti-39 kDa; complex II, anti-SDH 70 kDa; complex III, anti-core 2, complex IV, anti-COII. The blot accurately reflects three experiments. SDH is a complex only comprising proteins encoded in the cytosol. (**F**) Respiratory coupling is modestly affected in cells depleted of human mtRRF. HeLa cells were exposed (3 days) to *mtRRF*-or *NT*-targeted siRNA prior to high resolution respirometry (as in Methods), three measures of respiratory control and capacity were made.

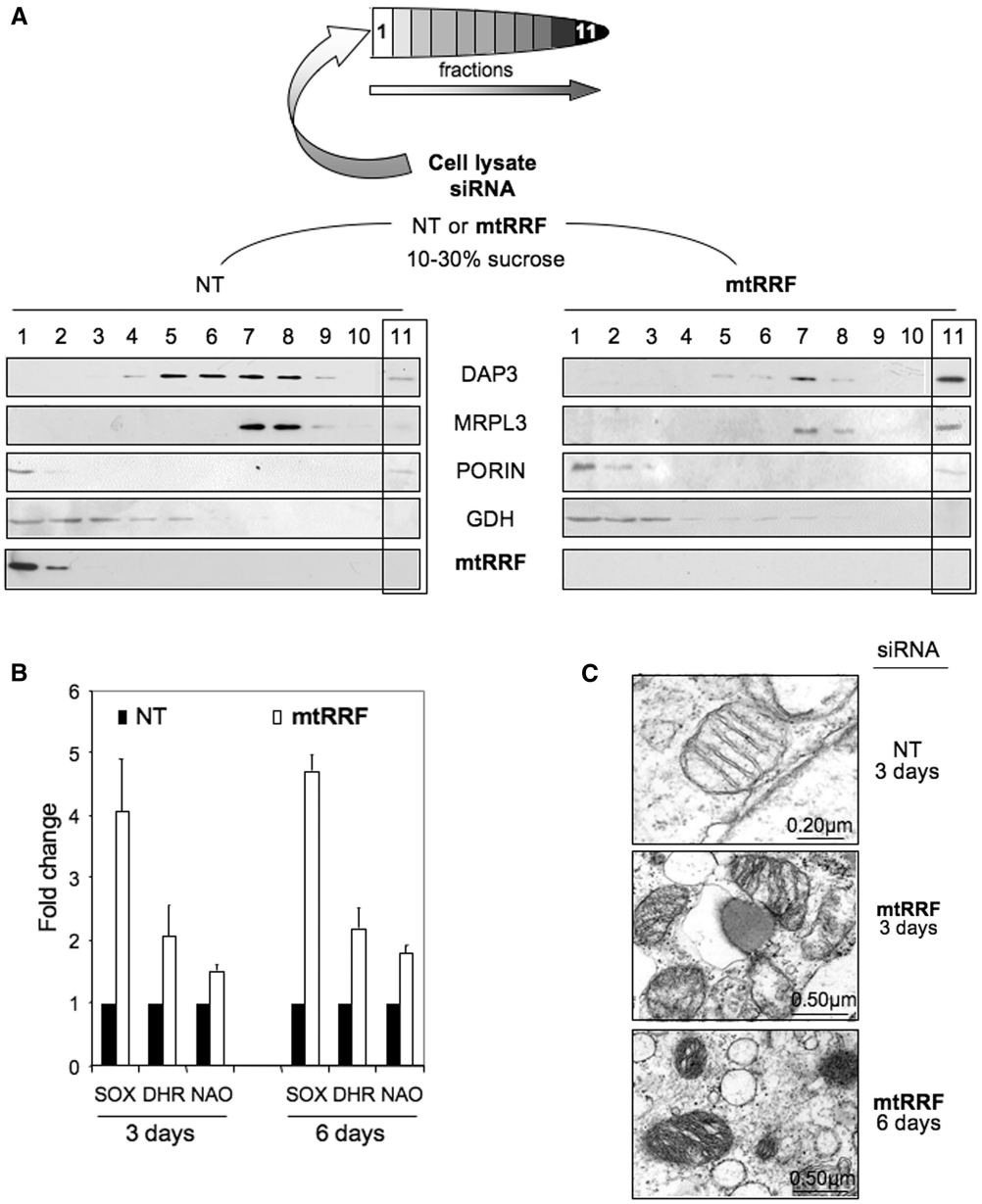

Figure 5. Reduction of mtRRF results in redistribution of ribosomal proteins, increased ROS and mitochondrial dysmorphism. (**A**). HeLa lysates were prepared from cells treated with mtRRF or non-targeted (NT) siRNA (3 days). After separation through 10–30% sucrose gradients, fractions were analysed by western blot using antibodies against the small (DAP3) and large (MRPL3) mitochondrial ribosomal subunits, mtRRF, porin as a mitochondrial membrane marker and glutamate dehydrogenase (GDH, matrix). (**B**) Superoxide levels are increased after mtRRF depletion. HeLa cells were exposed to *mtRRF* (white) or non-targeted (*NT*, black) siRNA over 6 days and superoxide and peroxide levels were measured with mitoSOX (superoxide) or DHR (peroxide) and compared to untreated controls. The fold increase is shown as a mean ± SEM from minimally three repeat experiments. Mitochondrial mass per cell was also measured using the cardiolipin selective dye NAO. (**C**) HeLa cells depleted of mtRRF show altered morphology. EM micrographs show HeLa cells treated with *mtRRF* (3 and 6 days) or non-targeted (NT, 3 days) siRNA. The images reflect mitochondria from two preparations.

DISCUSSION

Our studies presented here provide the first evidence that this candidate functions as the human mitochondrial ribosome recycling factor: (i) mtRRF is a mitochondrial protein, (ii) mtRRF is able to bind bacterial ribosomes *in vitro* and can tightly associate with human mitoribosomes *in vivo*, (iii) expression of human mtRRF suppresses the partial Δ*rrf1* respiratory deficiency in fission yeast *in vivo* and (iv) upon depletion of mtRRF, the relative level of mitochondrial monosomes increases whereas the free ribosomal subunits are reduced, indicating a defect in ribosome disassembly as has previously been reported on depletion of the bacterial counterpart (12).

Our results show that although mtRRF can associate tightly with mitoribosomes, the amount of interaction is enormously increased by pre-incubation. There are many possible hypotheses to explain this observation, but it is interesting to note that high resolution studies have shown

that RRF binds bacterial ribosomes that have adopted a ratchet conformation at a site spanning both P and A site (15). Therefore, it may be speculated that tRNA bound to these sites may prevent interaction with mtRRF allowing occupancy only when these sites become vacant.

Why does expression of human mtRRF restore the respiratory function of an *rrf1* mutant only in *S. pombe* and not in *S. cerevisiae*? Human mtRRF shows a stronger identity to *S. pombe* than the *S. cerevisiae* orthologue (EBI tools 21.1% versus 16.8%; Figure S4). There is an overall greater similarity between fission yeast and human mtRNAs (30) and these two species share a highly conserved set of general translation factors (18). In bacterial systems, functional studies with heterologous RRF and EFG proteins showed poor activity on the post-termination ribosomal complex compared to assays using RRF and EFG from the same species, underlining the importance of interplay between RRF and EFG [for example, (31,32)]. In light of these findings, it is also possible that human mtRRF was unable to rescue the growth phenotype of *S. cerevisiae* Δ*rrf1* due to a weak interaction with the budding yeast 70S mitoribosome or mtEFG that also has only limited similarity with the human mtEFG.

Depletion experiments revealed that mtRRF is essential for cell viability, with depletion causing gross mitochondrial dysmorphology and dysfunction. One of the primary effects of mtRRF depletion, which seemed to precede measurable translation abnormalities, was elevated ROS production (evident by day two post-transfection). The mechanisms that lead to mitochondrial ROS overproduction, although often associated with mitochondrial dysfunction are not always clear. Our recent work on depletion of the mitochondrial release factor mtRF1a also resulted in a profound increase in mitochondrial ROS without any measurable effect on mitochondrial translation (6). It is possible that increased ROS production could be a direct result of mitoribosome aggregation, but other subtle indirect effects cannot be ruled out. Our results are another example that even a small disruption of interplay between mitochondrial translation, respiration and ROS production may lead to profound cellular dysfunction.

In this study, lack of ribosome recycling led to a variety of deleterious downstream consequences. Shortage of available functionally active mitoribosomes eventually affected translation, and subsequently resulted in decreased steady-state levels of mitochondrially encoded proteins, hence reduced amounts of fully assembled complexes (6 days post-transfection). It was surprising, however, that a measurable decrease in mitochondrial protein synthesis took so long to manifest. It is possible that mitoribosomes are in excess in human organelles (33) with translation being initiated by mitoribosomes that had spontaneously disassembled. A similar process could explain the partial growth defect in yeasts lacking RRF. Another intriguing explanation could be that translation may be able to initiate from monosomes that have terminated translation, processed back along the mt-mRNA in a 3′ to 5′manner to reach the 5′-terminus and then scanned to locate the closest initiation codon, all without the monosome being dissociated. Although controversial, it must be considered that there is currently no model to explain how the mitoribosome naturally locates to the mt-mRNA initiation codon in the absence of a 5′-cap or Shine–Dalgarno sequence.

Finally, proteomic analysis of the factors that were eluted from immunoprecipitated mtRRF-FLAG, revealed 73 MRPs, several translation-associated factors and putative nucleoid proteins on the production and protease/DNase treatment of mitoplasts (Table 1). Nucleoids are dynamic structures containing mtDNA and proteins involved in maintenance, replication and transcription of the mitochondrial genome [reviewed in (34)]. These structures are well described in bacteria and close association between nucleoids and ribosomes has been previously measured in the Gram positive bacteria *Bacillus subtilis*, with this association being dependent on active transcription (35). Coupling of transcription and translation in human mitochondria has been frequently suggested (36,37), but there has been only one report showing interaction of mtRNA polymerase with a mitoribosomal protein, MRPL12, an interaction that was shown *in vitro* to stimulate transcription (38). In a recent report on proteins associated with nucleoids, 15 mitoribosomal proteins were identified, along with assorted factors that also function in protein synthesis (25). This observation is consistent with our data, but the authors were concerned that MRPs may have been present due to adventitious co-purification. Such a criticism could also be levelled at our observation, particularly as we were unable to completely remove cytosolic contamination, even in the mitoplasting experiments. Without further experimentation, this remains only tentative evidence of a direct physical link between mitoribosome and nucleoid. However, these proteomic studies also revealed several other candidate proteins that may be associated with the translational machinery and/or nucleoids. These findings open exciting avenues for further investigations.

SUPPLEMENTARY DATA

Supplementary Data are available at NAR Online.

ACKNOWLEDGEMENTS

We wish to thank L Spremulli (North Carolina, USA) for the initial construct. TD Fox for anti-Arg8Sc antibody and M Yoshida for the S. pombe RRF-FLAG2His6 plasmid. R.N.L. and Z.M.A.C.-L. wish to thank the Wellcome Trust for continuing support.

FUNDING

AFM and ANR (grant JCJC06-0163 to I.K., M.G. and N.B.); MEST-CT-FP6-503684 (to J.R. and M.W.); EUMITOCOMBAT (LSHM-CT-2004-503116 to J.W., J.S. and R.N.L.). Funding for open access charge: Wellcome Trust Grant 074454/Z/04/Z.

Conflict of interest statement. None declared.

REFERENCES

1. Anderson,S., Bankier,A.T., Barrell,B.G., De Bruijn,M.H.L., Coulson,A.R., Drouin,J., Eperon,I.C., Nierlich,D.P., Roe,B.A., Sanger,F. *et al.* (1981) Sequence and organization of the human mitochondrial genome. *Nature*, **290**, 457–465.
2. Pel,H.J. and Grivell,L.A. (1994) Protein synthesis in mitochondria. *Mol. Biol. Rep.*, **19**, 183–194.
3. Chung,H.K. and Spremulli,L.L. (1990) Purification and characterization of elongation factor G from bovine liver mitochondria. *J. Biol. Chem.*, **265**, 21000–21004.
4. Koc,E.C. and Spremulli,L.L. (2002) Identification of mammalian mitochondrial translational initiation factor 3 and examination of its role in initiation complex formation with natural mRNAs. *J. Biol. Chem.*, **277**, 35541–35549.
5. Schwartzbach,C.J. and Spremulli,L.L. (1989) Bovine mitochondrial protein synthesis elongation factors. Identification and initial characterization of an elongation factor Tu-elongation factor Ts complex. *J. Biol. Chem.*, **264**, 19125–19131.
6. Soleimanpour-Lichaei,H.R., Kuhl,I., Gaisne,M., Passos,J.F., Wydro,M., Rorbach,J., Temperley,R., Bonnefoy,N., Tate,W., Lightowlers,R. *et al.* (2007) mtRF1a is a human mitochondrial translation release factor decoding the major termination codons UAA and UAG. *Mol. Cell*, **27**, 745–757.
7. Zhang,Y. and Spremulli,L.L. (1998) Identification and cloning of human mitochondrial translational release factor 1 and the ribosome recycling factor. *Biochim. Biophys. Acta*, **1443**, 245–250.
8. Petry,S., Weixlbaumer,A. and Ramakrishnan,V. (2008) The termination of translation. *Curr. Opin. Struct. Biol.*, **18**, 70–77.
9. Agrawal,R.K., Sharma,M.R., Kiel,M.C., Hirokawa,G., Booth,T.M., Spahn,C.M., Grassucci,R.A., Kaji,A. and Frank,J. (2004) Visualization of ribosome-recycling factor on the Escherichia coli 70S ribosome: functional implications. *Proc. Natl Acad. Sci. USA*, **101**, 8900–8905.
10. Janosi,L., Shimizu,I. and Kaji,A. (1994) Ribosome recycling factor (ribosome releasing factor) is essential for bacterial growth. *Proc. Natl Acad. Sci. USA*, **91**, 4249–4253.
11. Janosi,L., Ricker,R. and Kaji,A. (1996) Dual functions of ribosome recycling factor in protein biosynthesis: disassembling the termination complex and preventing translational errors. *Biochimie*, **78**, 959–969.
12. Hirokawa,G., Demeshkina,N., Iwakura,N., Kaji,H. and Kaji,A. (2006) The ribosome-recycling step: consensus or controversy? *Trends Biochem. Sci.*, **31**, 143–149.
13. Peske,F., Rodnina,M.V. and Wintermeyer,W. (2005) Sequence of steps in ribosome recycling as defined by kinetic analysis. *Mol. Cell*, **18**, 403–412.
14. Zavialov,A.V., Hauryliuk,V.V. and Ehrenberg,M. (2005) Splitting of the posttermination ribosome into subunits by the concerted action of RRF and EF-G. *Mol. Cell*, **18**, 675–686.
15. Barat,C., Datta,P.P., Raj,V.S., Sharma,M.R., Kaji,H., Kaji,A. and Agrawal,R.K. (2007) Progression of the ribosome recycling factor through the ribosome dissociates the two ribosomal subunits. *Mol. Cell*, **27**, 250–261.
16. Weixlbaumer,A., Petry,S., Dunham,C.M., Selmer,M., Kelley,A.C. and Ramakrishnan,V. (2007) Crystal structure of the ribosome recycling factor bound to the ribosome. *Nat. Struct. Mol. Biol.*, **14**, 733–737.
17. Minet,M., Dufour,M.E. and Lacroute,F. (1992) Cloning and sequencing of a human cDNA coding for dihydroorotate dehydrogenase by complementation of the corresponding yeast mutant. *Gene*, **121**, 393–396.
18. Chiron,S., Suleau,A. and Bonnefoy,N. (2005) Mitochondrial translation: elongation factor tu is essential in fission yeast and depends on an exchange factor conserved in humans but not in budding yeast. *Genetics*, **169**, 1891–1901.
19. Chiron,S., Gaisne,M., Guillou,E., Belenguer,P., Clark-Walker,G.D. and Bonnefoy,N. (2007) Studying mitochondria in an attractive model: Schizosaccharomyces pombe. *Methods Mol. Biol.*, **372**, 91–105.
20. Gaisne,M. and Bonnefoy,N. (2006) The COX18 gene, involved in mitochondrial biogenesis, is functionally conserved and tightly regulated in humans and fission yeast. *FEMS Yeast Res.*, **6**, 869–882.
21. Steele,D.F., Butler,C.A. and Fox,T.D. (1996) Expression of a recoded nuclear gene inserted into yeast mitochondrial DNA is limited by mRNA-specific translational activation. *Proc. Natl Acad. Sci. USA*, **93**, 5253–5257.
22. Nijtmans,L.G., Henderson,N.S. and Holt,I.J. (2002) Blue native electrophoresis to study mitochondrial and other protein complexes. *Methods*, **26**, 327–334.
23. Chomyn,A. (1996) In vivo labeling and analysis of human mitochondrial translation products. *Methods Enzymol.*, **264**, 197–211.
24. Ishino,T., Atarashi,K., Uchiyama,S., Yamami,T., Saihara,Y., Yoshida,T., Hara,H., Yokose,K., Kobayashi,Y. and Nakamura,Y. (2000) Interaction of ribosome recycling factor and elongation factor EF-G with E. coli ribosomes studied by the surface plasmon resonance technique. *Genes Cells*, **5**, 953–963.
25. Bogenhagen,D.F., Rousseau,D. and Burke,S. (2008) The layered structure of human mitochondrial DNA nucleoids. *J. Biol. Chem.*, **283**, 3665–3675.
26. He,J., Mao,C.C., Reyes,A., Sembongi,H., Di Re,M., Granycome,C., Clippingdale,A.B., Fearnley,I.M., Harbour,M., Robinson,A.J. *et al.* (2007) The AAA+ protein ATAD3 has displacement loop binding properties and is involved in mitochondrial nucleoid organization. *J. Cell. Biol.*, **176**, 141–146.
27. Wang,Y. and Bogenhagen,D.F. (2006) Human mitochondrial DNA nucleoids are linked to protein folding machinery and metabolic enzymes at the mitochondrial inner membrane. *J. Biol. Chem.*, **281**, 25791–25802.
28. Kanai,T., Takeshita,S., Atomi,H., Umemura,K., Ueda,M. and Tanaka,A. (1998) A regulatory factor, Fil1p, involved in derepression of the isocitrate lyase gene in Saccharomyces cerevisiae–a possible mitochondrial protein necessary for protein synthesis in mitochondria. *Eur. J. Biochem.*, **256**, 212–220.
29. Teyssier,E., Hirokawa,G., Tretiakova,A., Jameson,B., Kaji,A. and Kaji,H. (2003) Temperature-sensitive mutation in yeast mitochondrial ribosome recycling factor (RRF). *Nucleic Acids Res.*, **31**, 4218–4226.
30. Schafer,B., Hansen,M. and Lang,B.F. (2005) Transcription and RNA-processing in fission yeast mitochondria. *RNA*, **11**, 785–795.
31. Ito,K., Fujiwara,T., Toyoda,T. and Nakamura,Y. (2002) Elongation factor G participates in ribosome disassembly by interacting with ribosome recycling factor at their tRNA-mimicry domains. *Mol. Cell*, **9**, 1263–1272.
32. Rao,A.R. and Varshney,U. (2001) Specific interaction between the ribosome recycling factor and the elongation factor G from Mycobacterium tuberculosis mediates peptidyl-tRNA release and ribosome recycling in Escherichia coli. *EMBO J.*, **20**, 2977–2986.
33. King,M.P. and Attardi,G. (1993) Post-transcriptional regulation of the steady-state levels of mitochondrial tRNAs in HeLa cells. *J. Biol. Chem.*, **268**, 10228–10237.
34. Kucej,M. and Butow,R.A. (2007) Evolutionary tinkering with mitochondrial nucleoids. *Trends Cell. Biol.*, **17**, 586–592.
35. Mascarenhas,J., Weber,M.H. and Graumann,P.L. (2001) Specific polar localization of ribosomes in Bacillus subtilis depends on active transcription. *EMBO Rep.*, **2**, 685–689.
36. Bonawitz,N.D., Clayton,D.A. and Shadel,G.S. (2006) Initiation and beyond: multiple functions of the human mitochondrial transcription machinery. *Mol. Cell*, **24**, 813–825.
37. Fontanesi,F., Soto,I.C., Horn,D. and Barrientos,A. (2006) Assembly of mitochondrial cytochrome c-oxidase, a complicated and highly regulated cellular process. *Am. J. Physiol. Cell Physiol.*, **291**, C1129–C1147.
38. Wang,Z., Cotney,J. and Shadel,G.S. (2007) Human mitochondrial ribosomal protein MRPL12 interacts directly with mitochondrial RNA polymerase to modulate mitochondrial gene expression. *J. Biol. Chem.*, **282**, 12610–12618.
39. Koc,E.C., Burkhart,W., Blackburn,K., Moyer,M.B., Schlatzer,D.M., Moseley,A. and Spremulli,L.L. (2001) The large subunit of the mammalian mitochondrial ribosome. Analysis of the complement of ribosomal proteins present. *J. Biol. Chem.*, **23**, 43958–69.
40. CadverKoc,E., Burkhart,W., Blackburn,K., Moseley,A. and Spremulli,L. L. (2001) The small subunit of the mammalian mitochondrial ribosome. Identification of the full complement of ribosomal proteins present. *J. Biol. Chem.*, **276**, 19363–19374.